NUREG/IA-0027
AEEW-M2464

International Agreement Report

TRAC-PF1/MOD1 Calculations of LOFT Experiment LP-02-6

Prepared by
P. Coddington, C. Gill

Winfrith Technology Centre
United Kingdom Atomic Energy Authority
Winfrith, Dorchester
Dorset, England DT 28 DH

Office of Nuclear Regulatory Research
U.S. Nuclear Regulatory Commission
Washington, DC 20555

April 1992

Prepared as part of
The Agreement on Research Participation and Technical Exchange
under the International Thermal-Hydraulic Code Assessment
and Application Program (ICAP)

Published by
U.S. Nuclear Regulatory Commission

Available from

Superintendent of Documents
U.S. Government Printing Office
P.O. Box 37082
Washington, D.C. 20013-7082

and

National Technical Information Service
Springfield, VA 22161

NUREG/IA-0027
AEEW-M2464

International Agreement Report

TRAC-PF1/MOD1 Calculations of LOFT Experiment LP-02-6

Prepared by
P. Coddington, C. Gill

Winfrith Technology Centre
United Kingdom Atomic Energy Authority
Winfrith, Dorchester
Dorset, England DT 28 DH

Office of Nuclear Regulatory Research
U.S. Nuclear Regulatory Commission
Washington, DC 20555

April 1992

Prepared as part of
The Agreement on Research Participation and Technical Exchange
under the International Thermal-Hydraulic Code Assessment
and Application Program (ICAP)

Published by
U.S. Nuclear Regulatory Commission

NOTICE

This report is based on work performed under the sponsorship of the United Kingdom Atomic Energy Authority. The information in this report has been provided to the USNRC under the terms of the International Code Assessment and Application Program (ICAP) between the United States and the United Kingdom (Administrative Agreement - WH 36047 between the United States Nuclear Regulatory Commission and the United Kingdom Atomic Energy Authority Relating to Collaboration in the Field of Modelling of Loss of Coolant Accidents, February 1985). The United Kingdom has consented to the publication of this report as a USNRC document in order to allow the widest possible circulation among the reactor safety community. Neither the United States Government nor the United Kingdom or any agency thereof, or any of their employees, makes any warranty, expressed or implied, or assumes any legal liability of responsibility for any third party's use, or the results of such use, or any information, apparatus, product or process disclosed in this report, or represents that its use by such third party would not infringe privately owned rights.

TRAC-PF1/MOD1 CALCULATIONS OF LOFT EXPERIMENT LP-02-6

P CODDINGTON
C GILL

SUMMARY

The report describes four TRAC-PF1/MOD1 calculations modelling the OECD-LOFT experiment LP-02-6. This was a 200% double-ended cold leg break experiment performed at nearly full power (47 MW) and with a loop mass flow of 248 kg/s. In the experiment the pumps were tripped and then allowed to coast down naturally after the start of the transient. Two of the calculations compared the results of two versions of the code (12.2 and 13.0), one incorporated a reduced gap between the fuel and the cladding to reduce the initial fuel stored energy, and the other had the TRAC interface sharpener model switched off.

Following the opening of the quick acting blowdown relief valves to initiate the transient there is a net flow out of the vessel until about 4 seconds, at which time the broken loop cold leg flow out of the vessel drops below the flow into the vessel from the intact loop cold leg, being driven by the pumps' inertia. This net flow into the vessel, enhanced by flashing of subcooled liquid in the downcomer and lower plenum, causes a bottom-up flow of liquid and quenches about 2/3 of the core. Additionally a top-down partial quench, extending to about the 30 inch elevation, is observed at about 15 seconds. This corresponds to fluid running back into the upper plenum and down into the core as the fluid in the pressurizer and steam generator begins to flow back along the intact loop hot leg.

The nature of the observed quenching is not entirely clear: it may be genuine fuel pin quenching or simply localised quenching of the thermocouples.

At 17.5 seconds, the primary system pressure reaches 42 bars, at which point the Emergency Core Cooling System trips. Measurements suggest oscillatory flow immediately upstream of the accumulator injection point in the intact loop cold leg. Except for two slugs of liquid, totalling about 200-250 kg, compared to a total accumulator flow of about 1,690 kg, no continuous bypassing of the downcomer by the accumulator fluid occurs. Most of it finds its way to the lower plenum. As the water level here rises, it begins to quench the bottom of the core at about 37 seconds and the quench moves progressively upwards. The final quench of the uppermost elevations is coincident with the entry of accumulator nitrogen into the intact loop cold leg and the consequent rise in the primary system pressure.

SUMMARY (Continued)

All four TRAC calculations predict similar hydraulic behaviour to each other. The bottom-up liquid flow at 4 seconds extends to the top of the core, as opposed to just 2/3 of the way up as in the experiment. The TRAC modelling does not predict either the bottom-up or the top-down quench at 15 seconds and following the subsequent fuel rod dryout the calculated temperatures are too high, particularly at the top and bottom of the fuel rods. The reduced fuel-gap calculations (ZEROGAP and ISHARP) are considerably better in this respect due to their lower stored energy. The calculations predict no bypass of ECCS fluid in line with the experiment and all predict oscillatory core inlet flow. There were differences, however, in the behaviour of fluid in the intact loop cold leg, for in some of the calculations the production of liquid slugs was predicted, in others it was not. These differences are believed to be due to the sensitivity of the TRAC condensation model rather than any specific changes to the models.

All the calculations predict a surge of fluid into the core on the entry of nitrogen into the intact loop cold leg. However, the higher rod temperatures in the calculations mean that the final quench is delayed longer than in the experiment.

The main differences between the calculations are therefore restricted to the thermal behaviour of the fuel rods due for example to the different dispersed flow heat transfer used in versions 12.2 and 13.0 and the reduced fuel stored energy in the ZEROGAP and ISHARP calculations.

Reactor Systems Analysis Division
AEE Winfrith

August 1987

CONTENTS

FIGURES

FIGURES (Continued)

FIGURES (Continued)

FIGURES (Continued)

TABLES

1 INTRODUCTION

This report provides a description of the results of four TRAC-PF1/MOD1 calculations of the OECD-LOFT experiment LP-02-6. This experiment was the third of the high power LOFT large break experiments (L2-3 and L2-5 being the previous two experiments) and although it was performed at the beginning of the OECD-LOFT project, the boundary conditions for the experiment were specified by the USNRC. The primary boundary conditions that distinguish this experiment from the previous experiments L2-3 and L2-5 were the increased power, ie 47 MW and the fact that the primary coolant pumps were tripped but not decoupled from their flywheel systems at the start of the transient. This resulted in a positive (bottom-up) core flow during the blowdown period, ie at about 5 secs, but the magnitude of this flow was less than that observed in the earlier experiment L2-3 where the pumps where kept running, such that the fuel rod external thermocouples quenched immediately only in the bottom 2/3 rds of the central fuel assembly. The remainder of the core (ie the top 1/3 rd) quenched subsequently during the top-down flow period after about 12 secs.

A description of the LP-02-6 experiment can be found in the Quick Look Report, Ref 1.

2 TRAC INPUT MODEL AND NODALISATION

Diagrams showing the LOFT facility and instrument locations are given in Figs 1 and 2 while noding diagrams of the TRAC representation of the LOFT facility are shown in Figs 3, 4, 5 and 6 for all the calculations presented in this report, all of which used the same nodal representation. The noding scheme and input model is based upon the original TRAC-PD2 model which was modified for TRAC-PF1/MOD1 at LANL for the analysis of L2-3 and at AEEW for the analysis of LP-LB-1 (Ref 2). However subsequent to the analysis of LP-LB-1 the input deck was modified (Ref 3) to improve the modelling in the areas of:-

(i) Primary coolant loop and vessel flow resistance.

(ii) Renodalisation of the ECCS injection line (Ref 4).

(iii) Revision of the fluid volumes and flow areas within the reactor vessel.

(iv) Inclusion of core bypass paths in the reactor vessel (lower plenum and core to upper plenum and downcomer to upper plenum).

(v) Revision of the vessel metal-work heat structures (Ref 5).

(vi) A revision and inclusion of ambient heat losses.

All of the above are likely to have an influence on the calculated results when compared to those calculated for experiment LP-LB-1 and in fact some of the revisions, eg (i),

(ii) and (v) were a result of recognised inadequacies of that analysis (see Refs 2 and 3).
The results of the renodalisation of the ECCS line can be seen in Fig 3, and the inclusion of the lower plenum and core to upper plenum bypass in Fig 6i. Also shown in Figs 3 and 4 is the location of the experimental measurement rakes in the intact and broken loop hot and cold legs.

3 TRAC CALCULATIONS

As stated above, this report contains the results of four TRAC-PF1/MOD1 calculations, these were performed sequentially and the results of the calculations are presented in three groups each containing a pair of calculations together with the experimental data where appropriate. This report therefore provides both the results of a limited sensitivity study together with a comparison of the TRAC calculations with the experimental data.

The four TRAC calculations, identified by their differences, are as follows:-

(1) A calculation using the 'Standard' Winfrith version of TRAC-PF1/MOD1, Version 12.2 (ie code version UK reference X26). This calculation used the "as manufactured" fuel-clad gap of 100 µm, on the figures this calculation is labelled "JON'S" and is the subject of a separate report (Ref 6).

(2) The above calculation was repeated using the Winfrith version of TRAC-PF1/MOD1 Version 13.0 (ie code version UK Reference B03). This calculation is labelled "ORIGINAL" on the figures.

(3) Calculation (2) was repeated but with the "fuel-clad" gap reduced to zero to reduce the steady state fuel stored energy and hence the peak cladding temperatures during blowdown. This calculation is labelled "ZERO-GAP" on the figures.

(4) Finally calculation (3) was repeated but with the TRAC-PF1/MOD1 core interface sharpener logic <u>removed</u>. The core interface sharpener logic is a facility for overwriting the axial mass flux in the core calculated from the constitutive relations with an externally imposed model to produce a "sharp" core liquid level. The interface sharpener restricts the axial flow of liquid in the core by limiting the core cell exit void fraction to be greater than 90% irrespective of that calculated by the constitutive relations. The operation of the interface sharpener has been seen to produce unphysical behaviour during blowdown when applied to reactor calculations and to produce too sharp a liquid vapour interface during reflood (Ref 7). Its use is therefore <u>not</u> currently recommended. This calculation is labelled "ISHARP" in the figures.

A review of the four calculations is given in Table 1.

4 INITIAL CONDITIONS

The initial conditions for experiment LP-02-6 and the calculated transients are given in Table 2. The data for the experiment was taken from the Experiment Quick LooK Report (Ref 1) and the Experiment Specification Document (Ref 8). The data for the TRAC calculations was taken from the "ZERO-GAP" calculation which was the calculation used as the submission to the OECD-LOFT LP-02-6 experiment comparison exercise (Ref 9). There are no significant differences between the initial conditions of the four calculations and in fact transient calculations 3 and 4 used the same steady-state calculation.

One major difference between this series of calculations and all previous TRAC calculations, ie PD2 L2-3 and L2-5 (Ref 10) and PF1/MOD1 LP-LB-1 (Ref 2) and LP-02-6 (Ref 11) calculations is the improvement in the bypass modelling. As we see from Table 2, for example, the total calculated bypass of ~ 10% is divided into a lower plenum to upper plenum bypass of 2.6%, a downcomer to upper plenum bypass of 2.26% with the remainder, 5.25%, flowing through the Reflood Assist Bypass Valves (RABV). Previously only the flow through the RABVs was represented.

The power was increased in experiment LP-02-6 from the 36 MW used in L2-3 and L2-5, to 47 MW, an increase of ~ 1.3. However the flow rate was only increased by ~ 25% from 200 kg/sec to 250 kg/sec, producing therefore a slightly increased temperature rise across the core. The contrasts with experiment LP-LB-1 where the loop flow rate was increased to ~ 300 kg/sec for a small (49 compared to 47 MW) increase in core power, producing a significantly smaller core ΔT.

The relative magnitude of loop flow and core power is likely to influence the vessel hydraulic behaviour during blowdown, as is the bypass representation for the calculated transients.

The total accumulator liquid available in experiment LP-02-6 was ~ 1.69 m^3 which is lower than that for experiments L2-5 (1.96 m^3) and L2-3 (2.166 m^3), but higher than that of experiment LP-LB-1 (1.18 m^3) (Ref 12). These numbers should be compared with the vessel volumes of 0.68 m^3 for the lower plenum, 1.017 m^3 for the downcomer (this number was significantly increased from that of 0.672 m^3 used in previous TRAC analyses of LOFT) and 0.272 m^3 for the core.

As will be seen from Table 2 the accumulator gas volume used in the calculation is significantly smaller than the experimental value (0.642 m^3 compared to 0.95 m^3). This difference was introduced into the input deck to compensate for the fact that the TRAC code places a lower limit on the Nitrogen gas temperature of 273 k (0°C) ie the freezing point of water, and that the gas temperature will fall well below this value during the emptying of the accumulators.

Apart from the above accumulator gas volume difference, Table 2 shows that the TRAC calculated initial conditions for the primary circuit are within the uncertainty levels of the corresponding measured quantities. There is however a small difference in the pressuriser volumes used in the calculations (liquid 0.555, steam 0.376 m^3) compared to those for the experiment (liquid 0.607, steam 0.39 m^3).

5 ANALYSIS OF LP-02-6 TRANSIENT

5(i) Sequence of Events

The sequence of the significant events for LOFT experiment LP-02-6 are listed in Table 3, where the times of occurrence are compared with the times predicted by the "ZERO-GAP" TRAC calculation. This is the same calculation as that for which the initial conditions were presented in Table 2.

Experiment LP-02-6 was initiated (0.0 secs) by the opening of the quick-opening blowdown valves in the broken loops. The reactor was scrammed on low hot leg pressure at 0.1 secs and the pumps were tripped at 0.8 secs. (The pumps were not immediately decoupled from their flywheels as in experiment L2-5, but allowed to coast down naturally). The pumps coasted down until 16.5 secs when their rotational speed fell below the trip point and they were decoupled from their flywheels. Following the opening of the blowdown valves the system pressure falls rapidly to the saturation pressure of the hot leg fluid and voids form in the upper plenum, core and hot leg. The flow into the core quickly reverses as a result of the large subcooled critical flow out of the broken loop cold leg. The core therefore rapidly voids such that the fuel rods begin to dryout in the centre of the core at about 0.9 secs. The fuel rod cladding temperatures (recorded by the thermocouples located on the outside of the cladding) rise as the energy stored within the UO_2 is equalised radially across the whole of the fuel rod. The fuel rod cladding temperatures continue to rise until approximately 5 secs when a positive flow through the core was re-established. This flow through the core at about 5 secs, occurs as the flow into the vessel downcomer from the intact loop, which remains almost constant as a result of the high pump inertia and single-phase nature of the cold leg fluid, exceeds the falling flow out of the vessel downcomer through the broken loop cold leg. The broken loop cold leg flow falls as the system pressure falls from hot leg saturation pressure to the cold leg saturation pressure. The flow through the core at 5 secs is enhanced by the flashing of the cold leg fluid in the vessel lower plenum and downcomer and the intact loop cold leg. The positive flow through the core cools the core and produces a rapid quench of the cladding (external) thermocouples in the lower ~ 2/3 rds of the central fuel assembly. After the system pressure falls below the cold leg saturation pressure the flow of liquid into the downcomer decreases as the intact loop cold leg voids, so that this flow quickly falls below that out of the broken loop cold leg, and the core once again empties. After ~ 10 secs therefore the fuel rods in the core begin to heat up again. A partial top-down quench is initiated at about 15 secs and lasts until ~ 18.5 secs as liquid flowing out of the pressuriser and along the hot leg into the upper plenum flows down into the core.

The system pressure falls below the accumulator trip point at ~ 17.5 secs and the ECCS liquid begins to flow into the primary circuit, the HPIS and LPIS began at 21.8 and 34.8 secs respectively. The flow out of the broken loop continues to fall as the primary system pressure falls with no obvious direct bypass of liquid (ie subcooled liquid in the broken loop cold leg), except for one slug of liquid between 30 and 32.5 secs.

The lower plenum was estimated to have filled at 30.7 secs (Ref 1) which is the time that the lowest core thermocouple (ie at a 2 inch elevation) is observed to quench. This is well in advance of the time that the accumulator empties. The accumulator tank for example empties at about 48 secs, while an additional ~ 7 secs is required to clear the ECCS line, so that the ECCS accumulator liquid flow into the intact loop cold leg is not complete until about 55 secs. Following this the effect of the accumulator nitrogen flow into the primary circuit is seen as part of the slug of subcooled liquid, resident in the intact loop cold leg, is swept out of the broken loop cold leg.

Following the cooling of the fuel rods during the blowdown period, once the cladding thermocouples dry out they heat up rapidly in the centre of the core to a temperature of about 800 K, which is close to the corresponding fuel temperature. The cladding temperatures then increase slowly as a result of the fuel decay heat until the bottom of the core begins to quench at about 31 secs as outlined above. Following this, liquid flows into the bottom of the core and begins to cool the lower parts of the fuel rods while the fuel rod quench progresses intermittently up the bottom part of the core reaching the 21 inch elevation at about 48 secs. Above the peak power elevation ie at a height of greater than about 30 inches, the fuel rods do not begin to cool until about 42 secs at which time the cladding temperatures range from ~ 750 K at 31 inches to ~ 500 K at 62 inches. The quench time of the fuel rods at these elevations corresponds to the end of the accumulator liquid flow, with for example times of 54.5 secs at 31 inches, 56 secs at 43.8 inches and 49 inches and 54.5 secs again at 62 inches. (The end of the accumulator liquid flow into the primary circuit is estimated to occur at about 55 secs - see above). It is postulated therefore that the flow of accumulator nitrogen into the intact loop cold leg initates the flow of a slug of liquid into the core as well as one out of the broken loop cold leg as described above. The mechanism that leads to this is described in Ref 13 for example. The flow of liquid into the core at the time is able to quench the upper parts of the fuel rods as the majority of the cladding is at a temperature below the minimum film boiling point of ~ 650 K. The quench of the core therefore was complete by 56 secs and occurs as a direct result of the flow of a slug of liquid into the bottom of the core driven by the system pressurisation as the flow into the primary circuit from the accumulator changes from water to nitrogen.

5(ii) TRAC Calculations

In the following three Sections of the report we present the results of the four TRAC calculations of experiment LP-02-6 described in Section 3 and Table 1. The results of the four calculations are presented in the following three groups of Figures together with the experimental measurements where appropriate.

GROUP 1, Figure 7 to 77

Calculations (see Section 3 and Table 1)

- "JON'S", "ORIGINAL"

and the experimental data.

GROUP 2, Figures 78 to 148

Calculations; "ORIGINAL", "ZERO-GAP"

and the experimental data.

GROUP 3, Figures 149 to 219

Calculations; "ZERO-GAP", "ISHARP"

and the experimental data.

The results from each of the above groups is described in turn in the following Sections. In the first Section a detailed description of the experimental measurements together with a comparison with the general results of the TRAC calculations is provided in addition to comments on the differences between the two calculations. The subsequent Sections just review the differences between the calculations and how these influence the main elements of the calculated transient.

5(iii) "JONS" and "ORIGINAL" Calculations

LOOP BEHAVIOUR

These two calculations of the LOFT large break transient experiment LP-02-6 are identical in the sense that they used exactly the same input deck. The difference between the two calculations being that the "JON'S" calculation was performed using code version X26 (UK version of LANL code version 12.2) and the "ORIGINAL" calculation was performed using code version B03 (UK version of LANL code version 13.0). There are obviously likely to be many differences between the two code versions - in spite of the fact that the code from version 12.1 was formally a frozen code, however it is thought that none of these changes, except for one, are likely to have a significant influence on the behaviour of a large break calculated transient. We consider that this observation is confirmed by the results presented in Figures 7 to 77. The one area in which there is a known difference between the two code versions that is likely to influence large break calculations are the changes made the post-dryout heat transfer. This accounts for the difference in the calculated cladding temperatures which occur primarily during the reflood period. In code version X26 the "error" in the Forslund-Rohsenow dispersed flow heat transfer coefficient (ie the use of the liquid thermal conductivity instead of the vapour conductivity) had been corrected by the UK. In version B03 the Forslund-Rohsenow relation had been changed by LANL in such away as to correct the "error" in the value of the thermal conductivity used but to also increase the numerical coefficient in order to preserve the resultant value of the heat transfer coefficient. This revised value of the Forslund-Rohsenow dispersed flow heat transfer coefficient introduced by LANL in version 13.0 was kept in the equivalent UK version B03. The result of this change can be seen as a more rapid cooling of the cladding temperatures during reflood with the revised form of the heat transfer term in the "ORIGINAL" ie B03 calculation.

The first observation from the results of these two calculations is that their behaviour particularly that reflected by the global parameters is very similar especially during the blowdown period (ie 0.0 to 20.0 secs), where the results of the two calculations are almost indistinguishable. The calculated and experimental pressure decay, shown for example in Fig 7 for the broken loop cold leg and Fig 30 for the intact loop hot leg shows a very good comparison between the two calculations and the experiment, and a significant improvement over that calculated for LOFT experiment LP-LB-1 (Ref 2). For experiment LP-LB-1 the TRAC calculation underestimated the primary system pressure after approximately 13 secs. The improvement in the calculation for LP-02-6 is ascribed to the revised vessel metal heat structures contained within the LP-02-6 input deck as these produce a significant increase in the heat released from the vessel metal-work to the fluid (see Fig 51). There is a small difference in the calculated system pressure between about 26 and 33 secs, with the "JON'S" calculation providing a better comparison with the experimental data. It is thought that this difference is possibly due to different condensation rates in the intact loop cold leg and Fig 20 for example shows that during the approximate same time period in the "JON'S" calculation a liquid slug forms upstream of the ECCS injection point whereas one is not formed in the "ORIGINAL" calculation. Previous experience of large break TRAC calculations has shown that the details of the intact loop cold leg behaviour during the accumulator flow period is both difficult to predict and very sensitive to the details of the loop and ECCS flows. This of course is always likely to be the situation when large changes in condensation rates are involved.

The broken loop cold leg density and mass flow shown in Figs 8 and 9 show that although the density is well calculated during the blowdown period the calculated mass flow is overestimated both during the subcooled period and during the saturated flow period when the calculations are approximately 20 kg/sec higher than the experimental value. This is a consistent feature of all of the calculated transients, but is different to that of the LP-LB-1 comparison (Ref 2), however that probably just reflects the difference in the calculated primary system pressures for LP-LB-1 and LP-02-6 (see above). The calculated mass flow during the saturated blowdown period is high in spite of the fact that a critical flow multiplier of 0.84 is used, a value of 1.0 is used during the subcooled blowdown. (These numbers were inherited from LANL and have not been the subject of a study in the UK, however it would not be possible to justify a number of less than 0.84 for the saturated flow period). As observed in Section 5(i), neither of the calculated transients shows any direct ECCS bypass, until the accumulator empties at about 53 secs, whereas the experiment shows the flow of two distinct slugs of subcooled water through the broken loop cold leg (Figs 8, 9, 10) the first betwen 29 and 33 secs and the second between 49.5 and 51.5 secs. Both the calculations and the experiment show the flow of a slug of subcooled liquid coincident with nitrogen entering the intact loop cold leg from the accumulator, however, the calculated flow is much more extensive than that observed in the experiment.

Rather surprisingly both of the calculations show some reverse flow at the measurement location in the broken loop cold leg, during the bypass phase of the transient. The "JON'S" calculation shows some reverse flow at ~ 43 secs while the "ORIGINAL" calculation shows reverse flow at ~ 42.5 secs and 46.5 secs, whereas none is observed in the experiment. Given the good agreement between the calculated and experimental primary system pressure during this period it is possible that the reverse flow results from an error in the break pressure used in the calculation to simulate the presure in the blowdown suppression tank.

The calculated and experimental intact loop cold leg behaviour is shown in Figs 20 to 26, the first point to note is the different pump behaviour as shown in Fig 25. The "ORIGINAL" calculation used the INEL specified pump inertia and so produces a long coast down such that the pump is not calculated to decouple from its flywheel system (ie at a velocity of 75 rads/sec) until after 70 secs, this is consistent with other calculations of the pump behaviour, see for example Ref 11, Fig 79. The experimental curve shows a much faster initial rundown of the pump such that the pump decouples from its flywheel at ~ 16.5 secs, because of the subsequent reduced inertia the pump velocity increases during the bypass phase of the transient as a result of the ECCS related condensation induced pressure drop across the intact loop. The main feature of the pump velocity curve for the "JON'S" calculation is that the pumps were tripped to decouple from their flywheels at the experimental time of 16.5 secs. In spite of the different pump behaviour seen in the two calculations there is almost no observable difference in the intact loop cold leg flow, see for example Fig 21 which shows the cold leg mass flow.

The intact loop cold leg calculated and experimental fluid densities show very good agreement up to ~ 12.5 secs, both

showing for example the start of the voiding in the cold leg at ~ 6 secs. Between 12.5 and 20 secs the calculated densities are slightly higher than the average experimental value, but well within the range of the experimental error. The calculated velocity and hence mass flow are however lower than the experimental values (by about 25 kg/sec in the case of the mass flow) during the first 6 secs when the flow is single-phase liquid. Following this the experimental fluid velocity and therefore mass flow falls rather more abruptly than the calculated values.
Following the initiation of the flow of liquid from the accumulators into the intact loop cold leg at ~ 17.5 secs, the formation of oscillating slugs of subcooled liquid immediately upstream of the ECCS injection point are observed starting at about 21 secs. The oscillatory nature of the liquid slugs can be seen in the measurements of fluid density, mass flow, fluid velocity and temperature. These observations are consistent with the behaviour of all of the other LOFT large break experiments, although as was mentioned in the analysis of experiment LP-LB-1 (Ref 2) a detailed analysis of the individual density and momentum flux measurements (not shown here) shows that the fluid flow is unlikely to be one of a simple 1-D slug moving back and forth along the cold leg pipe. The calculated behaviour is not one of an oscillatory slug although the calculated fluid densities, Fig 20, show that in the case of the "JON'S" calculation there is some intermittent slug flow upstream of the ECCS injection point but almost none in the case of the "ORIGINAL" calculation. It is not possible currently to offer an explanantion for the different behaviours. Both calculations produce a stable liquid slug downstream of ECCS injection location.

The broken and intact loop hot leg comparisons are shown in Figs 14 to 19 and 26 to 32 respectively. The differences in the behaviour of the two calculations in both the broken loop and intact loop hot legs is almost negligable. However both calculations underestimate the broken loop hot leg fluid density and mass flow after the first few seconds, although the errors on both measurements are quite large.

The flow in the intact loop hot leg remains in a positive direction for approximately the first 9 secs as a result of the pressure drop provided by the slow rundown of the pumps. (This is in contrast to a positive flow period of approximately 4.5 secs for experiment LP-LB-1 where the pumps were decoupled from their flywheels at the start of the transient). After 9 secs the flow reverses and two peaks in the mass flow are observed, the first at ~ 12 secs occurs as liquid flows out of the pressuriser and back along the hot leg to the upper plenum and the second at ~ 16.5 secs when liquid from the upside of the steam generator tubes flows back along the hot leg. In both of these instances Fig 27 shows that the magnitude of the reverse flow peaks is much greater in the calculation than in the experiment. During the initial (0 to 9 secs) positive flow period an increase in flow is observed, ie at about 6.5 secs in the experiment but not in the calculations this attributed

(Ref 1) to be a consequence of the bottom-up flow through the core at this time. However no significant hot leg flow is calculated even when the core interface sharpner is turned off - see Section 5(v). As the hot leg side of the reactor drains the hot leg mass flow falls, and the flow becomes positive again at about 30 secs. However in the experiment a surge in the hot leg flow is seen at about 26.5 secs, and several peaks in the flow are observed between 42 and 51 secs. These later ones presumably occur as a result of liquid carry over from the core as the lower part of the core quenches during the period. An increase in the hot leg flow is seen at ~ 54 secs in both the experiment and the calculations coincident with the surge of liquid into the core following the initial injection of accumulator nitrogen into the intact loop cold leg.

The depressurisation and water level of the pressuriser is shown in Figs 31 and 32, the calculated depressurisation rate is slightly faster than the experimental value as a result of the underestimation of the initial pressuriser liquid level.

The accumulator level and pressure is shown in Figs 33 and 34, the agreement between the calculations and the experimental values is now very good following the renodalisation of the ECCS line (Ref 3). However no explanation can be found for the discrepancy between the calculated and measured accumulator pressure during the period when nitrogen flows from the tank.

VESSEL HYDRAULIC AND THERMAL BEHAVIOUR

The vessel hydraulic and thermal behaviour is shown in Figs 35 to 52, while the fuel rod cladding temperatures are shown in Figs 53 to 77. The global vessel behaviour, ie vessel mass, lower plenum liquid volume fraction etc is shown in Figs 43 to 48, for the two calculations, there is of course no direct experimental equivalent data. The results from the two calculations are virtually identical during the first 20 secs, while after this there is a slight delay in the filling of the vessel in the "JON'S" calculation as the ECCS liquid accumulates as a slug in the intact loop cold leg extending upstream of the injection point.

The calculated behaviour of the vessel during blowdown shows that the core, lower plenum and downcomer void during the first 3 to 4 secs as subcooled liquid flows out of the broken loop cold leg. The core rapidly empties while the lower plenum and downcomer liquid volume fractions fall to about 0.7. As the flow of subcooled liquid out of the broken loop cold leg falls it is exceeded by the flow of liquid into the vessel from the intact loop cold leg so that the liquid volume fractions of the lower plenum and downcomer increase. These then fall again after about 6 secs when the flow of liquid into the vessel decreases as the fluid in the intact loop cold leg flashes. The increase in the flow of liquid into the vessel produces a flow of liquid into the bottom of the core beginning at about 4 secs. The flow through the core is enhanced by the flashing of the liquid in the lower plenum and downcomer at about 6 secs and then falls to zero again between about 9 and 10 secs as the lower plenum and downcomer void. (See Fig 35). In addition to the above flow of liquid into the bottom of the core a flow of liquid from the upper plenum down through the core is observed to occur between about 16 and 22 secs. This is shown as a reverse flow in the core outlet mass flow, Fig 44.

As stated above, the calculations show that, following the initiation of the accumulator flow at about 17 secs, the accumulator liquid flows into and down the vessel downcomer to fill the vessel lower plenum, and there is no observed direct bypass of the accumulator liquid out of the broken loop cold leg. Although of course fluid continues to flow out of the broken loop cold leg this fluid is saturated and is provided by the flashing of the liquid in the lower plenum as the pressure falls. The flow of accumulator liquid into the lower plenum produces an increase in the liquid volume fraction beginning at about 25 secs. Almost immediately some small quantity of liquid enters the bottom of the core and its influence can be seen on the cladding temperature (thermocouples) located at the bottom of the core. Initially all the accumulator liquid flows down the downcomer into the lower plenum so that the liquid volume fraction rises to ~ 0.75 at about 33 secs. Following this the liquid flow into the core increases and some liquid begins to accumulate in the downcomer. At about 40 secs in both calculations the lower plenum is liquid full and the core liquid volume fraction is ~ 0.2. (Note this is still some ~ 15 secs before the end of accumulator injection). After 40 secs when the lower plenum is full the accumulator liquid continues to flow into the downcomer which therefore rapidly fills, with the downcomer in the version 13.0 (ie "ORIGINAL") calculation filling somewhat faster than in the version 12.2 (ie "JON'S") calculation. The downcomer continues to fill in the calculation well above the level of the nozzles as a consequence of the fact that the primary system pressure falls below the boundary pressure used to model that in the blowdown suppression tank. The downcomer begins to empty at about 52 to 53 secs which is coincident with the end of the accumulator liquid flow as the primary system pressure once more exceeds that at the break. Following this there is a rapid increase in the liquid content of the core.

As stated above there is no detectable difference in the vessel behaviour between the two calculations during the blowdown period, and although there are some differences in detail between the two calculations following the initiation of the accumulator liquid the global behaviour is the same. The differences in behaviour almost certainly arise from the extreme sensitivity of the 1-D condensation model which as we have seen produces an upstream liquid plug in one instance but not in the other, rather than a specific difference between the two code versions.

As has been stated in relation to the analysis of other LOFT large break experiments (see Ref 2), the level and interpretation of the LOFT vessel instrumentation is both limited and difficult. However the lower plenum velocity and mommentum flux measurements (Figs 36 and 42) do confirm the bottom up flow of liquid observed during blowdown, ie between about 4.5 and 9 secs. Also it is possible to estimate that the peak velocity and mass flux of the flow was > 1 m/sec and between 500 and 1000 kg/m^2 sec respectively. The downcomer fluid temperature measurements, located on the broken loop side, also confirm the broken loop cold leg measurements in that there was only a small amount of direct subcooled liquid bypass. Fig 38 for example shows liquid subcooling only, between 31 and 33 secs and between 50 and 53 secs, prior to the end of the accumulator liquid injection.

CORE THERMAL RESPONSE

Central Bundle

The fuel rod cladding temperatures for the "JON'S" and "ORIGINAL" calculations together with the experiment are shown if Figs 53 to 63 for the central fuel assembly (ie LOFT assembly 5) and in Figs 64 to 67 for the instrumented peripheral fuel bundles (ie LOFT fuel assemblies 2, 4 and 6). In addition Table 4 shows the axial location of the calculational fine mesh together with the relative power density at the coarse mesh boundaries.

Two features of the calculated temperature transients are immediately obvious, (1) is the fact that during blowdown (and therefore for the remainder of the transient) the calculated peak clad temperatures are more than 100K too high and (2) the fact that the "ORIGINAL" calculation (version 13.0) cools faster than the "JON'S" calculation (version 12.2).

The peak clad temperature of a fuel rod during the initial blowdown period of a large break transient is determined primarily by the transfer of heat from the centre of the fuel to the cladding as the cladding to fluid heat transfer falls following dryout and as the heat generated within the core falls to the decay heat level. This means that the peak cladding temperature is particularly sensitive to the fuel rod pre-transient (steady state) stored energy, ie fuel rod centre temperature. The only unknown parameter of any significance in the calculation of the steady state fuel stored energy is the fuel to cladding heat transfer, ie the fuel-clad gap conductance. In the TRAC code this is determined from the input value of the fuel-clad gap width, and in both of these calculations this was set to the "as manufactured" value of ~ 100 μons. Because of the obvious error in the resultant peak clad temperatures particularly at the bottom of the fuel rods, the influence of changing the fuel clad gap to fully closed, ie no gap, is evaluated as part of this sensitivity study (see Section 5.iv). Calculations of the initial cladding temperature response over the whole core is made more difficult because of the limitations of the TRAC fuel pin model, for example there is only a single fuel pin representation for the whole of the core and for this pin only a single set of radial dimensions can be input. So that changes in the pin dimensions both axially and between pins cannot be modelled. Also changes in the fuel clad gap width and the fuel and clad dimensions generally, due to mechanical effects, cannot be modelled, only changes due to thermal effects are considered.

From Figs 53 and 54 we see that the fuel rod cladding temperatures during blowdown of the two calculations are identical and although there are some small differences in the cladding temperatures during the refill period the largest and most consistent difference is the fact that during reflood the "ORIGINAL" calculation (version 13.0) cools faster than the "JON'S" calculation (version 12.2). The major identifiable difference between the two code versions as was reviewed in Section 3, is that the dispersed flow (ie void fraction > 0.5) heat transfer coefficients in the UK version of 13.0 were significantly higher than those in the UK version of 12.2. (For the reasons mentioned in Section 3 the LANL version of both codes would have given the higher of the two heat transfer coefficients). The higher heat transfer for the "ORIGINAL", ie v13.0 calculation would of course produce the observed earlier cooling of the cladding for identical core fluid conditions. Although as we see from Fig 48 for example, there are some small differences in the core liquid mass during reflood, but these on their own are not enough to be responsible for the different cladding behaviour.

The experimental cladding temperatures in LOFT are those recorded by thermocouples attached to the surface of the cladding. This has lead to intense speculation both to whether they truly reflect the temperature of the cladding particularly during the very rapid quench periods and to whether the thermocouples themselves induce additional cooling that would not be present on uninstrumented fuel rods. Both of these questions have been subject to separate effects experimental investigations at both high and low pressures (Ref 14 and 15) and a review of this information is currently taking place at AEEW (Ref 16).

The general response of the calculated and experimental cladding temperatures during the transient just reflects the vessel hydraulic behaviour described above. The cladding temperatures rise rapidly after about 1 sec as the fuel rods in the central assembly begin to dry out, increasing to over 1000K after about 3 secs in the experiment at the peak power location. The calculated peak temperatures are higher by up to 100K, because of the too large a value of the steady state stored energy, as explained above. After approximately 5 secs the surge of liquid into the bottom of the core produces a rapid cool down (quench) of the experimentally observed temperatures at all elevations up to and including the 39 inch level, but not at elevations above this. In the calculation the cladding is cooled by more than 200K at the 24 and 27 inch elevations, but of course this is not sufficient to produce a quench. More significant is that in the calculation the cooling extends all the way to the top of the fuel assembly so that at the 62 inch elevation for example, where the temperatures are low because of the lower power, a quench occurs in the calculation but not in the experiment.

Following the rapid cool down (quench) of the thermocouple-cladding in the experiment, dryout occurs again at the centre of the core after about 11 secs, and the temperature across the the fuel rod is once again re-equalised as the observed temperatures rise rapidly to about 800K. This behaviour is confirmed by the limited fuel rod centre line temperature measurements which show the centre of the fuel at the 27 inch elevation (Fig 63) to cool slowly to ~ 800K at about 15 secs. In the calculated transients following the blowdown cooling of the fuel rods the cladding temperatures rise to ~ 1000K, ie some 200K higher than the experimental values.

At the higher elevations in the central fuel assembly for the experiment the influence of the top down flow of liquid from the upper plenum is seen as the fuel rods quench from the top downwards between about 15 and 19 seconds. Although a small downflow of liquid is observed in the calculations (Fig 44) between 16 and 22 secs. This does not appear to have a major influence on the cladding temperatures except at the highest (62 inch) elevation (Fig 62).

Following the blowdown cooling and the re-equalisation of the fuel rod temperatures, ie after ~ 15 secs, the cladding temperatures rise slowly as the core is steam cooled and the vessel fills with water from the accumulator. This continues until the first sign of reflood cooling occurs at about 30 secs which is well before the accumulator empty time of ~ 54 secs. The temperature rise turns over at about the same time in both the experiment and the calculations (particularly the "ORIGINAL" v13.0 calculation) especially towards the bottom of the core, ie below ~ 21 inches. Above this, ie up to 31 inch level the cooling effect of the core flows is seen in the experiment, but not in the calculation until ~ 40 secs, when as Fig 48 shows there is an increase in the flow of water into the core. Above the 31 inch elevation both the experiment and calculations show a cooling of the fuel rods after 40 secs. The cooling of the cladding particularly in the experiment is distinctly oscillatory in nature, indicating an oscillating flow at the core inlet, this is likely to arise both as a result of increases in the core pressure as steam is produced and as a reduction in the pressure in the intact loop cold leg as steam condenses on the subcooled accumulator liquid.

The fuel rod cladding in the central fuel assembly continues to cool and subsequently quenche, such that, except at the very bottom of the core, the quench takes place coherently over significant lengths of the core. The following for example shows the quench times at the various elevations in the central assembly, and we see that

Elevation	Quench Time
2"	31 secs
11"	46.7 secs
21"	46.7 secs
24"	54.2 secs
27"	54.2 secs
31"	55.8 secs
43.8"	55.8 secs
49"	55.8 secs
62"	54.6 secs

the core quenches at the 11 and 21 inch elevation at ~ 47 secs while the remainder of the core, ie 24 to 62 inches quenches between 54 and 56 secs. The final core quench (ie between 54 and 56 secs) occurs at the same time as the termination of the accumulator liquid flow and the initiation of the accumulator nitrogen flow, and as is explained in Refs 13 and 17 and above this produces a surge of liquid both out of the broken loop cold leg and into the core. The coherency of the final quenches indicate that for this experiment, and for LOFT in general, the quench process is dictated by the fluid conditions, rather than thermal conditions within the fuel rod. In this sense it is different from the propagating quench fronts observed in slow forced reflood experiments. The experimental quench temperatures in this experiment are by and large determined by the fuel rod temperatures at the time of the "end of accumulator" inflow of liquid into the core, but are typically less than 700K even at the peak power elevation. As explained above the relation of the observed quench temperatures in LOFT to a minimum in the boiling "Tmin" has been the subject of several separate effects studies, some of which (Ref 15) have shown that at reflood pressures (typically ~ 3 bars) the presence of the external thermocouples can promote quenches at temperatures higher that "Tmin". The fuel centre line temperatures (Fig 63) show that in line with the separate effects studies (Ref 15) that the quench of the external thermocouples quickly promotes cooling radially across the fuel.

In the calculations the surge of liquid into the core at ~ 54 secs (Fig 48) which results from the termination in the accumulator liquid flow, produces an increase in the cooling of the cladding; but because the temperatures are typically 200K too high at this time and no account of the influence of the external thermocouples on the quench process is allowed for, the final calculated quench is delayed by some 40 to 50 secs.

<u>Peripheral Bundles</u>

The fuel rod cladding temperatures for the three LOFT peripheral instrumented bundles 2, 4 and 6 are shown in Figs 64 to 77. Fuel assembly 4 is located between the intact loop hot leg and the broken loop cold leg, fuel assembly 2, between the broken loop cold leg and the broken loop hot leg and fuel assembly 6 between the broken loop hot leg and the intact loop cold leg, this arrangement is shown in Fig 6ii. All of the instrumented rods except one, 4G08-21 (Fig 70), are located on the side of the peripheral bundles adjacent to the central bundle, whereas rod 4G08 is located towards the middle of assembly 4.

The thermal behaviour of the peripheral bundles, particularly that of 2 and 6, for the most part just mirrors the behaviour of the central bundle, except that the temperatures are lower as the result of the lower power level. The fuel rods dryout as the core voids during blowdown, reaching a peak temperature of ~ 900K at the peak power elevation in all 3 bundles. The bottom-up core liquid flow produces a rapid cooldown (quench) of all of the instrumented rods, even at the highest elevation of 49 inches, between 6 and 8 secs. In bundle 6 the fuel rods dryout again after about 12 secs rising rapidly to a temperature of ~ 650K to 700K then more slowly to a peak reflood temperature of ~ 750K (Fig 75, rod 6H12-026). In bundle 2 the fuel rods dryout at about 12 secs, but are then "quenched" again at all but the bottom elevation from the top-downwards between 14.5 and 18 secs. These rods then dryout between 18 and 21 secs rising to a peak temperature of ~ 700K (rod 2614-011, Fig 64). In fuel assembly 4, Figs 69 to 72, we see that following the blowdown "quenching" the fuel rods do not immediately dryout again, so that the resultant reflood peak temperatures are significantly lower, ie less than 600K. From the instrumented rod located in the middle of assembly 4 (ie rod 4G08, Fig 70), we see that at this location the fuel rods do not dryout during the blowdown period. The lowest elevation on assembly 4 dryout at about 18 secs in line with the fuel rods in assembly 2, while the higher elevations do not dryout until about 29 to 30 secs.

Cooling of the rods during reflood begins at about 29 to 30 secs at the 11 inch elevation (Figs 64, 73) in bundles 2 and 6 and this is consistent with the temperature measurements for the central bundle (see previous Section). Following this the thermocouples show an oscillatory behaviour similar to that observed in the cetral bundle, and again provide a confirmation of the likely oscillatory flow conditions at the core inlet. The cladding temperatures for bundles 2 and 6, during this reflood period lie between ~ 600K (2H13-049, Fig 68) and 750K (6H15-026, Fig 75) and these therefore are the temperatures from which the fuel rods quench. The quench times for assemblies 2 and 6 are given below; these as with the quench of the central fuel assembly show that the quench (of the thermocouples) is determined by the fluid conditions rather than the thermal behaviour of the fuel rods. For example the quenches occur coherently and are most likely coincident with the flow of liquid into the bottom of the core. In addition the final quench at the top of the peripheral fuel rod bundles occurs at ~ 55 secs, which again is in line with the data from the central fuel assembly, and

Height	ASSEMBLY 2	ASSEMBLY 6
11 inch	46.7 secs	40.8 secs
21 inch	43.3 secs	-
26 inch	-	47 secs
30 inch	49 secs	49 secs
39 inch	54.6 secs	54.6 secs
45 inch	-	54.6 secs
49 inch	52.5 secs	-

results from the surge of liquid into the core following the change of fluid flow, from the accumulator into the intact loop cold leg from that of water to nitrogen.

The calculated cladding temperatures for the peripheral bundles just reflect the general behaviour of those for the central bundle, ie (1) the blowdown peaks are too high because of the "high" initial fuel stored energy and (2) the "ORIGINAL" (ie v13.0) calculation cools quicker during reflood than the "JON'S" (v12.2) calculation. In addition to these, the first of the above leads to an overestimation of the cladding temperatures for bundle 6 during reflood of between 100 and 200K (eg Figs 74 to 77). Finally in bundles 2 and particularly 4 where in addition to the experimental bottom-up blowdown quench the fuel rods are subsequently quenched from the top downwards, the calculated temperatures which do not show this asymmetric top-down cooling are some 300K too high.

5(iv) "ORIGINAL" and "ZERO-GAP" Calculations

The "ZERO-GAP" calculation was the second in the series of TRAC sensitivities performed as part of the comparison with LOFT experiment.LP-02-6. This calculation was performed because of the obvious overestimation of the steady-state fuel stored energy calculated in the first two calculations when the "as manufactured" fuel clad gap was used. In the "ZERO-GAP" calculation the fuel clad gap was set to zero, while in all other ways the calculation was identical to the "ORIGINAL" calculation (ie it used code version B03, the UK version of LANL code version 13.0). As would be expected the major effect of the above change is to the calculated core cladding temperatures, however it might be anticipated that this change could influence the heat transferred to the fluid and hence the hydraulic behaviour.

The improvement in the calculated cladding temperatures during blowdown for the "ZERO-GAP" calculation can be easily seen in Figs 124 etc for the central fuel bundle, and Figs 136 etc for the peripheral bundles. However one consequence of reducing the fuel clad gap over the whole length of the fuel rod, as is required by the TRAC simplified fuel rod model, is that the peak temperature during blowdown at the top of the core is now underestimated. This can be seen particularly in the central fuel bundle at all elevations above about 40 inches.

Note Comparisons of the TRAC calculations with the experimental results for the peripheral bundles is made difficult in some instances because of an error in the TRAC (v13.0) heat transfer logic that artificially quenches some rods during the blowdown period (Ref 18), see for example Fig 146.

An improved fit to the overall blowdown temperatures could obviously be made by adjusting the fuel clad gap along the length of the fuel rods, ie a closed up gap at the bottom and a partially open one at the top. However for this to be more than just a "fitting" exercise additional information ought to be available either from fuel PIE or a fuels code.

In the centre of the core, eg Figs 127, 128, where the "ZERO-GAP" blowdown peak temperatures are now well-represented, the calculated temperatures fall to ~ 800K as a result of the bottom-up core cooling, and subsequently rise to about 850K as the cooling diminishes and the temperatures across the fuel rod equalise out. In the experiment the recorded temperatures on the external thermocouples cool down rapidly to the saturation temperature as a consequence of the bottom-up liquid flow, but then rise to ~ 800K as the cooling diminishes and the temperatures across the rod re-equalise. The average rod temperature therefore after the blowdown cooling is only some 50K higher in the "ZERO-GAP" calculation than in the experiment. This shows therefore that at this elevation the net heat transfer from the cladding to the coolant is only marginally smaller in the case of TRAC compared to the experiment. The difference in the net cooldown of the fuel rod could therefore be well-accommodated within the uncertainty of the inlet fluid conditions, without requiring major changes to the TRAC heat transfer package. The above observations also apply in general to the lower core elevations, although the difference between the TRAC "ZERO-GAP" and experiment clad temperatures after the end of the blowdown cooling are in some instances somewhat higher.

In the upper part of the central fuel bundle and generally across the peripheral bundles, differences between the calculated and experimental fluid conditions make comparisons more difficult. At the 43.8 inch elevation (Fig 131) for example, we see that

(1) The calculated cladding temperature shows dryout well in advance of the experiment.

(2) As mentioned above the "ZERO-GAP" calculated peak clad temperature is lower than the measured value (assumed to be due to a partially open gap towards the top of the core).

(3) In the experiment the bottom-up liquid flow is limited so that the temperature of thermocouple does not fall to saturation, whereas in the calculation more extensive cooling is observed, and finally;

(4) The rod thermocouple cools to saturation at ~ 19 secs due to the top-down flow of liquid from the upper plenum and this is not predicted in either calculation except at the highest elevation (ie at 62 inches, see Fig 133).

As stated above differences 1, 3 and 4 arise because of inaccuracies in the calculated core blowdown fluid conditions and the sensitivity of the thermal response to them, and for this reason it is not easy to see how to improve the accuracy of the calculation. However it does go to show that an accurate calculation of the core blowdown hydraulics is a pre-requisit to the calculation of the core blowdown cooling.

As a full review of the loop and vessel behaviour is contained in the previous Section we only comment here on the observed differences between the two calculations and their relation to the experimental data. As might be expected there are only minor differences in both the loop and vessel hydraulic conditions between the "ORIGINAL" and "ZERO-GAP" calculations. In line with the comments in the previous Section we see that neither calculation produces any direct bypass of subcooled ECCS liquid, whereas the experiment shows subcooled bypass at ~ 31 secs, estimated to be between 80 and 130 kg. The calculated broken loop mass flow (Fig 80) also shows that there is no reverse flow, ie flow from the BST to the reactor vessel in the "ZERO-GAP" calculation, as there is in the "ORIGINAL" calculation between ~ 42 and 48 secs. This results from the fact that the system pressure is fractionally higher in the "ZERO-GAP" calculation due to the increased heat transfer from the core fuel rods to the coolant.

The calculated intact loop cold leg behaviour during refill, as explained in the previous Section, is very sensitive to the details of the calculated transient particularly through the condensation model and this can then feed back and influence the vessel refill and early core reflood behaviour. Figs 91 and 92 which show the intact loop cold leg density and mass flow, upstream of the ECCS injection point, show that there is a difference in the behaviour of the two calculations during the refill (accumulator flow) period, with the "ZERO-GAP" calculation producing some rapid liquid slugs after ~ 38 secs. This movement and accumulation of the ECCS liquid in the intact loop cold leg, through the behaviour of the condensation model, then modifies the subsequent core reflood. An additional consequence of the different intact loop cold leg behaviour is that the pump in the "ZERO-GAP" calculation runs down slightly quicker after ~ 45 secs, (Fig 96).

One interesting feature of both the calculation and the experiment observed in the intact loop cold leg is that following the exhaustion of the nitrogen from the accumulators, the liquid begins to accumulate, producing an increase in the intact loop cold leg density, (Fig 91), at about 85 secs.

Finally the other observable difference between the two calculations, is that following the end of the accumulator liquid flow, the pressure drop from the reactor vessel to the BST produced by the flow of nitrogen steam and water is smaller in the "ZERO-GAP" calculation than in the "ORIGINAL" calculation. So that after 55 secs the system pressure (see Fig 114 for example) is lower in the "ZERO-GAP" calculation. Fig 114 however also shows that it is now closer to the experimental value. The difference in this pressure rise results from the different mass flow and densities calculated along the broken loop cold leg (Figs 80 and 79) after 55 secs, and these differences result from the way liquid has accumulated in the intact and broken loop cold legs and along the top of the downcomer prior to this time.

5(v) "ZERO-GAP" and "ISHARP" Calculations

The fourth TRAC-PF1/MOD1 calculation ("ISHARP") of experiment LP-02-6 performed was a repeat of the previous "ZERO-GAP" calculation (code version UK B03, LANL 13.0) except that the core interface sharpener logic was bypassed. The reason for carrying out this calculation was to examine the effect of bypassing this logic in an integral calculation. Previous analysis of separate effects reflood experiments (Ref 7) had recommended bypassing this logic as the best way of modelling the core void fraction above the quench front and previous plant studies had also shown that the interface sharpener logic could produce unphysical liquid holdup in the core during blowdown. As the differences between the "ZERO-GAP" and "ISHARP" calculations relate to the core hydraulics, one would expect to see differences primarily in the core flows and from these differences in the fuel rod cladding temperatures, and possibly via the heat input to the fluid from the fuel rods, differences in the loop behaviour.

The results from the two calculations together with the experimental data, where appropriate are shown in Figs 149 to 219. The most striking feature of the comparison taken as a whole is that the difference between the two calculations is relatively small. The resultant cladding temperatures for example (Figs 195 to 219) are very similar, this just amplifies the fact that for large break transients performed in LOFT (primarily because of the size and location of the core) the cooling of the fuel rods during both blowdown and reflood is dictated by the system hydraulics in the loops and the vessel downcomer.

It should be noted, that as for the previous calculations performed with code verison 13.0, the "ISHARP" calculated cladding temperatures are subject to the error in the heat transfer logic (Ref 18) described in the previous Section. (See for example Figs 195, 206, 207, 212, 213 and 217).

The core inlet and outlet flows together with the core liquid mass (Figs 185, 186 and 189), show for the ISHARP calculation, as would be expected, that during blowdown more of the liquid flowing into the bottom of the core flow out of the top and so less accumulates in the core. After the flow into the core during blowdown, liquid re-enters the core just after 30 secs in both calculations, as the lower plenum fills. After ~ 40 secs the core flow oscillations for the "ISHARP" calculation increase in magnitude with the liquid fraction (Fig 190) oscillating between ~ 0.2 and zero, this is also reflected in the behaviour of the downcomer and lower plenum volume fractions (Figs 189 and 188), so that the average quantity of liquid in the core after

40 secs is slightly less for the "ISHARP" calculation. Following the end of the accumulator liquid flow at ~ 54 secs the surge of liquid into the core occurs in both calculations, only the absence of the interface sharpener logic in the "ISHARP" calculation allows more of the liquid to flow out of the top of the core and so the mass of liquid retained in the core is slightly less. Also the subsequent oscillations in the core liquid content that result from the fuel rods quenching are greater in magnitude for the "ISHARP" calculation.

As stated above, the above differences in the core hydraulics produce only small changes to the cladding temperatures. At the peak power elevation of the central fuel assembly, Figs 197 to 200, we see that during blowdown the "ISHARP" transient cools somewhat quicker following the bottom-up flow of liquid as liquid flows through the core rather than being retained at the bottom. However the period of cooling is slightly shorter so that the net heat loss from the fuel rod to the coolant is about the same. So that following the blowdown cooling the calculated cladding temperatures in the centre of the core rise to about the same value, ie ~ 50K higher than those in the experiment. If anything the "ISHARP" calculated blowdown temperature transient is in close agreement with the experimental data.

At these elevations (ie 20 to 30 inches) reflood cooling in the calculations begins just prior to 40 secs and although the cladding temperatures level off they do not fall (in the "ISHARP" calculation) until after the "post accumulator" flow of liquid into the core at ~ 54 secs. This just reflects the slightly lower average core liquid content in the "ISHARP" calculation during this period. However following 54 secs the cooling is such that both calculations have near identical quench times.

At the bottom of the central fuel assembly (Figs 195 and 196) the initial dryout of the "ISHARP" calculated fuel rod is delayed, due in part to the heat transfer error described above, so that the resultant cladding temperatures during blowdown are lower than both the "ZERO-GAP" calculation and the experiment. Towards the top of the core (Figs 201 to 204) the overcooling and resultant quenching of the fuel rods due to the bottom-up flow of liquid is even more exaggerated for the "ISHARP" calculation (see Fig 203) and although some influence of the top-down flow of liquid is seen this is not enough to extend the area of quenching below that resulting from the bottom-up liquid flow.

A comparison between the two calculated cladding temperature transients for the peripheral fuel bundles is made almost impossible because of the error in the heat transfer logic described above and in Ref 18. The spurious cooling produced by this error which is restricted to high void fractions is more prevalent in the "ISHARP" calculation than in the other 13.0 calculations because of the changed core hydraulic conditions.

The changes in the loop flows produced by the change in the core hydraulic modelling are very small. As a result of the slightly lower quantity of heat transferred from the core to the coolant during the early part of reflood the system pressure falls just below that used to represent the BST, so that liquid flows back along the broken loop cold leg at ~ 48 secs. As a consequence of the increased flow out of the top of the core during blowdown for the "ISHARP" calculation one might expect to see a change in the intact and broken loop hot leg flows, and although a small increase in the broken loop hot leg flow is seen (Fig 158) at ~ 9.5 secs the change is very small.

As might be expected there are some changes to the intact loop cold leg behaviour during reflood (Figs 162, 163) but again these are small and the flow of liquid up-stream of the ECCS injection point is limited to a short period of between ~ 38 to 48 secs for both the "ISHARP" and "ZERO-GAP" calculations. These cold leg flow oscillations occur either in part or whole as a consequence of the pressure induced oscillations in the core flow rather than being induced by changes in the cold leg condensation. This contrasts with the experimentally observed intact loop cold leg flow oscillations which extend for most of the accumulator flow period, ie from ~ 21 to 54.5 secs, and must arise at least initially from the condensation of the intact loop steam flow by the subcooled ECCS liquid.

6 SUMMARY AND CONCLUSIONS

This report compares the results of four TRAC-PF1/MOD1 calculations with the experimental data for the LOFT large break experiment LP-02-6. The four calculations compare changes to; code version, ie versions 12.2 and 13.0, fuel pin modelling, ie "as manufactured" and zero steady state fuel clad gap and to core hydraulic modelling, ie with and without the core interface sharpener logic.

The features that distinguish the LOFT LP-02-6 experiment from the previous 200% double-ended cold leg break experiments L2-3 and L2-5 and the subsequent experiment LP-LB-1 were the fact that it was performed at near full power (ie 47 MW) with a relatively low loop flow (248 kg/sec) and therefore a high core ΔT and the fact that the pumps were tripped and allowed to coast down naturally at the start of the transient. This contrasts with L2-3 where the pumps were kept running and L2-5 and LP-LB-1 where the pumps were decoupled from their flywheels at the start of the transient.

The transient was initiated at time zero by the opening of the quick acting blowdown refief valves, and the upper plenum and core rapidly void as subcooled liquid flows out of the broken loop cold leg. As the core voids the reactor power falls and the fuel rods dry out. The cladding temperatures rise as the stored energy in the fuel equalises out across the fuel pin. The subsequent behaviour of the fuel rods during blowdown in LP-02-6 is dictated by the core hydraulics as for the other LOFT large break experiments. The balance of liquid flow into the vessel downcomer is such that after ~ 4 secs there is a net inflow as the broken loop cold leg flow falls, as the system pressure falls to the 'cold leg' saturation pressure, and the inertia of the pumps produce a flow of liquid along the intact loop cold leg close to the steady state value. The net inflow into the vessel produces a small bottom-up core flow which is enhanced by the flashing of the cold liquid in lower plenum and downcomer. The core flow primarily cools the lower 2/3 rds of the fuel rods - to the extent that the recorded temperatures on the external thermocouples fall to saturation. However in addition to the bottom-up flow there is a significant downflow at about 15 secs, as liquid flowing back along the intact loop hot leg from the pressuriser and the up (hot) side of the steam generator tubes accumulates in the upper plenum. This downflow is sufficient to cool the external thermocouples to saturation at all elevations from the top of the core down to about 30 inches. Therefore the whole of the core is subjected to blowdown cooling either from the bottom-up flow or the top-down flow and the central region from ~ 30 to 40 inches experiences both. This "double" cooling is unique to experiment LP-02-6 and reduces significantly the core stored energy.

There has been considerable speculation as to whether the observed LOFT fuel rod behaviour is indicative of what is happening on the unistrumented fuel rods, and this is currently the subject of a separate investigation. However an indication of the heat removed from the instrumented fuel rods can be obtained from the thermocouple temperatures flowing the blowdown cooling, when the fuel rod temperatures are once again re-equalised. At the peak power elevations, ie between about 24 and 30 inches the cladding temperature rises to ~ 800K.

The primary system pressure falls to the accumulator trip point of 42 bars (600 psi) at about 17.5 secs and accumulator liquid begins to flow into the intact loop cold leg. In line with all the other LOFT large break experiments the measurement rake immediately upstream of the ECCS injection location indicates an oscillatory flow of subcooled liquid along the intact loop cold leg starting at about 21 secs. This flow continues until the flow of accumulator liquid into the intact loop cold leg terminates at ~ 54 secs. The accumulator liquid flows into and down the downcomer filling the lower plenum. The broken loop cold leg measurements supported by the downcomer measurements located on the broken loop side show that there is no continuous bypass of subcooled liquid. However a slug of subcooled liquid is observed to flow along the broken loop cold leg between ~ 29 and 32 secs, the total mass of this slug is estimated to be very roughly about 100 kg; compared to the total accumulator volume of 1.69 m^3, ie ~ 1,690 kg. An additional slug of subcooled liquid flows along the broken loop cold leg at ~ 50 secs, again with a total mass of roughly 100 to 150 kg. Because of the small scale of the LOFT facility and therefore the relatively high metal-work heat flux the primary system pressure never falls below that in the BST. So that in addition to the flow of the two slugs of subcooled liquid along the broken loop cold leg there is a flow of two-phase saturated fluid as the liquid in the lower plenum continues to flash and steam and entrained liquid flow from the vessel to the BST.

The lower plenum fills rapidly with ECCS liquid so that the bottom of the core begins to cool again at ~ 31 secs. Following this time cooling is observed progressively up the core with a turnover, in the cladding temperature rise above 30 inches occurring at about 40 secs. The most noticeable effect observed by the cladding thermocouples once reflood cooling starts is that they behave in an oscillatory manner. This is attributed to an oscillatory core flow which is likely to occur as a result of a combination of core-steam generation oscillations and intact loop cold leg condensation induced oscillations. Just as the core inlet hydraulics determines the fuel rod cooling it also determines the fuel rod quench. Except at the very bottom of the core a significant degree of coherency is seen in the fuel rod quench, for example in the central fuel assembly the 11 inch and 21 inch thermocouples and some of the 15 inch thermocouples all quench at ~ 46.7 secs, and above 24 inches the final quench occurs between 54 and 56 secs. The final quench coincides with the termination of the accumulator liquid flow, and results from a surge of liquid into the core as the reduction in condensation and the presence of the accumulator nitrogen causes the intact loop cold leg pressure to rise. The rise in the intact loop cold leg pressure also causes some of the ECCS liquid located in the intact loop cold leg and at the top of the downcomer to flow out of the broken loop cold leg to the BST. Because of the blowdown cooling of the core the maximum cladding temperature at ~ 54 secs when the surge of liquid into the core occurs is only ~ 700K, so that the whole of the core in experiment LP-02-6 is cooled and quenched by the liquid from the accumulator.

The results from the four TRAC-PF1/MOD1 calculations bear a large degree of similarity particulary in their hydraulic behaviour. They all therefore, in the main, produce the same global transient and suffer from the same modelling deficiencies. Those sensitivities performed for a specific reason, eg reducing the steady state fuel clad gap obviously produced the desired result of lower cladding temperatures.

In spite of the fact that the calculated transients overestimate the observed subcooled flow in the broken loop cold leg, flow into the core after ~ 4 secs extends to the top of the core and quenches the 62 inch elevation whereas in the experiment the "quench" only reaches the 45 inch level. However whereas in the experiment the subsequent top-down liquid flow "quenches" the top of the core particulary in the peripheral fuel bundles no such cooling is observed in the calculations. Therefore particularly towards the top and the bottom of the core the calculated fuel rod temperatures after blowdown are higher than the experimental values. In the centre of the core however (ie ~ 24 to 27 inches) for the "ZERO-GAP" calculations the calculated cladding temperatures are only about 50K too high showing that the net heat loss from the fuel rod for the calculations is only slightly lower than in the experiment.

In all four calculations there is no direct bypass of the ECCS subcooled liquid so that, as in the experiment, the lower plenum fills up rapidly with some liquid first entering the bottom of the core at ~ 28 secs. The subsequent core inlet flow is oscillatory as a result of steam production in the core, and the fuel rods begin to cool at ~ 32 secs at 11 inches and at ~ 39 secs at 21 inches.

One region where there is a difference in the behaviour of the four calculations is in the intact loop cold leg during the accumulator liquid flow period. In some cases liquid slugs form upstream of the ECCS injection point and in other cases not. These differences are attributed to the sensitivity of the TRAC condensation model to small changes in the steam and liquid flows rather than to any specific modelling changes between the four calculations. In none of the calculations however was the calculated flow similar to the experimental observations, and because no bypass was calculated the differences in the calculated intact loop cold leg behaviour only had a very minor effect on the vessel refill and subsequent core reflood.

In all of the calculations a surge of liquid into the core occurs as a result of the pressurisation of the intact loop cold leg as the flow from the accumulator changes from subcooled water to nitrogen. This liquid surge effectively fills the small LOFT core and so the fuel rods cool. The final quench is delayed because the cladding temperatures are at least 80 to 100K higher than the equivalent experimental values and no modelling of the influence of the external thermocouples on the quench process is included in the calculations.

One may conclude therefore that although small variations were observed in the hydraulic behaviour of the four calculations, because no changes were made to the following sensitive areas the general behaviour of all the calculations was the same; ie the nature of a LOFT transient is determined by:

- the blowdown cooling, in which the calculations show too much bottom-up flow and not enought top-down.

- ECCS bypass, none is calculated and only small slugs of direct bypass are observed in the experiment.

- the slug of liquid forced into the core following the termination of the accumulator liquid flow, which is sufficient to cool/quench the whole of the "short" LOFT core.

The thermal response of the core to the above hydraulics is of course different for the different calculations, with those calculations with the reduced fuel stored energy (ie zero fuel clad gap) producing results closest to the experiment. However the very limited fuel pin model available in TRAC restricts the modelling ability to better simulate the observed thermocouple behaviour.

7 ACKNOWLEDGEMENTS

The authors wish to acknowledge the valuable assistance of Dr J Birchley who adapted and modified the TRAC input deck for

LOFT from that used in the previous analysis of experiment LP-LB-1 and who performed the first of the calculations analysed in the report.

8 REFERENCES

(1) J P Adams, K G Condie, D L Blatt. Quick-Look Report on OECD LOFT Experiment LP-02-6. OECD LOFT-T-3404, October 1983.

(2) P Coddington. Analysis of LOFT Experiment LP-LB-1 Using the TRAC-PF1/MOD1 Code. UKAEA Internal Publication.

(3) J Birchley. Modifications to the TRAC-PF1/MOD1 Input Models for LOFT. UKAEA Internal Publication, March 1986.

(4) M Blackmore, J Birchley. Modelling of LOFT ECC Injection Line for TRAC-PF1/MOD1. UKAEA Internal Publication, May 1986.

(5) J Birchley. Heat Structures for the 3-D Vessel Representation of LOFT with TRAC-PF1/MOD1. UKAEA Internal Publication.

(6) J Birchley, P Coddington. Post Experimental Analysis of OECD-LOFT Experiment LP-02-6 with TRAC-PF1/MOD1. To be published.

(7) R O'Mahoney. A Study of the Reflood Characteristics of TRAC-PF1/MOD1. AEEW - M 2305, April 1986.

(8) E M Feldman. OECD LOFT Project Experiment Specification Document, Cold Leg Break Experiment LP-02-6. OECD LOFT-T-3402, July 1983.

(9) Private Communication. Letter: P Coddington to Salih Guntäy, EIR Switzerland, July 1987.

(10) TRAC-PD2 Independent Assessment. NUREG/CR-3866, LA-10166-MS, December 1984. Pages 234 to 291.

(11) T D Knight. TRAC Analysis of LOFT LP-02-6. LA-UR-85-3723, October 1985.

(12) A B Wahba. Emergency Core Coolant Systems and Their Effectiveness in Large Break LOCA. Paper presented to the OECD-LOFT Specialist Meeting on Large Break LOCA, 24-27 March 1987, Grindelwald, Switzerland.

(13) P Coddington. Comments on the Accumulator Nitrogen Injection Phase of a Large Cold Leg Break PWR Loss-of-Coolant Accident. UKAEA Internal Publication, August 1986.

(14) S N Aksan. Evaluation of Analytical Capability to Predict Cladding Quench. EGG-LOFT-5555, August 1982.

and

R C Gottula. Effects of Cladding Surface Thermocouples and Electrical Heater Rod Design on Quench Behaviour. NUREG/CR-2691, February 1984.

(15) S Yanar, S Guntay. Effect of External Thermocouples on Quench Temperatures Evidence From NEPTUN Reflooding Experiments. Paper presented at the OECD-LOFT Specialist Meeting on Large Break LOCA, Grindelwald, Switzerland. 24-27 March 1987.

G Class et al. Measurement of Cladding Temperatures with Loss-of-Fluid-Test Thermocouples in the COSIMA Blowdown Test Facility. Nuclear Technology, Vol 69 (April 1985) p 72.

and

G L Shires et al. An Experimental Study of the Effect of External Thermocouples on Rewetting During Reflood. AEEW - R 1357.

(16) R O'Mahoney, C Gill, P Coddington. Status of the High and Low Pressure Quenching Studies at AEEW, Spetember 1987. UKAEA Internal Publication.

(17) P Coddington. The Effect of Accumulator Nitrogen on the Reflood of a PWR Core During a Large Break LOCA. Paper presented to the IAEA Specialist Meeting on Fuel Behaviour Under Accident Conditions and Acceptance Creiteria, 30 September-4 October 1985, Warsaw, Poland.

(18) Private Communication. Letters: P Coddington to R Jenks, LANL, USA. 29 January 1987, and 7 and 24 April 1987.

TABLE 1

TRAC CALCULATIONS

NO	LABEL	CODE VERSION		FUEL CLAD GAP WIDTH	INTERFACE SHARPENER LOGIC
		LANL	UK		
1	"JONS"	12.2	X26	100 μon	Yes
2	"ORIGINAL"	13.0	B03	100 μon	Yes
3	"ZERO-GAP"	13.0	B03	0.0	Yes
4	"ISHARP"	13.0	B03	0.0	No

TABLE 2

INITIAL CONDITIONS FOR EXPERIMENT LP-02-6

Parameter	TRAC Calculated Value	Experimental Value
Primary Coolant System		
Temperature across core (K)	34.5	33.1±1.4
Hot leg pressure (MPa)	15.04	15.09±0.08
Cold leg temperature (K)	556.7	555.9±1.1
Mass flow rate (Kg/s)	248.1	248.7±2.6
Primary coolant pump injection (both pumps) (ℓ/s)	0.0	0.092±0.003
Core bypass pipe flow (Kg/s)	6.5	Not measured directly
Hot leg nozzles bypass flow (Kg/s)	5.6	
Reflood assist valve flow rate (Kg/s)	13.1	
Total core bypass flow (Kg/s)	25.2	
Reactor Vessel		
Power level (MW)	47.0	46.0±1.2
Maximum linear heat generation rate (KW/ft)	15.07 (Av rods) 16.20 (Peak rods)	14.9±1.1
Steam generator secondary side		
Pressure (MPa)	5.62	-
Steam generator feedwater flow rate (Kg/s)	2.53	-
Pressuriser		
Liquid volume (m^3)	0.555	0.607±0.02
Steam volume (m^3)	0.376	0.39±0.02

TABLE 2 (Continued)

Water temperature (K)	615.4	615.6±5.8
Pressure (MPa)	15.03	15.3±0.11
Liquid level (m)	1.26	1.04±0.04
Broken Loop		
Cold leg temperature (K)	556.7	553±6
Hot leg temperature (K)	556.1	560±6
Reflood assist valve leak flow rate (Kg/s)	13.1	-
Suppression Tank		
Pressure (gas space) (KPa)	15.04	
Emergency Core Cooling System		
Accumulator liquid level (m)	1.05	-
Accumulator liquid volume (m^3)	1.315 (tank)	1.2360
	0.36 (line)	0.4559
Accumulator gas volume (m^3)	0.642	0.9506
Accumulator pressure (MPa)	4.11	4.11±0.06
Accumulator liquid temperature (K)	302.0	302±6.1
High pressure injection flow rate (ℓ/s)	1.50	1.04±0.04
High pressure injection liquid temperature (K)	302.1	305±7
Low pressure injection flow Rate (ℓ)	5.5	-
Low pressure injection liquid temperature (K)	302.9	305±7

TABLE 3

CHRONOLOGY OF EVENTS FOR EXPERIMENT LP-02-6

Event	TRAC Calculated Value	Experimental Value
Blowdown valves opened	0.0	0
End of sub-cooled blowdown	0.05	0.05±0.05
Reactor scrammed	-	0.1±0.01
Primary coolant pumps tripped	0.8	0.8±0.01
Cladding temperatures initially deviated from saturation	0.32	0.9±0.01
End of sub-cooled break flow	4.9	4.0±0.5
Maximum cladding temperature (1061 K @ 24 in) reached (blowdown)	4.6	4.9±0.2
Bottom-up core rewet initiated	4.2	5.2±0.2
Bottom-up core rewet complete	13.1	9.1±0.2
Partial core top-down quench initiated		14.8±0.02
Pressuriser emptied	13.6	15.5±0.5
Primary coolant pumps disconnected from flywheels	-	16.5±0.01
Accumulator injection initiated	16.6	17.5±0.5
Partial core top-down quench complete		18.6±0.2
High pressure injection initiated	22.0	21.8±0.01
Lower plenum refill complete (from void)	36.5 to 48.2	
Lower plenum refill complete (thermocouple)	28.7	30.7±0.2
Low pressure injection initiated	35.1	34.8±0.01

TABLE 3 (Continued)

Maximum cladding temperature (929.7 K @ 24 in) reached (reflood)	40.5	41±0.2
Accumulator empty	48.0	
Accumulator injection complete	53.0	57±5[a]
Core quench complete	91.1	56±0.2

[a] Ref 1 calculates the accumulator injection complete time by extrapolating from the time the accumulator is empty to the time the connecting piping is empty assuming a constant mass flow

TABLE 4

CORE AXIAL FINE MESH ELEVATIONS AND RELATIVE POWER DENSITY

Fine Mesh	Height Metres	Height Inches	Power Density
* 1	0.0	0.0	0.59415
2	0.07625	3.0	
3	0.1525	6.0	
4	0.22875	9.0	
* 5	0.305	12.0	1.35550
6	0.362	14.25	
7	0.419	16.50	
8	0.476	18.75	
* 9	0.533	21.00	1.54060
10	0.59025	23.25	
11	0.6475	25.50	
12	0.70475	27.75	
* 13	0.762	30.00	1.47230
14	0.87625	34.5	
15	0.9905	39.0	
16	1.10475	43.5	
* 17	1.219	48.0	0.78851
18	1.33325	52.5	
19	1.4475	57.0	
20	1.56175	61.5	
* 21	1.676	66.0	0.029708

* Fluid dynamic cell boundaries

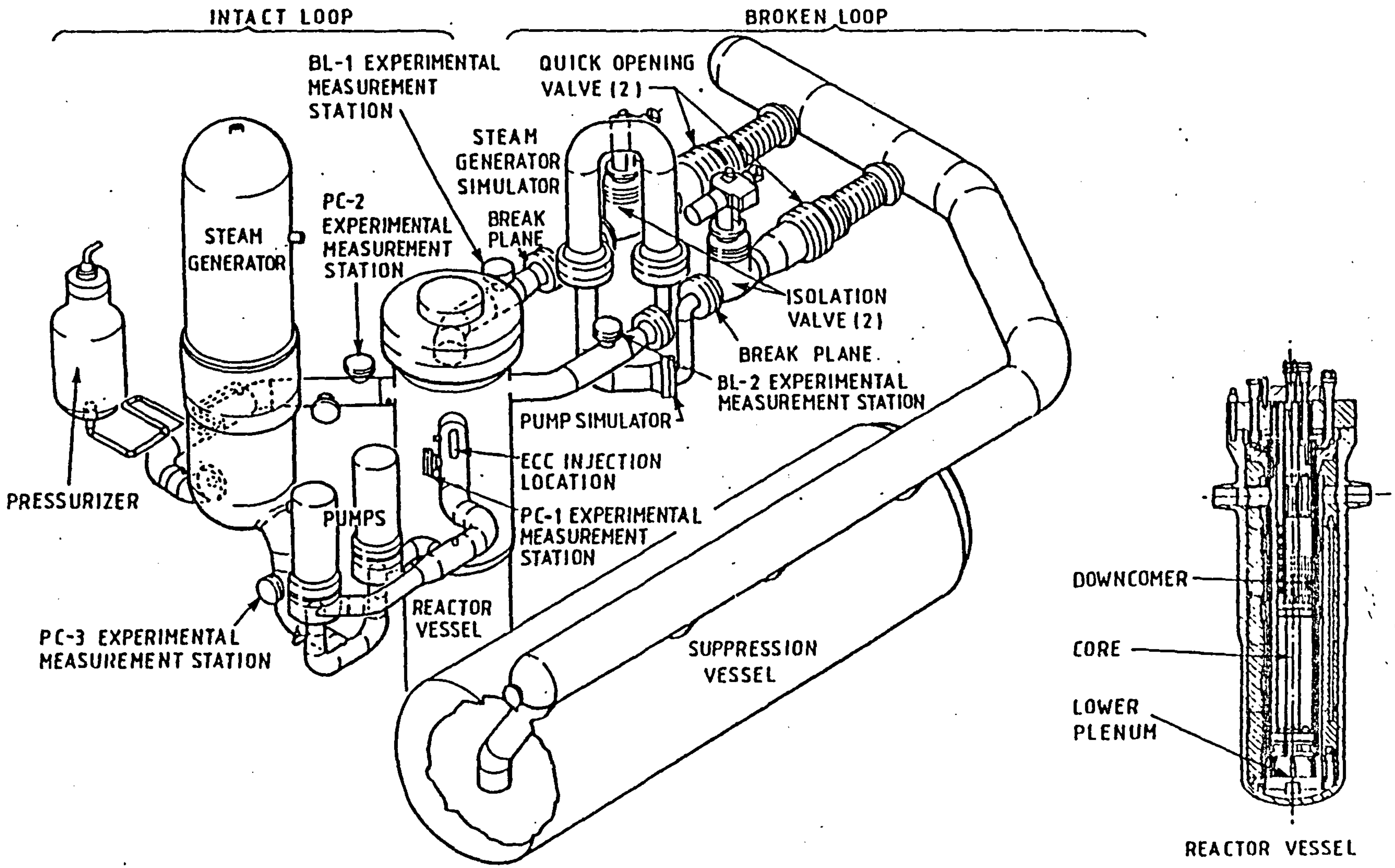

FIG.1. MAJOR COMPONENTS OF LOFT SYSTEM

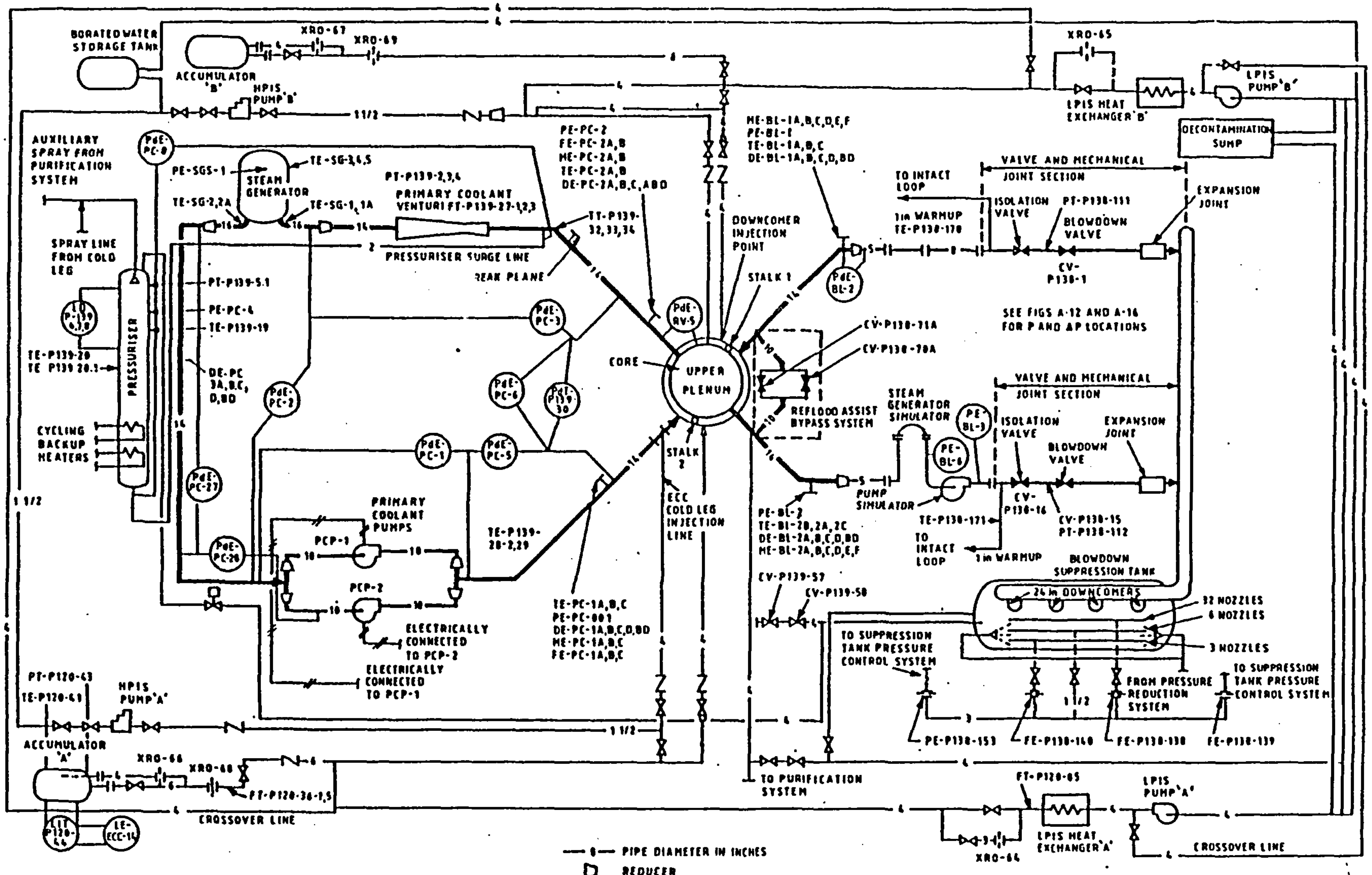

FIG. 2. LOFT PIPING SCHEMATIC WITH INSTRUMENTATION

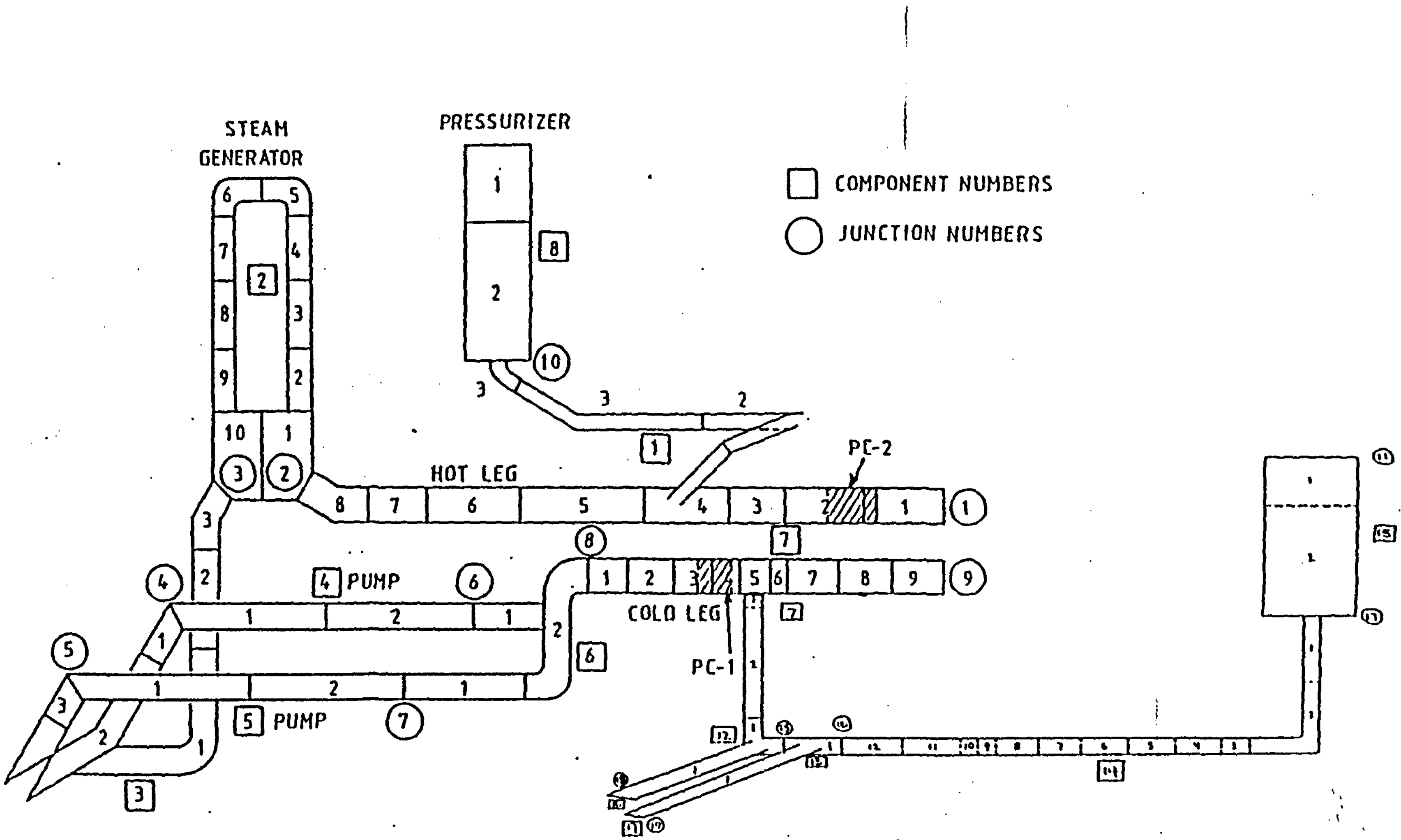

FIG.3. INTACT LOOP NODALISATION

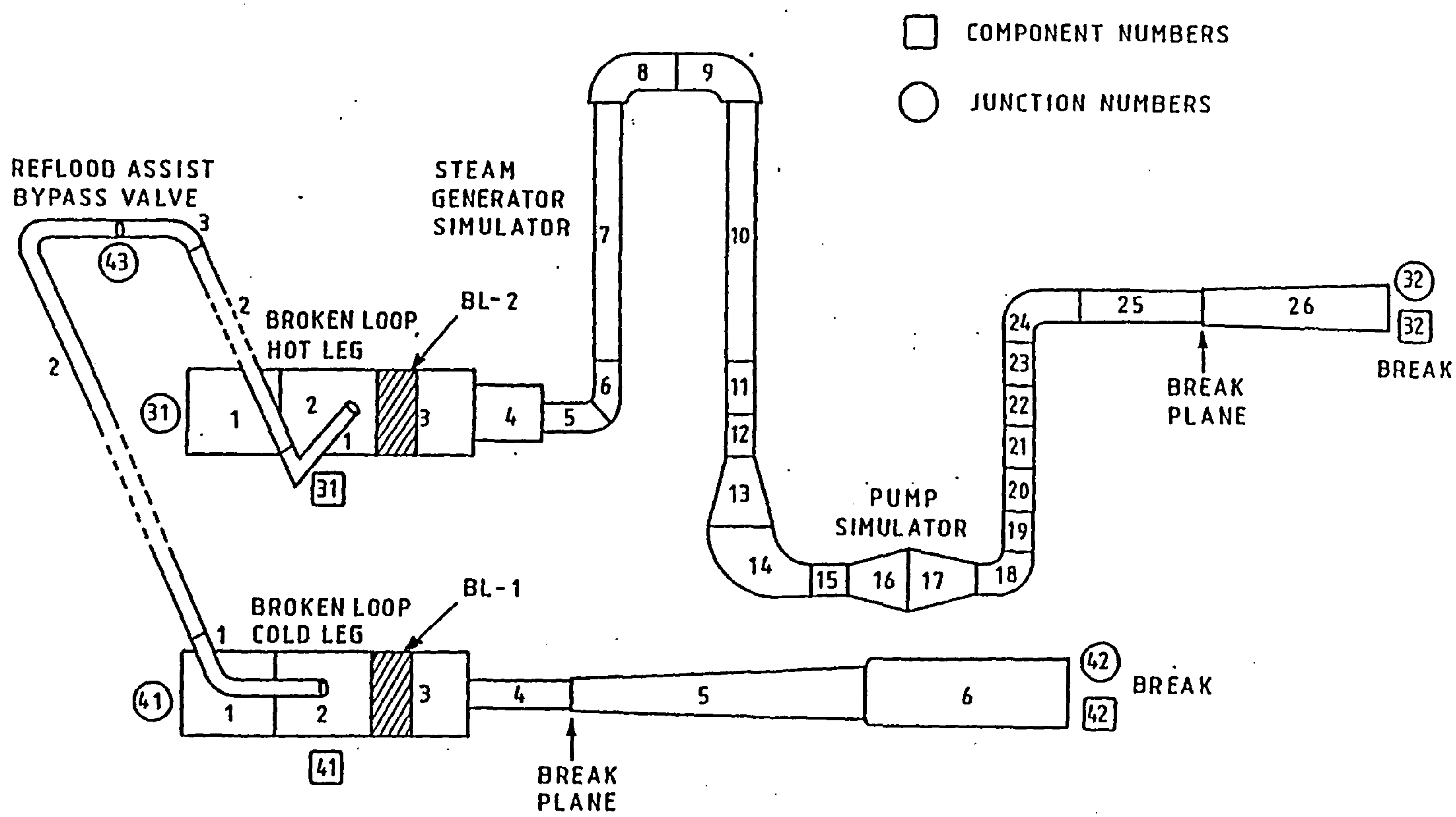

FIG. 4. BROKEN LOOP NODALIZATION

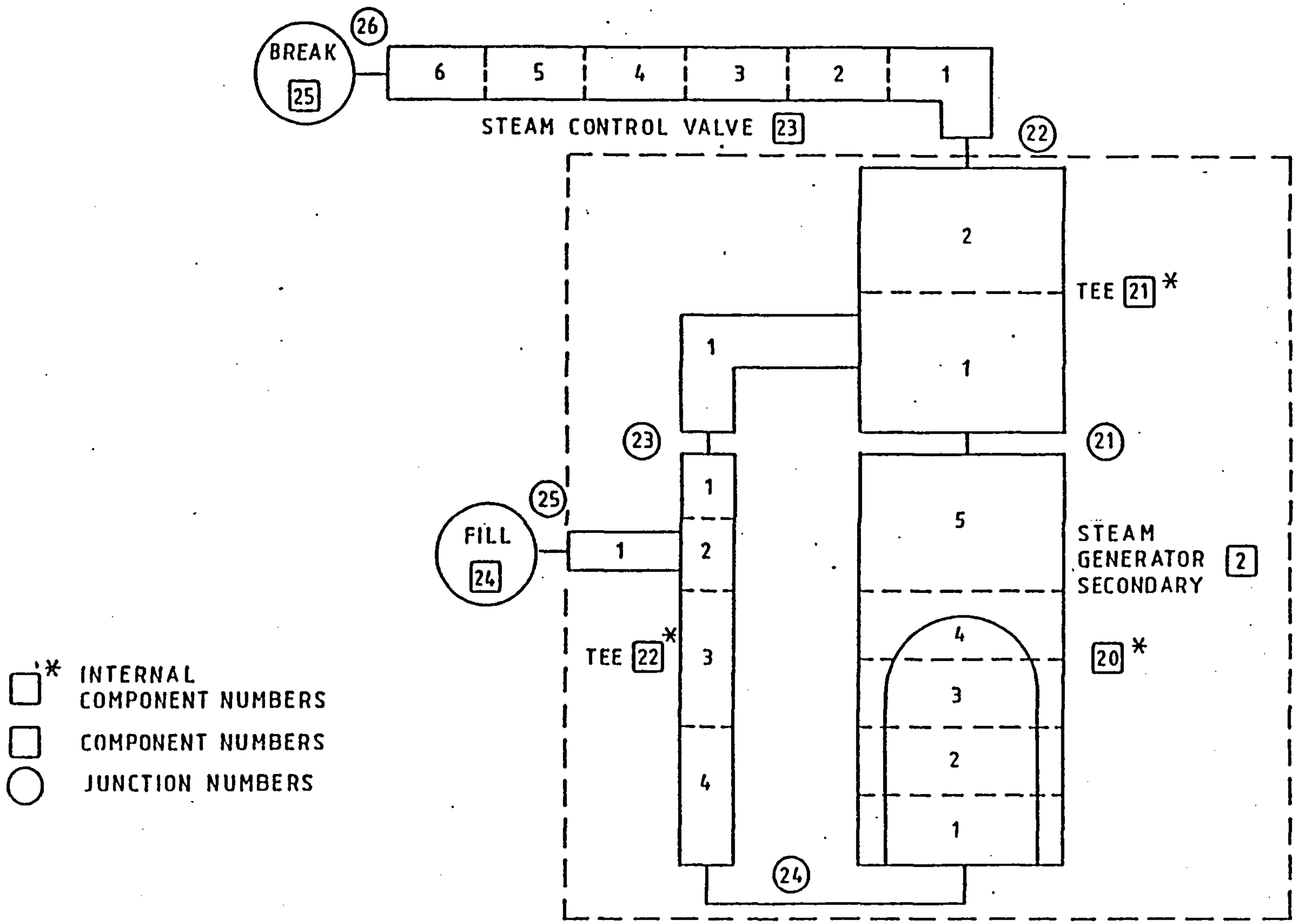

FIG. 5. STEAM GENERATOR SECONDARY NODALIZATION

CORE BYPASS COMPONENTS

The top of level 3, third radial ring, is linked for each of the four azimuthal sectors to the bottom of level 11 (rings 2 and 3) by four TEE components. The horizontal side arms of the TEEs are connected to the outer surface (ring 3) of level 8.

The arrangement is such that Bypass TEE Components 101 and 103 are connected to $r = 3$, $\theta = 1$ (3) at levels 3 and 11, while Bypass TEE Components 102 and 104 are connected to $r = 3$, $\theta = 2$ (4) at level 3 and $r = 2$, $\theta = 2$, (4) at level 11. (This is to allow for the Upper Plenum Hot Leg connections in radial ring 3 azimuthal sectors 2, 4 at level 11).

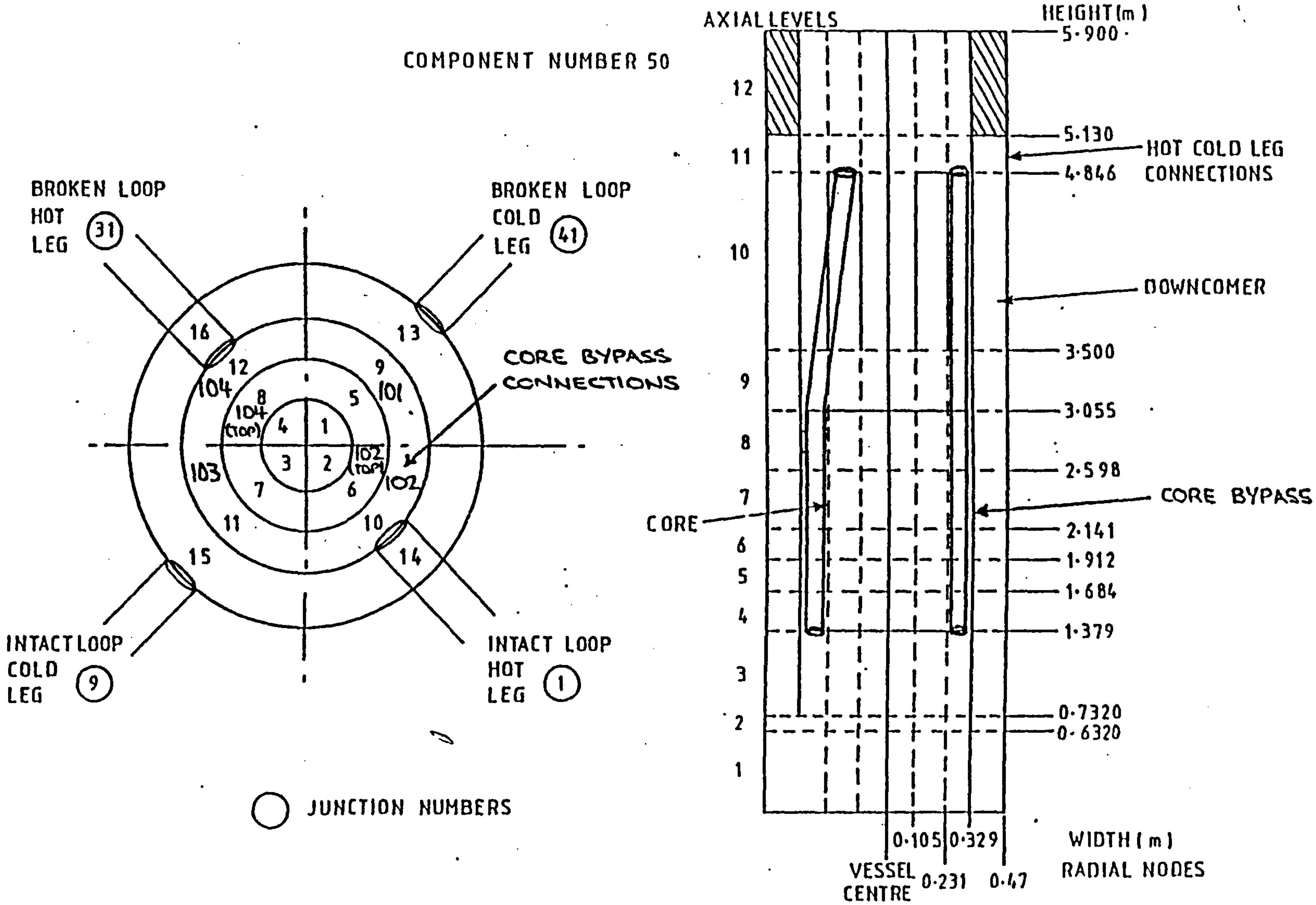

FIG.6i REACTOR VESSEL NODALISATION

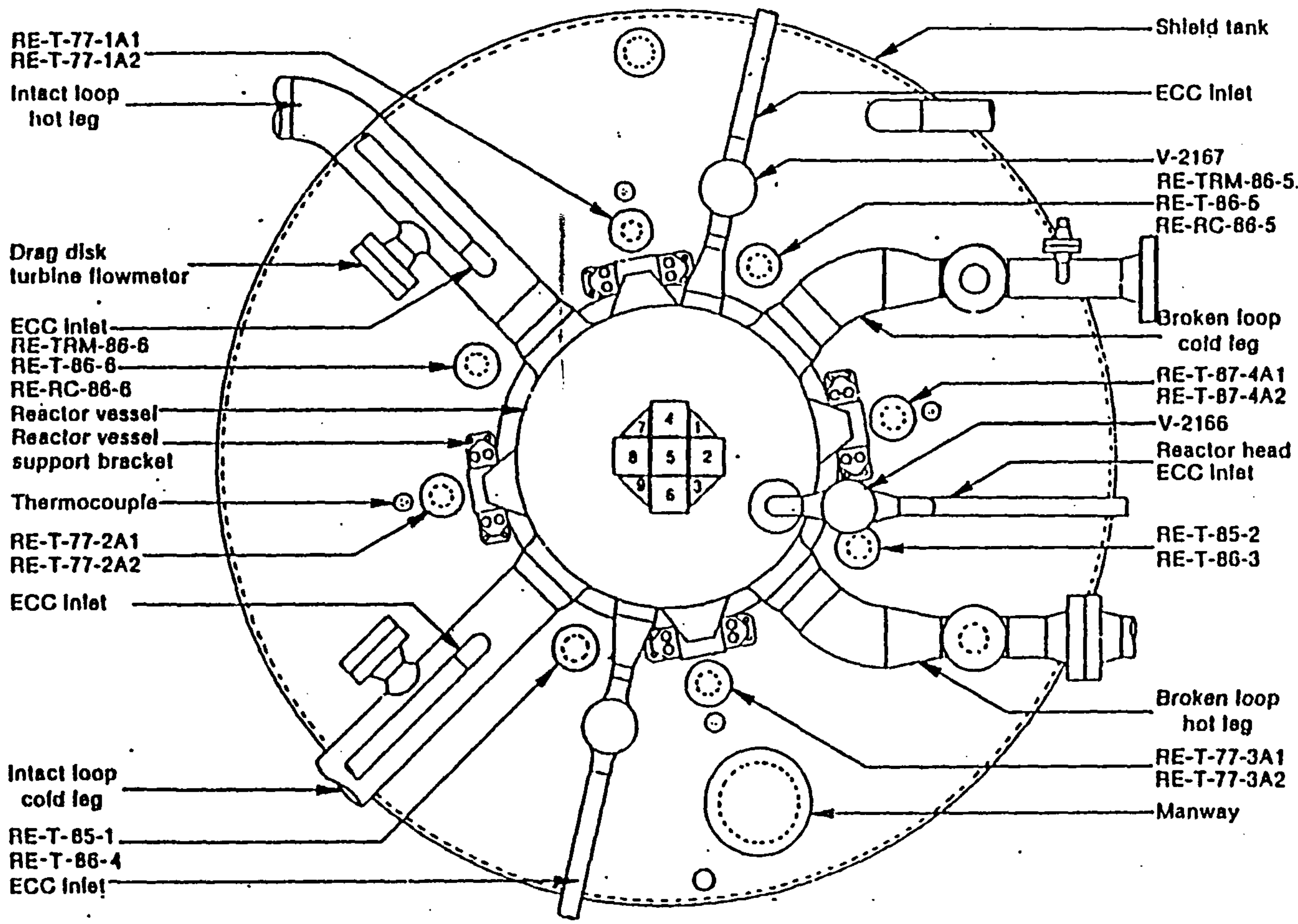

Figure 6.11 Reactor Vessel Instrument Locations

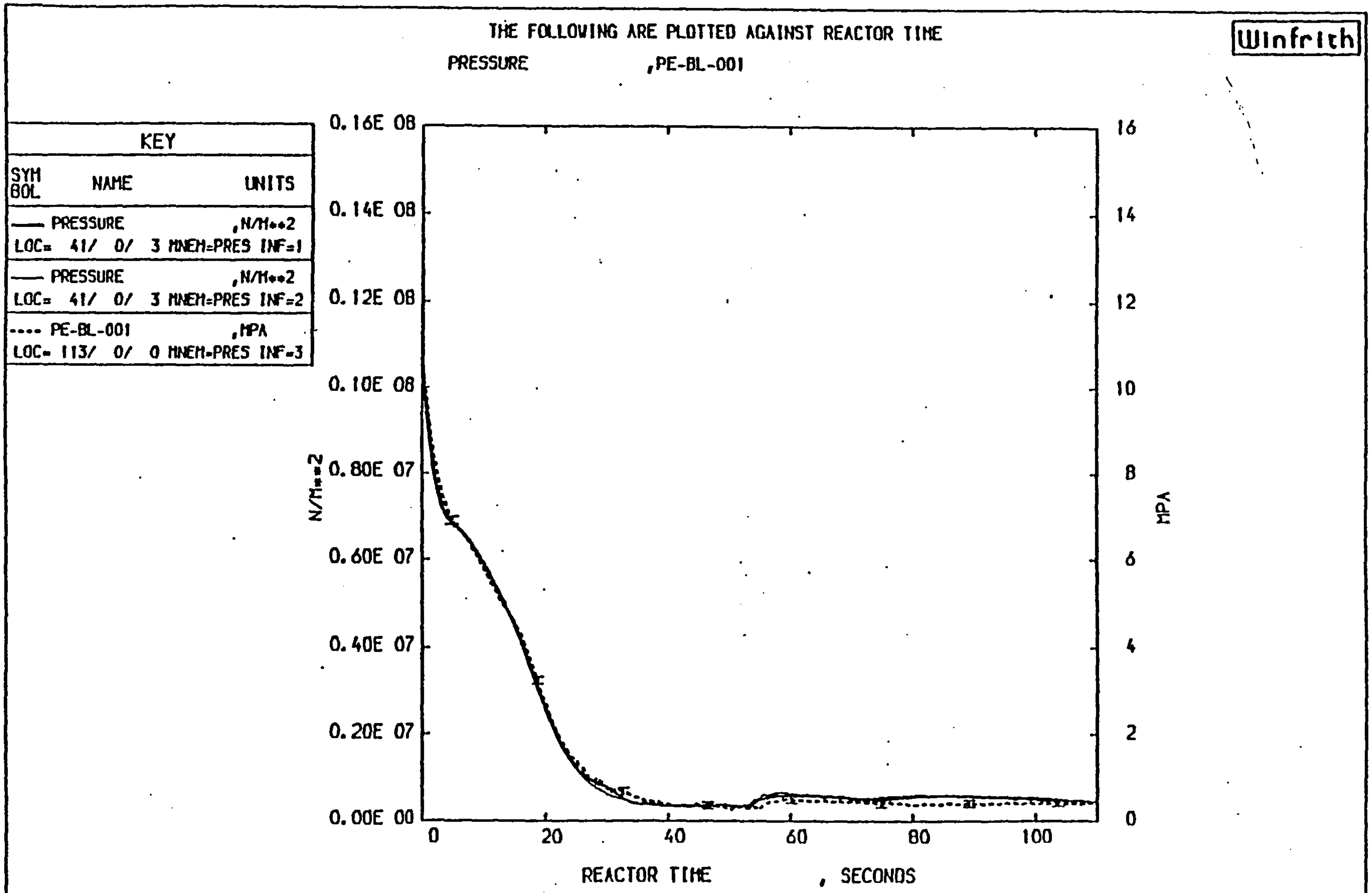

FIGURE 7 INF 1 JON'S, INF 2 ORIG, INF 3 EXP
BROKEN LOOP COLD LEG - EXPERIMENTAL LOCATION BL-1

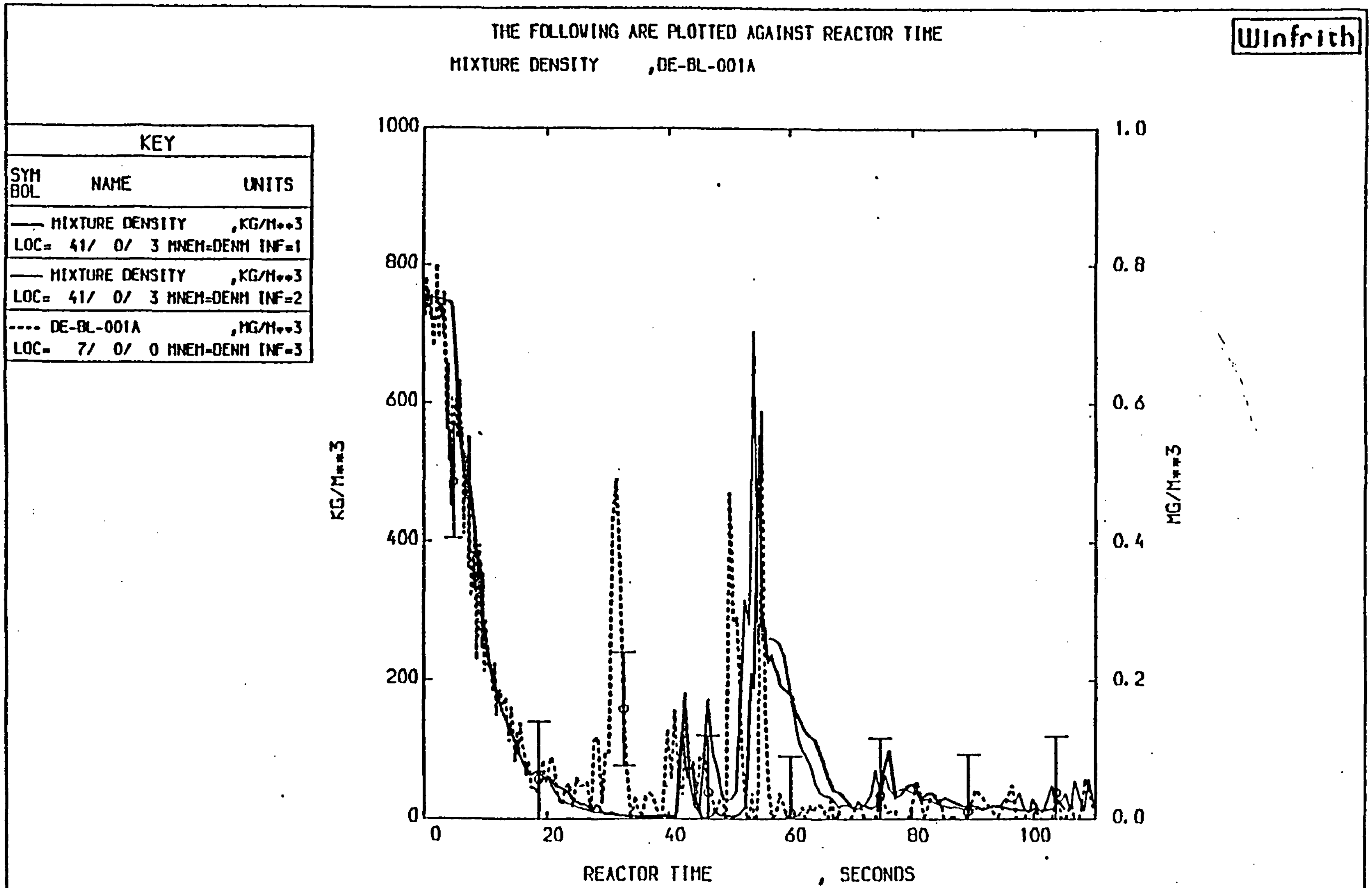

FIGURE 8 INF 1 JON'S, INF 2 ORIG, INF 3 EXP
BROKEN LOOP COLD LEG - EXPERIMENTAL LOCATION BL-1

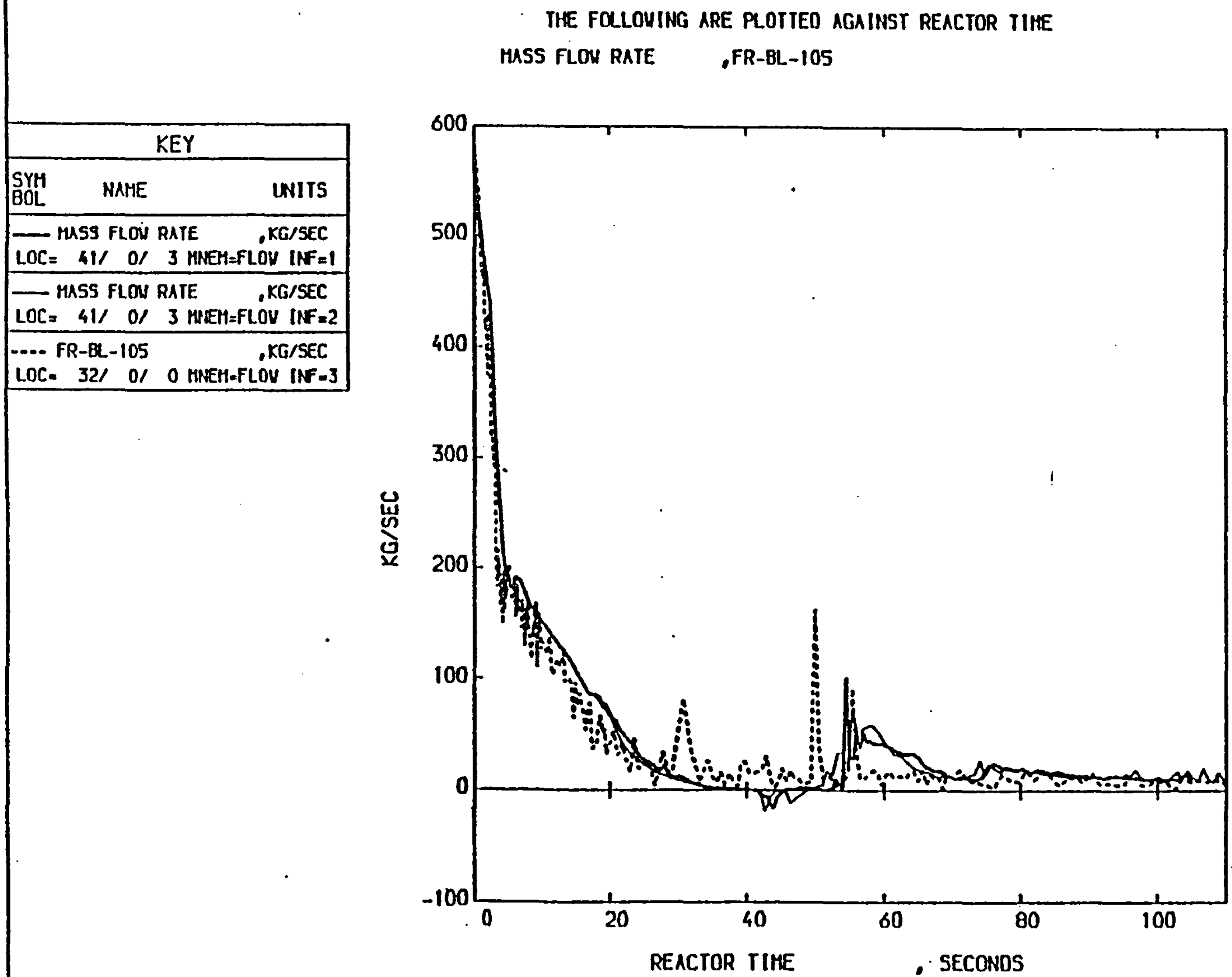

FIGURE 9 INF 1 JON'S, INF 2 ORIG, INF 3 EXP
BROKEN LOOP COLD LEG - EXPERIMENTAL LOCATION BL-1

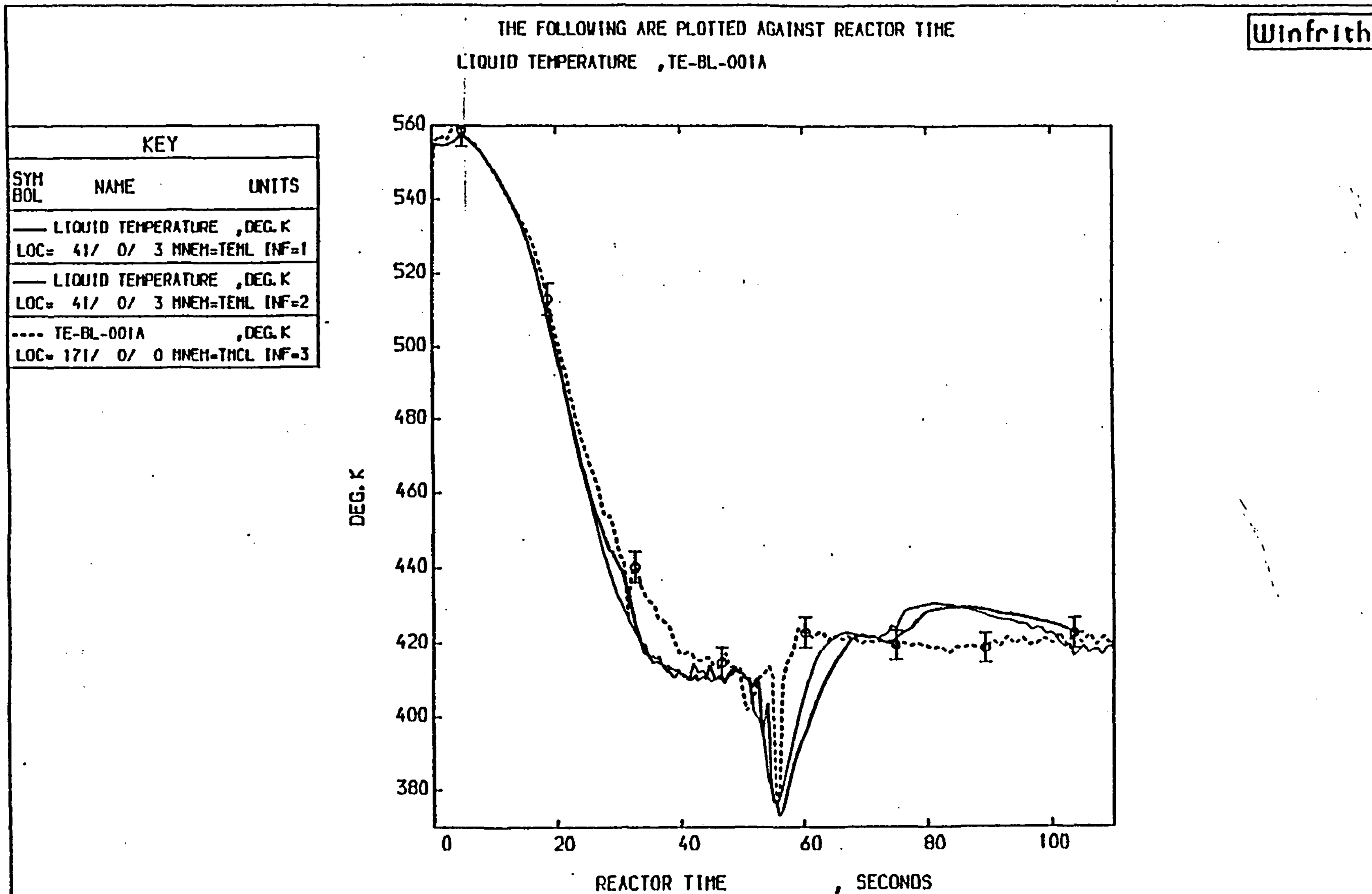

FIGURE 10 INF 1 JON'S, INF 2 ORIG, INF 3 EXP
BROKEN LOOP COLD LEG - EXPERIMENTAL LOCATION BL-1

Winfrith

THE FOLLOWING ARE PLOTTED AGAINST REACTOR TIME

VAPOR TEMPERATURE ,TE-BL-001C

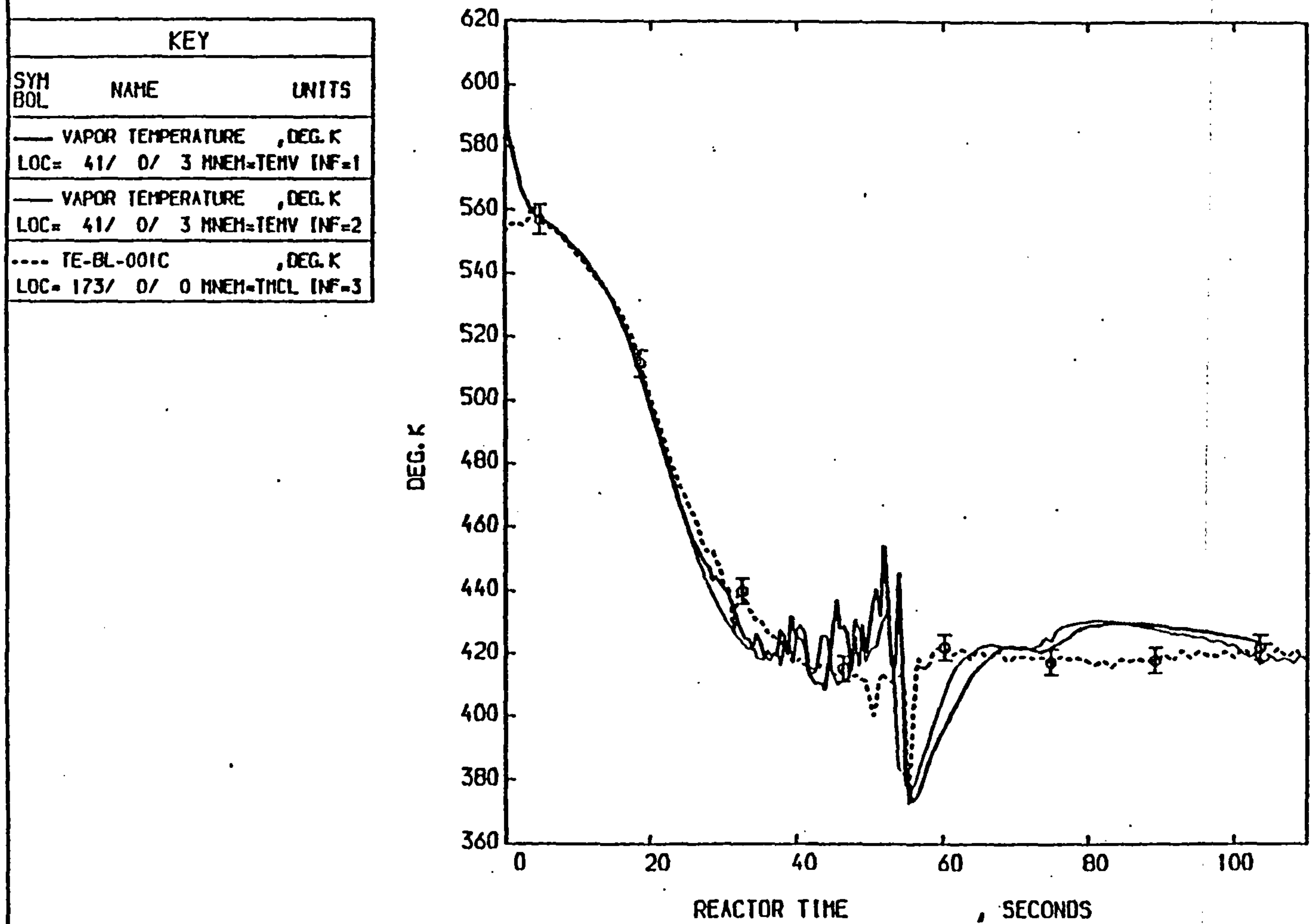

FIGURE 11 INF 1 JON'S, INF 2 ORIG, INF 3 EXP
BROKEN LOOP COLD LEG - EXPERIMENTAL LOCATION BL-1

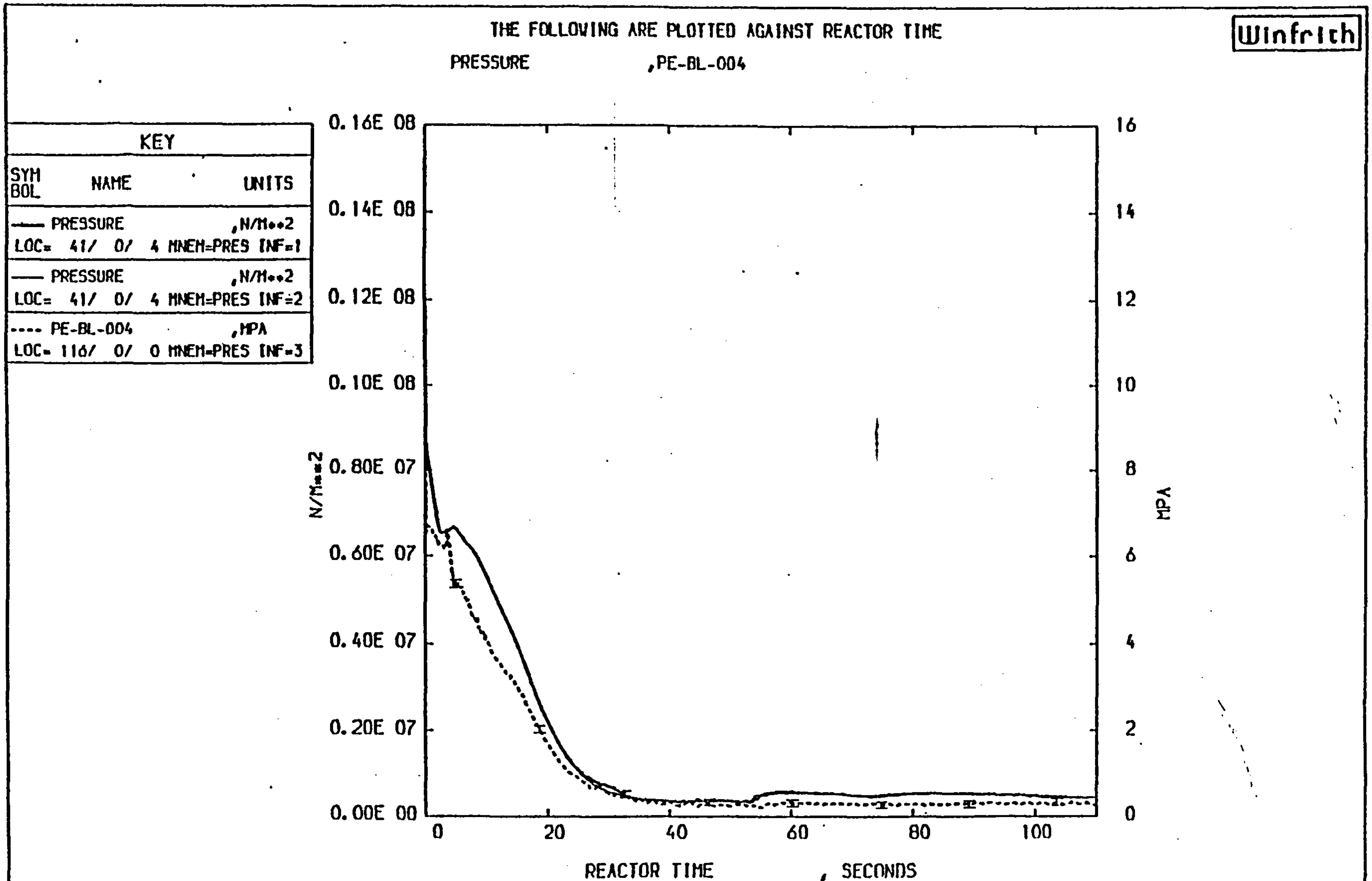

FIGURE 12 INF 1 JON'S, INF 2 ORIG, INF 3 EXP
BROKEN LOOP COLD LEG - EXPERIMENTAL LOCATION BL-4

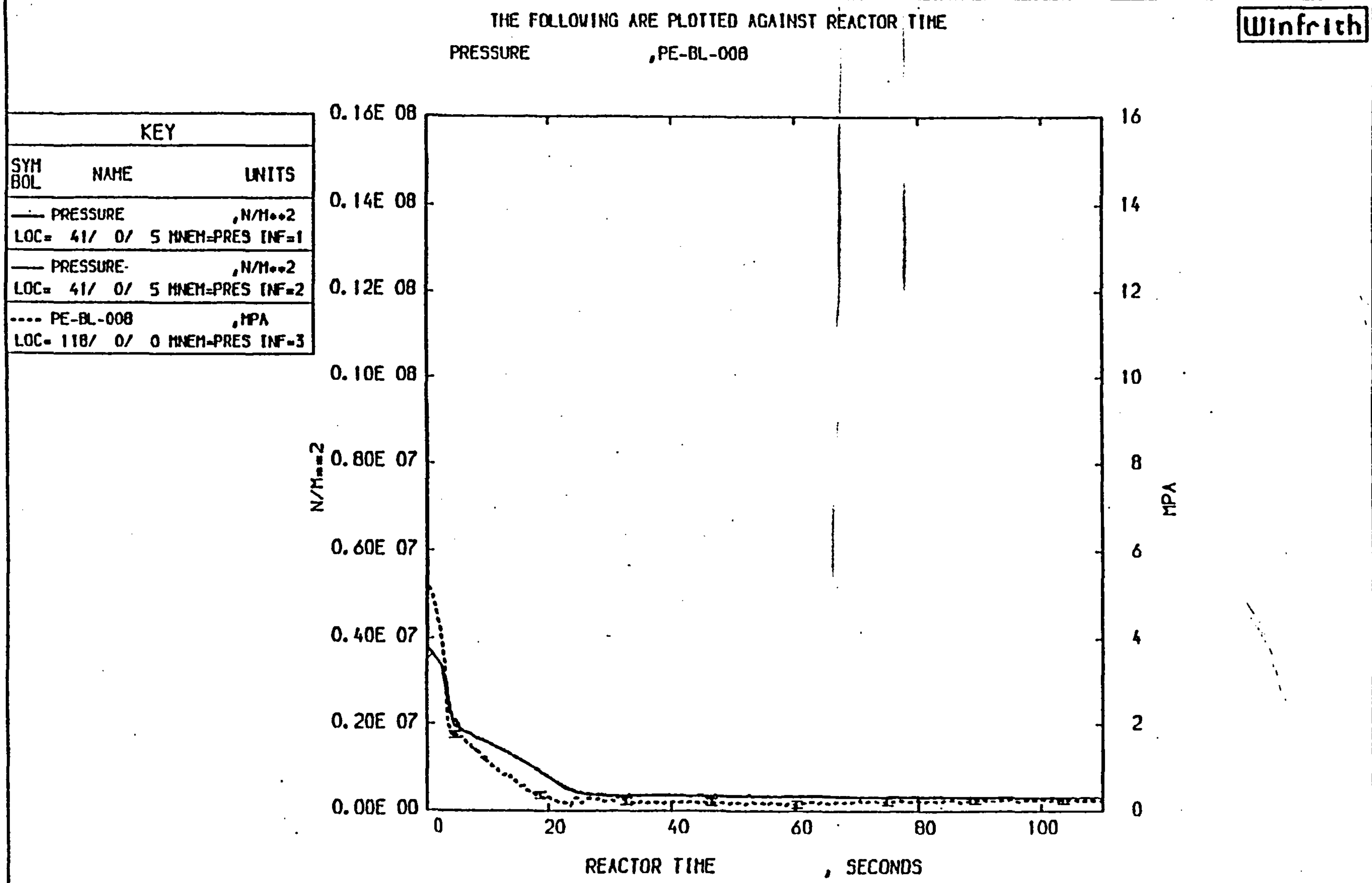

FIGURE 13 INF 1 JON'S, INF 2 ORIG, INF 3 EXP
BROKEN LOOP COLD LEG - EXPERIMENTAL LOCATION BL-8

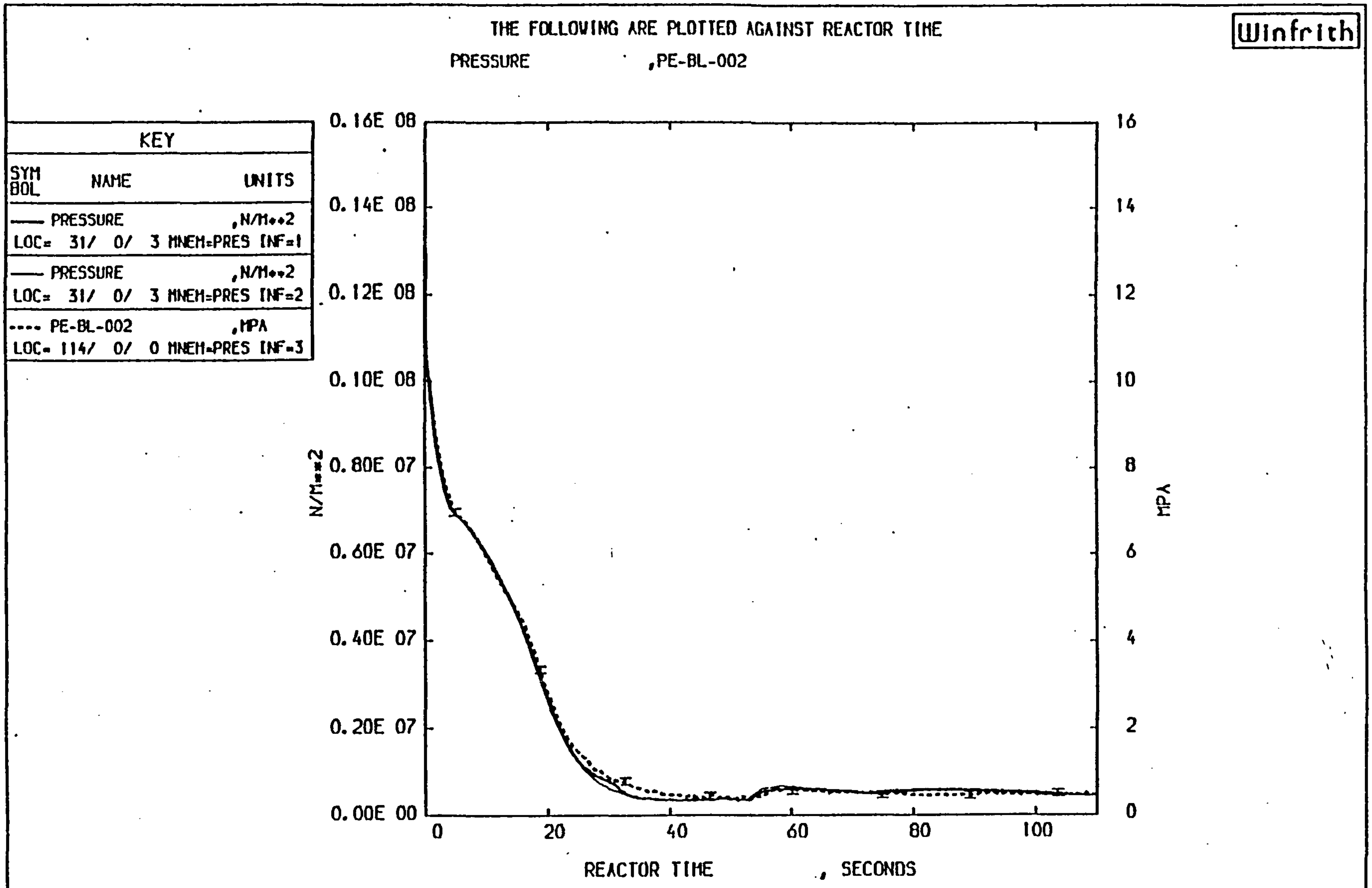

FIGURE 14 INF 1 JON'S, INF 2 ORIG, INF 3 EXP
BROKEN LOOP HOT LEG - EXPERIMENTAL LOCATION BL-2

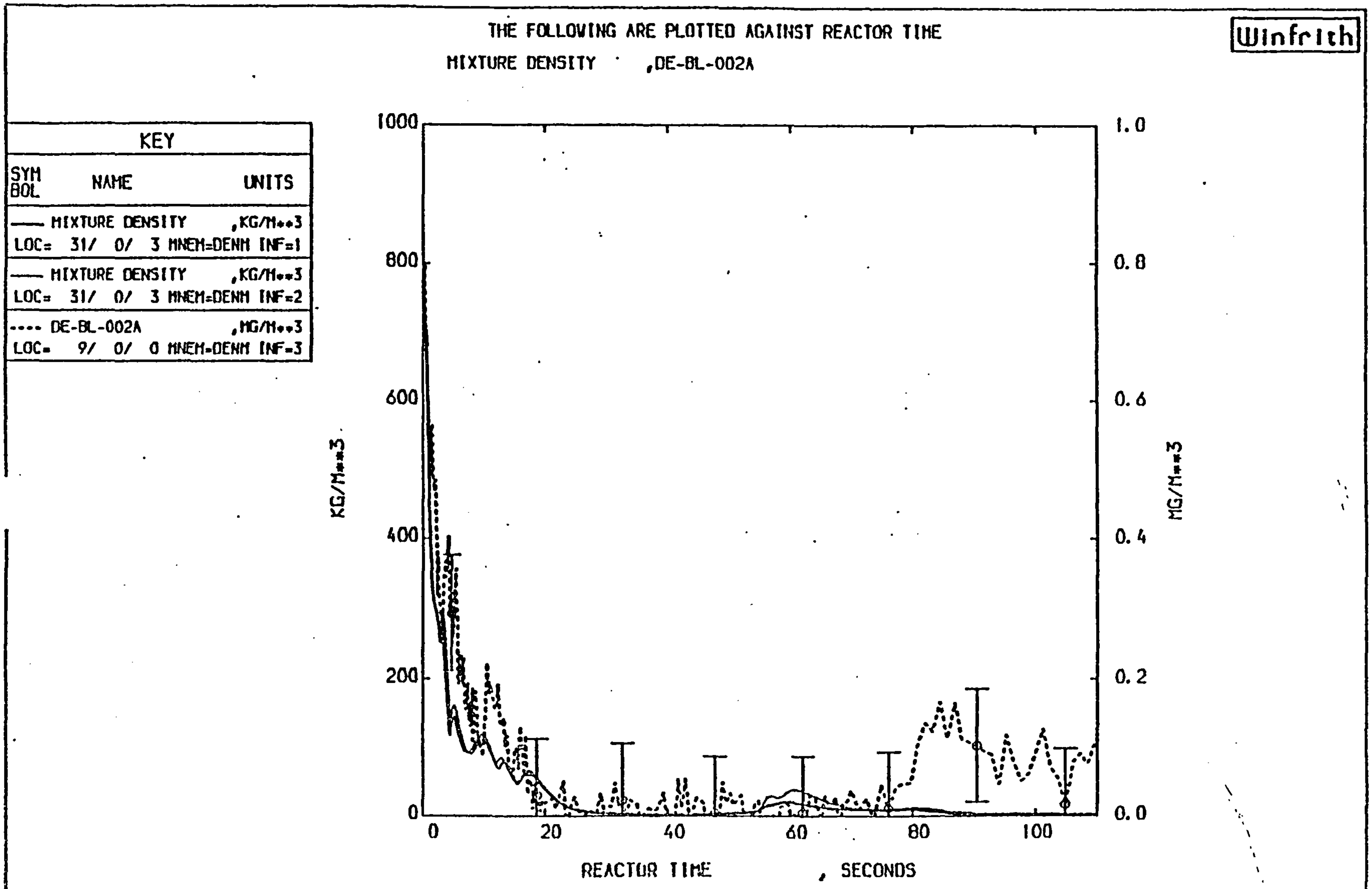

FIGURE 15 INF 1 JON'S, INF 2 ORIG, INF 3 EXP
BROKEN LOOP HOT LEG - EXPERIMENTAL LOCATION BL-2

THE FOLLOWING ARE PLOTTED AGAINST REACTOR TIME

MASS FLOW RATE ,FR-BL-205

Winfrith

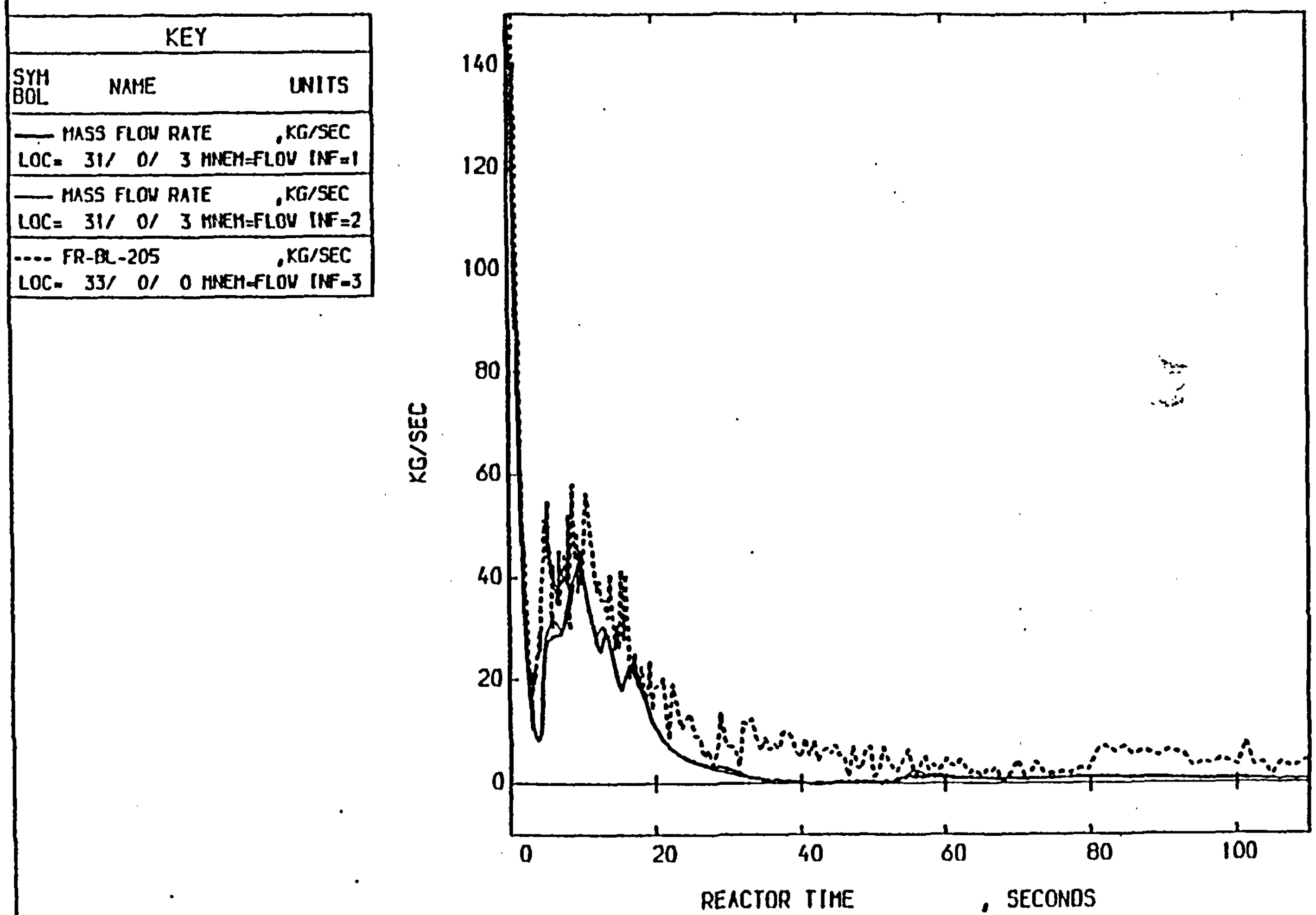

FIGURE 16 INF 1 JON'S, INF 2 ORIG, INF 3 EXP
BROKEN LOOP HOT LEG - EXPERIMENTAL LOCATION BL-2

THE FOLLOWING ARE PLOTTED AGAINST REACTOR TIME

LIQUID TEMPERATURE ,TE-BL-002B

KEY		
SYM BOL	NAME	UNITS
——	LIQUID TEMPERATURE LOC= 31/ 0/ 3 MNEM=TEML INF=1	,DEG.K
——	LIQUID TEMPERATURE LOC= 31/ 0/ 3 MNEM=TEML INF=2	,DEG.K
----	TE-BL-002B LOC= 174/ 0/ 0 MNEM=TMCL INF=3	,DEG.K

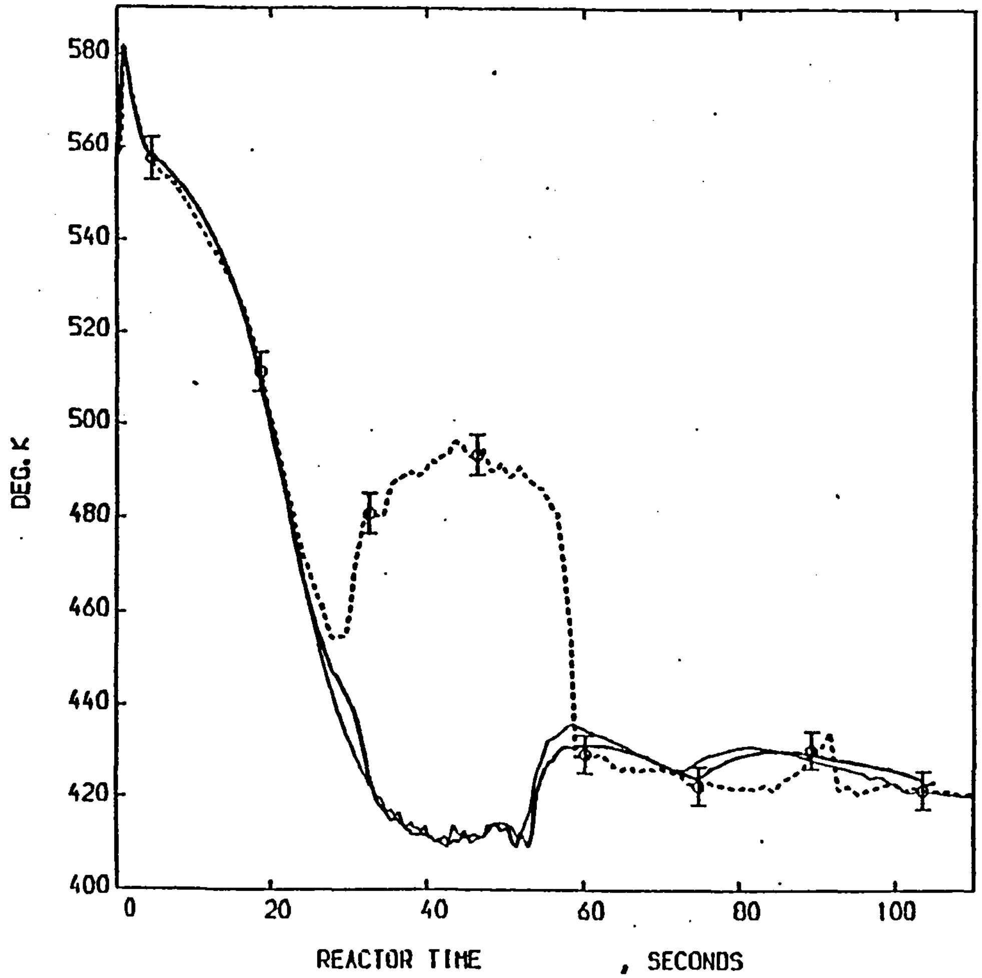

FIGURE 17 INF 1 JON'S, INF 2 ORIG, INF 3 EXP
BROKEN LOOP HOT LEG - EXPERIMENTAL LOCATION BL-2

Winfrith

THE FOLLOWING ARE PLOTTED AGAINST REACTOR TIME

VAPOR TEMPERATURE . ,TE-BL-002B ,TE-BL-002C

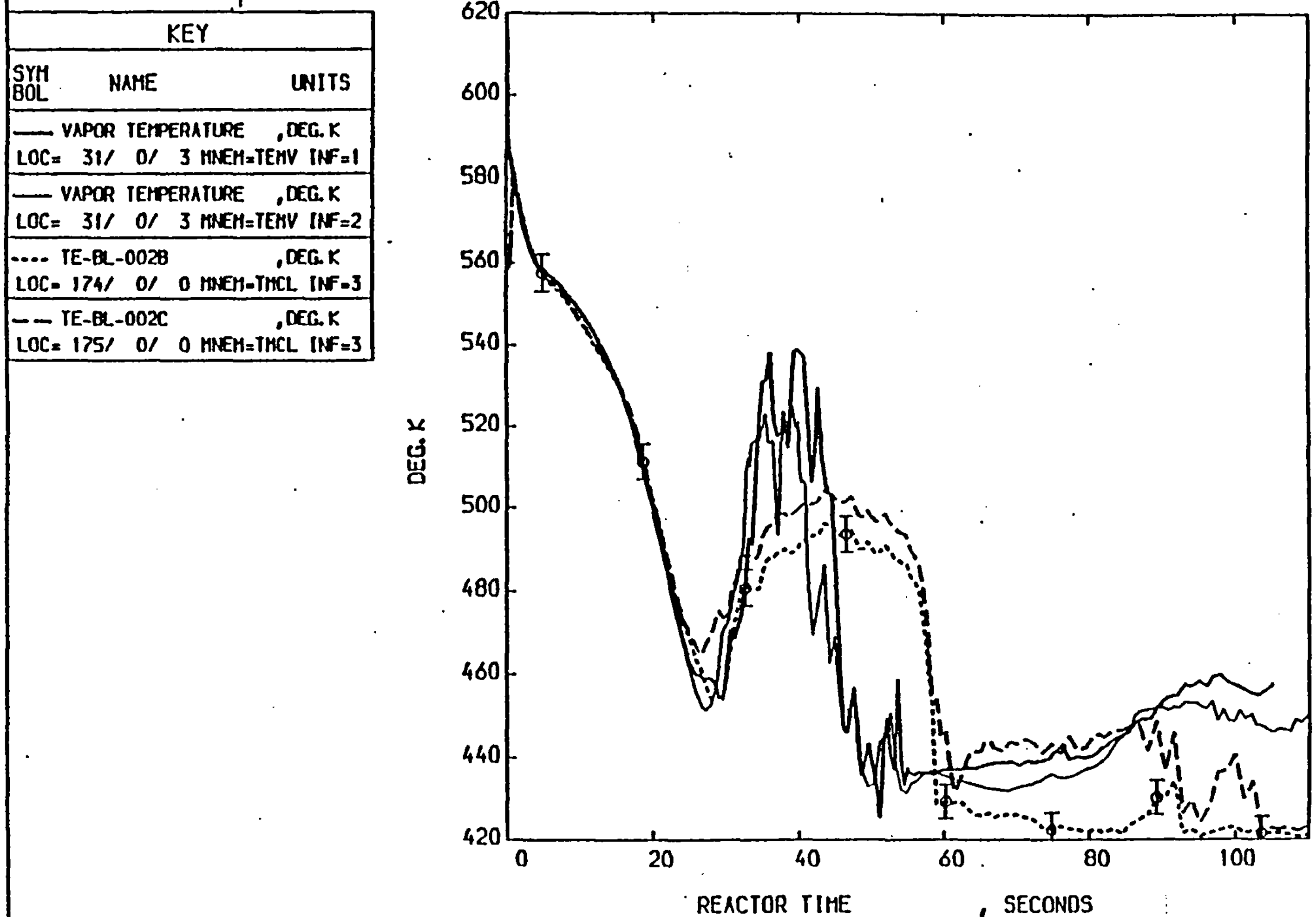

FIGURE 18 INF 1 JON'S, INF 2 ORIG, INF 3 EXP
BROKEN LOOP HOT LEG - EXPERIMENTAL LOCATION BL-2

Winfrith

THE FOLLOWING ARE PLOTTED AGAINST REACTOR TIME

PRESSURE ,PE-BL-003

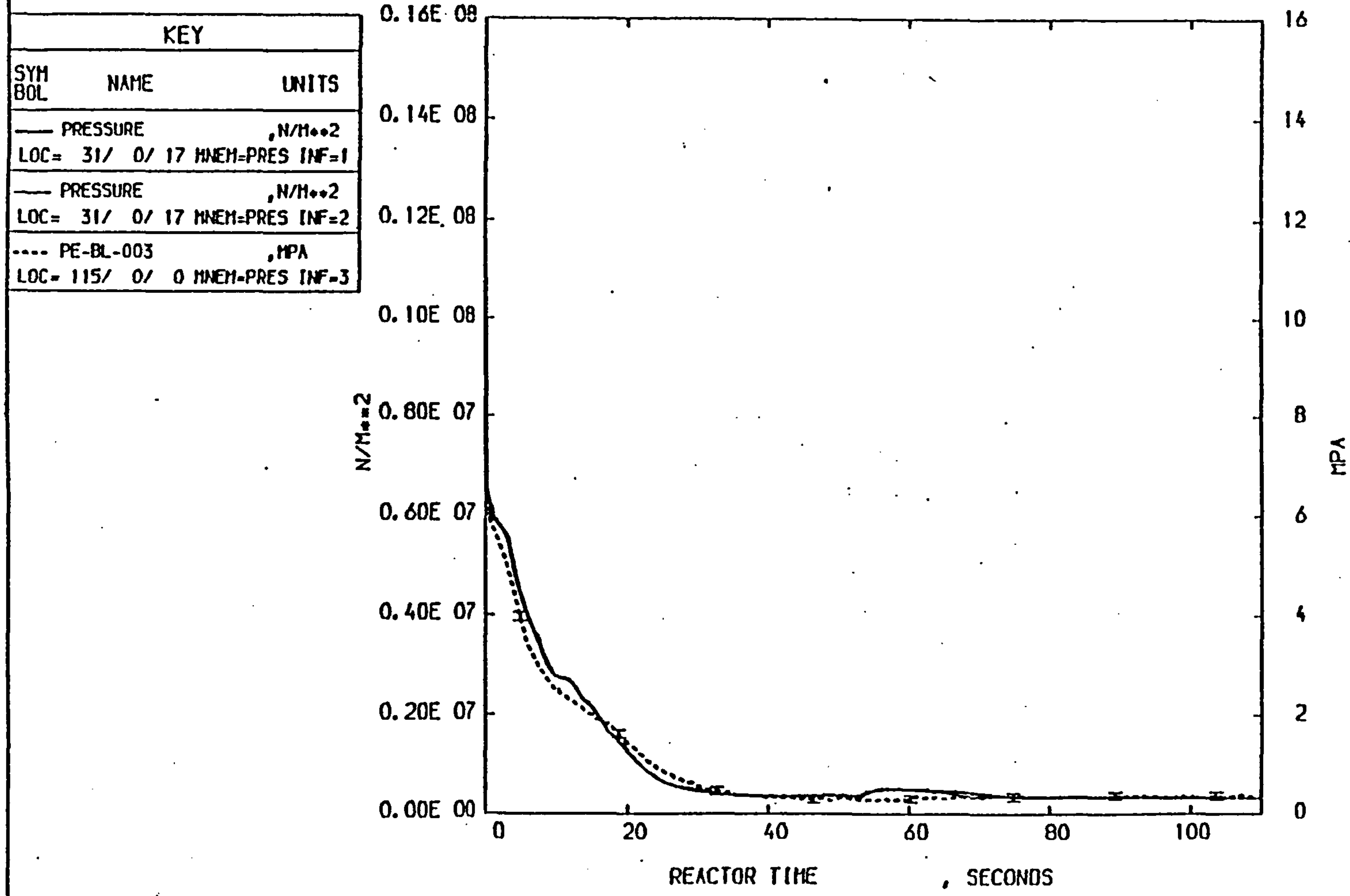

FIGURE 19 INF 1 JON'S, INF 2 ORIG, INF 3 EXP
BROKEN LOOP HOT LEG - EXPERIMENTAL LOCATION BL-3

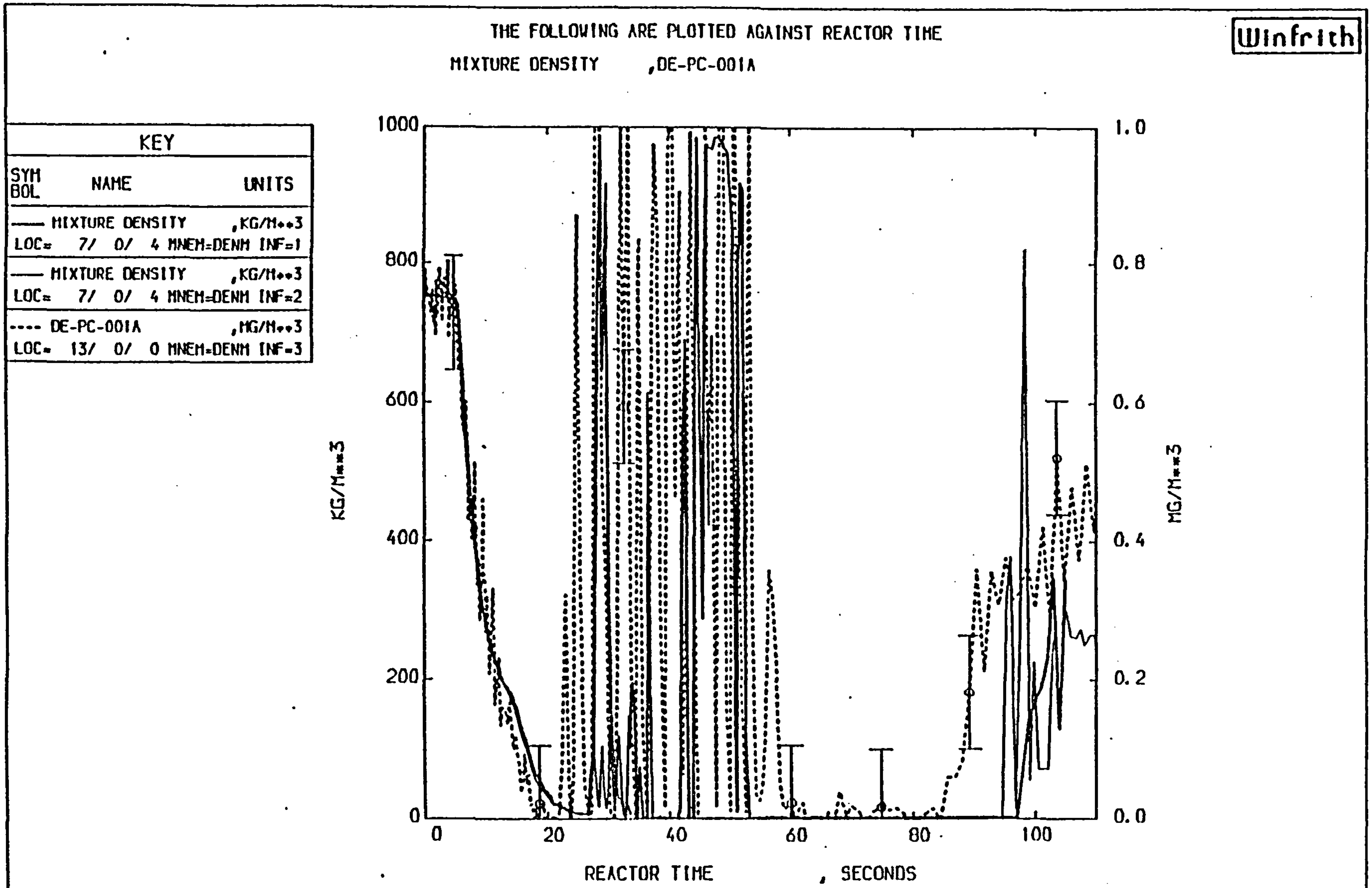

FIGURE 20 INF 1 JON'S, INF 2 ORIG, INF 3 EXP
INTACT LOOP COLD LEG - EXPERIMENTAL LOCATION PC-1

Winfrith

THE FOLLOWING ARE PLOTTED AGAINST REACTOR TIME

MASS FLOW RATE ,FR-PC-100

KEY		
SYMBOL	NAME	UNITS
——	MASS FLOW RATE	,KG/SEC
LOC= 7/ 0/ 4 MNEM=FLOW INF=1		
——	MASS FLOW RATE	,KG/SEC
LOC= 7/ 0/ 4 MNEM=FLOW INF=2		
----	FR-PC-100	,KG/SEC
LOC= 34/ 0/ 0 MNEM=FLOW INF=3		

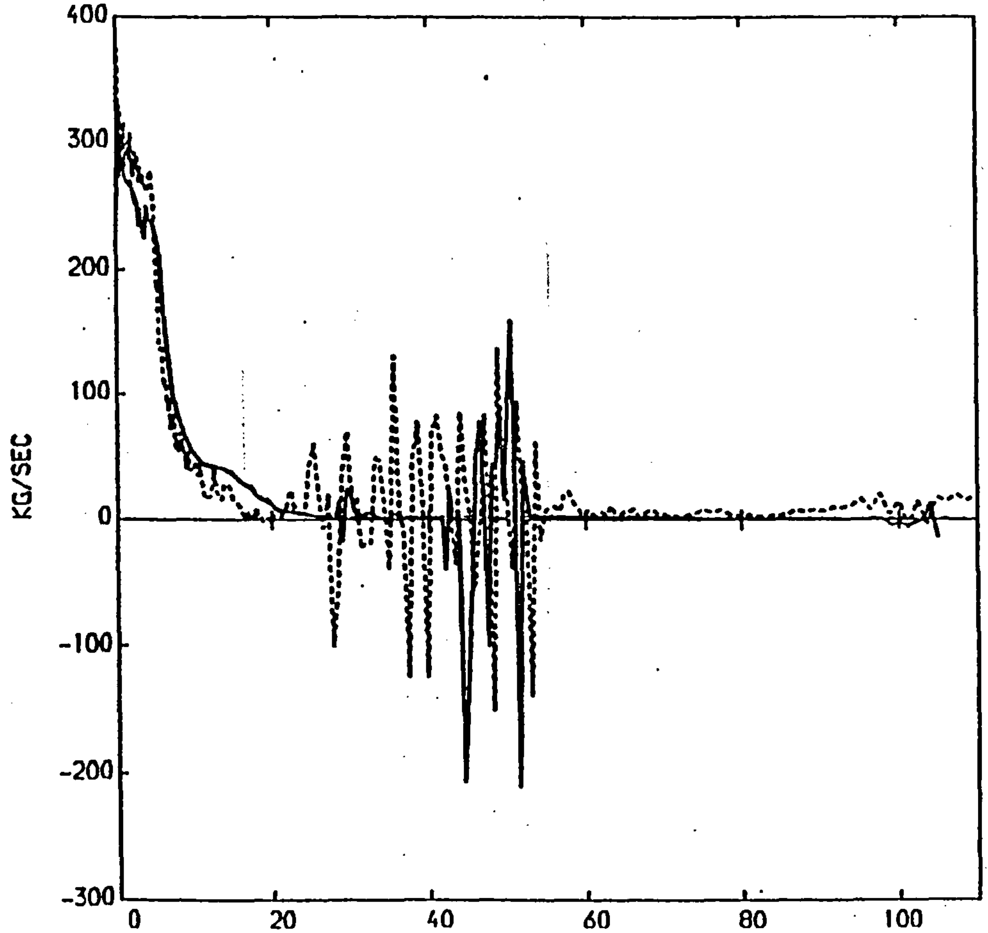

FIGURE 21 INF 1 JON'S, INF 2 ORIG, INF 3 EXP
INTACT LOOP COLD LEG - EXPERIMENTAL LOCATION PC-1

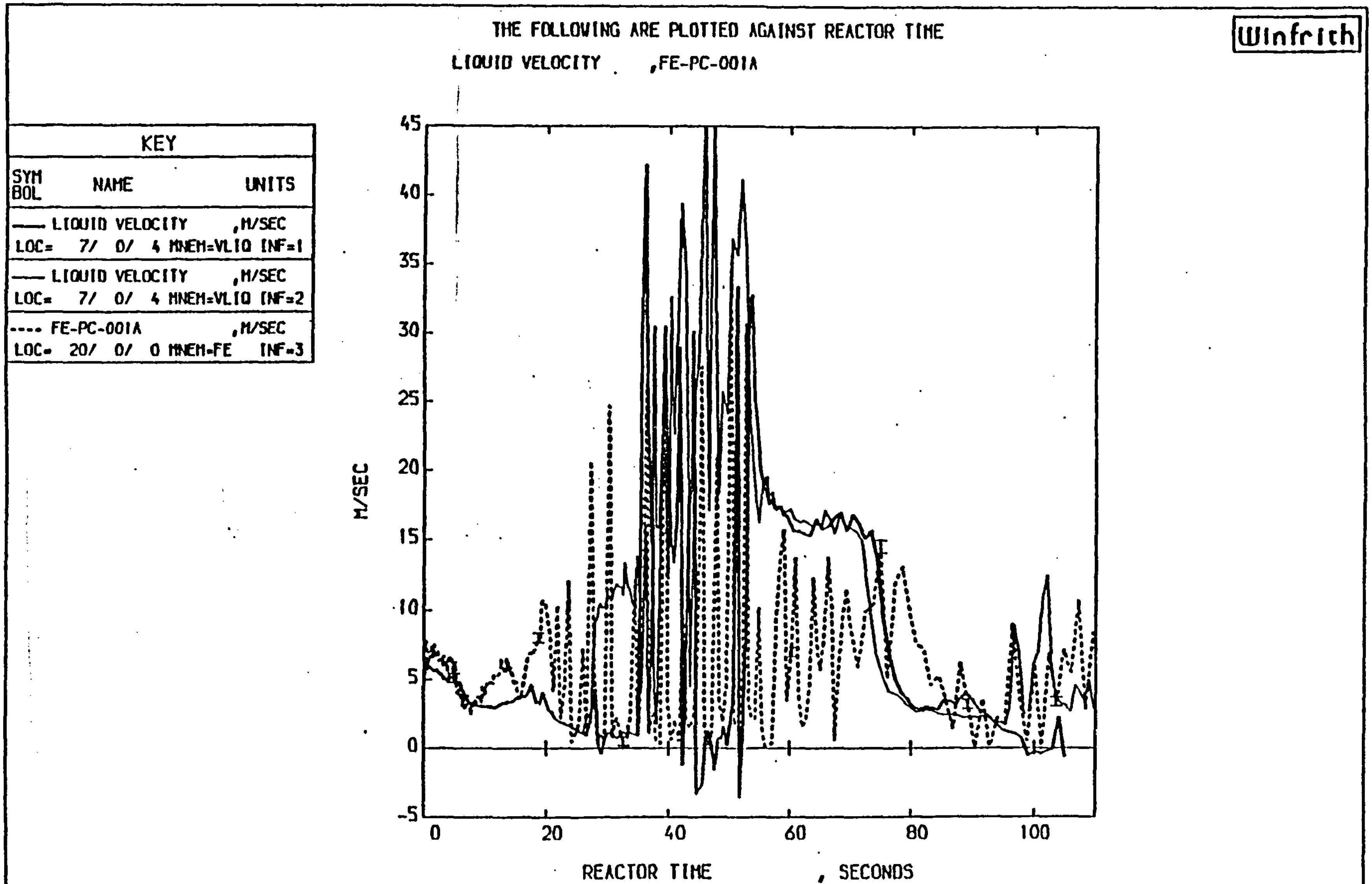

FIGURE 22 INF 1 JON'S, INF 2 ORIG, INF 3 EXP
INTACT LOOP COLD LEG - EXPERIMENTAL LOCATION PC-1

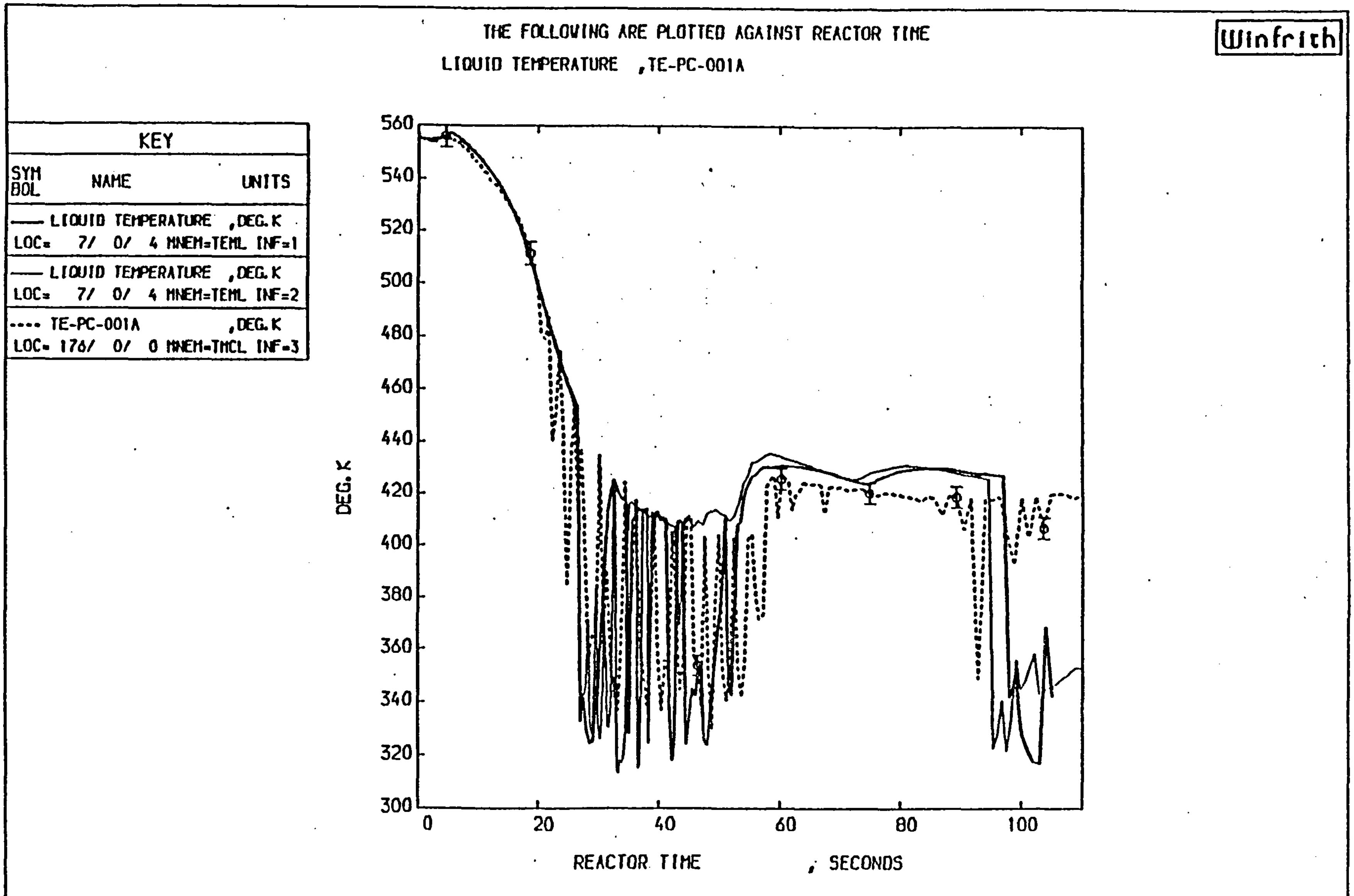

FIGURE 23 INF 1 JON'S, INF 2 ORIG, INF 3 EXP
INTACT LOOP COLD LEG - EXPERIMENTAL LOCATION PC-1

Winfrith

THE FOLLOWING ARE PLOTTED AGAINST REACTOR TIME
VAPOR TEMPERATURE ,TE-PC-001C

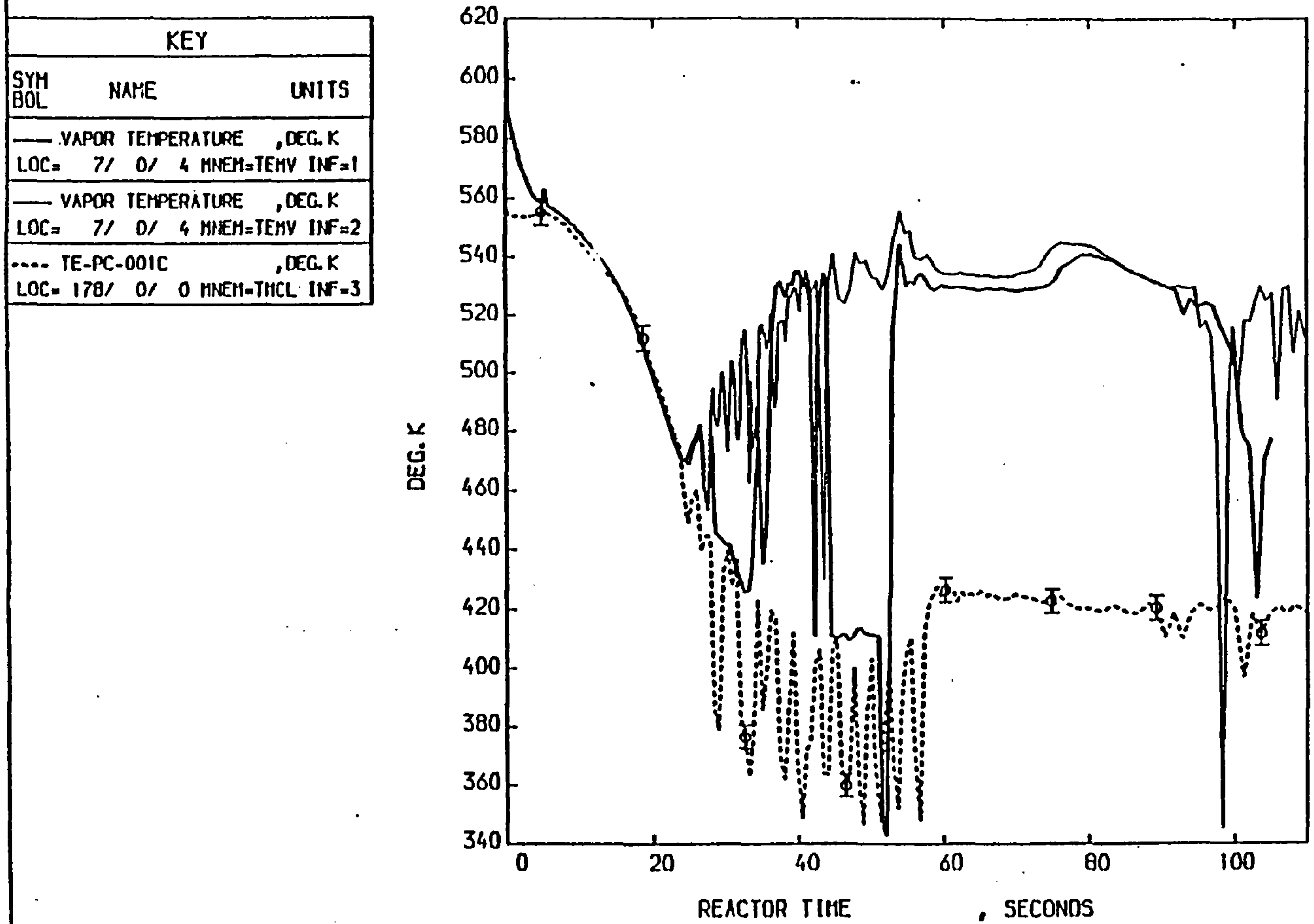

FIGURE 24 INF 1 JON'S, INF 2 ORIG, INF 3 EXP
INTACT LOOP COLD LEG - EXPERIMENTAL LOCATION PC-1

Winfrith

THE FOLLOWING ARE PLOTTED AGAINST REACTOR TIME
PUMP SPEED ,FUNCTION

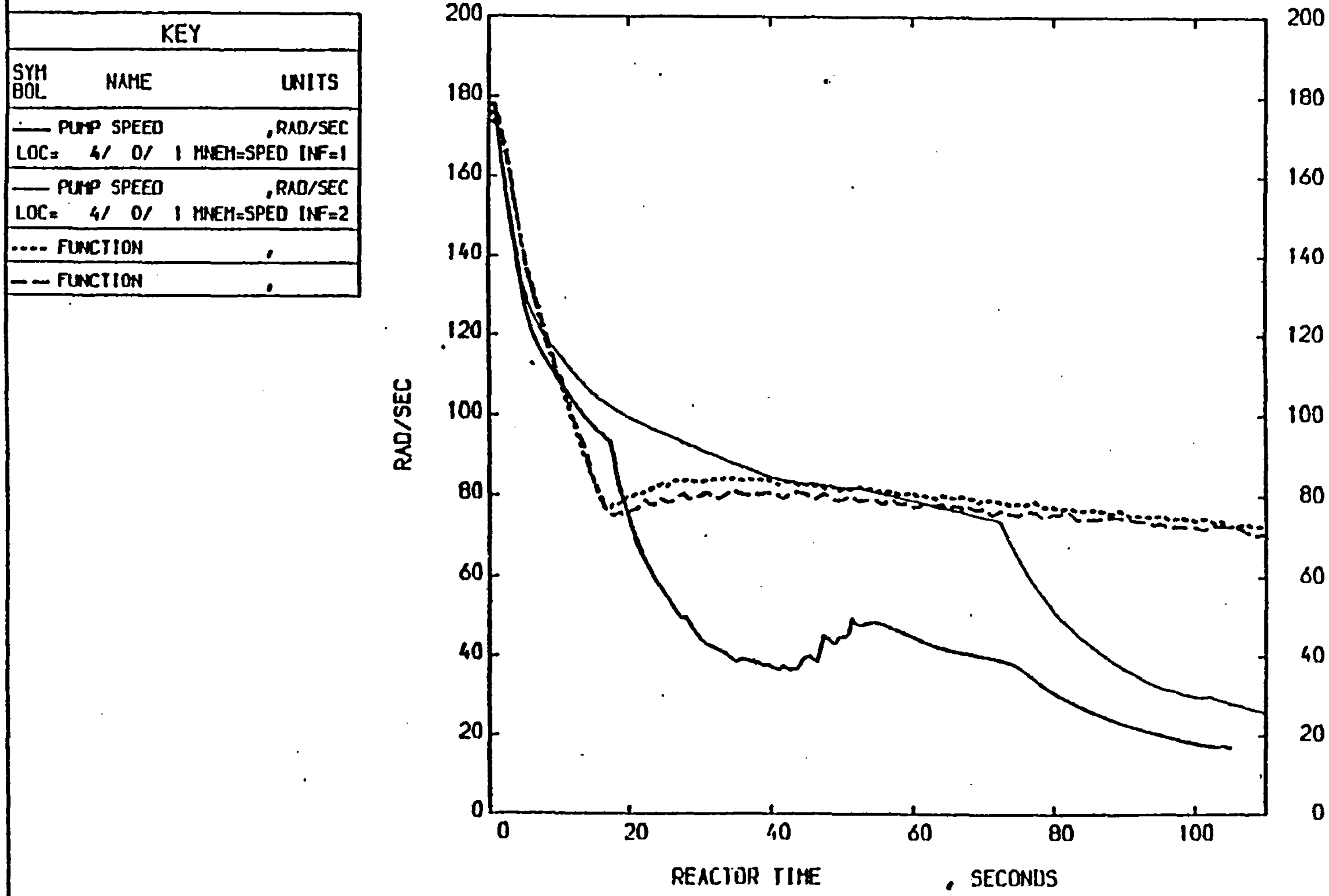

FIGURE 25 INF 1 JON'S, INF 2 ORIG, INF 3 EXP
PUMP SPEED

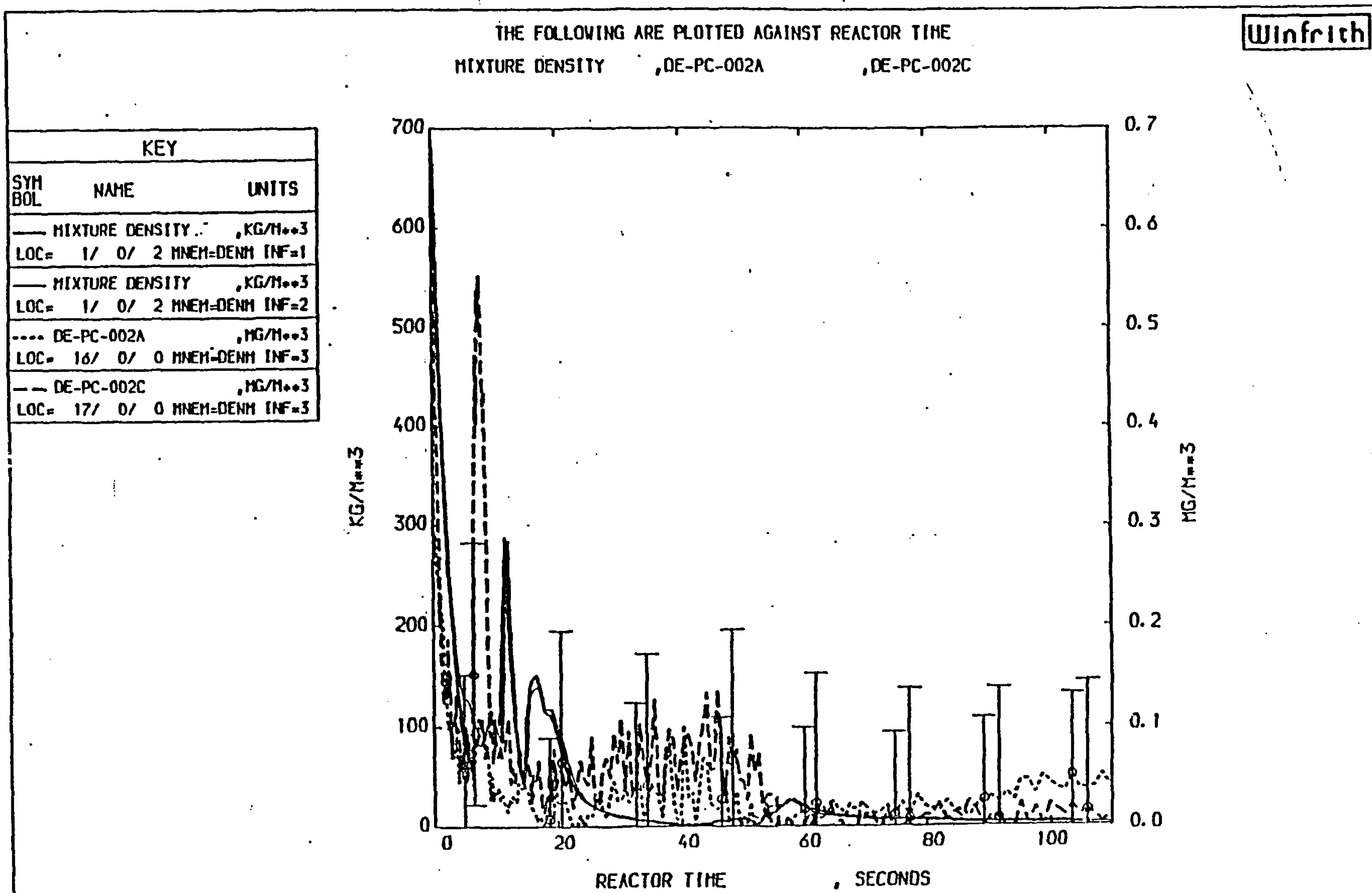

FIGURE 26 INF 1 JON'S, INF 2 ORIG, INF 3 EXP
INTACT LOOP HOT LEG - EXPERIMENTAL LOCATION PC-2

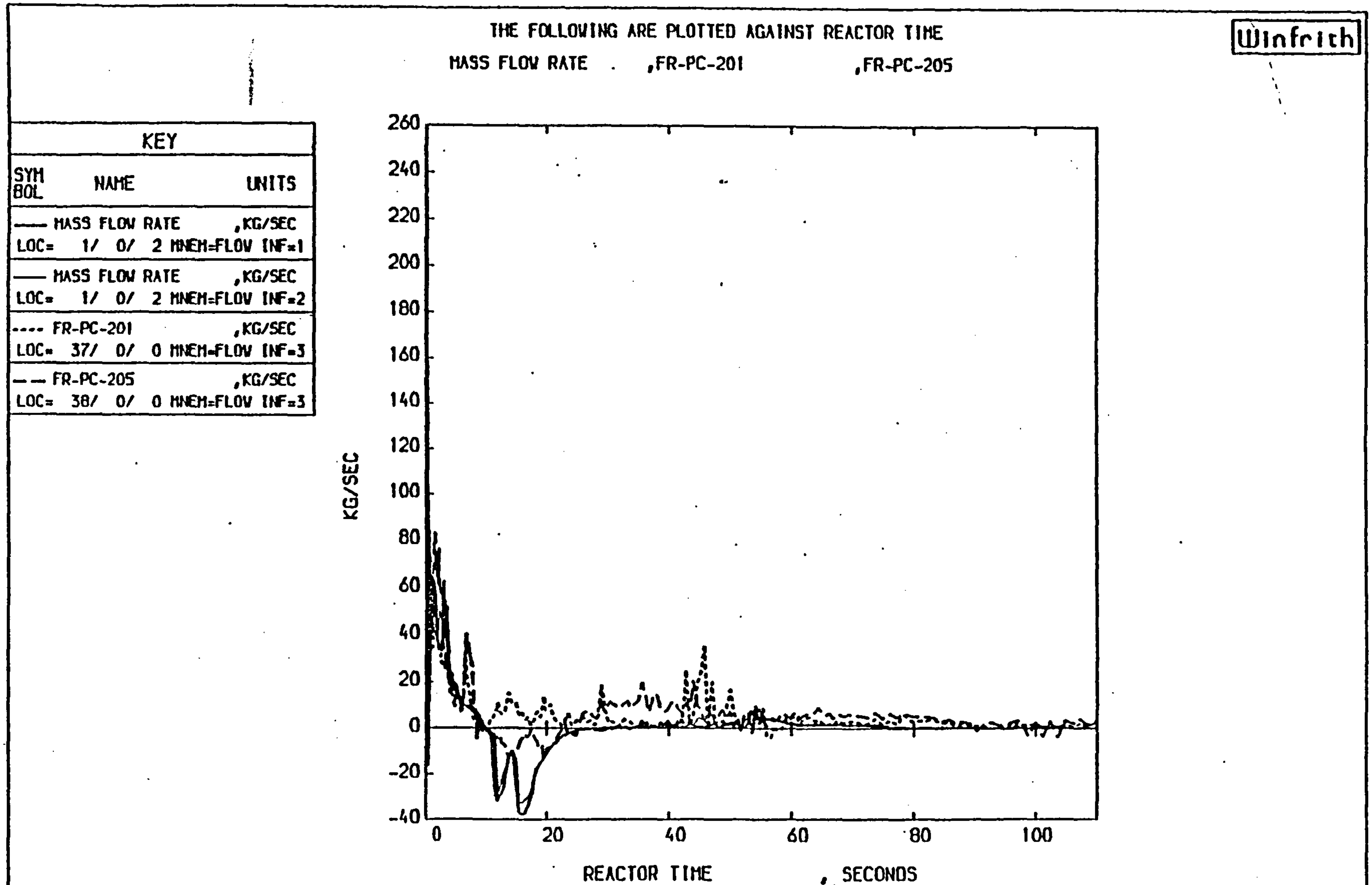

FIGURE 27 INF 1 JON'S, INF 2 ORIG, INF 3 EXP
INTACT LOOP HOT LEG - EXPERIMENTAL LOCATION PC-2

Winfrith

THE FOLLOWING ARE PLOTTED AGAINST REACTOR TIME

LIQUID TEMPERATURE ,TE-PC-002A

KEY		
SYM BOL	NAME	UNITS
—— LIQUID TEMPERATURE		,DEG.K
LOC= 1/ 0/ 2 MNEM=TEML INF=1		
—— LIQUID TEMPERATURE		,DEG.K
LOC= 1/ 0/ 2 MNEM=TEML INF=2		
---- TE-PC-002A		,DEG.K
LOC= 179/ 0/ 0 MNEM=TMCL INF=3		

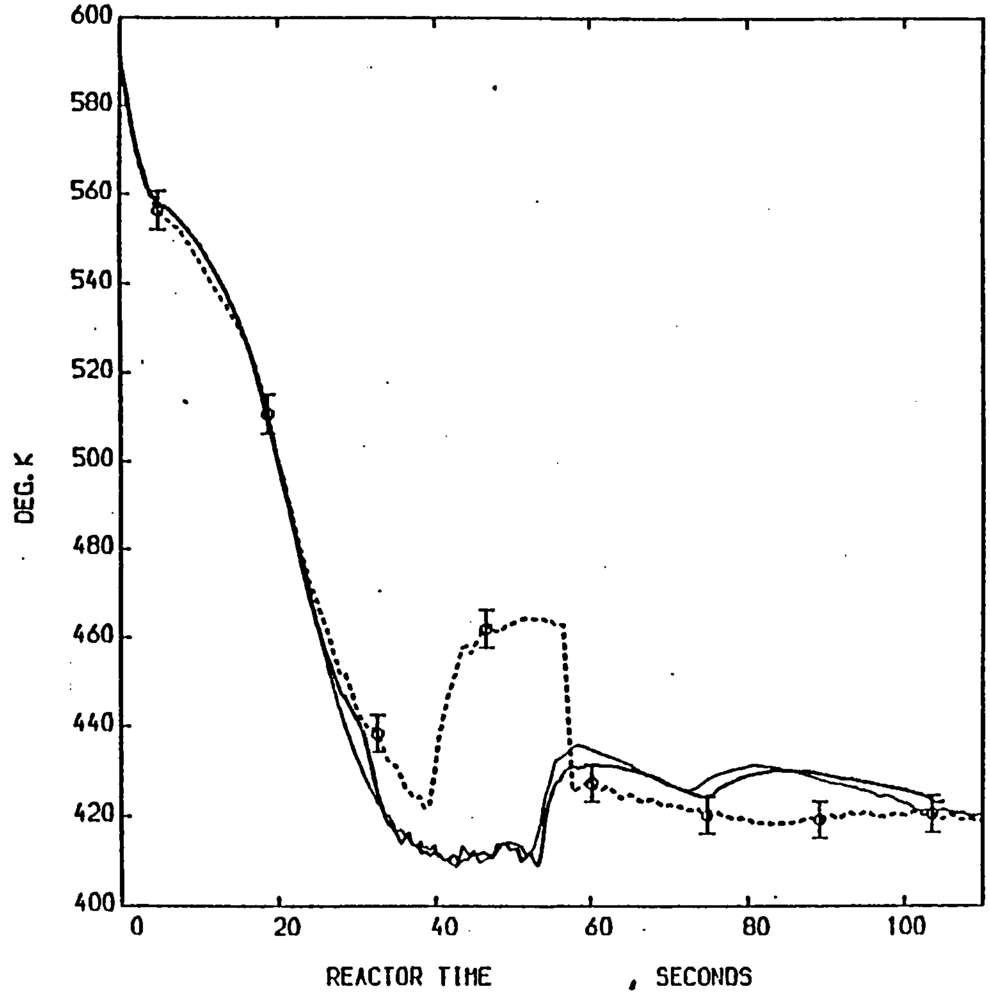

FIGURE 28 INF 1 JON'S, INF 2 ORIG, INF 3 EXP
INTACT LOOP HOT LEG - EXPERIMENTAL LOCATION PC-2

Winfrith

THE FOLLOWING ARE PLOTTED AGAINST REACTOR TIME

VAPOR TEMPERATURE ,TE-PC-002A ,TE-PC-002B
TE-PC-002C

KEY		
SYMBOL	NAME	UNITS
——	VAPOR TEMPERATURE	,DEG.K
LOC= 1/ 0/ 2 MNEM=TEMV INF=1		
——	VAPOR TEMPERATURE	,DEG.K
LOC= 1/ 0/ 2 MNEM=TEMV INF=2		
----	TE-PC-002A	,DEG.K
LOC= 179/ 0/ 0 MNEM=TMCL INF=3		
— —	TE-PC-002B	,DEG.K
LOC= 180/ 0/ 0 MNEM=TMCL INF=3		
——	TE-PC-002C	,DEG.K
LOC= 181/ 0/ 0 MNEM=TMCL INF=3		

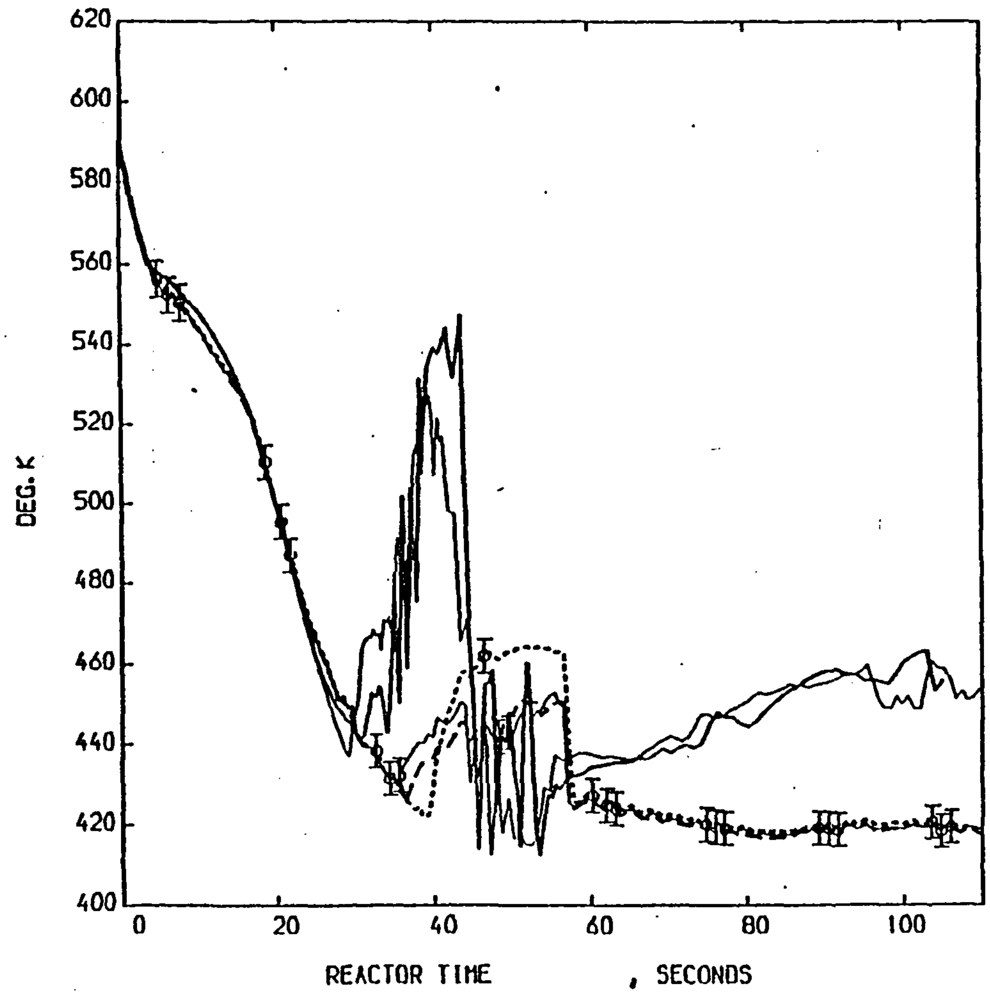

FIGURE 29 INF 1 JON'S, INF 2 ORIG, INF 3 EXP
INTACT LOOP HOT LEG - EXPERIMENTAL LOCATION PC-2

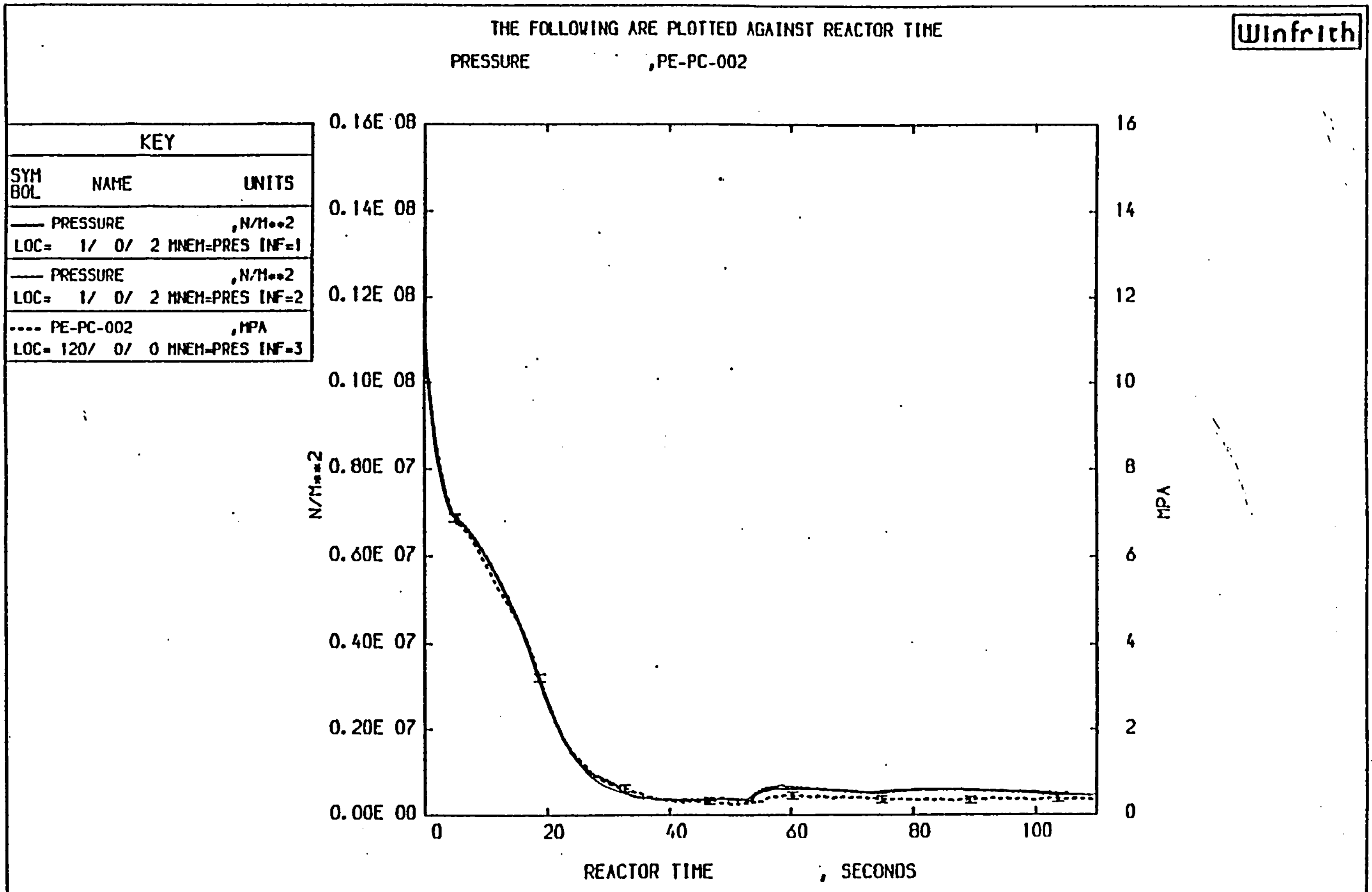

FIGURE 30 INF 1 JON'S, INF 2 ORIG, INF 3 EXP
INTACT LOOP HOT LEG - EXPERIMENTAL LOCATION PC-2

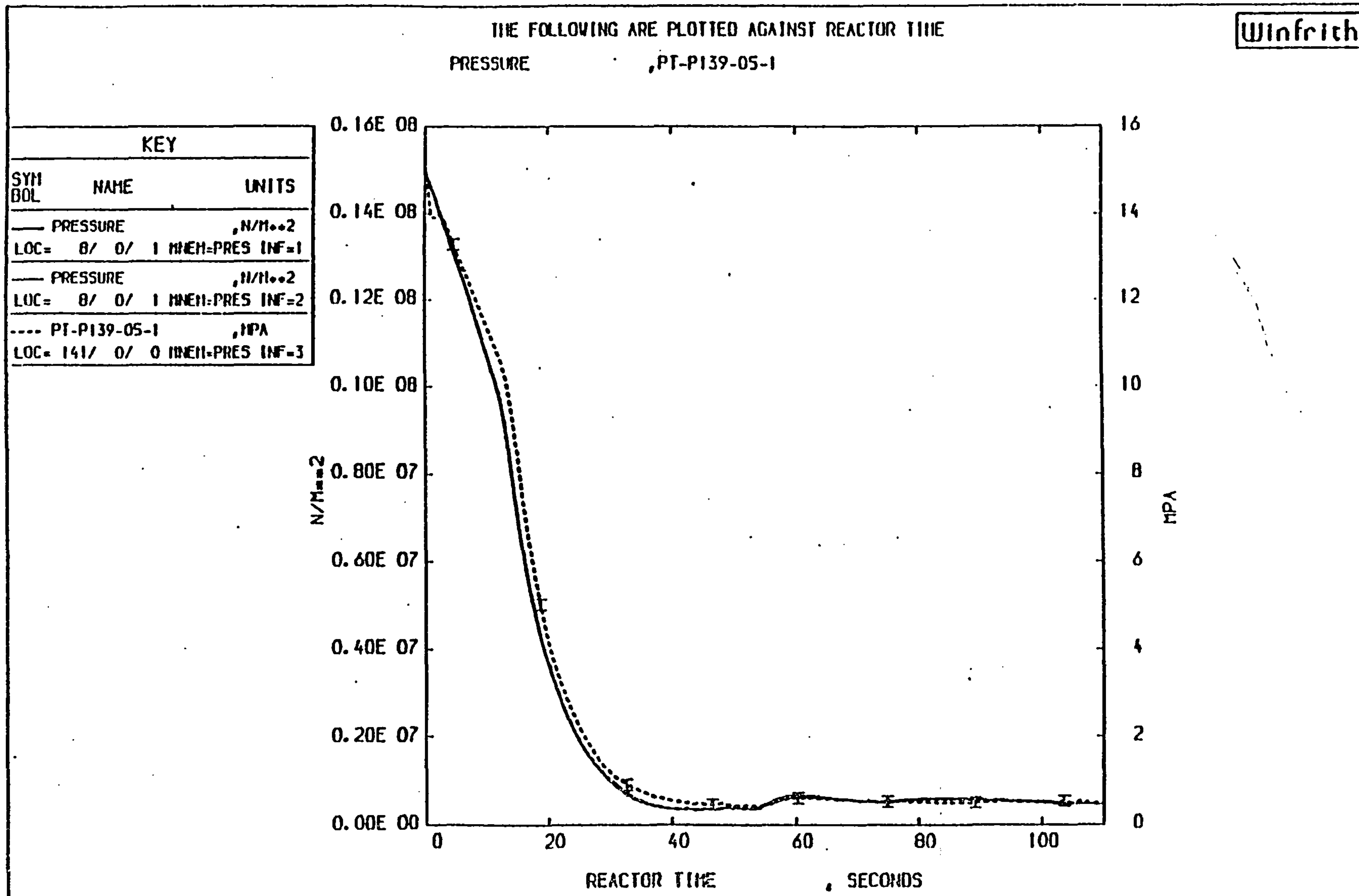

FIGURE 31 INF 1 JON'S, INF 2 ORIG, INF 3 EXP
INTACT LOOP HOT LEG - PRESSURIZER

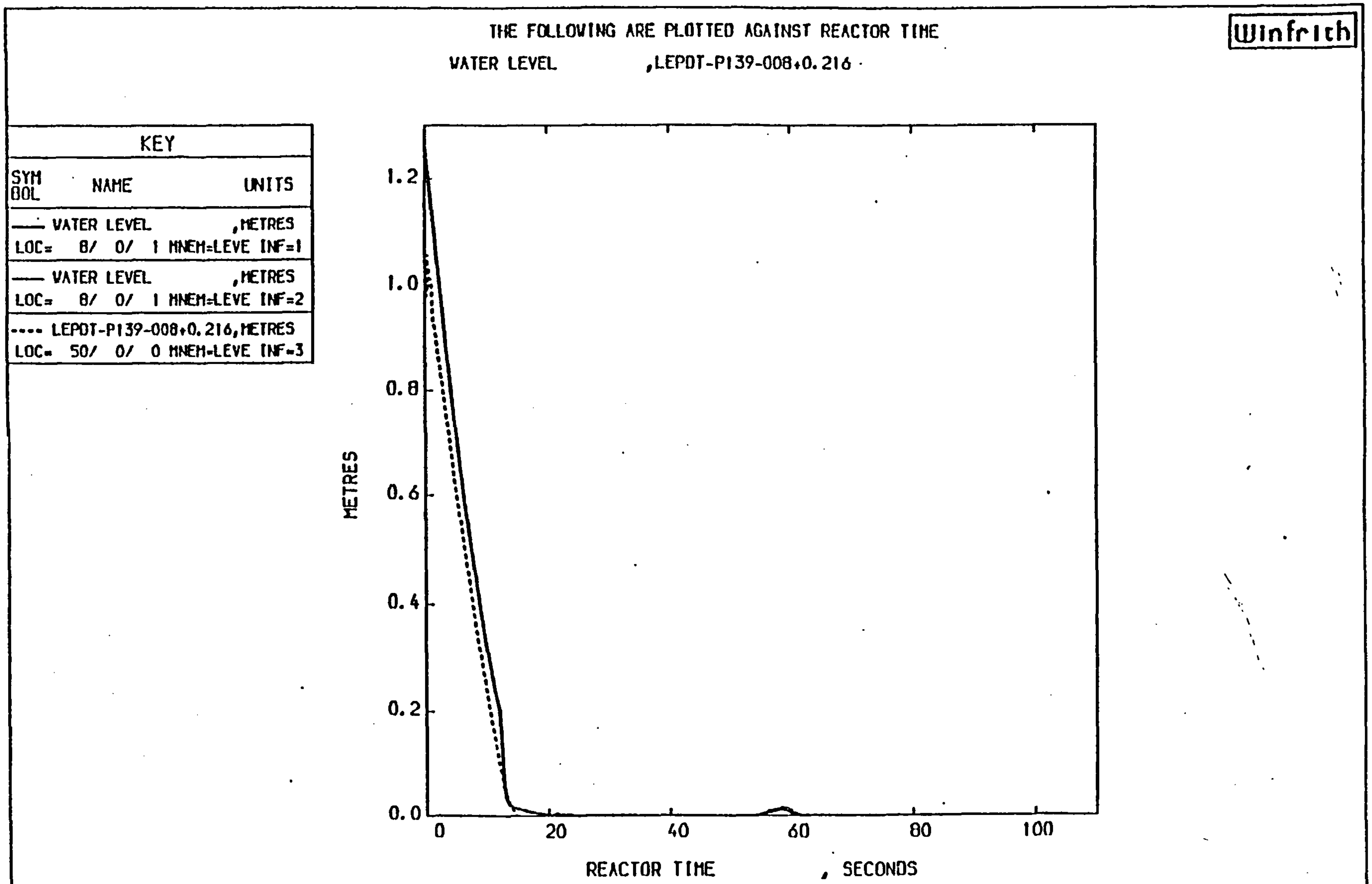

FIGURE 32 INF 1 JON'S, INF 2 ORIG, INF 3 EXP
INTACT LOOP HOT LEG - PRESSURIZER

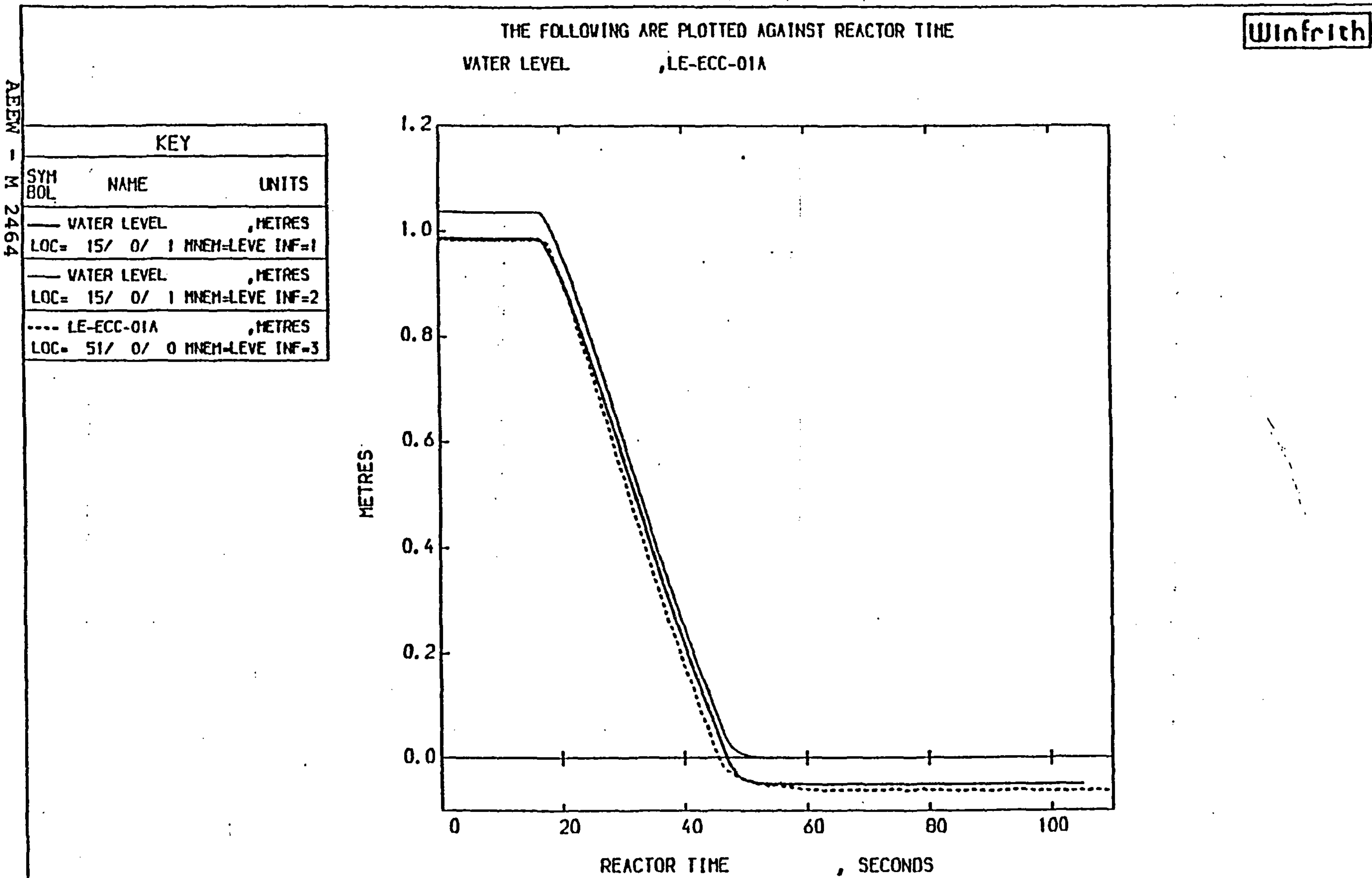

FIGURE 33 INF 1 JON'S, INF 2 ORIG, INF 3 EXP
EMERGENCY CORE COOLING SYSTEM

Winfrith

THE FOLLOWING ARE PLOTTED AGAINST REACTOR TIME

PRESSURE ,PT-P120-043

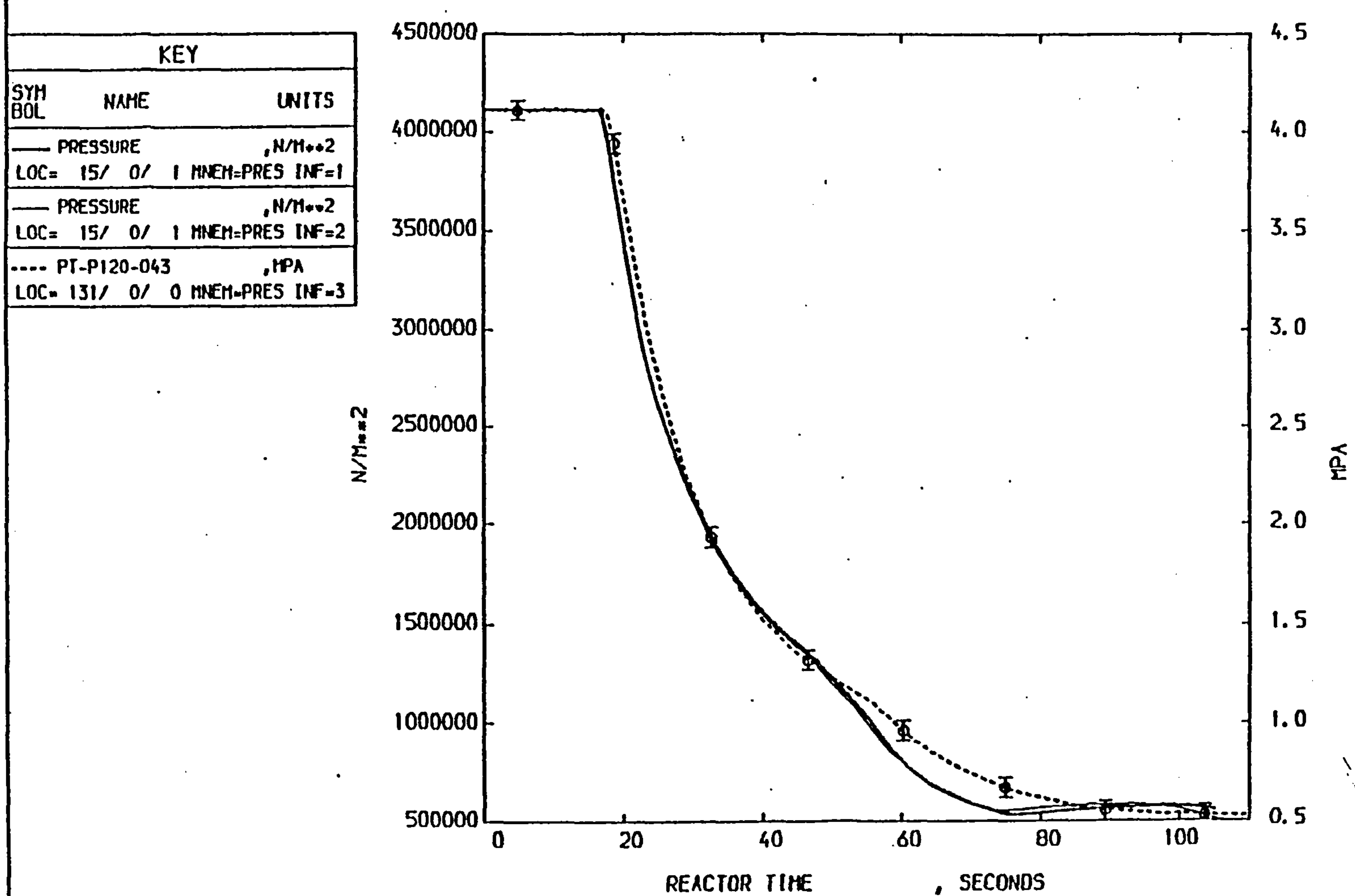

FIGURE 34 INF 1 JON'S, INF 2 ORIG, INF 3 EXP
EMERGENCY CORE COOLING SYSTEM

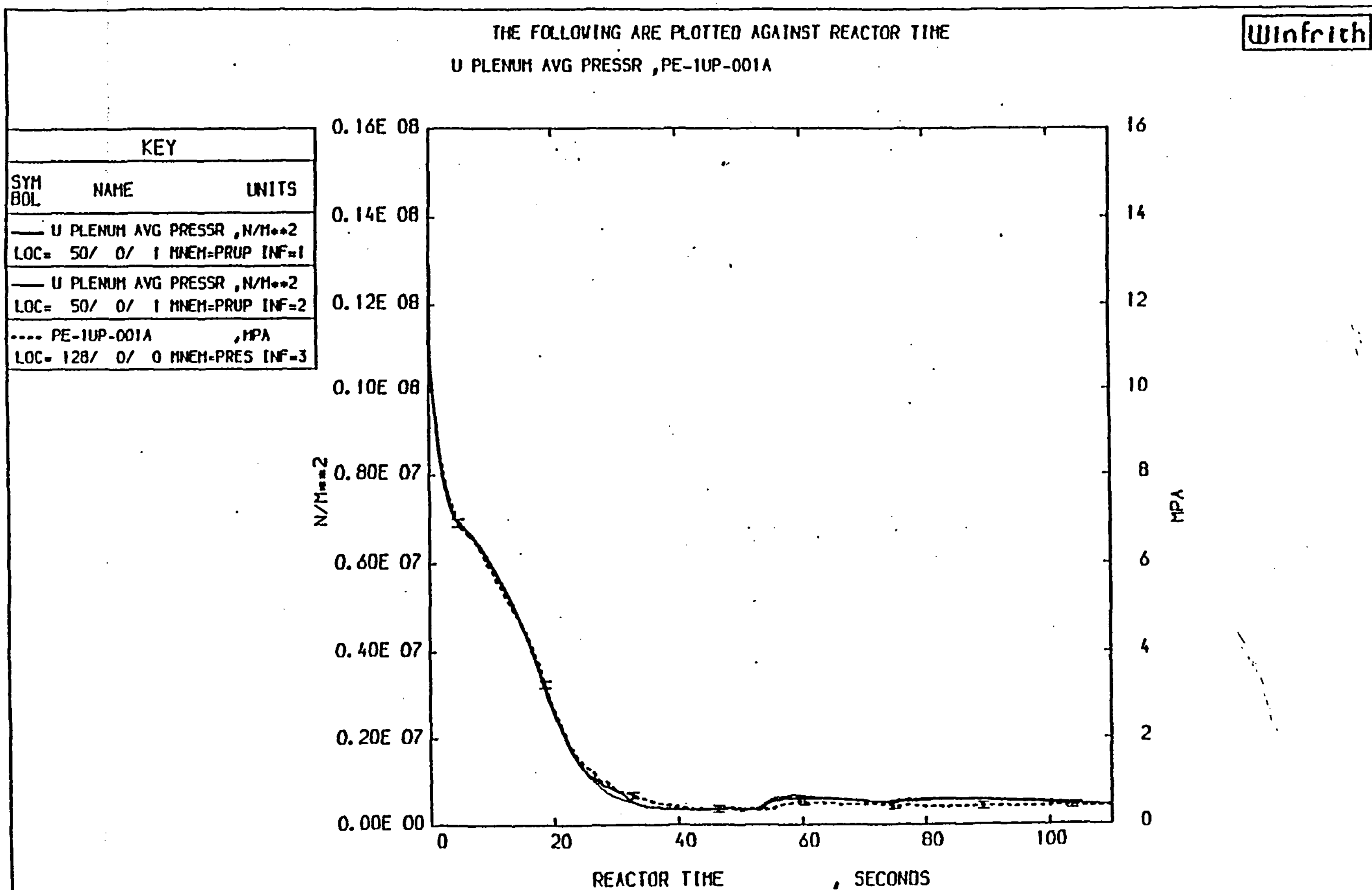

FIGURE 35 INF 1 JON'S, INF 2 ORIG, INF 3 EXP
UPPER PLENUM PRESSURE

Winfrith

THE FOLLOWING ARE PLOTTED AGAINST REACTOR TIME

LIQ AXIAL VELOCITY ,FE-5LP-001

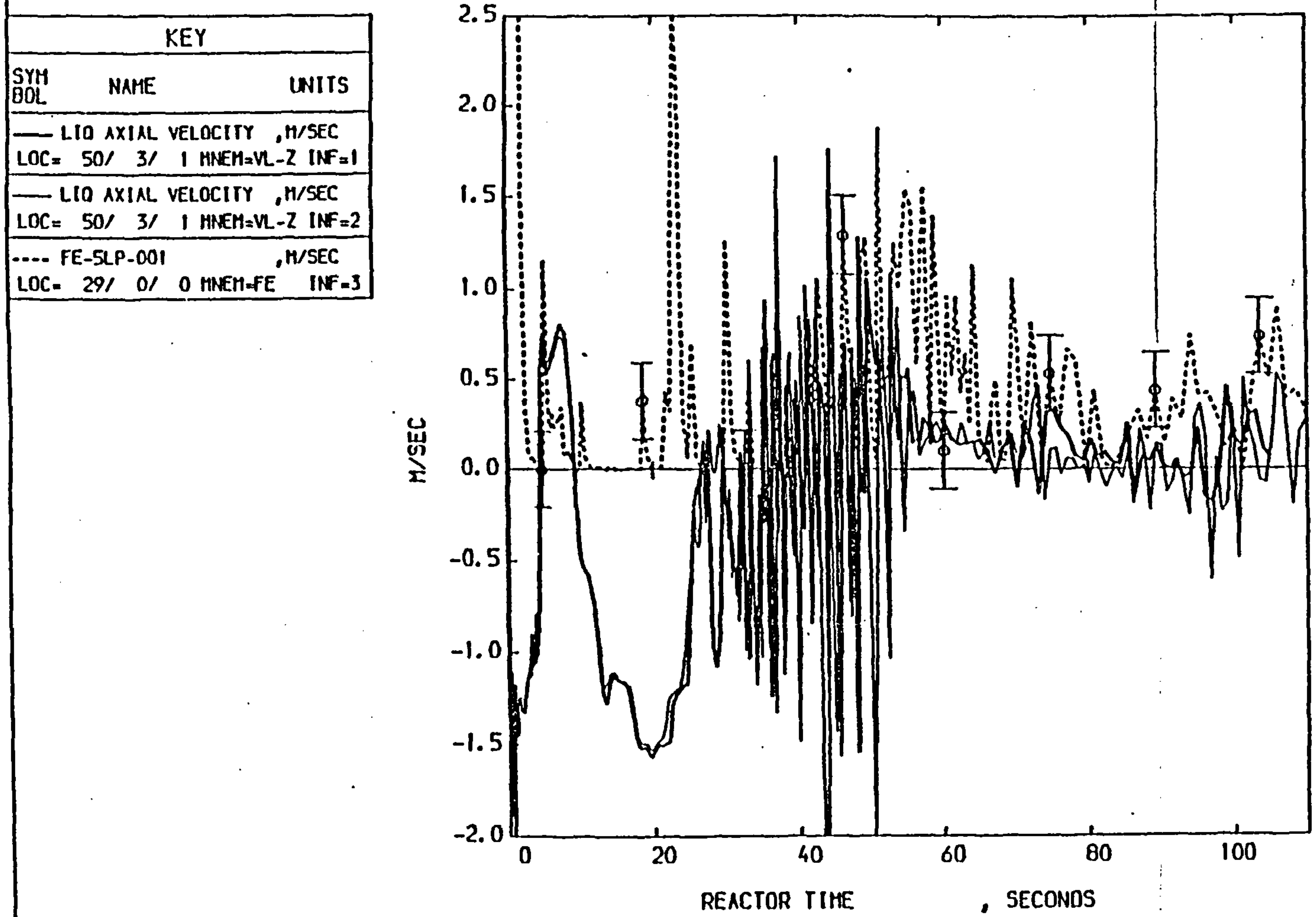

FIGURE 36 INF 1 JON'S, INF 2 ORIG, INF 3 EXP
LOWER PLENUM LIQUID AXIAL VELOCITY

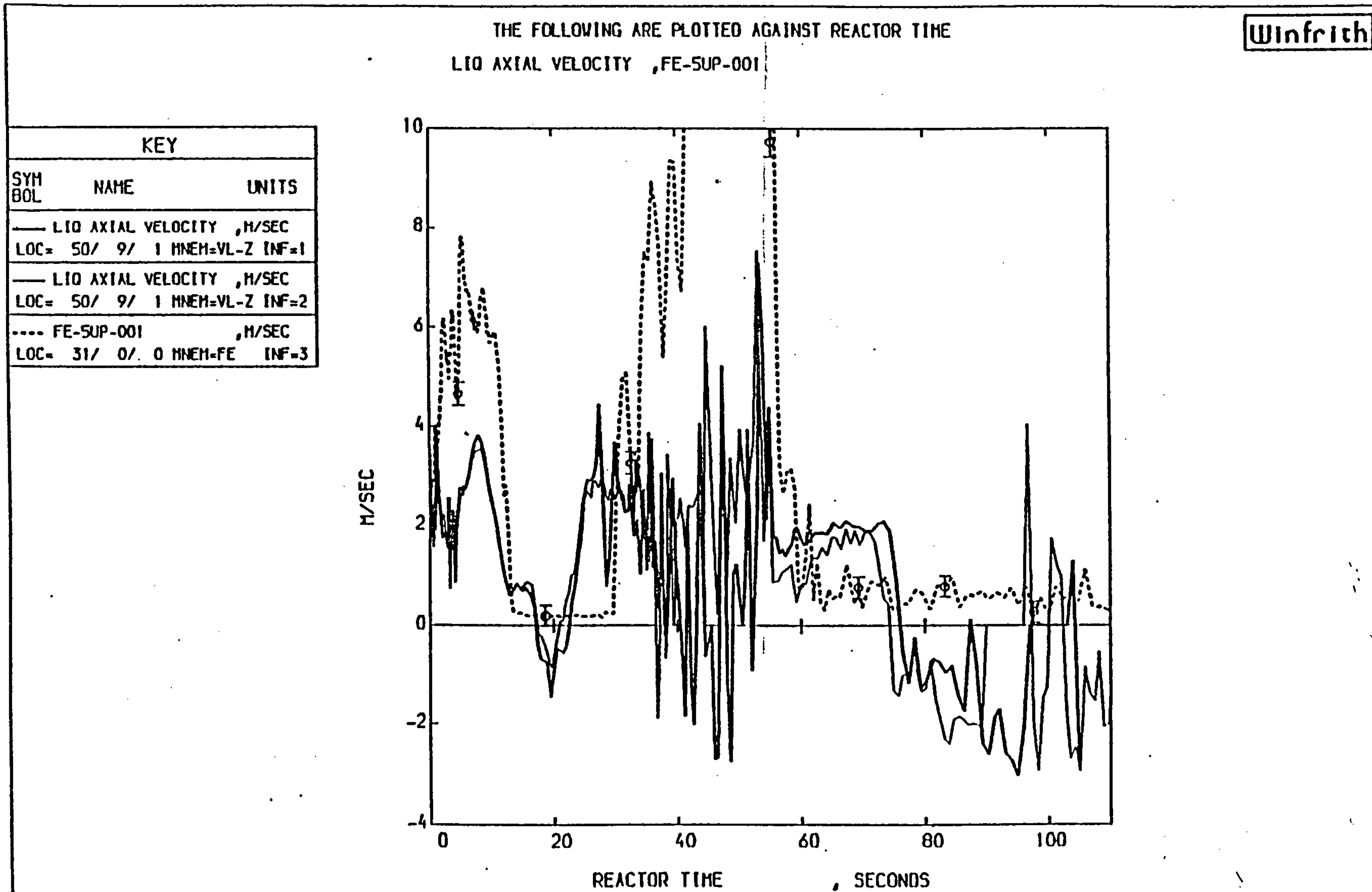

FIGURE 37 INF 1 JON'S, INF 2 ORIG, INF 3 EXP
UPPER PLENUM LIQUID AXIAL VELOCITY

THE FOLLOWING ARE PLOTTED AGAINST REACTOR TIME
LIQUID TEMPERATURE ,TE-1ST-001

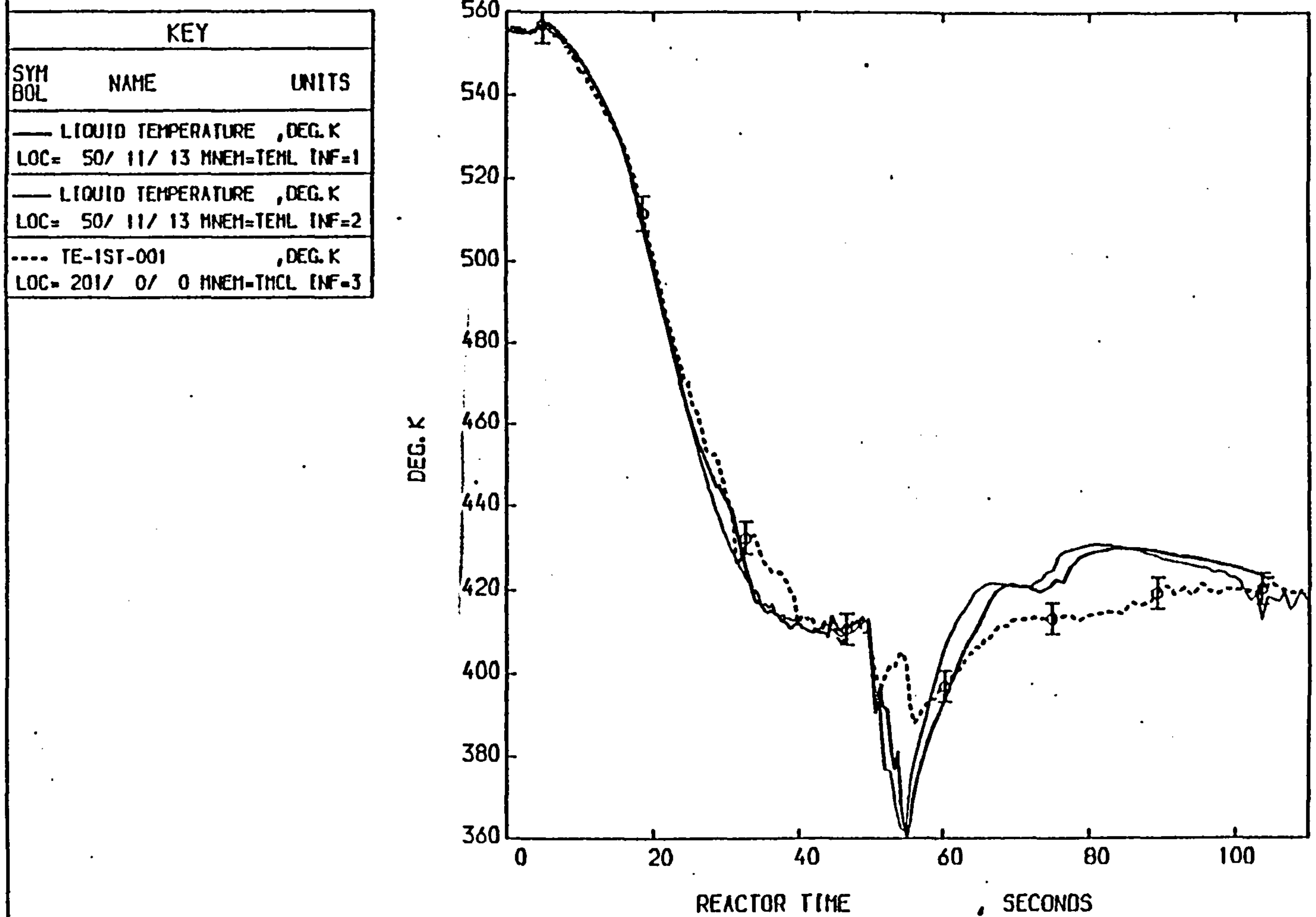

FIGURE 38 INF 1 JON'S, INF 2 ORIG, INF 3 EXP
DOWNCOMER LIQUID TEMPERATURE AT 5.0 METRES

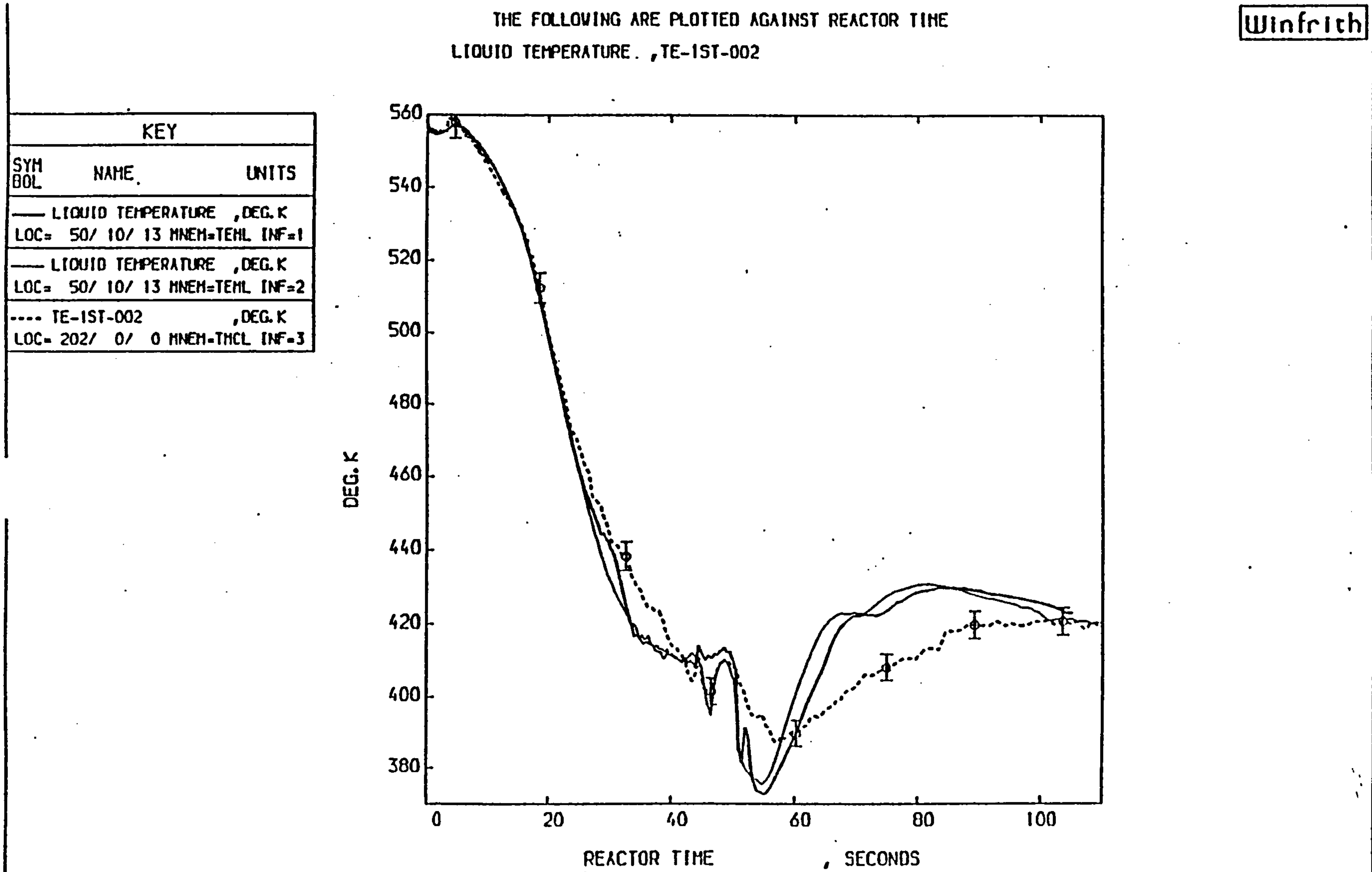

FIGURE 39 INF 1 JON'S, INF 2 ORIG, INF 3 EXP
DOWNCOMER LIQUID TEMPERATURE AT 4.2 METRES

THE FOLLOWING ARE PLOTTED AGAINST REACTOR TIME

LIQUID TEMPERATURE ,TE-1ST-005

Winfrith

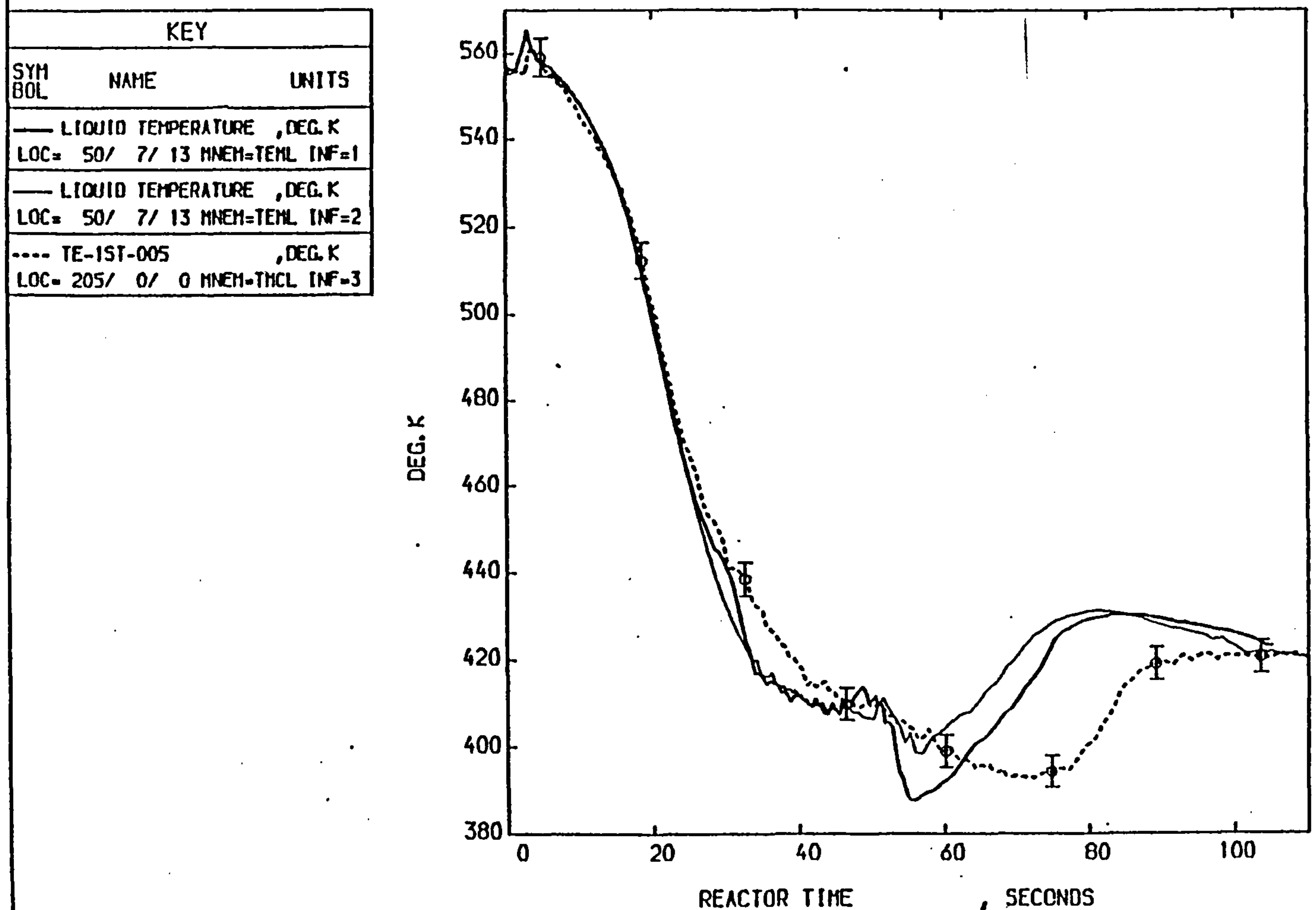

FIGURE 40 INF 1 JON'S, INF 2 ORIG, INF 3 EXP
DOWNCOMER LIQUID TEMPERATURE AT 2.4 METRES

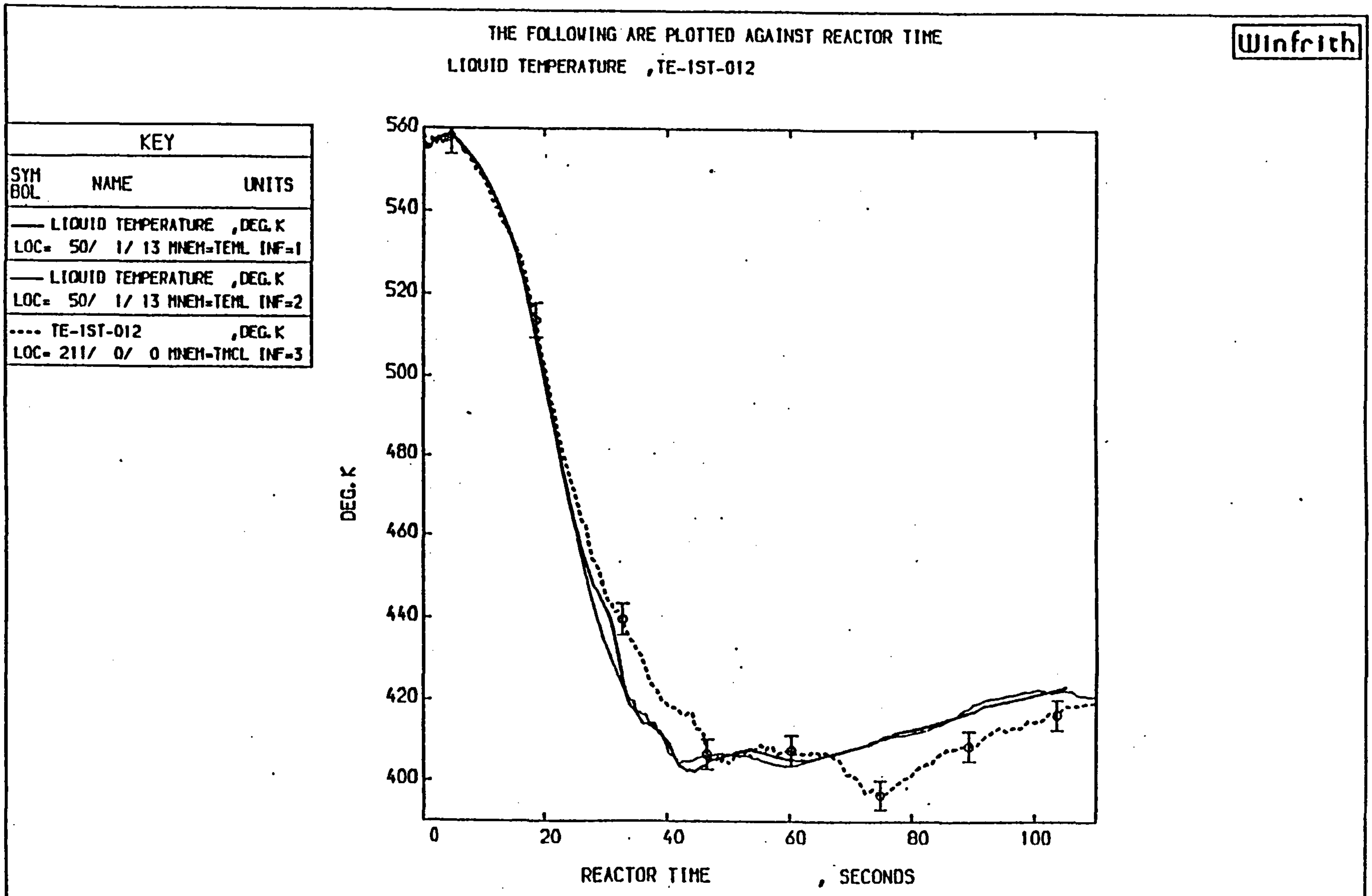

FIGURE 41 INF 1 JON'S, INF 2 ORIG, INF 3 EXP
DOWNCOMER LIQUID TEMPERATURE AT 0.3 METRES

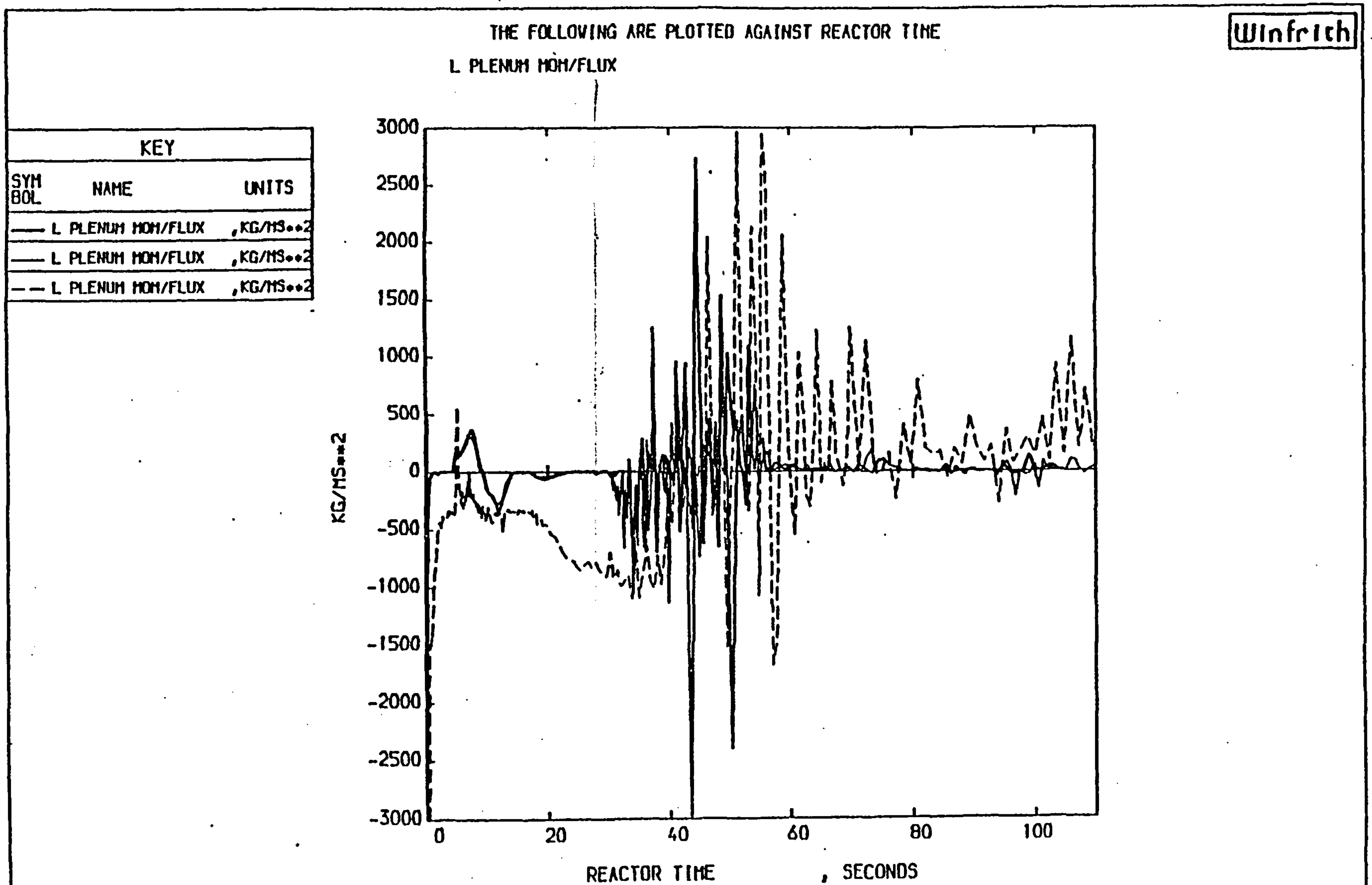

FIGURE 42 LINE 1 JON'S, LINE 2 ORIG, LINE 3 EXP
LOWER PLENUM MOMENTUM FLUX

THE FOLLOWING ARE PLOTTED AGAINST REACTOR TIME

CORE INLET MASS FLOW

Winfrith

KEY		
SYM BOL	NAME	UNITS
——	CORE INLET MASS FLOW,	KG/SEC
LOC= 50/ 0/ 1 MNEM=FLCI INF=1		
——	CORE INLET MASS FLOW,	KG/SEC
LOC= 50/ 0/ 1 MNEM=FLCI INF=2		

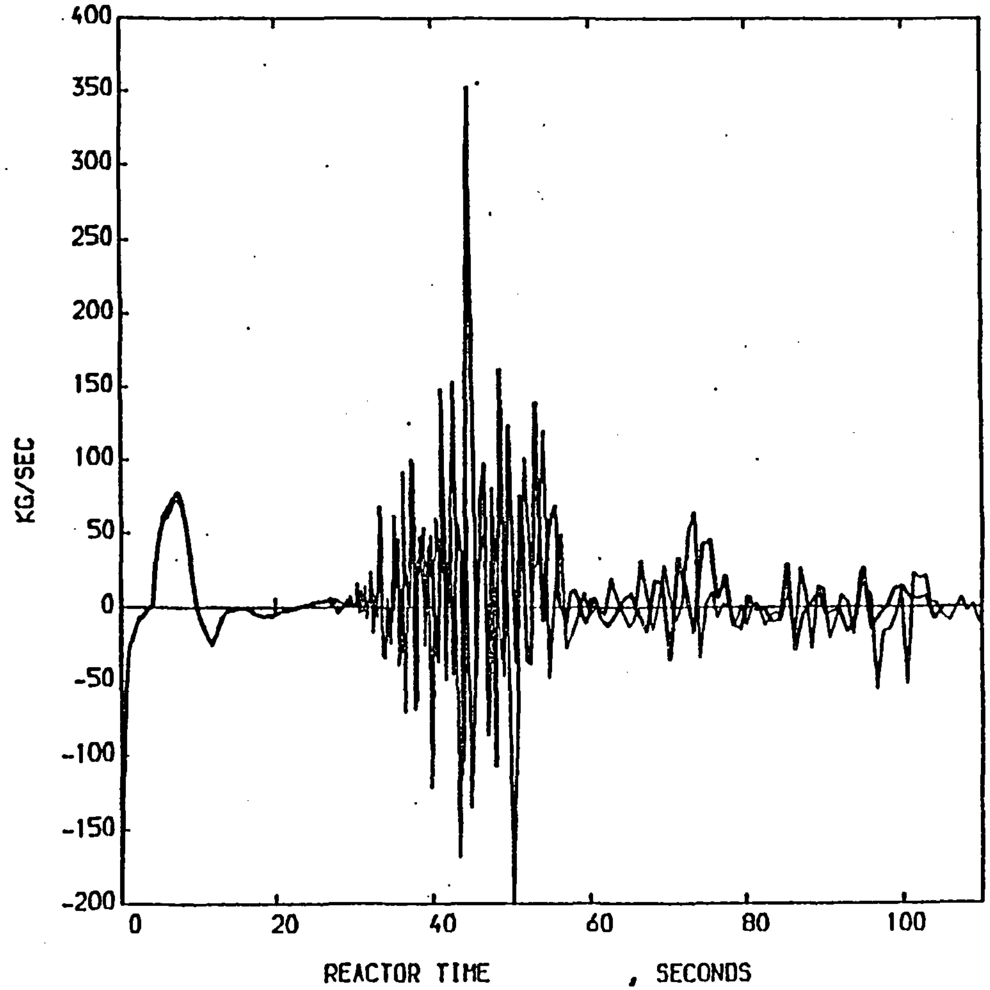

FIGURE 43 INF 1 JON'S, INF 2 ORIG
VESSEL GLOBALS

Winfrith

THE FOLLOWING ARE PLOTTED AGAINST REACTOR TIME

CORE OUTLET MASSFLOW

KEY		
SYMBOL	NAME	UNITS
——	CORE OUTLET MASSFLOW,	KG/SEC
	LOC= 50/ 0/ 1 MNEM=FLCO INF=1	
——	CORE OUTLET MASSFLOW,	KG/SEC
	LOC= 50/ 0/ 1 MNEM=FLCO INF=2	

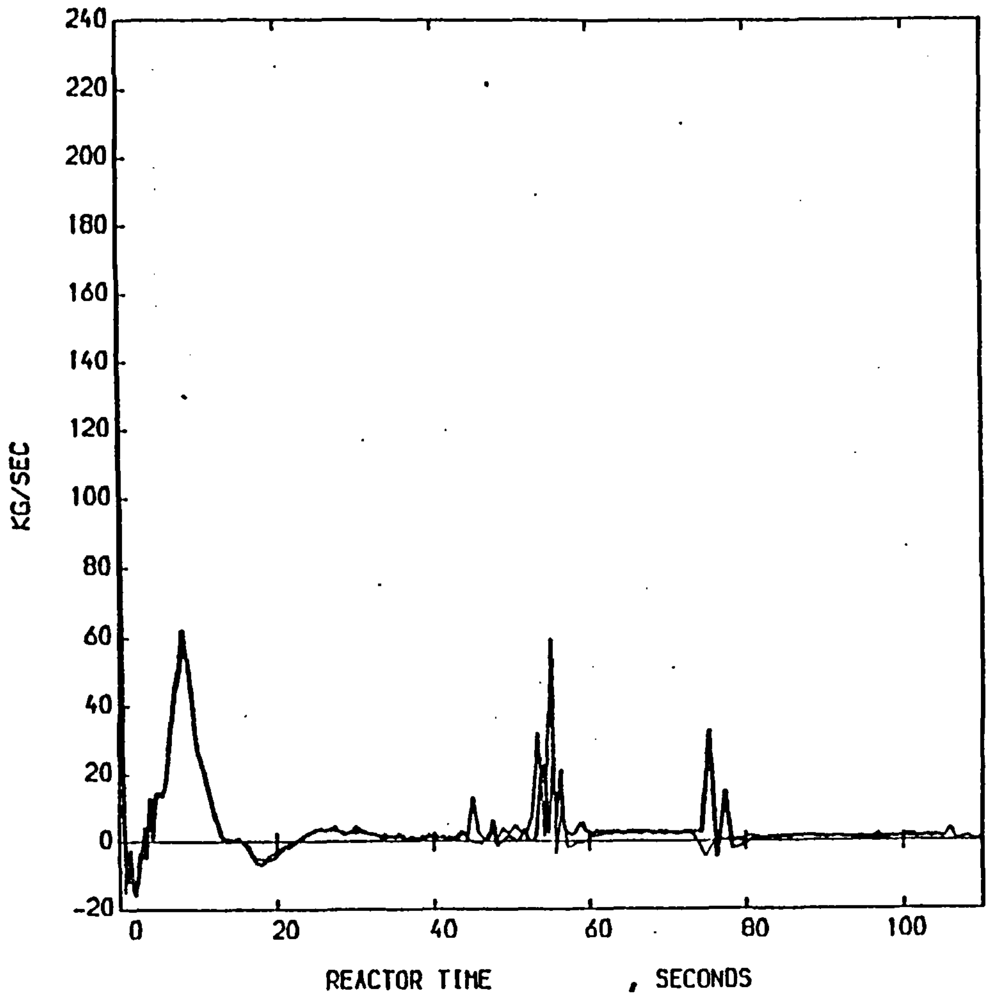

FIGURE 44 INF 1 JON'S, INF 2 ORIG
VESSEL GLOBALS

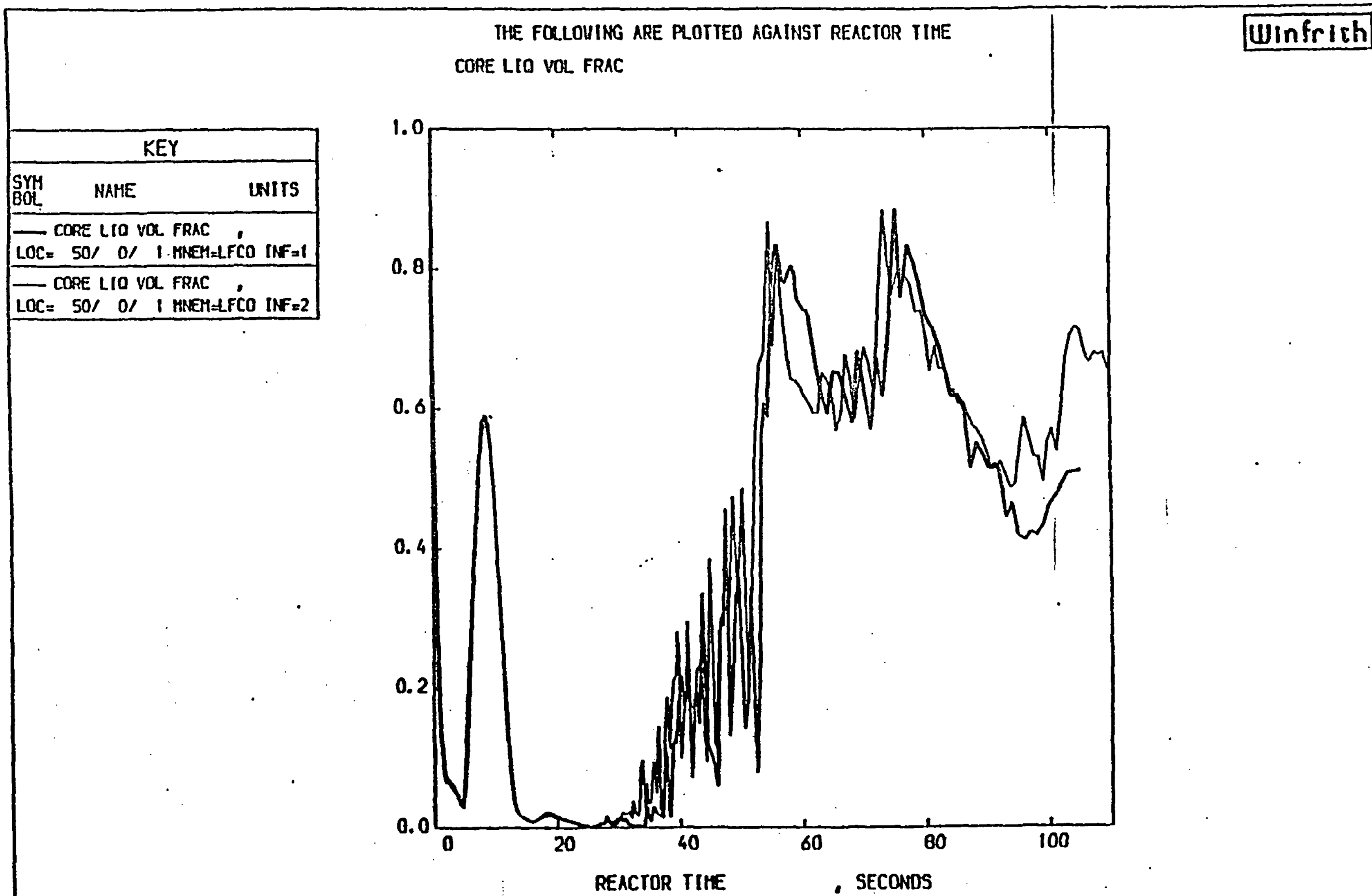

FIGURE 45 INF 1 JON'S, INF 2 ORIG
VESSEL GLOBALS

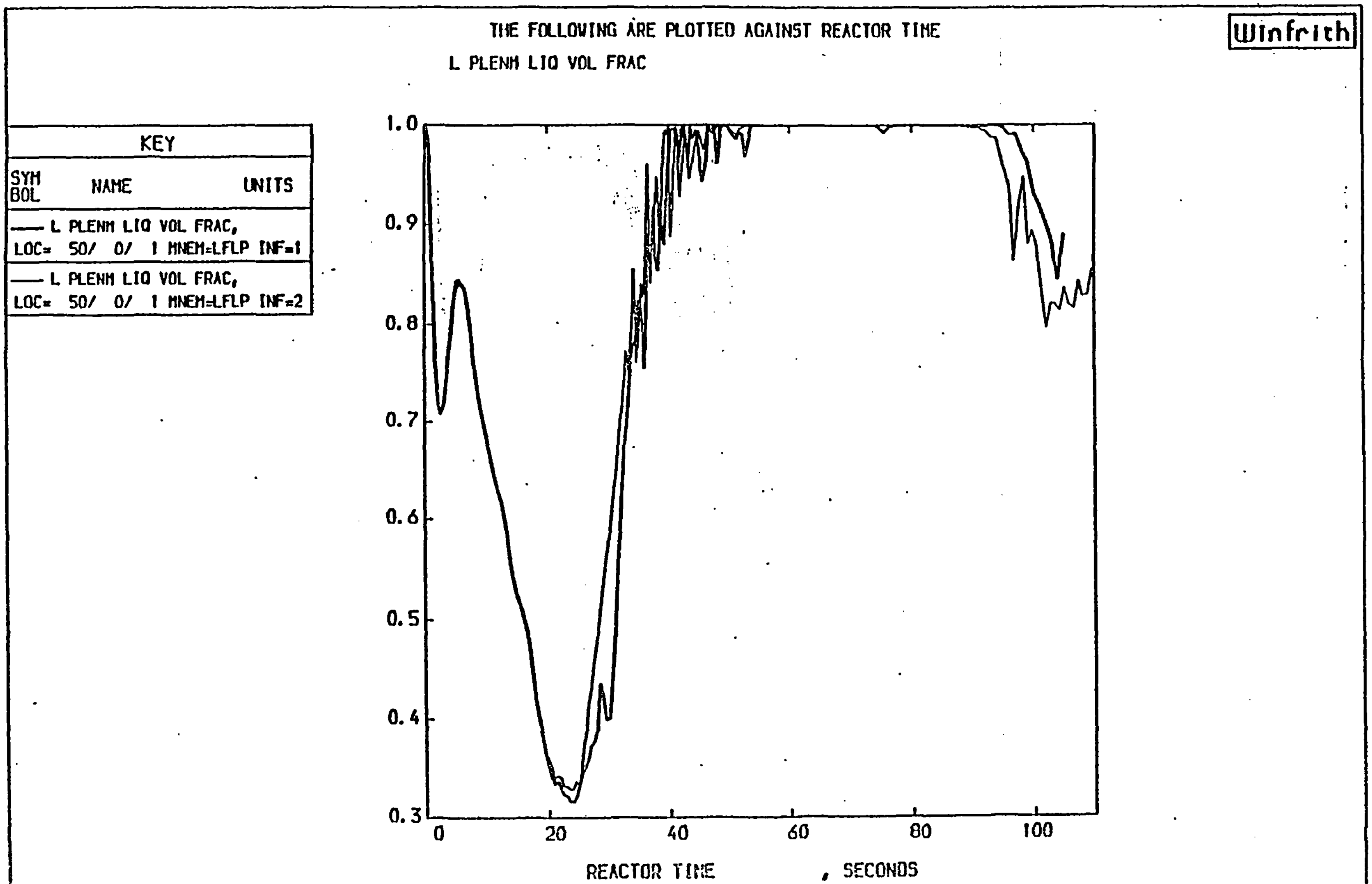

FIGURE 46 INF 1 JON'S, INF 2 ORIG
VESSEL GLOBALS

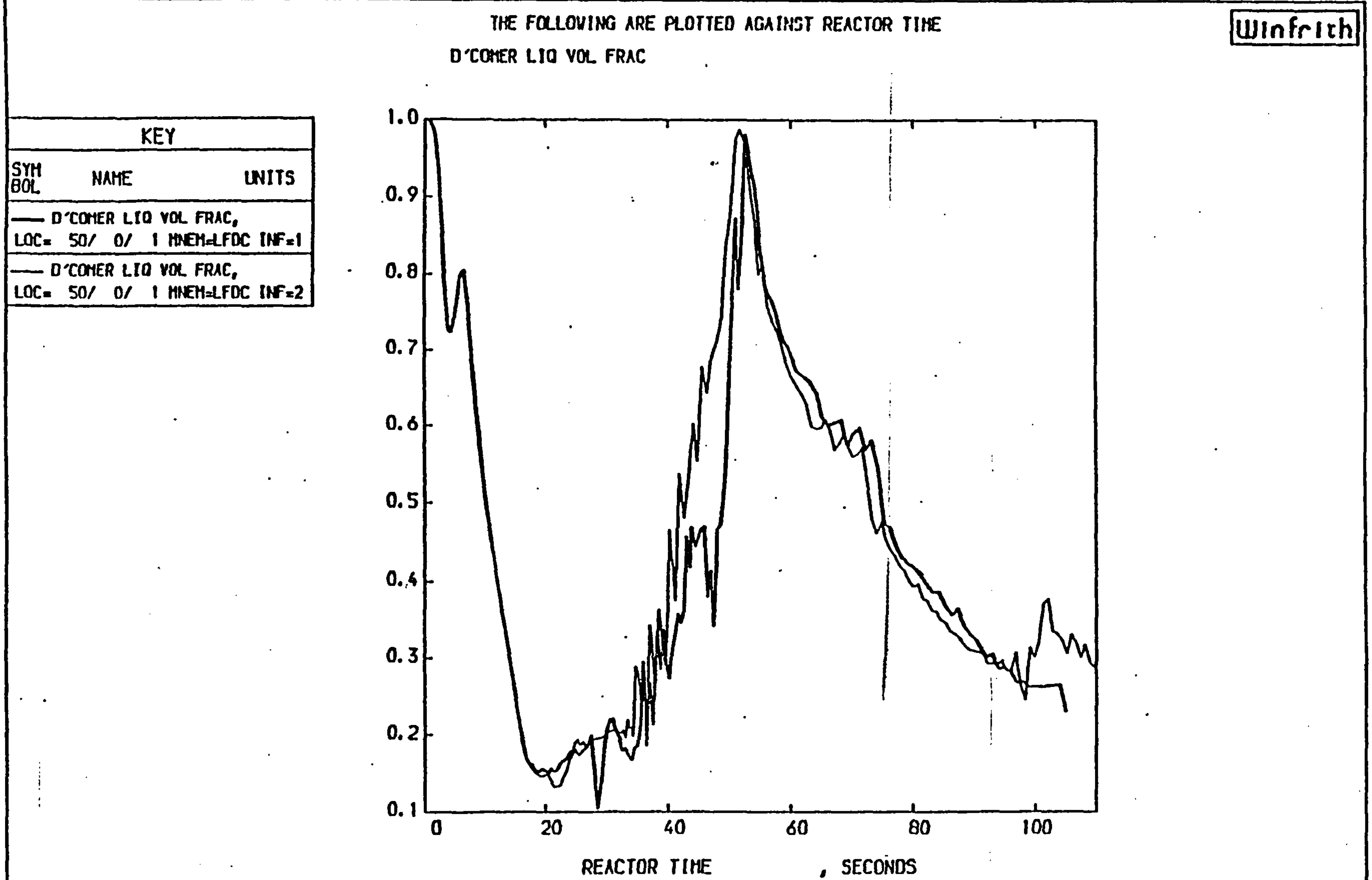

FIGURE 47 INF 1 JON'S, INF 2 ORIG
VESSEL GLOBALS

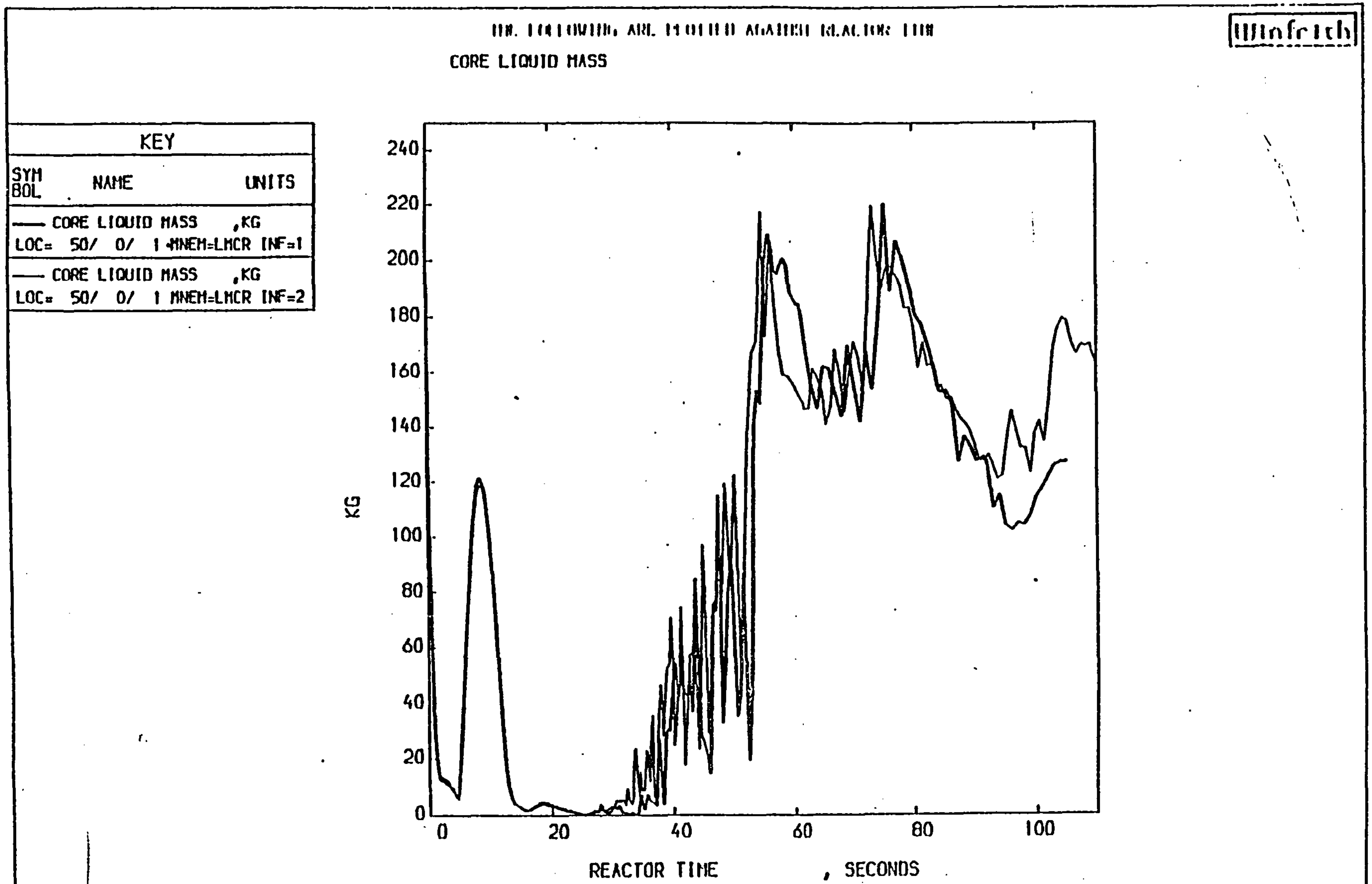

FIGURE 48 INF 1 JON'S, INF 2 ORIG
VESSEL GLOBALS

Winfrith

THE FOLLOWING ARE PLOTTED AGAINST REACTOR TIME

VESSEL LIQUID MASS

KEY		
SYM BOL	NAME	UNITS
——	VESSEL LIQUID MASS	,KG
LOC= 50/ 0/ 1 MNEM=LMVS INF=1		
——	VESSEL LIQUID MASS	,KG
LOC= 50/ 0/ 1 MNEM=LMVS INF=2		

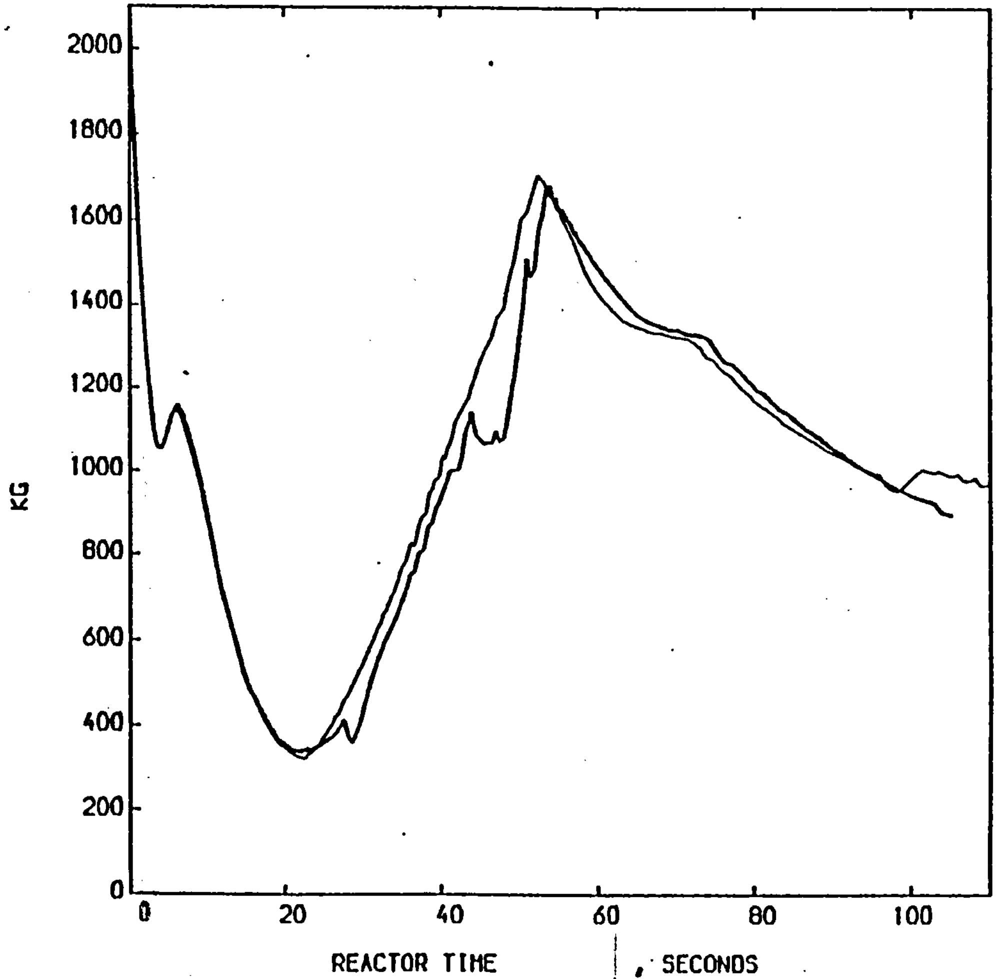

FIGURE 49 INF 1 JON'S, INF 2 ORIG
VESSEL GLOBALS

THE FOLLOWING ARE PLOTTED AGAINST REACTOR TIME

TOT ROD HEAT FLUX

Winfrith

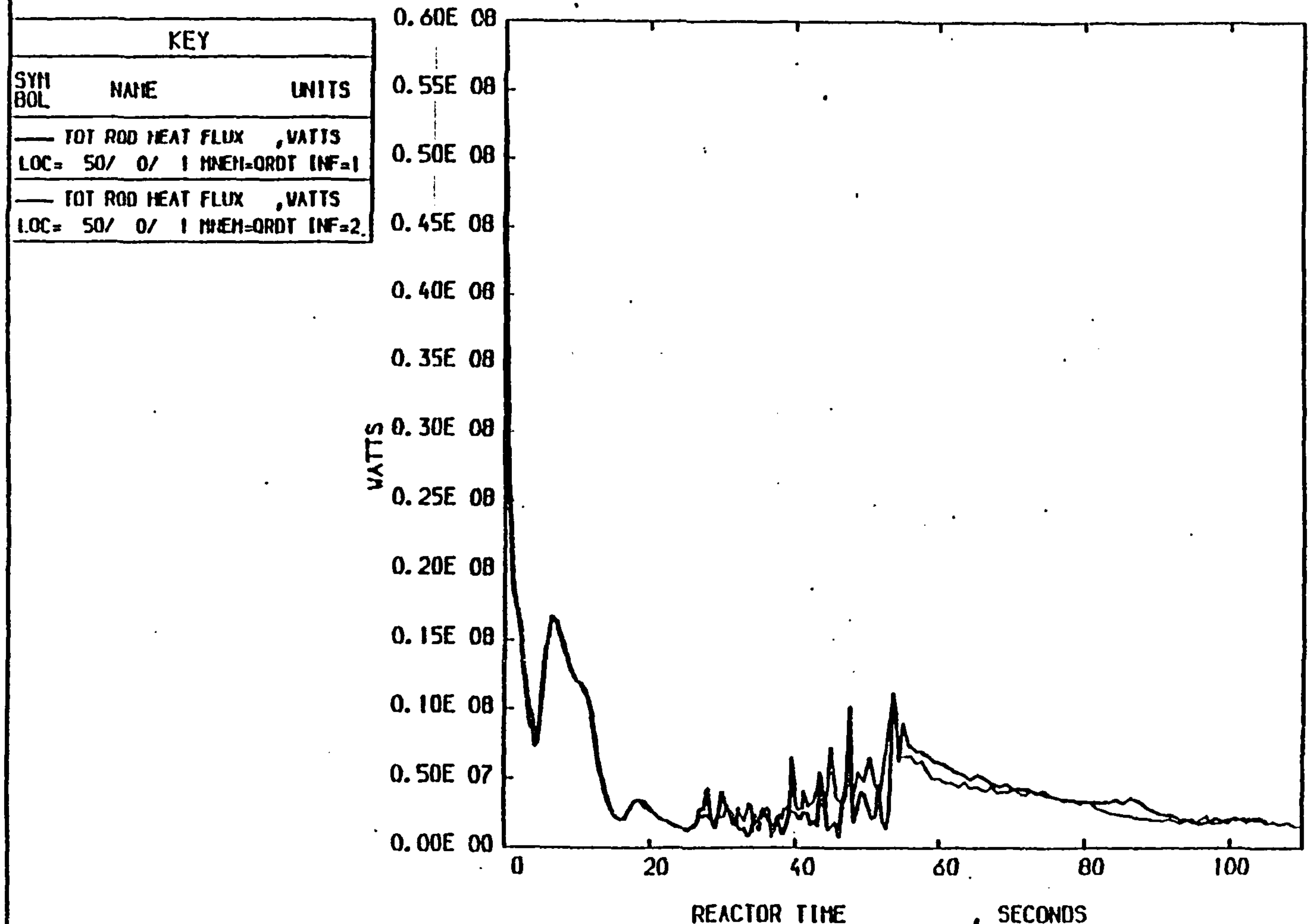

FIGURE 50 INF 1 JON'S, INF 2 ORIG
VESSEL GLOBALS

THE FOLLOWING ARE PLOTTED AGAINST REACTOR TIME

TOT SLAB HEAT FLUX

Winfrith

KEY		
SYM BOL	NAME	UNITS
——	TOT SLAB HEAT FLUX	,WATTS
	LOC= 50/ 0/ 1 MNEM=QSLT INF=1	
——	TOT SLAB HEAT FLUX	,WATTS
	LOC= 50/ 0/ 1 MNEM=QSLT INF=2	

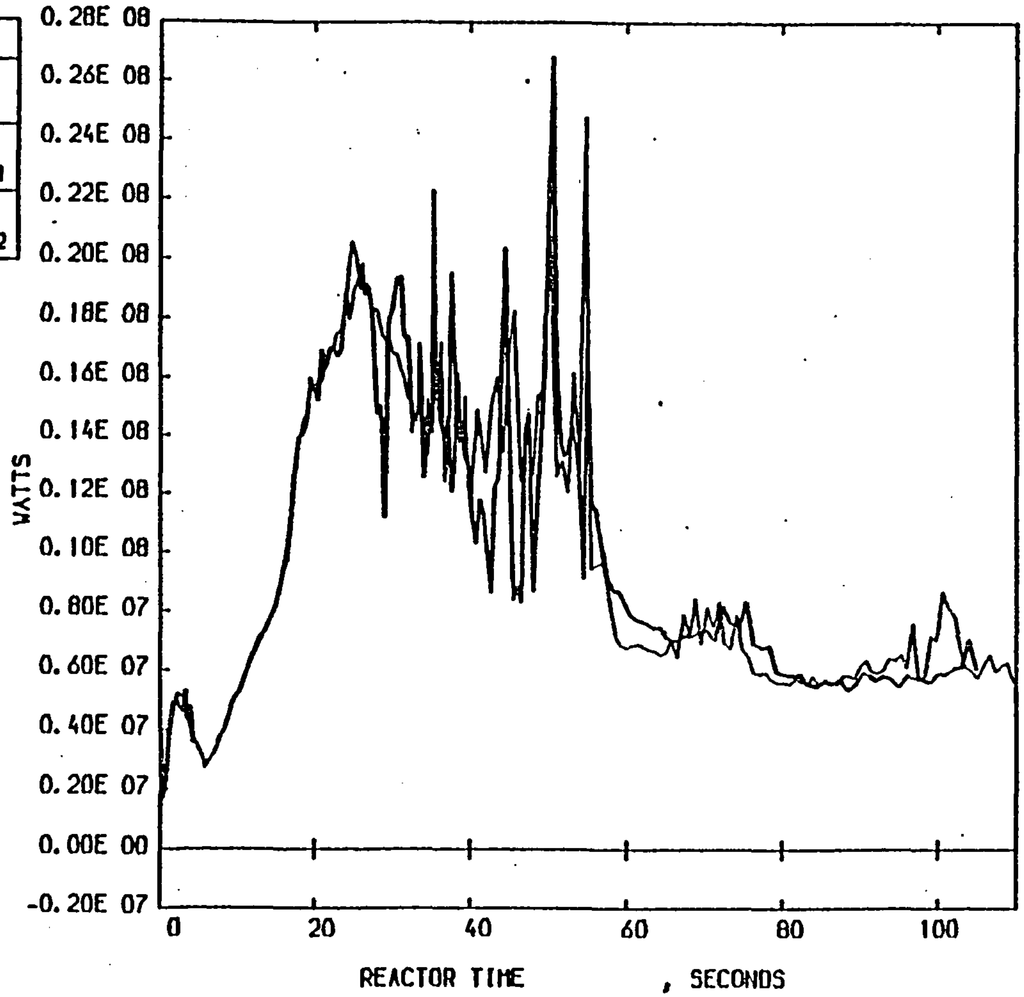

FIGURE 51 INF 1 JON'S, INF 2 ORIG
VESSEL GLOBALS

Winfrith

THE FOLLOWING ARE PLOTTED AGAINST REACTOR TIME

L PLENUM AVG LIQ TEM

KEY		
SYM BOL	NAME	UNITS
—·—	L PLENUM AVG LIQ TEM,	DEG.K
LOC= 50/ 0/ 1	MNEM=THLP	INF=1
——	L PLENUM AVG LIQ TEM,	DEG.K
LOC= 50/ 0/ 1	MNEM=THLP	INF=2

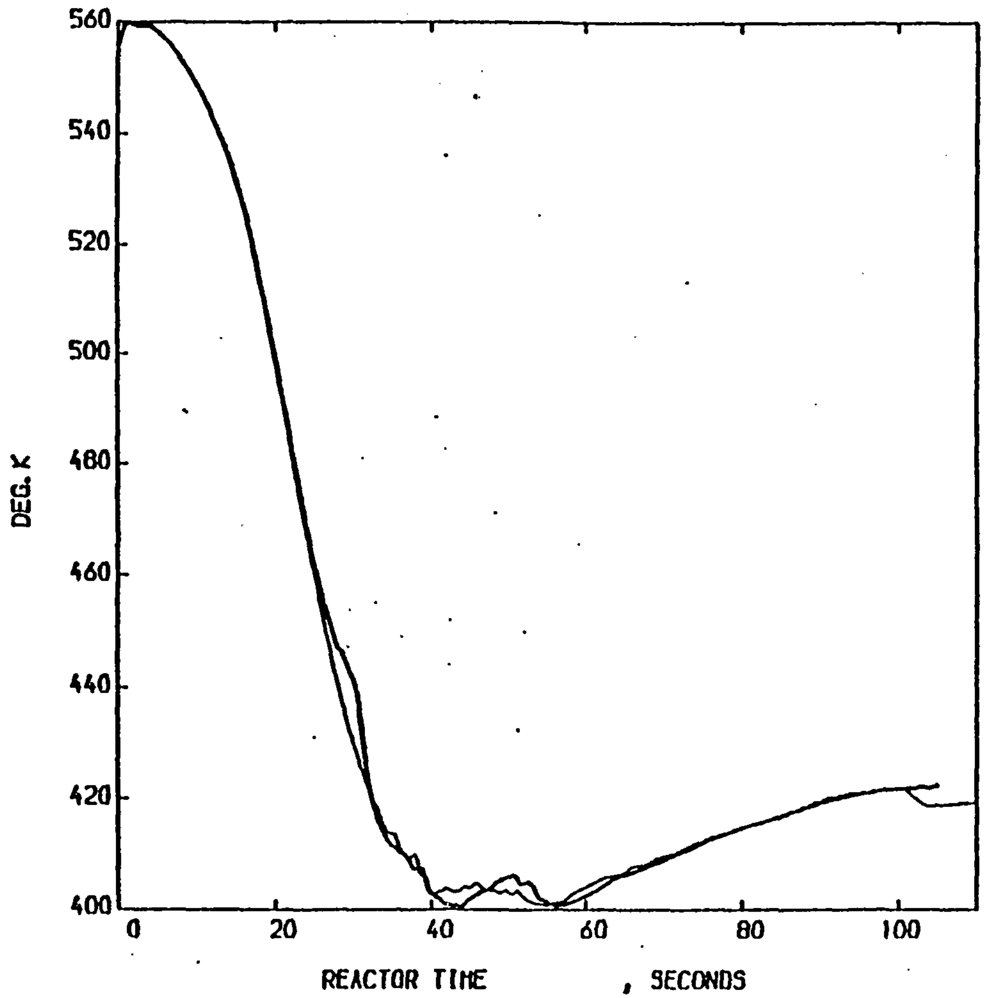

FIGURE 52 INF 1 JON'S, INF 2 ORIG
VESSEL GLOBALS

THE FOLLOWING ARE PLOTTED AGAINST REACTOR TIME

CLADDING TEMP -FINE,TE-5H05-002

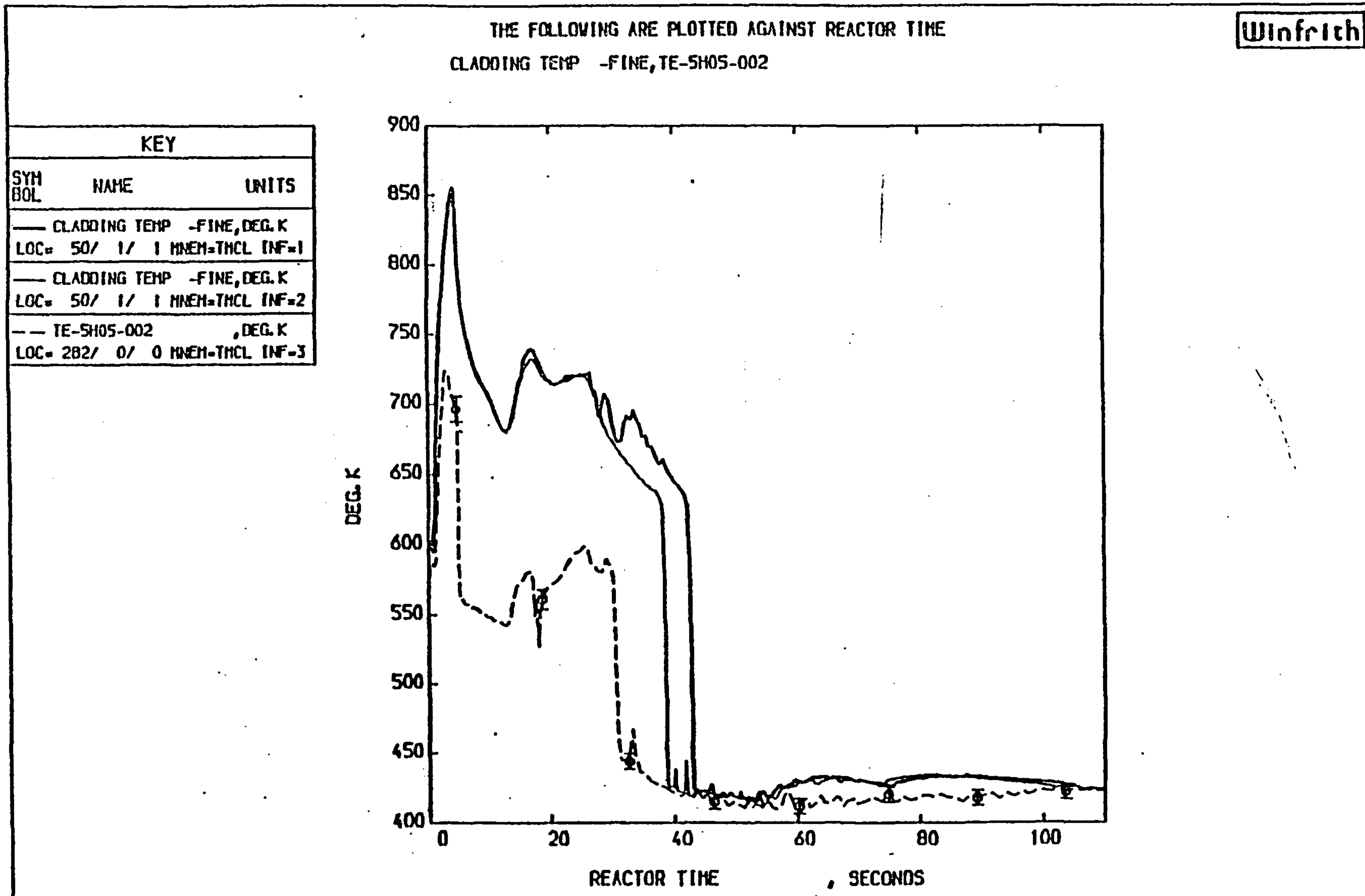

FIGURE 53 INF 1 JON'S, INF 2 ORIG, INF 3 EXP
CENTRAL FUEL BUNDLE CLADDING TEMPERATURES

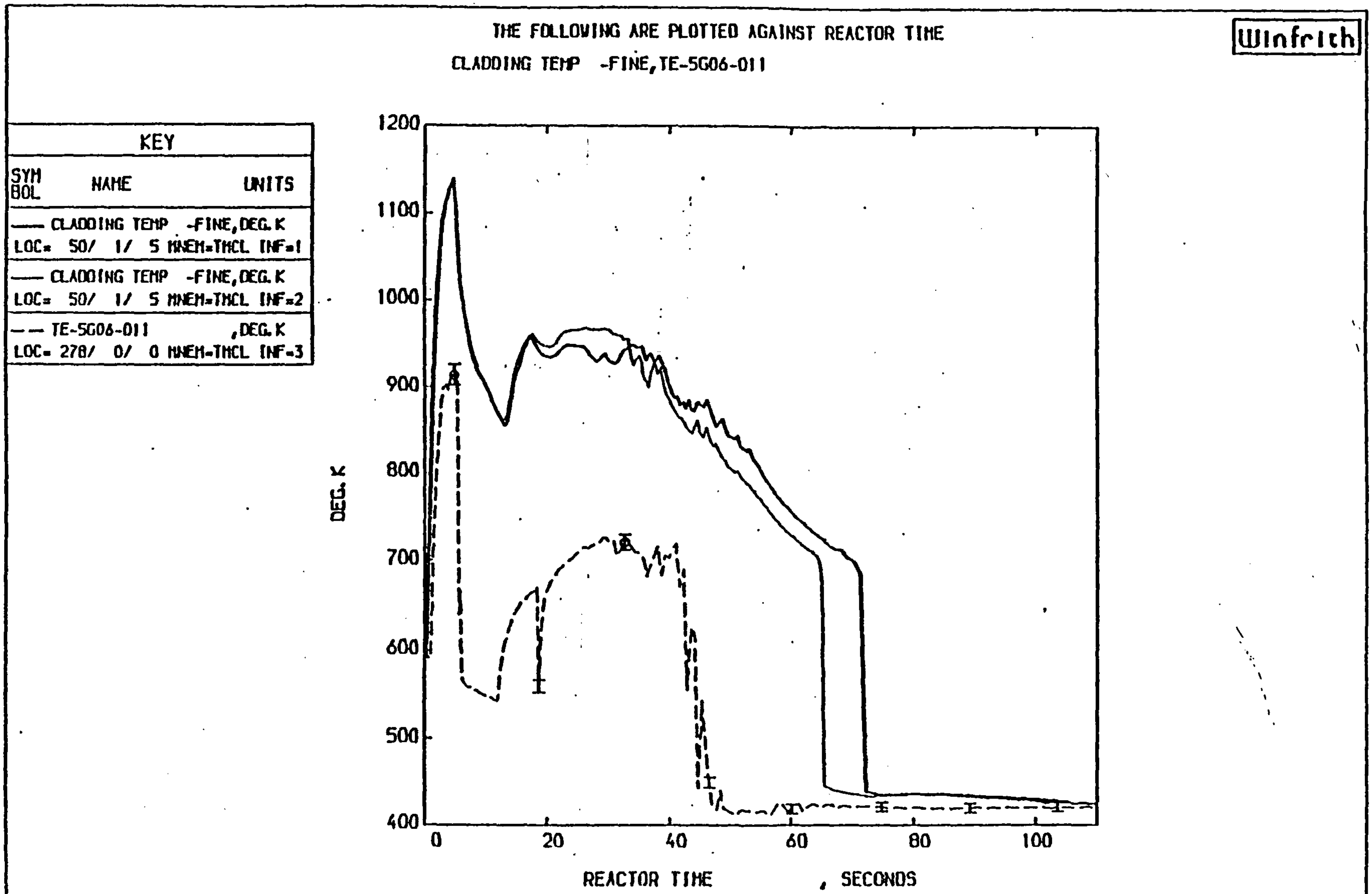

FIGURE 54 INF 1 JON'S, INF 2 ORIG, INF 3 EXP
CENTRAL FUEL BUNDLE CLADDING TEMPERATURES

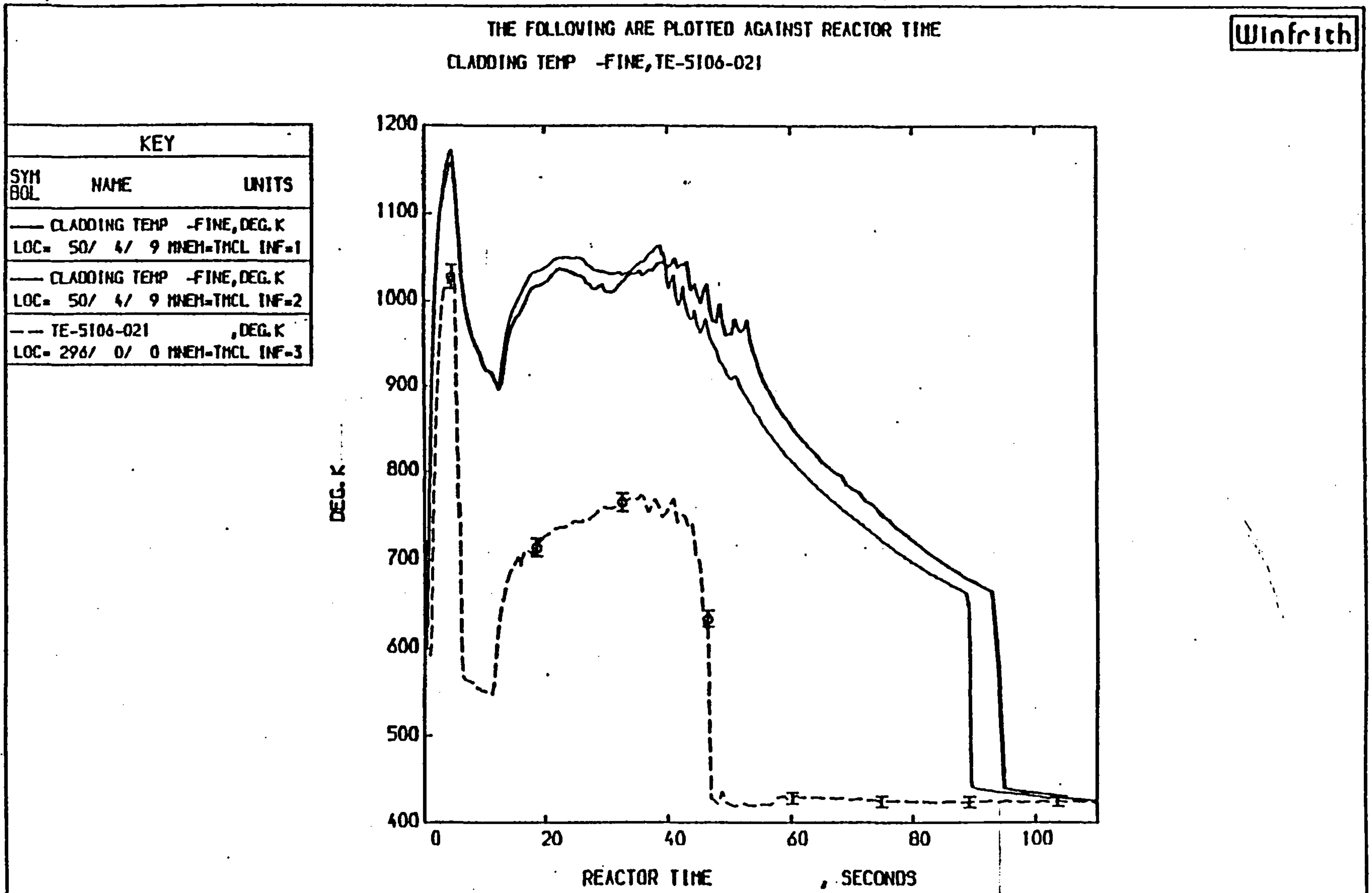

FIGURE 55 INF 1 JON'S, INF 2 ORIG, INF 3 EXP
CENTRAL FUEL BUNDLE CLADDING TEMPERATURES

Winfrith

THE FOLLOWING ARE PLOTTED AGAINST REACTOR TIME

CLADDING TEMP -FINE,TE-5H06-024

KEY		
SYMBOL	NAME	UNITS
——	CLADDING TEMP -FINE, LOC= 50/ 1/ 10 MNEM=TMCL INF=1	DEG.K
——	CLADDING TEMP -FINE, LOC= 50/ 1/ 10 MNEM=TMCL INF=2	DEG.K
– –	TE-5H06-024, LOC= 285/ 0/ 0 MNEM=TMCL INF=3	DEG.K

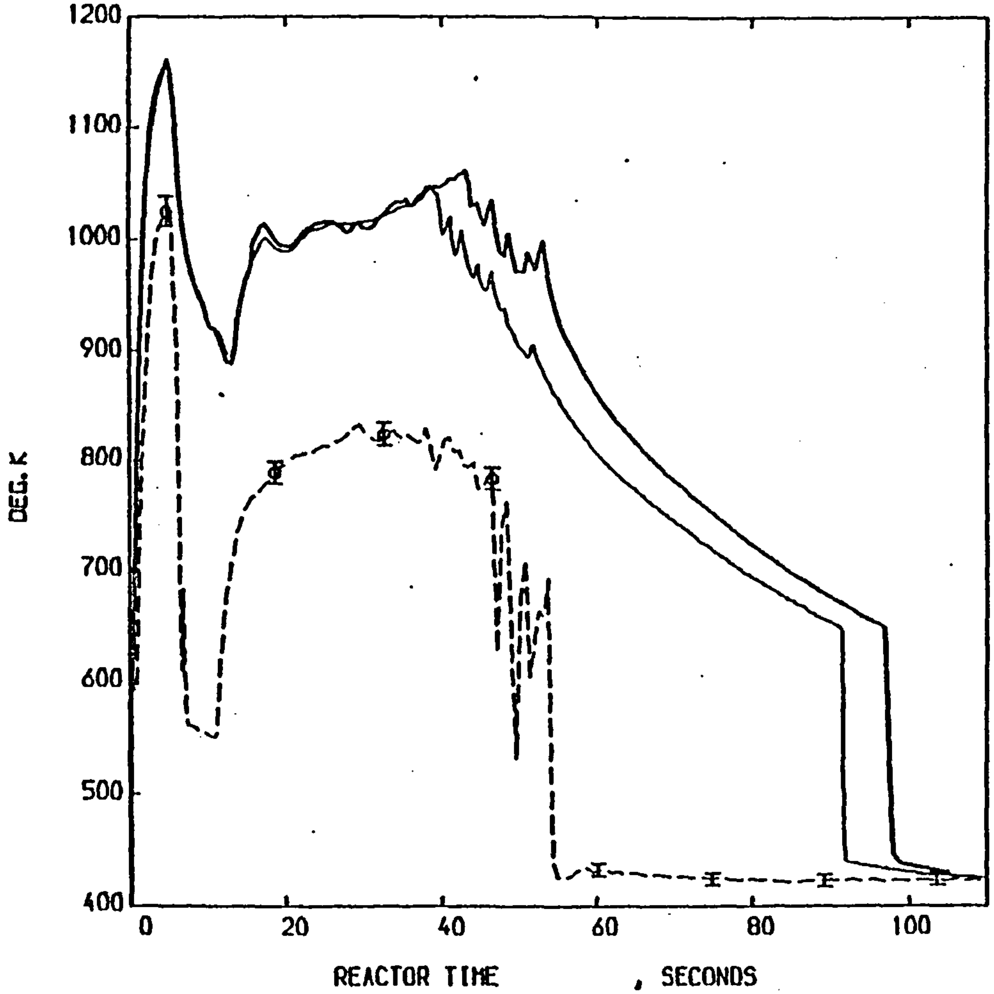

FIGURE 56 INF 1 JON'S, INF 2 ORIG, INF 3 EXP
CENTRAL FUEL BUNDLE CLADDING TEMPERATURES

THE FOLLOWING ARE PLOTTED AGAINST REACTOR TIME

CLADDING TEMP -FINE,TE-5104-027

Winfrith

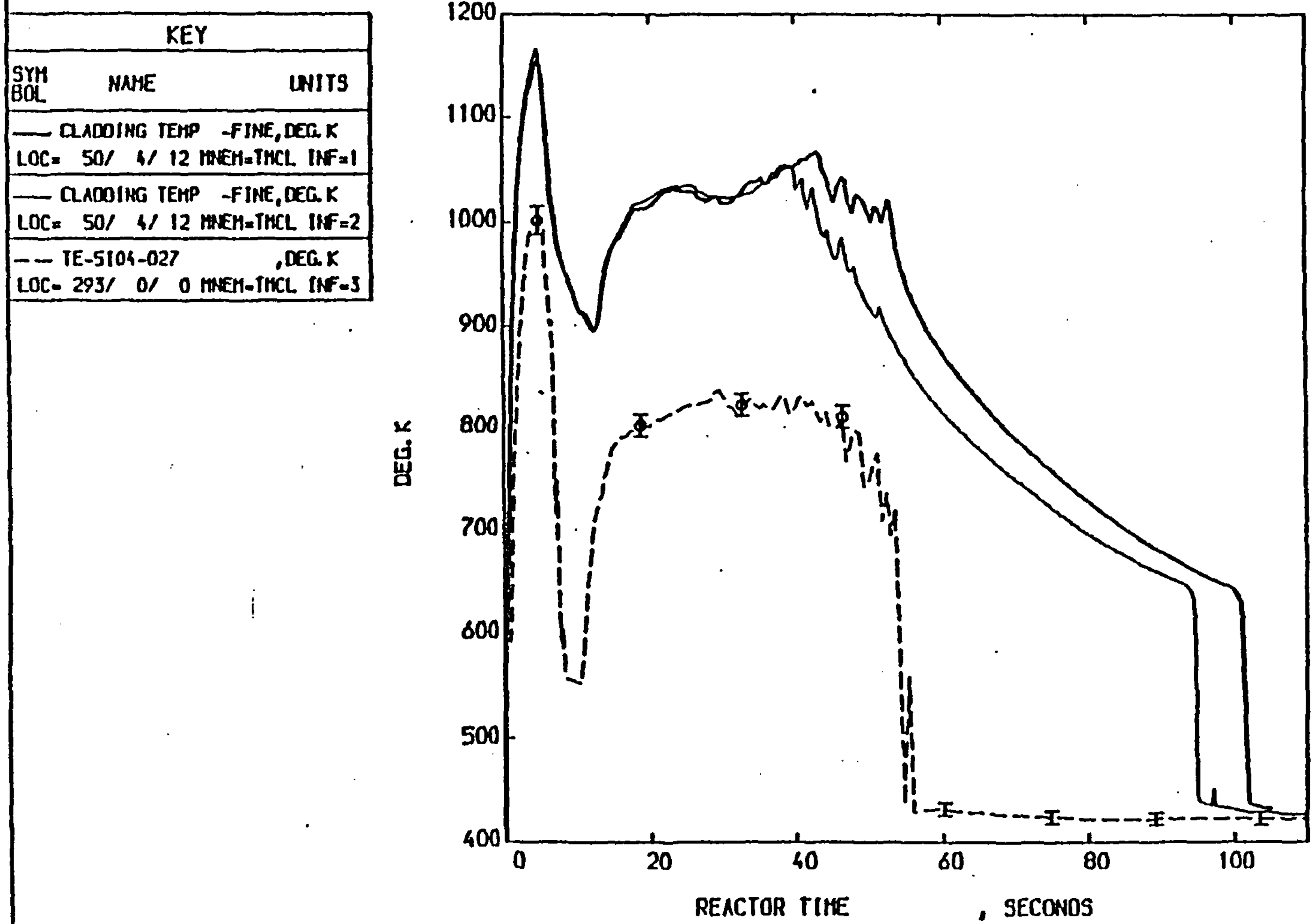

FIGURE 57 INF 1 JON'S, INF 2 ORIG, INF 3 EXP
CENTRAL FUEL BUNDLE CLADDING TEMPERATURES

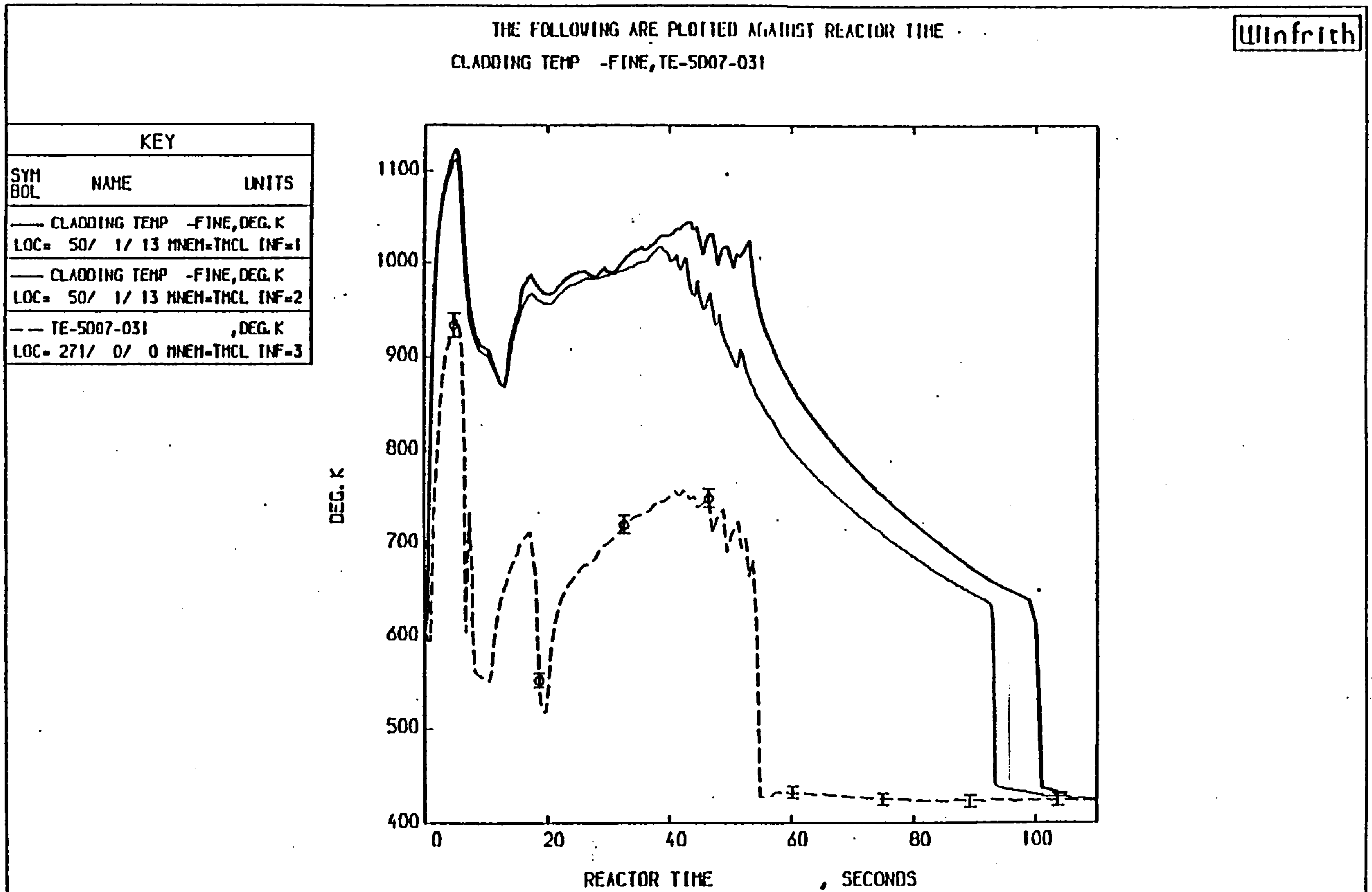

FIGURE 58 INF 1 JON'S, INF 2 ORIG, INF 3 EXP
CENTRAL FUEL BUNDLE CLADDING TEMPERATURES

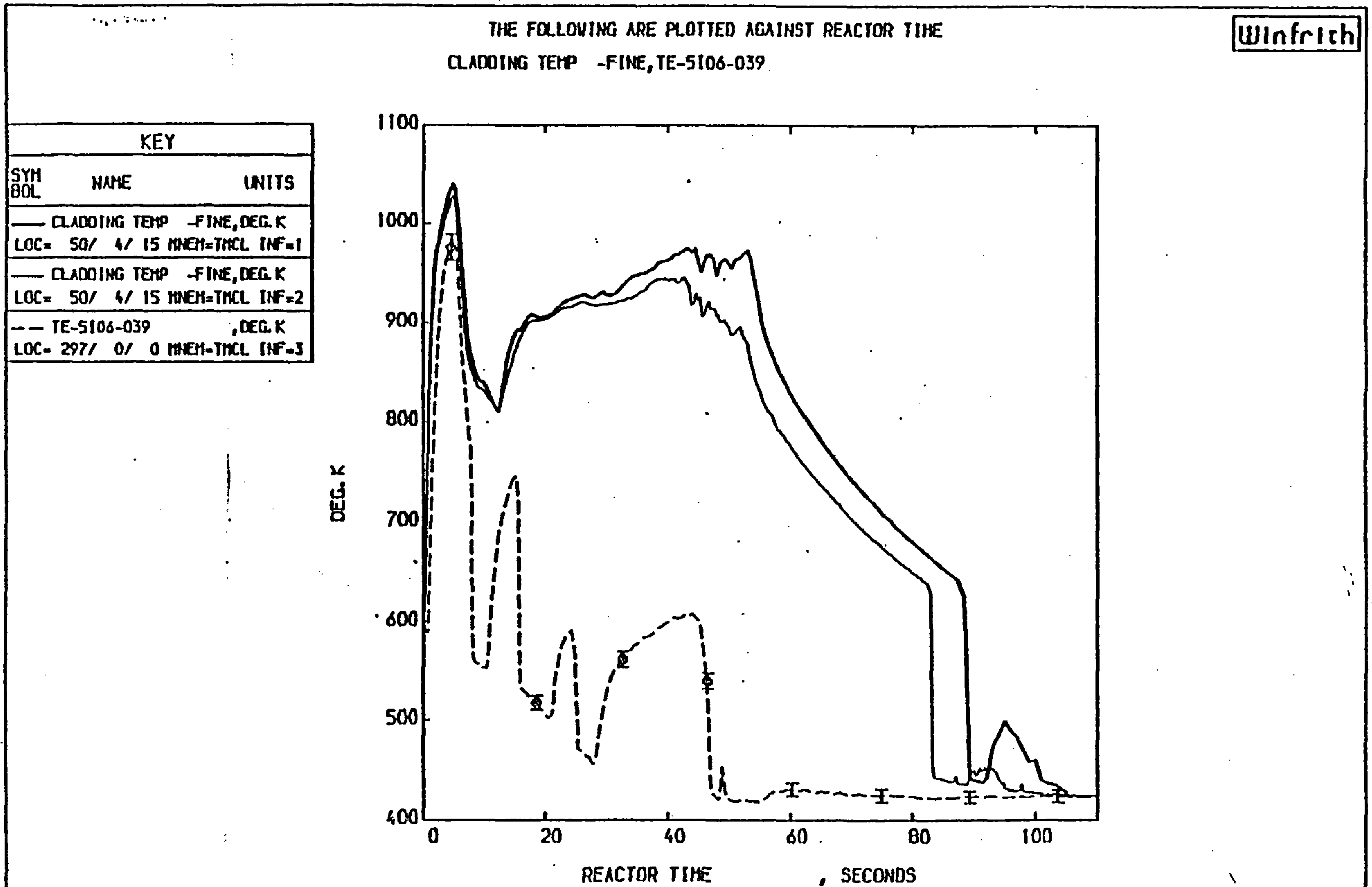

FIGURE 59 INF 1 JON'S, INF 2 ORIG, INF 3 EXP
CENTRAL FUEL BUNDLE CLADDING TEMPERATURES

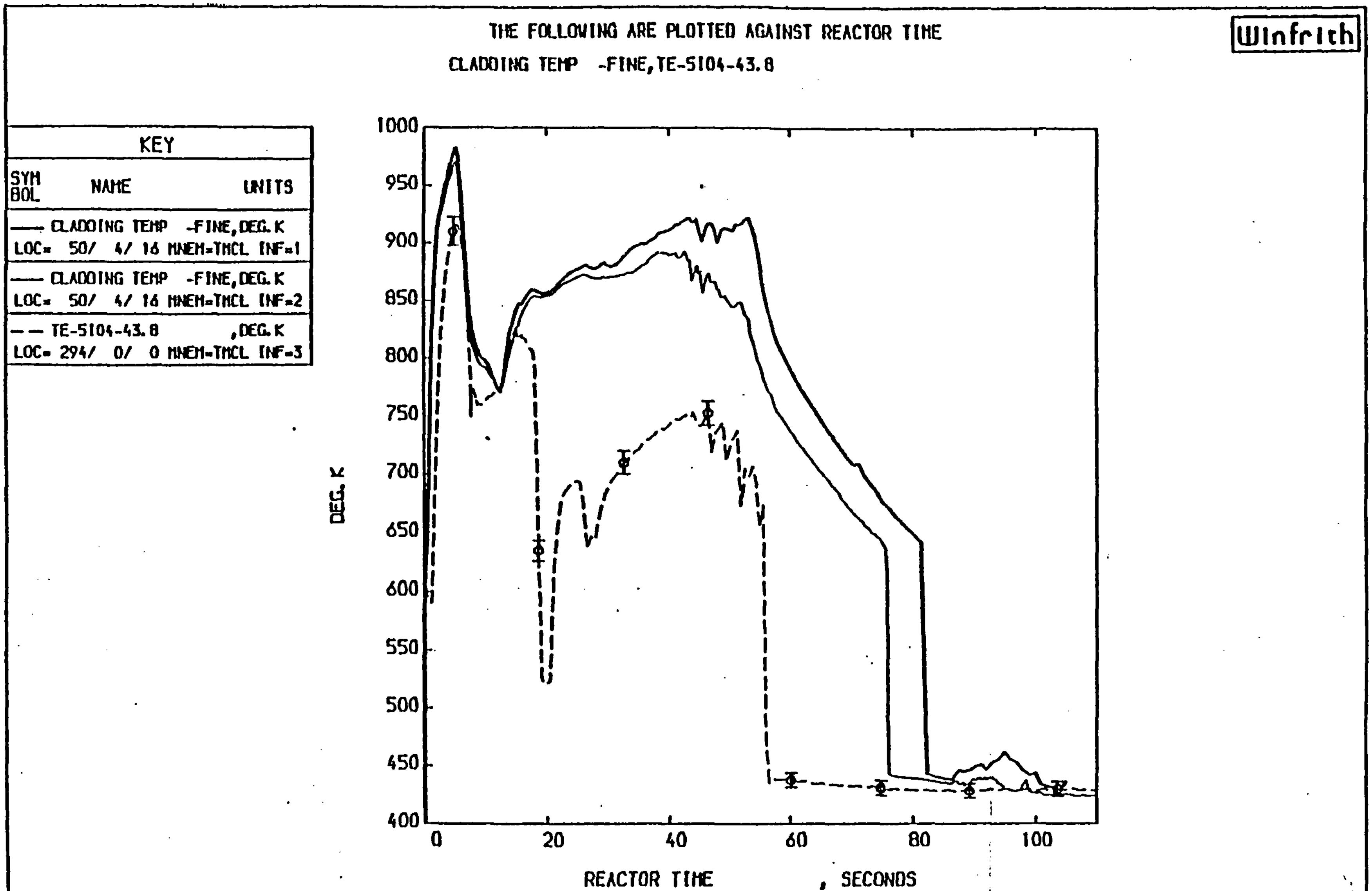

FIGURE 60 INF 1 JON'S, INF 2 ORIG, INF 3 EXP
CENTRAL FUEL BUNDLE CLADDING TEMPERATURES

THE FOLLOWING ARE PLOTTED AGAINST REACTOR TIME

CLADDING TEMP -FINE,TE-5H05-049

Winfrith

KEY		
SYMBOL	NAME	UNITS
——	CLADDING TEMP -FINE,	DEG.K
LOC= 50/ 1/ 17 MNEM=TMCL INF=1		
——	CLADDING TEMP -FINE,	DEG.K
LOC= 50/ 1/ 17 MNEM=TMCL INF=2		
– –	TE-5H05-049	,DEG.K
LOC= 284/ 0/ 0 MNEM=TMCL INF=3		

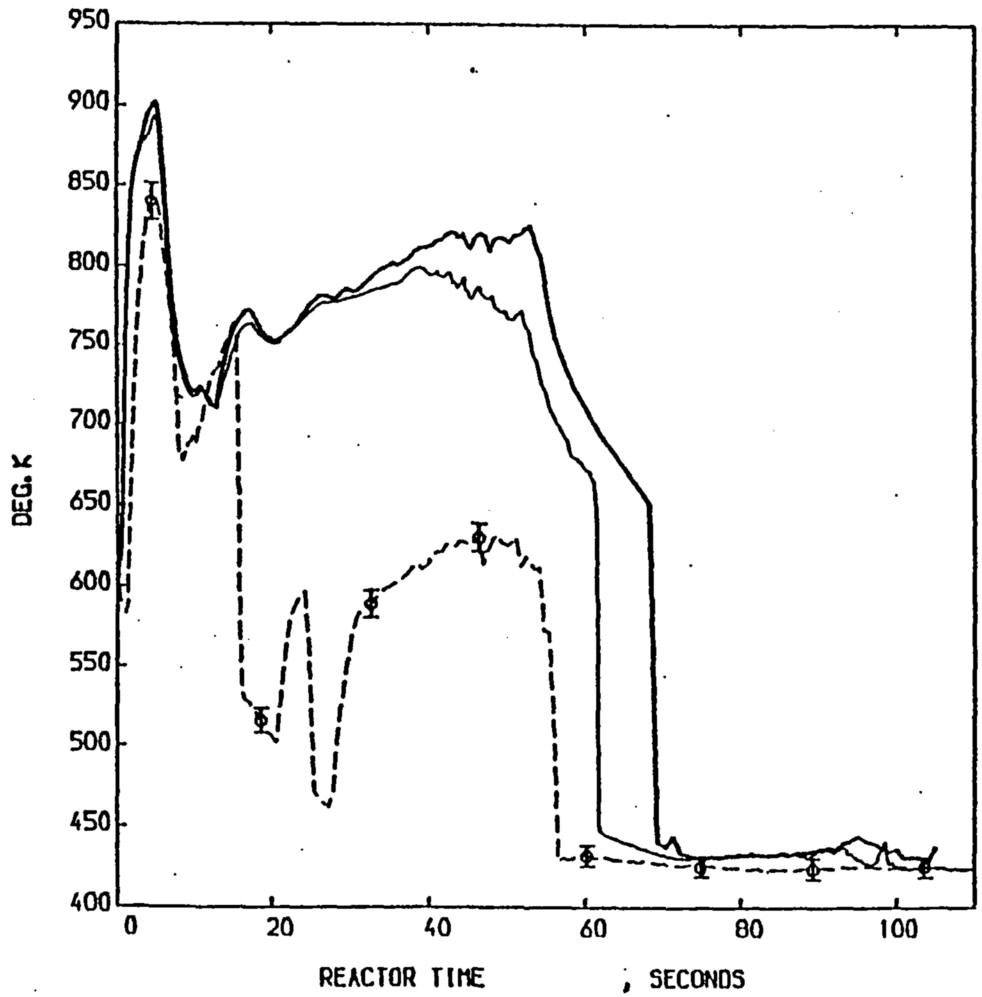

FIGURE 61 INF 1 JON'S, INF 2 ORIG, INF 3 EXP
CENTRAL FUEL BUNDLE CLADDING TEMPERATURES

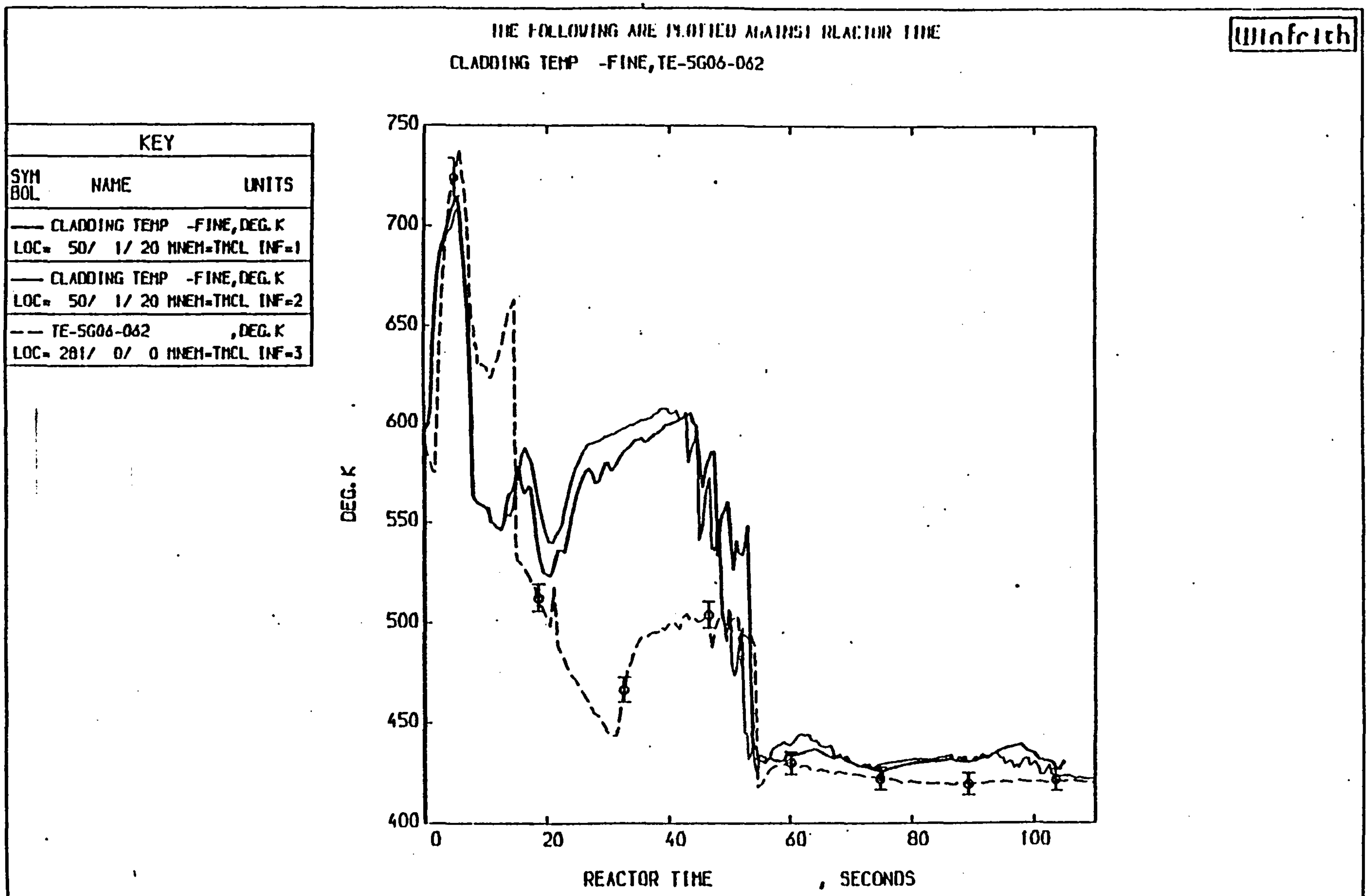

FIGURE 62 INF 1 JON'S, INF 2 ORIG, INF 3 EXP
CENTRAL FUEL BUNDLE CLADDING TEMPERATURES

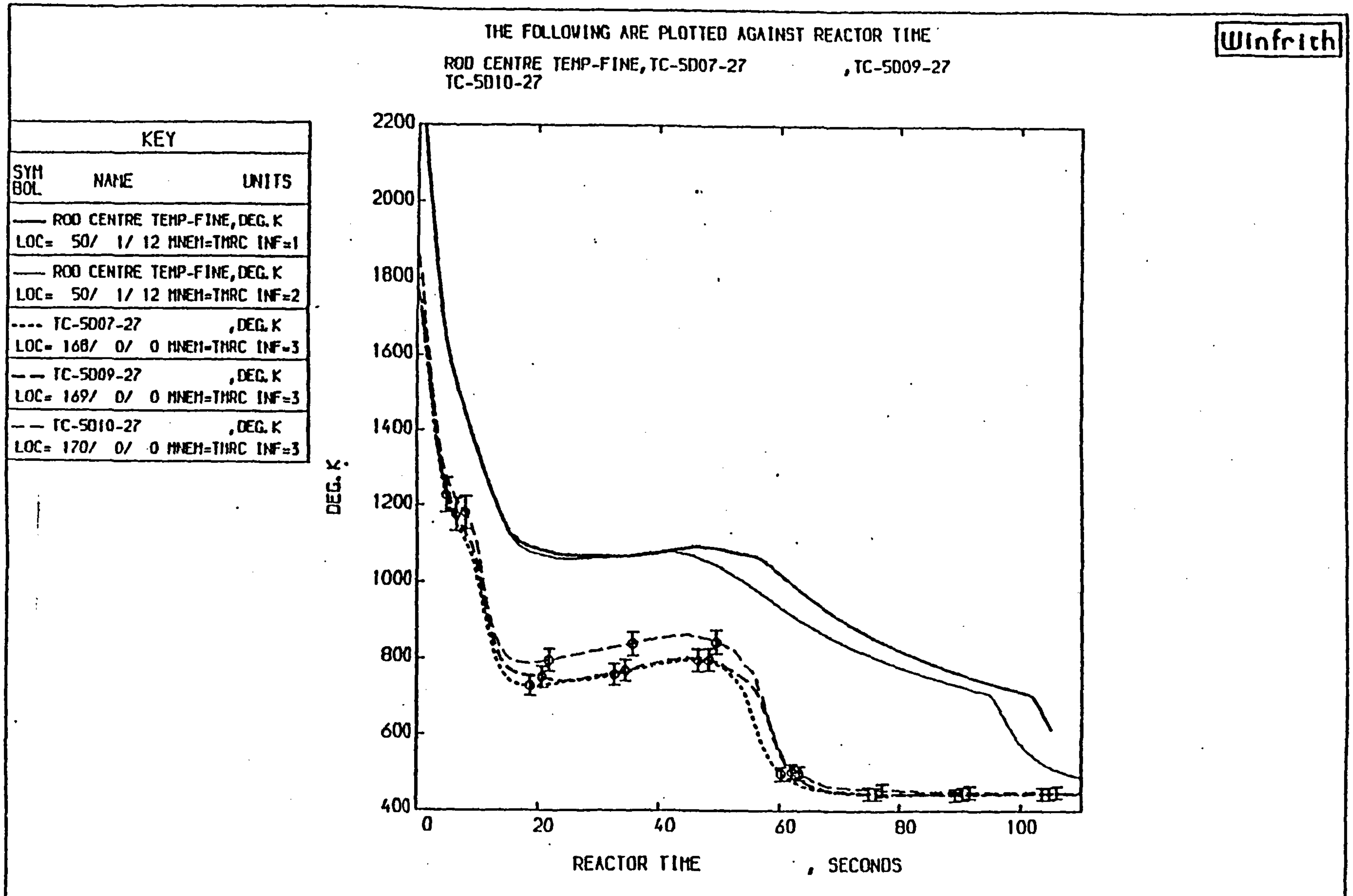

FIGURE 63 INF 1 JON'S, INF 2 ORIG, INF 3 EXP
CENTRELINE FUEL TEMPERATURE

Winfrith

THE FOLLOWING ARE PLOTTED AGAINST REACTOR TIME

CLADDING TEMP -FINE,TE-2G14-011

KEY		
SYMBOL	NAME	UNITS
——	CLADDING TEMP -FINE	DEG.K
LOC= 50/ 5/ 5 MNEM=THCL INF=1		
——	CLADDING TEMP -FINE	DEG.K
LOC= 50/ 5/ 5 MNEM=THCL INF=2		
----	TE-2G14-011	DEG.K
LOC= 220/ 0/ 0 MNEM=THCL INF=3		

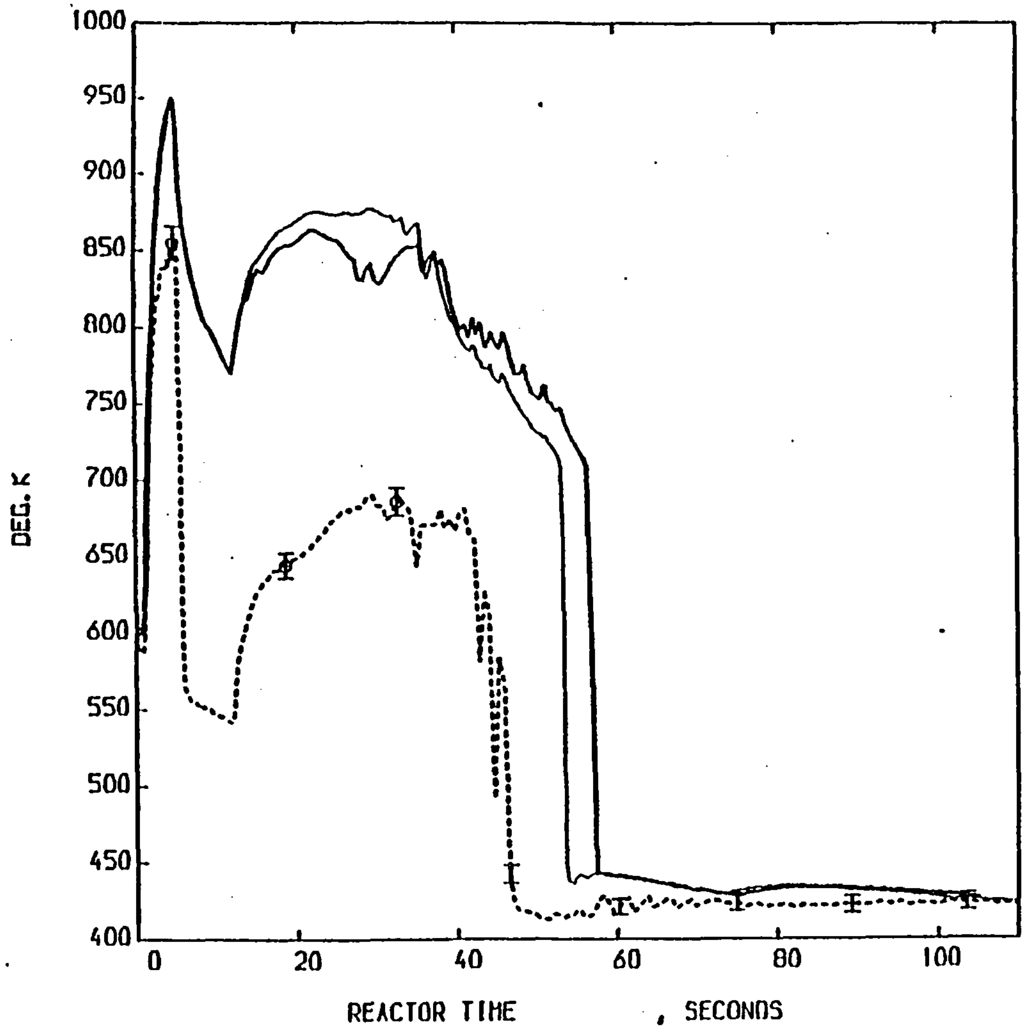

FIGURE 64 INF 1 JON'S, INF 2 ORIG, INF 3 EXP
FUEL ROD CLADDING TEMPERATURES - PERIPHERAL BUNDLES

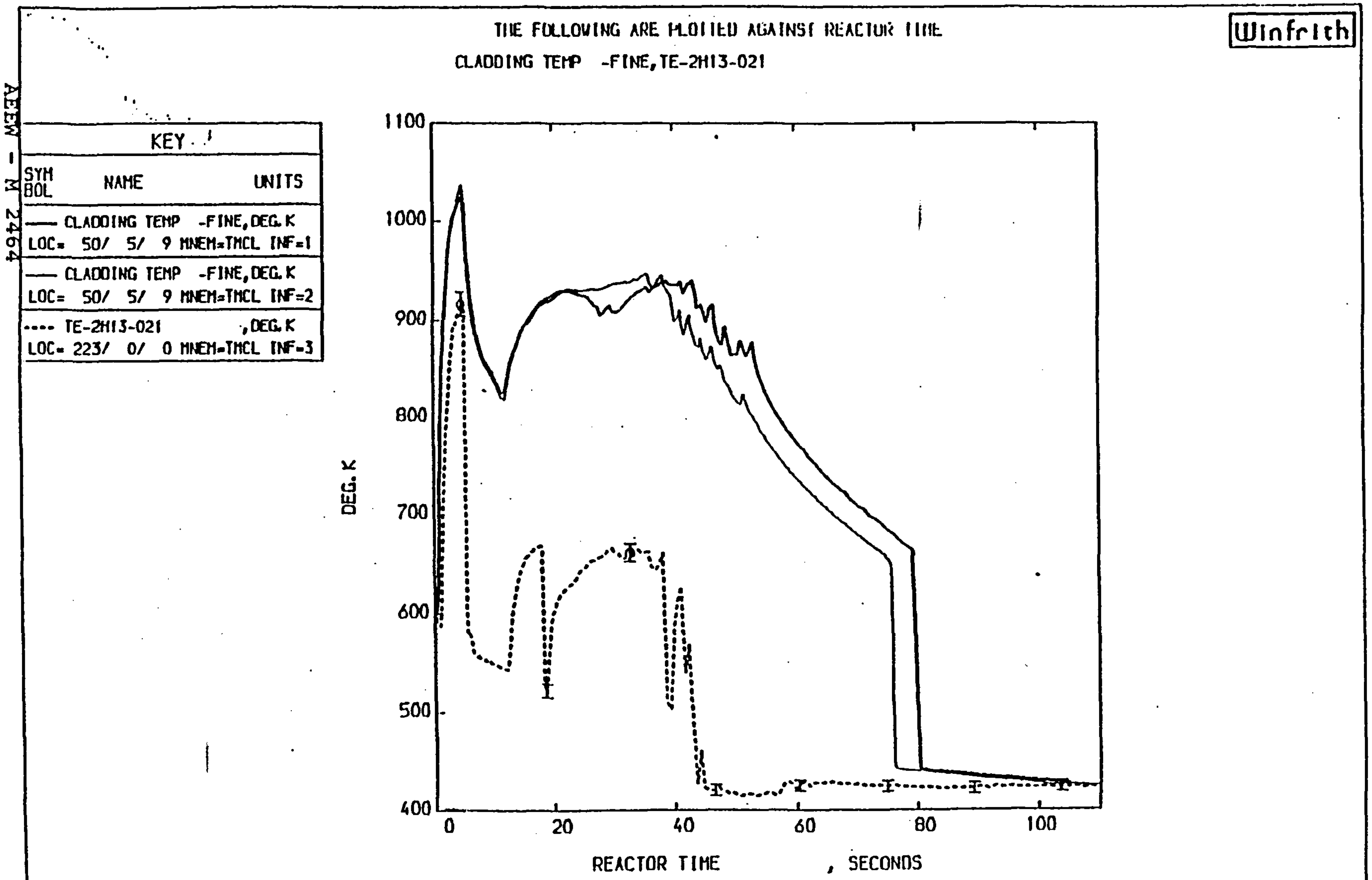

FIGURE 65 INF 1 JON'S, INF 2 ORIG, INF 3 EXP
FUEL ROD CLADDING TEMPERATURES - PERIPHERAL BUNDLES

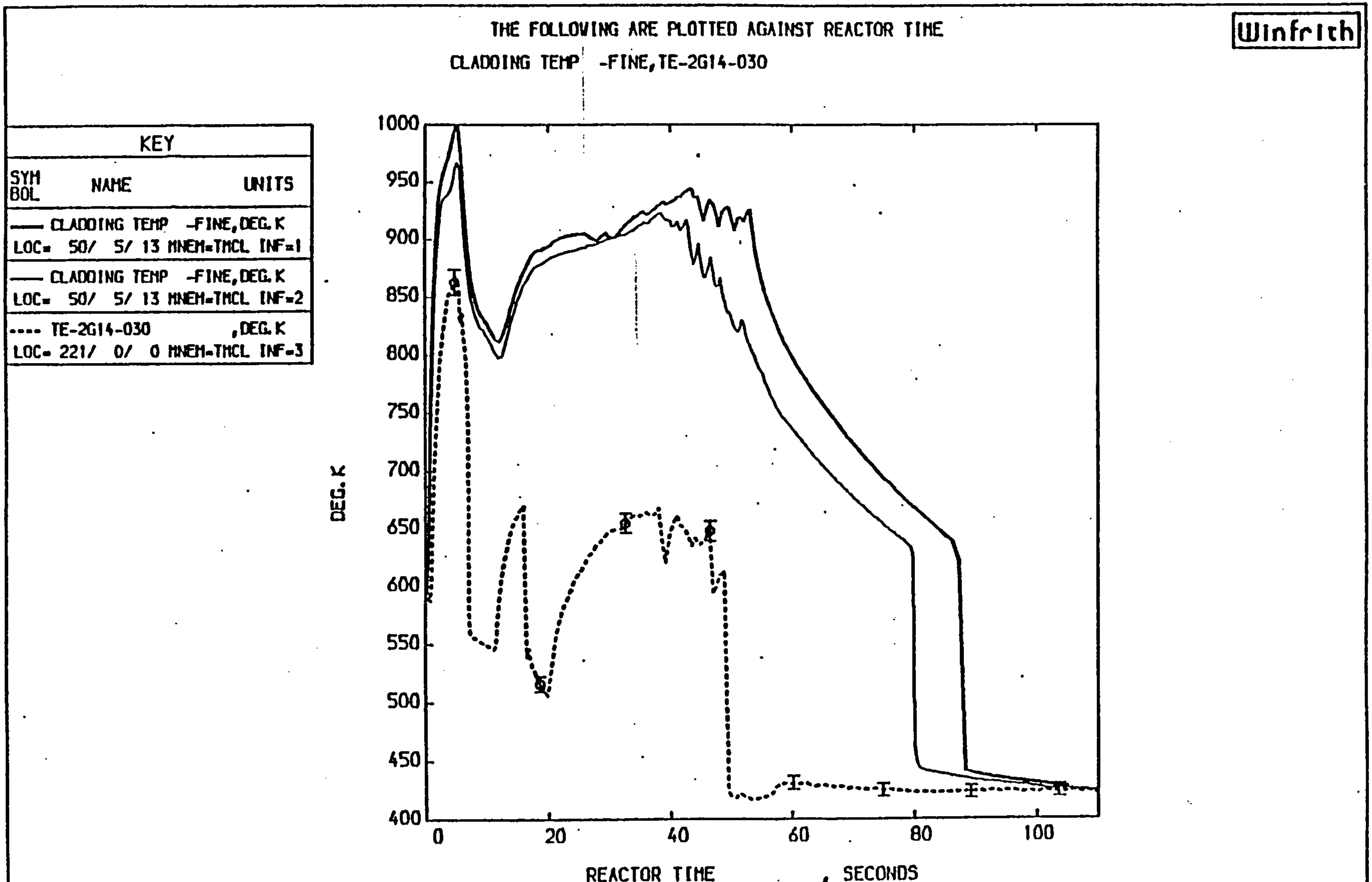

FIGURE 66 INF 1 JON'S, INF 2 ORIG, INF 3 EXP
FUEL ROD CLADDING TEMPERATURES - PERIPHERAL BUNDLES

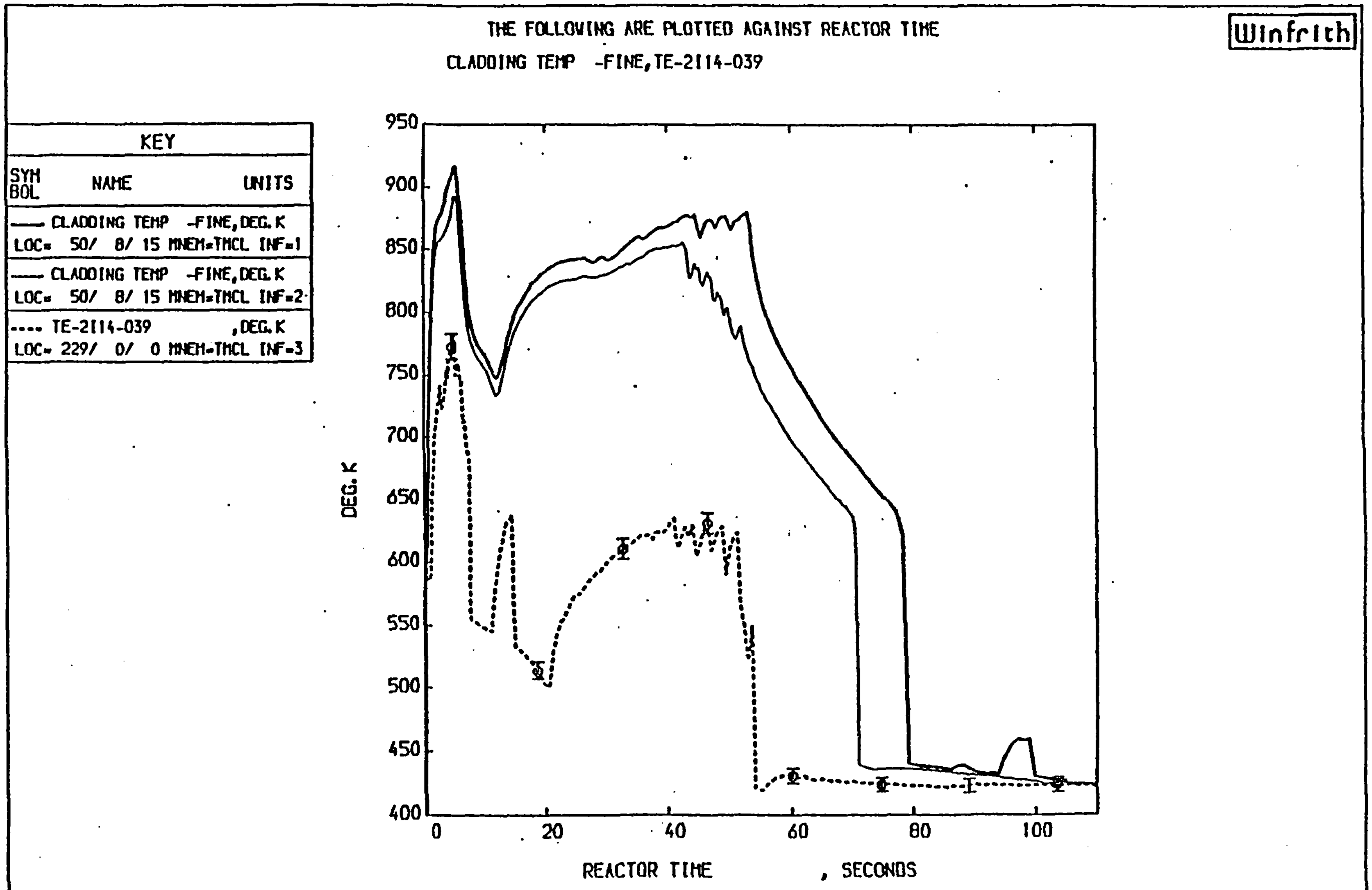

FIGURE 67 INF 1 JON'S, INF 2 ORIG, INF 3 EXP
FUEL ROD CLADDING TEMPERATURES - PERIPHERAL BUNDLES

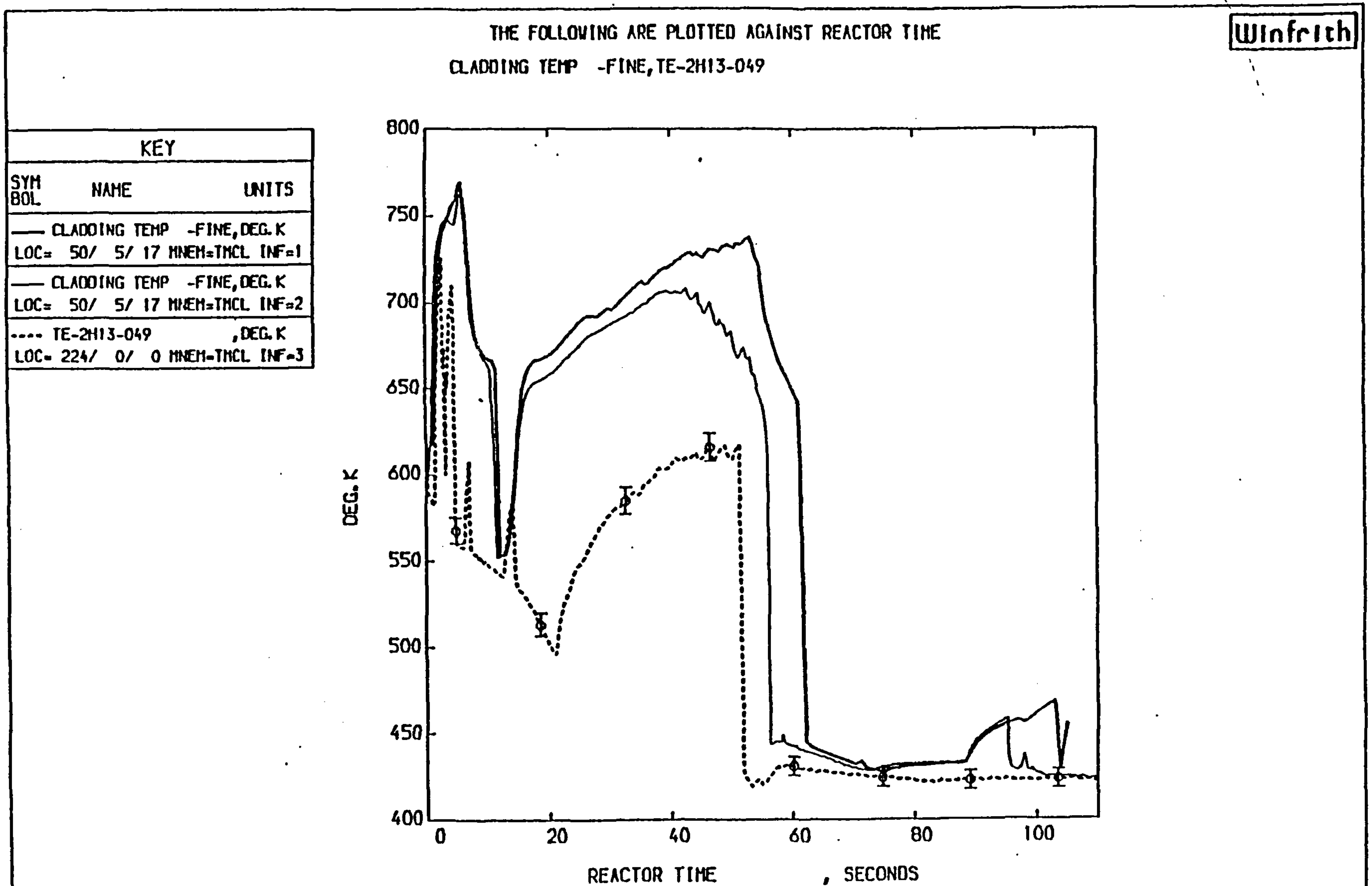

FIGURE 68 INF 1 JON'S, INF 2 ORIG, INF 3 EXP
FUEL ROD CLADDING TEMPERATURES - PERIPHERAL BUNDLES

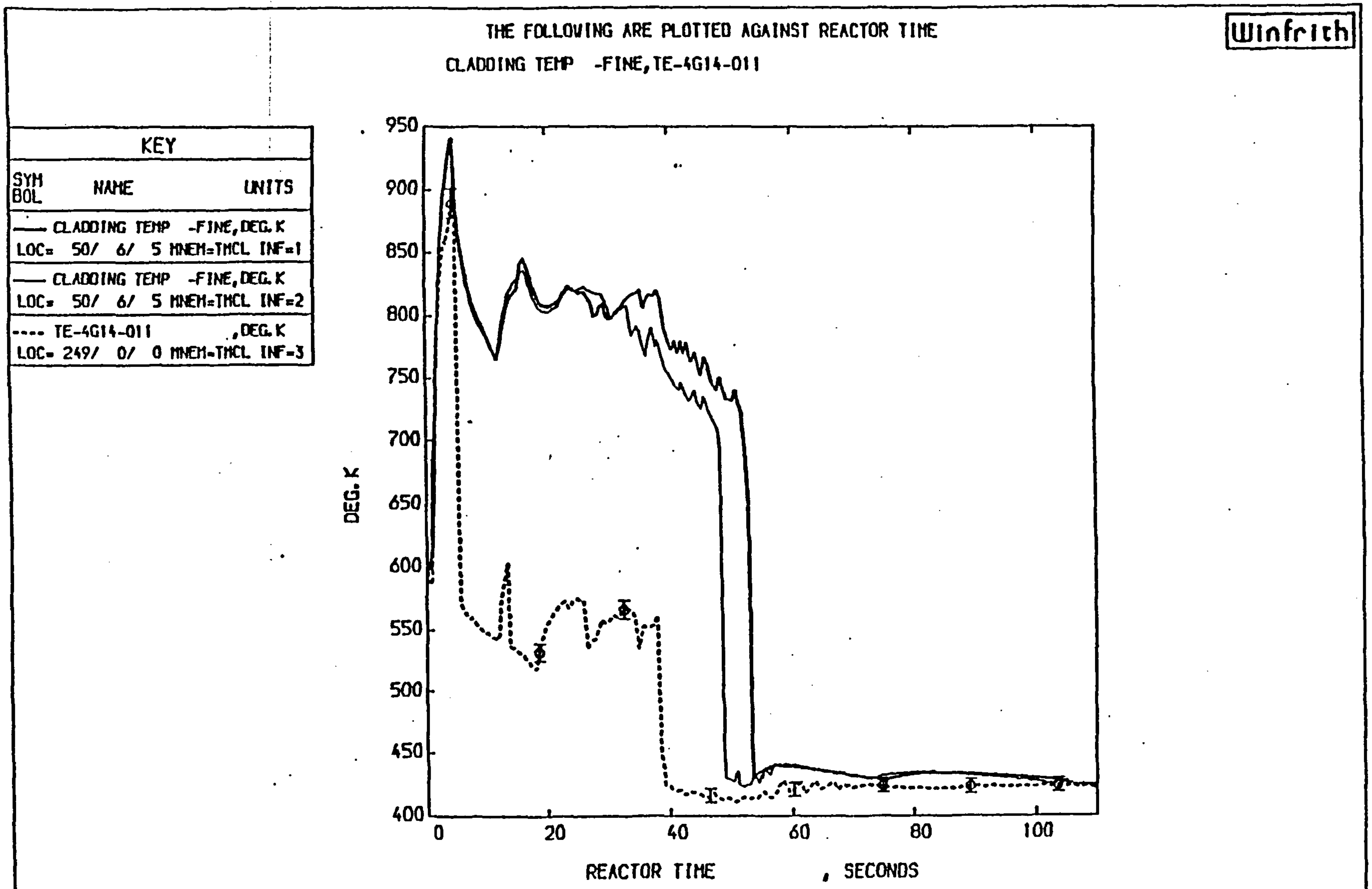

FIGURE 69 INF 1 JON'S, INF 2 ORIG, INF 3 EXP
FUEL ROD CLADDING TEMPERATURES - PERIPHERAL BUNDLES

THE FOLLOWING ARE PLOTTED AGAINST REACTOR TIME
CLADDING TEMP -FINE,TE-4G08-021

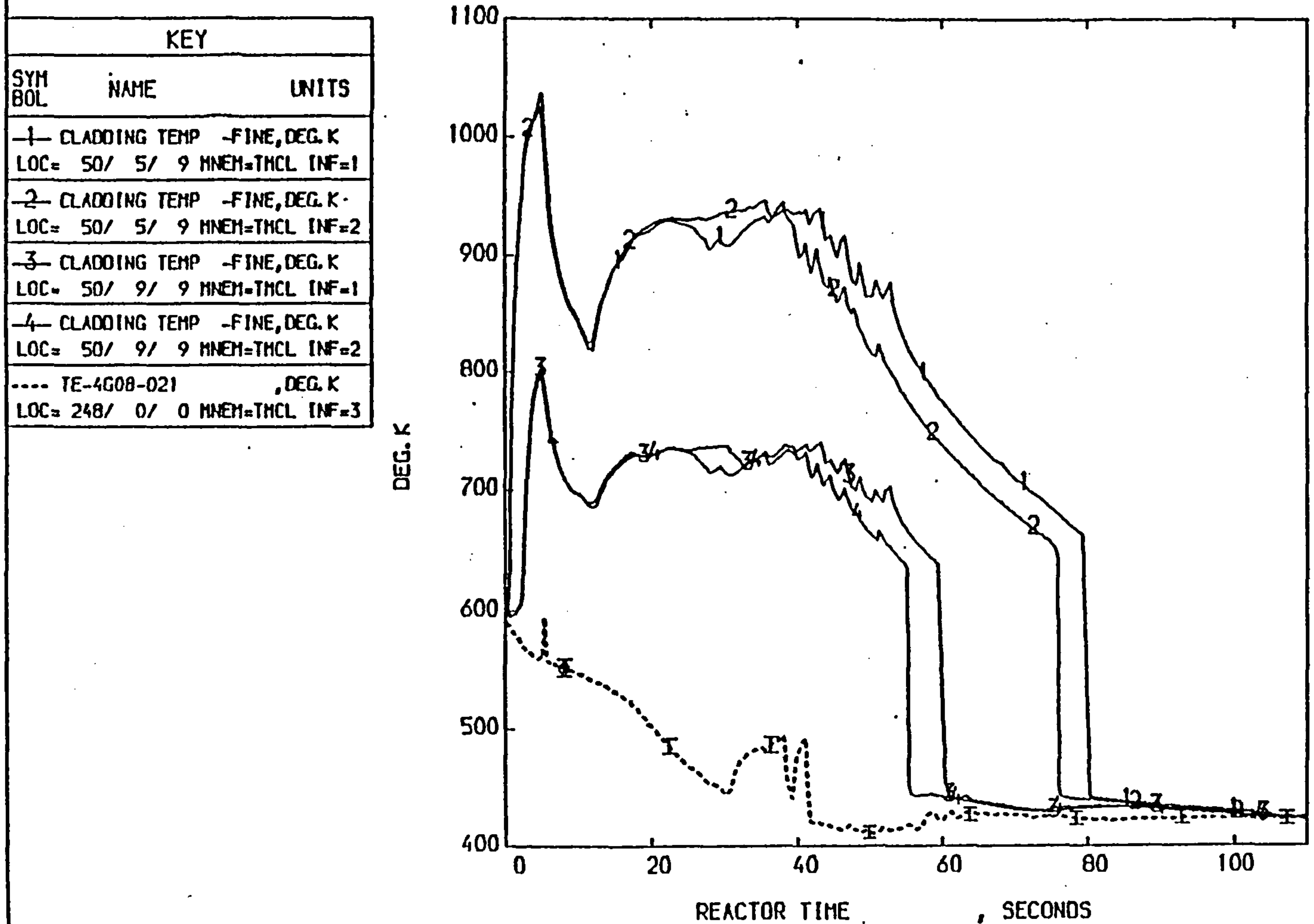

FIGURE 70 INF 1 JON'S, INF 2 ORIG, INF 3 EXP
FUEL ROD CLADDING TEMPERATURES - PERIPHERAL BUNDLES

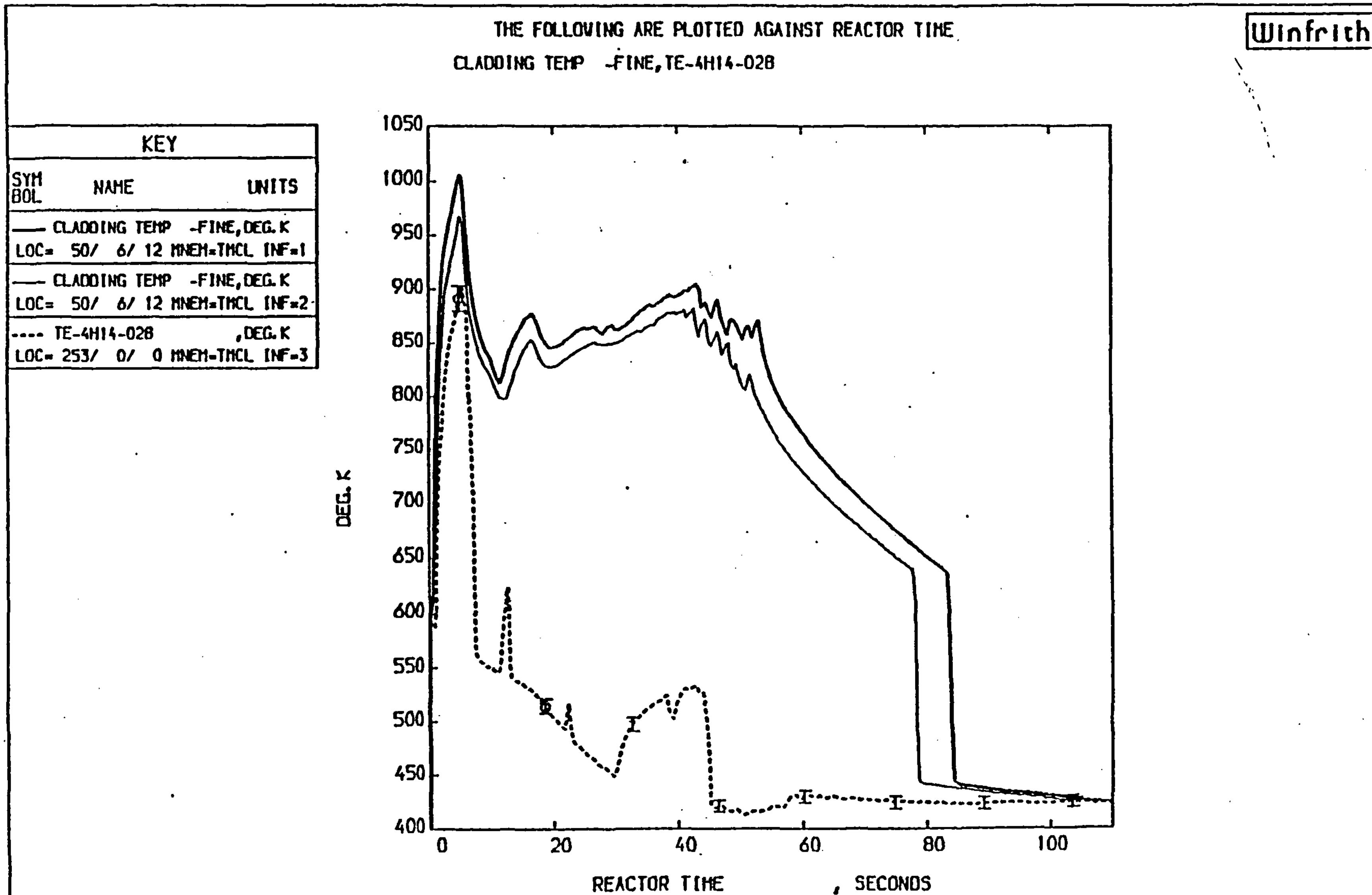

FIGURE 71 INF 1 JON'S, INF 2 ORIG, INF 3 EXP
FUEL ROD CLADDING TEMPERATURES - PERIPHERAL BUNDLES

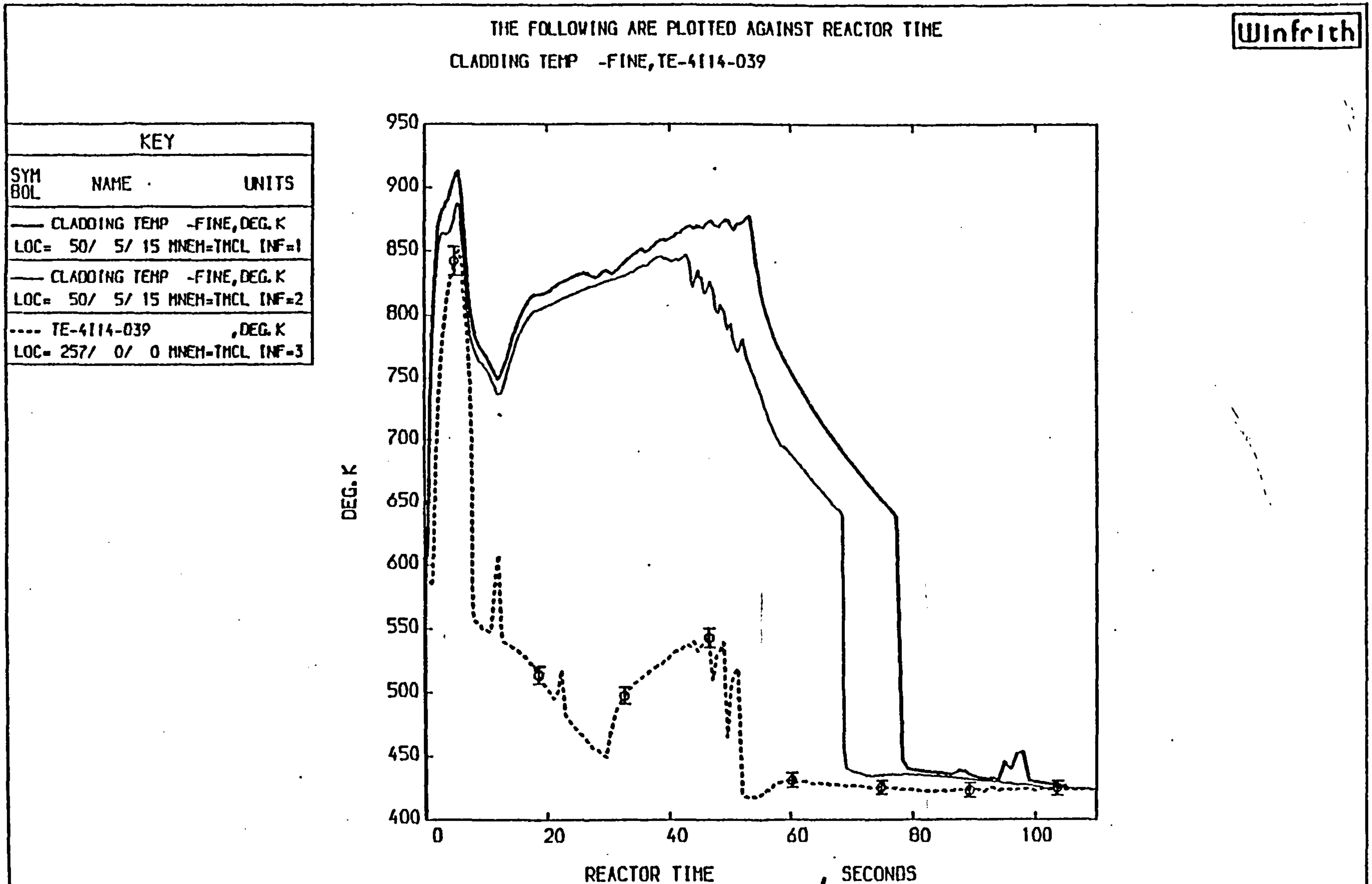

FIGURE 72 INF 1 JON'S, INF 2 ORIG, INF 3 EXP
FUEL ROD CLADDING TEMPERATURES - PERIPHERAL BUNDLES

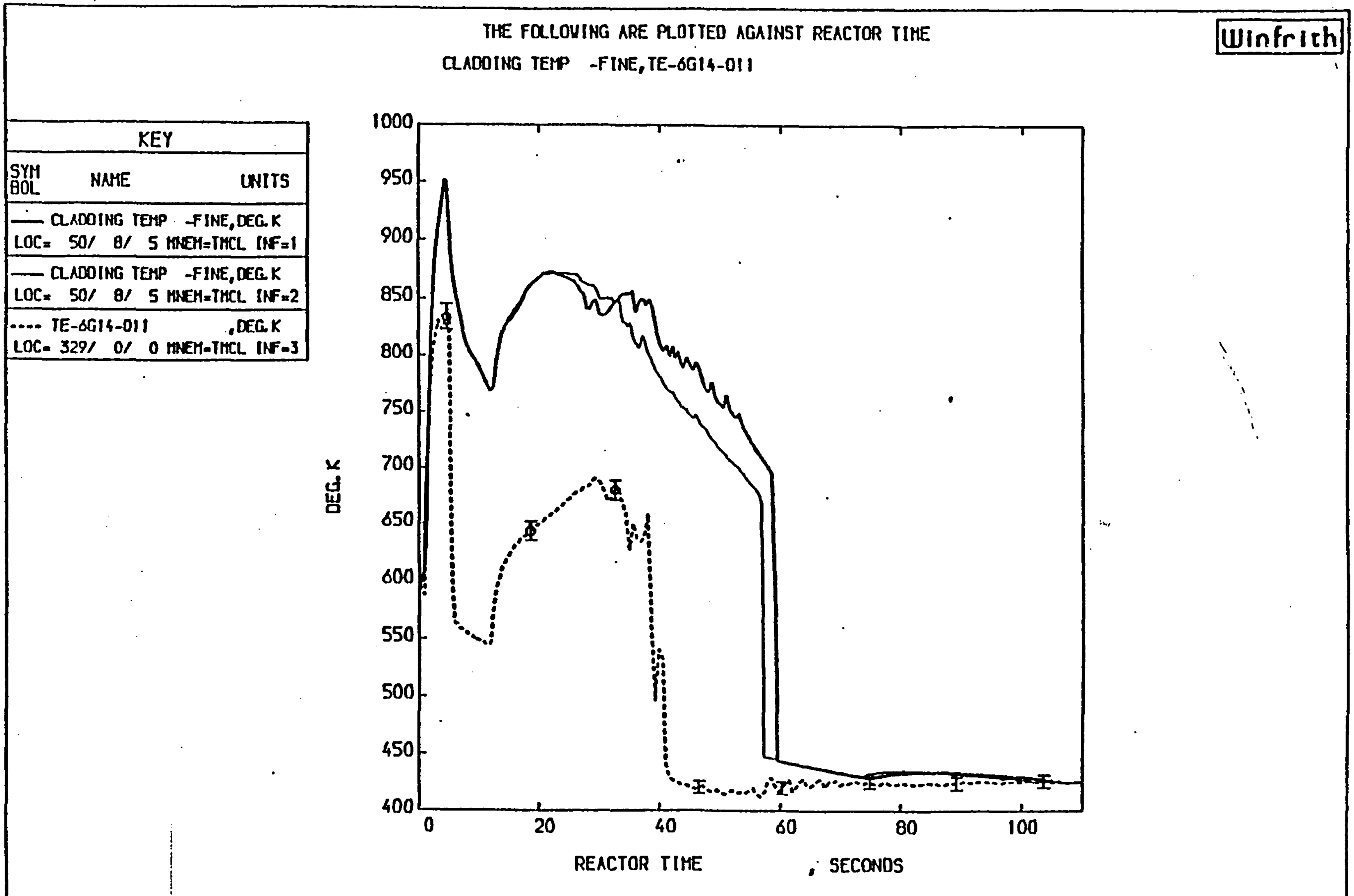

FIGURE 73 INF 1 JON'S, INF 2 ORIG, INF 3 EXP
FUEL ROD CLADDING TEMPERATURES - PERIPHERAL BUNDLES

Winfrith

THE FOLLOWING ARE PLOTTED AGAINST REACTOR TIME

CLADDING TEMP -FINE,TE-6G14-030

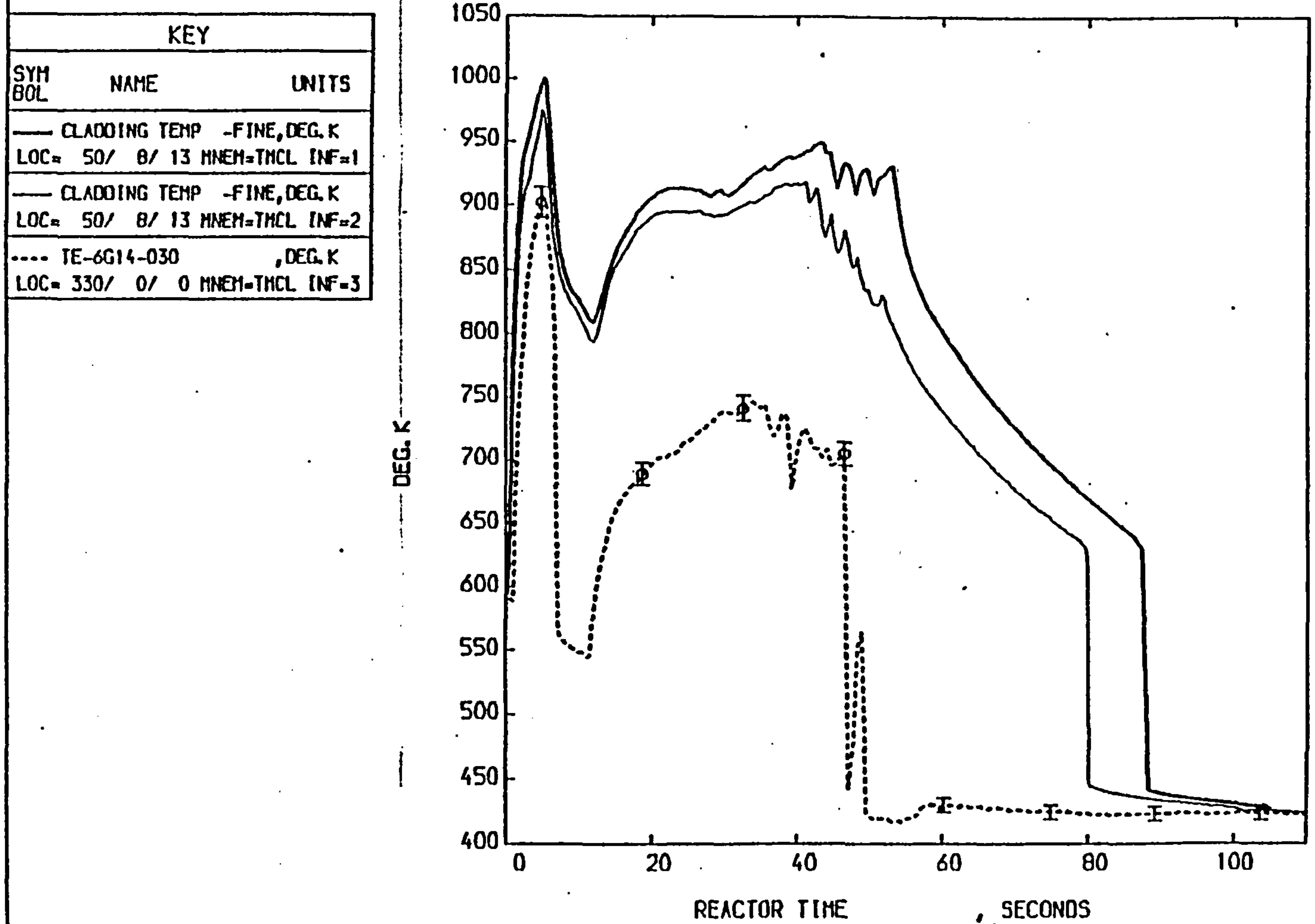

FIGURE 74 INF 1 JON'S, INF 2 ORIG, INF 3 EXP
FUEL ROD CLADDING TEMPERATURES – PERIPHERAL BUNDLES

THE FOLLOWING ARE PLOTTED AGAINST REACTOR TIME

CLADDING TEMP -FINE,TE-6H15-026

Winfrith

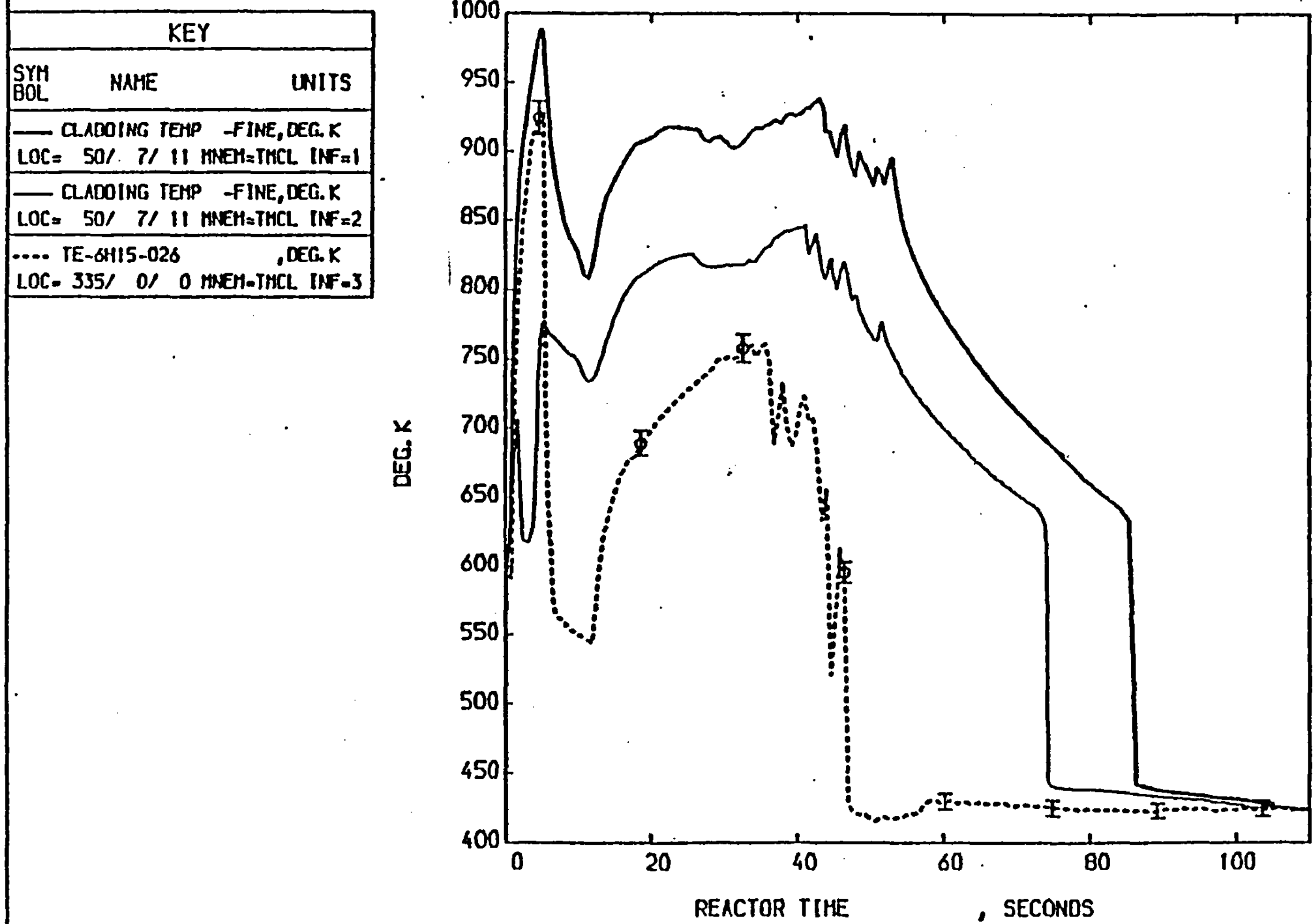

FIGURE 75 INF 1 JON'S, INF 2 ORIG, INF 3 EXP
FUEL ROD CLADDING TEMPERATURES - PERIPHERAL BUNDLES

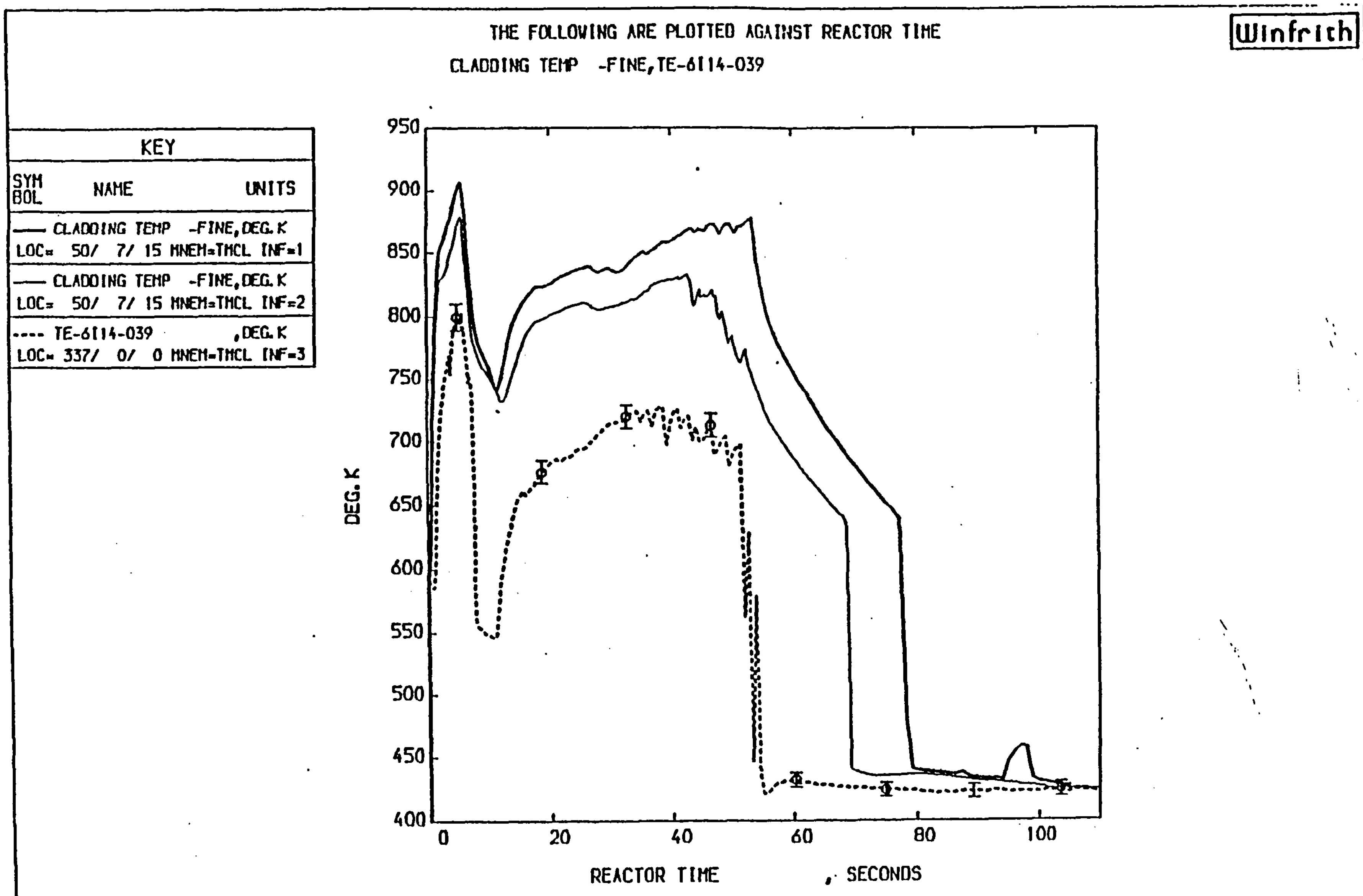

FIGURE 76 INF 1 JON'S, INF 2 ORIG, INF 3 EXP
FUEL ROD CLADDING TEMPERATURES - PERIPHERAL BUNDLES

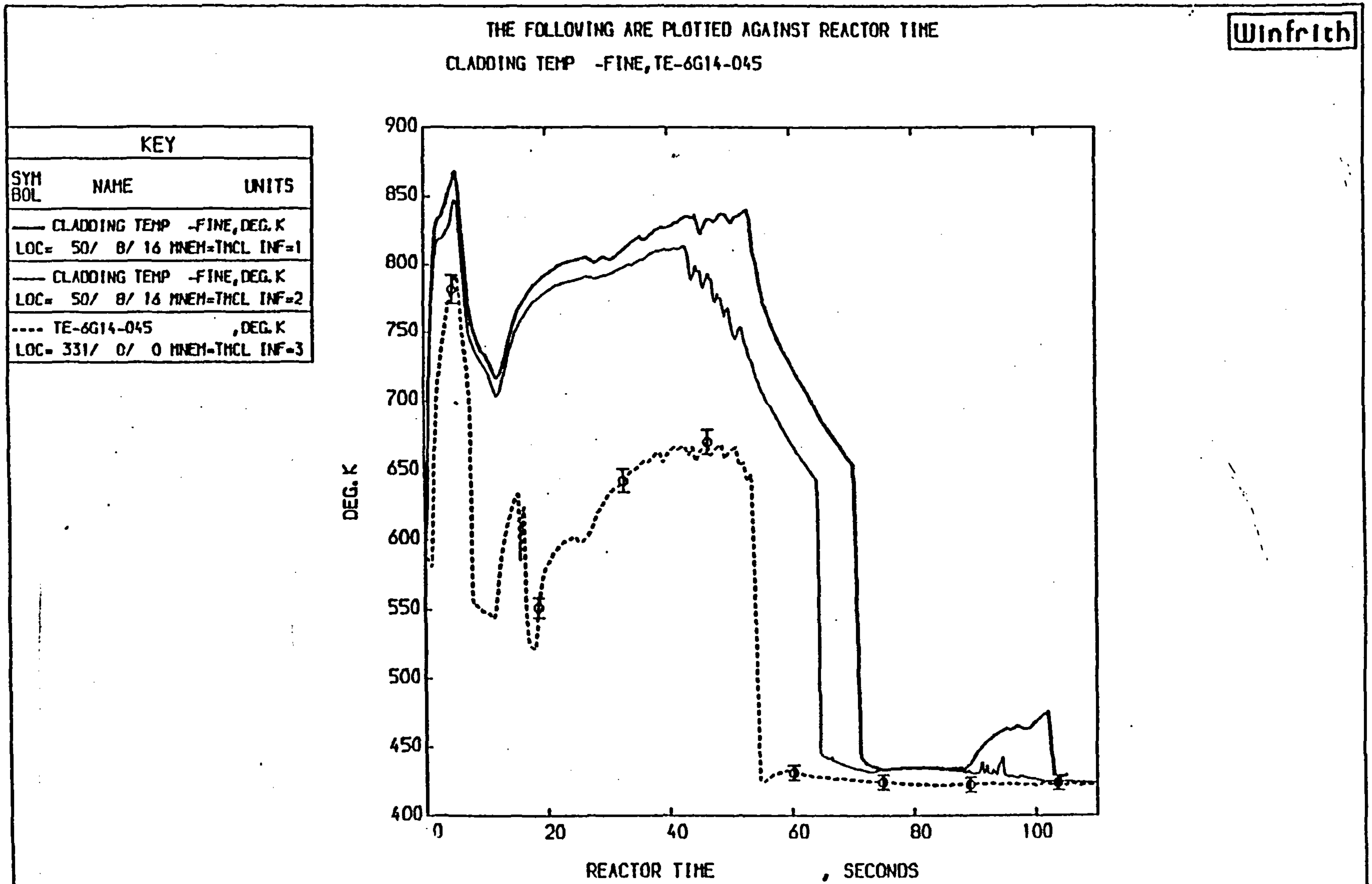

FIGURE 77 INF 1 JON'S, INF 2 ORIG, INF 3 EXP
FUEL ROD CLADDING TEMPERATURES - PERIPHERAL BUNDLES

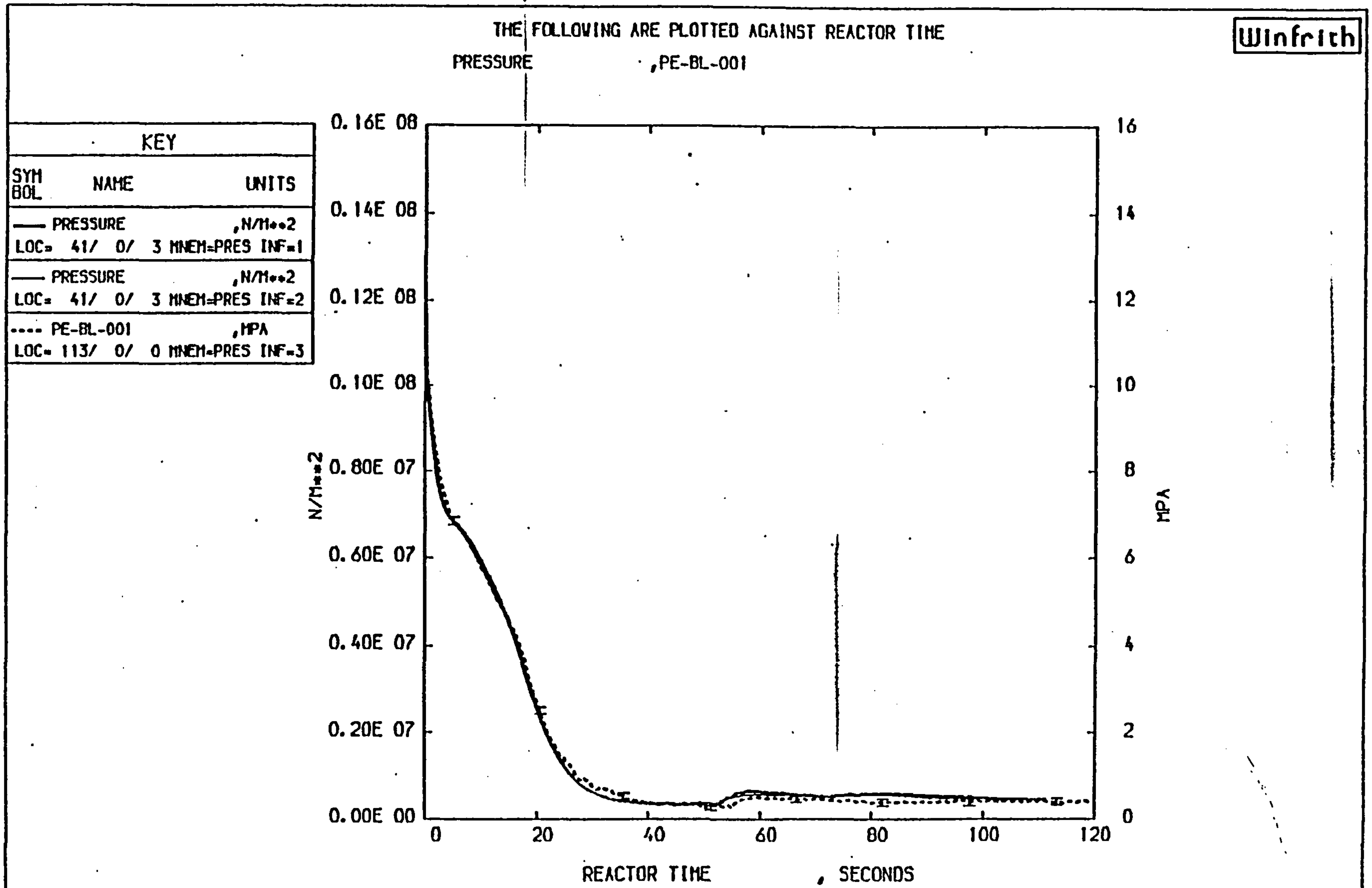

FIGURE 78 INF 1 ORIG, INF 2 ZEROGAP, INF 3 EXP
BROKEN LOOP COLD LEG - EXPERIMENTAL LOCATION BL-1

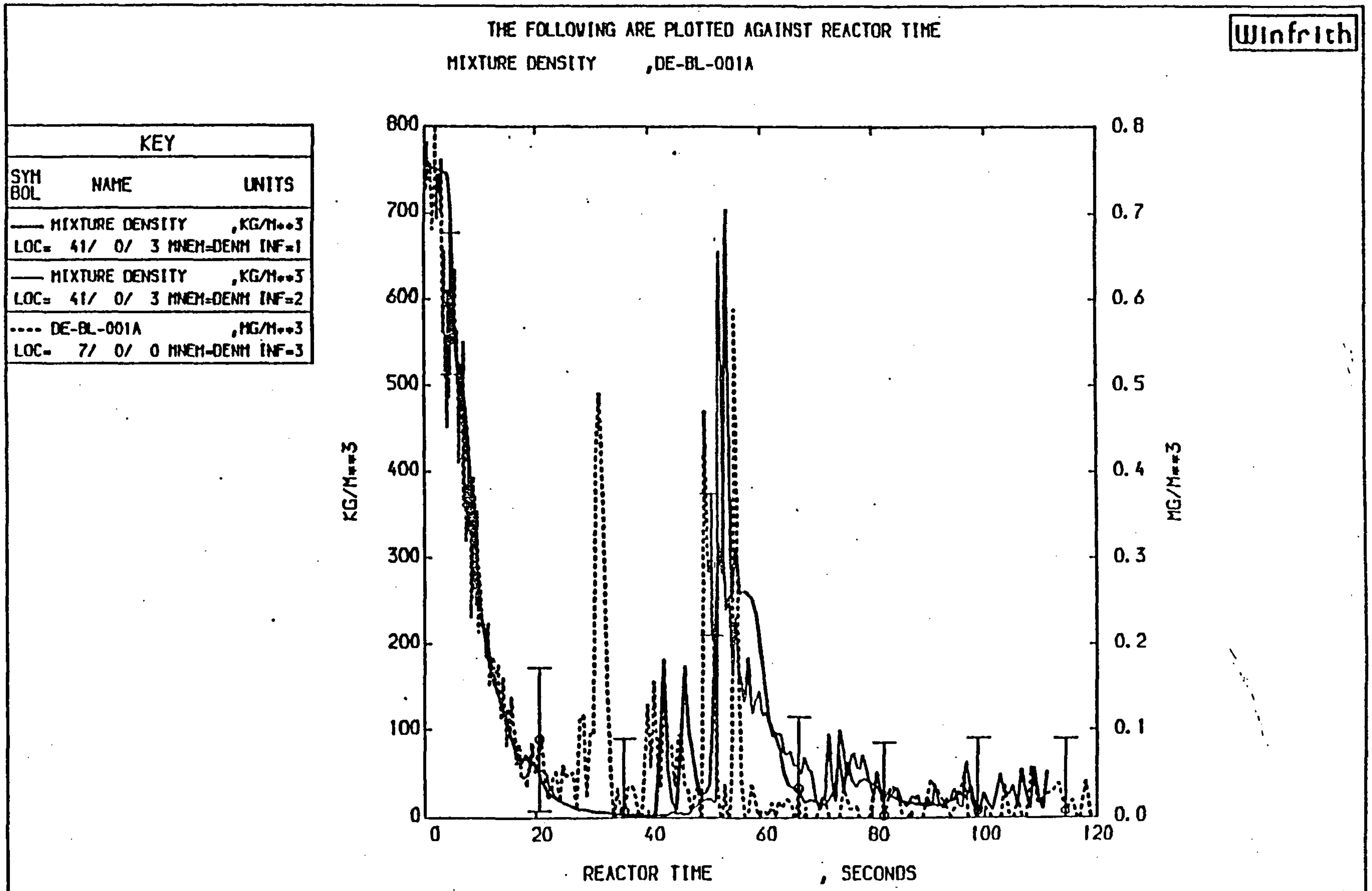

FIGURE 79 INF 1 ORIG, INF 2 ZEROGAP, INF 3 EXP
BROKEN LOOP COLD LEG - EXPERIMENTAL LOCATION BL-1

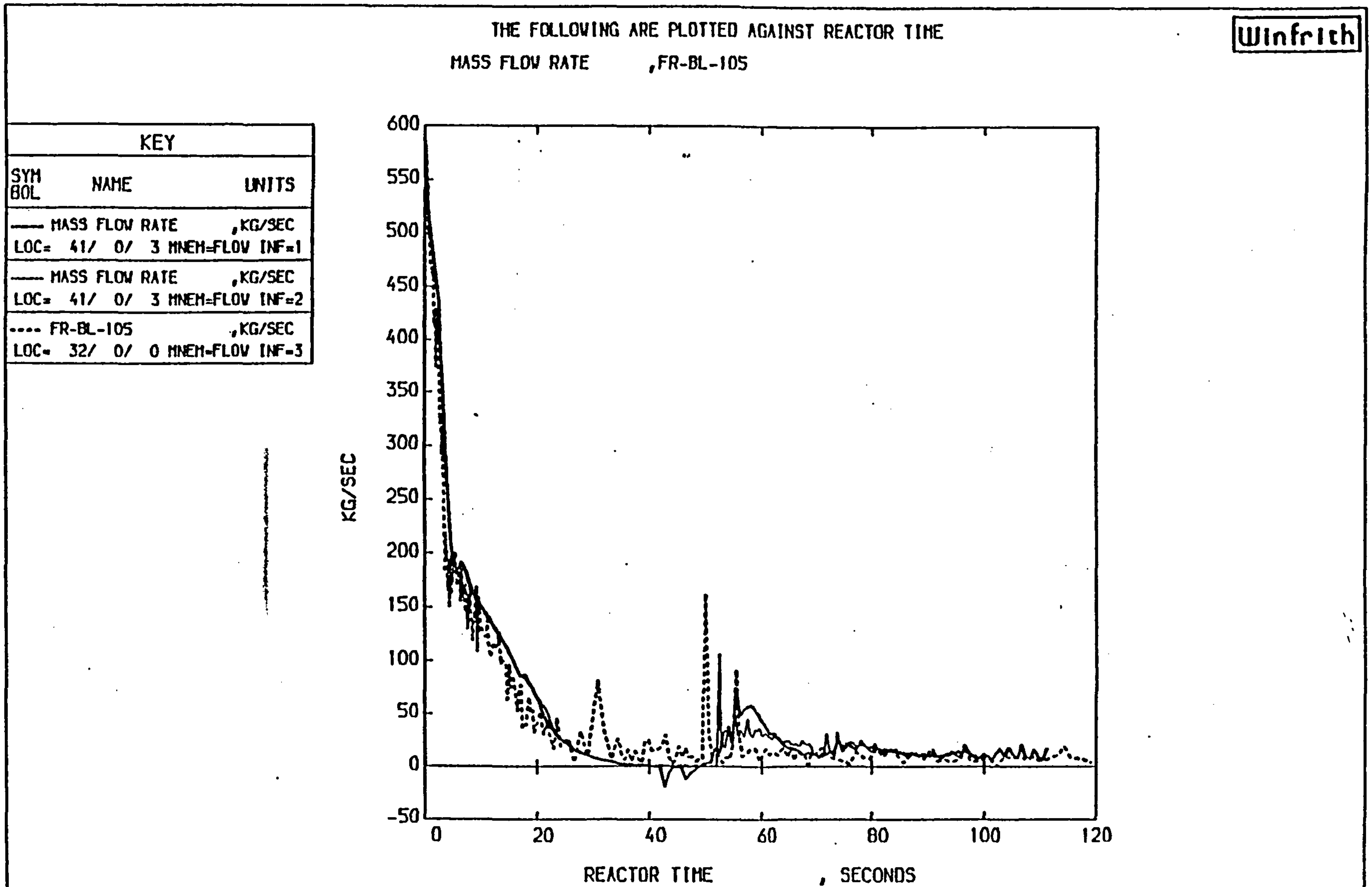

FIGURE 80 INF 1 ORIG, INF 2 ZEROGAP, INF 3 EXP
BROKEN LOOP COLD LEG – EXPERIMENTAL LOCATION BL-1

Winfrith

THE FOLLOWING ARE PLOTTED AGAINST REACTOR TIME

LIQUID TEMPERATURE ,TE-BL-001A

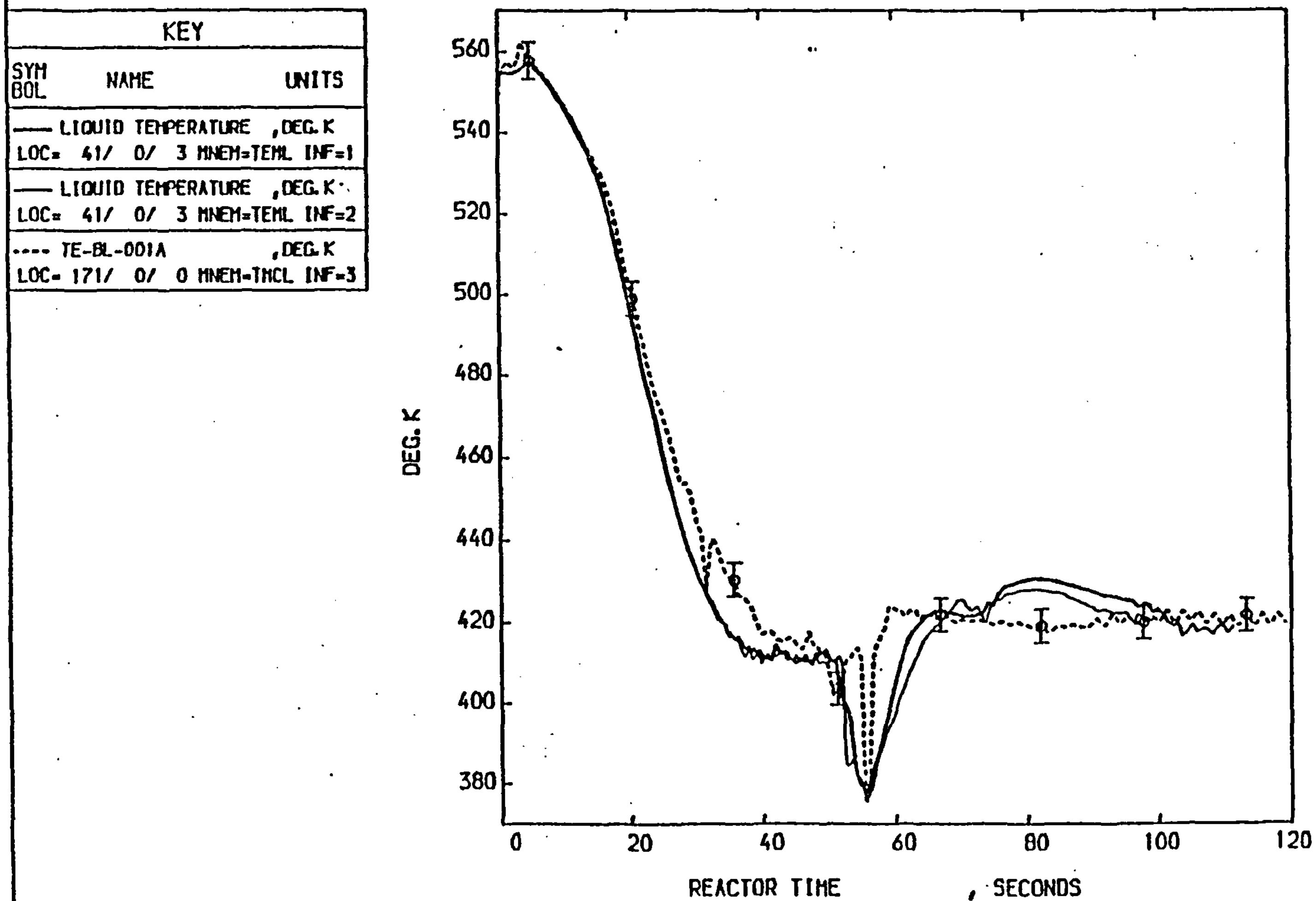

FIGURE 81 INF 1 ORIG, INF 2 ZEROGAP, INF 3 EXP
BROKEN LOOP COLD LEG - EXPERIMENTAL LOCATION BL-1

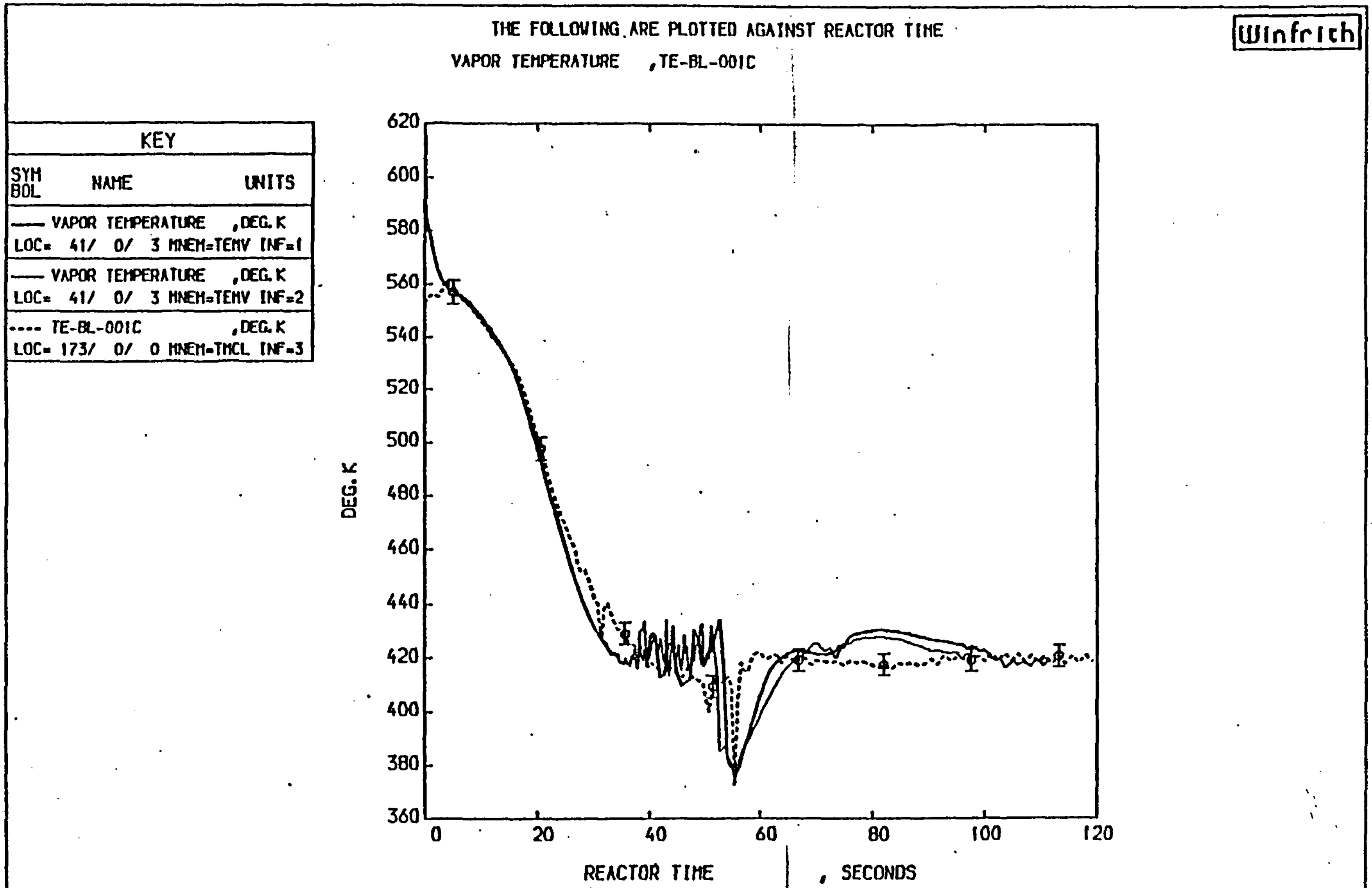

FIGURE 82 INF 1 ORIG, INF 2 ZEROGAP, INF 3 EXP
BROKEN LOOP COLD LEG - EXPERIMENTAL LOCATION BL-1

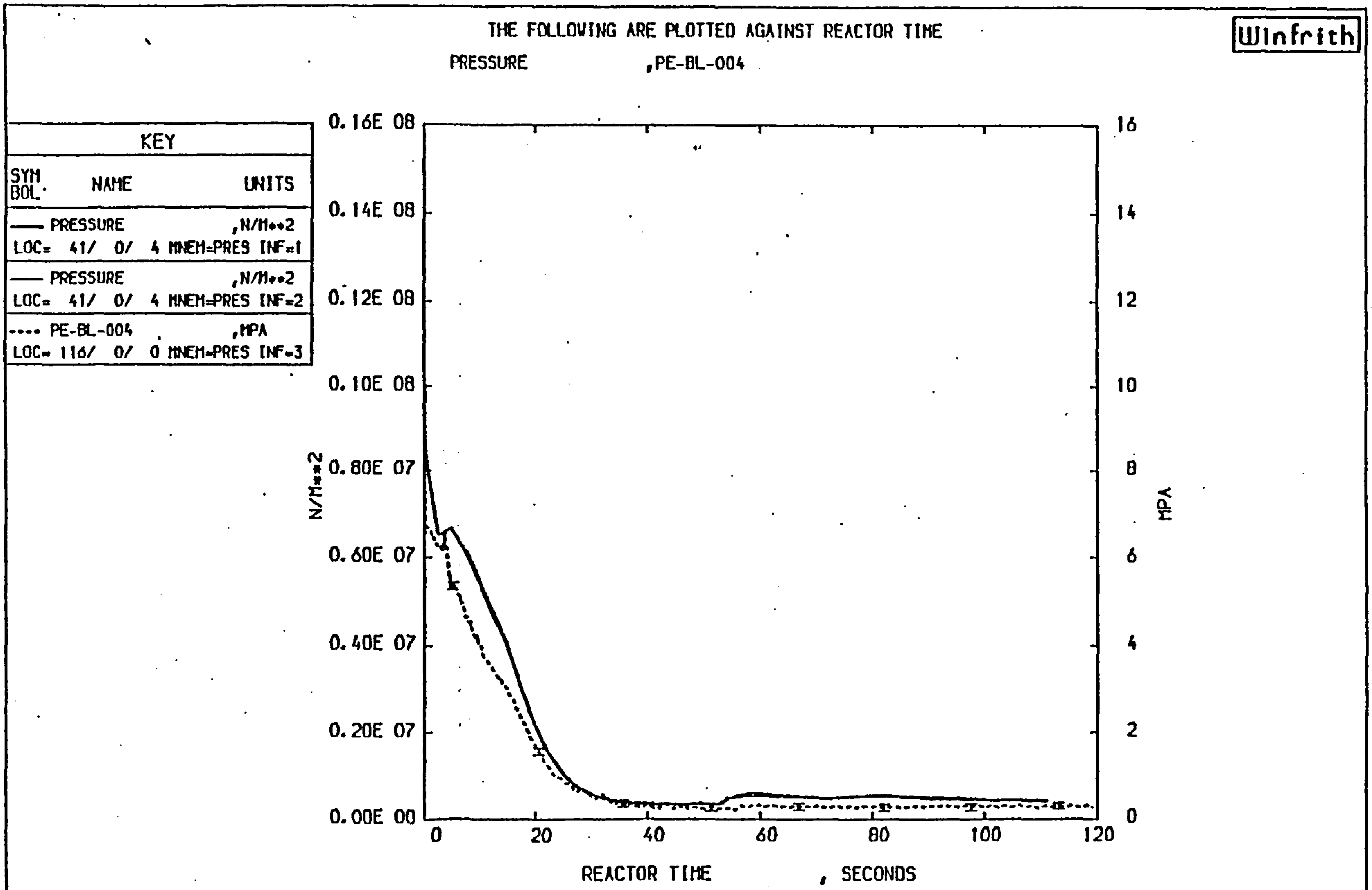

FIGURE 83 INF 1 ORIG, INF 2 ZEROGAP, INF 3 EXP
BROKEN LOOP COLD LEG - EXPERIMENTAL LOCATION BL-4

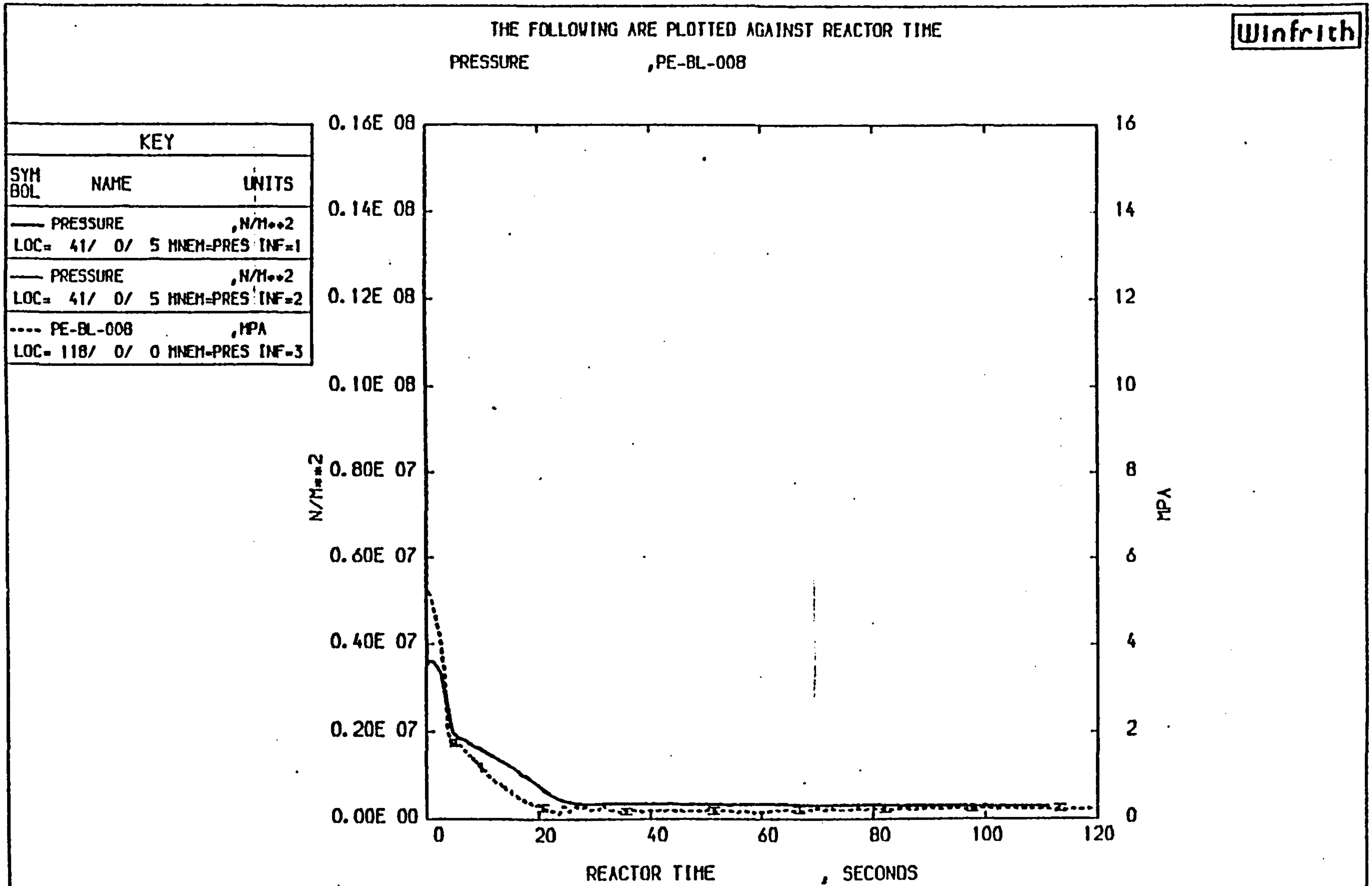

FIGURE 84 INF 1 ORIG, INF 2 ZEROGAP, INF 3 EXP
BROKEN LOOP COLD LEG - EXPERIMENTAL LOCATION BL-8

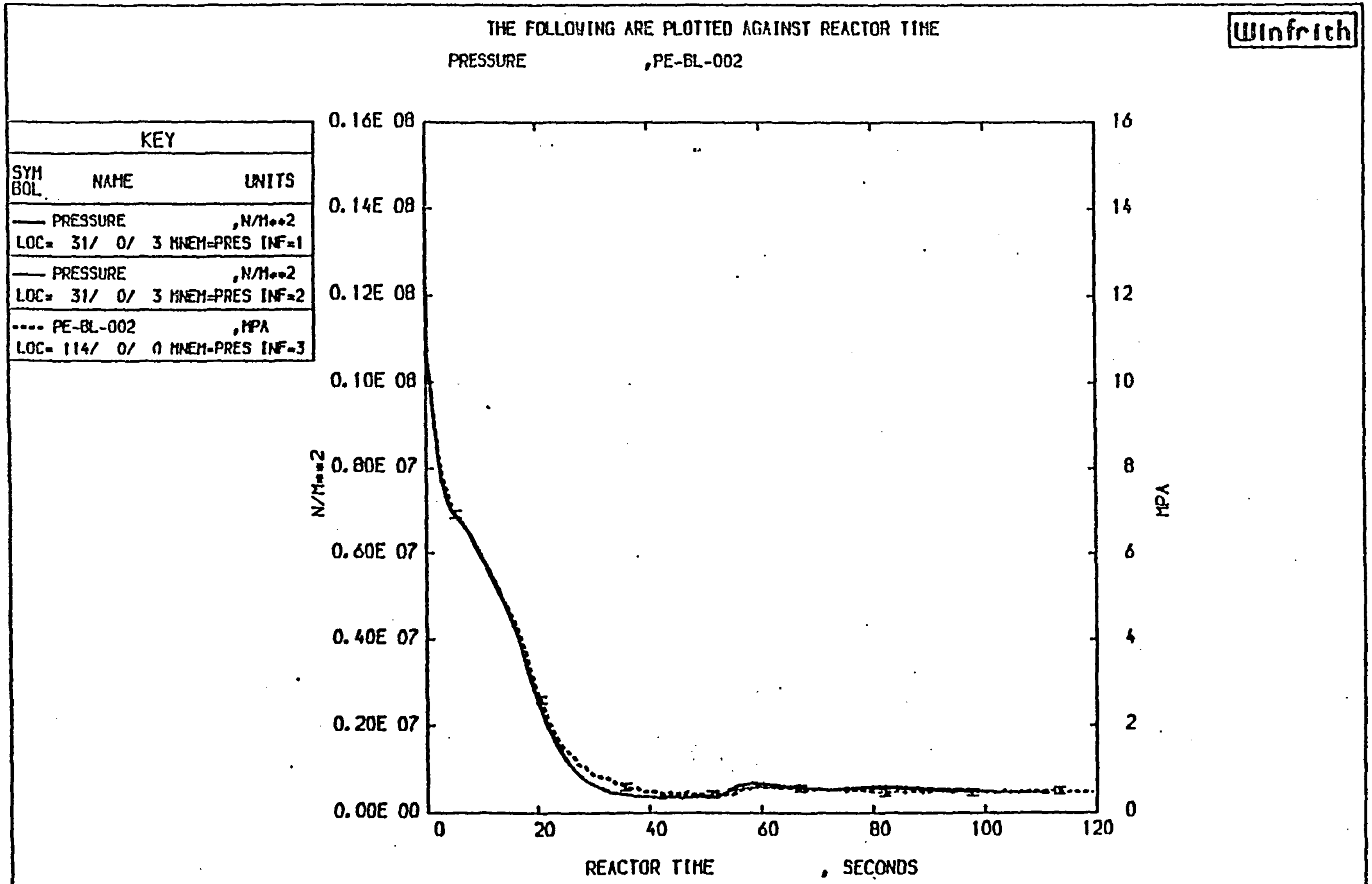

FIGURE 85 INF 1 ORIG, INF 2 ZEROGAP, INF 3 EXP
BROKEN LOOP HOT LEG - EXPERIMENTAL LOCATION BL-2

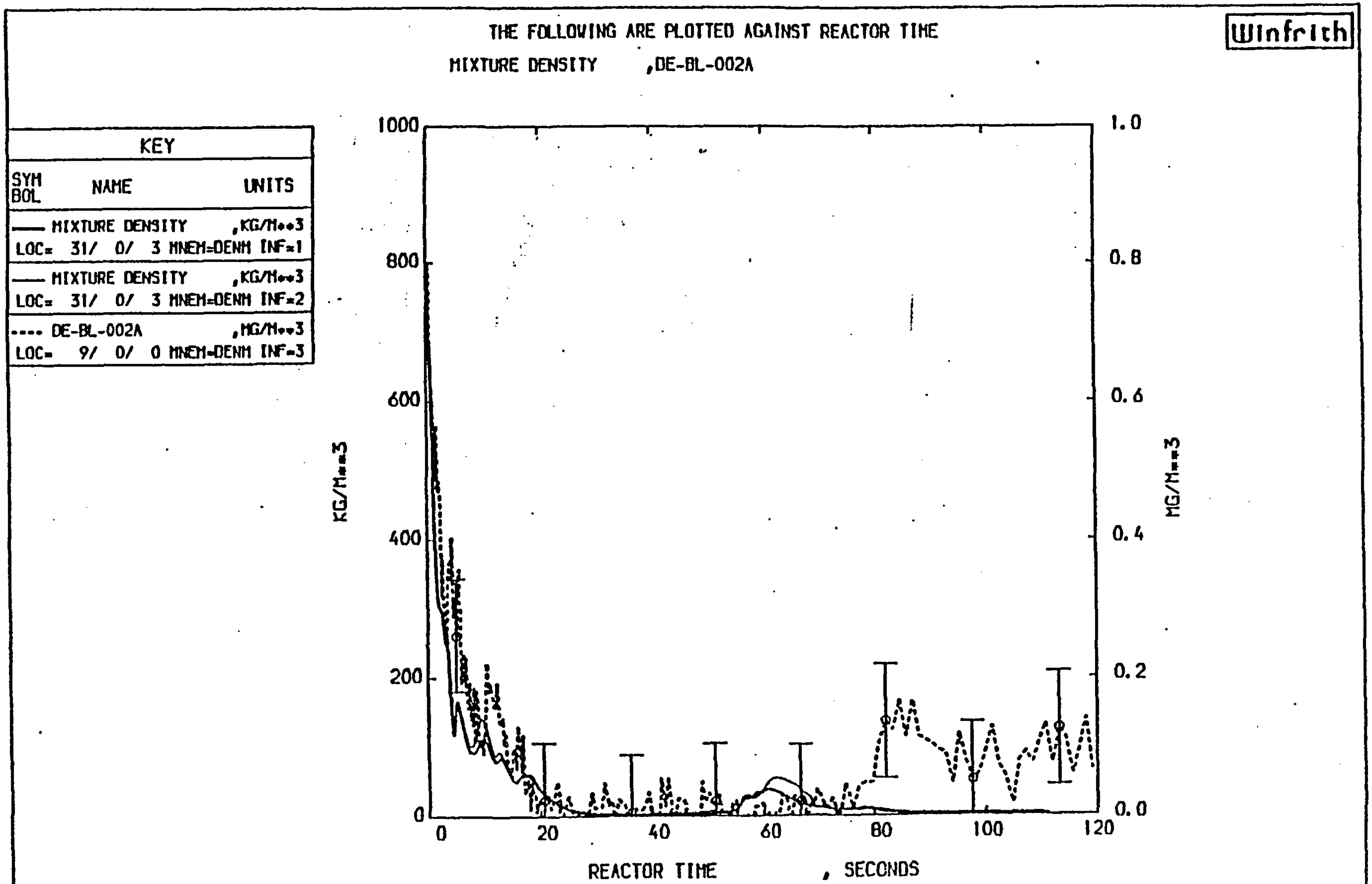

FIGURE 86 INF 1 ORIG, INF 2 ZEROGAP, INF 3 EXP
BROKEN LOOP HOT LEG - EXPERIMENTAL LOCATION BL-2

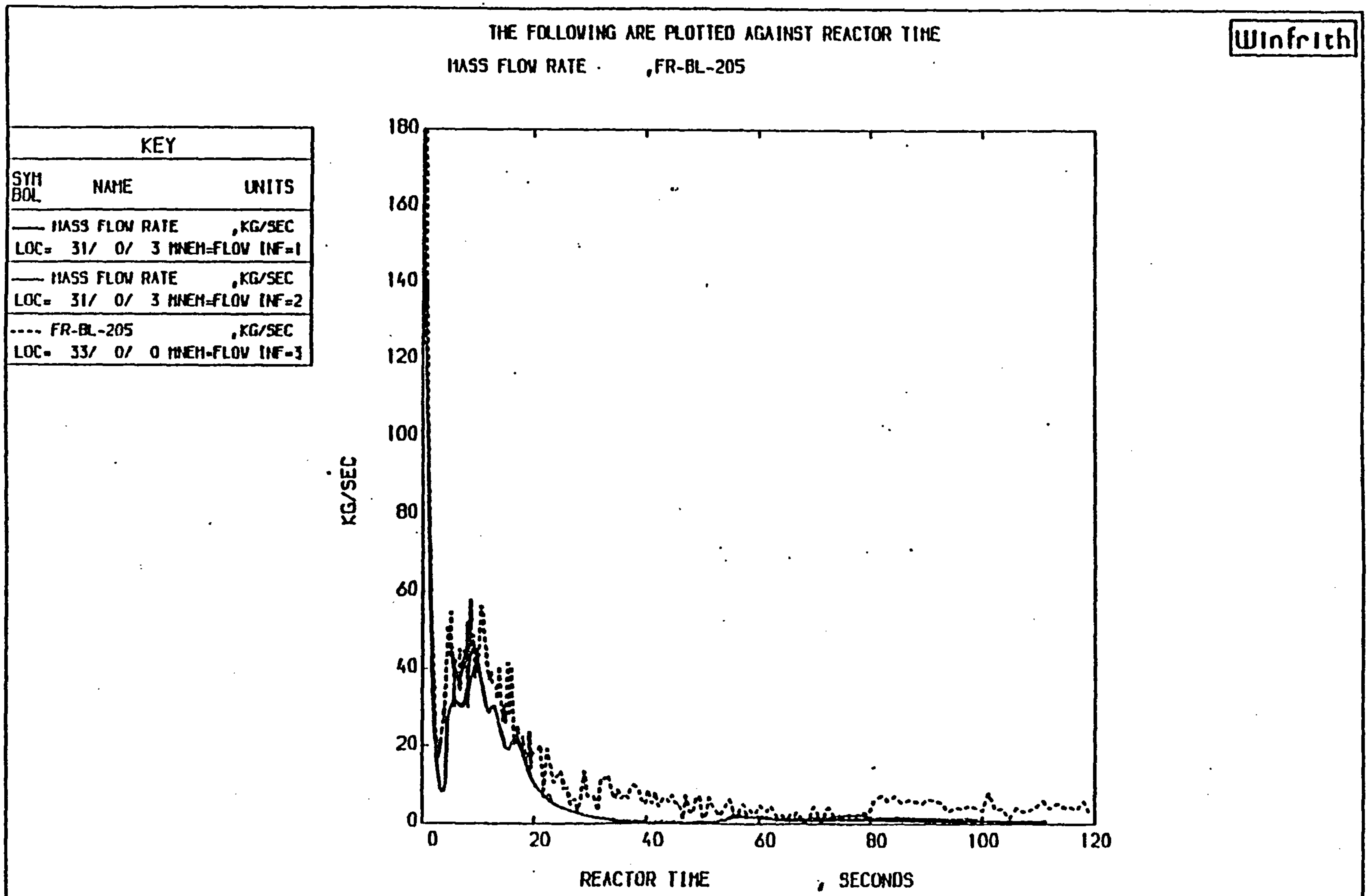

FIGURE 87 INF 1 ORIG, INF 2 ZEROGAP, INF 3 EXP
BROKEN LOOP HOT LEG - EXPERIMENTAL LOCATION BL-2

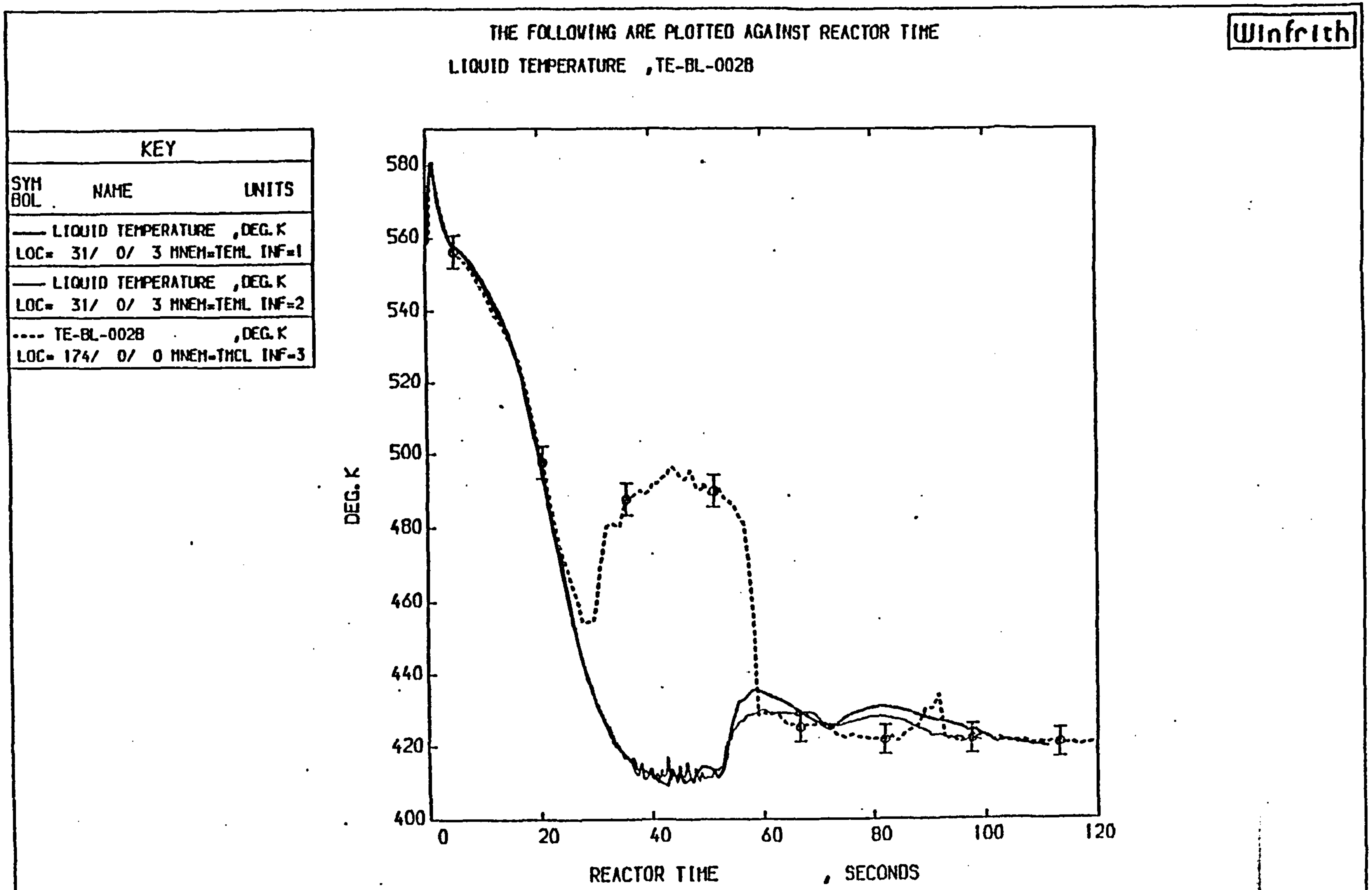

FIGURE 88 INF 1 ORIG, INF 2 ZEROGAP, INF 3 EXP
BROKEN LOOP HOT LEG - EXPERIMENTAL LOCATION BL-2

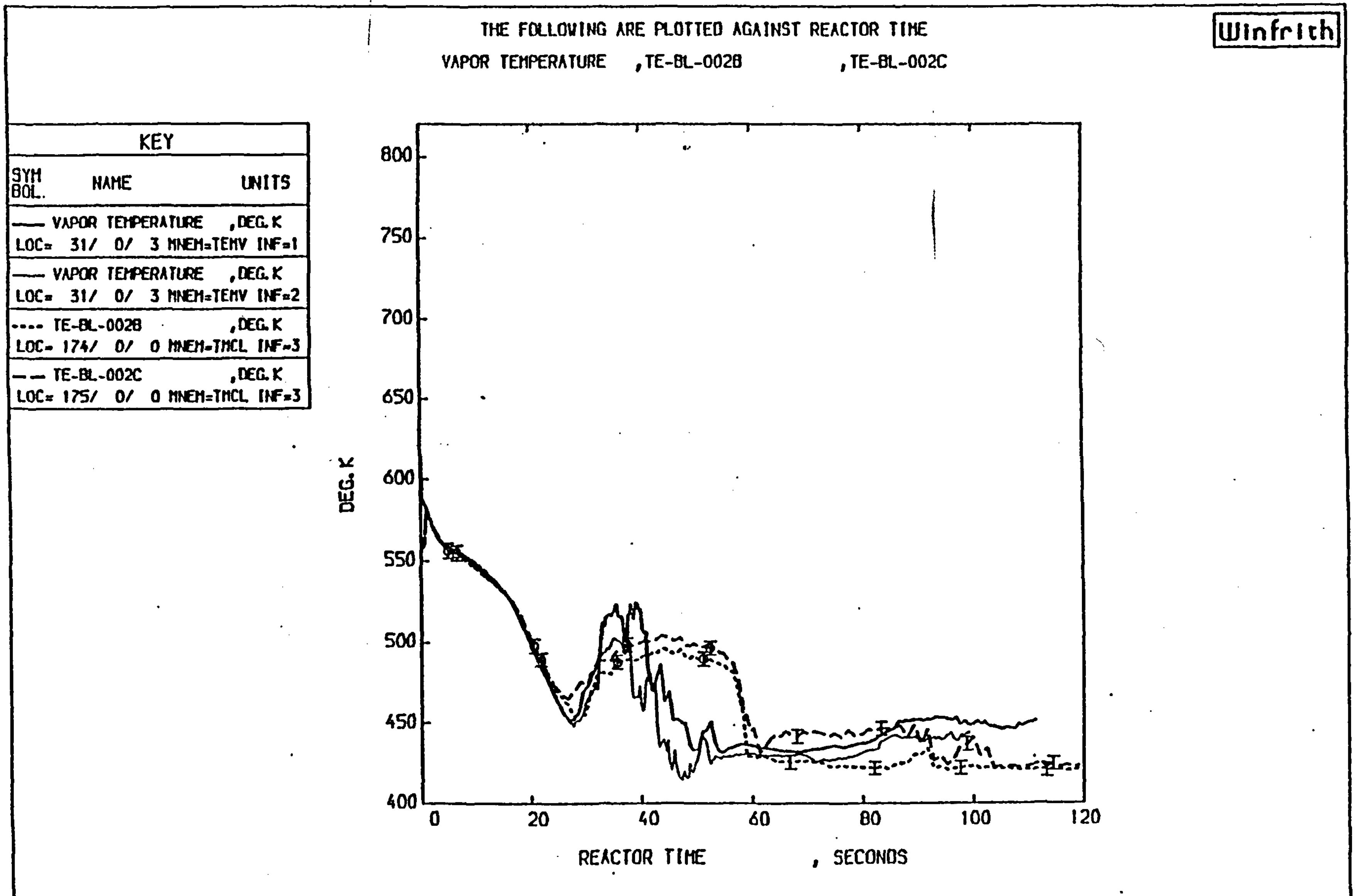

FIGURE 89 INF 1 ORIG, INF 2 ZEROGAP, INF 3 EXP
BROKEN LOOP HOT LEG - EXPERIMENTAL LOCATION BL-2

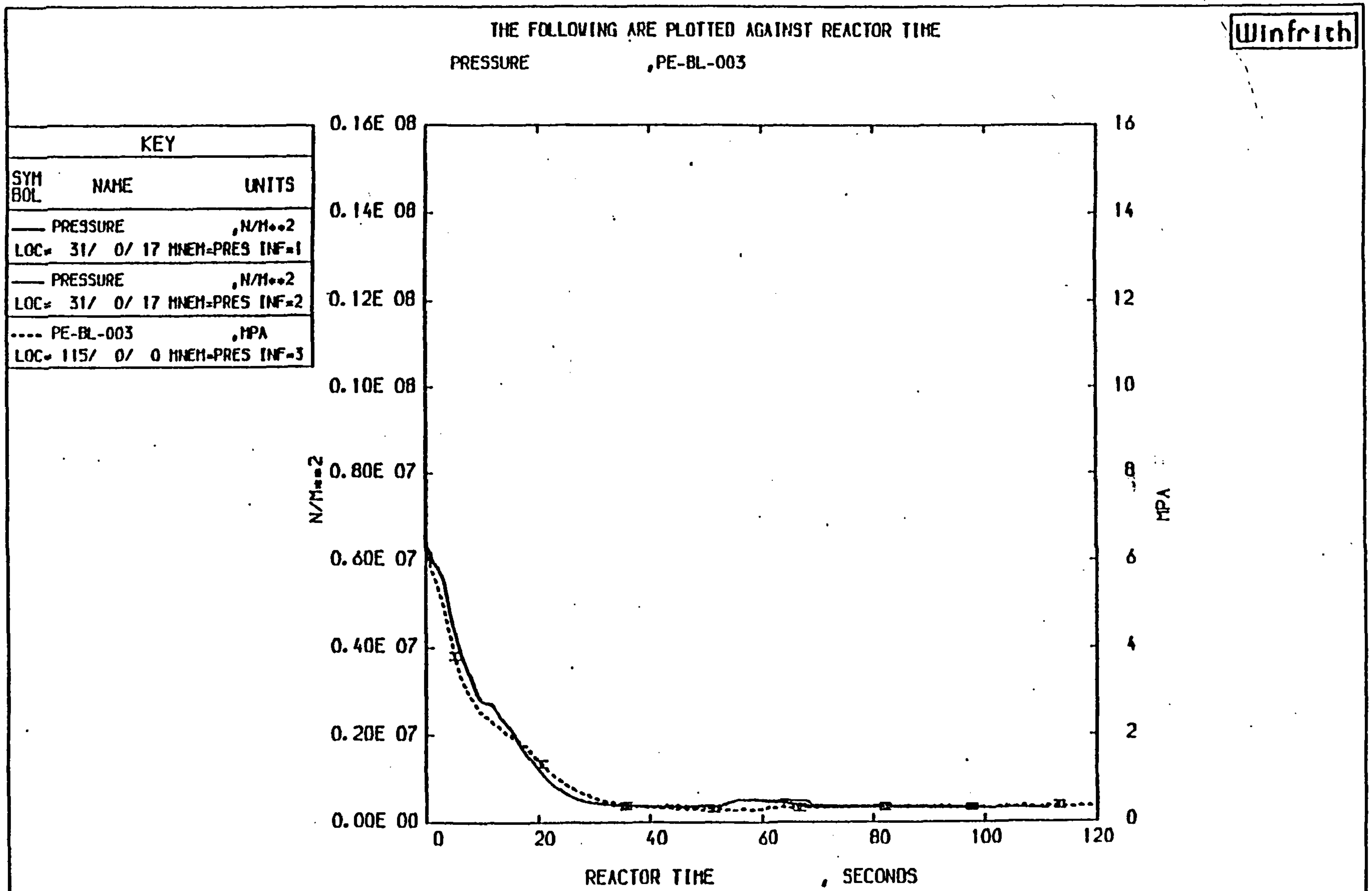

FIGURE 90 INF 1 ORIG, INF 2 ZEROGAP, INF 3 EXP
BROKEN LOOP HOT LEG - EXPERIMENTAL LOCATION BL-3

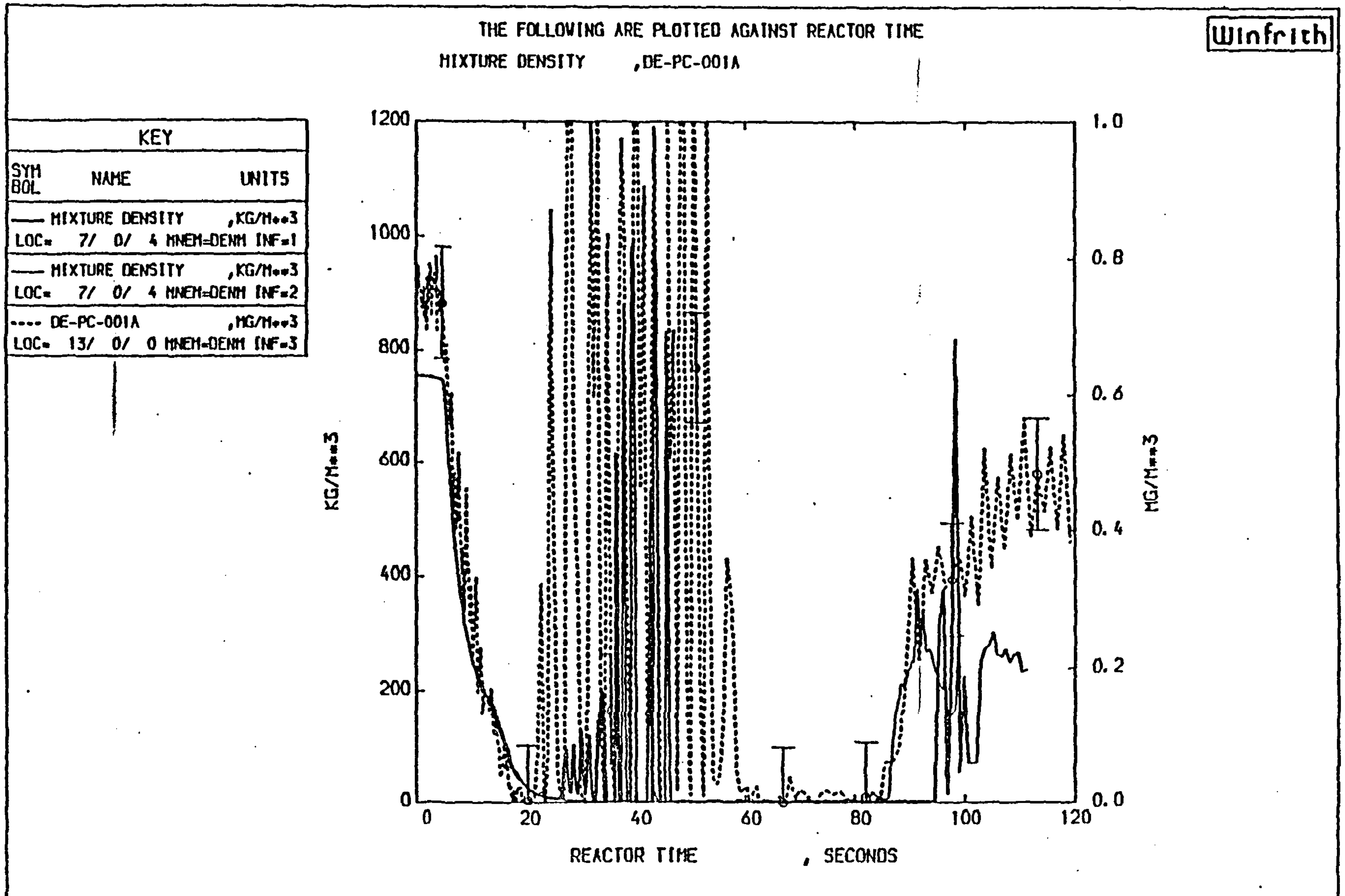

FIGURE 91 INF 1 ORIG, INF 2 ZEROGAP, INF 3 EXP
INTACT LOOP COLD LEG - EXPERIMENTAL LOCATION PC-1

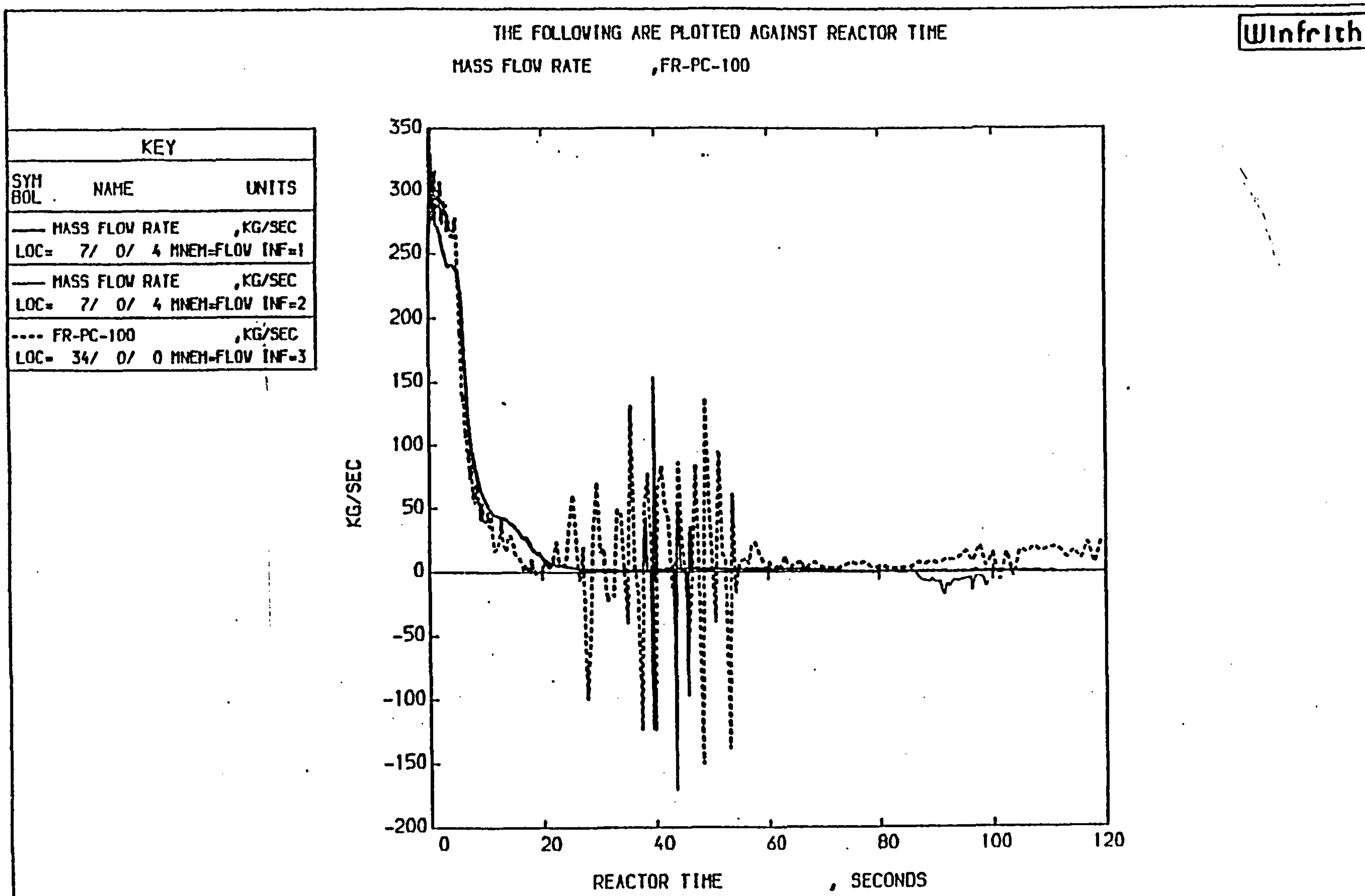

FIGURE 92 INF 1 ORIG, INF 2 ZEROGAP, INF 3 EXP
INTACT LOOP COLD LEG - EXPERIMENTAL LOCATION PC-1

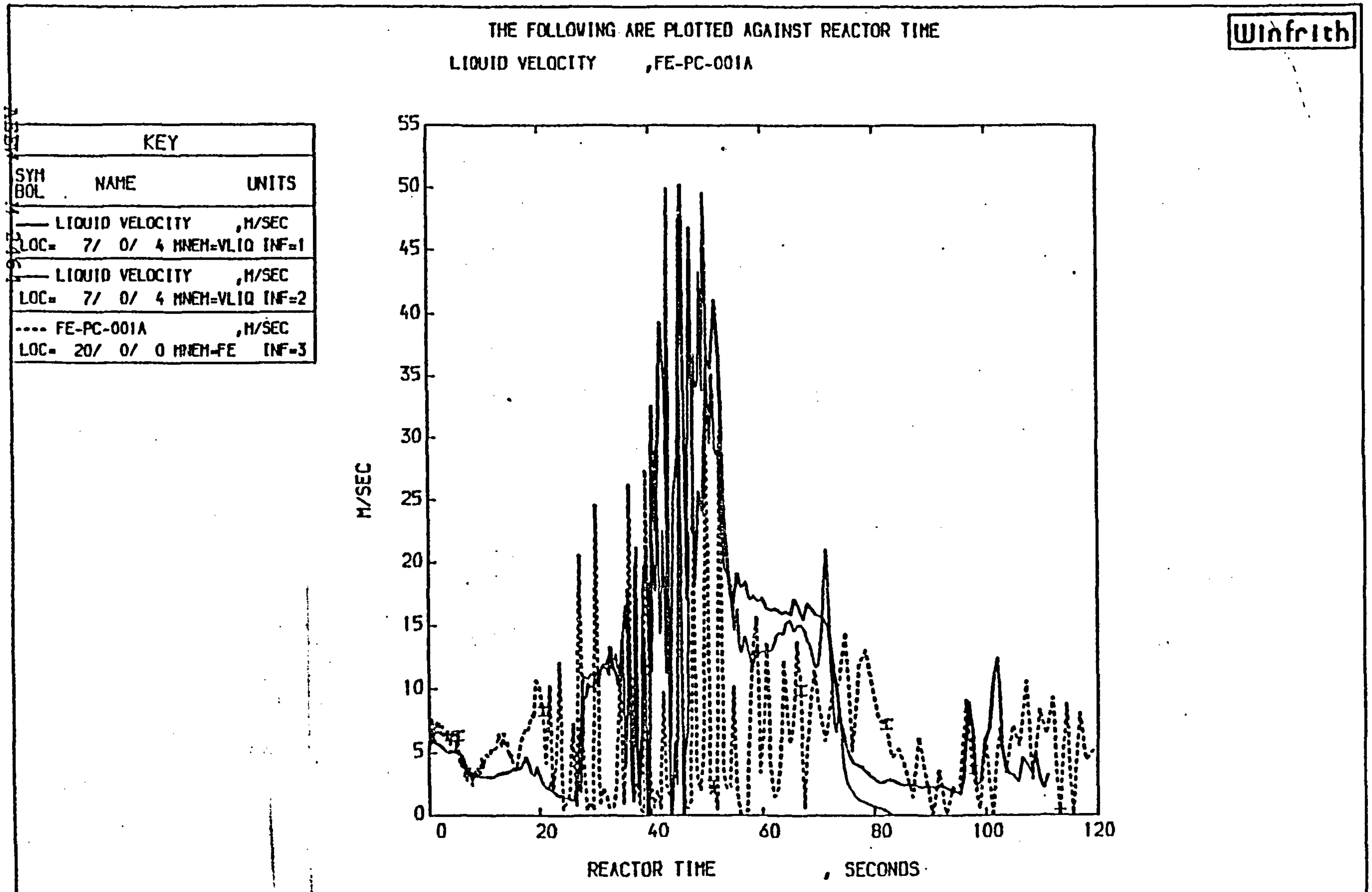

FIGURE 93 INF 1 ORIG, INF 2 ZEROGAP, INF 3 EXP
INTACT LOOP COLD LEG - EXPERIMENTAL LOCATION PC-1

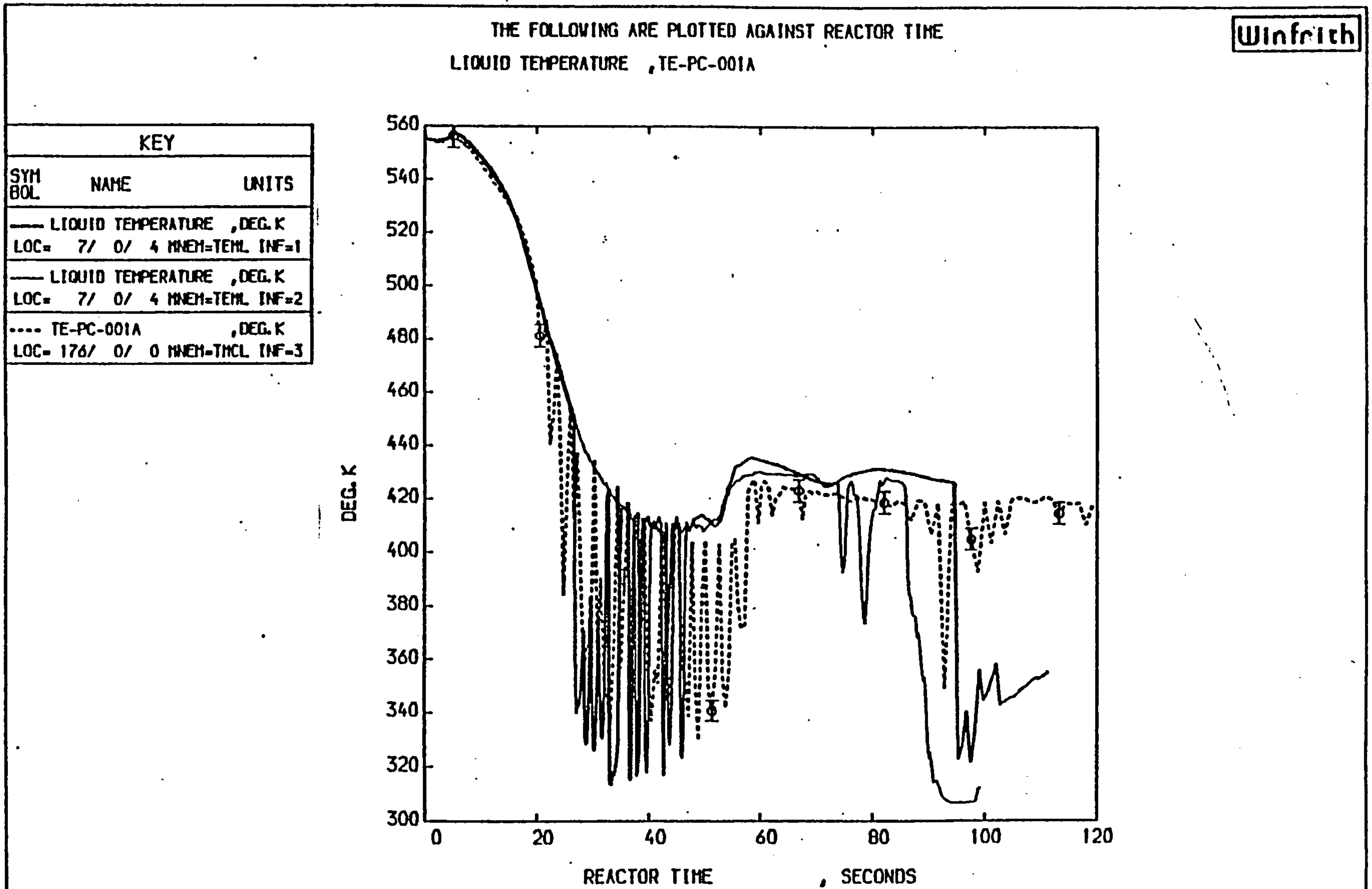

FIGURE 94 INF 1 ORIG, INF 2 ZEROGAP, INF 3 EXP
INTACT LOOP COLD LEG - EXPERIMENTAL LOCATION PC-1

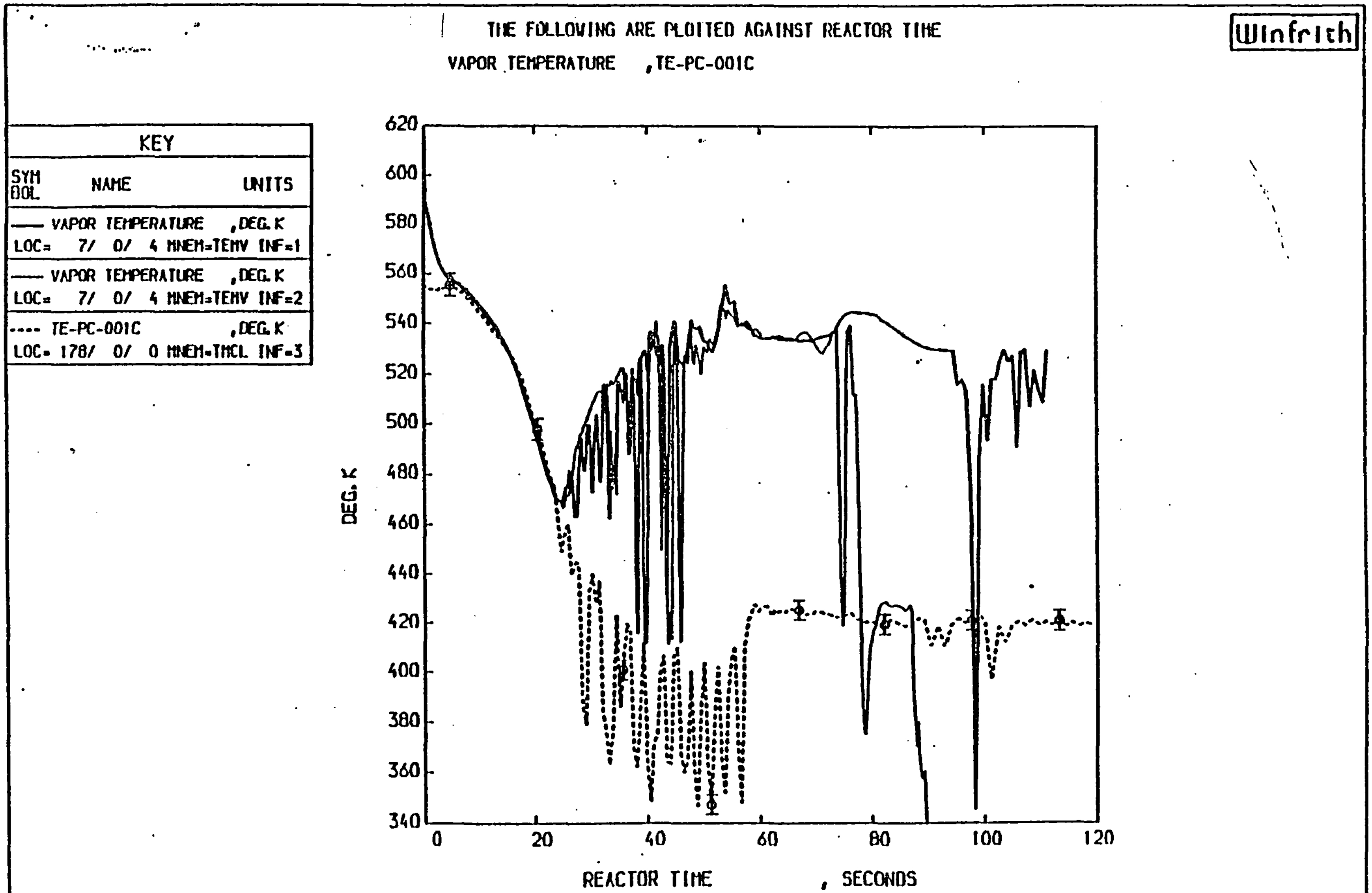

FIGURE 95 INF 1 ORIG, INF 2 ZEROGAP, INF 3 EXP
INTACT LOOP COLD LEG - EXPERIMENTAL LOCATION PC-1.

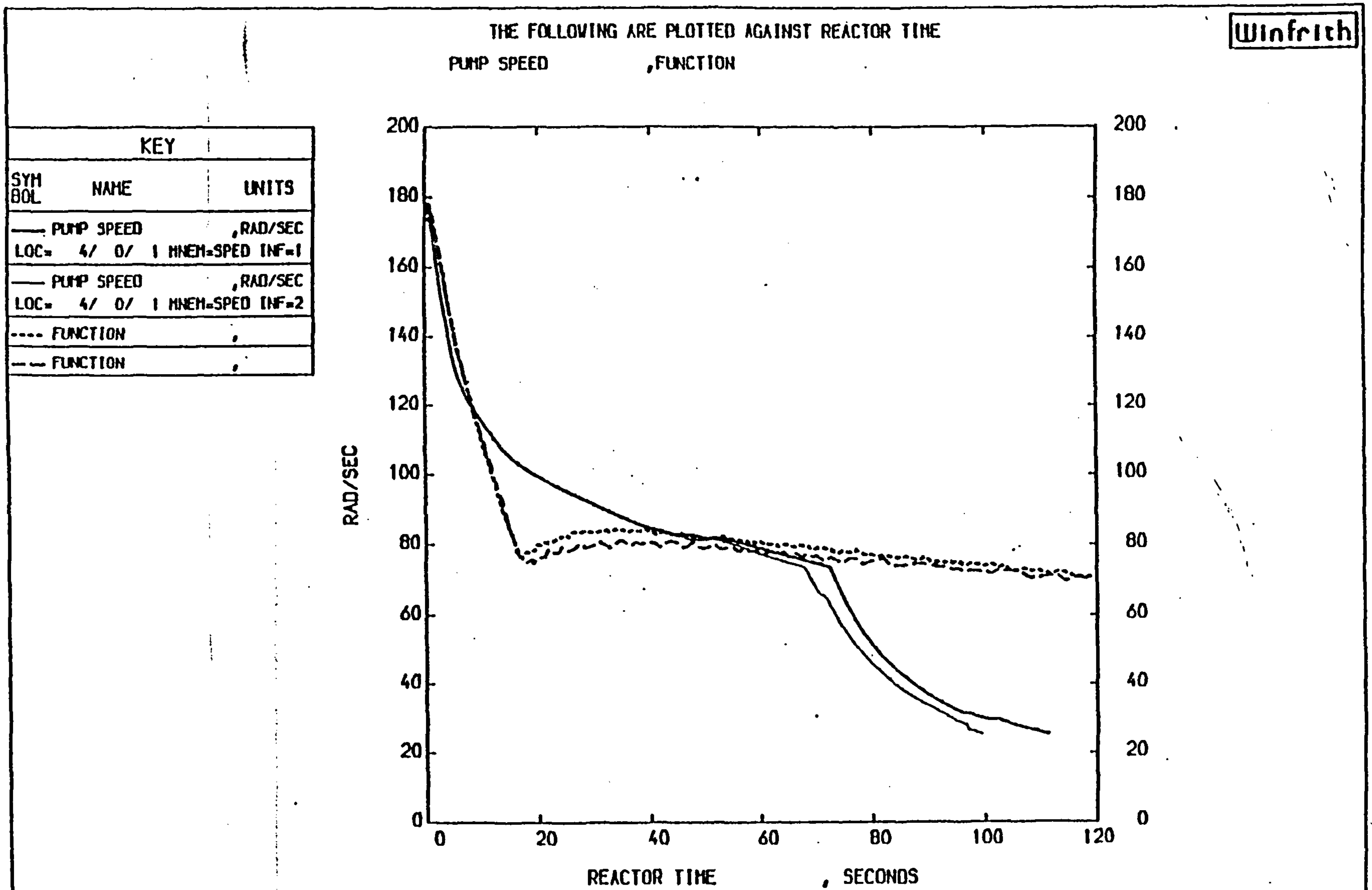

FIGURE 96 INF 1 ORIG, INF 2 ZEROGAP, INF 3 EXP
PUMP SPEED

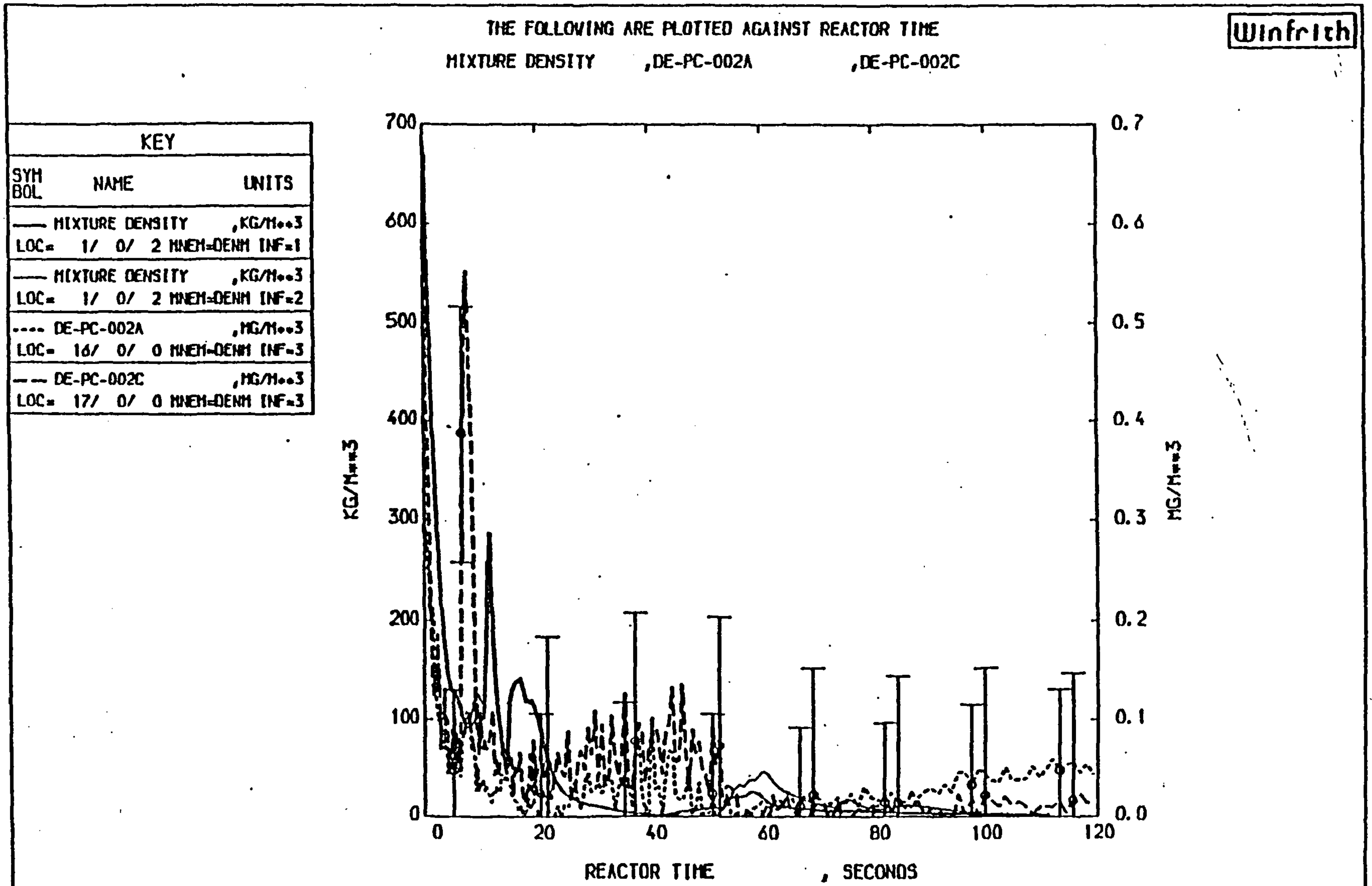

FIGURE 97 INF 1 ORIG, INF 2 ZEROGAP, INF 3 EXP
INTACT LOOP HOT LEG - EXPERIMENTAL LOCATION PC-2

Winfrith

THE FOLLOWING ARE PLOTTED AGAINST REACTOR TIME

MASS FLOW RATE ,FR-PC-201 ,FR-PC-205

KEY		
SYMBOL	NAME	UNITS
——	MASS FLOW RATE	,KG/SEC
	LOC= 1/ 0/ 2 MNEM=FLOW INF=1	
——	MASS FLOW RATE	,KG/SEC
	LOC= 1/ 0/ 2 MNEM=FLOW INF=2	
----	FR-PC-201	,KG/SEC
	LOC= 37/ 0/ 0 MNEM=FLOW INF=3	
— —	FR-PC-205	,KG/SEC
	LOC= 38/ 0/ 0 MNEM=FLOW INF=3	

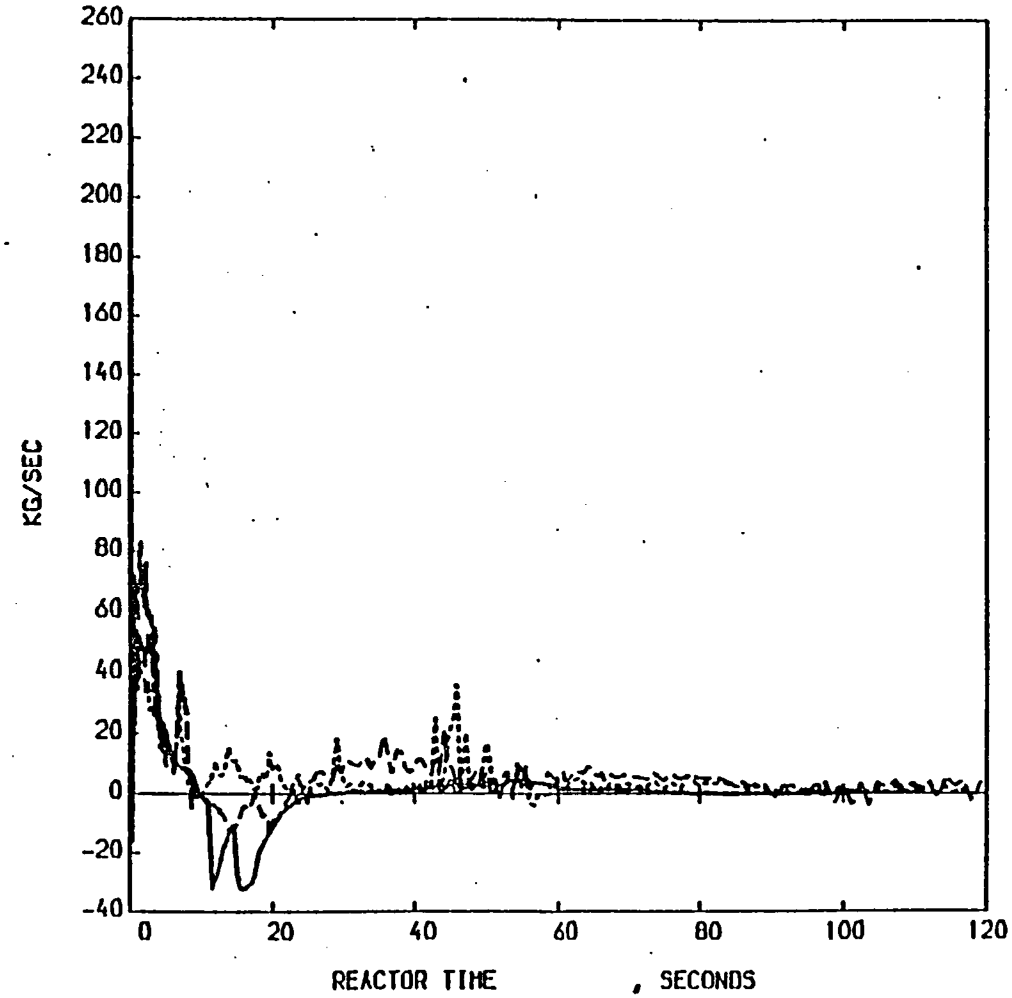

FIGURE 98 INF 1 ORIG, INF 2 ZEROGAP, INF 3 EXP
INTACT LOOP HOT LEG - EXPERIMENTAL LOCATION PC-2

THE FOLLOWING ARE PLOTTED AGAINST REACTOR TIME

LIQUID TEMPERATURE ,TE-PC-002A

Winfrith

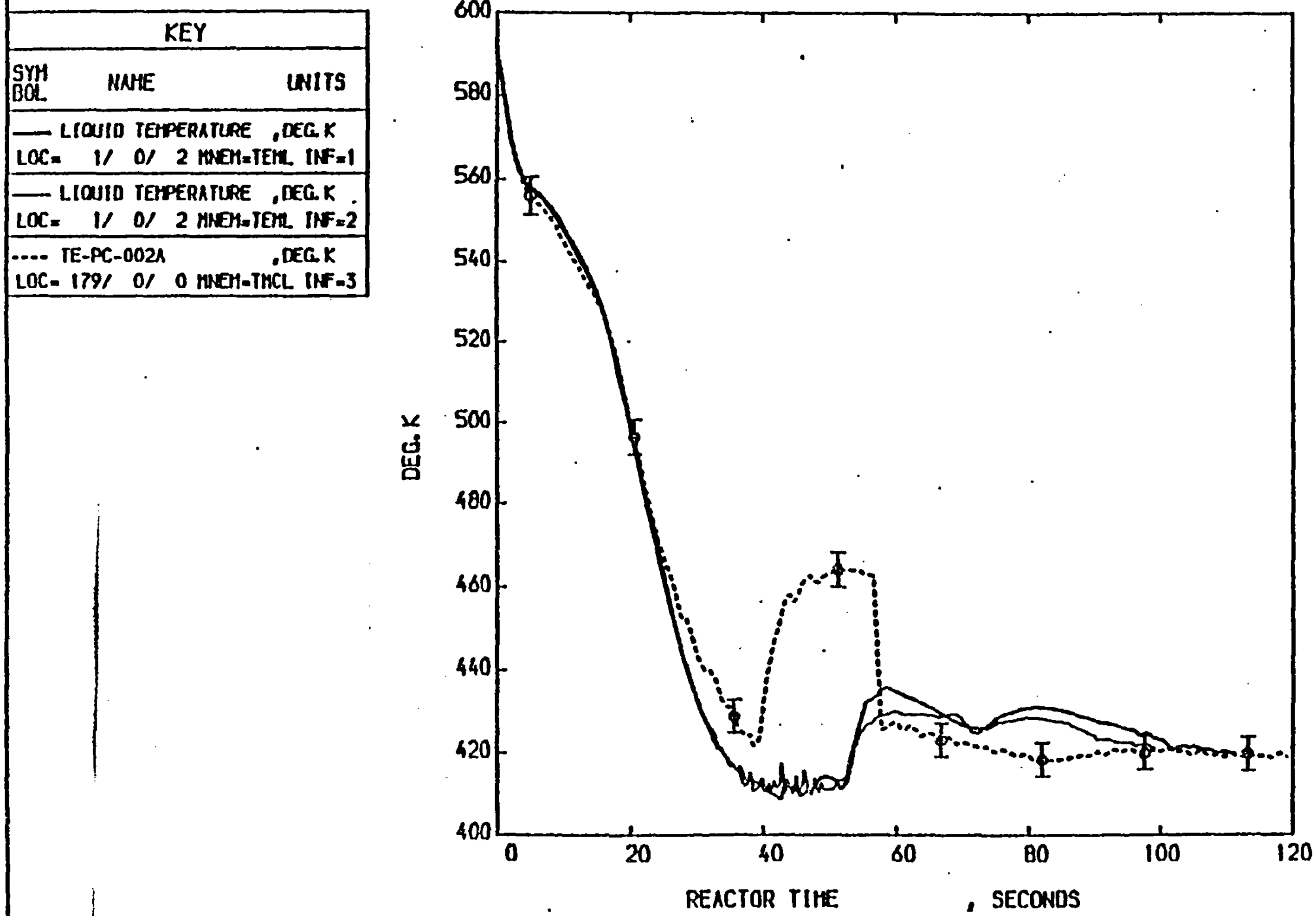

FIGURE 99 INF 1 ORIG, INF 2 ZEROGAP, INF 3 EXP
INTACT LOOP HOT LEG - EXPERIMENTAL LOCATION PC-2

Winfrith

THE FOLLOWING ARE PLOTTED AGAINST REACTOR TIME

VAPOR TEMPERATURE ,TE-PC-002A ,TE-PC-002B
TE-PC-002C

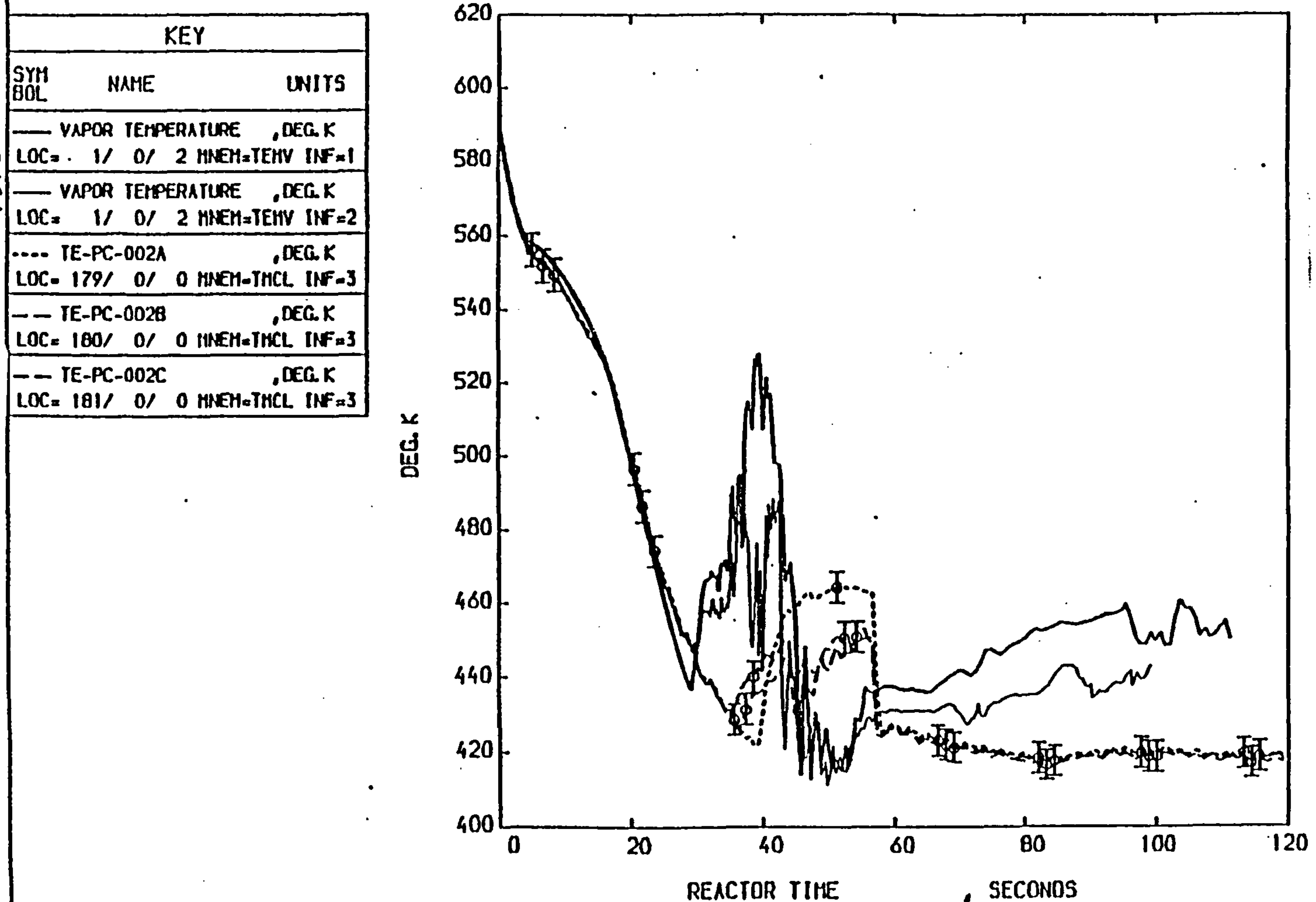

FIGURE 100 INF 1 ORIG, INF 2 ZEROGAP, INF 3 EXP
INTACT LOOP HOT LEG - EXPERIMENTAL LOCATION PC-2

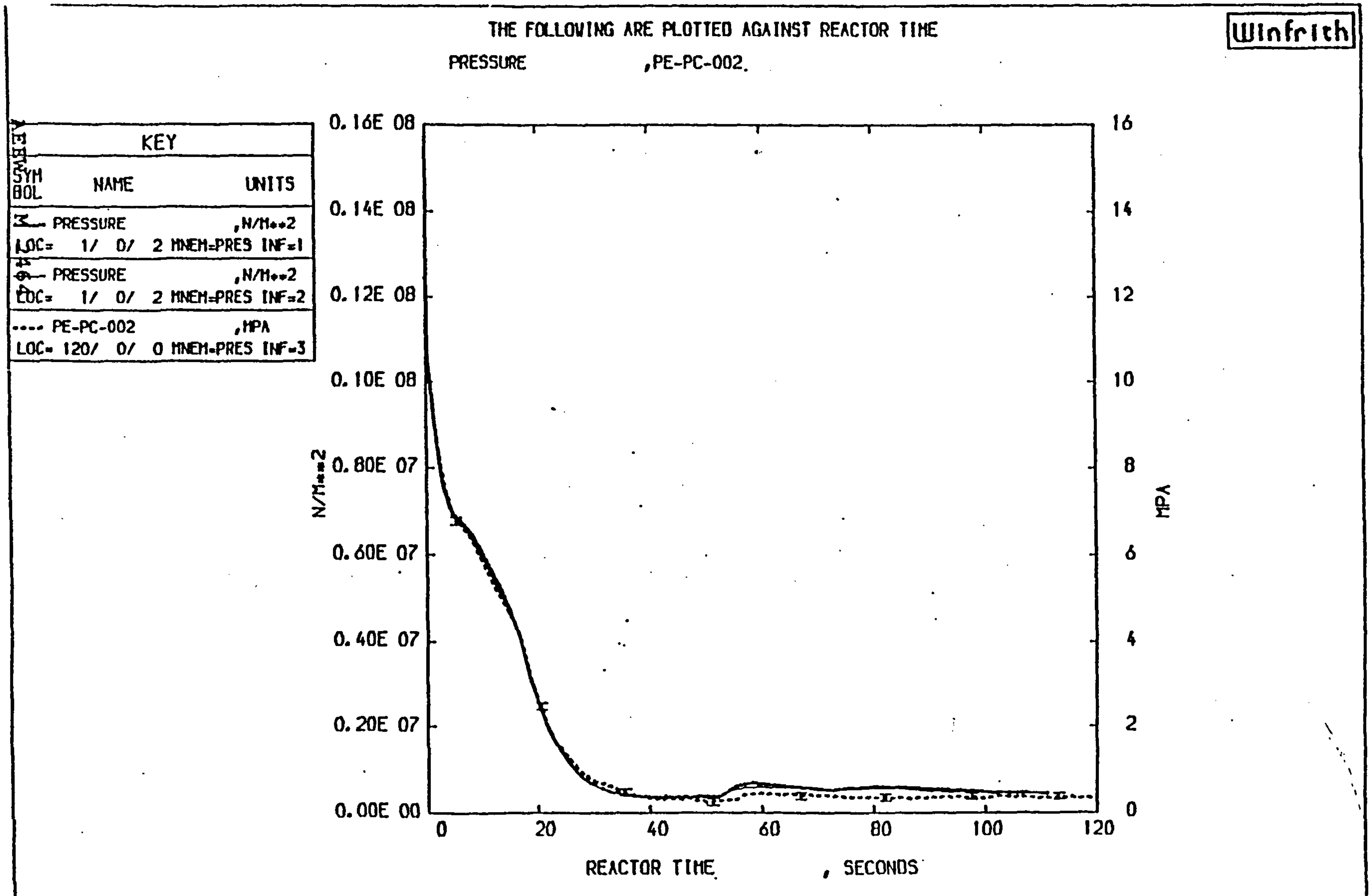

FIGURE 101 INF 1 ORIG, INF 2 ZEROGAP, INF 3 EXP
INTACT LOOP HOT LEG - EXPERIMENTAL LOCATION PC-2

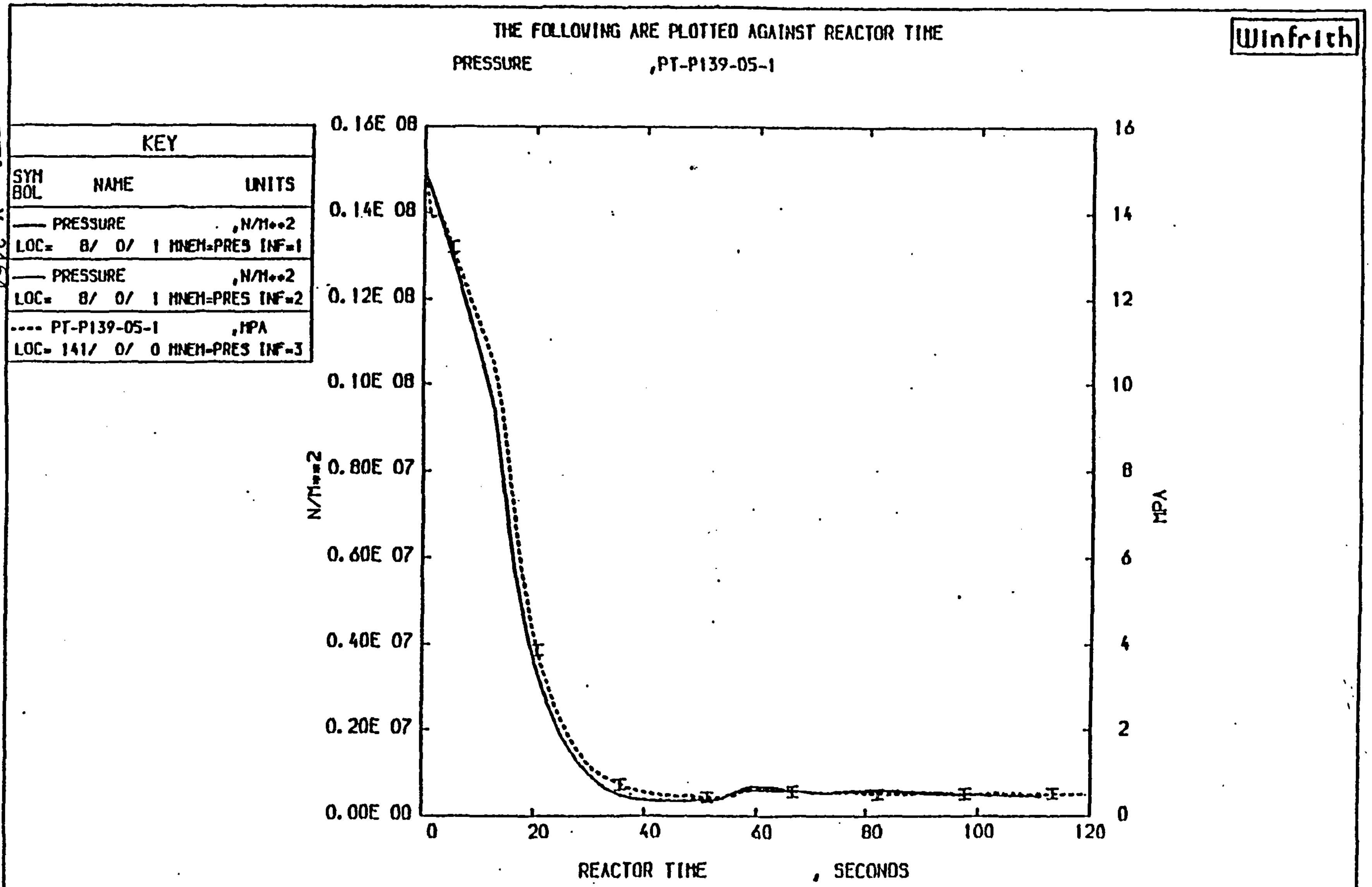

FIGURE 102 INF 1 ORIG, INF 2 ZEROGAP, INF 3 EXP
INTACT LOOP HOT LEG - PRESSURIZER

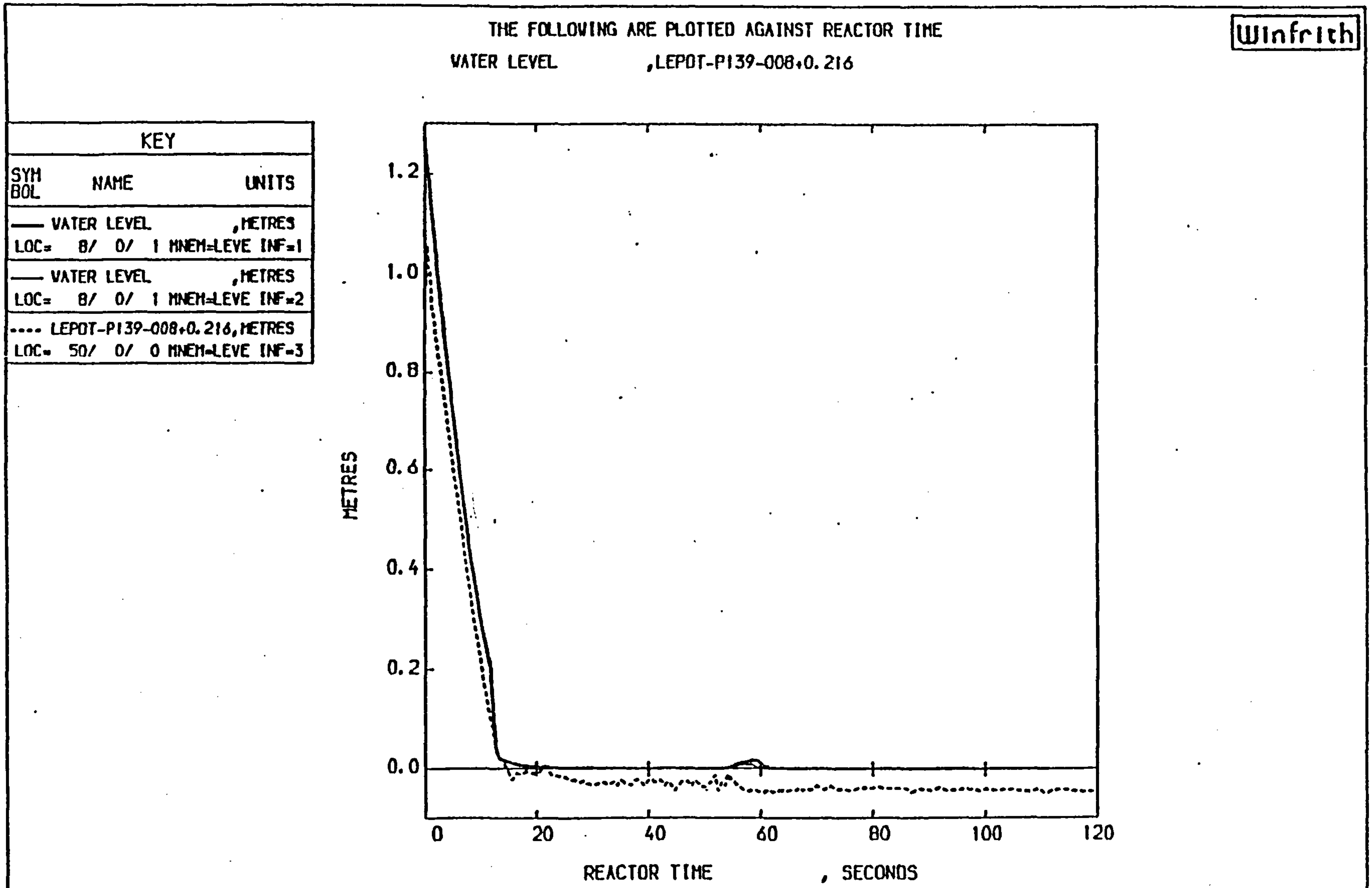

FIGURE 103 INF 1 ORIG, INF 2 ZEROGAP, INF 3 EXP
INTACT LOOP HOT LEG - PRESSURIZER

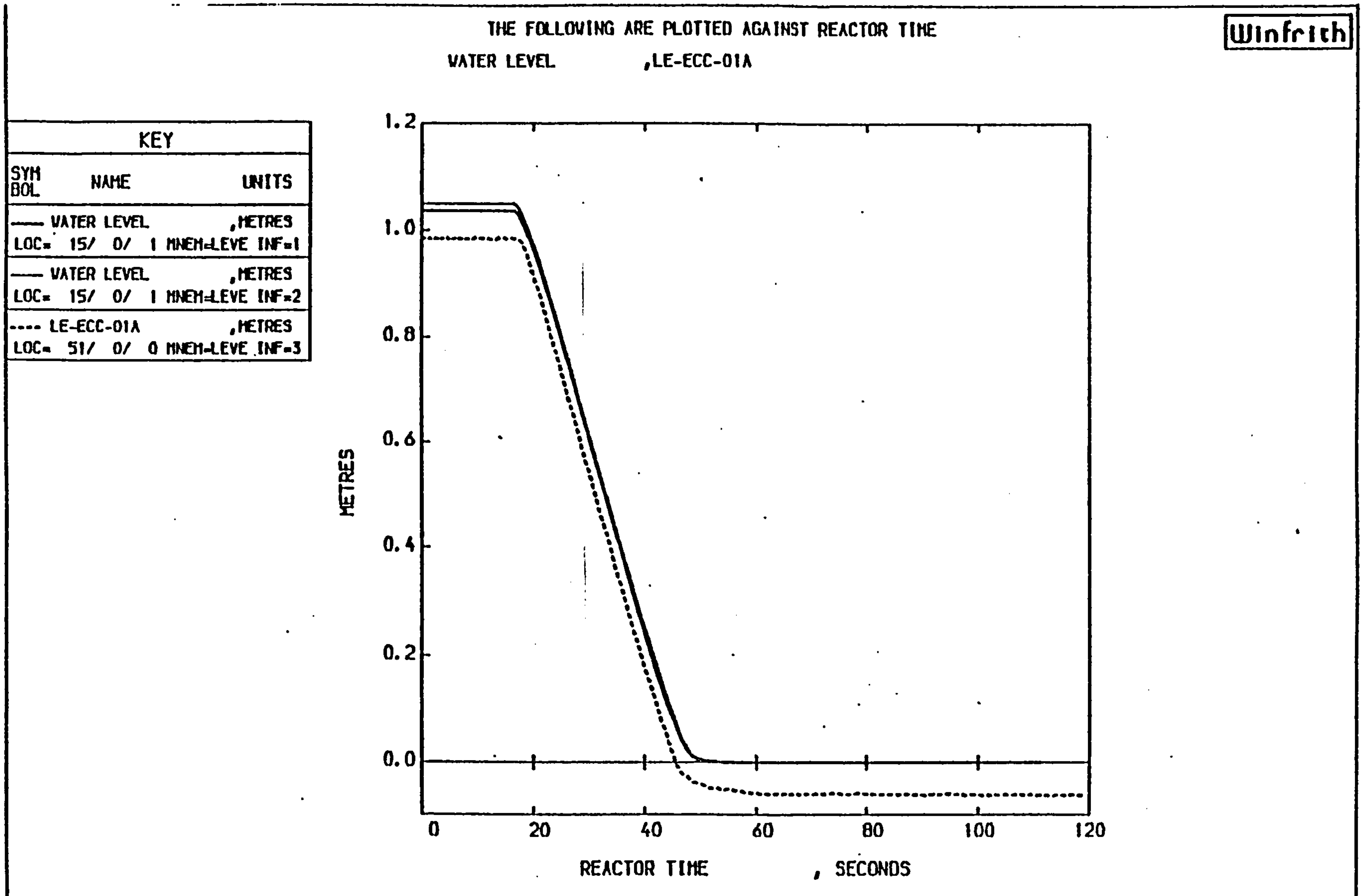

FIGURE 104 INF 1 ORIG, INF 2 ZEROGAP, INF 3 EXP
EMERGENCY CORE COOLING SYSTEM

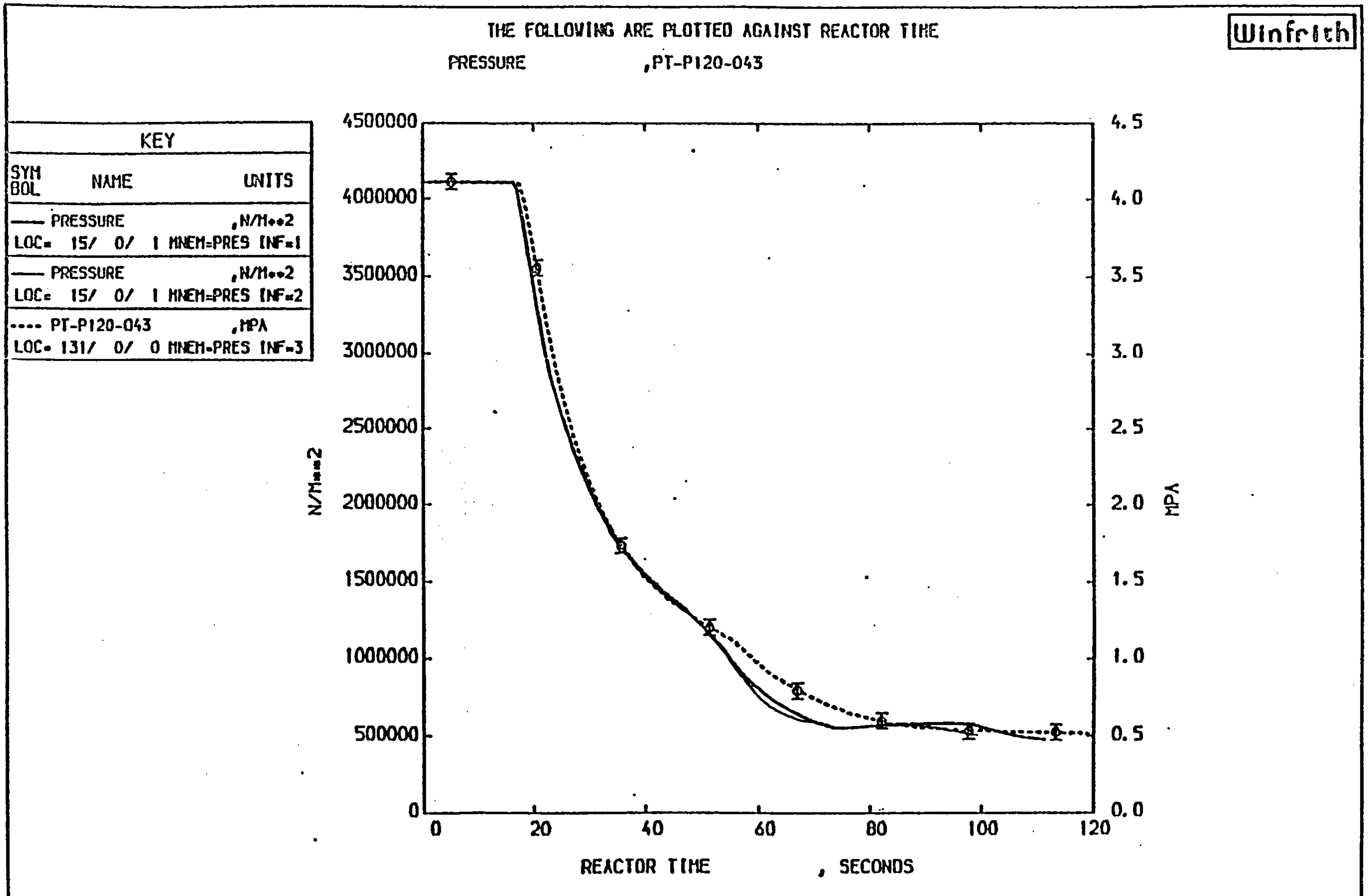

FIGURE 105 INF 1 ORIG, INF 2 ZEROGAP, INF 3 EXP
EMERGENCY CORE COOLING SYSTEM

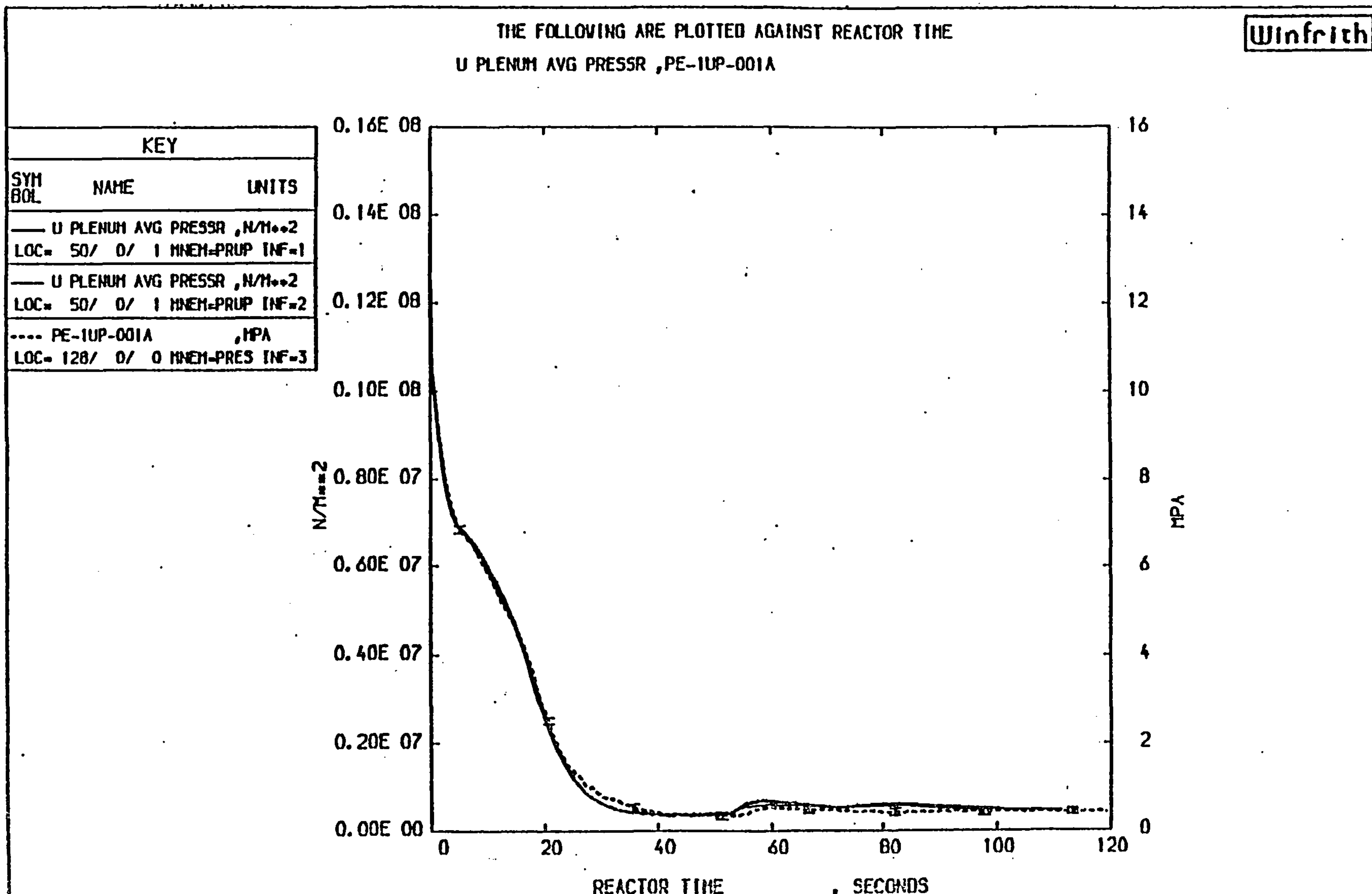

FIGURE 106 INF 1 ORIG, INF 2 ZEROGAP, INF 3 EXP
UPPER PLENUM PRESSURE

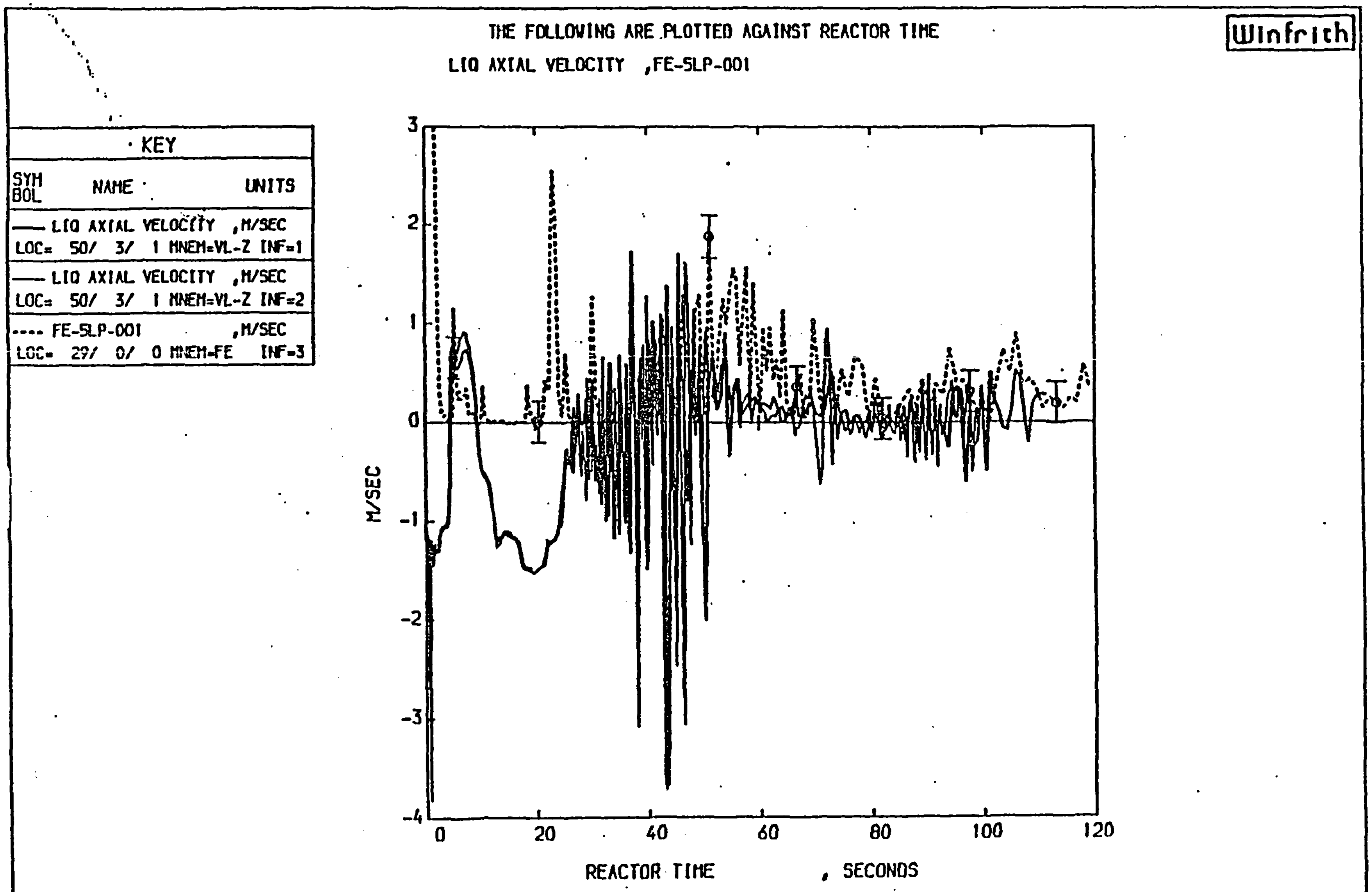

FIGURE 107 INF 1 ORIG, INF 2 ZEROGAP, INF 3 EXP
LOWER PLENUM LIQUID AXIAL VELOCITY

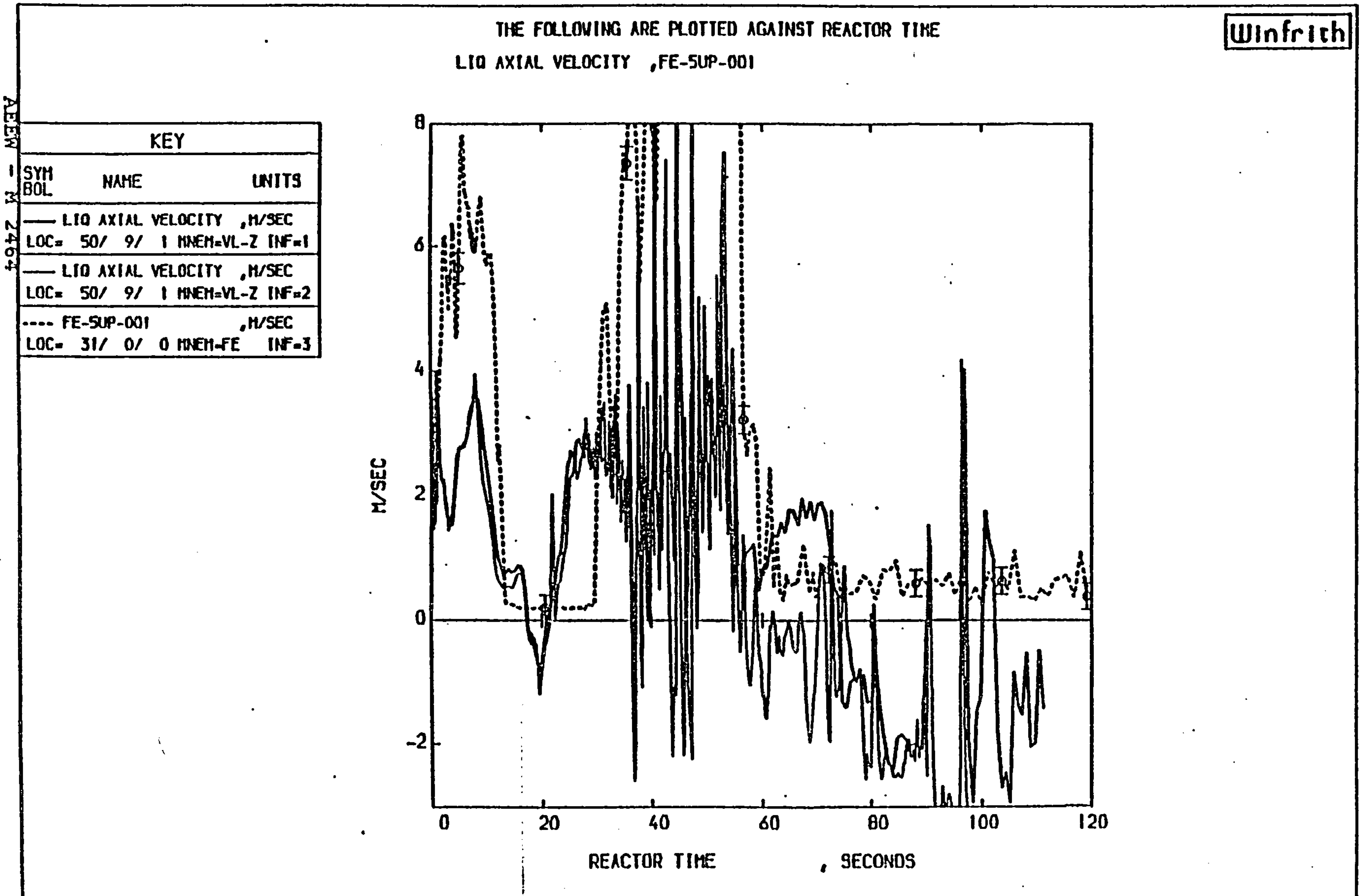

FIGURE 108 INF 1 ORIG, INF 2 ZEROGAP, INF 3 EXP
UPPER PLENUM LIQUID AXIAL VELOCITY

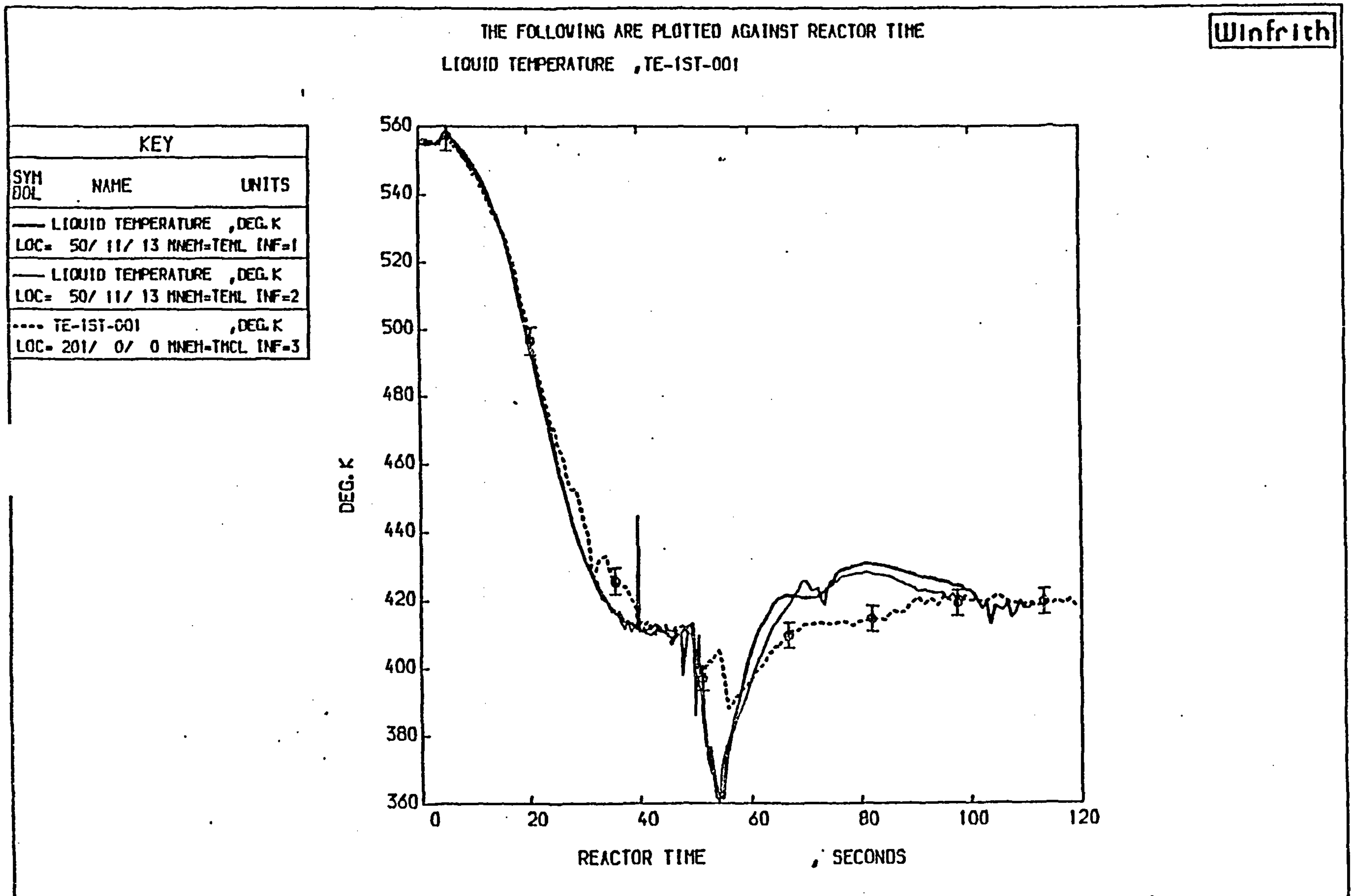

FIGURE 109 . INF 1 ORIG, INF 2 ZEROGAP, INF 3 EXP
DOWNCOMER LIQUID TEMPERATURE AT 5.0 METRES

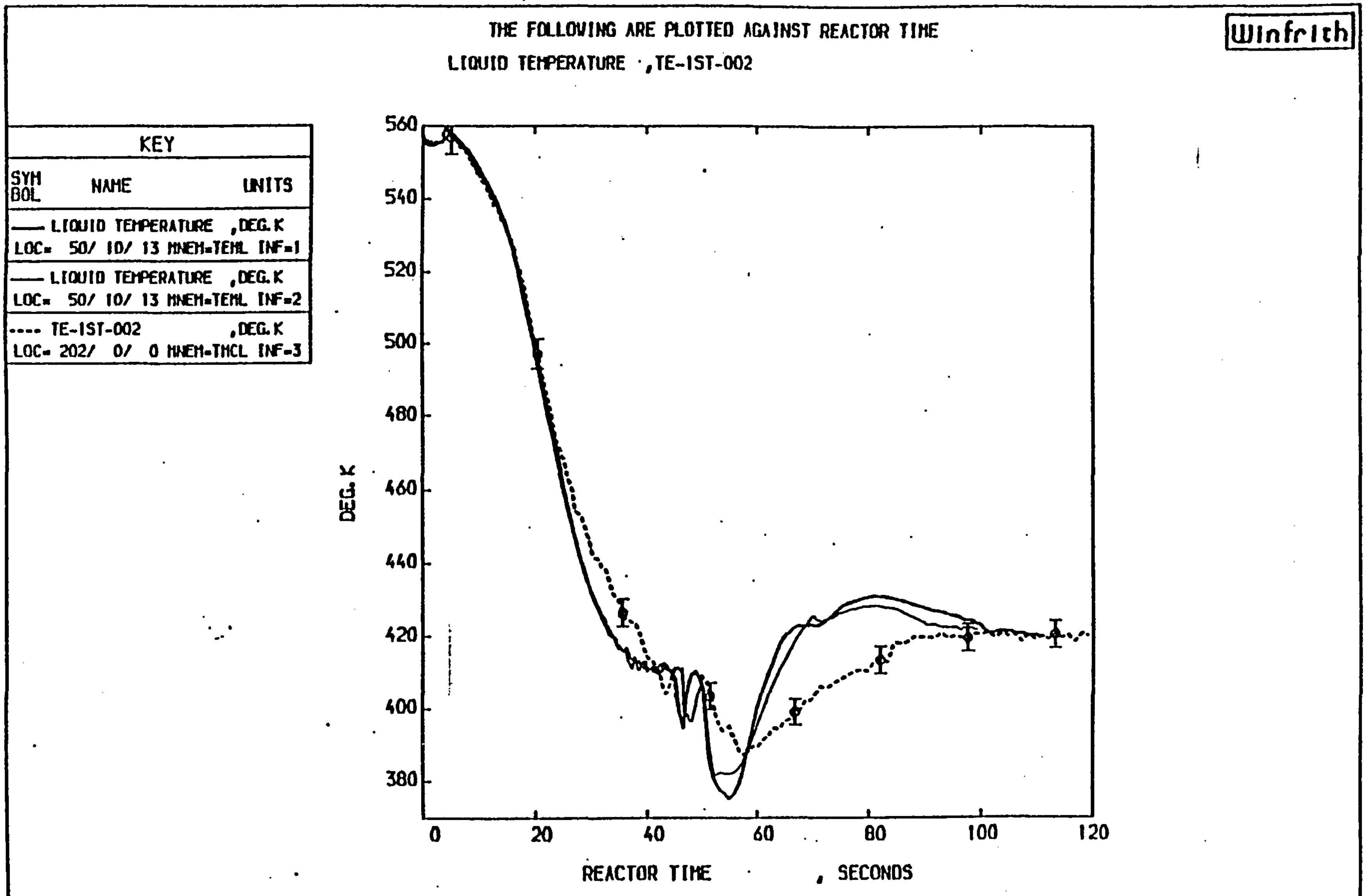

FIGURE 110 INF 1 ORIG, INF 2 ZEROGAP, INF 3 EXP
DOWNCOMER LIQUID TEMPERATURE AT 4.2 METRES

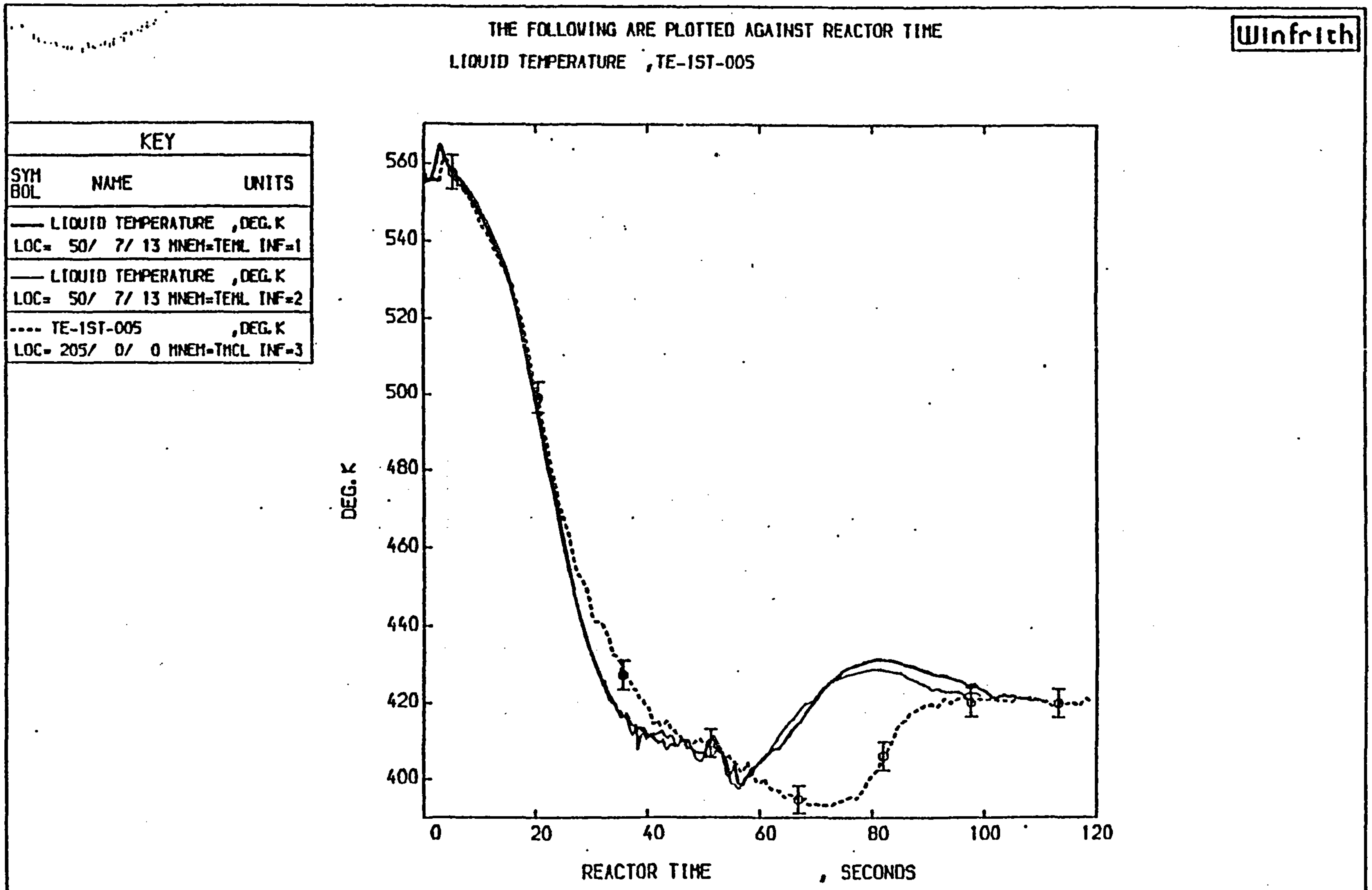

FIGURE 111 INF 1 ORIG, INF 2 ZEROGAP, INF 3 EXP
DOWNCOMER LIQUID TEMPERATURE AT 2.4 METRES

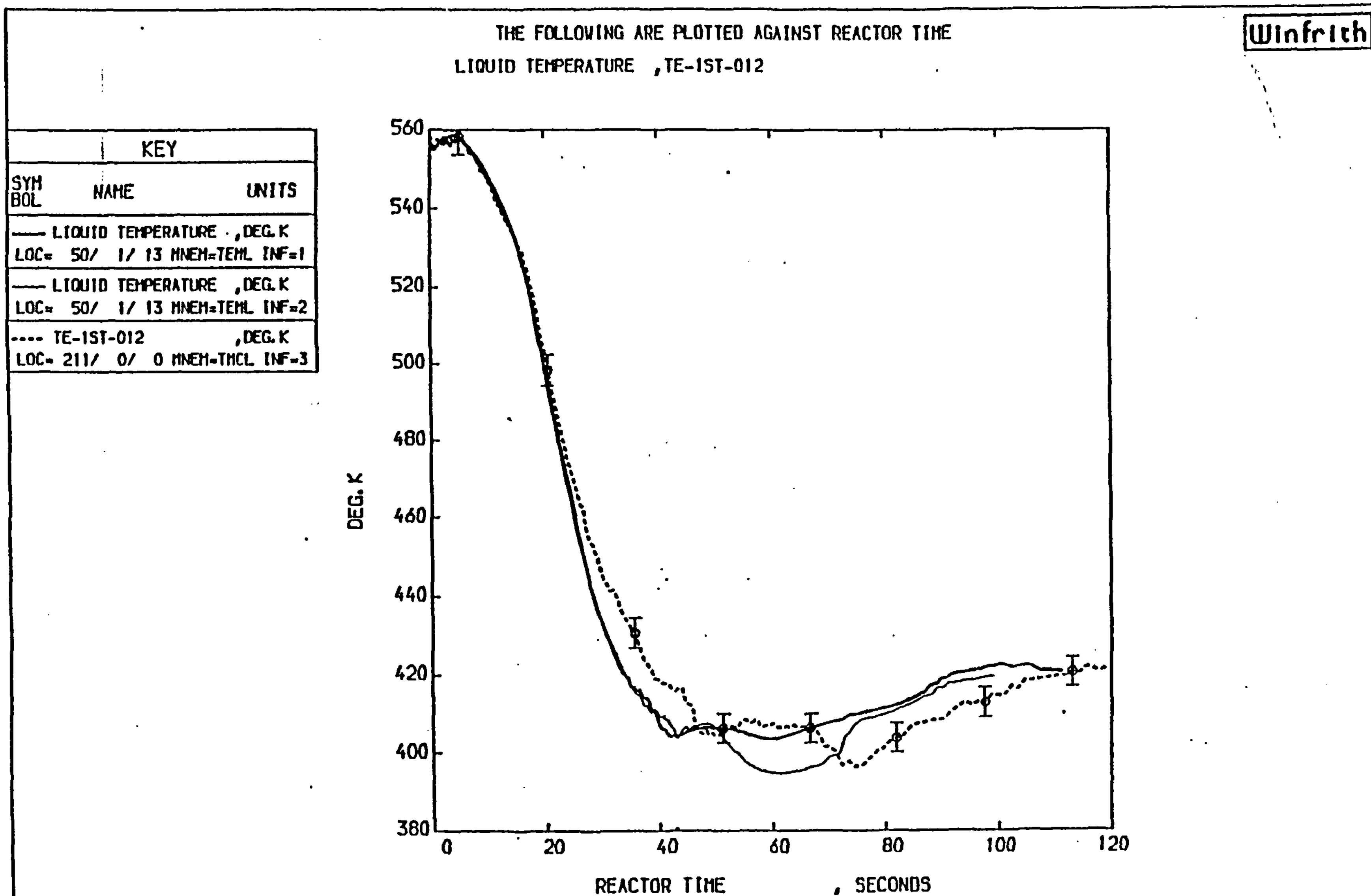

FIGURE 112 INF 1 ORIG, INF 2 ZEROGAP, INF 3 EXP
DOWNCOMER LIQUID TEMPERATURE AT 0.3 METRES

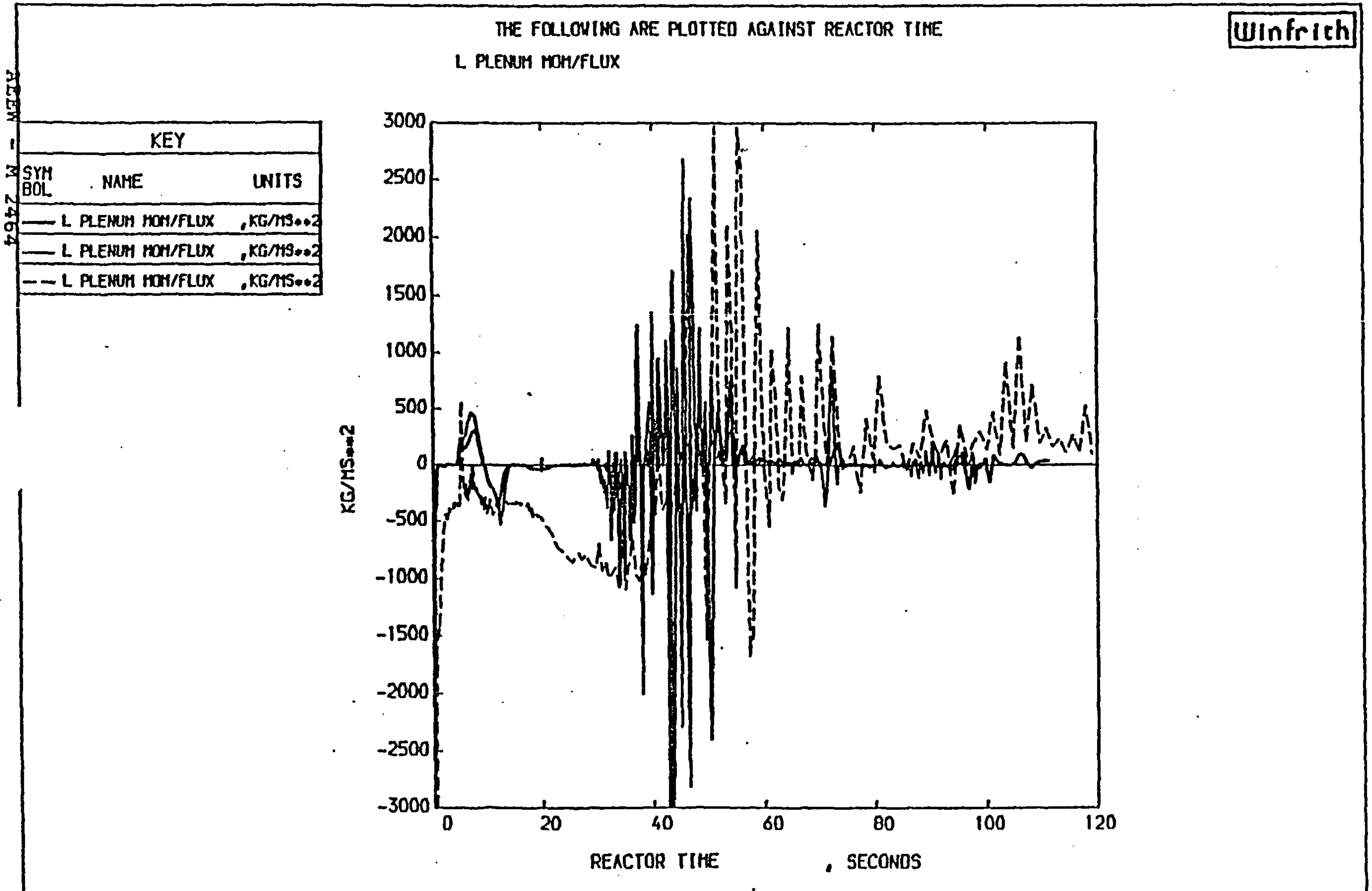

FIGURE 113 LINE 1 ORIG, LINE 2 ZEROGAP, LINE 3 EXP
LOWER PLENUM MOMENTUM FLUX

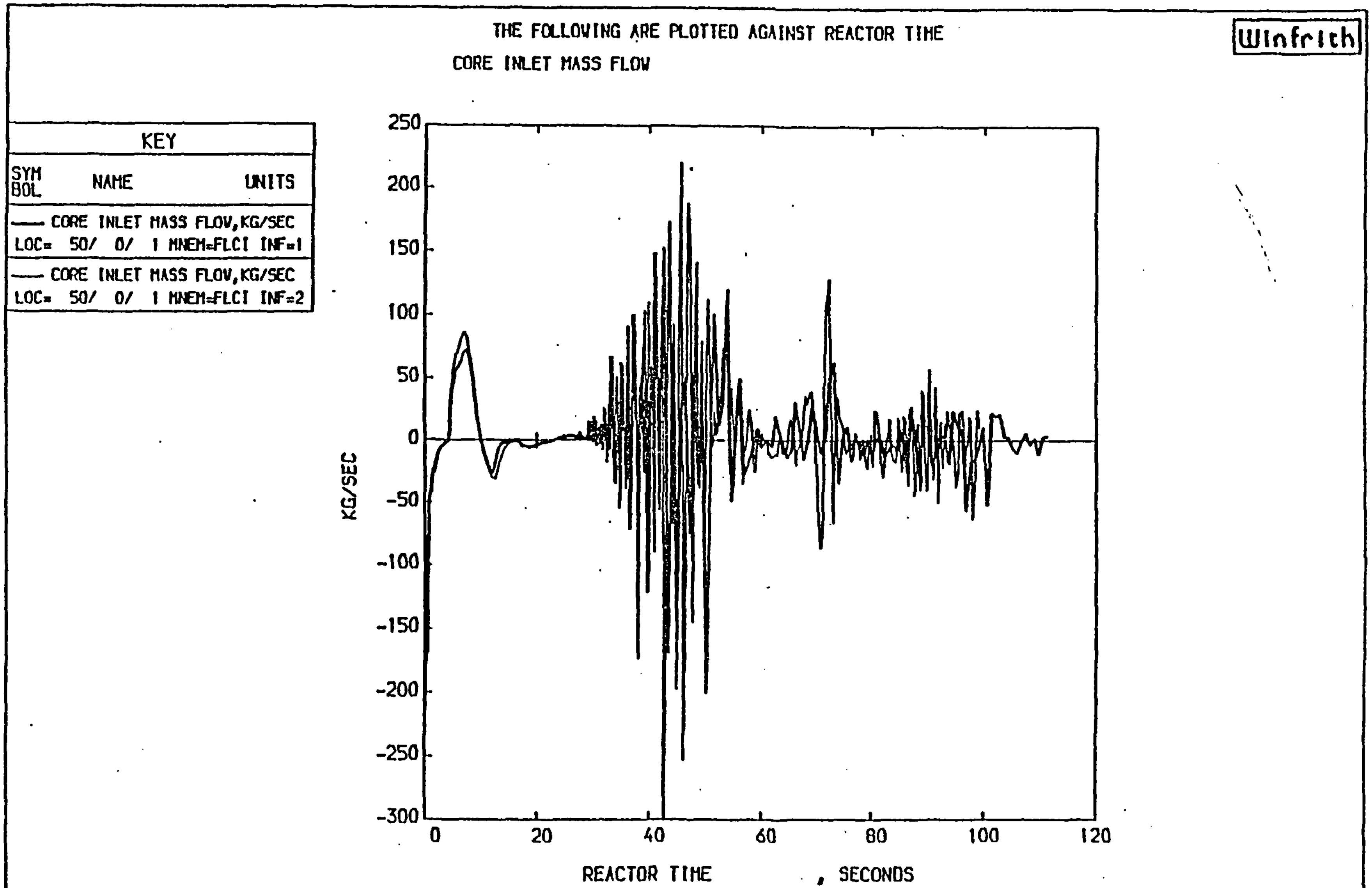

FIGURE 114 INF 1 ORIG, INF 2 ZEROGAP
VESSEL GLOBALS

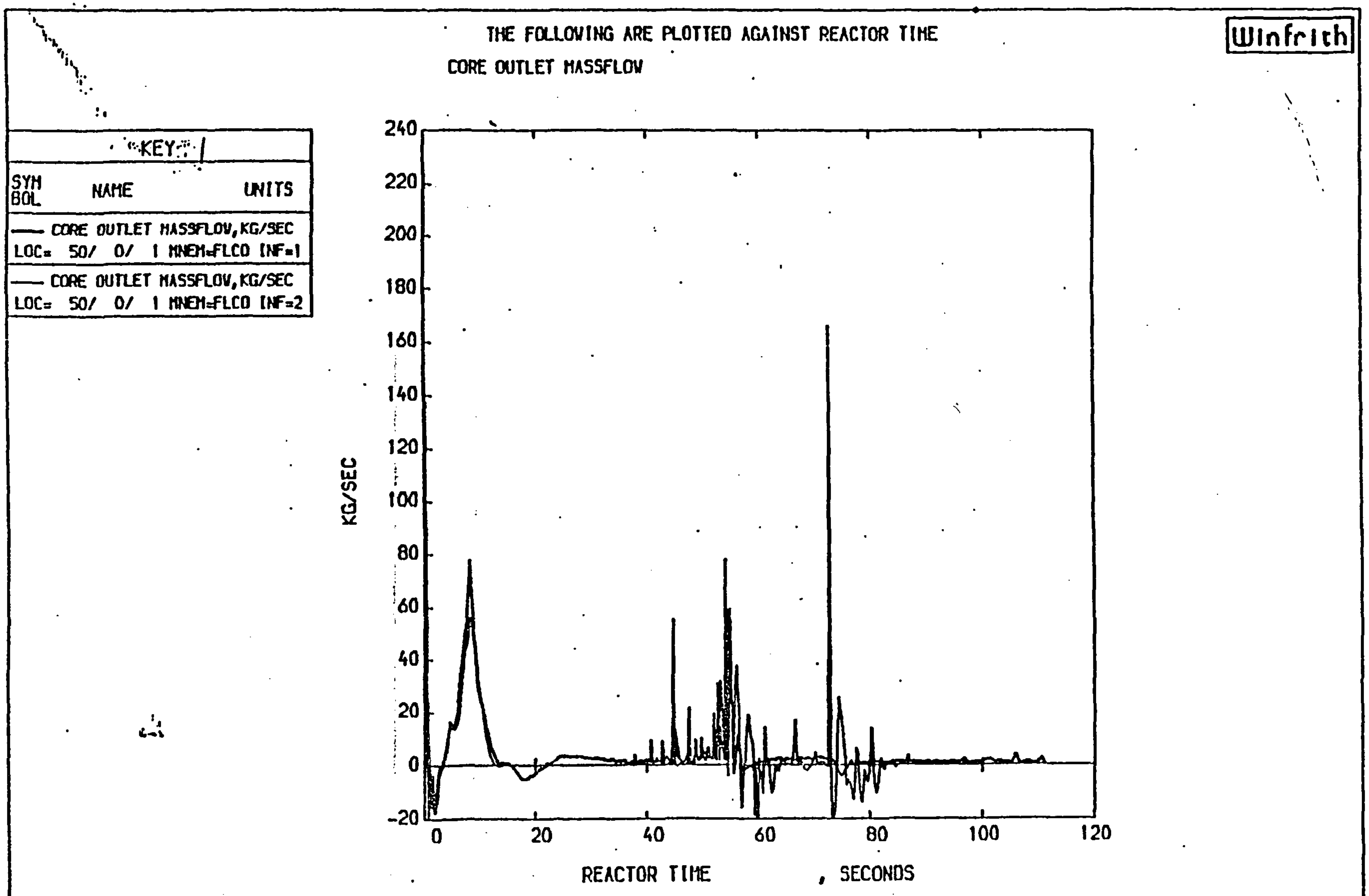

FIGURE 115 INF 1 ORIG, INF 2 ZEROGAP
VESSEL GLOBALS

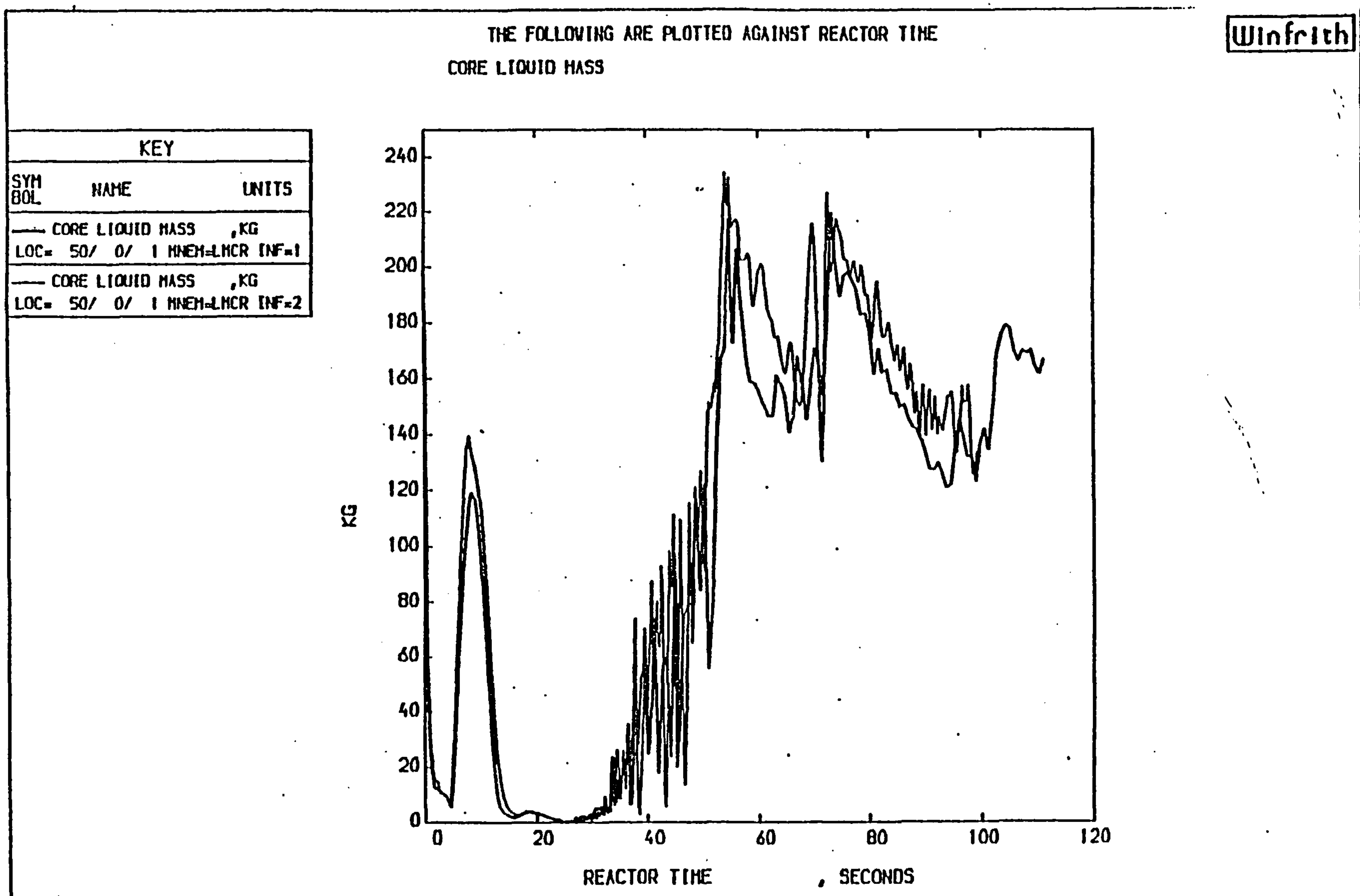

FIGURE 116 INF 1 ORIG, INF 2 ZEROGAP
VESSEL GLOBALS

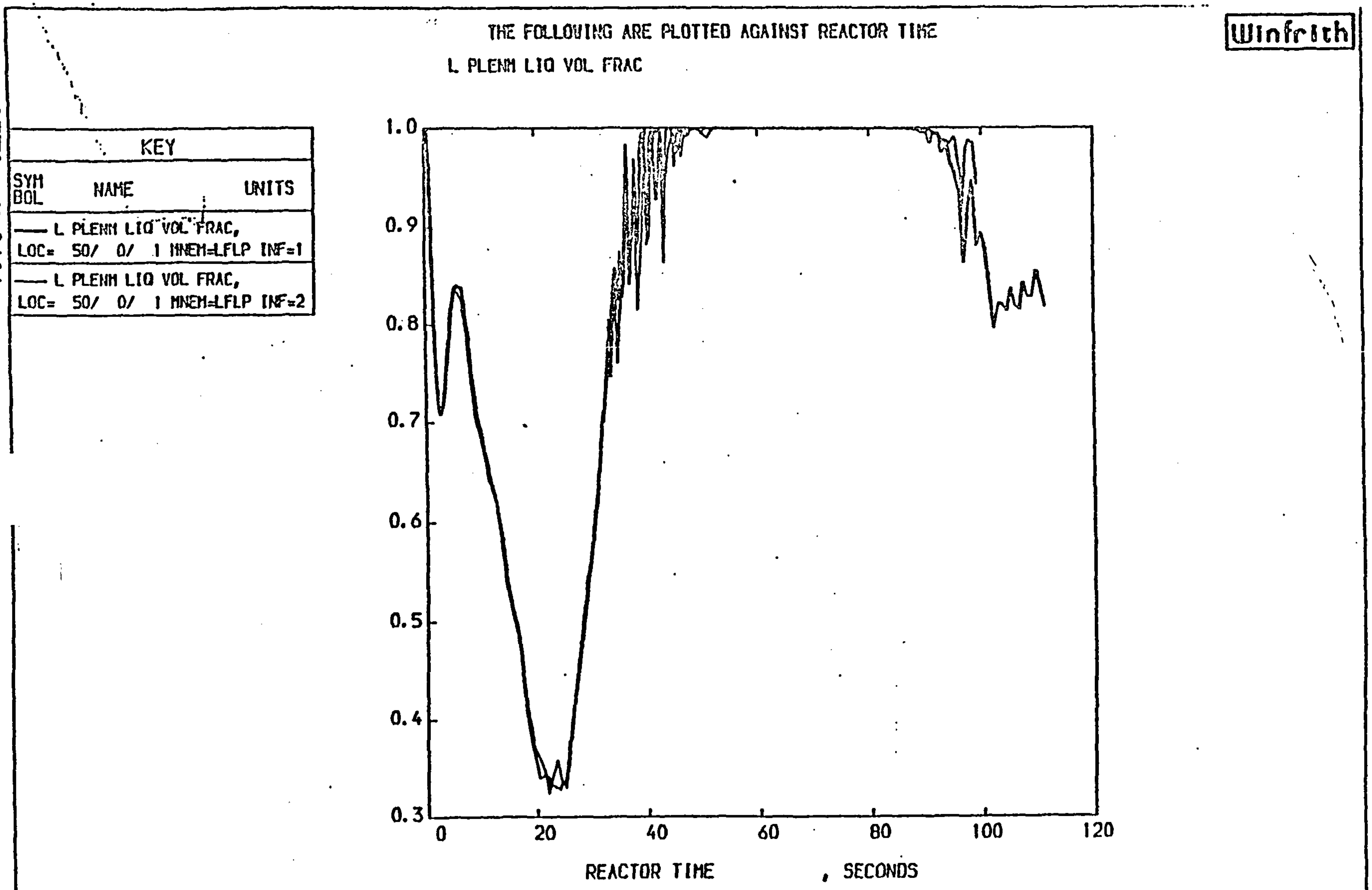

FIGURE 117 INF 1 ORIG, INF 2 ZEROGAP
VESSEL GLOBALS

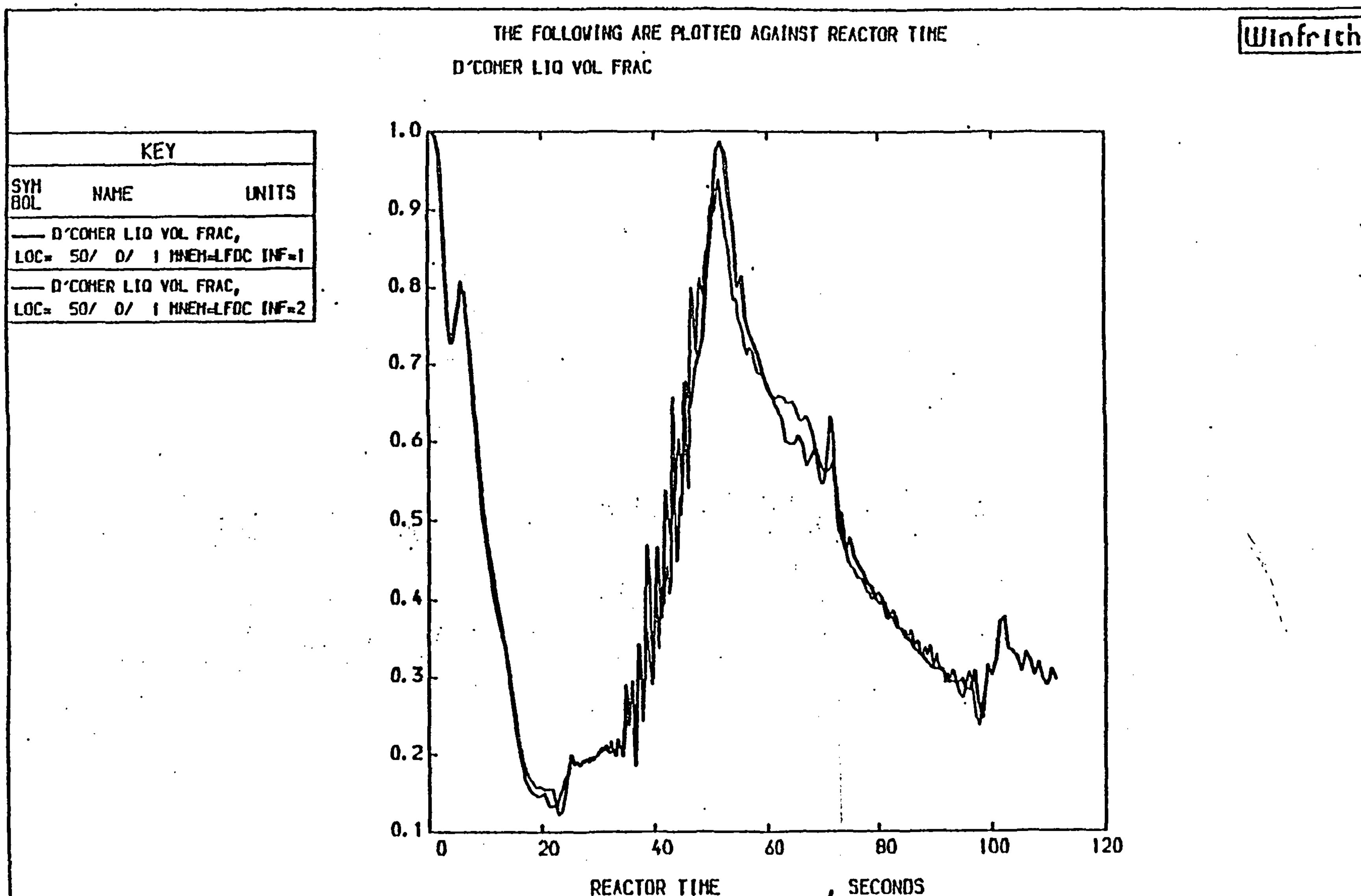

FIGURE 118 INF 1 ORIG, INF 2 ZEROGAP
VESSEL GLOBALS

THE FOLLOWING ARE PLOTTED AGAINST REACTOR TIME

CORE LIQ VOL FRAC

Winfrith

KEY		
SYMBOL	NAME	UNITS
——	CORE LIQ VOL FRAC , LOC= 50/ 0/ 1 MNEM=LFCO INF=1	
——	CORE LIQ VOL FRAC , LOC= 50/ 0/ 1 MNEM=LFCO INF=2	

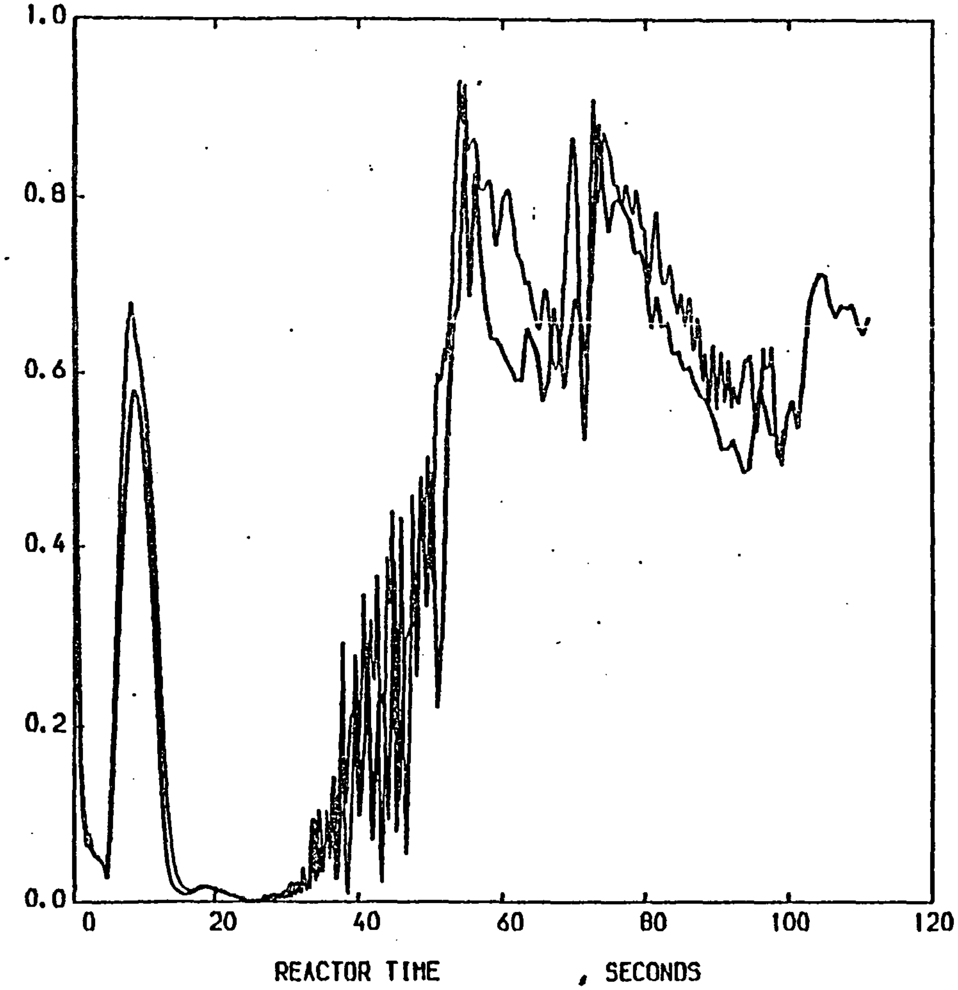

FIGURE 119 INF 1 ORIG, INF 2 ZEROGAP
VESSEL GLOBALS

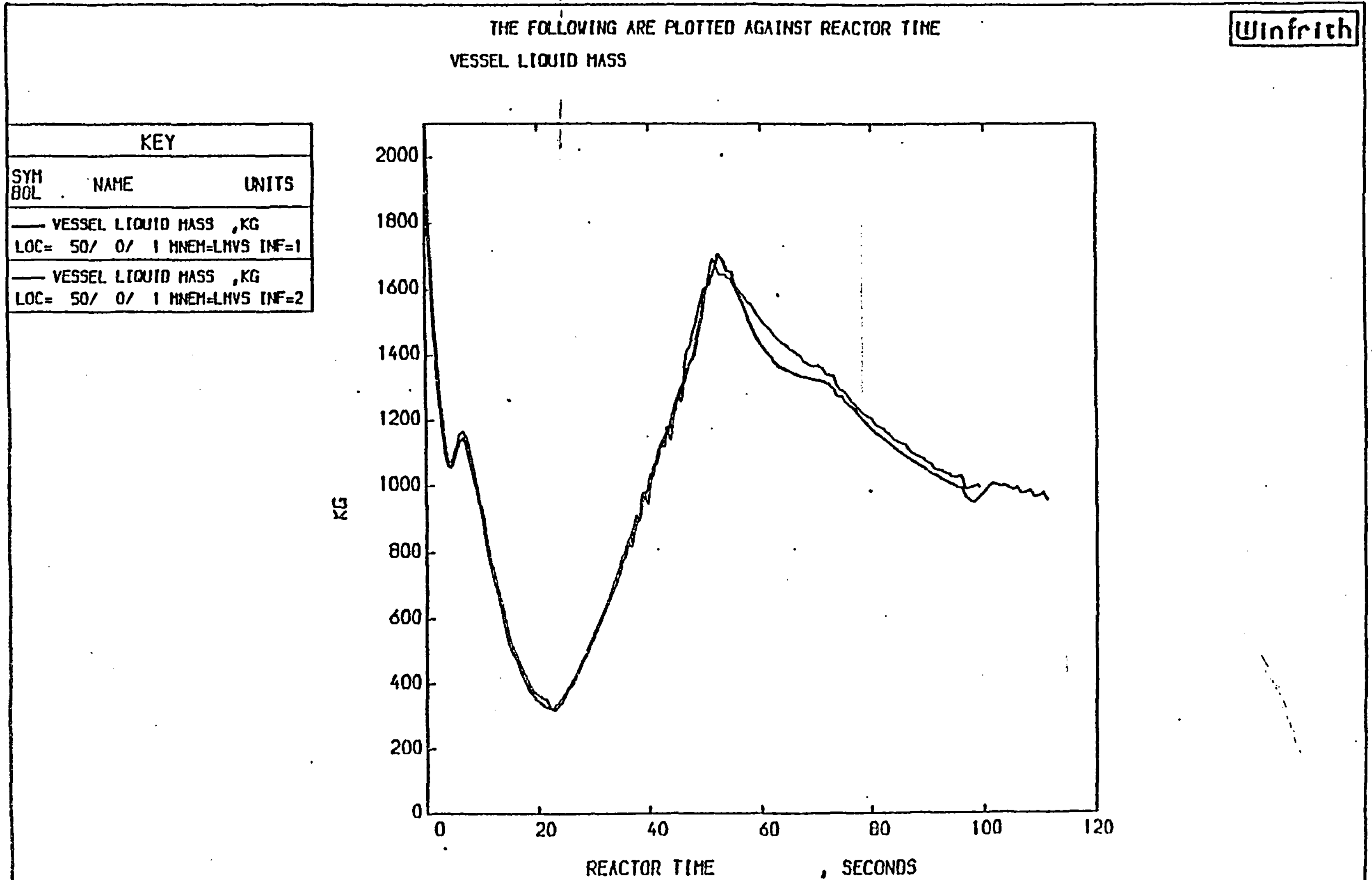

FIGURE 120 INF 1 ORIG, INF 2 ZEROGAP
VESSEL GLOBALS

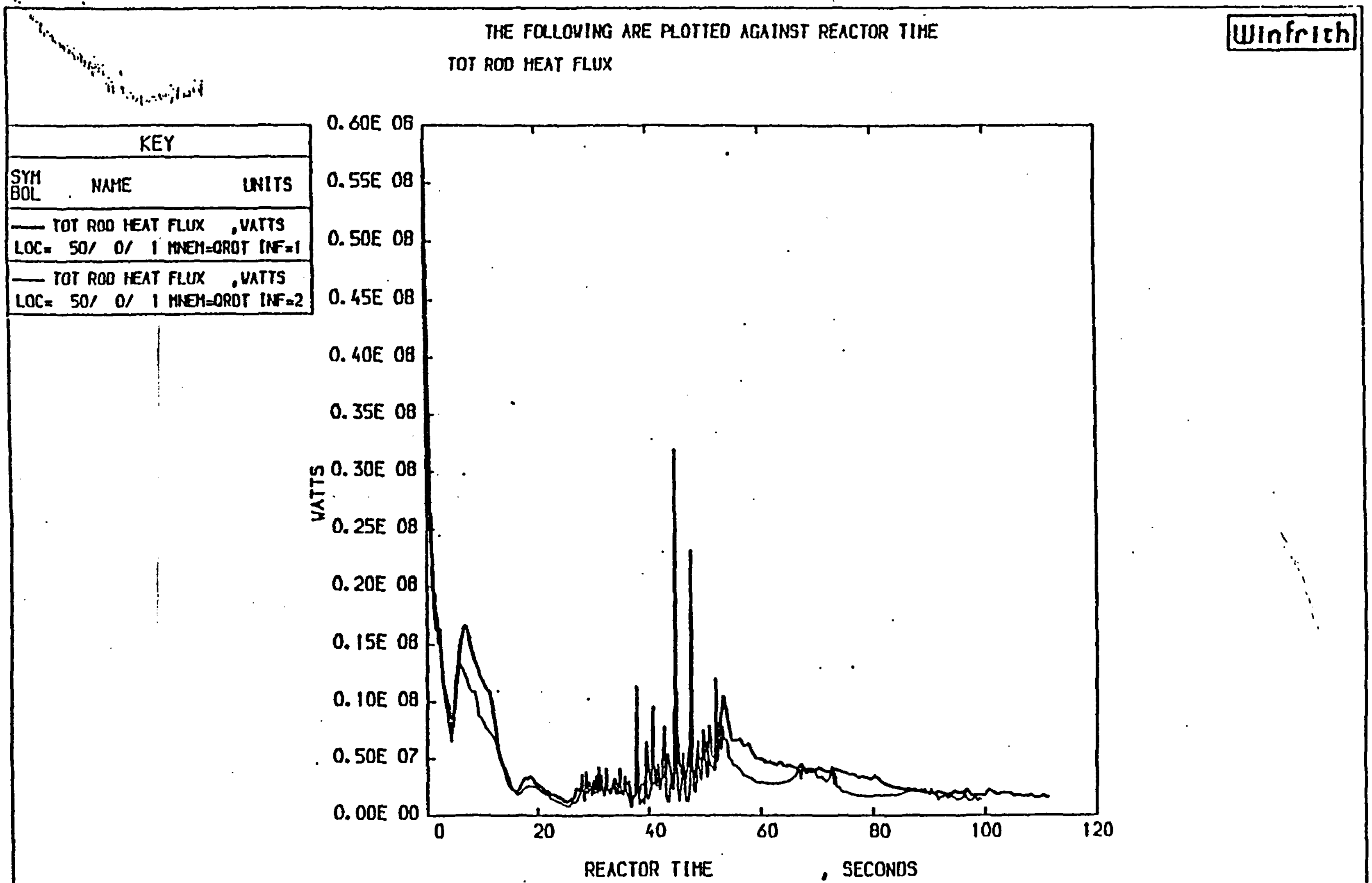

FIGURE 121. INF 1 ORIG, INF 2 ZEROGAP
VESSEL GLOBALS

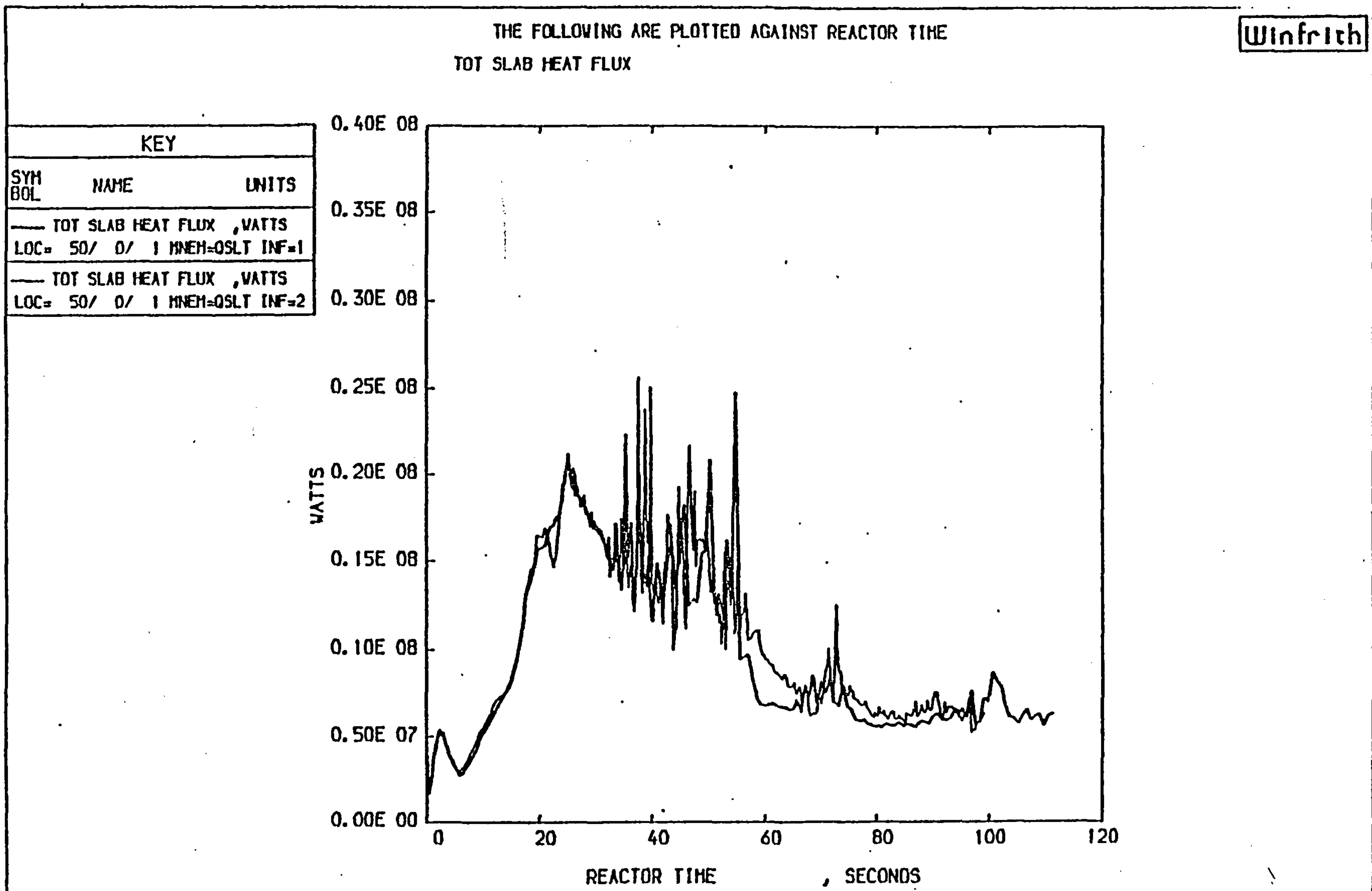

FIGURE 122 INF 1 ORIG, INF 2 ZEROGAP
VESSEL GLOBALS

THE FOLLOWING ARE PLOTTED AGAINST REACTOR TIME

Winfrith

L PLENUM AVG LIQ TEM

KEY		
SYM BOL	NAME	UNITS
——	L PLENUM AVG LIQ TEM,	DEG.K
LOC= 50/ 0/ 1	MNEM=TMLP	INF=1
——	L PLENUM AVG LIQ TEM,	DEG.K
LOC= 50/ 0/ 1	MNEM=TMLP	INF=2

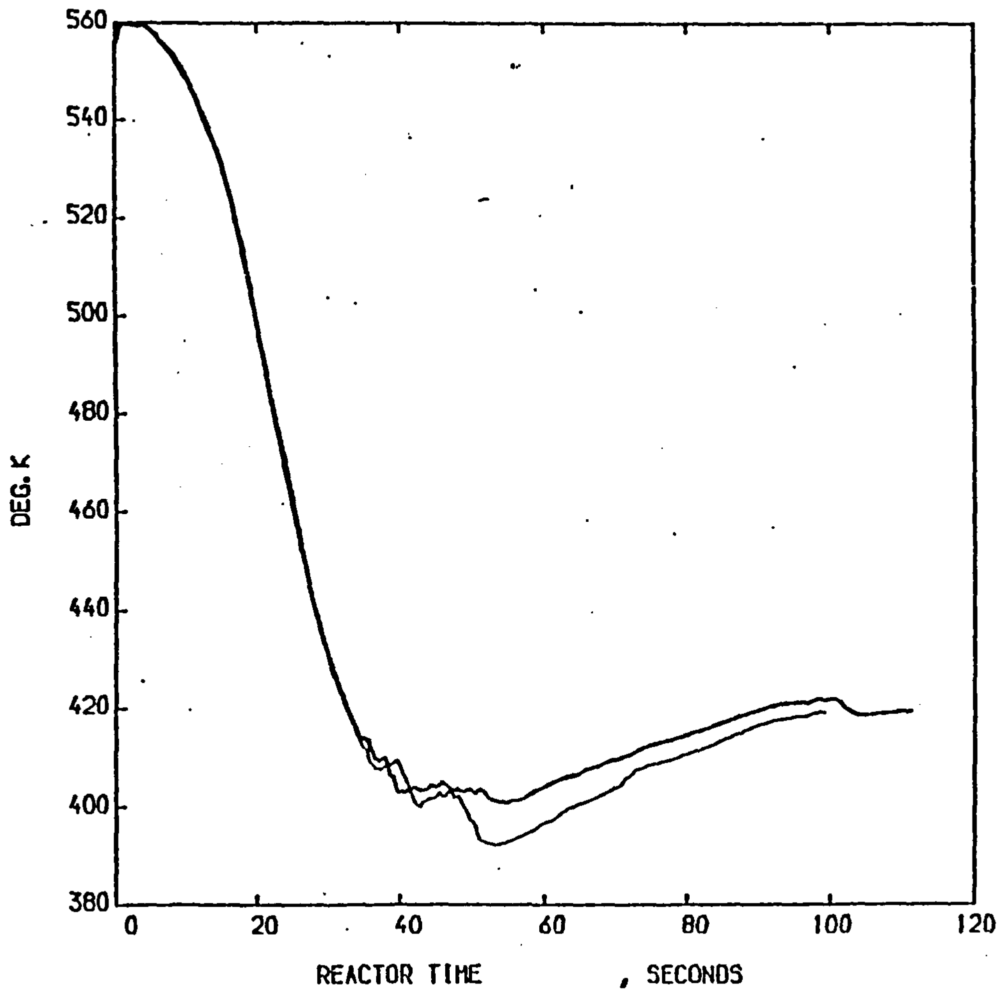

FIGURE 123 INF 1 ORIG, INF 2 ZEROGAP
VESSEL GLOBALS

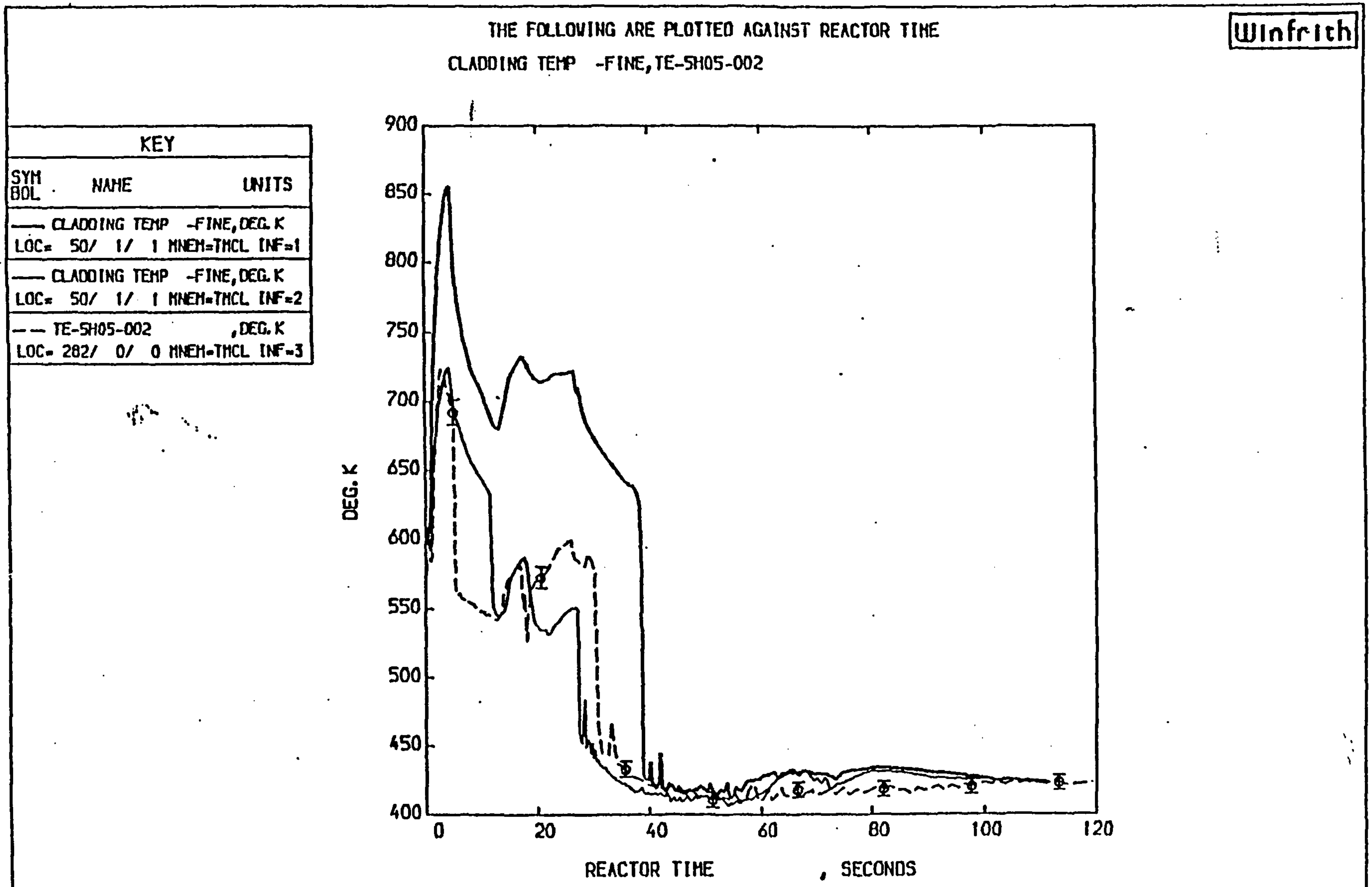

FIGURE 124 INF 1 ORIG, INF 2 ZEROGAP, INF 3 EXP
CENTRAL FUEL BUNDLE CLADDING TEMPERATURES

THE FOLLOWING ARE PLOTTED AGAINST REACTOR TIME

CLADDING TEMP -FINE,TE-5G06-011

Winfrith

KEY		
SYM BOL	NAME	UNITS
——	CLADDING TEMP -FINE,	DEG.K
	LOC= 50/ 1/ 5 MNEM=THCL INF=1	
——	CLADDING TEMP -FINE,	DEG.K
	LOC= 50/ 1/ 5 MNEM=THCL INF=2	
– –	TE-5G06-011	DEG.K
	LOC= 278/ 0/ 0 MNEM=THCL INF=3	

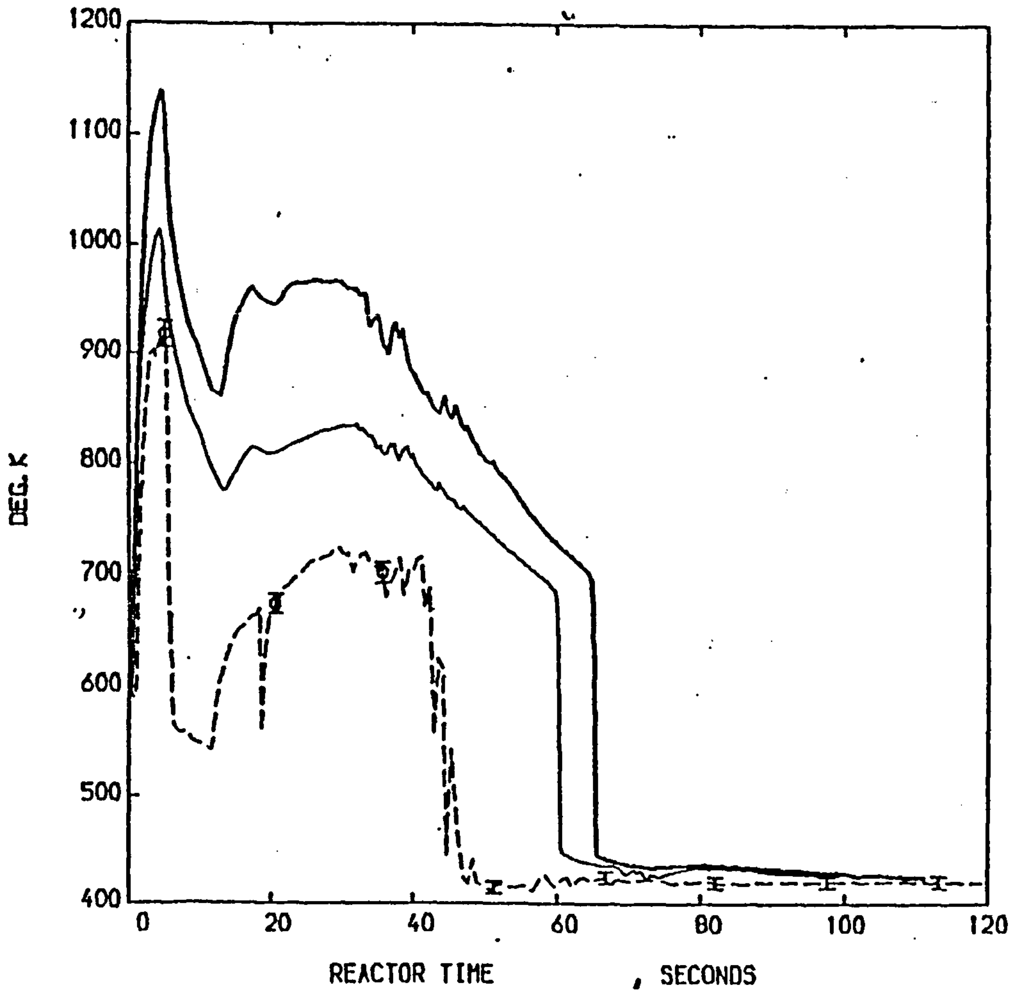

FIGURE 125 INF 1 ORIG, INF 2 ZEROGAP, INF 3 EXP
CENTRAL FUEL BUNDLE CLADDING TEMPERATURES

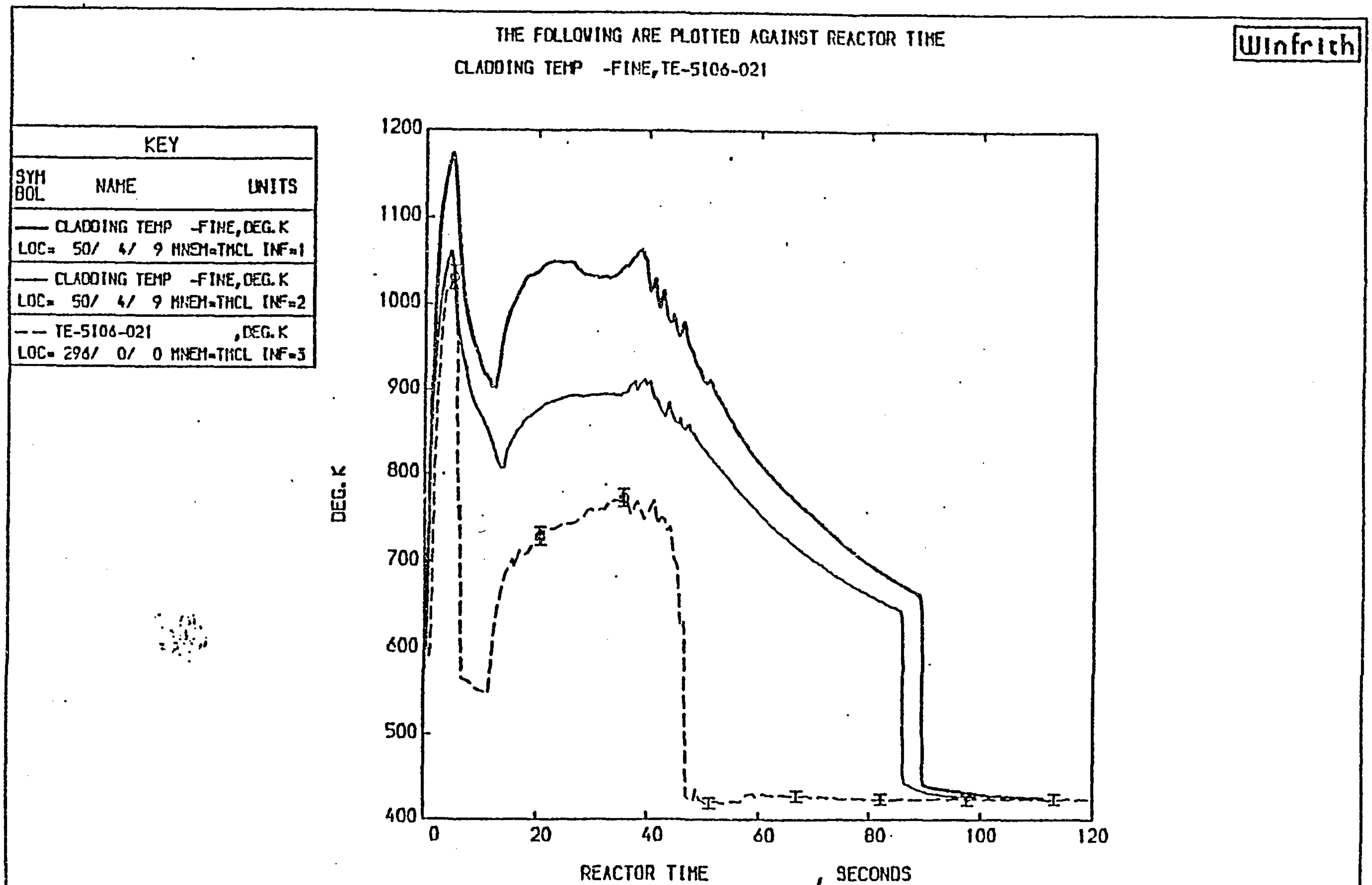

FIGURE 126 INF 1 ORIG, INF 2 ZEROGAP, INF 3 EXP
CENTRAL FUEL BUNDLE CLADDING TEMPERATURES

Winfrith

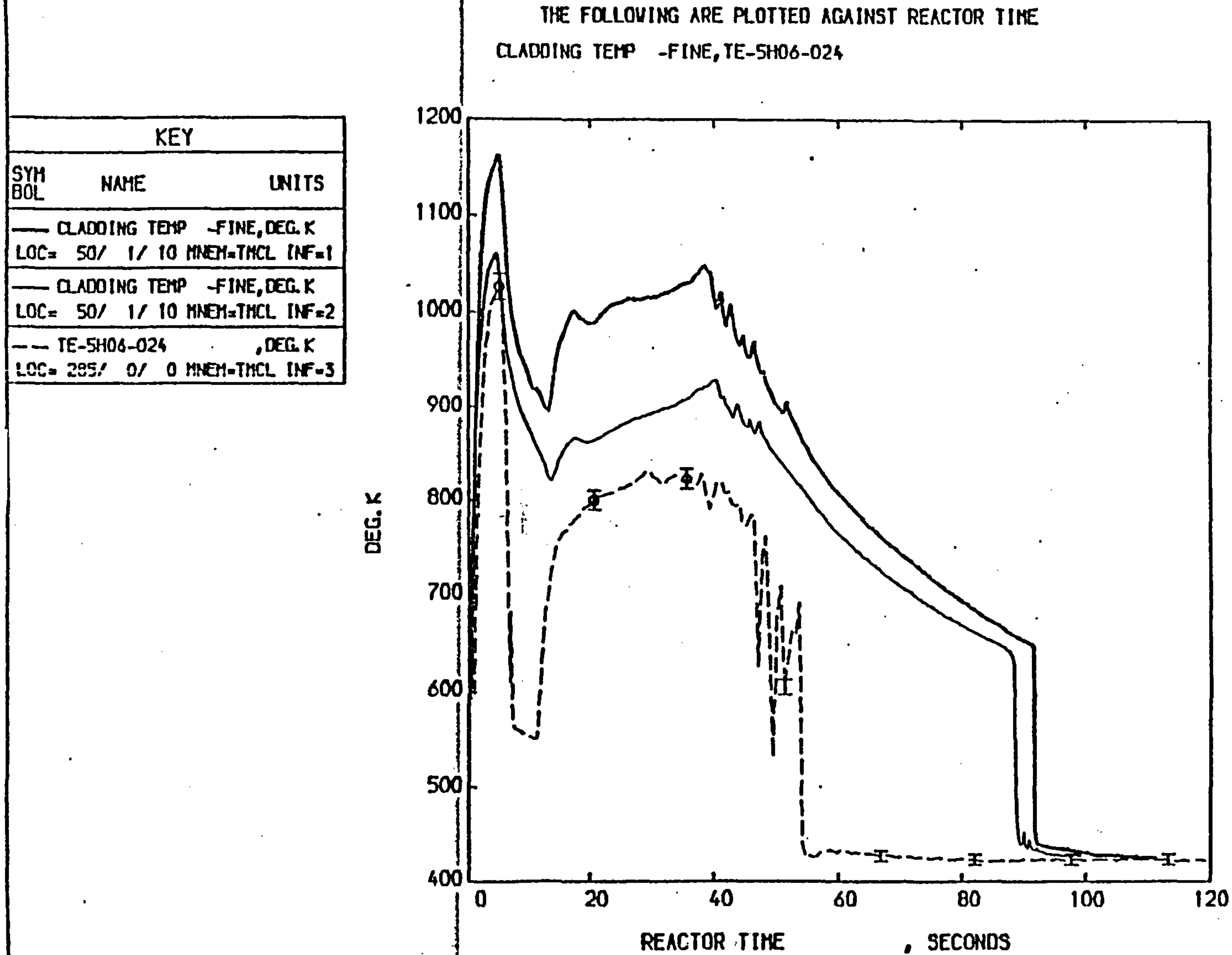

FIGURE 127 INF 1 ORIG, INF 2 ZEROGAP, INF 3 EXP
CENTRAL FUEL BUNDLE CLADDING TEMPERATURES

Winfrith

THE FOLLOWING ARE PLOTTED AGAINST REACTOR TIME
CLADDING TEMP -FINE,TE-5104-027

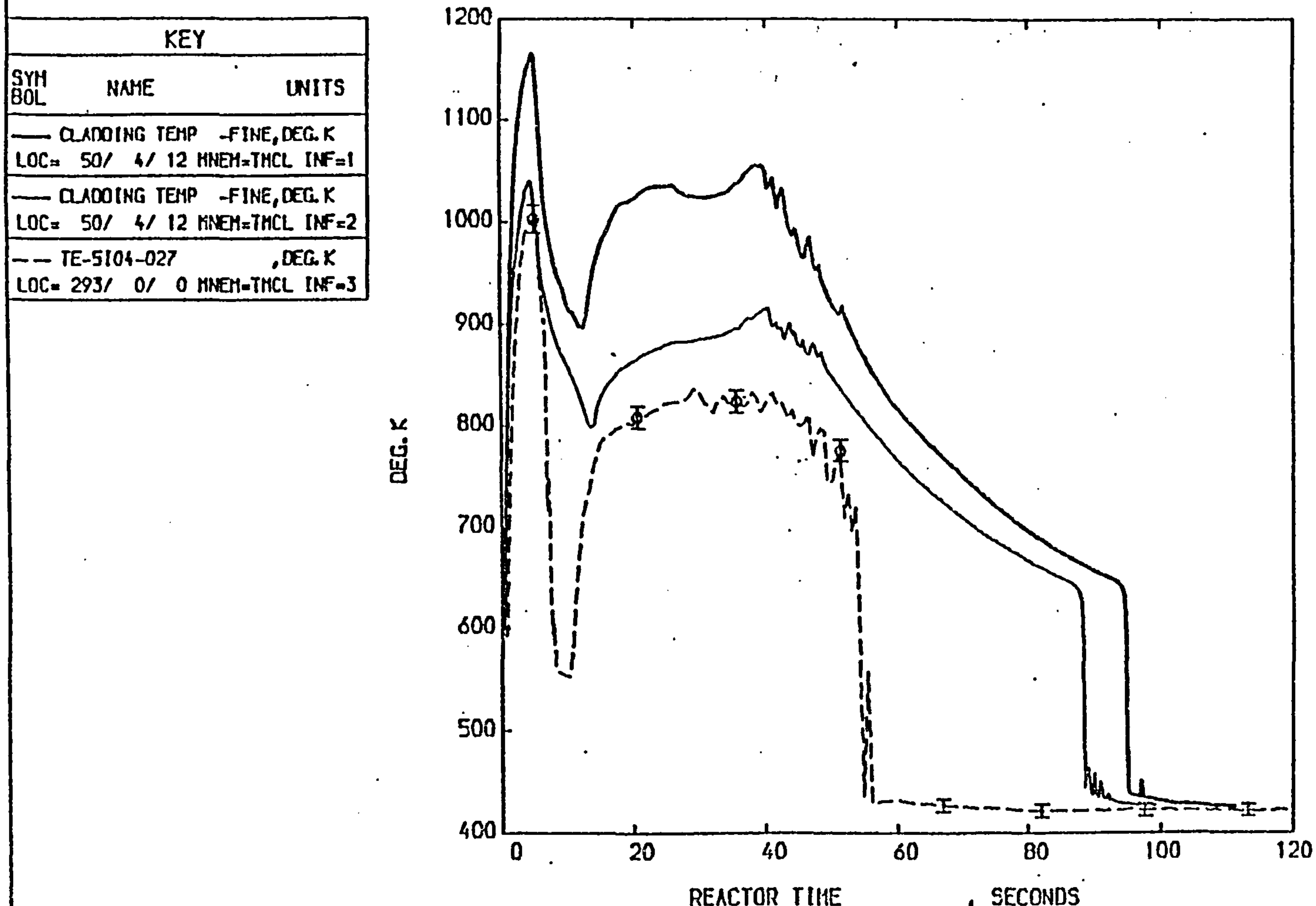

FIGURE 128 INF 1 ORIG, INF 2 ZEROGAP, INF 3 EXP
CENTRAL FUEL BUNDLE CLADDING TEMPERATURES

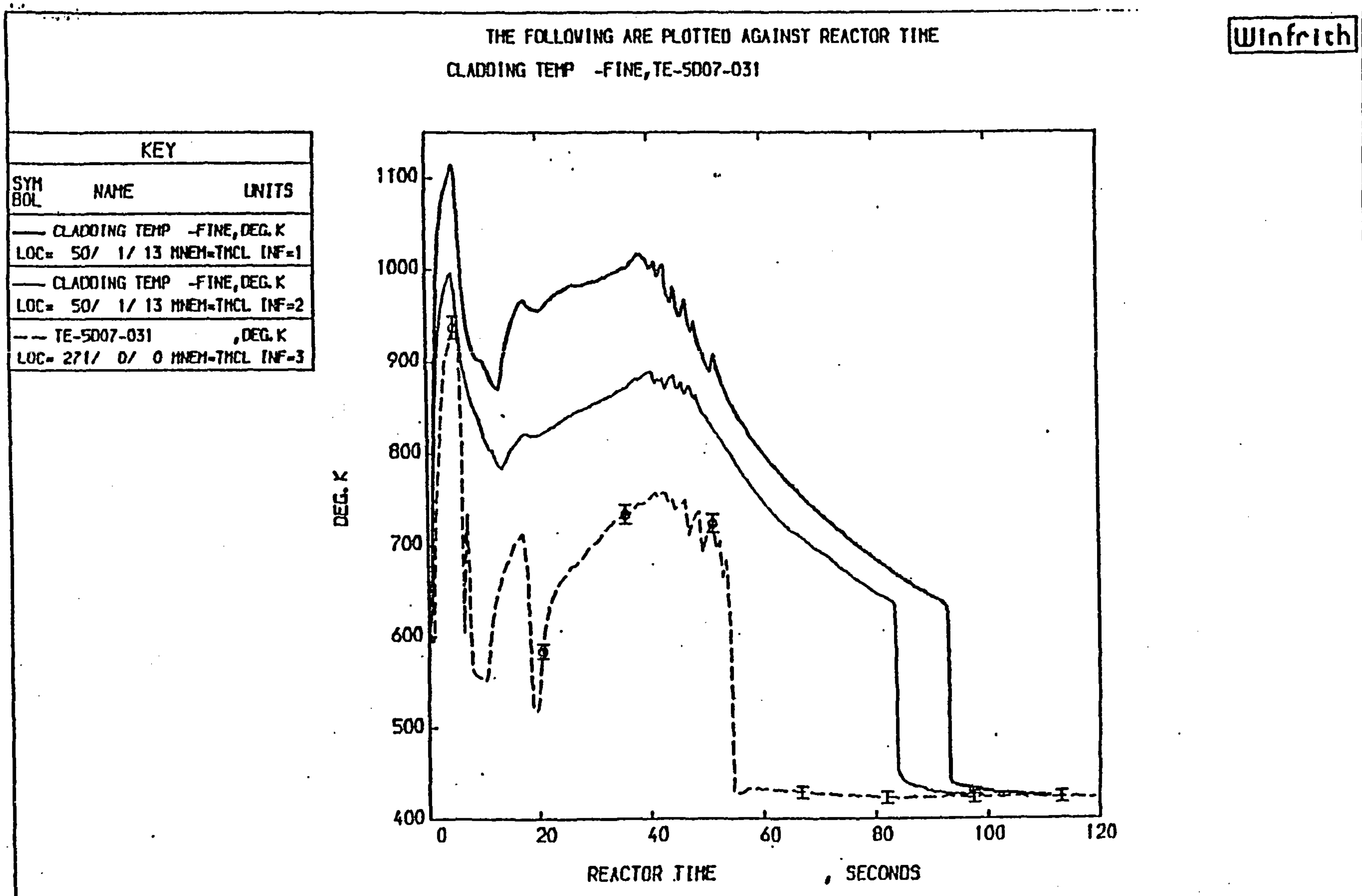

FIGURE 129 INF 1 ORIG, INF 2 ZEROGAP, INF 3 EXP
CENTRAL FUEL BUNDLE CLADDING TEMPERATURES

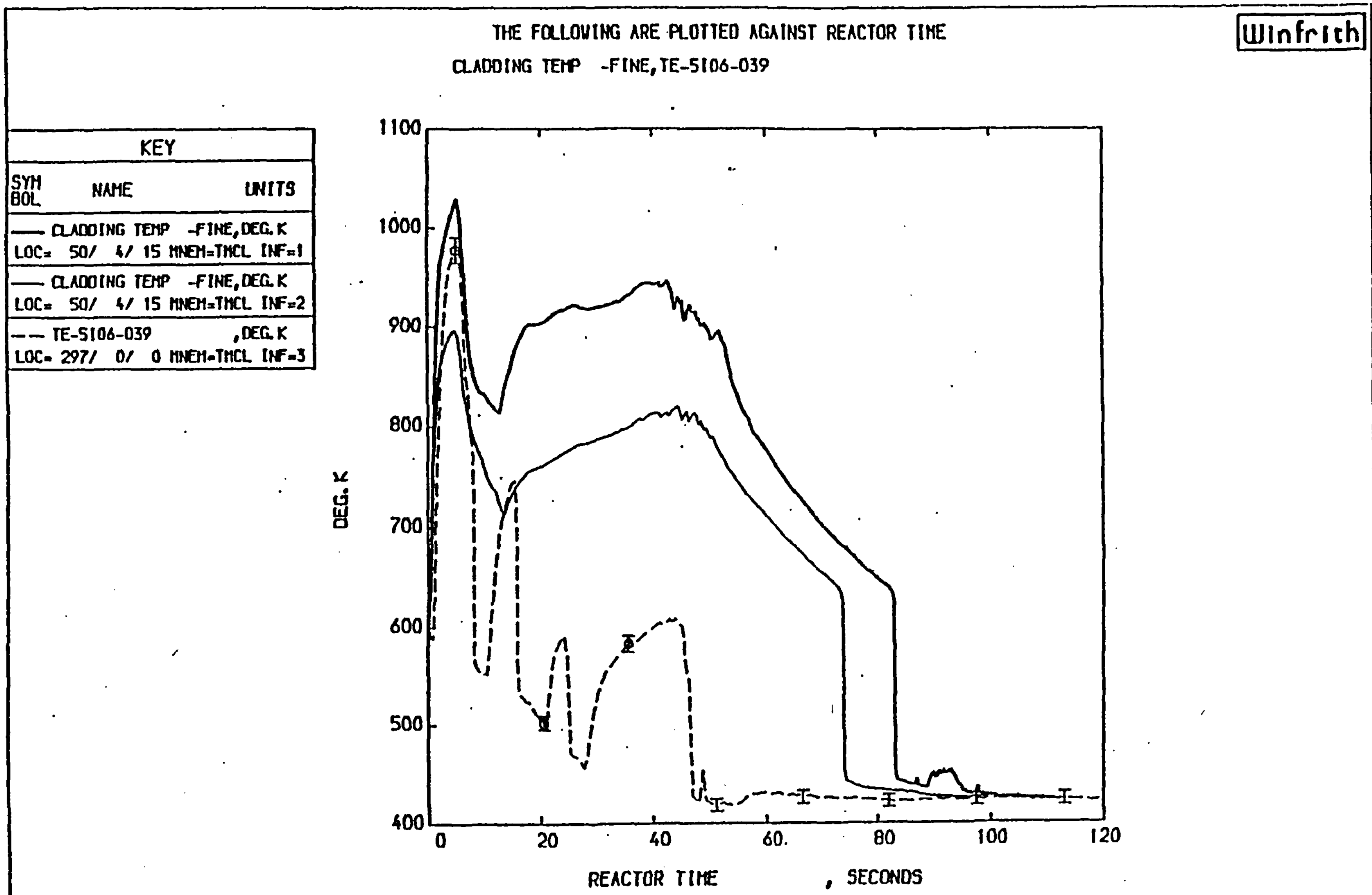

FIGURE 130 INF 1 ORIG, INF 2 ZEROGAP, INF 3 EXP
CENTRAL FUEL BUNDLE CLADDING TEMPERATURES

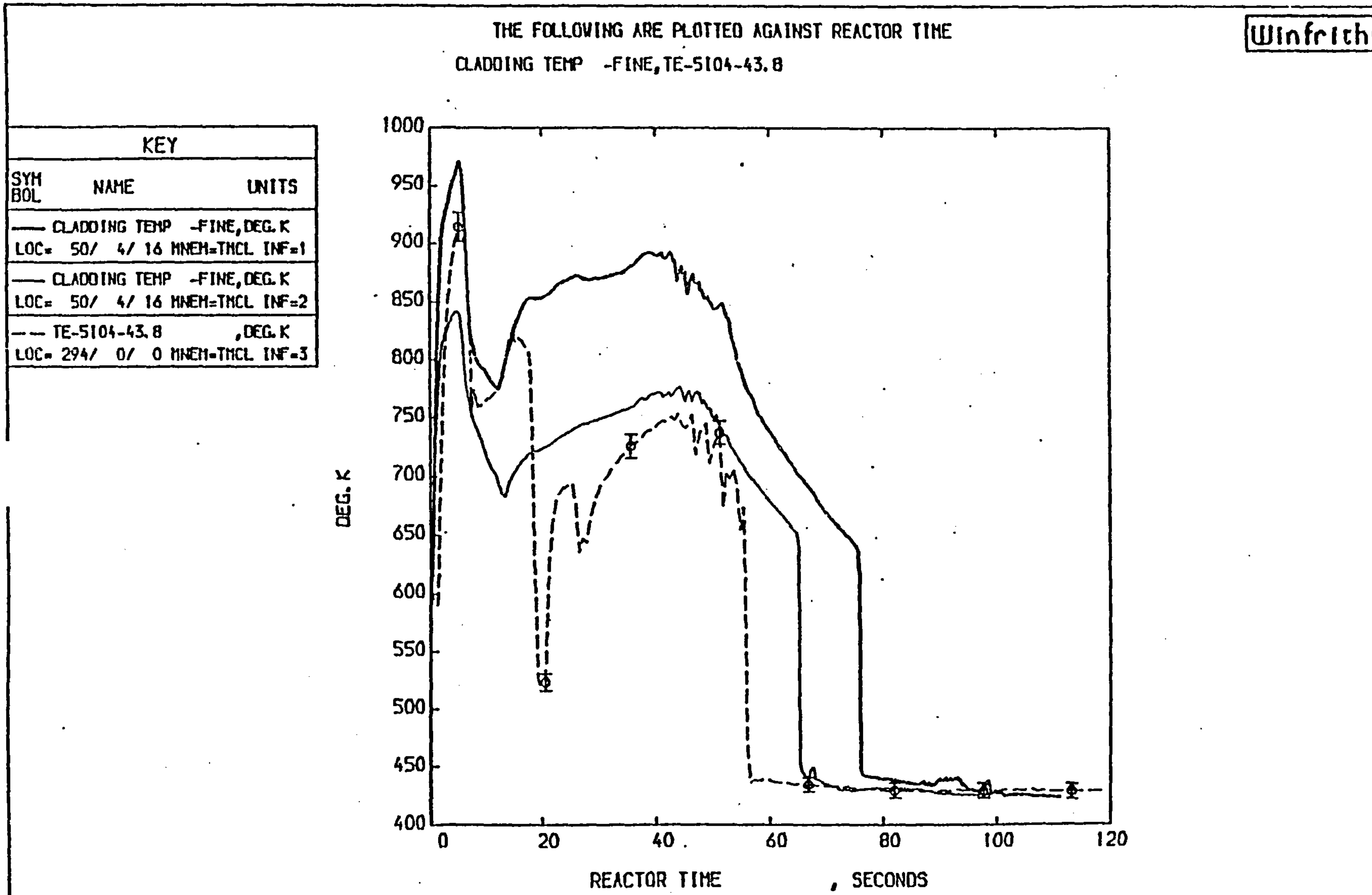

FIGURE 131 INF 1 ORIG, INF 2 ZEROGAP, INF 3 EXP
CENTRAL FUEL BUNDLE CLADDING TEMPERATURES

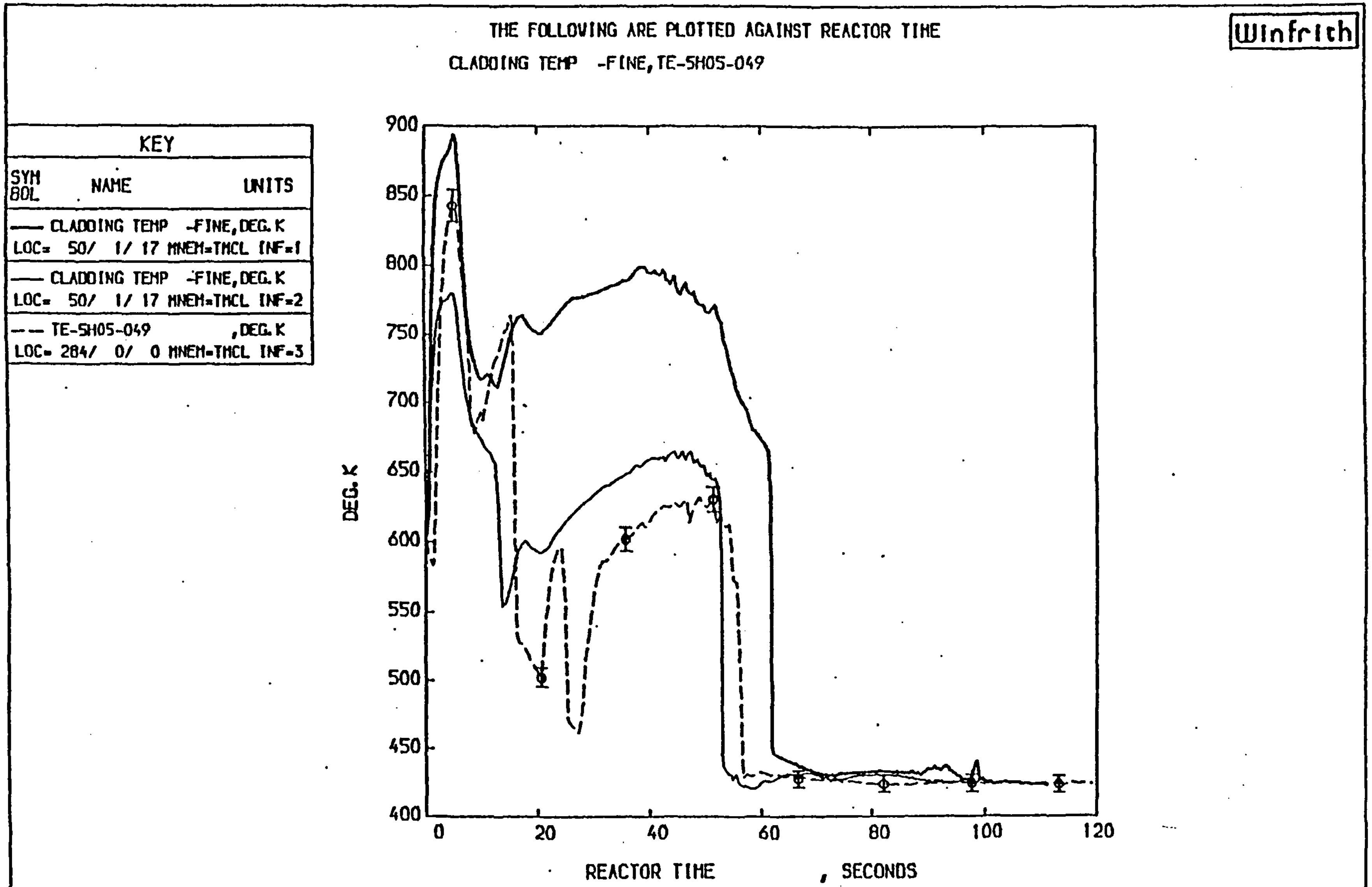

FIGURE 132 . INF 1 ORIG, INF 2 ZEROGAP, INF 3 EXP
CENTRAL FUEL BUNDLE CLADDING TEMPERATURES

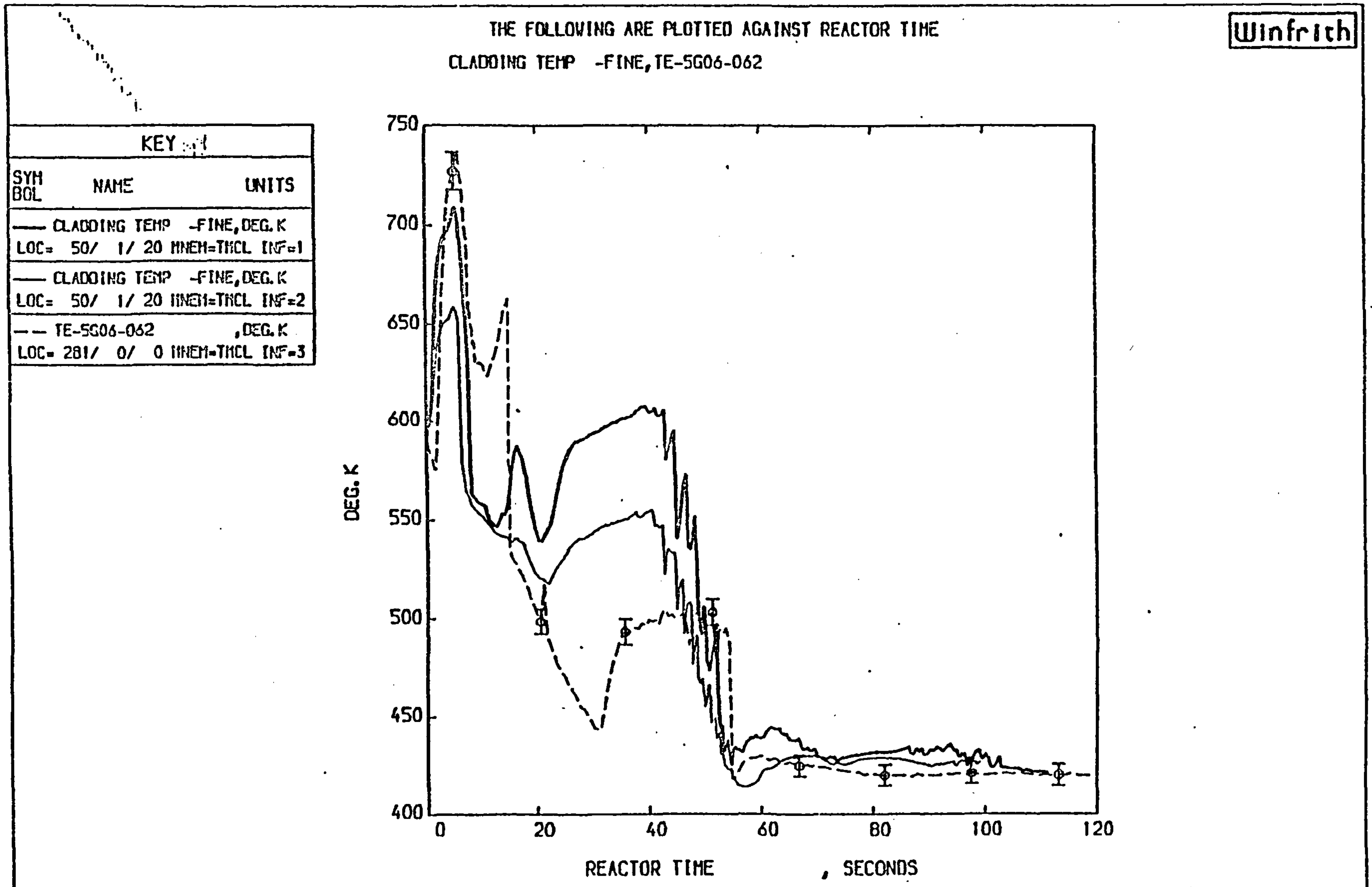

FIGURE 133 INF 1 ORIG, INF 2 ZEROGAP, INF 3 EXP
CENTRAL FUEL BUNDLE CLADDING TEMPERATURES

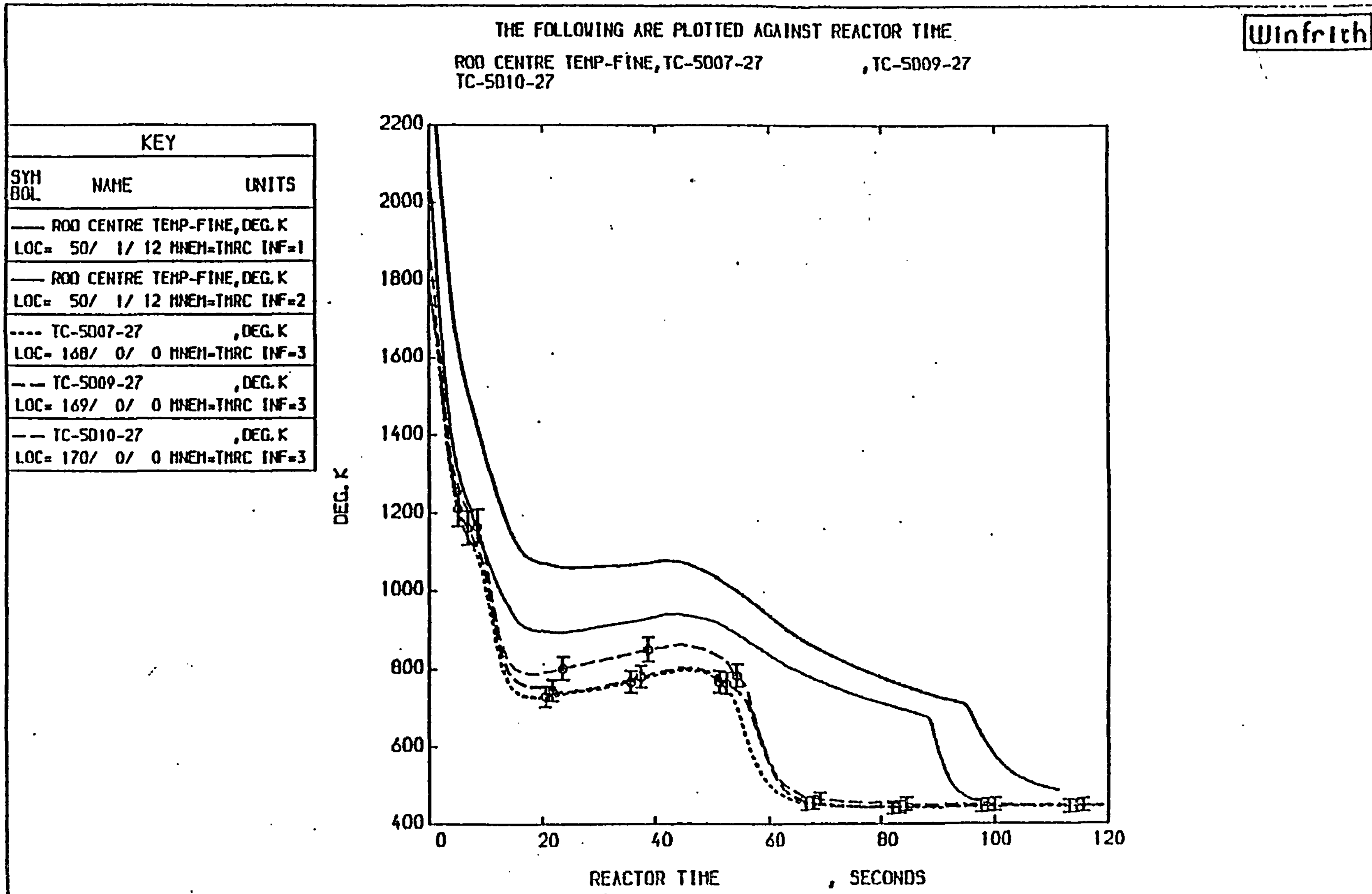

FIGURE 134 INF 1 ORIG, INF 2 ZEROGAP, INF 3 EXP
CENTRELINE FUEL TEMPERATURE

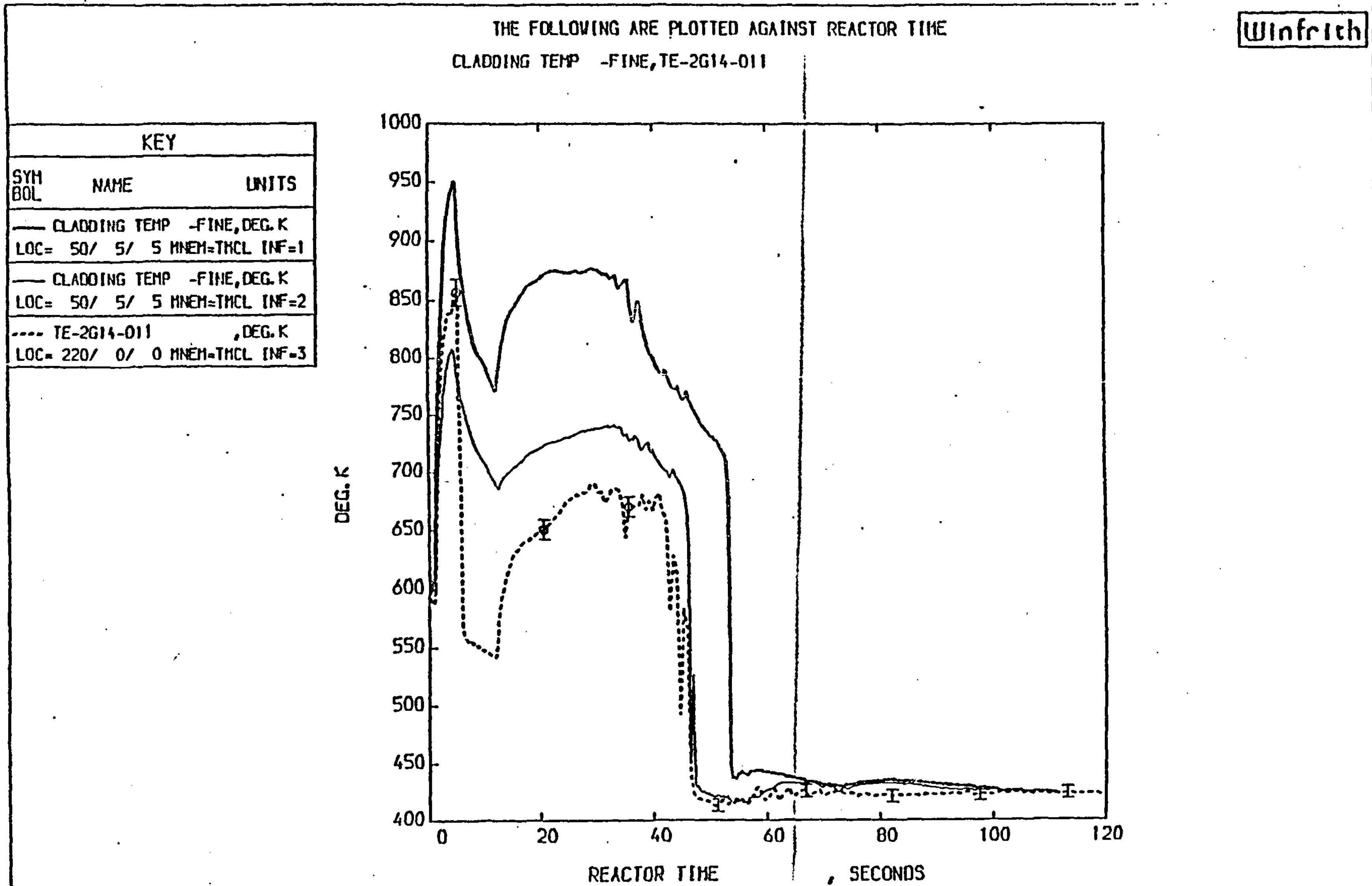

FIGURE 135 INF 1 ORIG, INF 2 ZEROGAP, INF 3 EXP
FUEL ROD CLADDING TEMPERATURES - PERIPHERAL BUNDLES

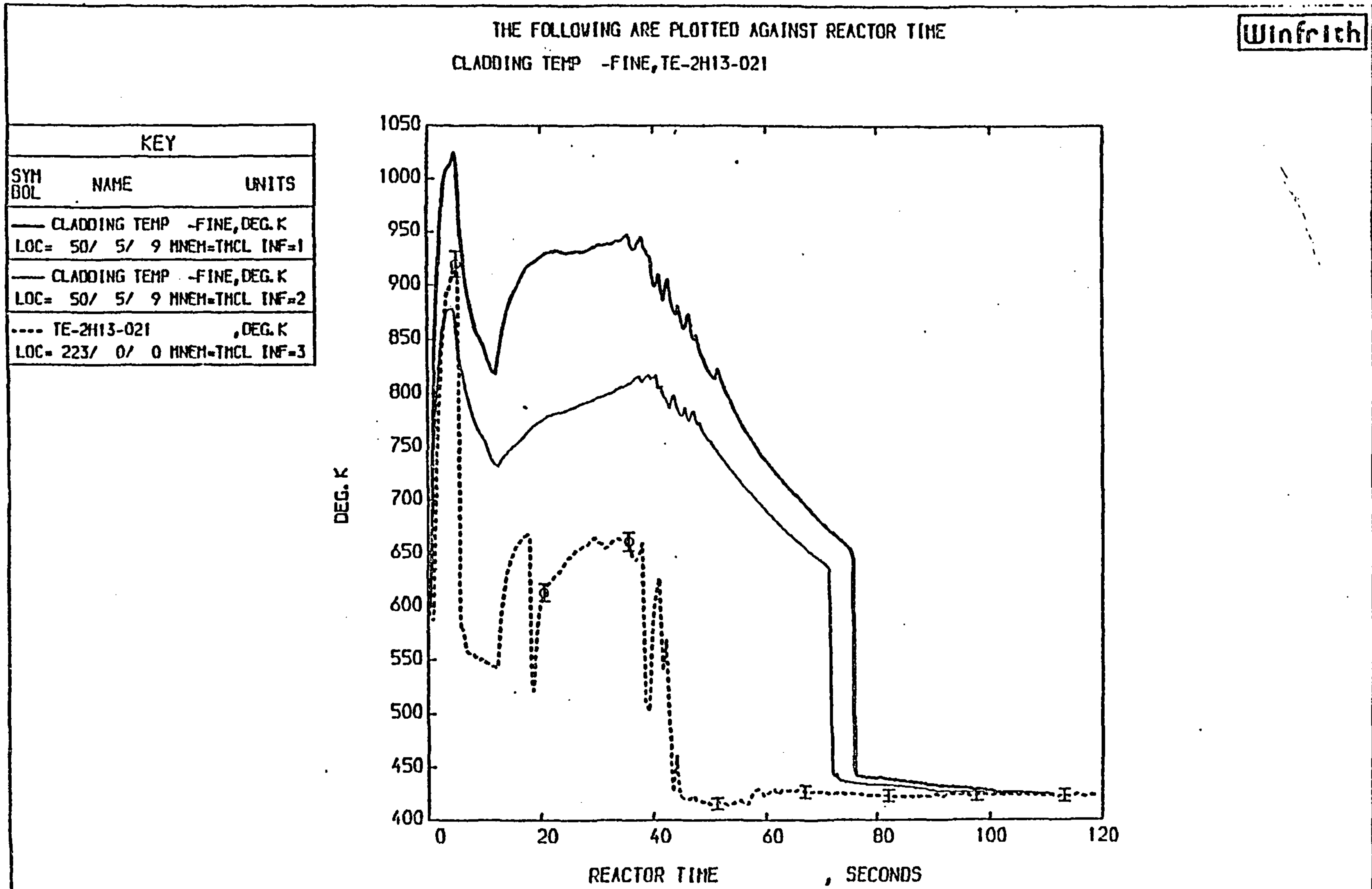

FIGURE 136 . INF 1 ORIG, INF 2 ZEROGAP, INF 3 EXP
FUEL ROD CLADDING TEMPERATURES - PERIPHERAL BUNDLES

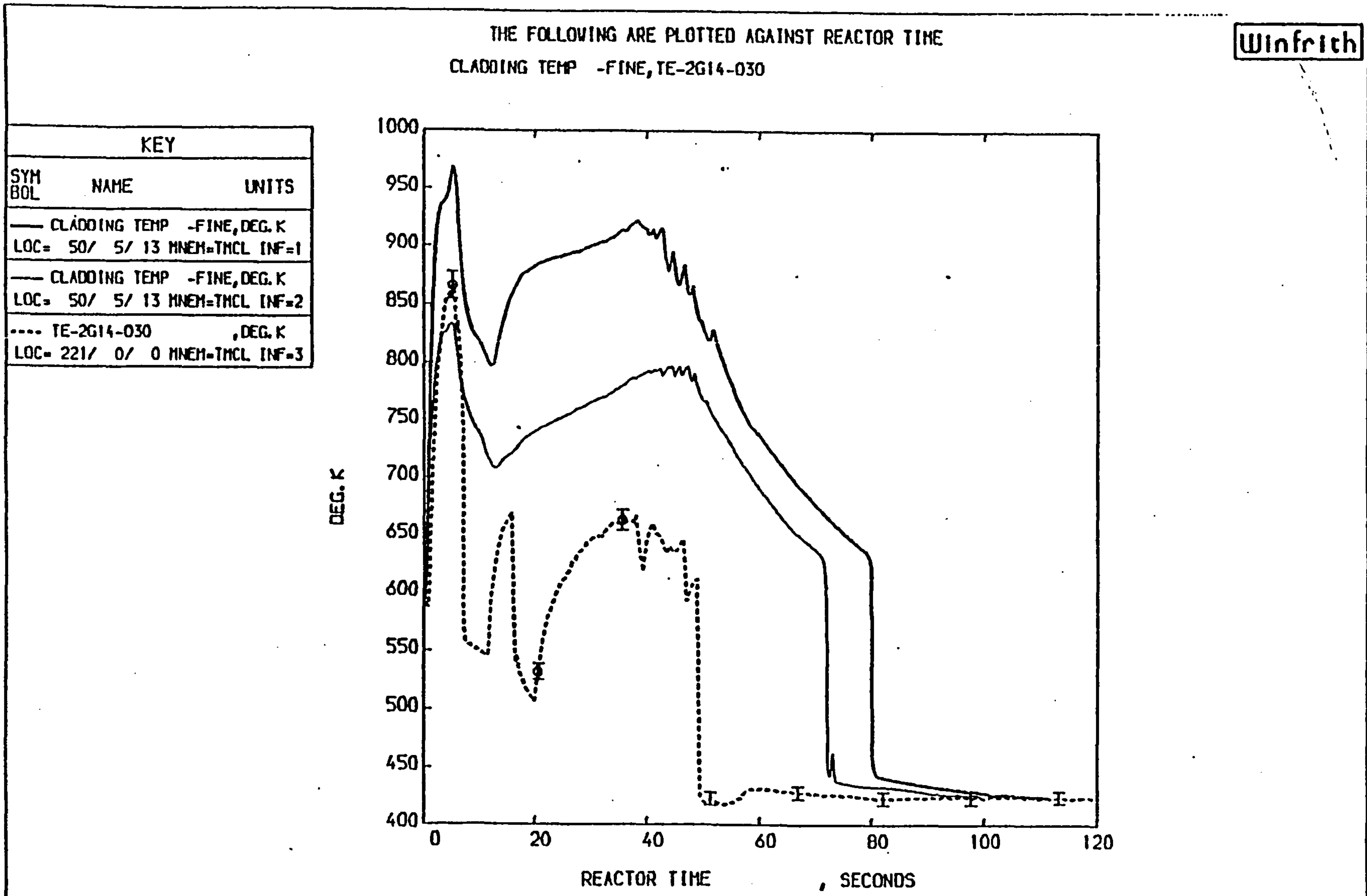

FIGURE 137 INF 1 ORIG, INF 2 ZEROGAP, INF 3 EXP
FUEL ROD CLADDING TEMPERATURES - PERIPHERAL BUNDLES

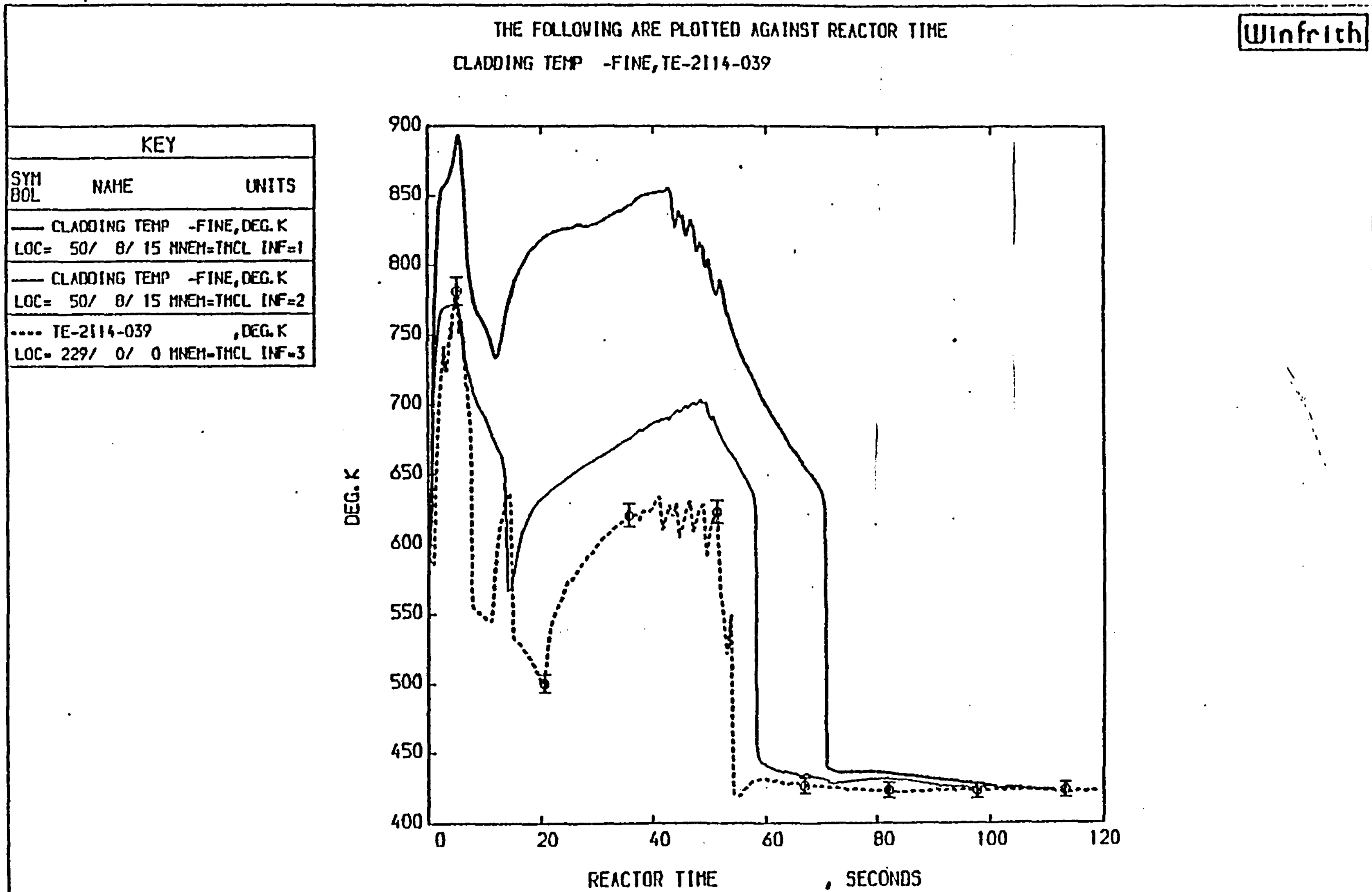

FIGURE 138 INF 1 ORIG, INF 2 ZEROGAP, INF 3 EXP
FUEL ROD CLADDING TEMPERATURES - PERIPHERAL BUNDLES

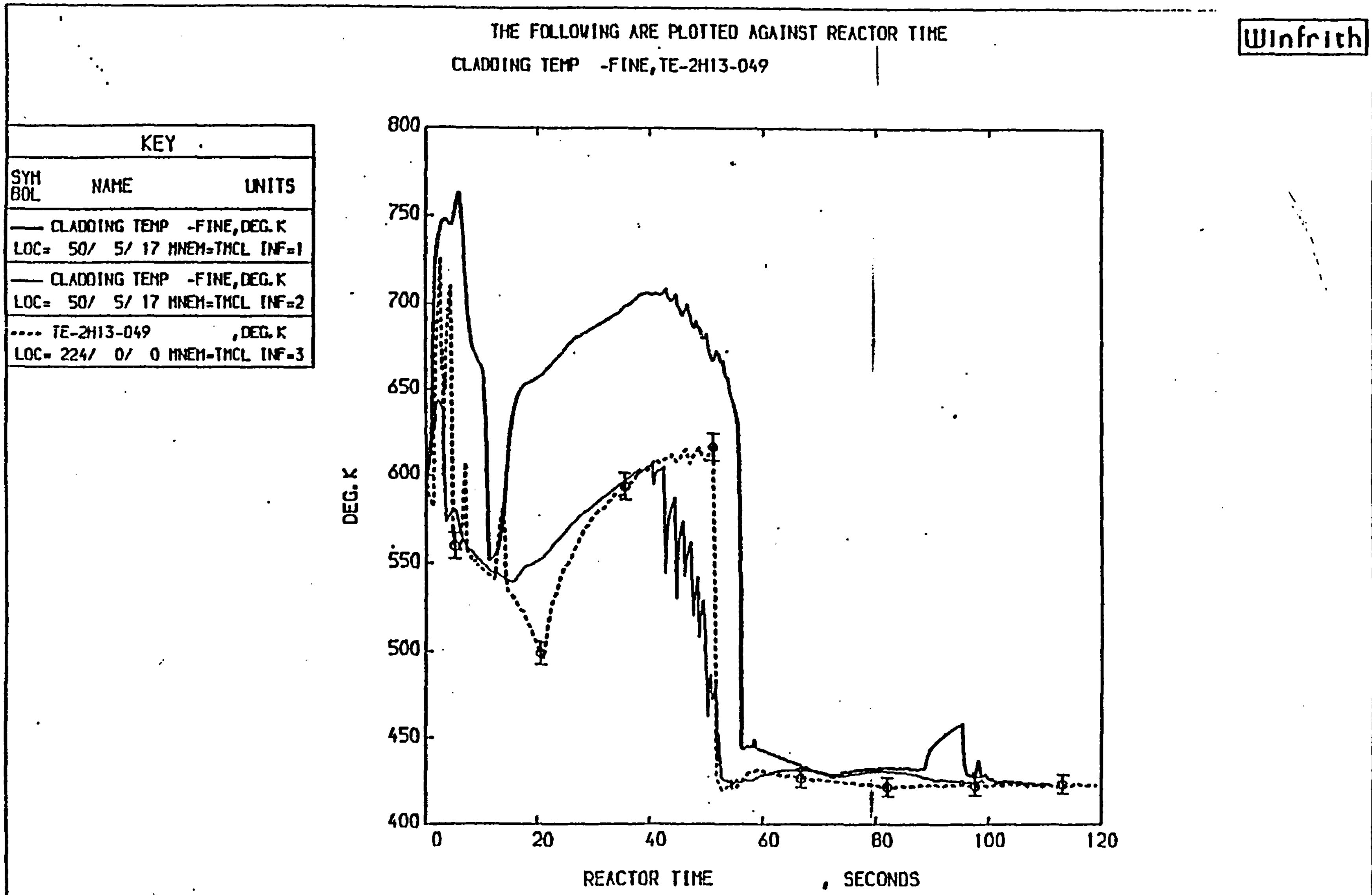

FIGURE 139 INF 1 ORIG, INF 2 ZEROGAP, INF 3 EXP
FUEL ROD CLADDING TEMPERATURES - PERIPHERAL BUNDLES

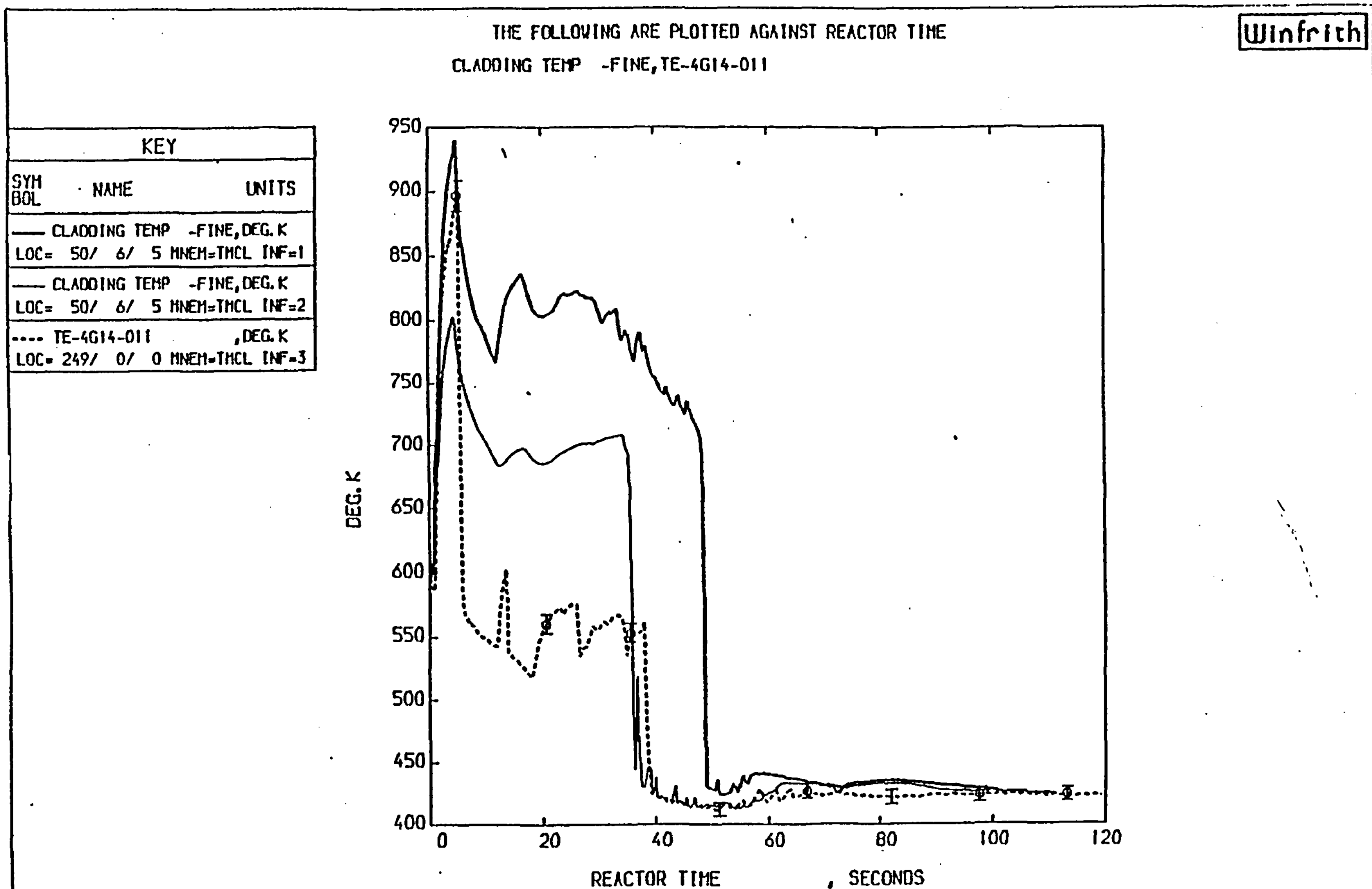

FIGURE 140 INF 1 ORIG, INF 2 ZEROGAP, INF 3 EXP
FUEL ROD CLADDING TEMPERATURES - PERIPHERAL BUNDLES

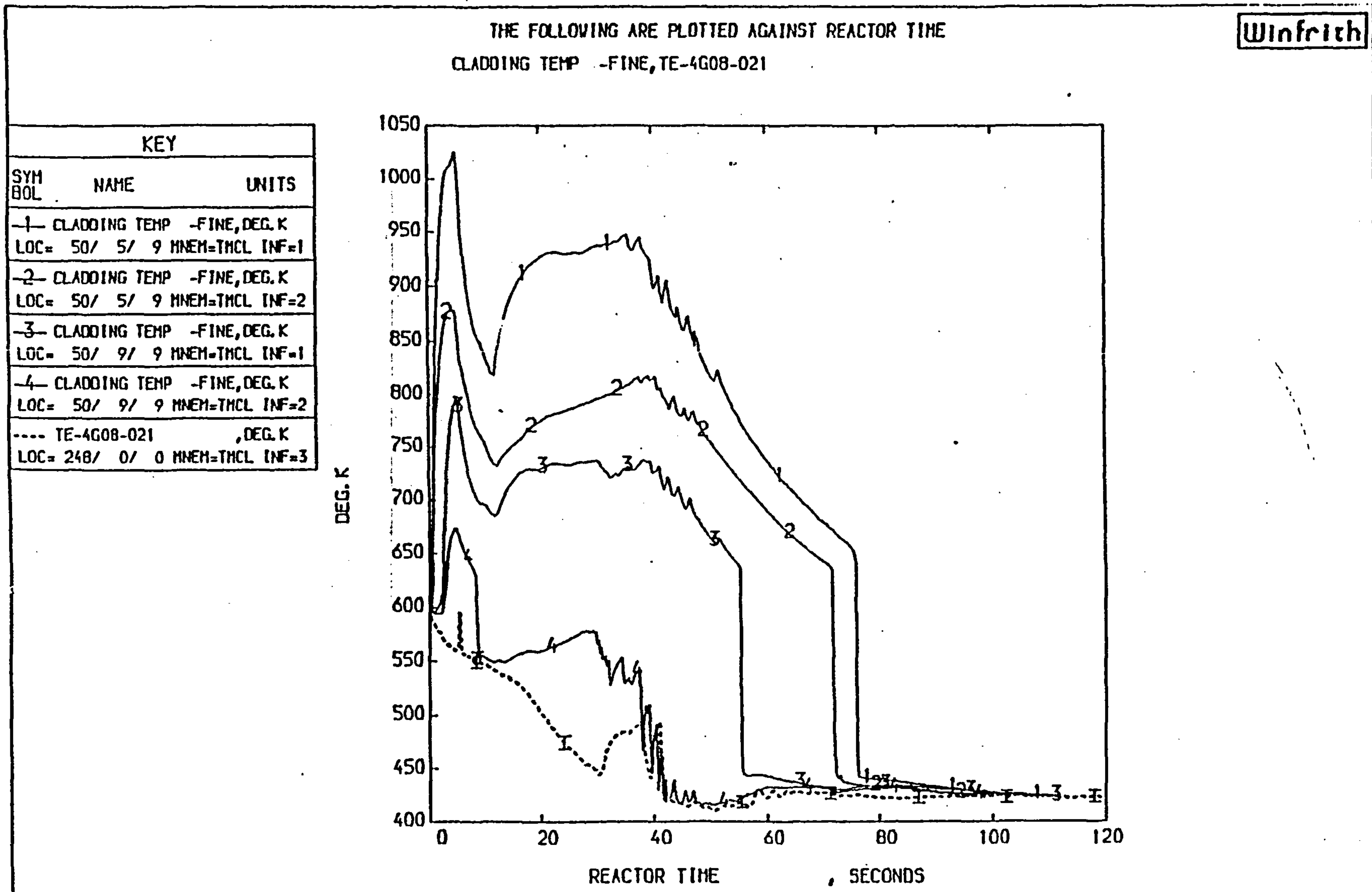

FIGURE 141 INF 1 ORIG, INF 2 ZEROGAP, INF 3 EXP
FUEL ROD CLADDING TEMPERATURES - PERIPHERAL BUNDLES

THE FOLLOWING ARE PLOTTED AGAINST REACTOR TIME

CLADDING TEMP -FINE, TE-4H14-028

Winfrith

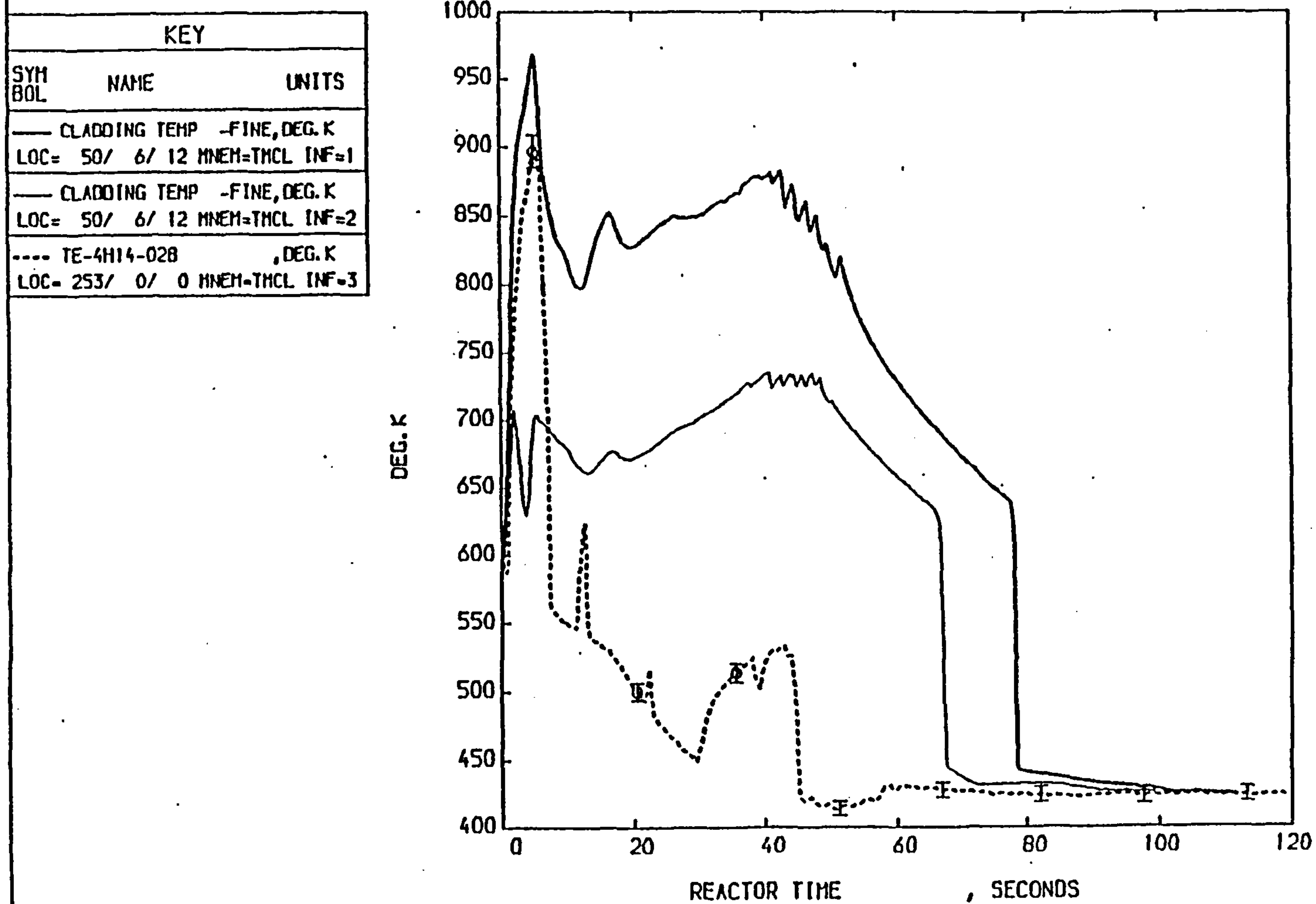

FIGURE 142 INF 1 ORIG, INF 2 ZEROGAP, INF 3 EXP
FUEL ROD CLADDING TEMPERATURES - PERIPHERAL BUNDLES

Winfrith

THE FOLLOWING ARE PLOTTED AGAINST REACTOR TIME
CLADDING TEMP -FINE,TE-4114-039

KEY		
SYMBOL	NAME	UNITS
——	CLADDING TEMP -FINE, LOC= 50/ 5/ 15 MNEM=THCL INF=1	DEG.K
——	CLADDING TEMP -FINE, LOC= 50/ 5/ 15 MNEM=THCL INF=2	DEG.K
----	TE-4114-039, LOC= 257/ 0/ 0 MNEM=THCL INF=3	DEG.K

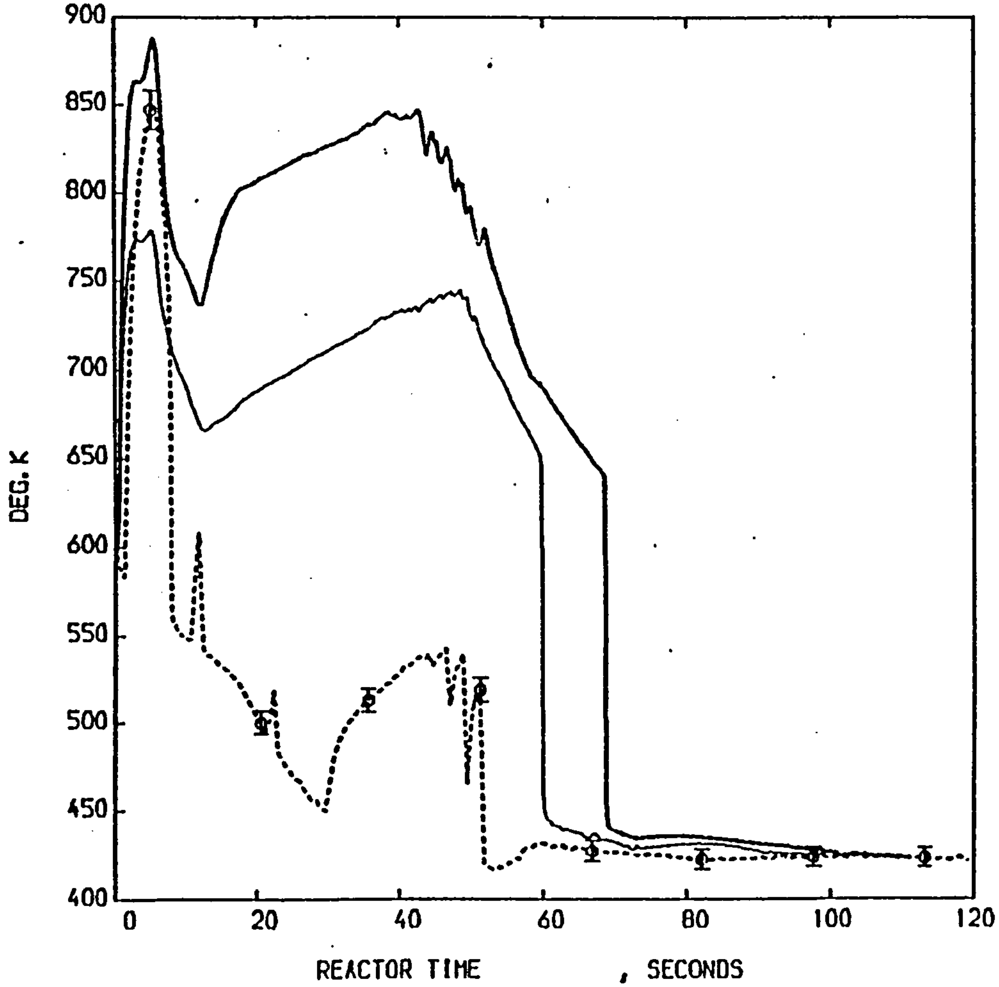

FIGURE 143 INF 1 ORIG, INF 2 ZEROGAP, INF 3 EXP
FUEL ROD CLADDING TEMPERATURES - PERIPHERAL BUNDLES

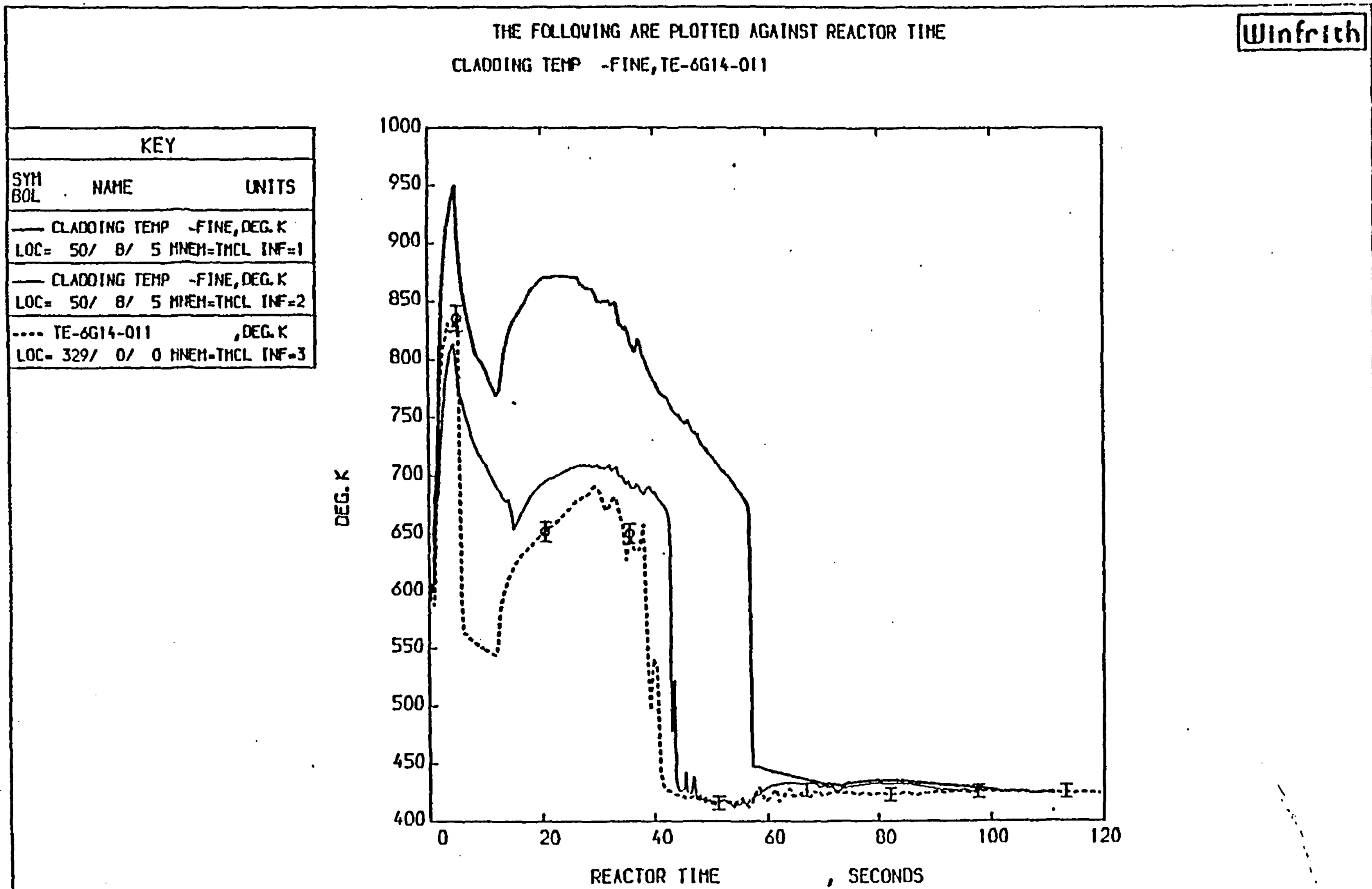

FIGURE 144 INF 1 ORIG, INF 2 ZEROGAP, INF 3 EXP
FUEL ROD CLADDING TEMPERATURES - PERIPHERAL BUNDLES

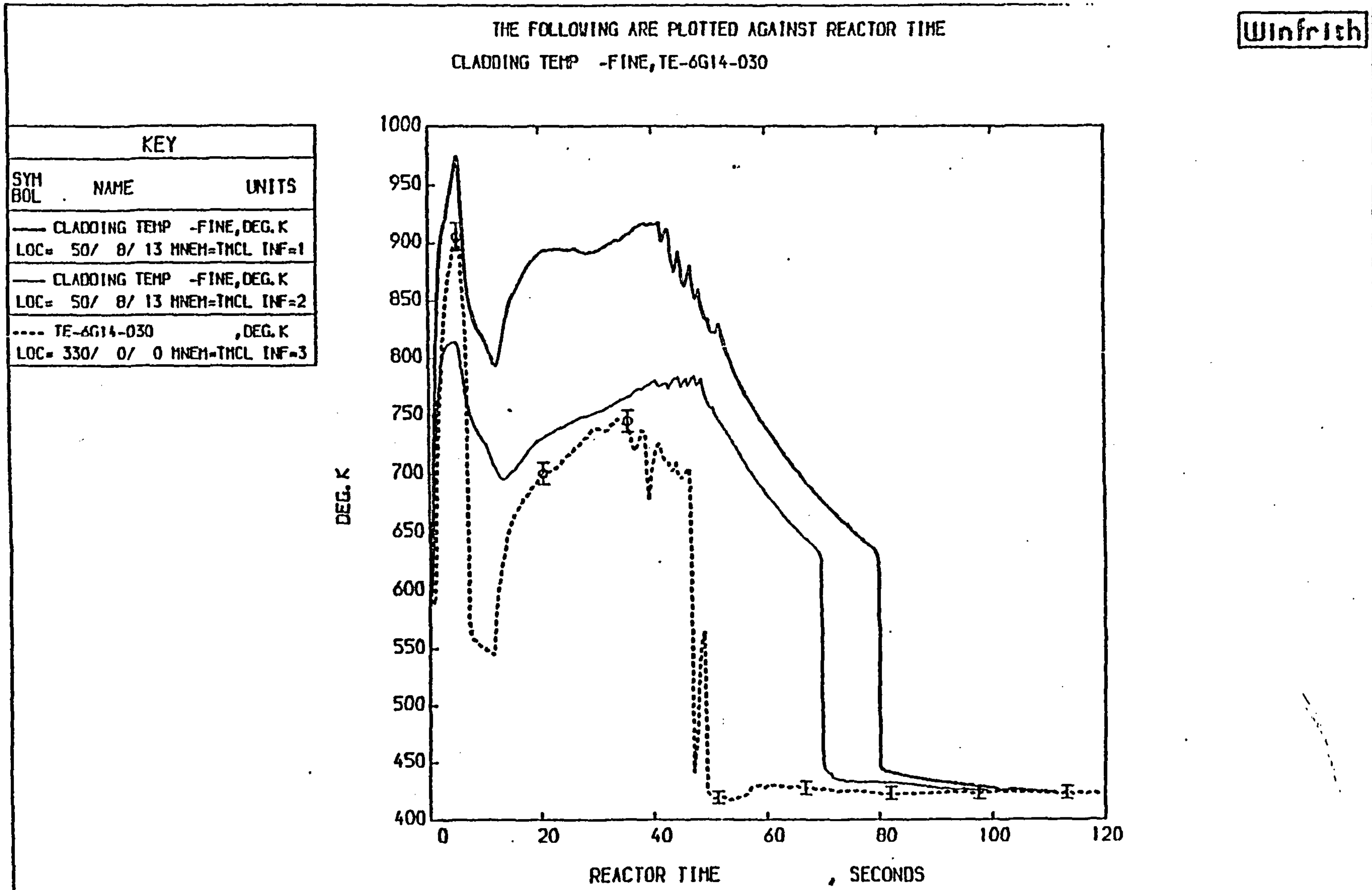

FIGURE 145 INF 1 ORIG, INF 2 ZEROGAP, INF 3 EXP
FUEL ROD CLADDING TEMPERATURES - PERIPHERAL BUNDLES

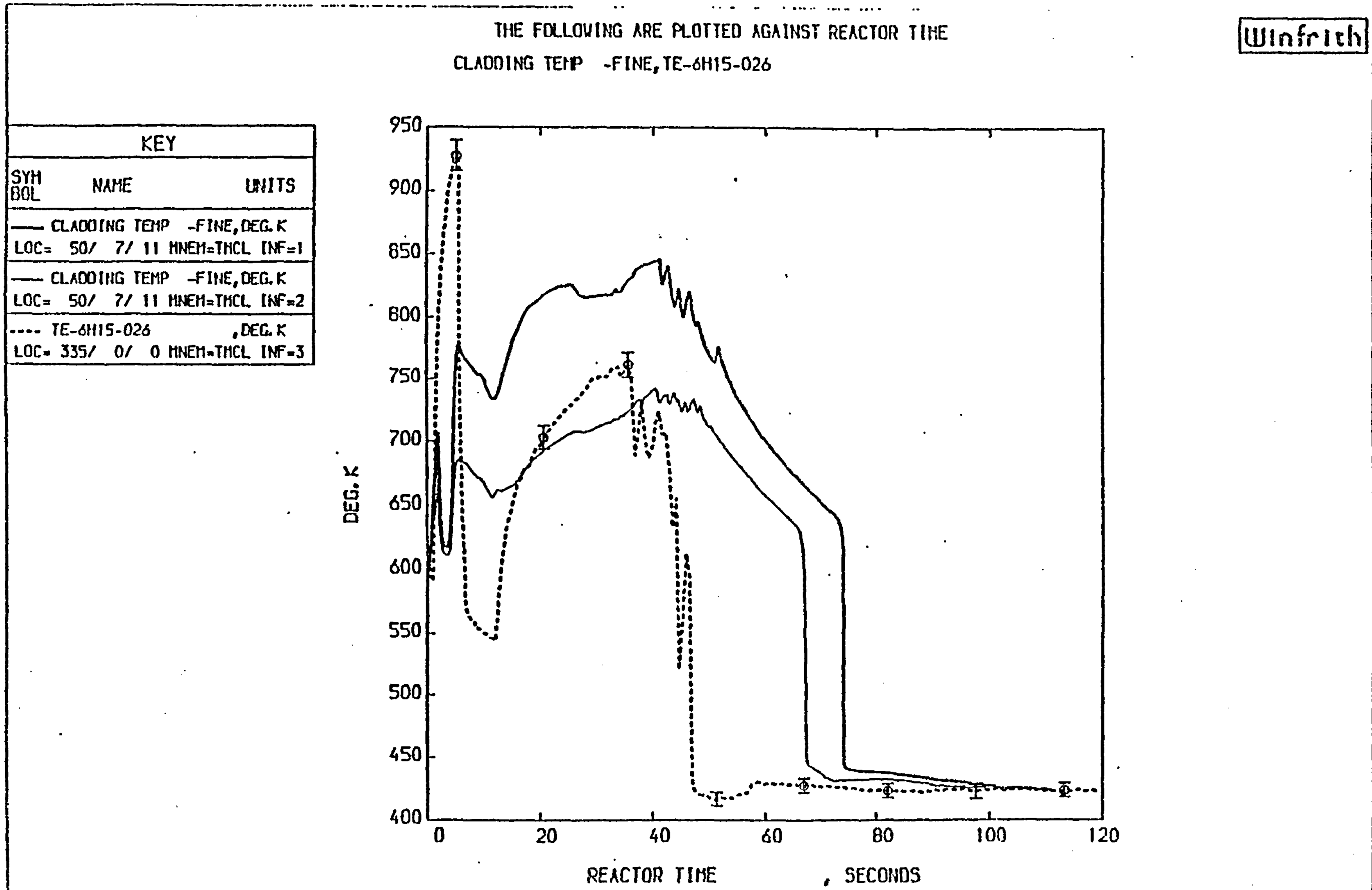

FIGURE 146 INF 1 ORIG, INF 2 ZEROGAP, INF 3 EXP
FUEL ROD CLADDING TEMPERATURES - PERIPHERAL BUNDLES

Winfrith

THE FOLLOWING ARE PLOTTED AGAINST REACTOR TIME
CLADDING TEMP -FINE,TE-6114-039

KEY		
SYMBOL	NAME	UNITS
——	CLADDING TEMP -FINE, LOC= 50/ 7/ 15 MNEM=TMCL INF=1	DEG.K
——	CLADDING TEMP -FINE, LOC= 50/ 7/ 15 MNEM=TMCL INF=2	DEG.K
----	TE-6114-039, LOC= 337/ 0/ 0 MNEM=TMCL INF=3	DEG.K

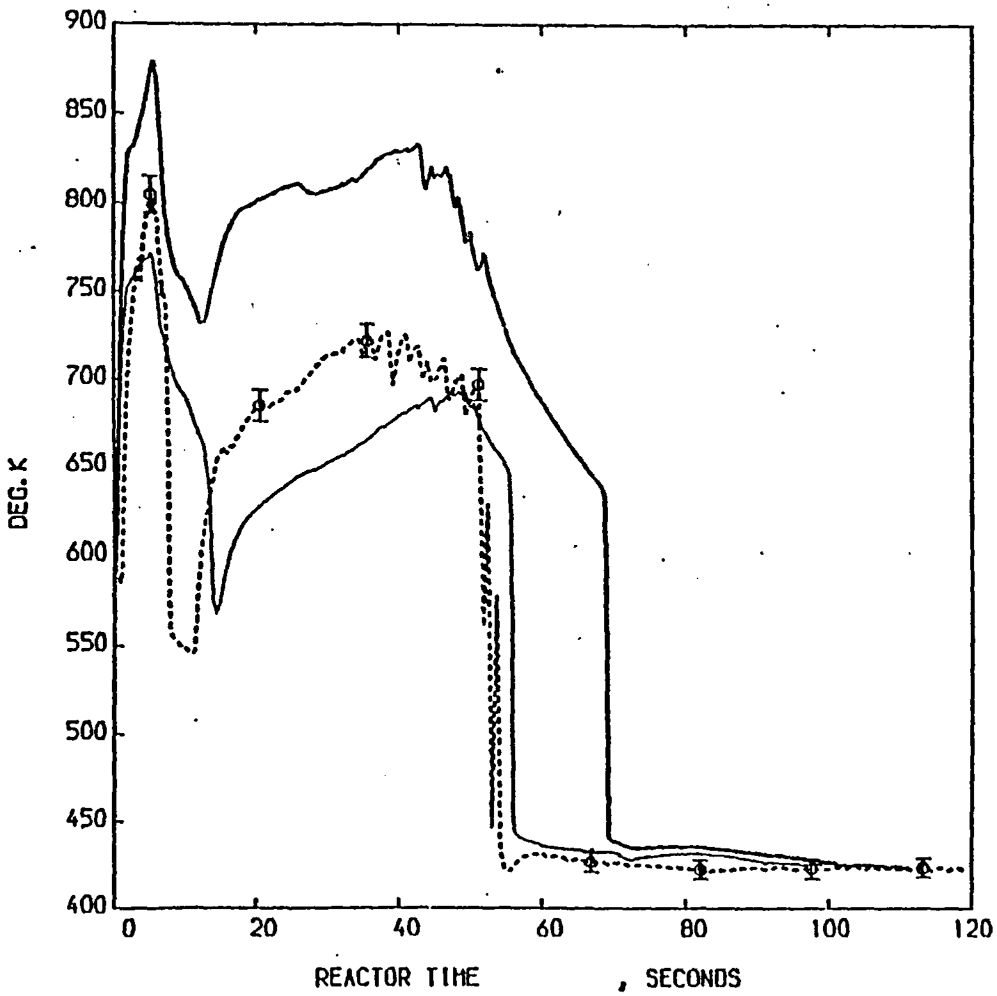

FIGURE 147 INF 1 ORIG, INF 2 ZEROGAP, INF 3 EXP
FUEL ROD CLADDING TEMPERATURES - PERIPHERAL BUNDLES

THE FOLLOWING ARE PLOTTED AGAINST REACTOR TIME

CLADDING TEMP -FINE,TE-6G14-045

Winfrith

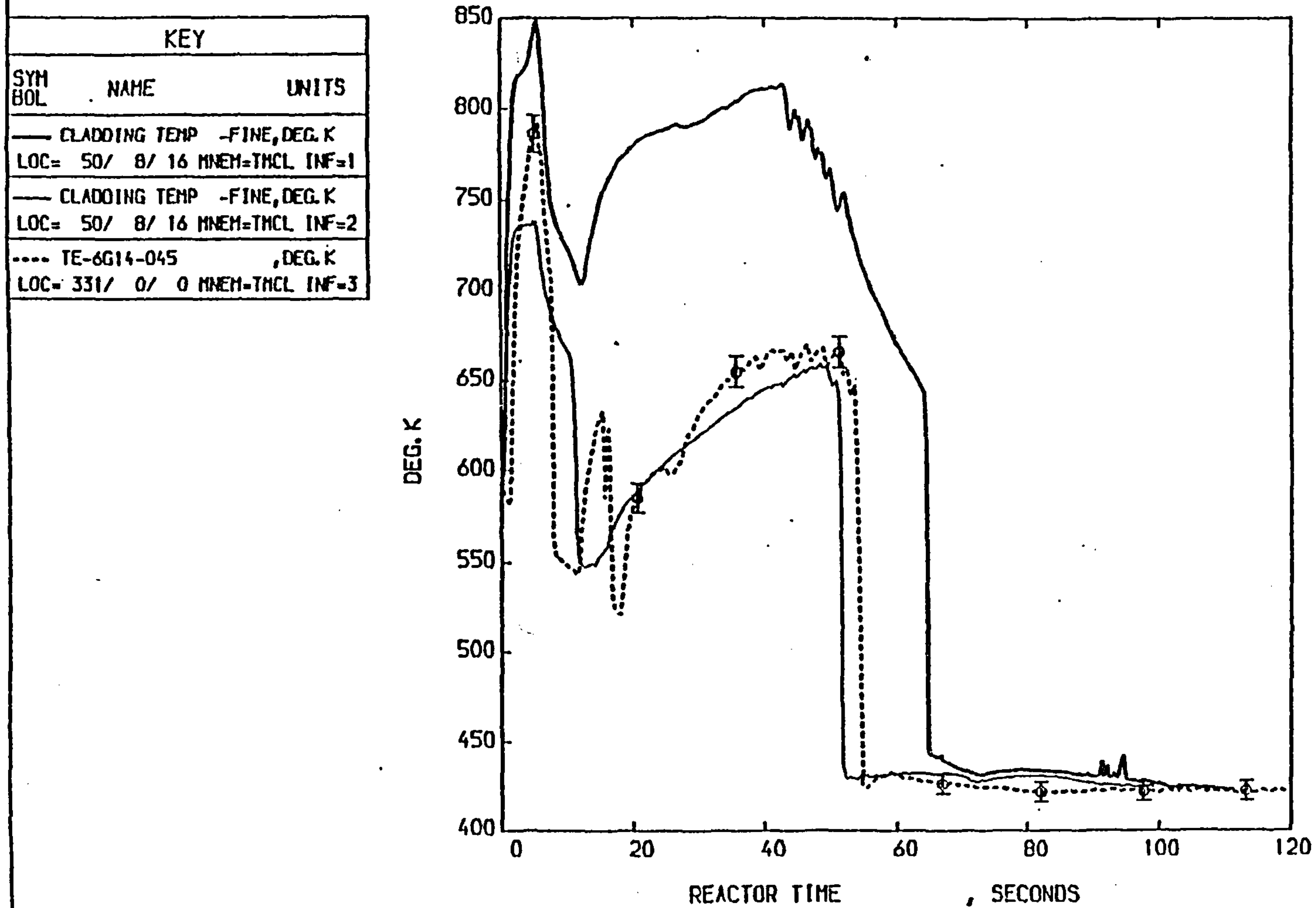

FIGURE 148 INF 1 ORIG, INF 2 ZEROGAP, INF 3 EXP
FUEL ROD CLADDING TEMPERATURES - PERIPHERAL BUNDLES

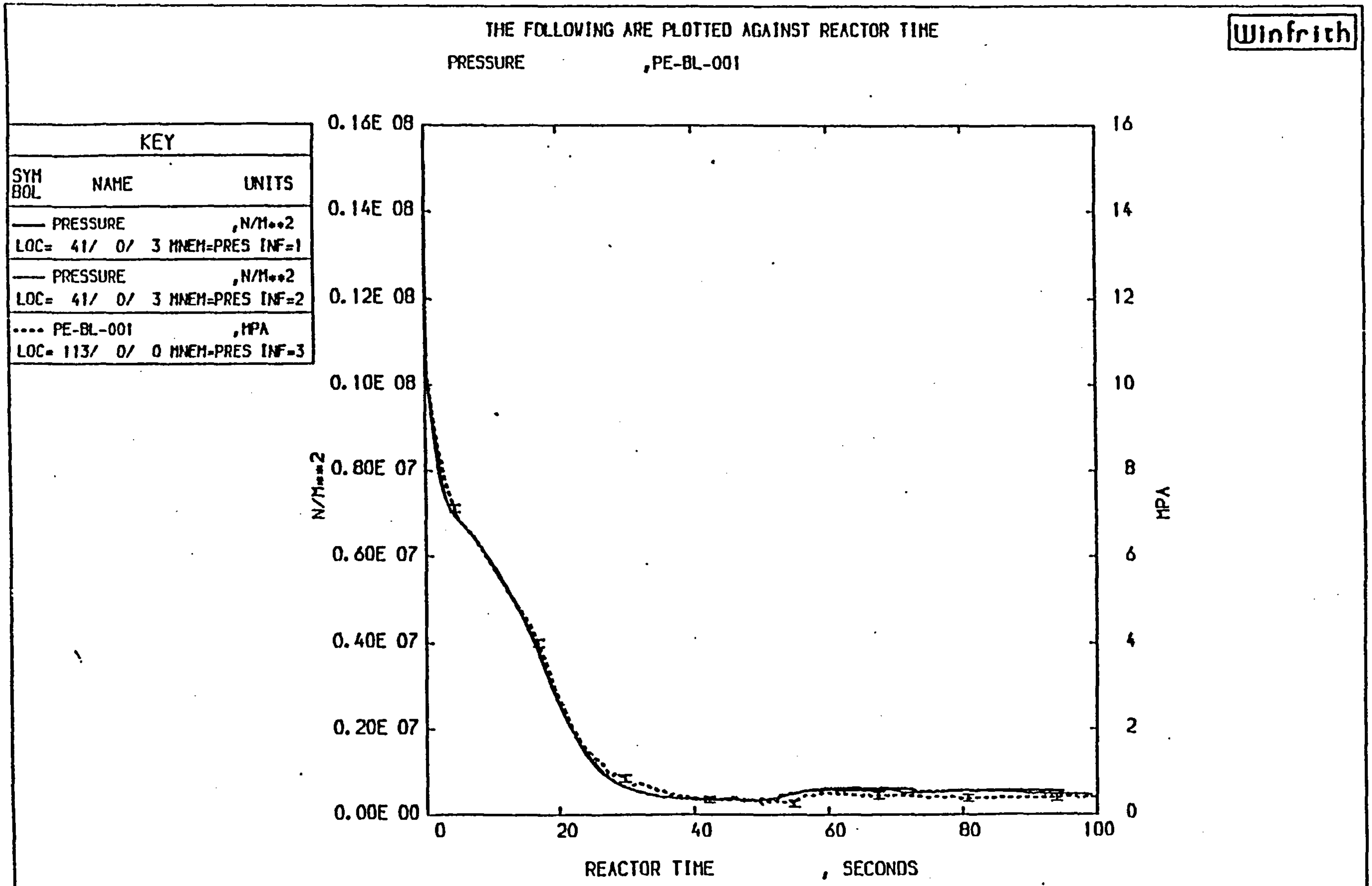

FIGURE 149 INF 1 ISHARP, INF 2 ZEROGAP, INF 3 EXP
BROKEN LOOP COLD LEG - EXPERIMENTAL LOCATION BL-1

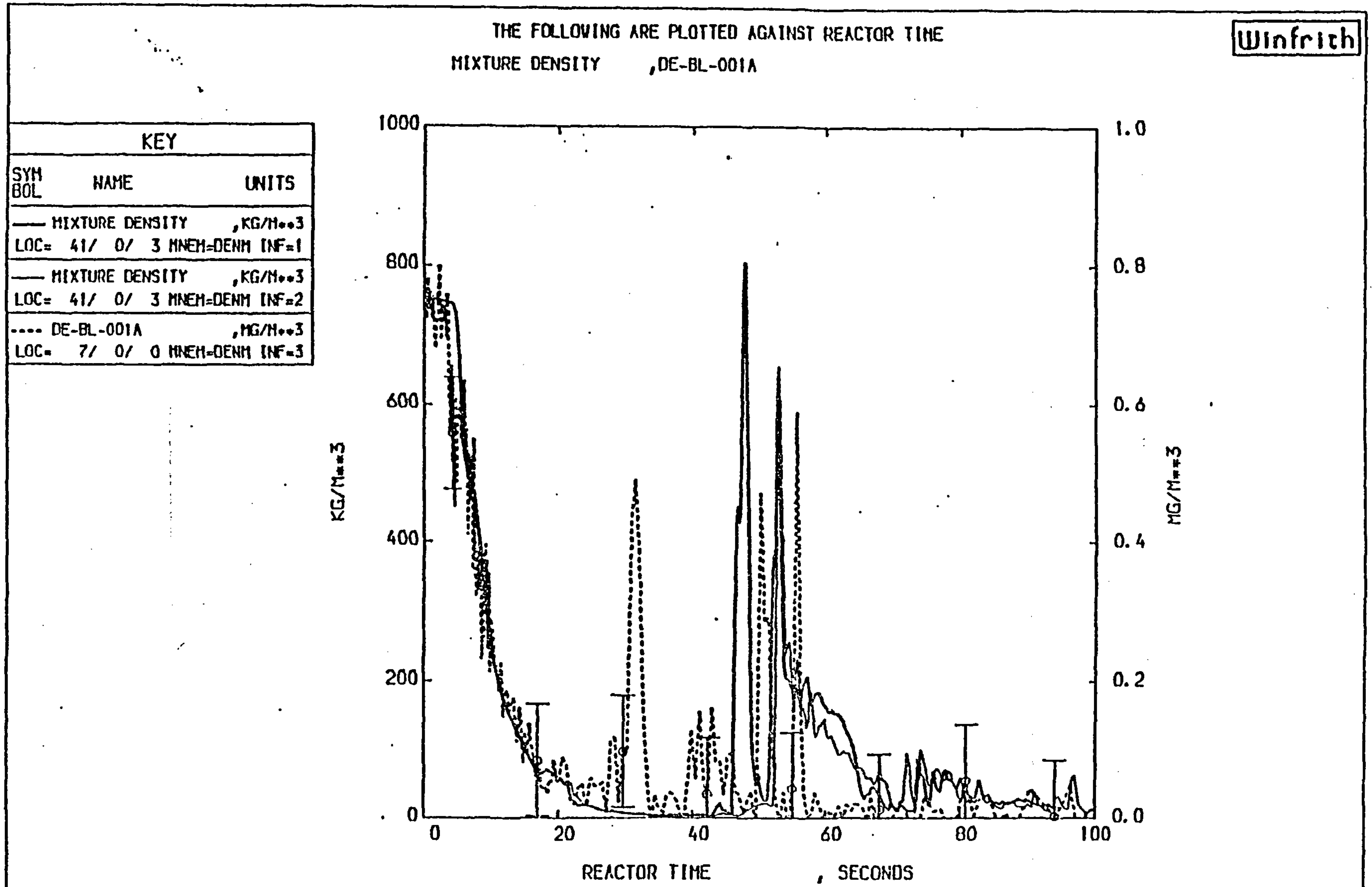

FIGURE 150 INF 1 ISHARP, INF 2 ZEROGAP, INF 3 EXP
BROKEN LOOP COLD LEG - EXPERIMENTAL LOCATION BL-1

Winfrith

THE FOLLOWING ARE PLOTTED AGAINST REACTOR TIME

MASS FLOW RATE ,FR-BL-105

KEY		
SYM BOL	NAME	UNITS
——	MASS FLOW RATE	,KG/SEC
LOC= 41/ 0/ 3 MNEM=FLOW INF=1		
——	MASS FLOW RATE	,KG/SEC
LOC= 41/ 0/ 3 MNEM=FLOW INF=2		
----	FR-BL-105	,KG/SEC
LOC= 32/ 0/ 0 MNEM=FLOW INF=3		

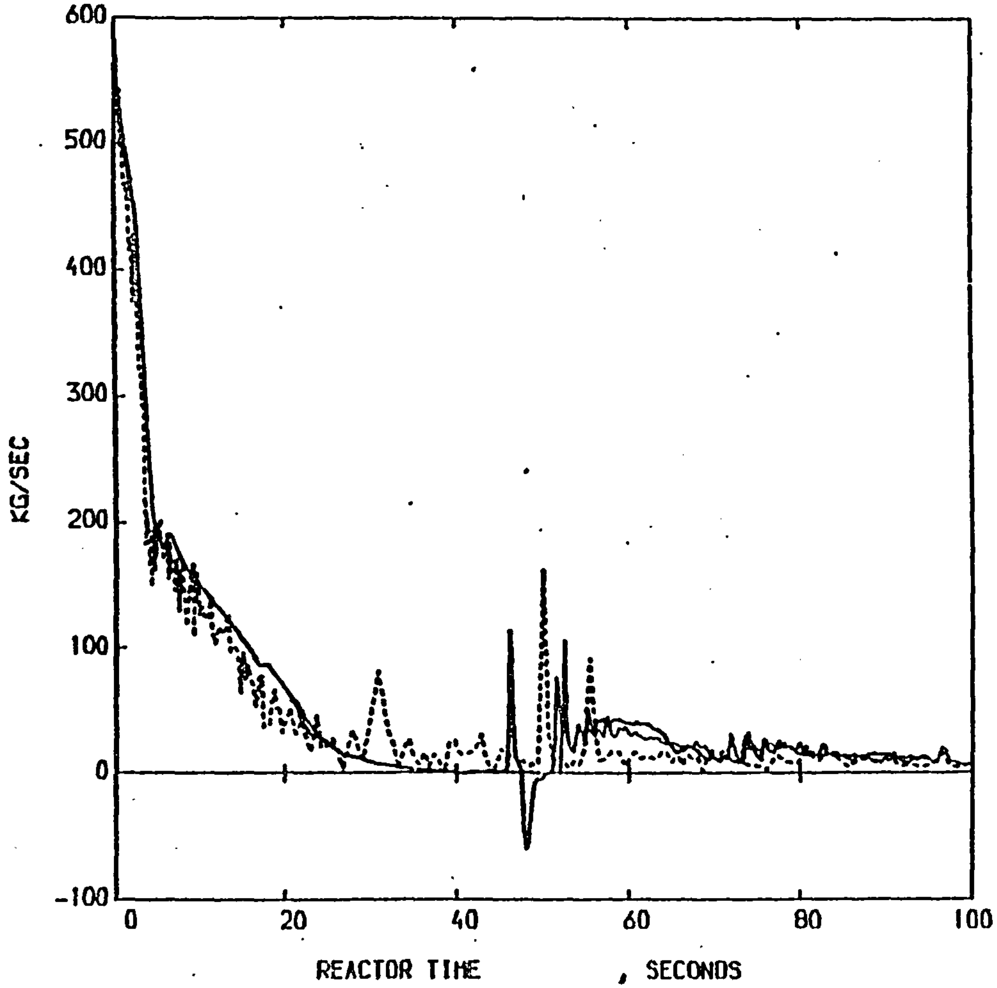

FIGURE 151 INF 1 ISHARP, INF 2 ZEROGAP, INF 3 EXP
BROKEN LOOP COLD LEG - EXPERIMENTAL LOCATION BL-1

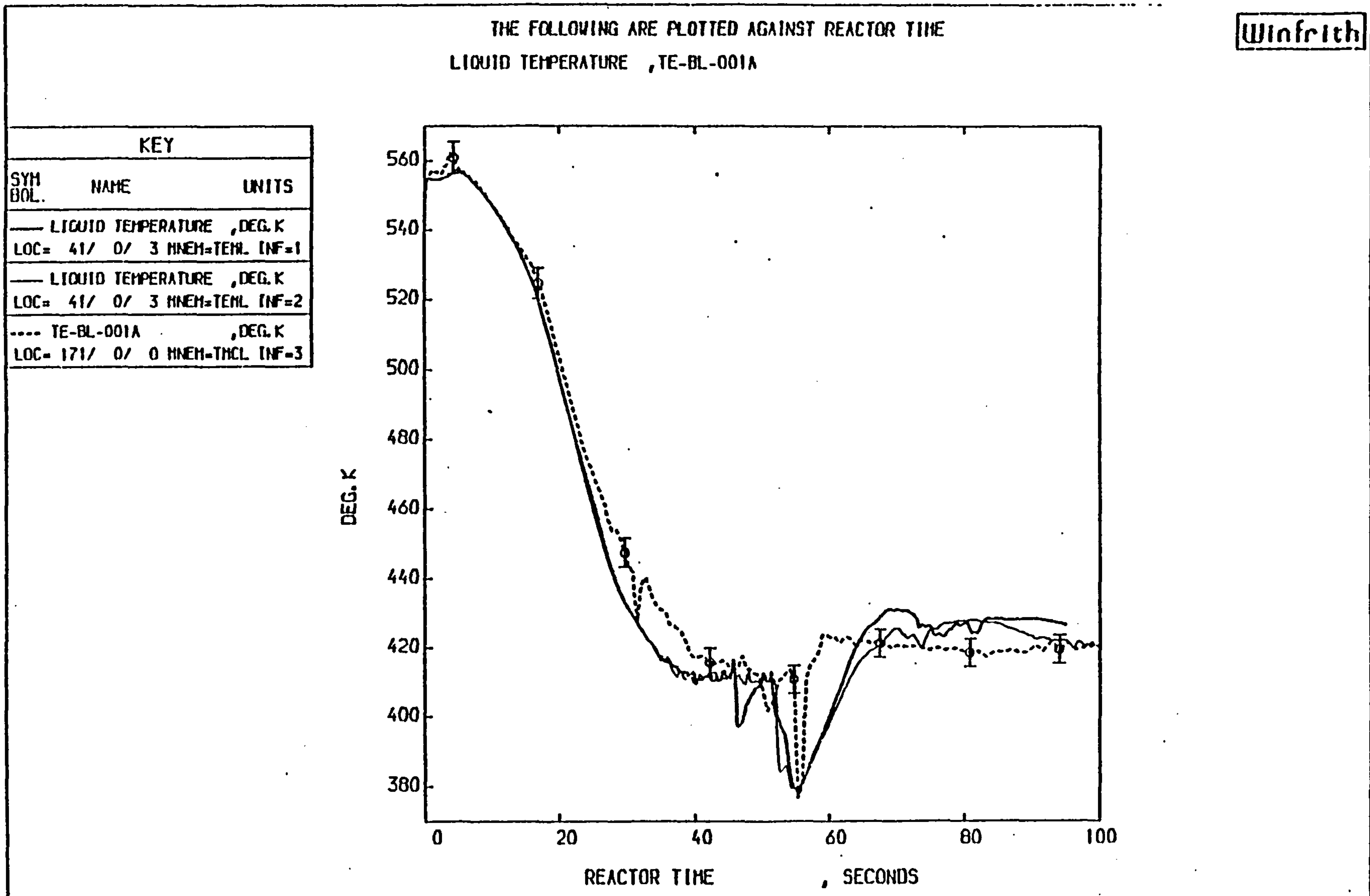

FIGURE 152 INF 1 ISHARP, INF 2 ZEROGAP, INF 3 EXP
BROKEN LOOP COLD LEG - EXPERIMENTAL LOCATION BL-1

THE FOLLOWING ARE PLOTTED AGAINST REACTOR TIME

VAPOR TEMPERATURE ,TE-BL-001C

Winfrith

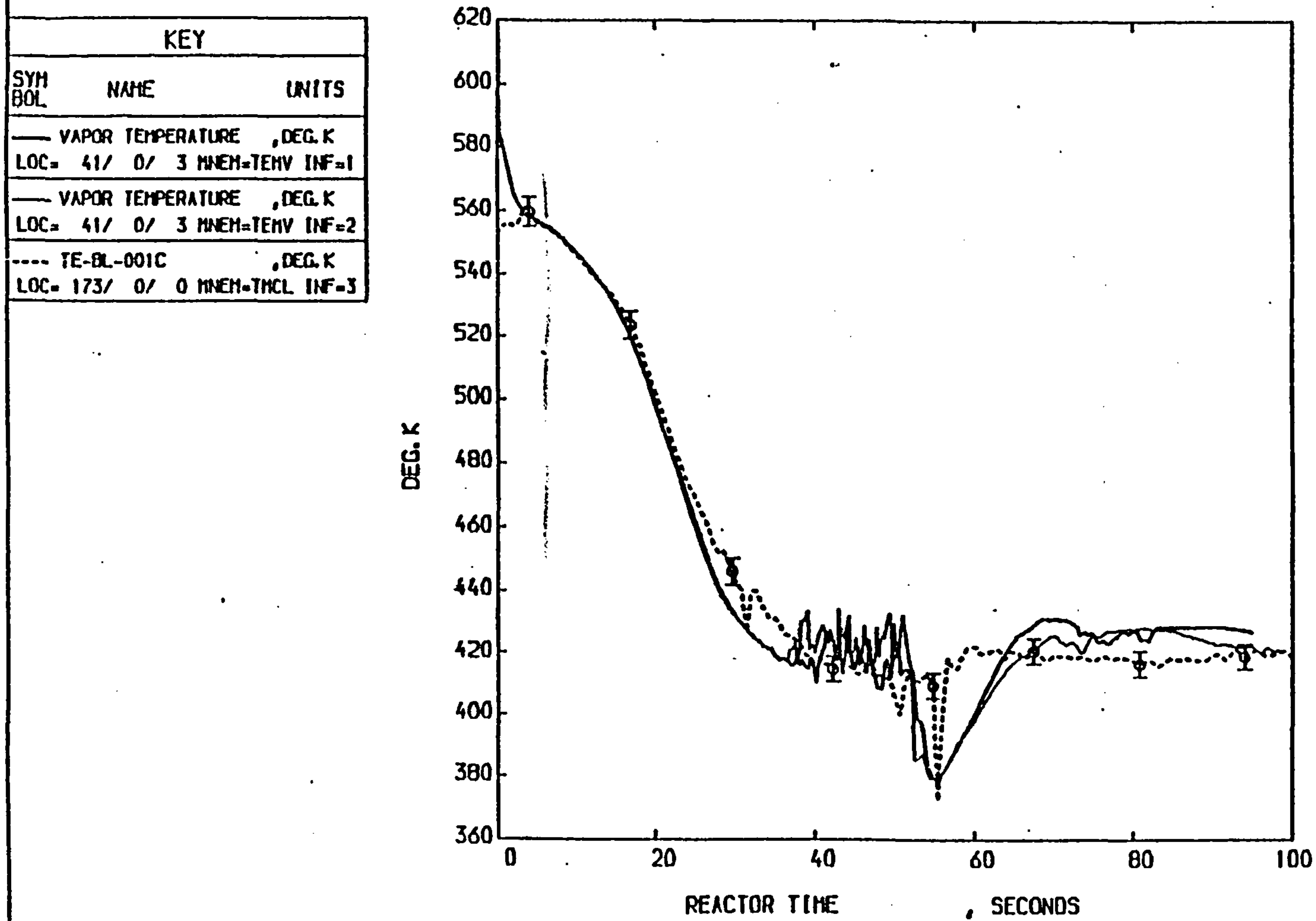

FIGURE 153 INF 1 ISHARP, INF 2 ZEROGAP, INF 3 EXP
BROKEN LOOP COLD LEG - EXPERIMENTAL LOCATION BL-1

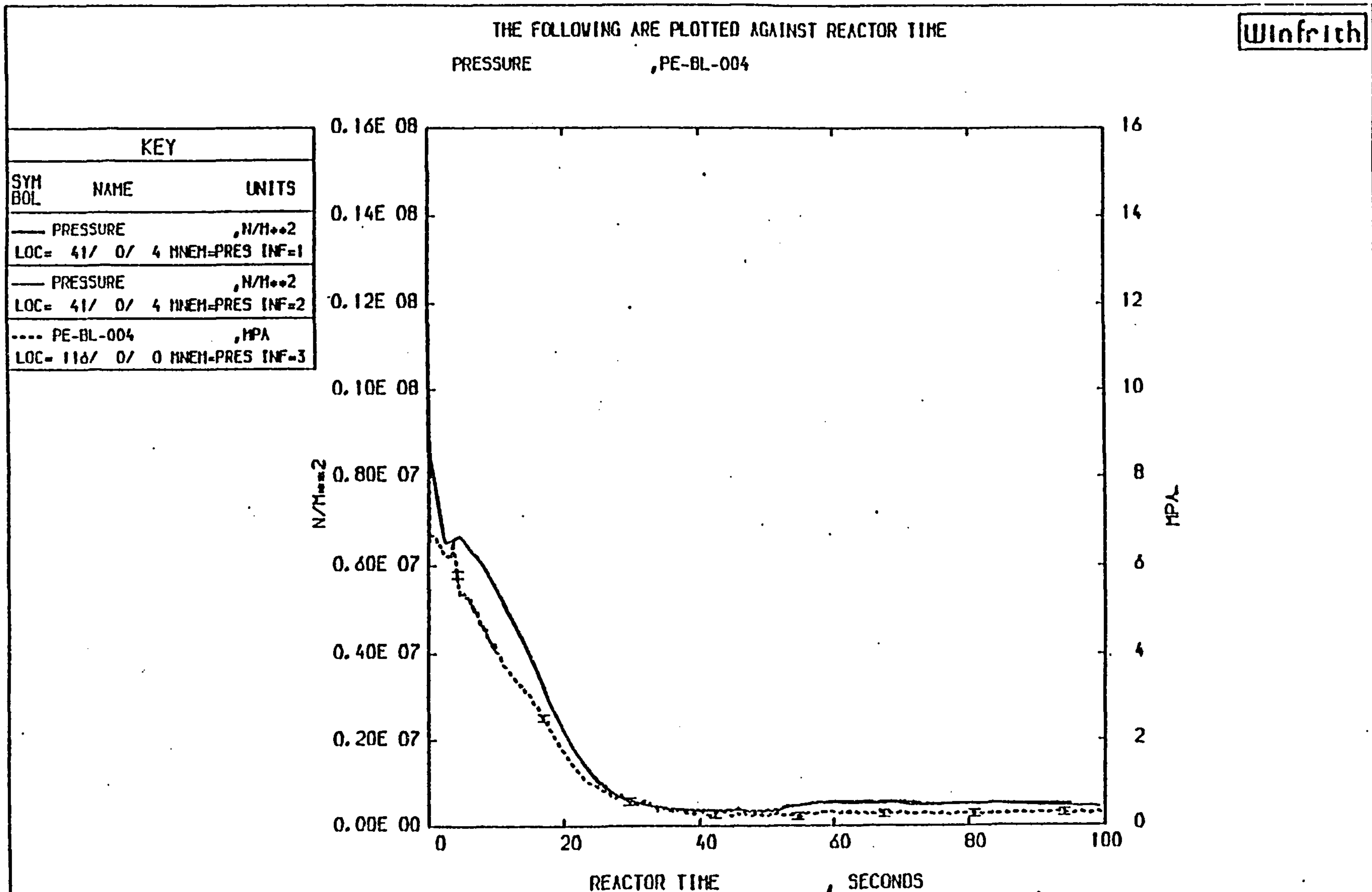

FIGURE 154 INF 1 ISHARP, INF 2 ZEROGAP, INF 3 EXP
BROKEN LOOP COLD LEG - EXPERIMENTAL LOCATION BL-4

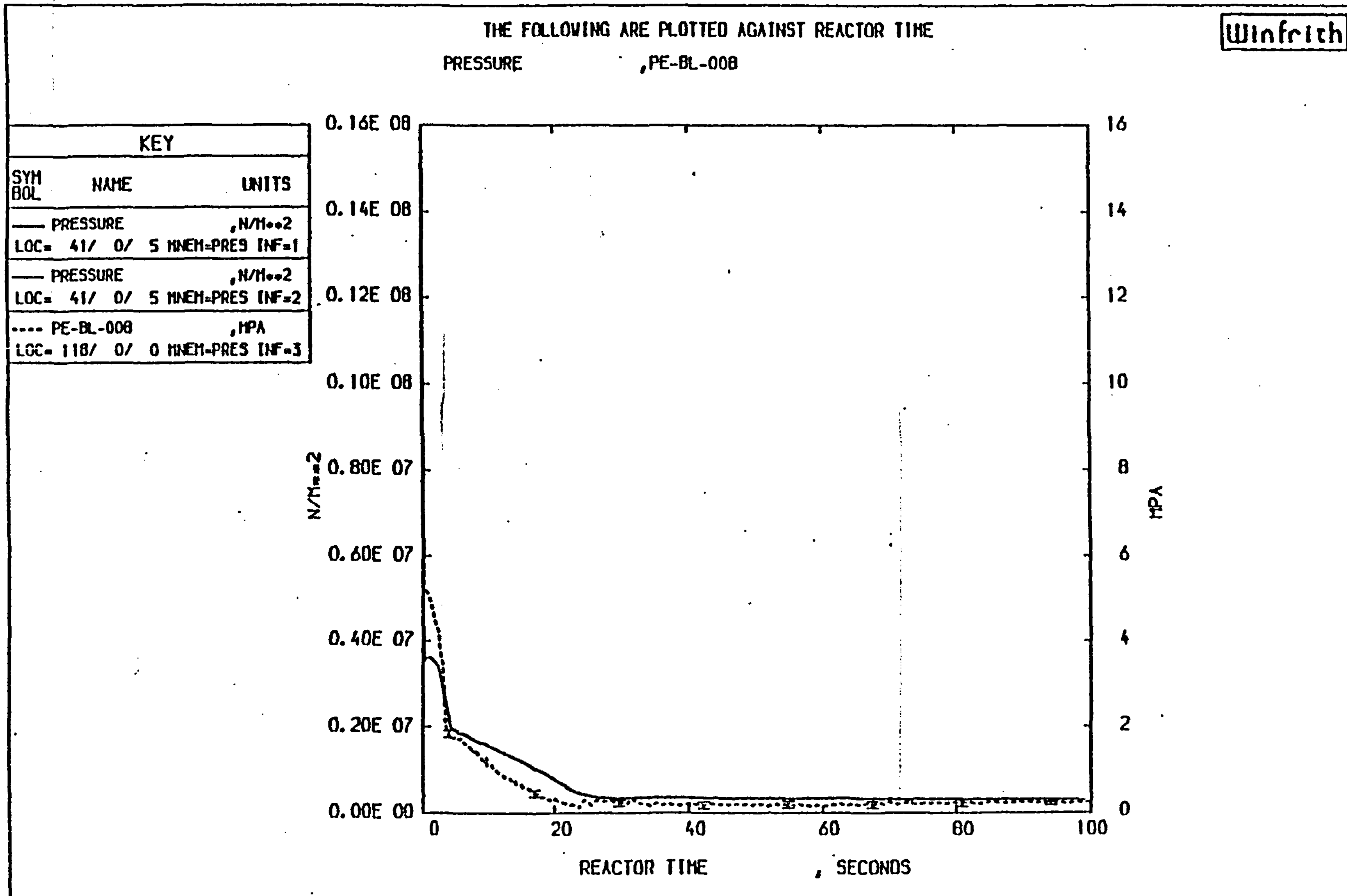

FIGURE 155 INF 1 ISHARP, INF 2 ZEROGAP, INF 3 EXP
BROKEN LOOP COLD LEG - EXPERIMENTAL LOCATION BL-8

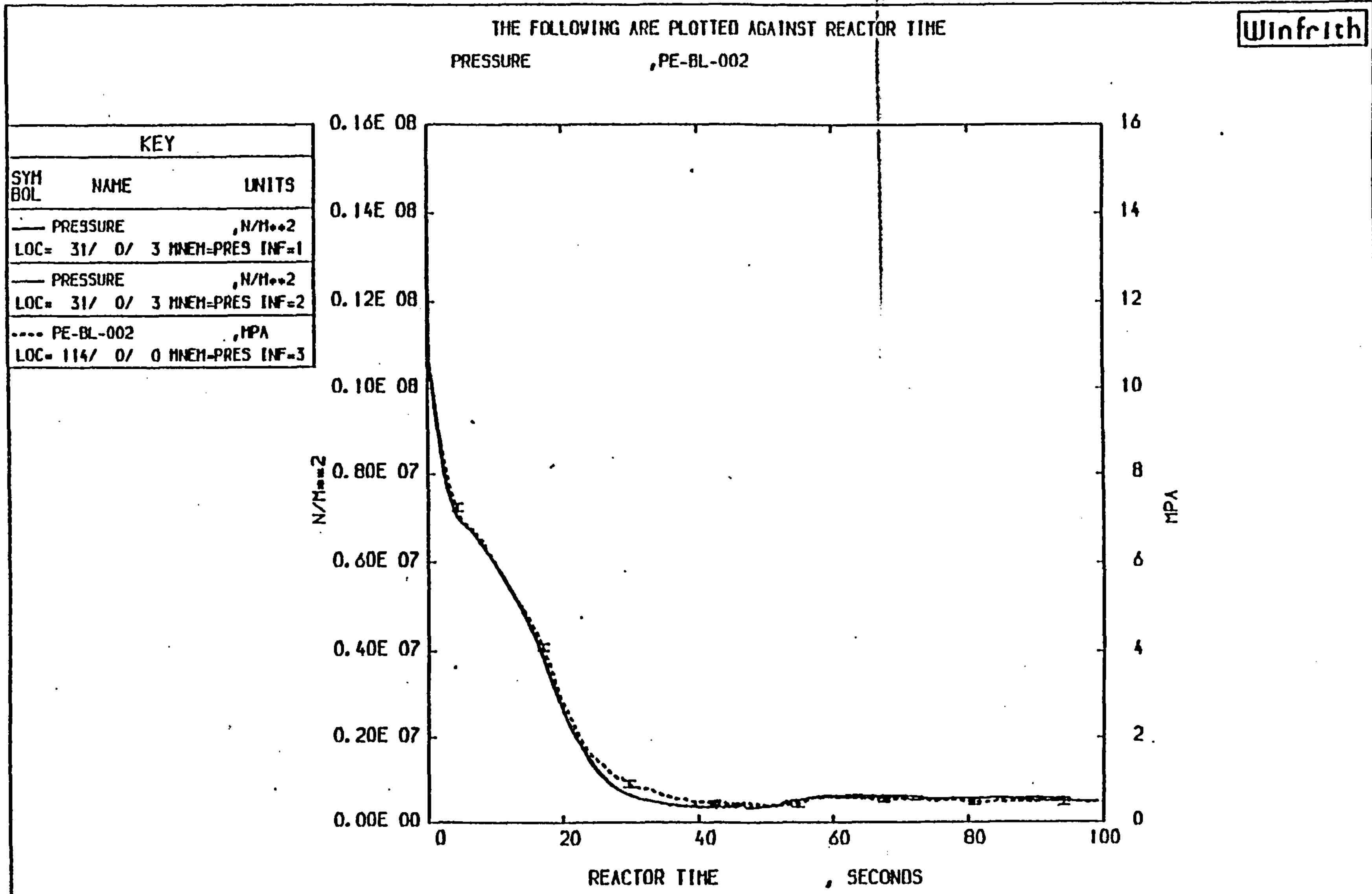

FIGURE 156 INF 1 ISHARP, INF 2 ZEROGAP, INF 3 EXP
BROKEN LOOP HOT LEG - EXPERIMENTAL LOCATION BL-2

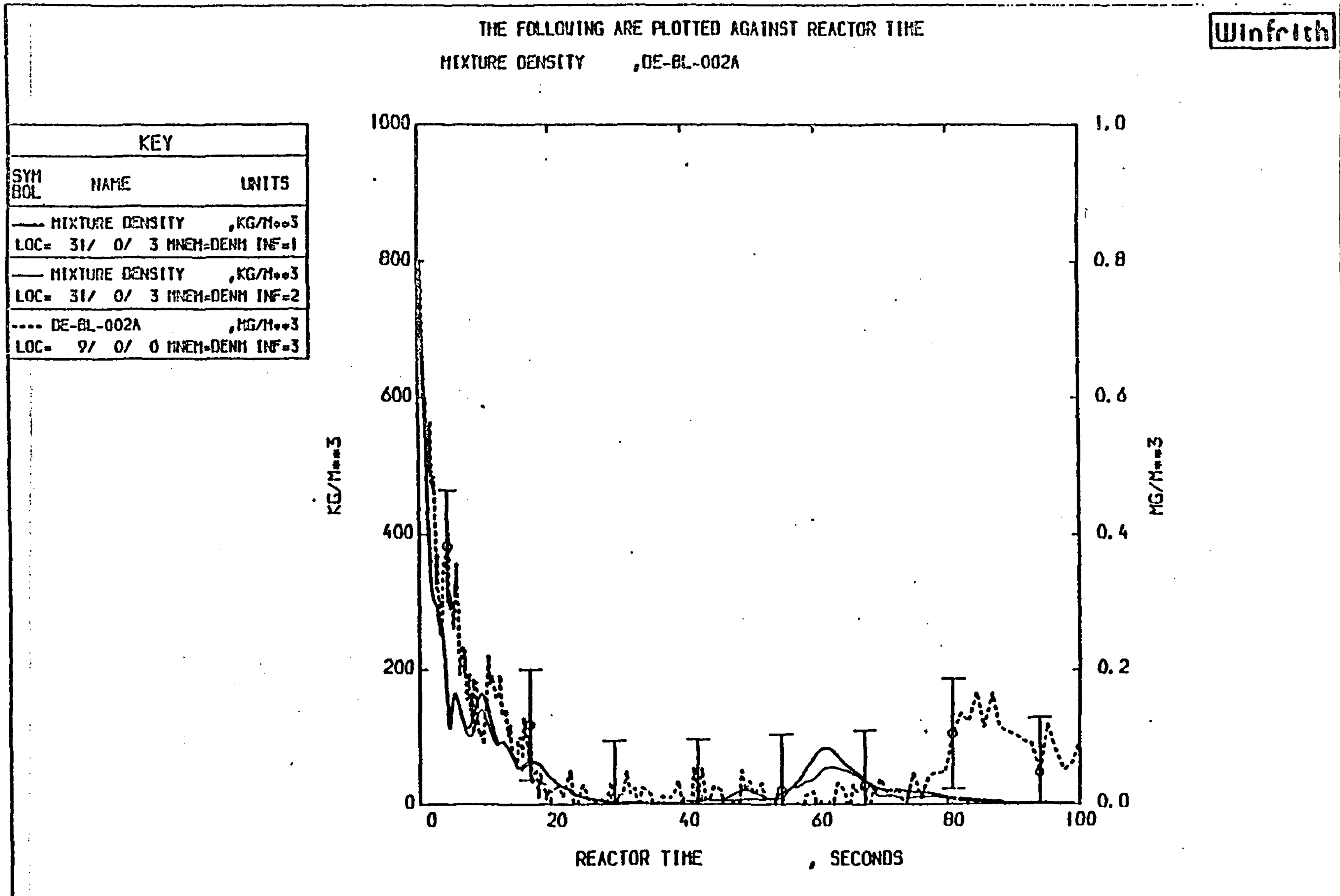

FIGURE 157 INF 1 ISHARP, INF 2 ZEROGAP, INF 3 EXP
BROKEN LOOP HOT LEG - EXPERIMENTAL LOCATION BL-2

Winfrith

THE FOLLOWING ARE PLOTTED AGAINST REACTOR TIME

MASS FLOW RATE ,FR-BL-205

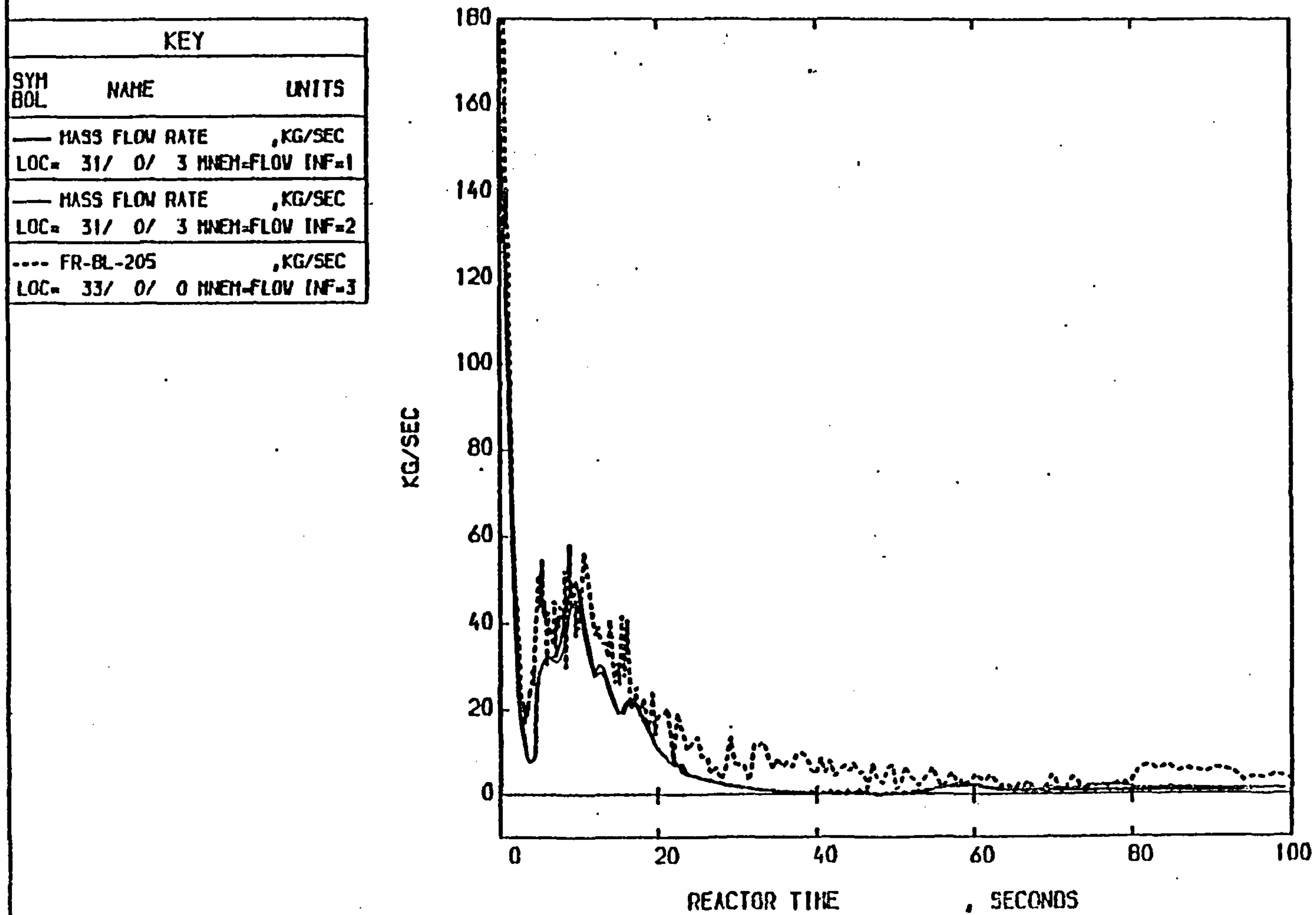

FIGURE 158 INF 1 ISHARP, INF 2 ZEROGAP, INF 3 EXP
BROKEN LOOP HOT LEG - EXPERIMENTAL LOCATION BL-2

Winfrith

THE FOLLOWING ARE PLOTTED AGAINST REACTOR TIME
LIQUID TEMPERATURE ,TE-BL-002B

KEY		
SYM BOL	NAME	UNITS
——	LIQUID TEMPERATURE	,DEG.K
	LOC= 31/ 0/ 3 MNEM=TEML INF=1	
——	LIQUID TEMPERATURE	,DEG.K
	LOC= 31/ 0/ 3 MNEM=TEML INF=2	
----	TE-BL-002B	,DEG.K
	LOC= 174/ 0/ 0 MNEM=TMCL INF=3	

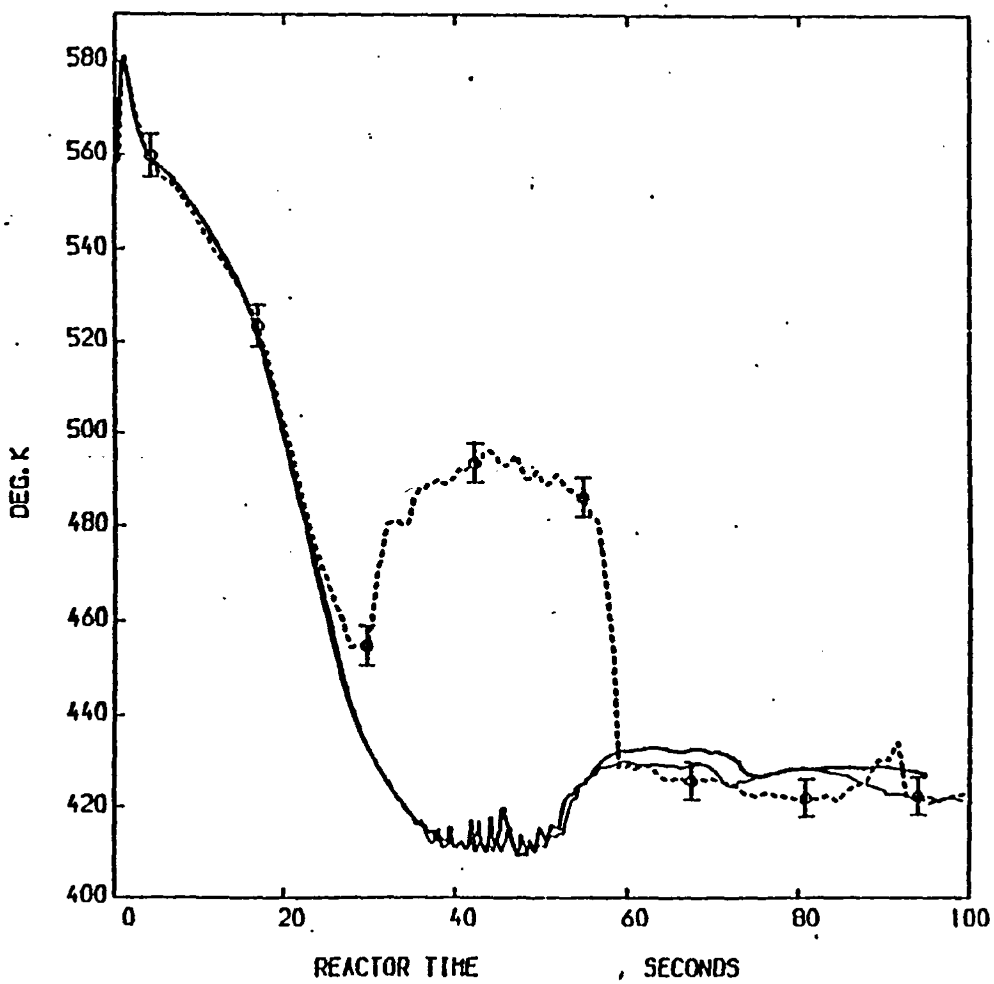

FIGURE 159 INF 1 ISHARP, INF 2 ZEROGAP, INF 3 EXP
BROKEN LOOP HOT LEG - EXPERIMENTAL LOCATION BL-2

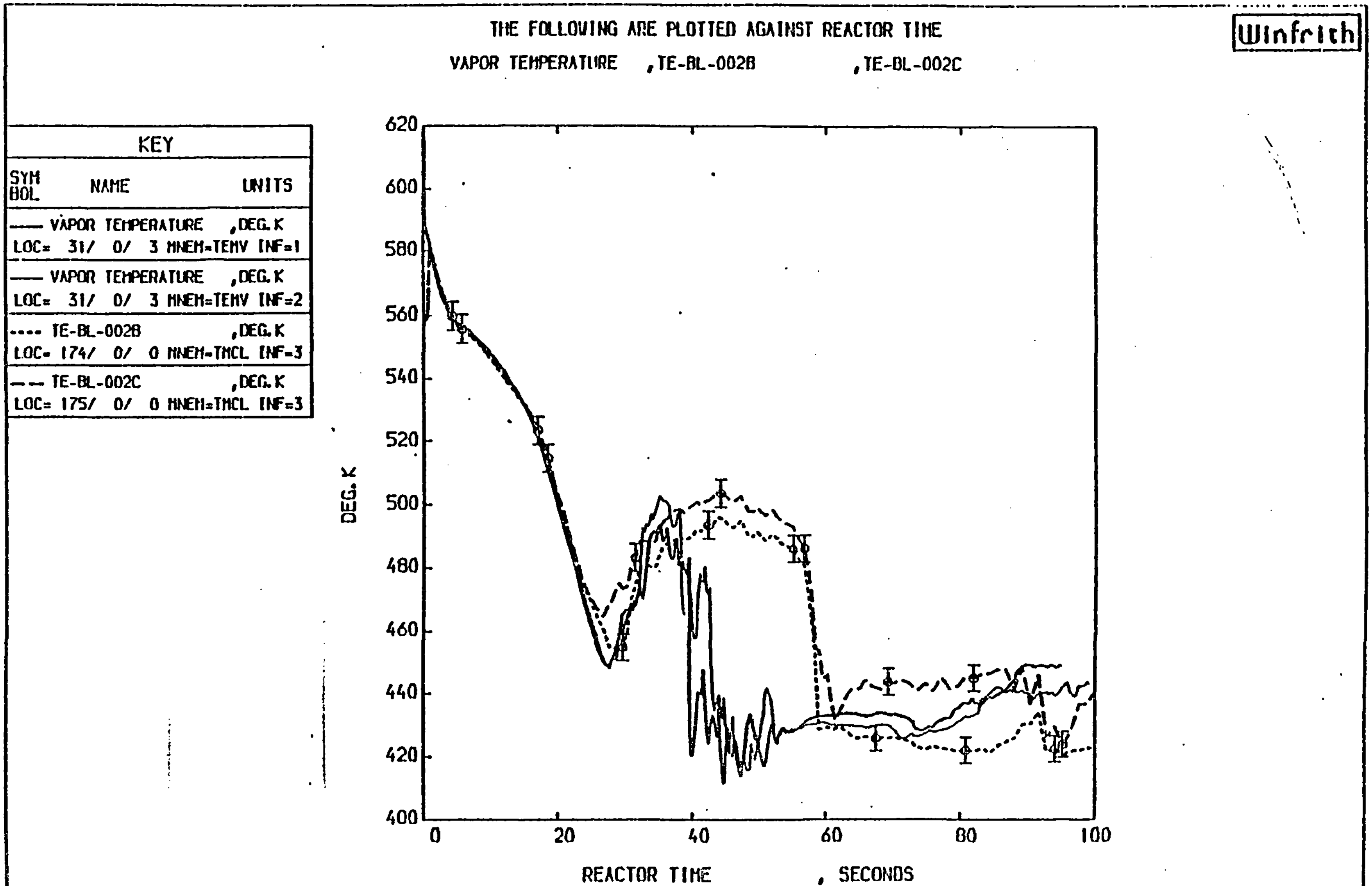

FIGURE 160 INF 1 ISHARP, INF 2 ZEROGAP, INF 3 EXP
BROKEN LOOP HOT LEG - EXPERIMENTAL LOCATION BL-2

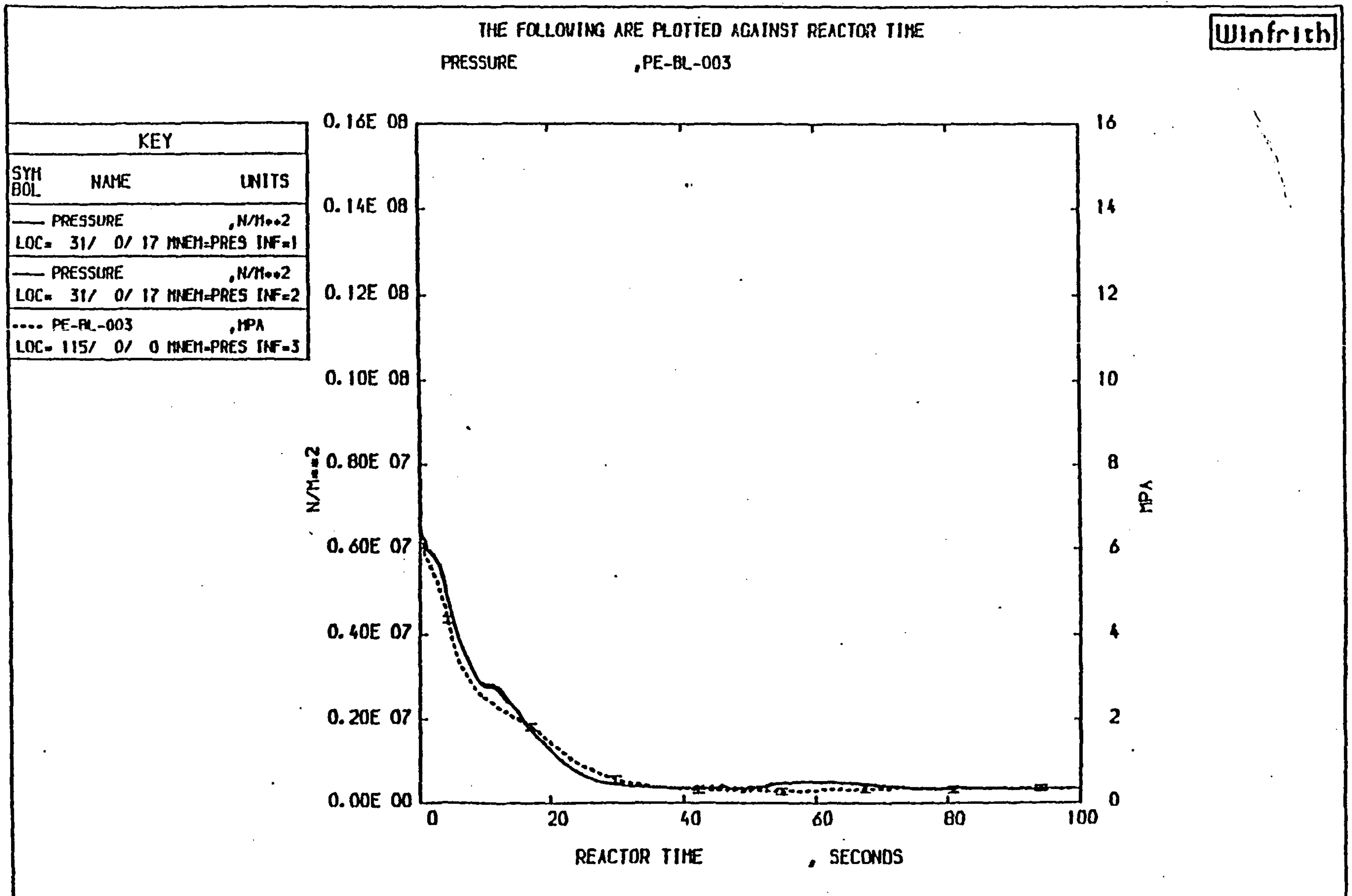

FIGURE 161 INF 1 ISHARP, INF 2 ZEROGAP, INF 3 EXP
BROKEN LOOP HOT LEG - EXPERIMENTAL LOCATION BL-3

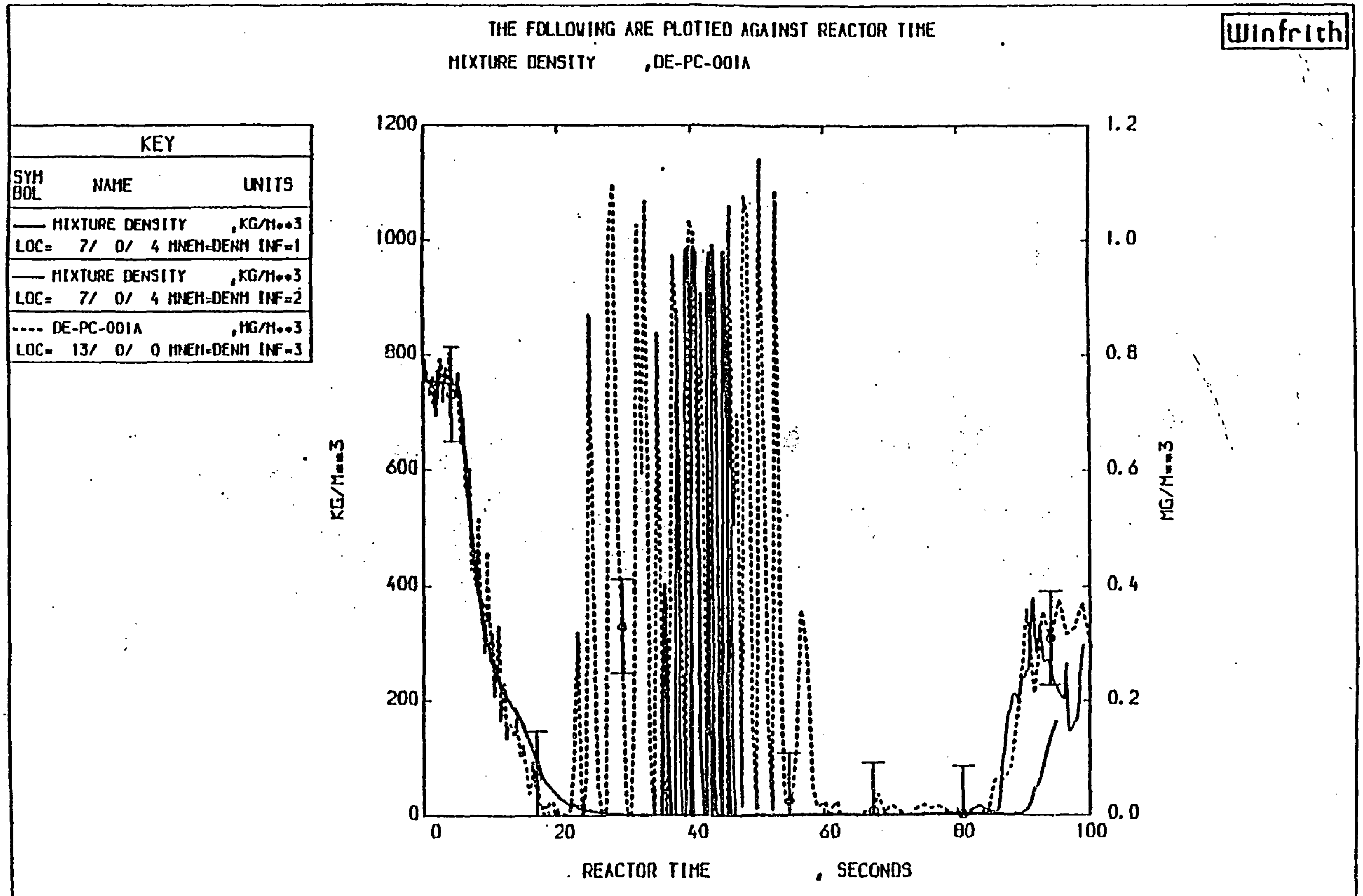

FIGURE 162 INF 1 ISHARP, INF 2 ZEROGAP, INF 3 EXP
INTACT LOOP COLD LEG - EXPERIMENTAL LOCATION PC-1

Winfrith

THE FOLLOWING ARE PLOTTED AGAINST REACTOR TIME

MASS FLOW RATE ,FR-PC-100

KEY		
SYMBOL	NAME	UNITS
——	MASS FLOW RATE LOC= 7/ 0/ 4 MNEM=FLOW INF=1	,KG/SEC
——	MASS FLOW RATE LOC= 7/ 0/ 4 MNEM=FLOW INF=2	,KG/SEC
----	FR-PC-100 LOC= 34/ 0/ 0 MNEM=FLOW INF=3	,KG/SEC

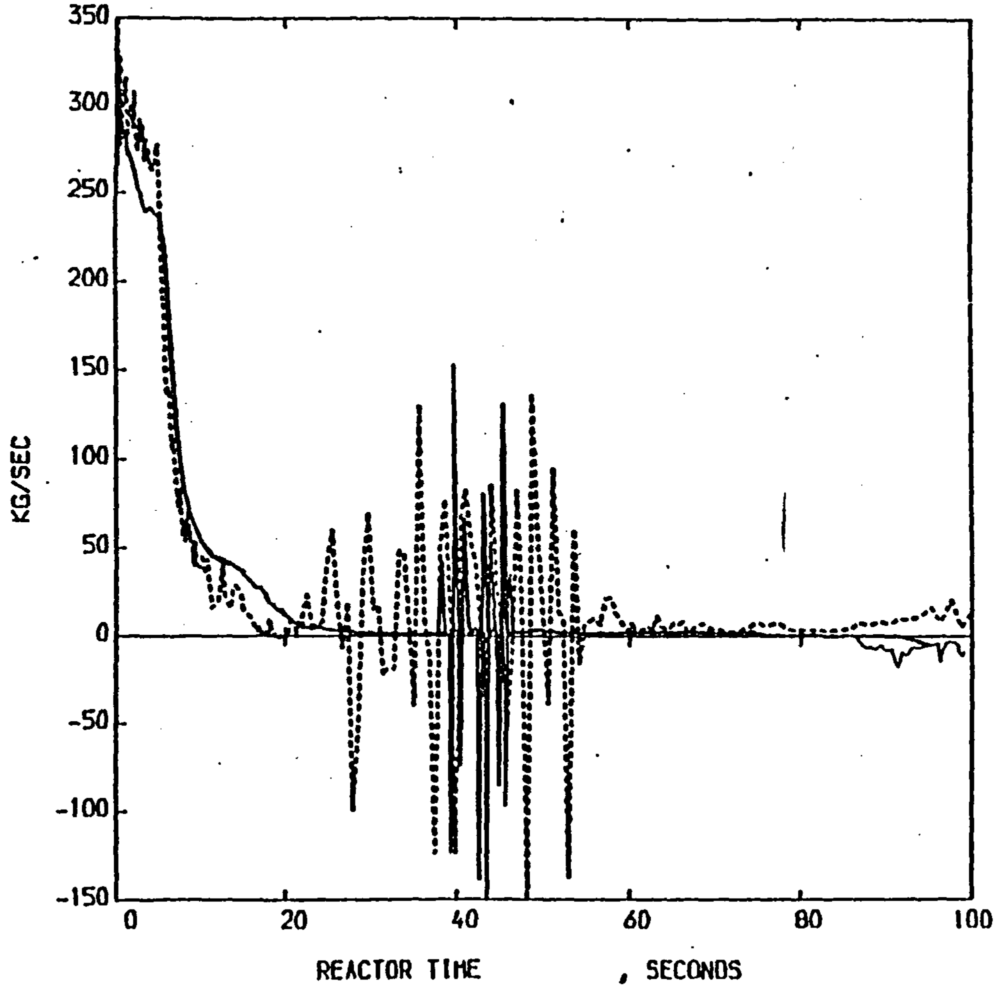

FIGURE 163 INF 1 ISHARP, INF 2 ZEROGAP, INF 3 EXP
INTACT LOOP COLD LEG - EXPERIMENTAL LOCATION PC-1

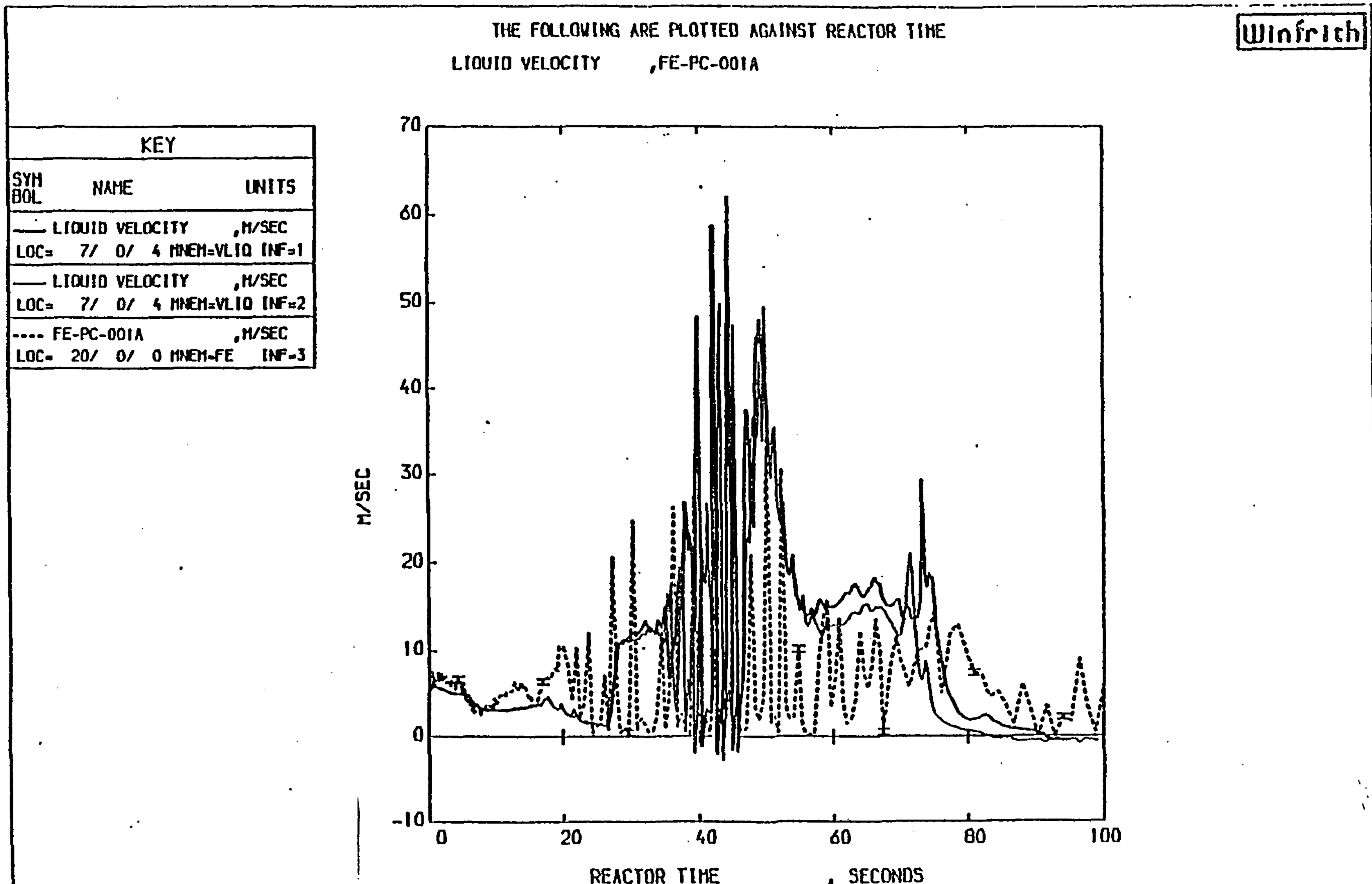

FIGURE 164 INF 1 ISHARP, INF 2 ZEROGAP, INF 3 EXP
INTACT LOOP COLD LEG - EXPERIMENTAL LOCATION PC-1

THE FOLLOWING ARE PLOTTED AGAINST REACTOR TIME

LIQUID TEMPERATURE ,TE-PC-001A

Winfrith

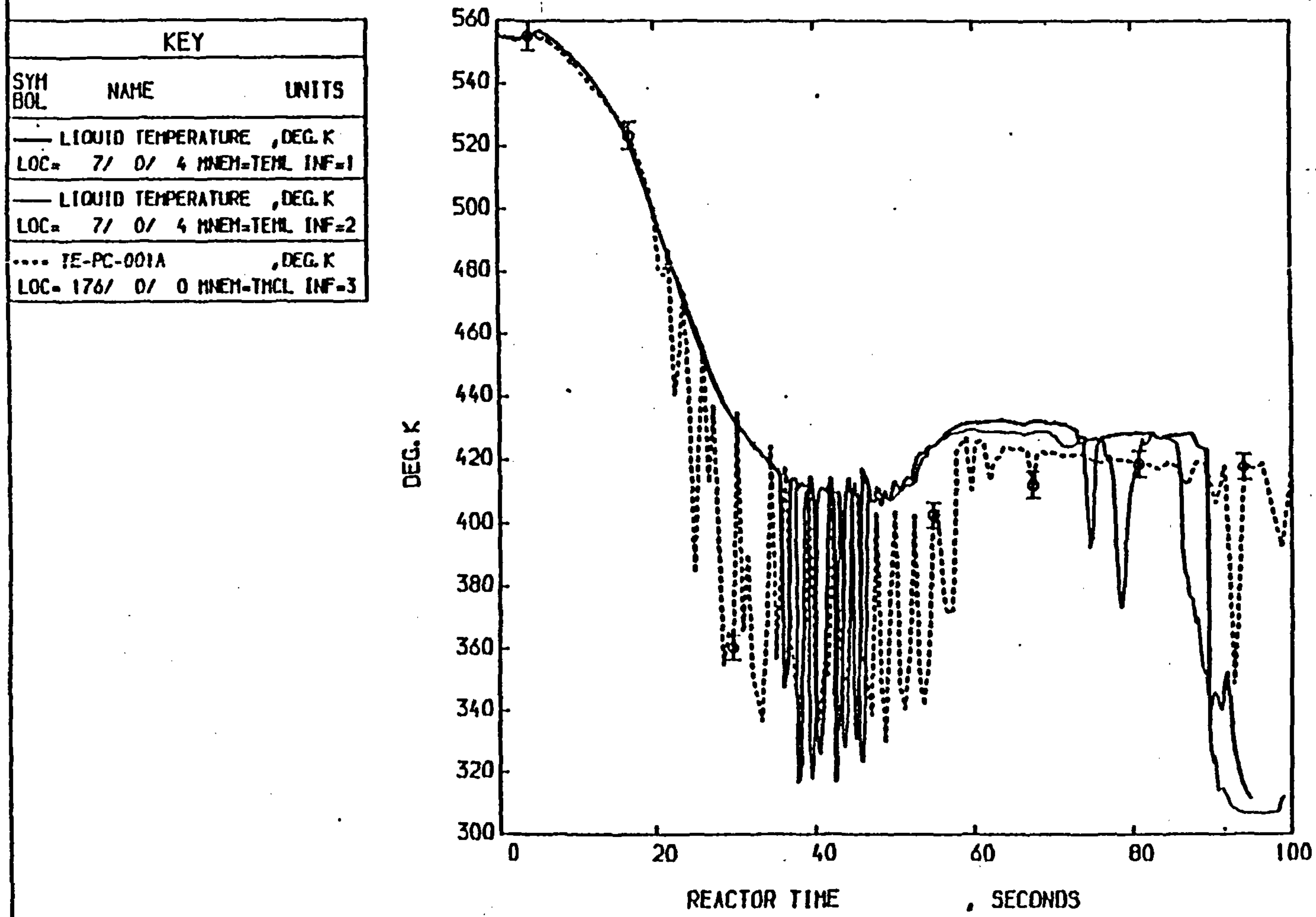

FIGURE 165 INF 1 ISHARP, INF 2 ZEROGAP, INF 3 EXP
INTACT LOOP COLD LEG - EXPERIMENTAL LOCATION PC-1

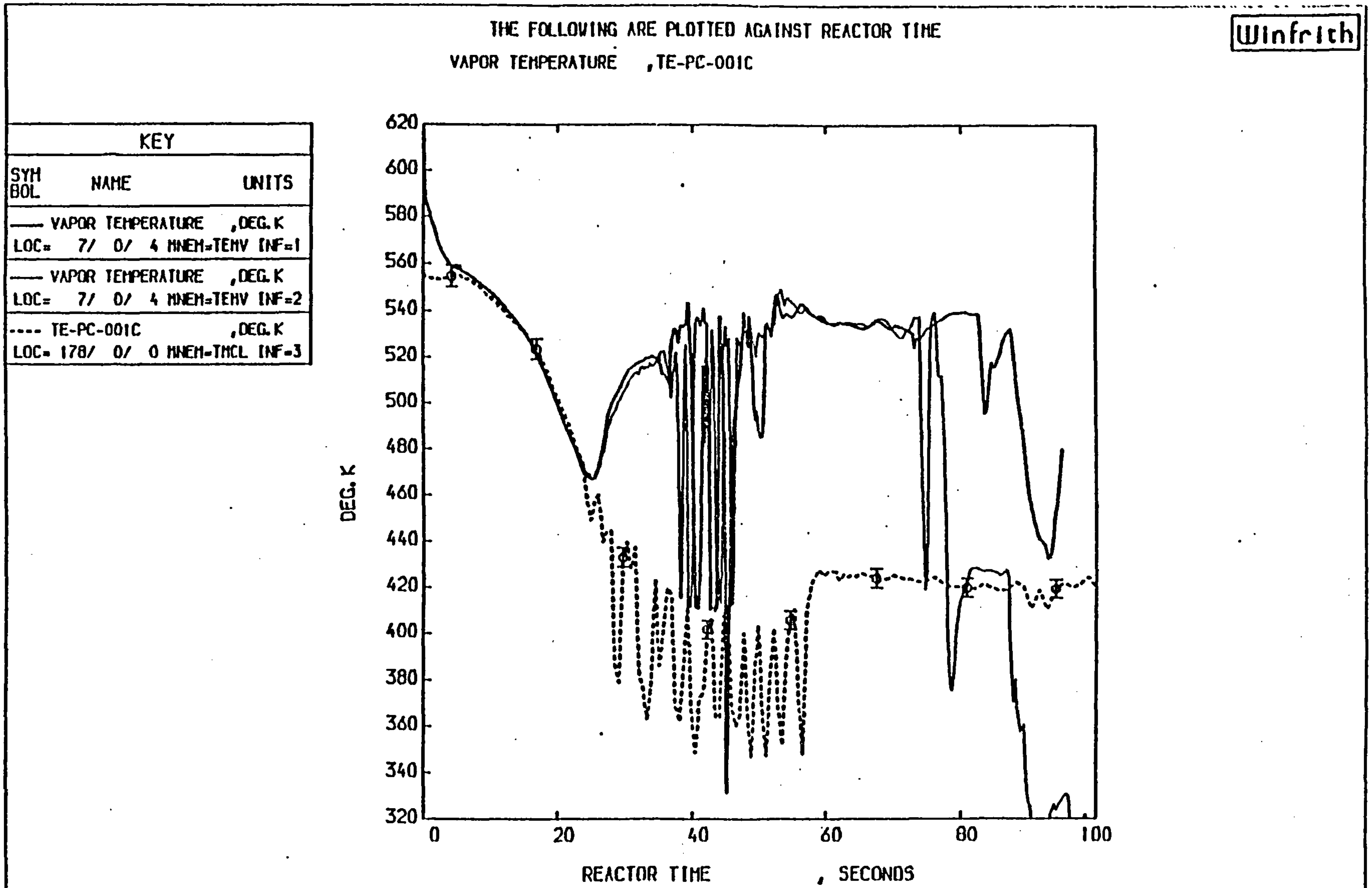

FIGURE 166 INF 1 ISHARP, INF 2 ZEROGAP, INF 3 EXP
INTACT LOOP COLD LEG - EXPERIMENTAL LOCATION PC-1

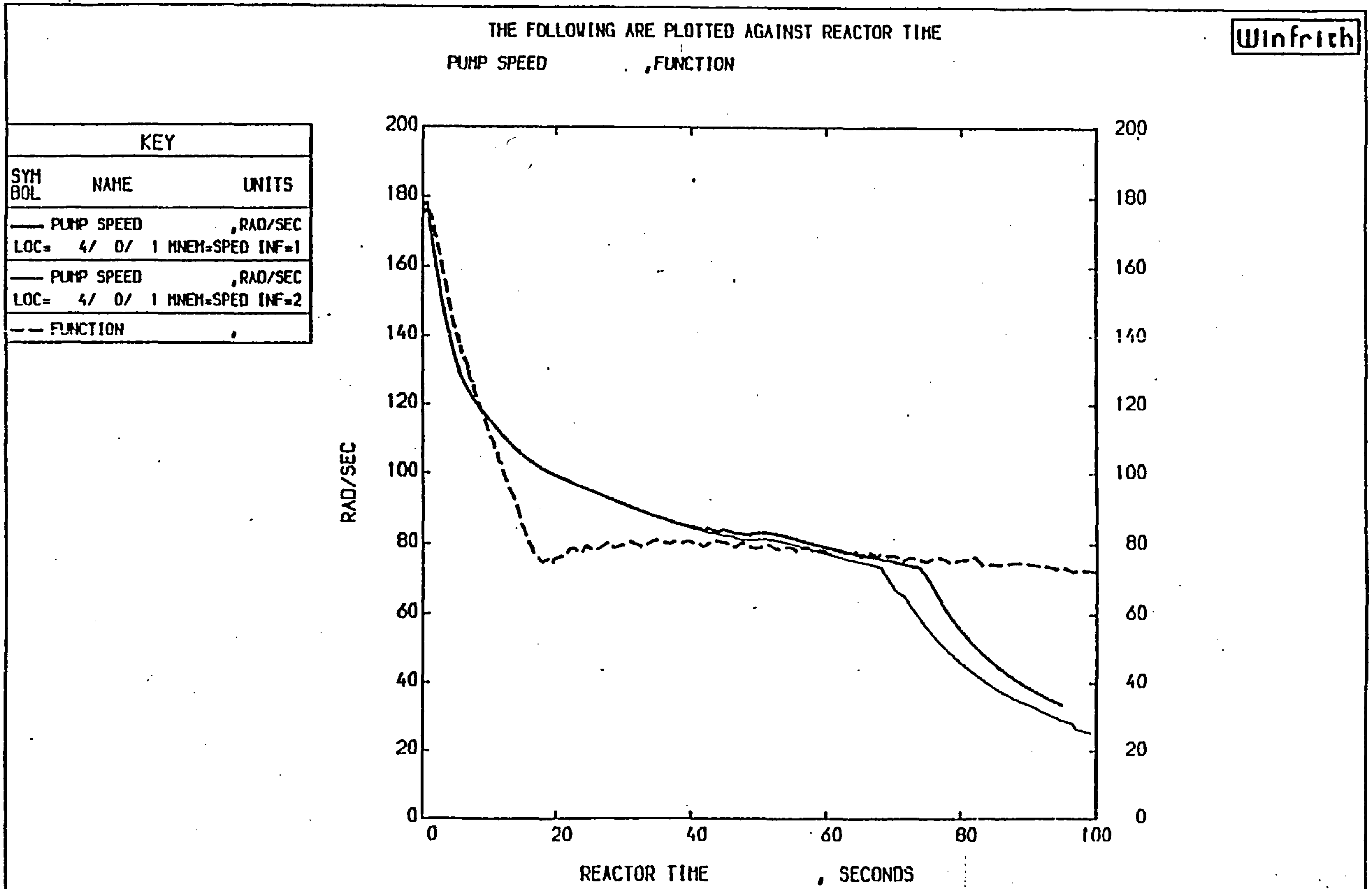

FIGURE 167 INF 1 ISHARP, INF 2 ZEROGAP, INF 3 EXP
PUMP SPEED

THE FOLLOWING ARE PLOTTED AGAINST REACTOR TIME

MIXTURE DENSITY ,DE-PC-002A ,DE-PC-002C

Winfrith

KEY		
SYMBOL	NAME	UNITS
——	MIXTURE DENSITY	,KG/M**3
	LOC= 1/ 0/ 2 MNEM=DENM INF=1	
——	MIXTURE DENSITY	,KG/M**3
	LOC= 1/ 0/ 2 MNEM=DENM INF=2	
----	DE-PC-002A	,MG/M**3
	LOC= 16/ 0/ 0 MNEM=DENM INF=3	
— —	DE-PC-002C	,MG/M**3
	LOC= 17/ 0/ 0 MNEM=DENM INF=3	

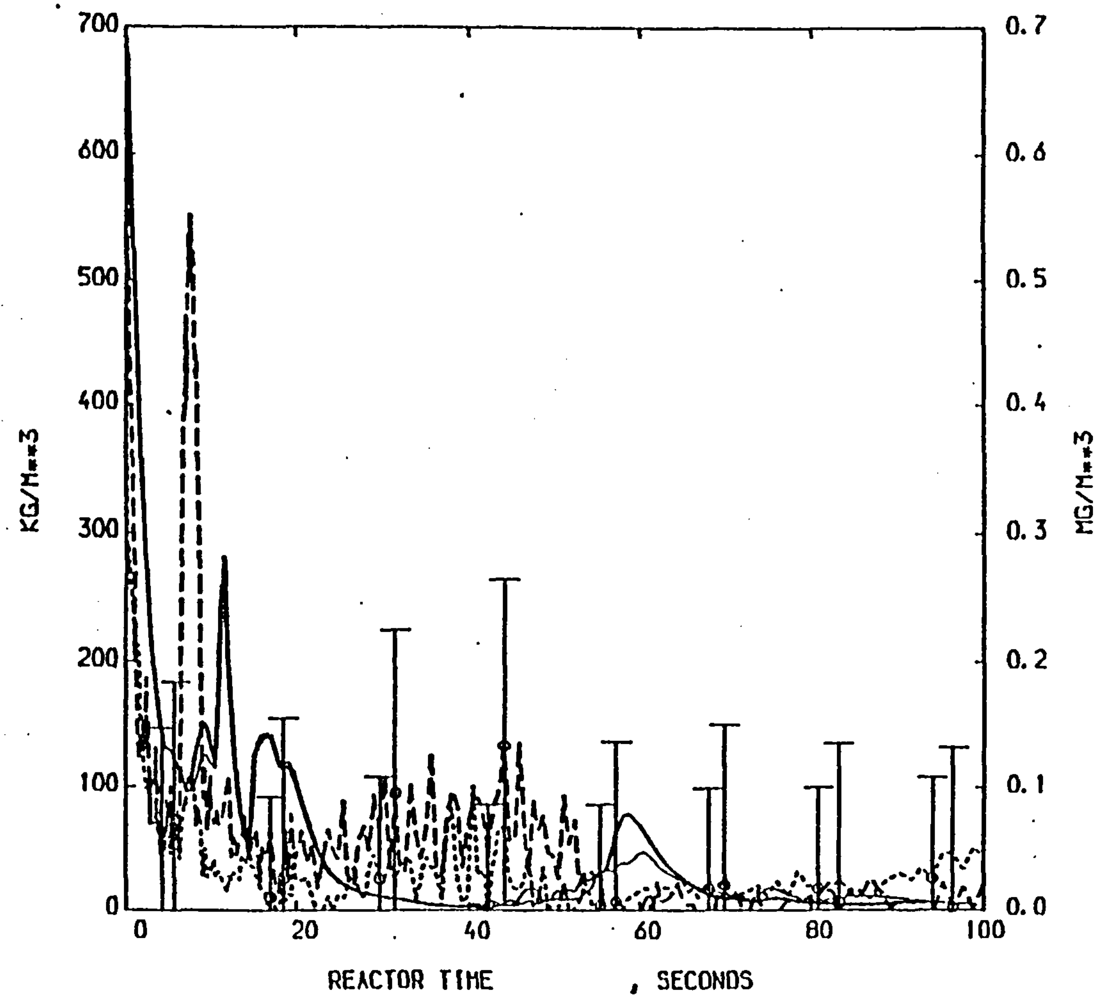

FIGURE 168 INF 1 ISHARP, INF 2 ZEROGAP, INF 3 EXP
INTACT LOOP HOT LEG - EXPERIMENTAL LOCATION PC-2

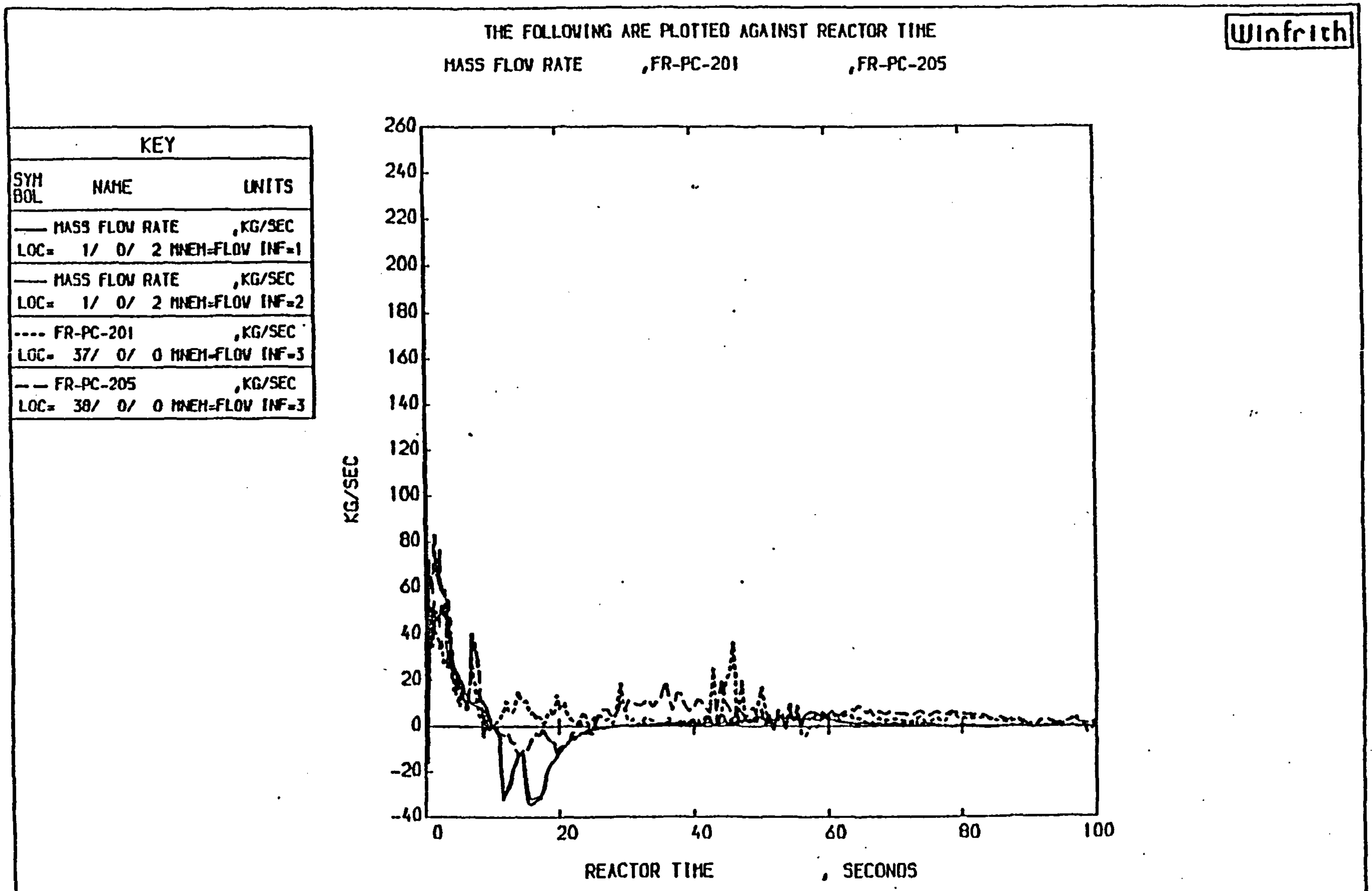

FIGURE 169 INF 1 ISHARP, INF 2 ZEROGAP, INF 3 EXP
INTACT LOOP HOT LEG - EXPERIMENTAL LOCATION PC-2

THE FOLLOWING ARE PLOTTED AGAINST REACTOR TIME

LIQUID TEMPERATURE ,TE-PC-002A

Winfrith

KEY

SYMBOL	NAME	UNITS
——	LIQUID TEMPERATURE LOC= 1/ 0/ 2 MNEM=TEML INF=1	,DEG.K
——	LIQUID TEMPERATURE LOC= 1/ 0/ 2 MNEM=TEML INF=2	,DEG.K
----	TE-PC-002A LOC= 179/ 0/ 0 MNEM=TMCL INF=3	,DEG.K

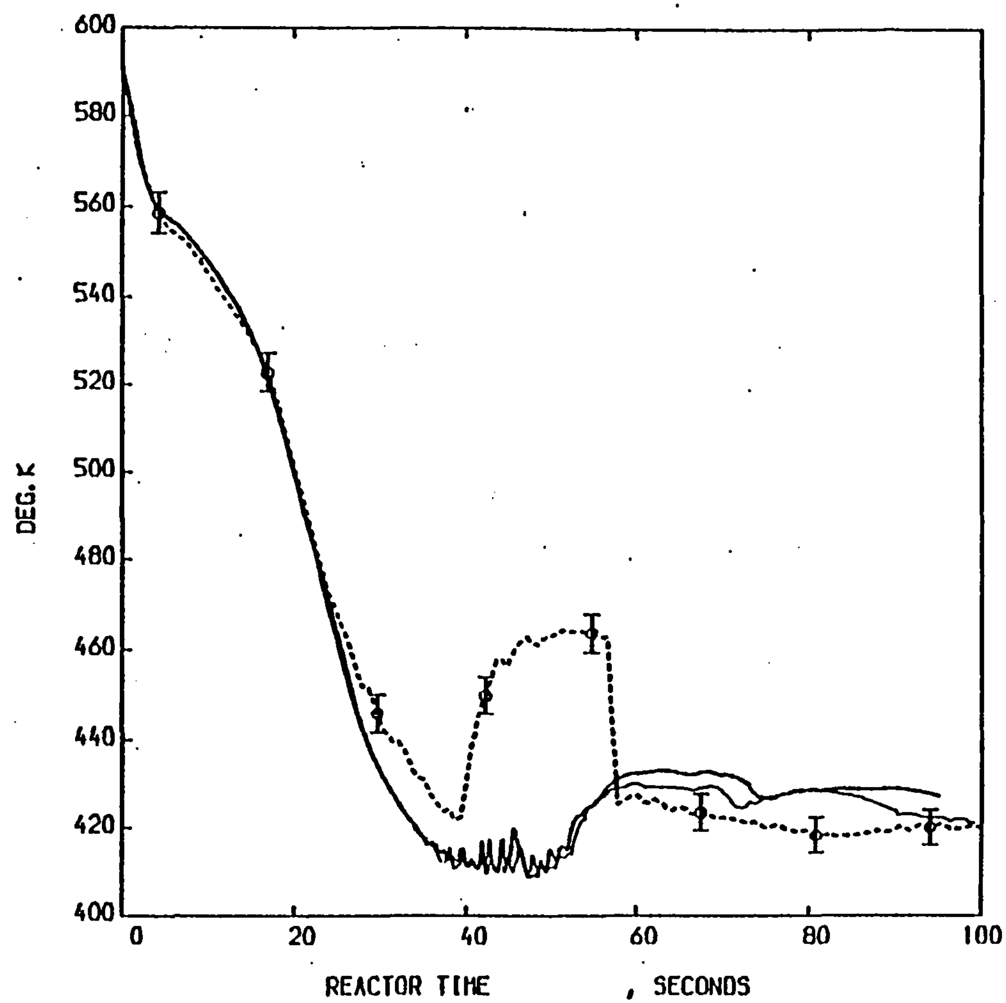

FIGURE 170 INF 1 ISHARP, INF 2 ZEROGAP, INF 3 EXP
INTACT LOOP HOT LEG - EXPERIMENTAL LOCATION PC-2

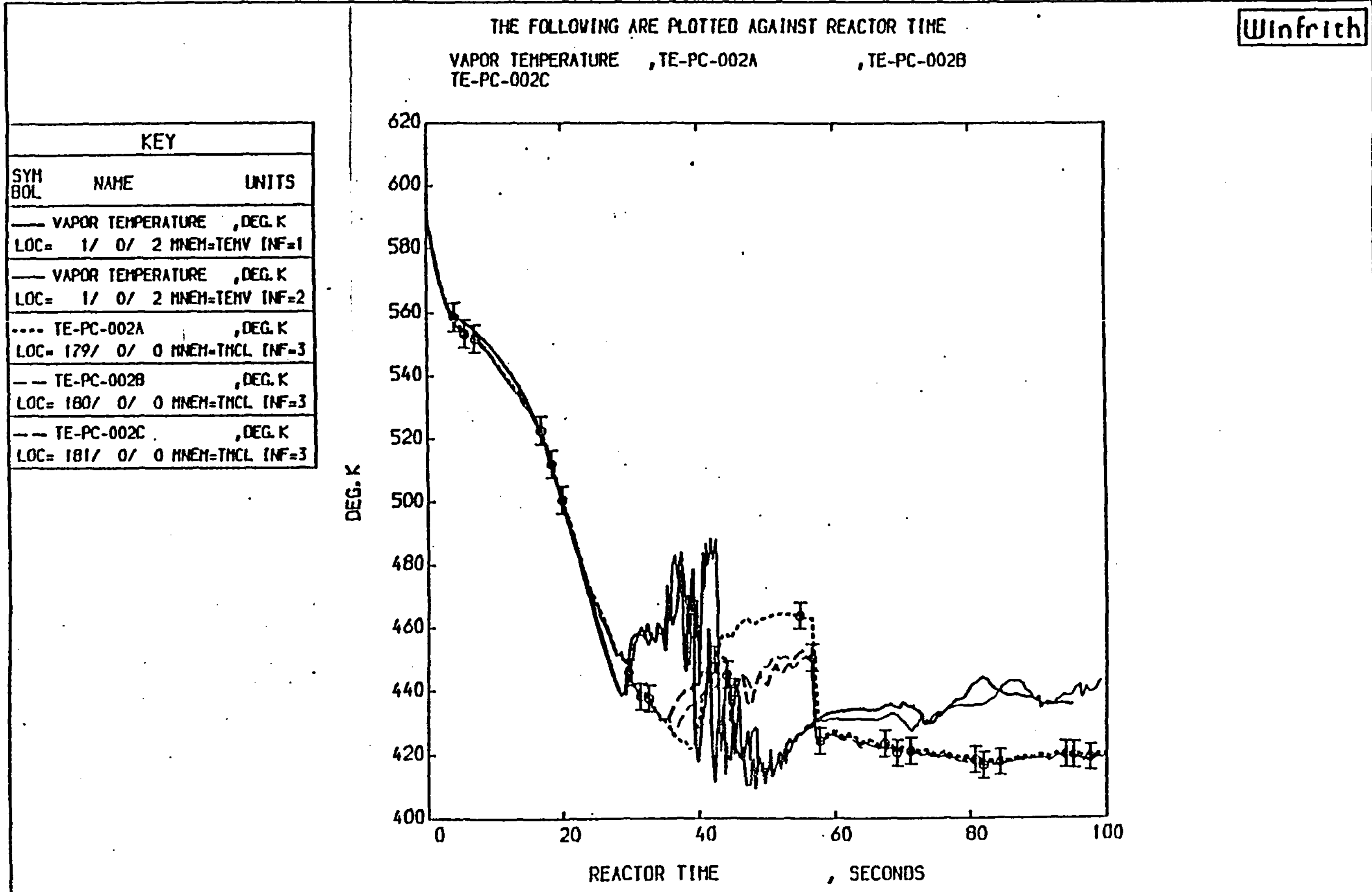

FIGURE 171 INF 1 ISHARP, INF 2 ZEROGAP, INF 3 EXP
INTACT LOOP HOT LEG - EXPERIMENTAL LOCATION PC-2

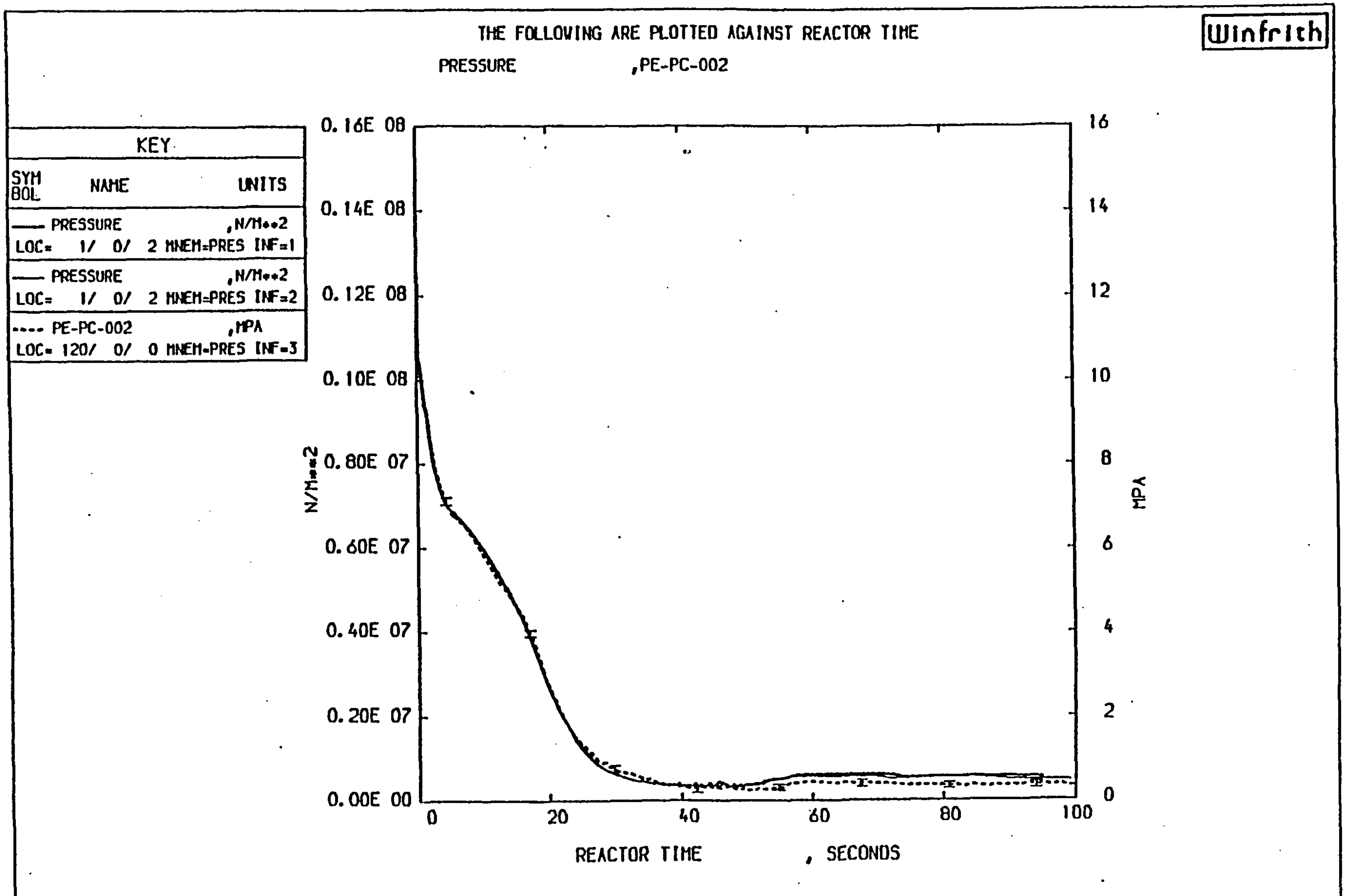

FIGURE 1.72 INF 1 ISHARP, INF 2 ZEROGAP, INF 3 EXP
INTACT LOOP HOT LEG - EXPERIMENTAL LOCATION PC-2

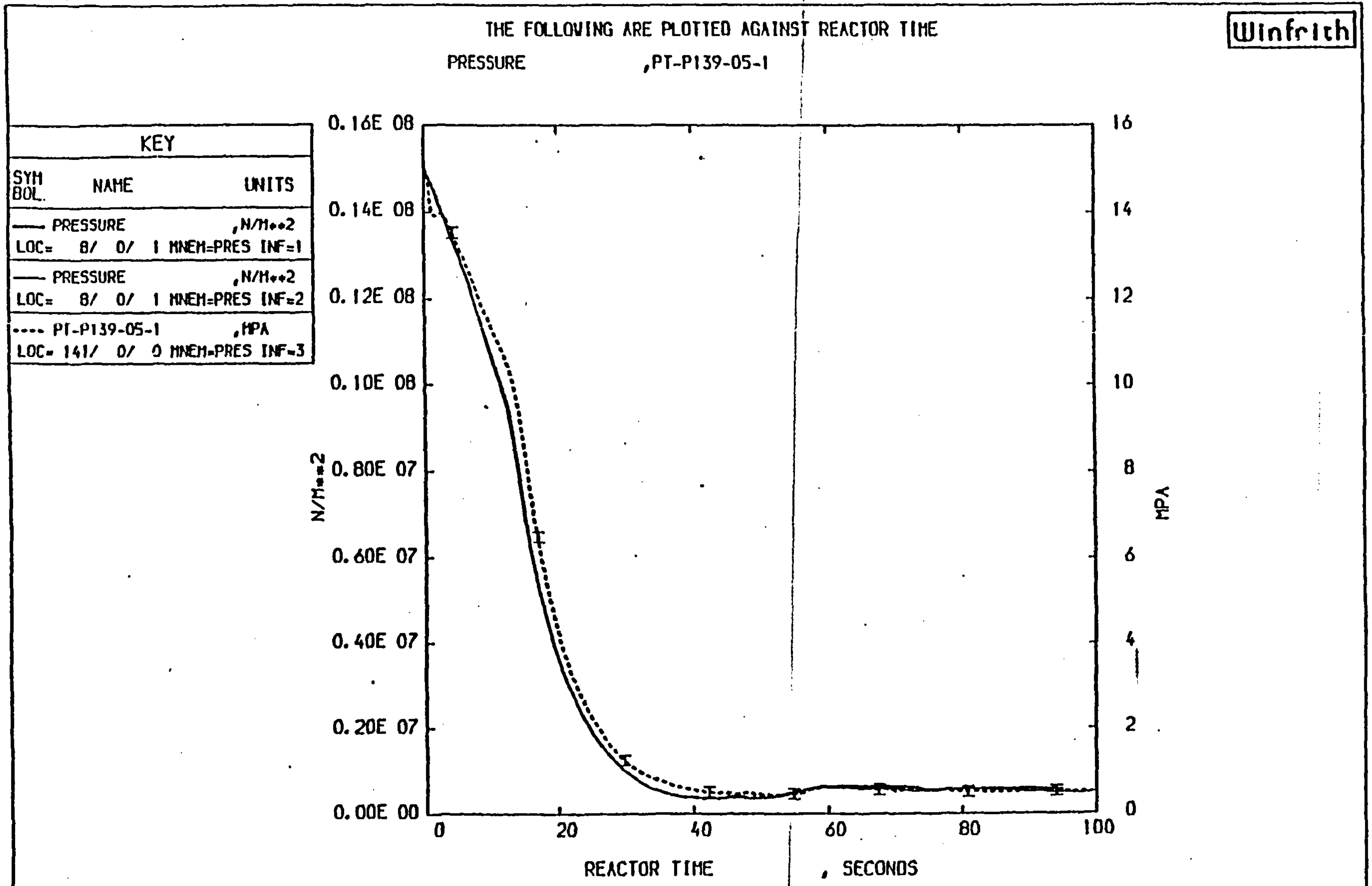

FIGURE 173 INF 1 ISHARP, INF 2 ZEROGAP, INF 3 EXP
INTACT LOOP HOT LEG - PRESSURIZER

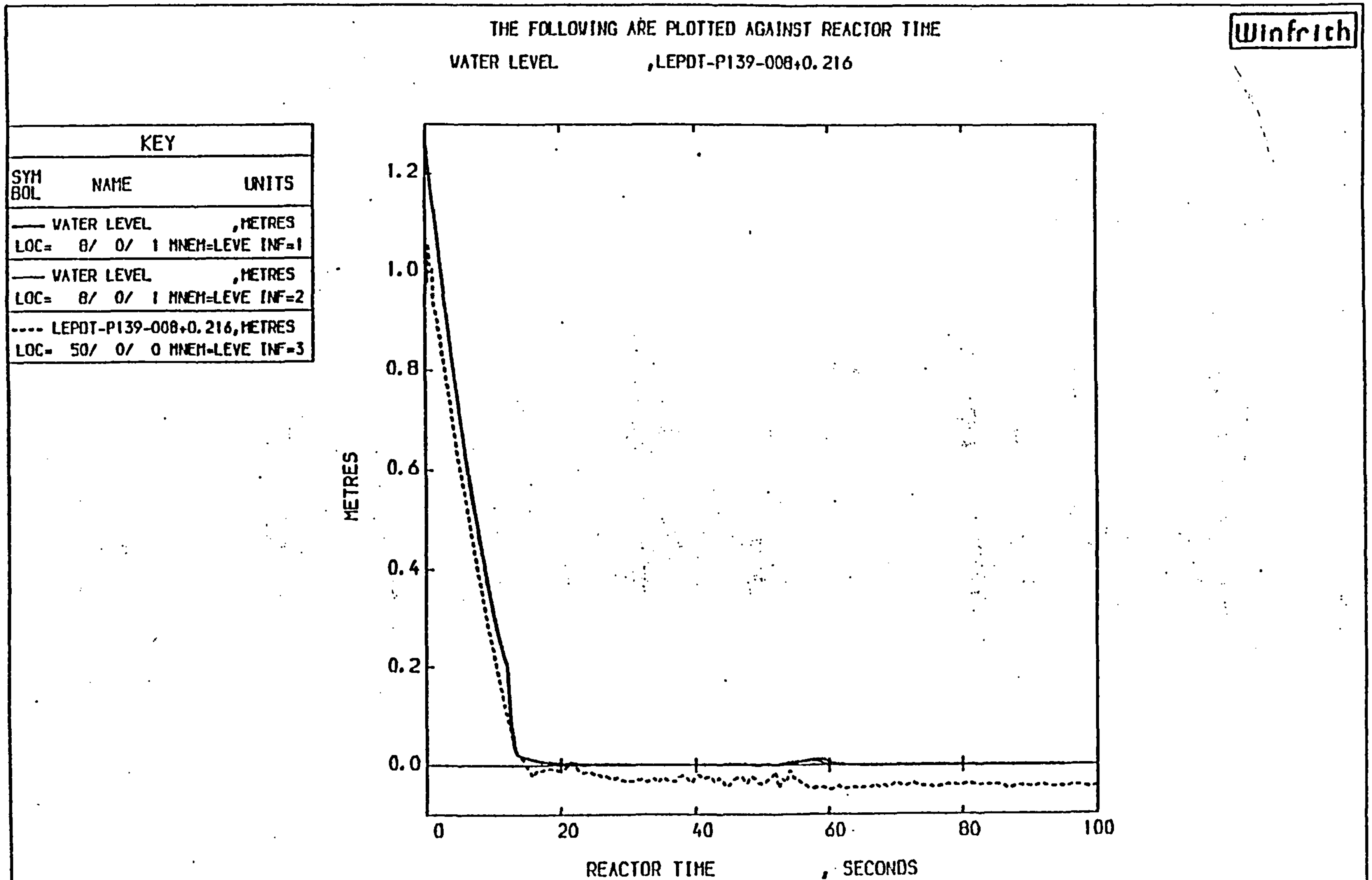

FIGURE 174 INF 1 ISHARP, INF 2 ZEROGAP, INF 3 EXP
INTACT LOOP HOT LEG - PRESSURIZER

THE FOLLOWING ARE PLOTTED AGAINST REACTOR TIME

WATER LEVEL ,LE-ECC-01A

Winfrith

KEY		
SYMBOL	NAME	UNITS
——	WATER LEVEL	,METRES
	LOC= 15/ 0/ 1 MNEM=LEVE INF=1	
——	WATER LEVEL	,METRES
	LOC= 15/ 0/ 1 MNEM=LEVE INF=2	
----	LE-ECC-01A	,METRES
	LOC= 51/ 0/ 0 MNEM=LEVE INF=3	

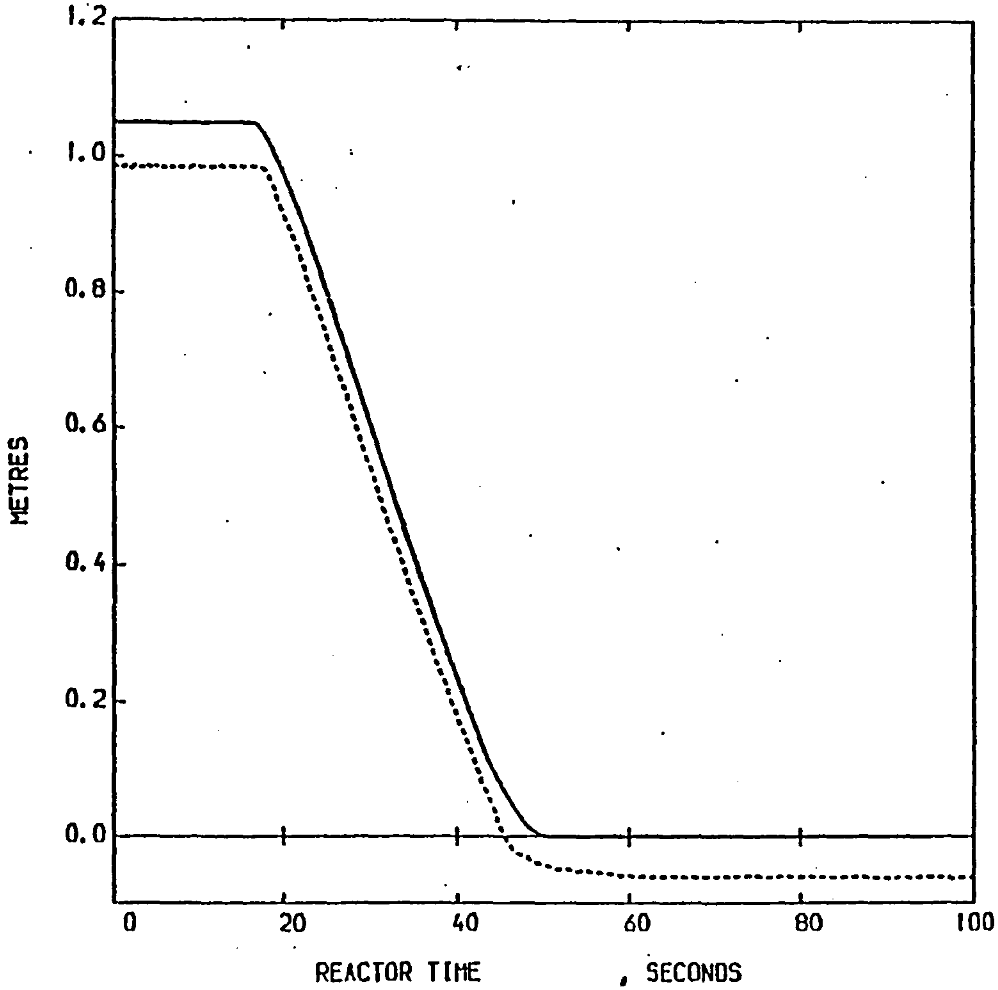

FIGURE 175 INF 1 ISHARP, INF 2 ZEROGAP, INF 3 EXP
EMERGENCY CORE COOLING SYSTEM

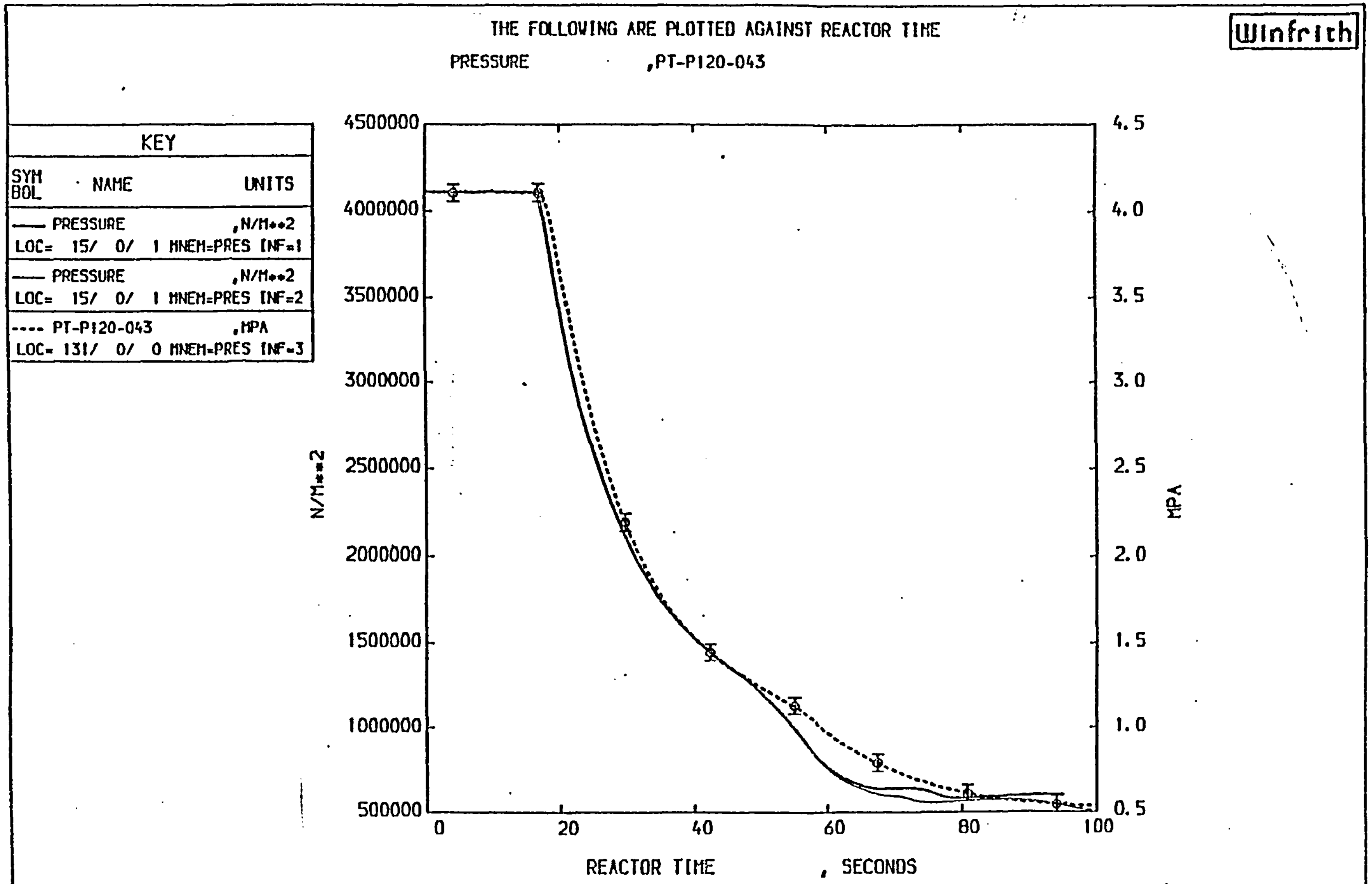

FIGURE 176 INF 1 ISHARP, INF 2 ZEROGAP, INF 3 EXP
INTACT LOOP HOT LEG - PRESSURIZER

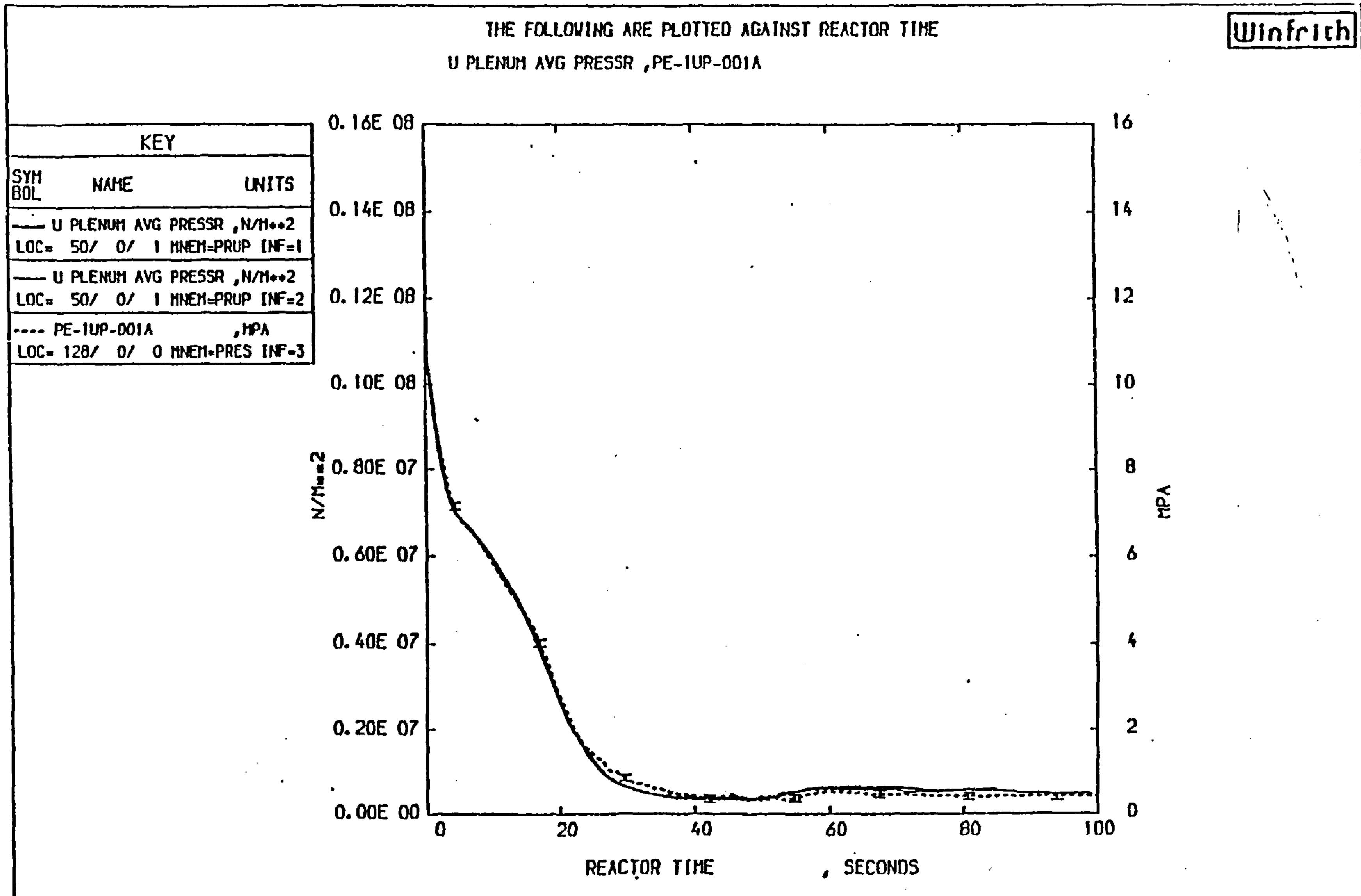

FIGURE 177 INF 1 ISHARP, INF 2 ZEROGAP, INF 3 EXP
UPPER PLENUM PRESSURE

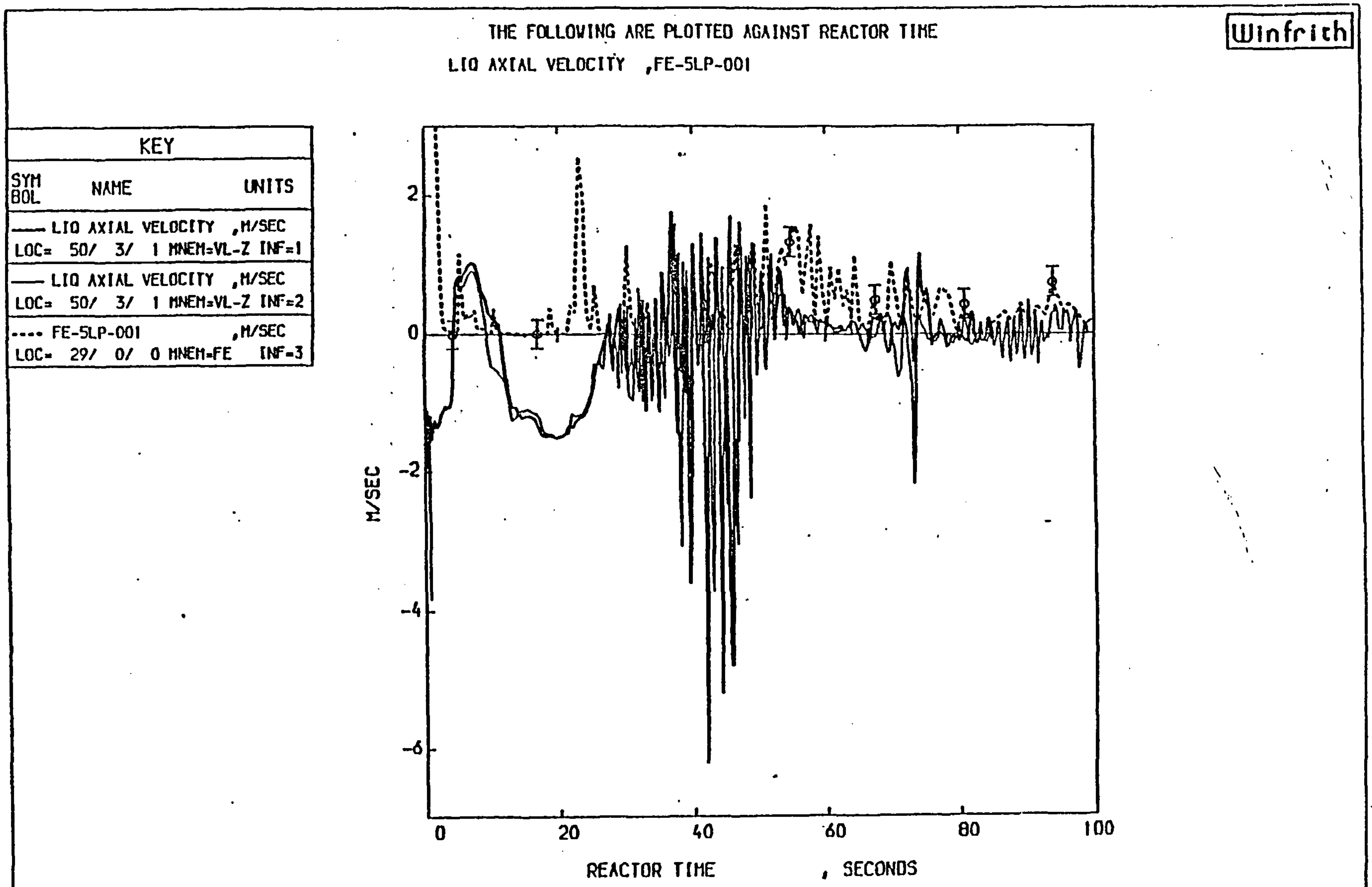

FIGURE 178 INF 1 ISHARP, INF 2 ZEROGAP, INF 3 EXP
LOWER PLENUM LIQUID AXIAL VELOCITY

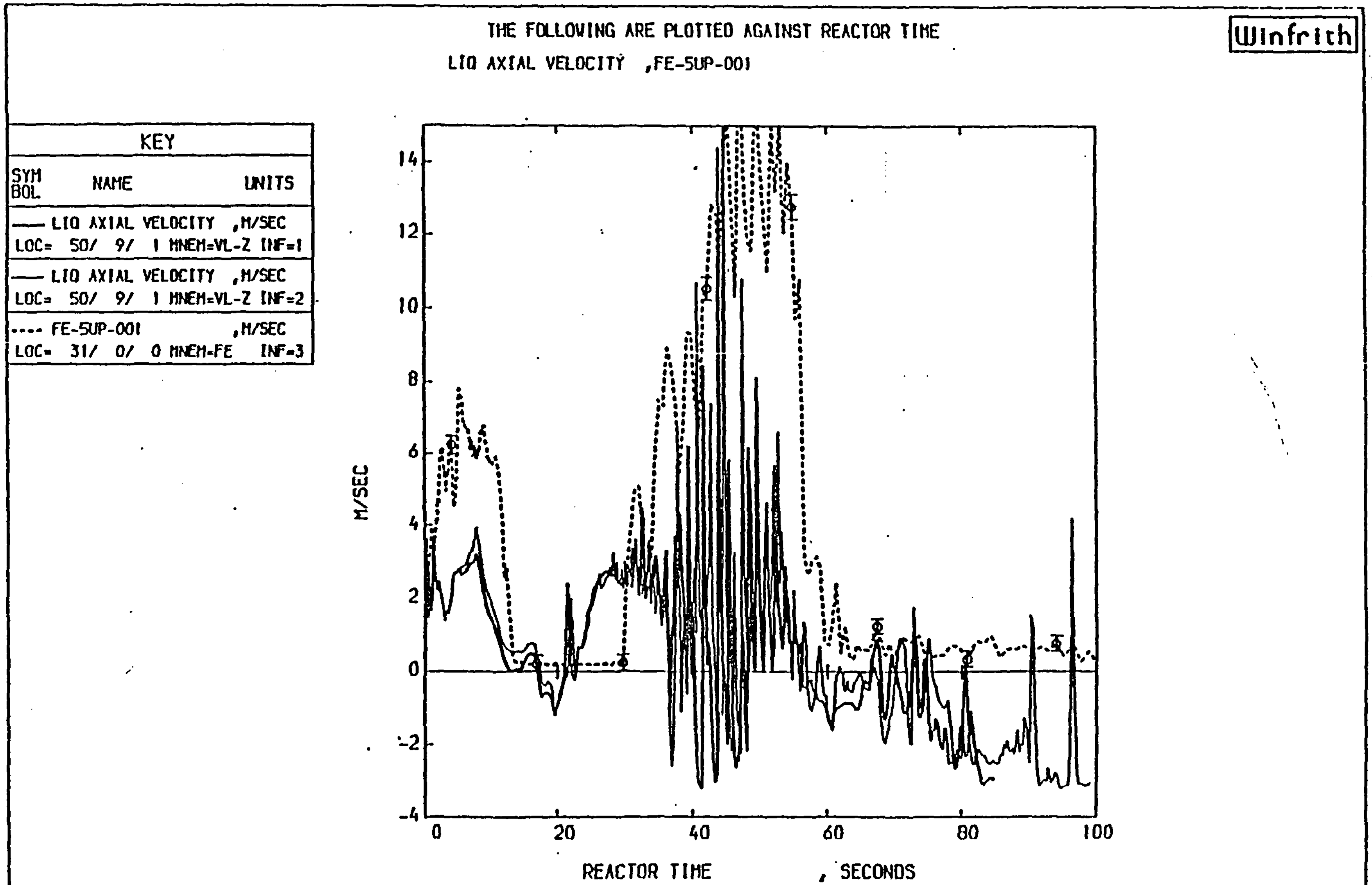

FIGURE 179 INF 1 ISHARP, INF 2 ZEROGAP, INF 3 EXP
UPPER PLENUM LIQUID AXIAL VELOCITY

Winfrith

THE FOLLOWING ARE PLOTTED AGAINST REACTOR TIME
LIQUID TEMPERATURE ,TE-1ST-001

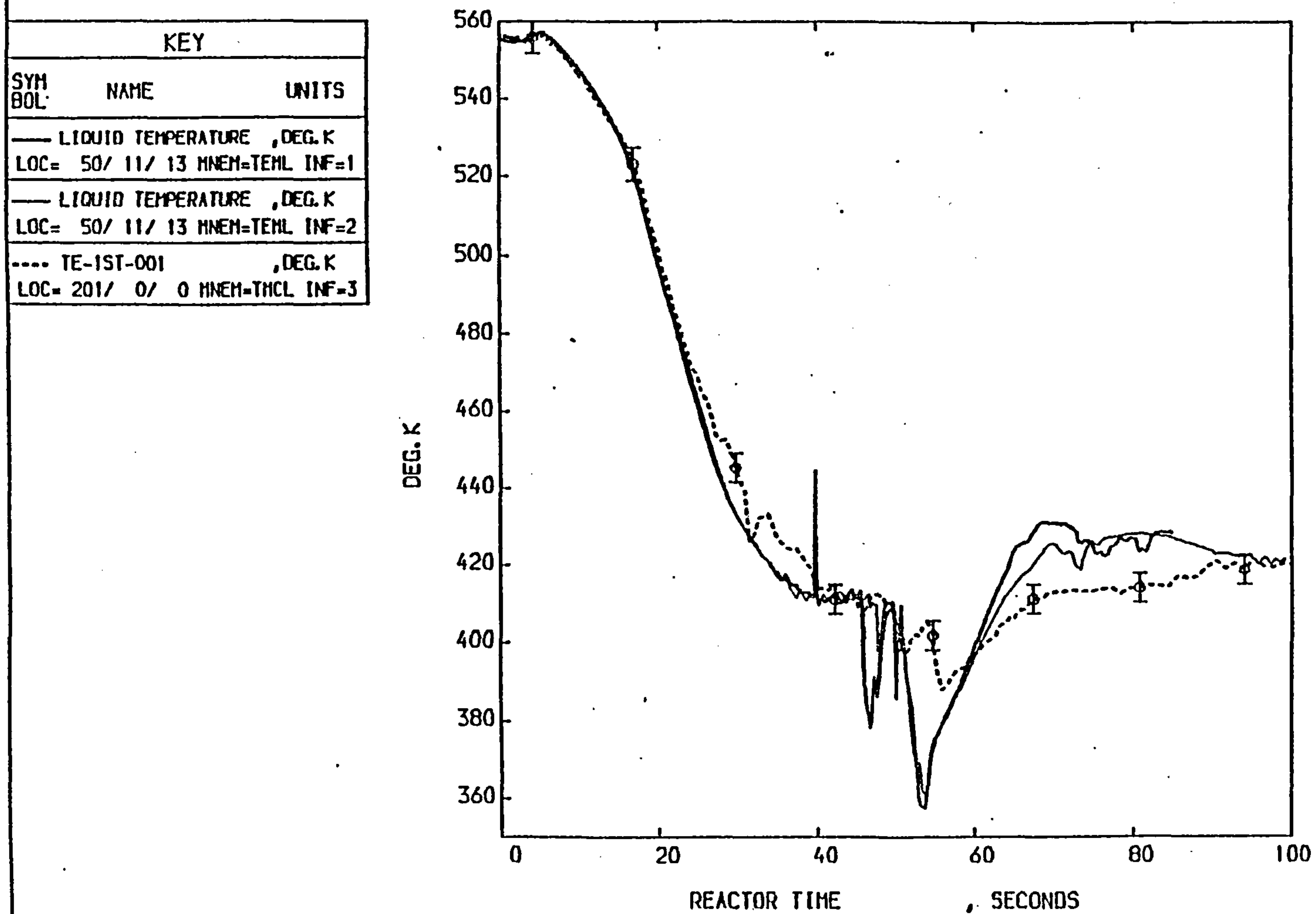

FIGURE 180 INF 1 ISHARP, INF 2 ZEROGAP, INF 3 EXP
DOWNCOMER LIQUID TEMPERATURE AT 5.0 METRES

Winfrith

THE FOLLOWING ARE PLOTTED AGAINST REACTOR TIME

LIQUID TEMPERATURE ,TE-1ST-002

KEY		
SYMBOL	NAME	UNITS
——	LIQUID TEMPERATURE	,DEG.K
	LOC= 50/ 10/ 13 MNEM=TEML INF=1	
——	LIQUID TEMPERATURE	,DEG.K
	LOC= 50/ 10/ 13 MNEM=TEML INF=2	
----	TE-1ST-002	,DEG.K
	LOC= 202/ 0/ 0 MNEM=THCL INF=3	

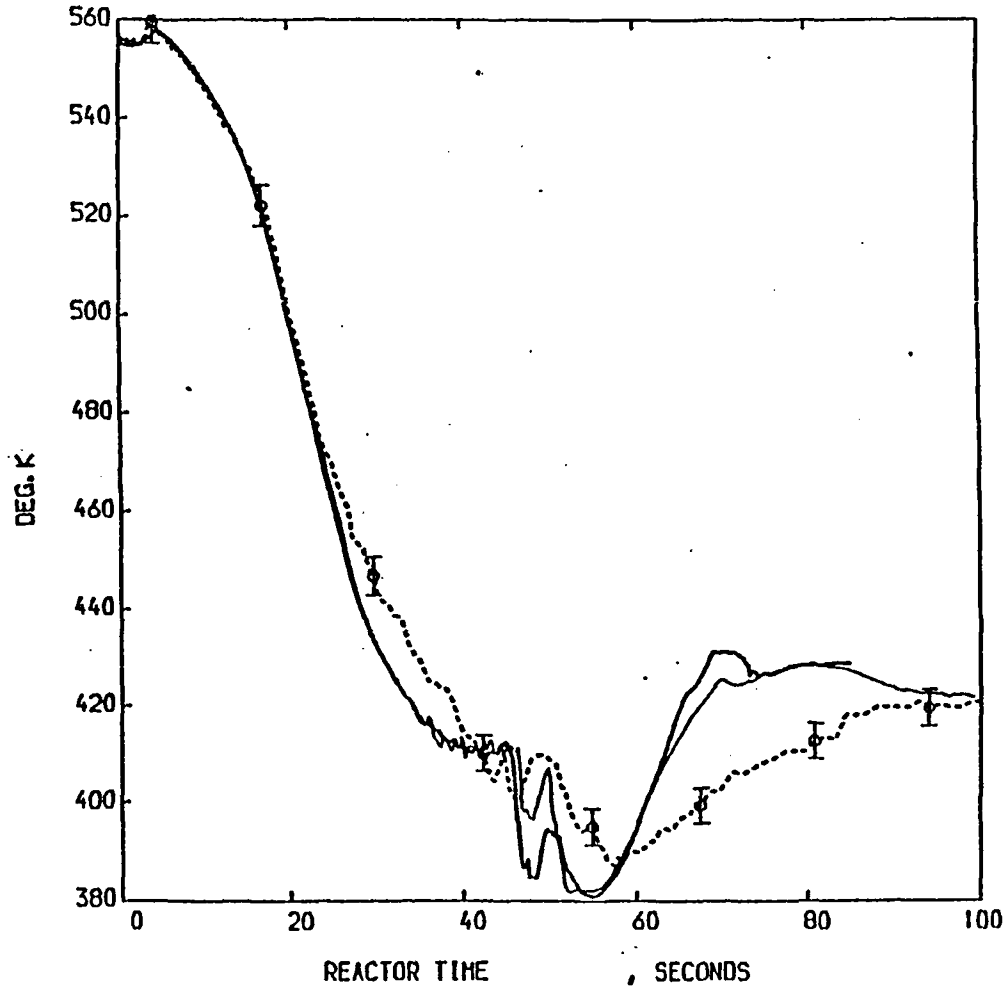

FIGURE 181 INF 1 ISHARP, INF 2 ZEROGAP, INF 3 EXP
DOWNCOMER LIQUID TEMPERATURE AT 4.2 METRES

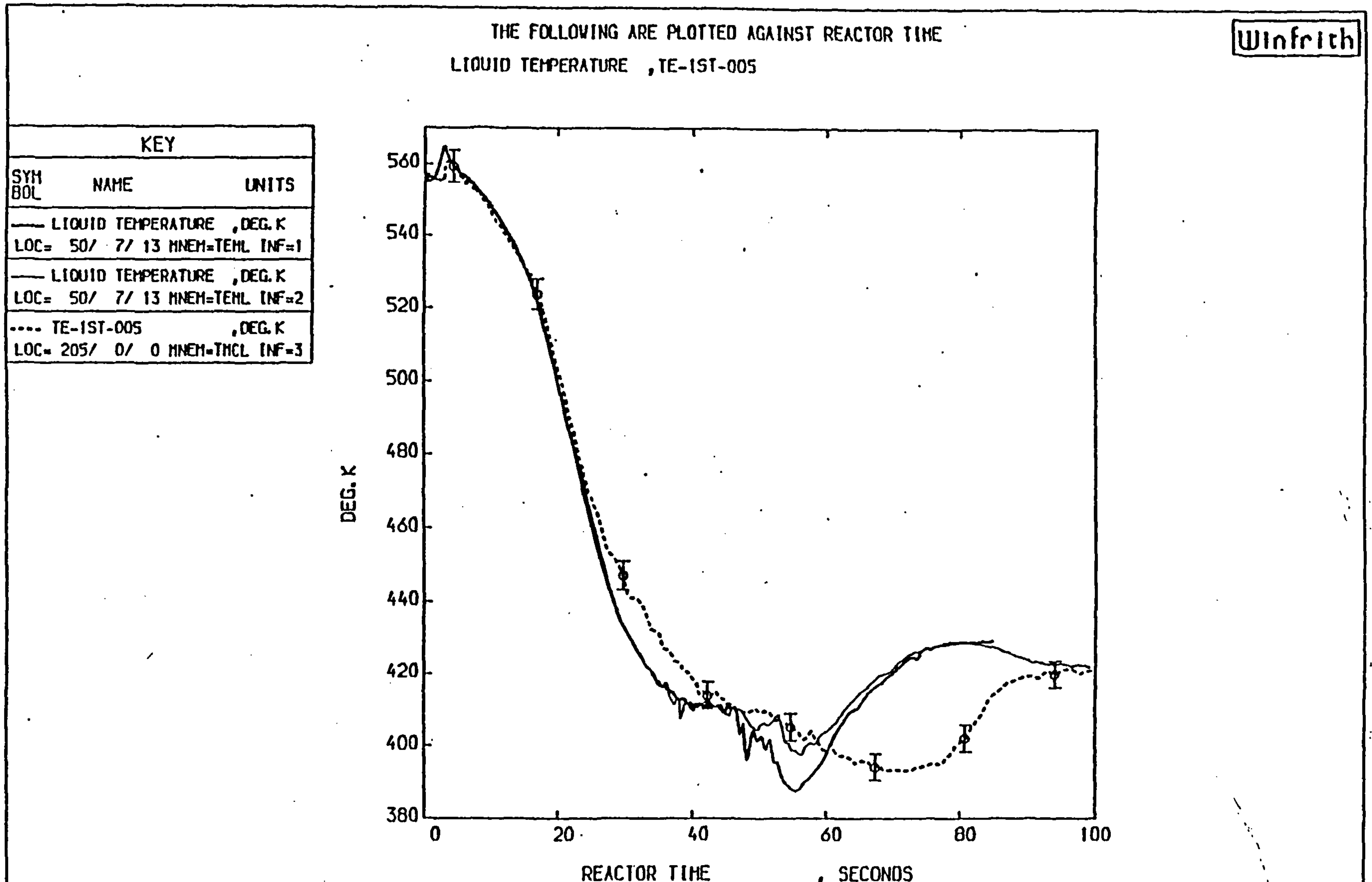

FIGURE 182 INF 1 ISHARP, INF 2 ZEROGAP, INF 3 EXP
DOWNCOMER LIQUID TEMPERATURE AT 2.4 METRES

THE FOLLOWING ARE PLOTTED AGAINST REACTOR TIME

LIQUID TEMPERATURE ,TE-1ST-012

Winfrith

KEY		
SYM BOL	NAME	UNITS
——	LIQUID TEMPERATURE LOC= 50/ 1/ 13 MNEM=TEML INF=1	,DEG.K
——	LIQUID TEMPERATURE LOC= 50/ 1/ 13 MNEM=TEML INF=2	,DEG.K
----	TE-1ST-012 LOC= 211/ 0/ 0 MNEM=THCL INF=3	,DEG.K

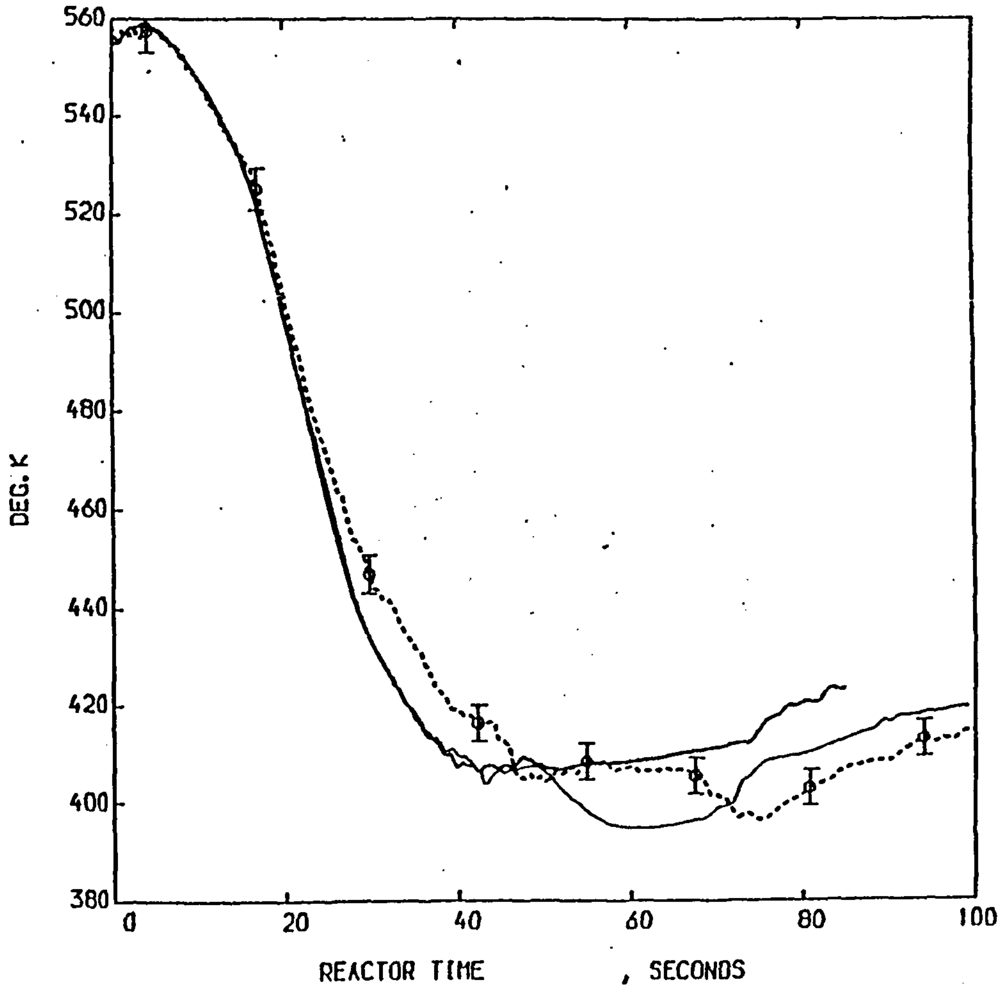

FIGURE 183 INF 1 ISHARP, INF 2 ZEROGAP, INF 3 EXP
DOWNCOMER LIQUID TEMPERATURE AT 0.3 METRES

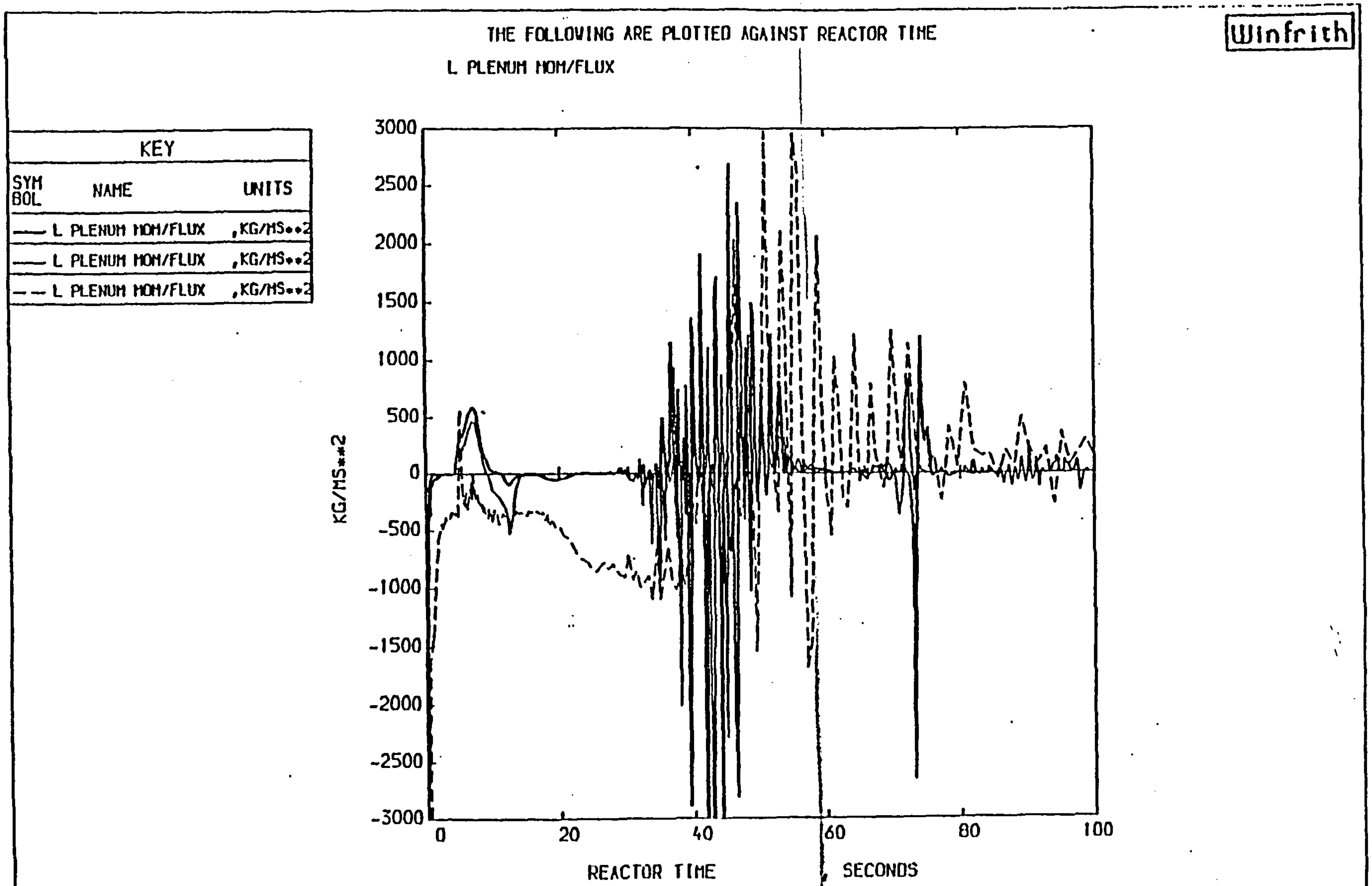

FIGURE 184 LINE 1 ISHARP, LINE 2 ZEROGAP, LINE 3 EXP
LOWER PLENUM MOMENTUM FLUX

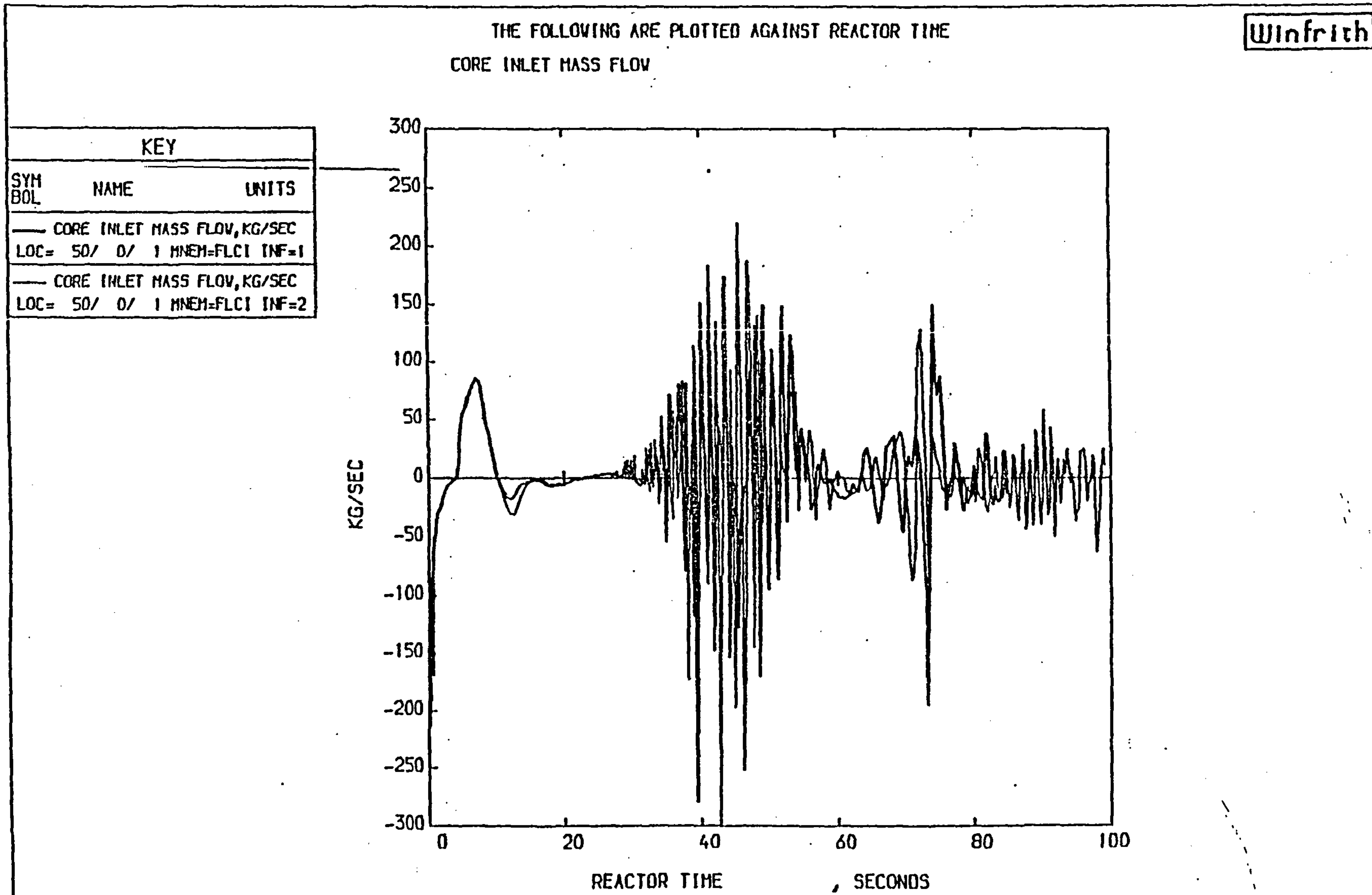

FIGURE 185 INF 1 ISHARP, INF 2 ZEROGAP
VESSEL GLOBALS

Winfrith

THE FOLLOWING ARE PLOTTED AGAINST REACTOR TIME

CORE OUTLET MASSFLOW

KEY		
SYM BOL	NAME	UNITS
——	CORE OUTLET MASSFLOW, KG/SEC LOC= 50/ 0/ 1 MNEM=FLCO INF=1	
——	CORE OUTLET MASSFLOW, KG/SEC LOC= 50/ 0/ 1 MNEM=FLCO INF=2	

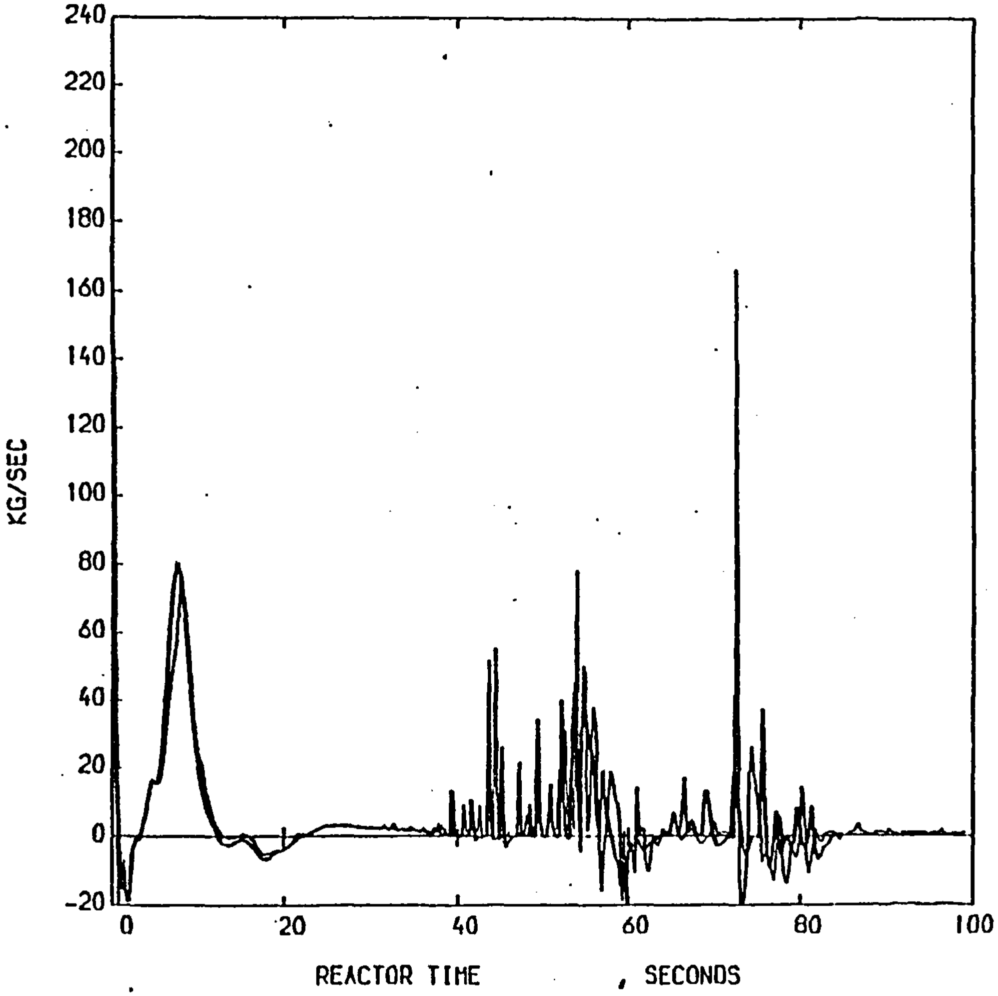

FIGURE 186 INF 1 ISHARP, INF 2 ZEROGAP
VESSEL GLOBALS

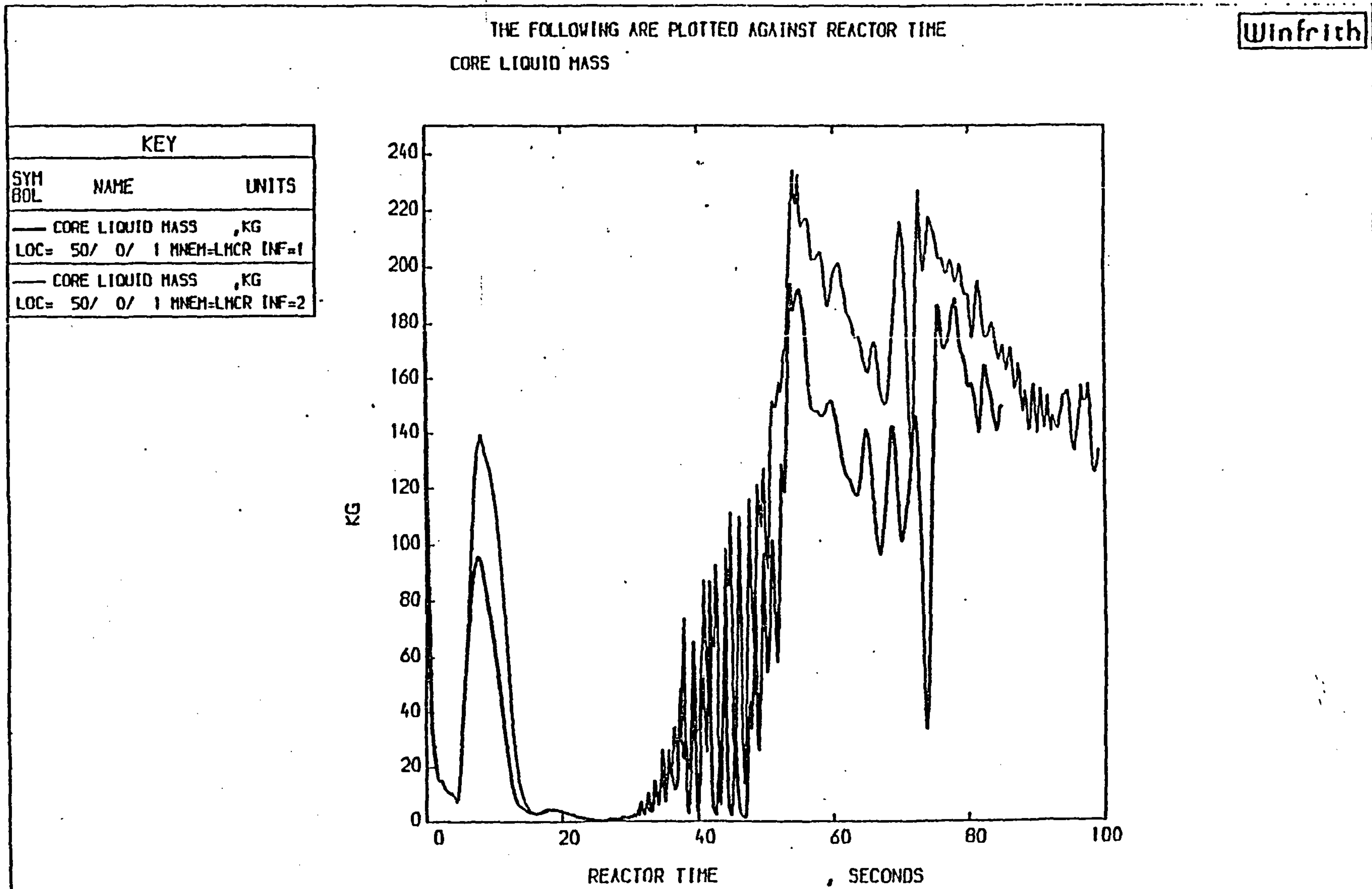

FIGURE 187 INF 1 ISHARP, INF 2 ZEROGAP
VESSEL GLOBALS

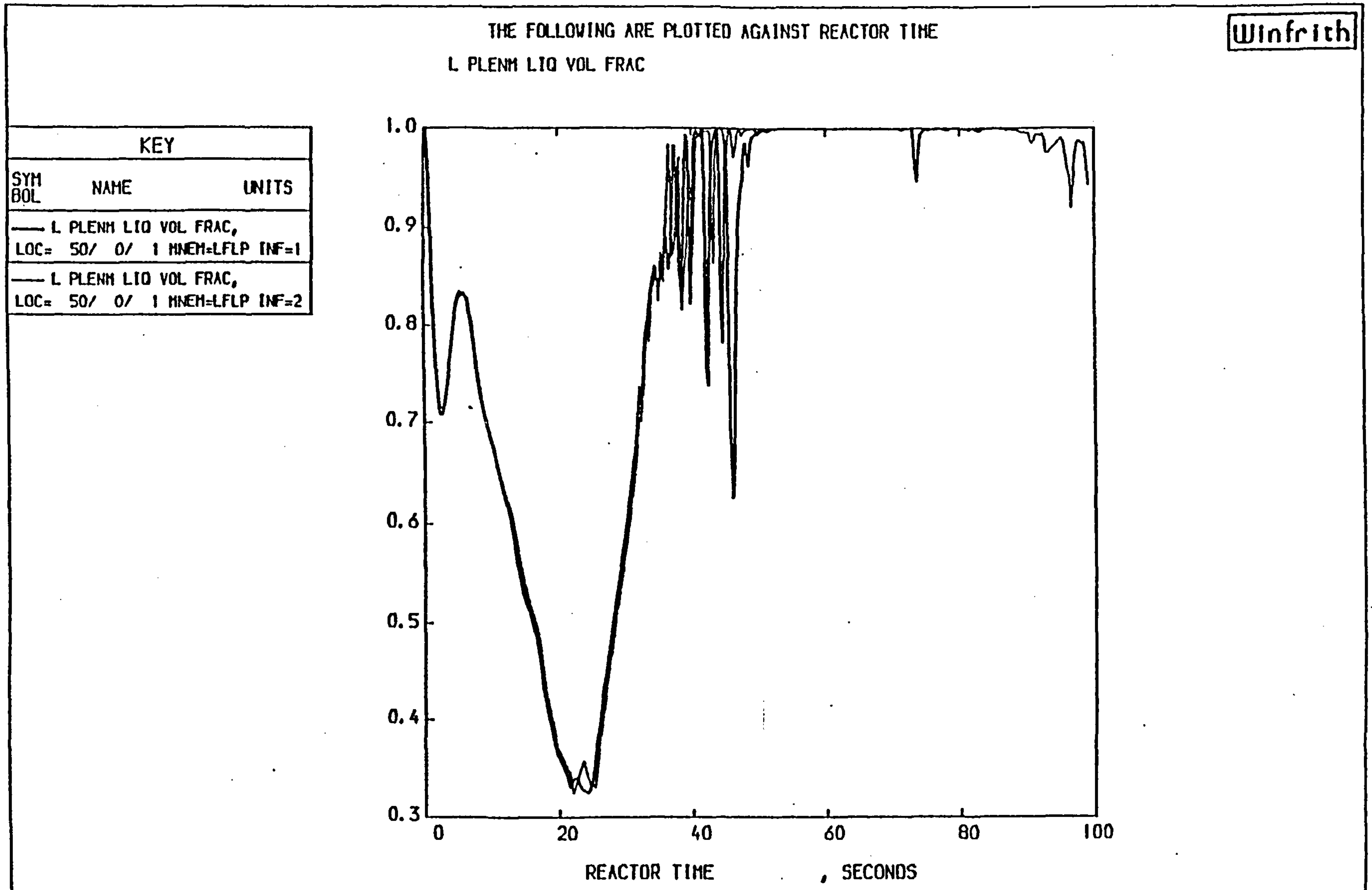

FIGURE 188 INF 1 ISHARP, INF 2 ZEROGAP
VESSEL GLOBALS

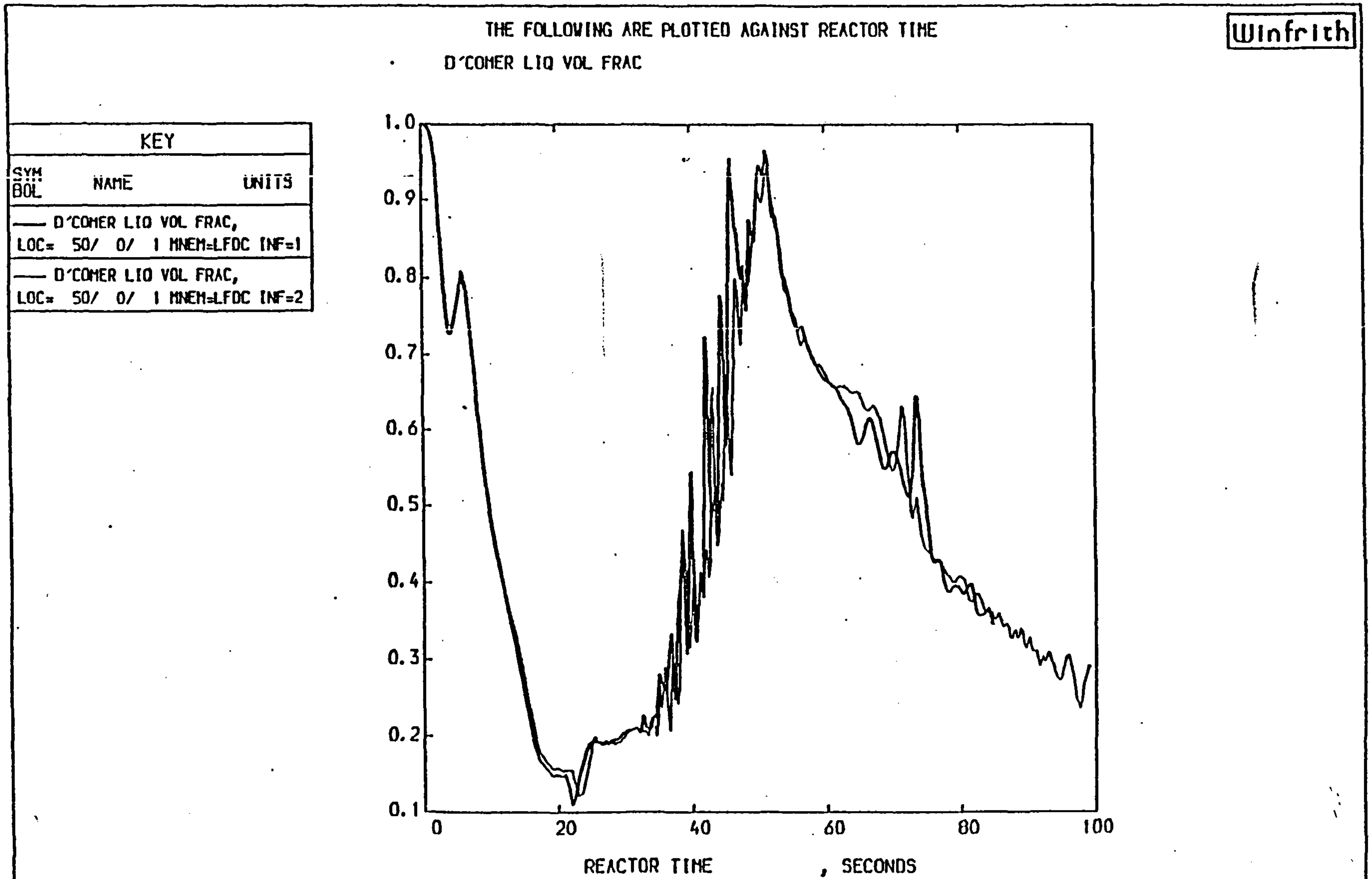

FIGURE 189 INF 1 ISHARP, INF 2 ZEROGAP
VESSEL GLOBALS

Winfrith

THE FOLLOWING ARE PLOTTED AGAINST REACTOR TIME

CORE LIQ VOL FRAC

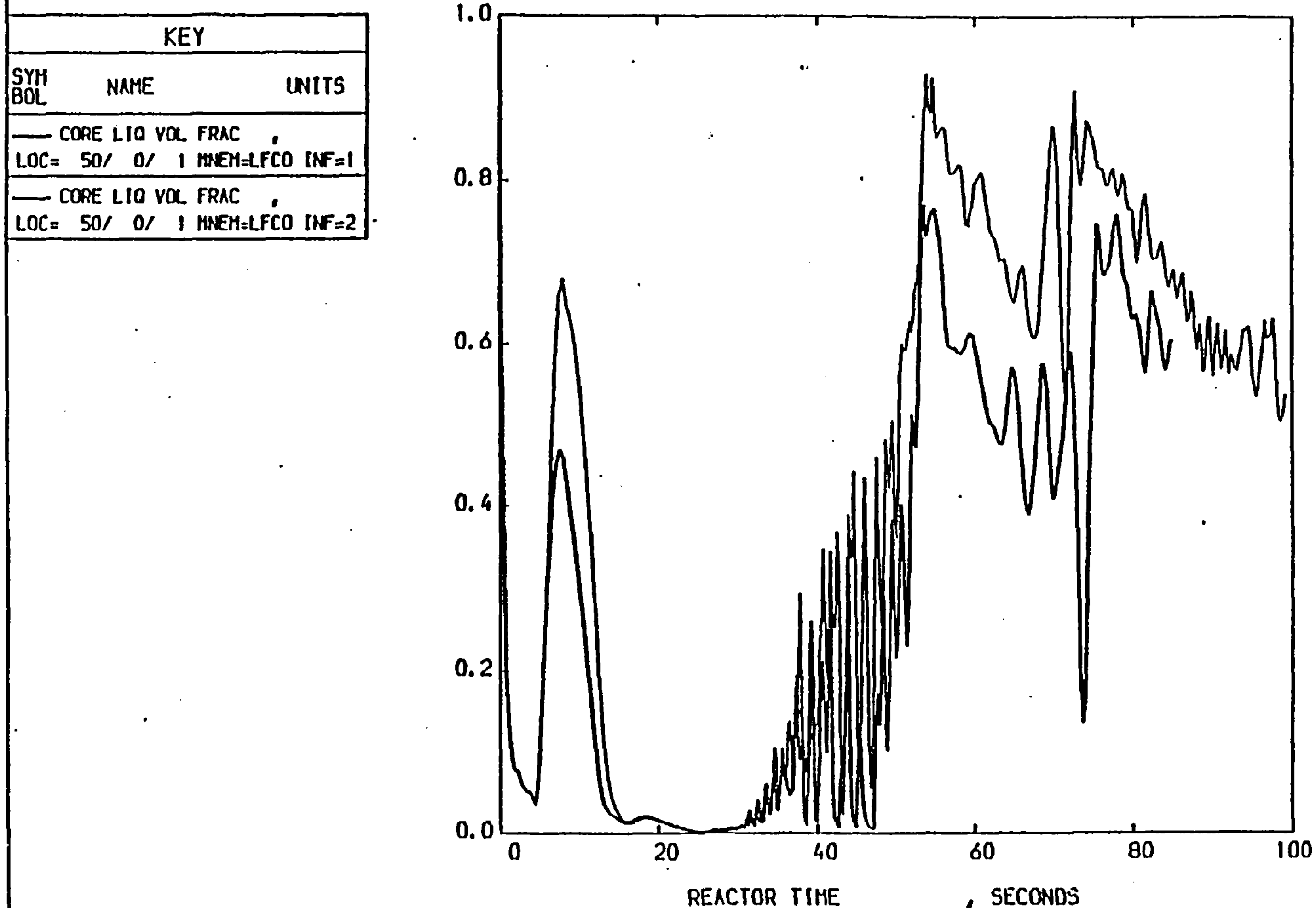

FIGURE 190 INF 1 ISHARP, INF 2 ZEROGAP
VESSEL GLOBALS

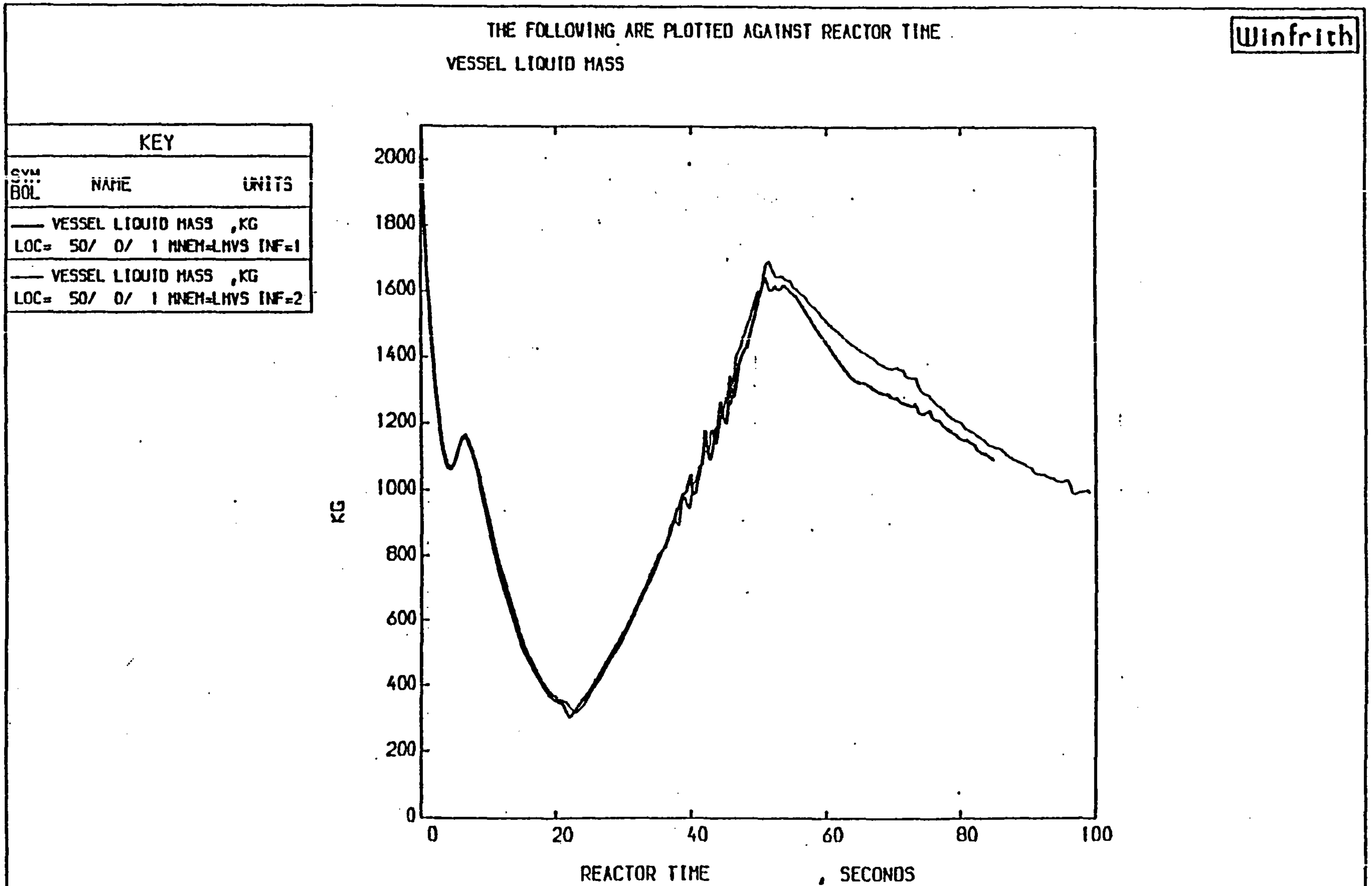

FIGURE 191 INF 1 ISHARP, INF 2 ZEROGAP
VESSEL GLOBALS

Winfrith

THE FOLLOWING ARE PLOTTED AGAINST REACTOR TIME

TOT ROD HEAT FLUX

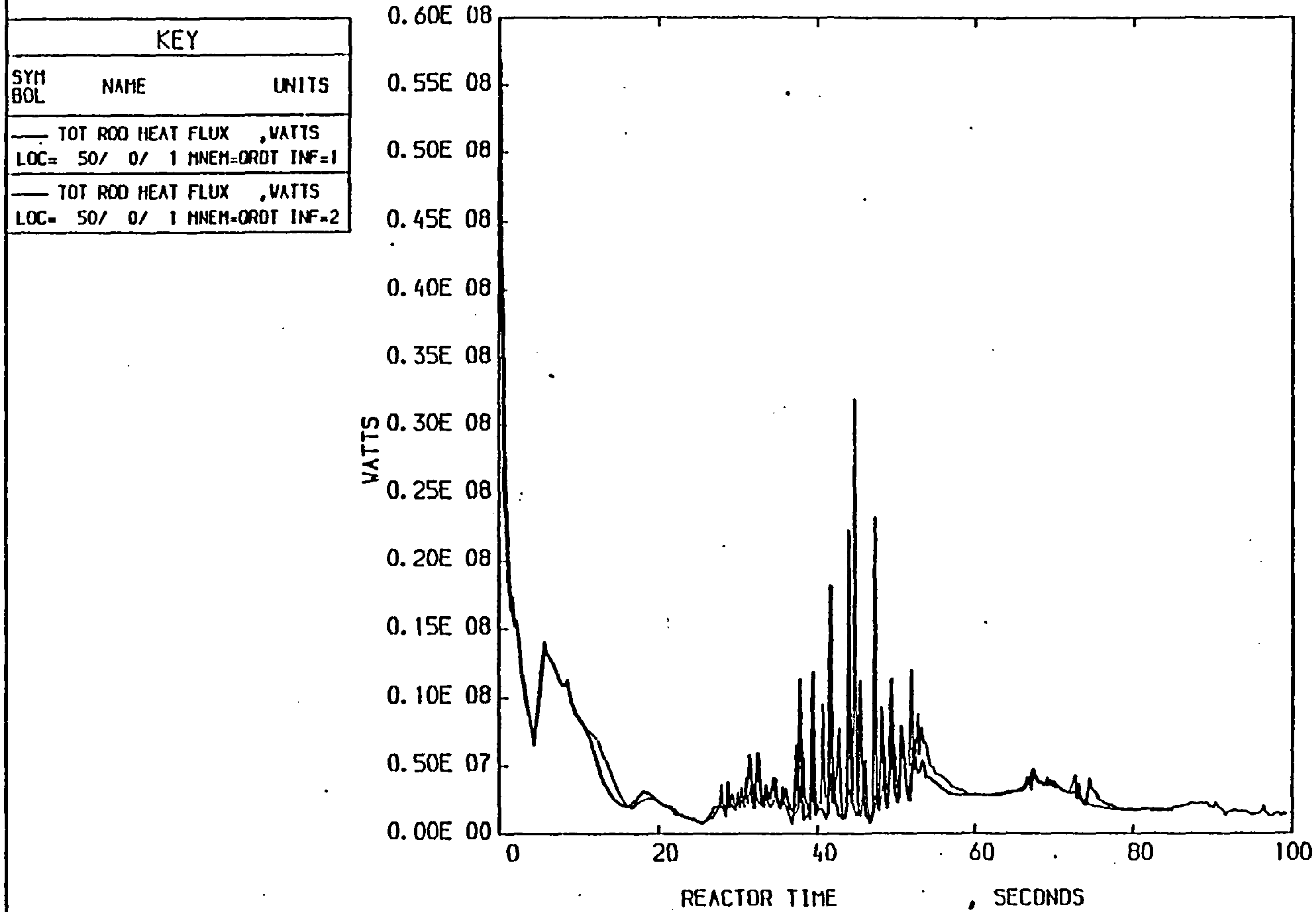

FIGURE 192 INF 1 ISHARP, INF 2 ZEROGAP

VESSEL GLOBALS

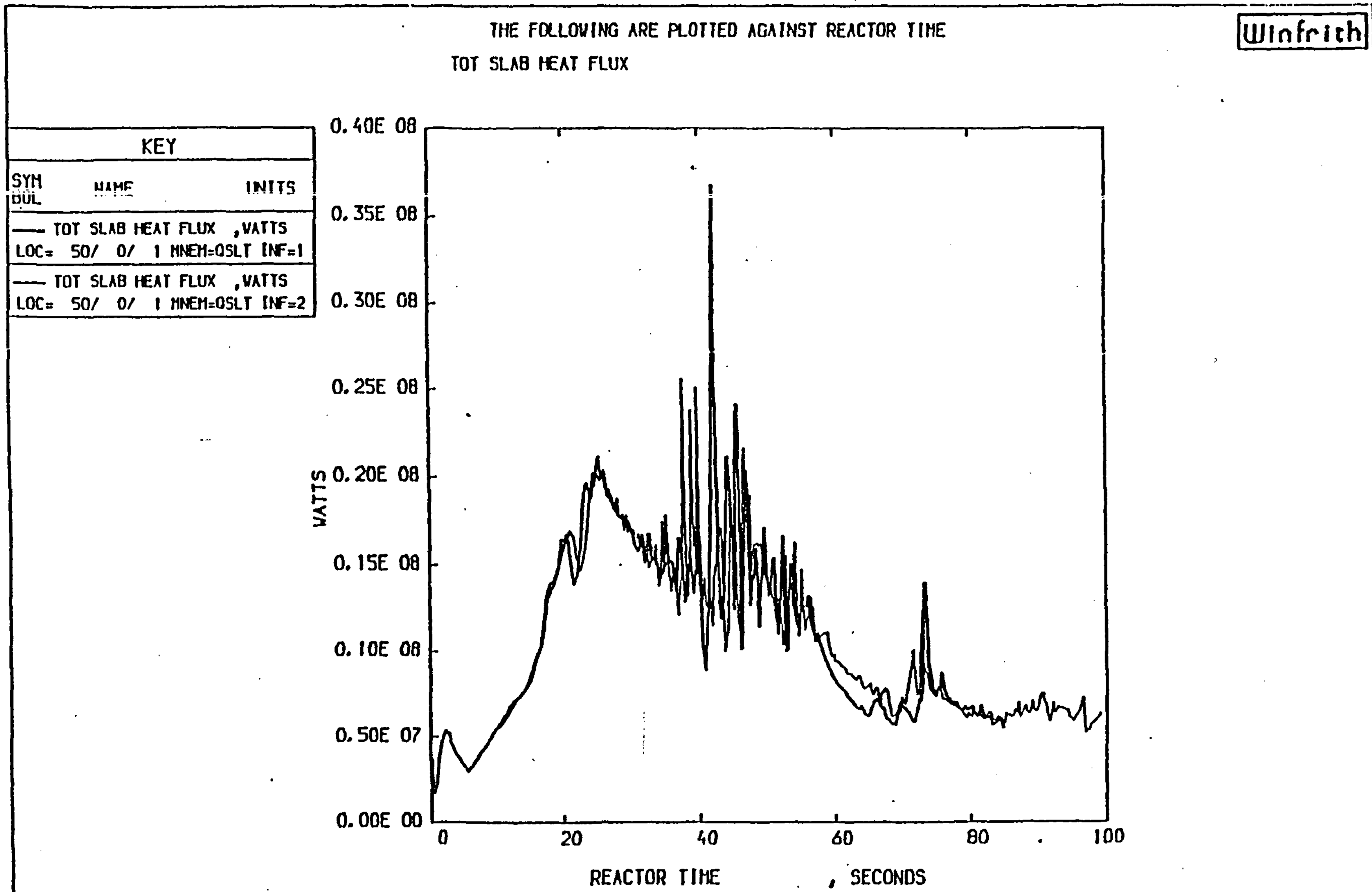

FIGURE 193 INF 1 ISHARP, INF 2 ZEROGAP
VESSEL GLOBALS

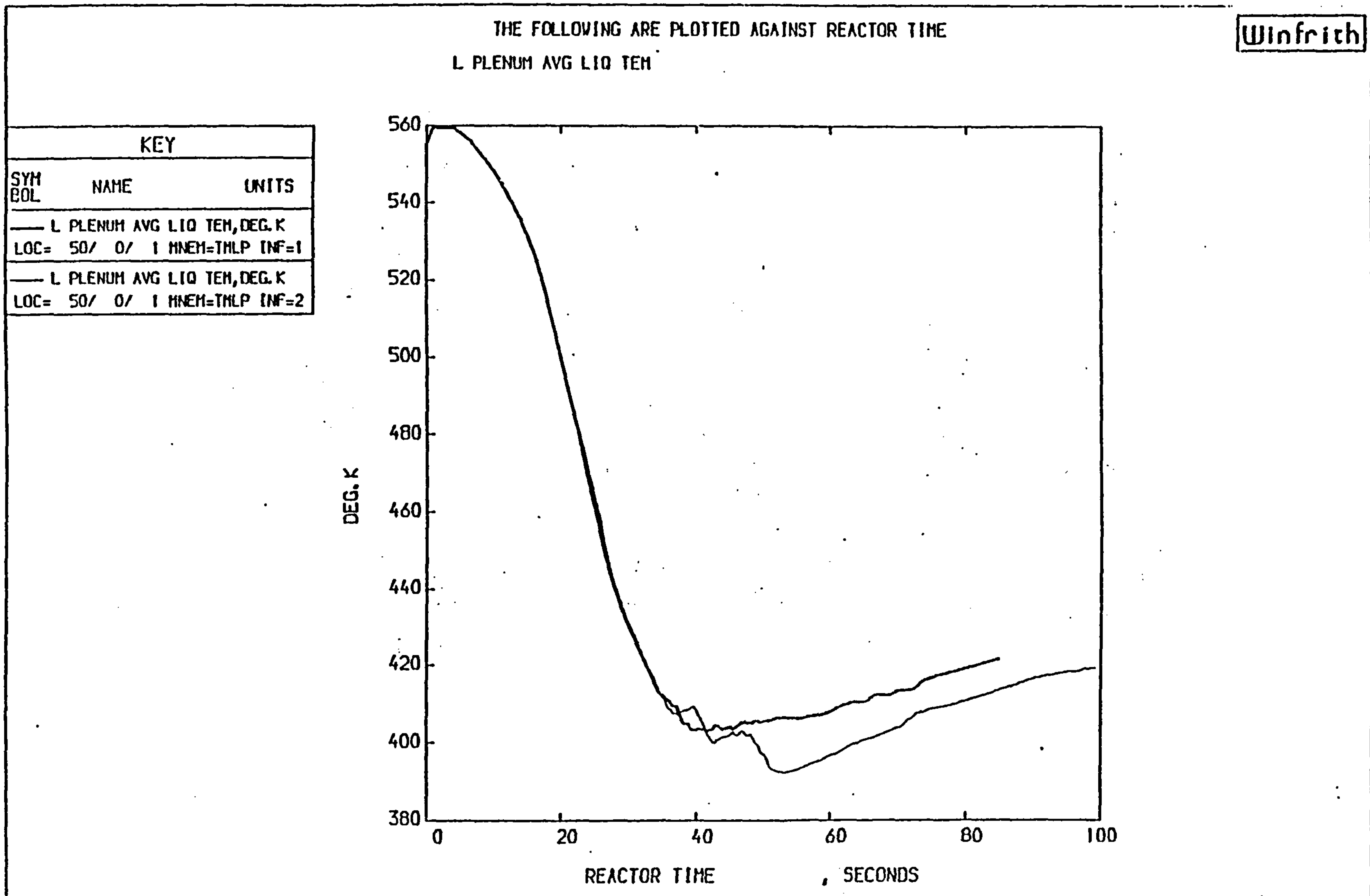

FIGURE 194 INF 1 ISHARP, INF 2 ZEROGAP
VESSEL GLOBALS

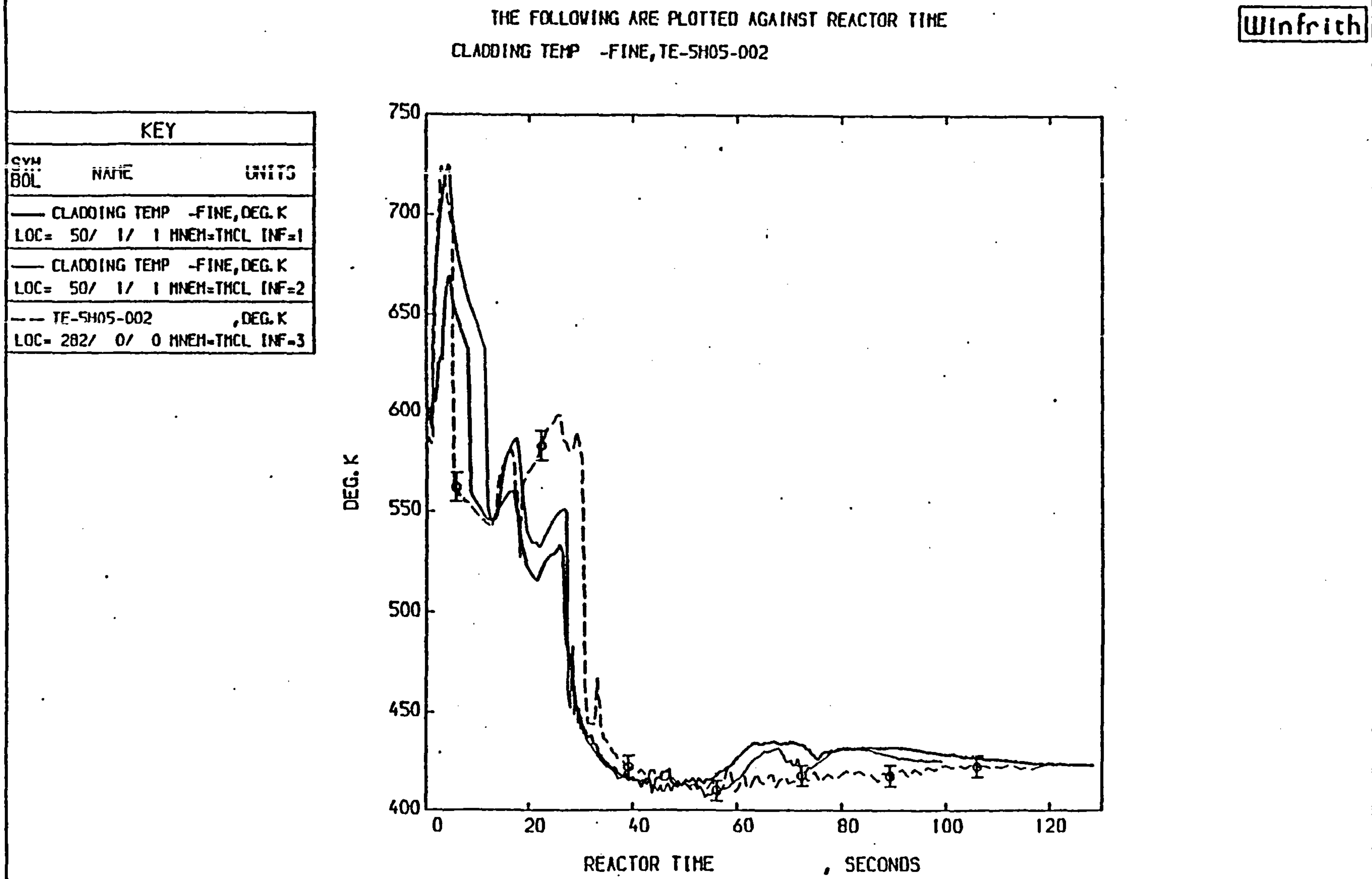

FIGURE 195 INF 1 ISHARP, INF 2 ZEROGAP, INF 3 EXP
CENTRAL FUEL BUNDLE CLADDING TEMPERATURES

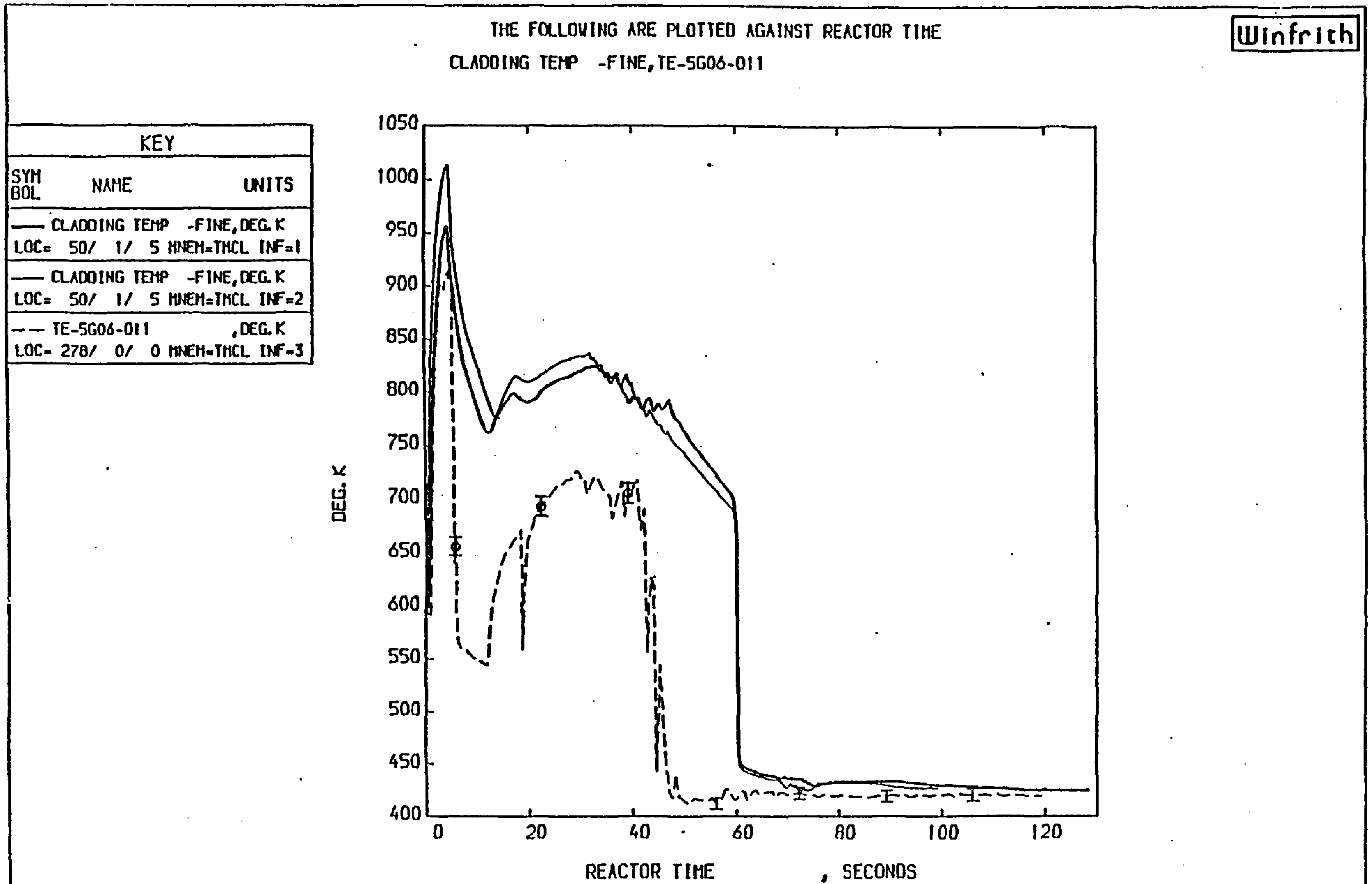

FIGURE 196 INF 1 ISHARP, INF 2 ZEROGAP, INF 3 EXP
CENTRAL FUEL BUNDLE CLADDING TEMPERATURES

Winfrith

THE FOLLOWING ARE PLOTTED AGAINST REACTOR TIME
CLADDING TEMP -FINE,TE-5106-021

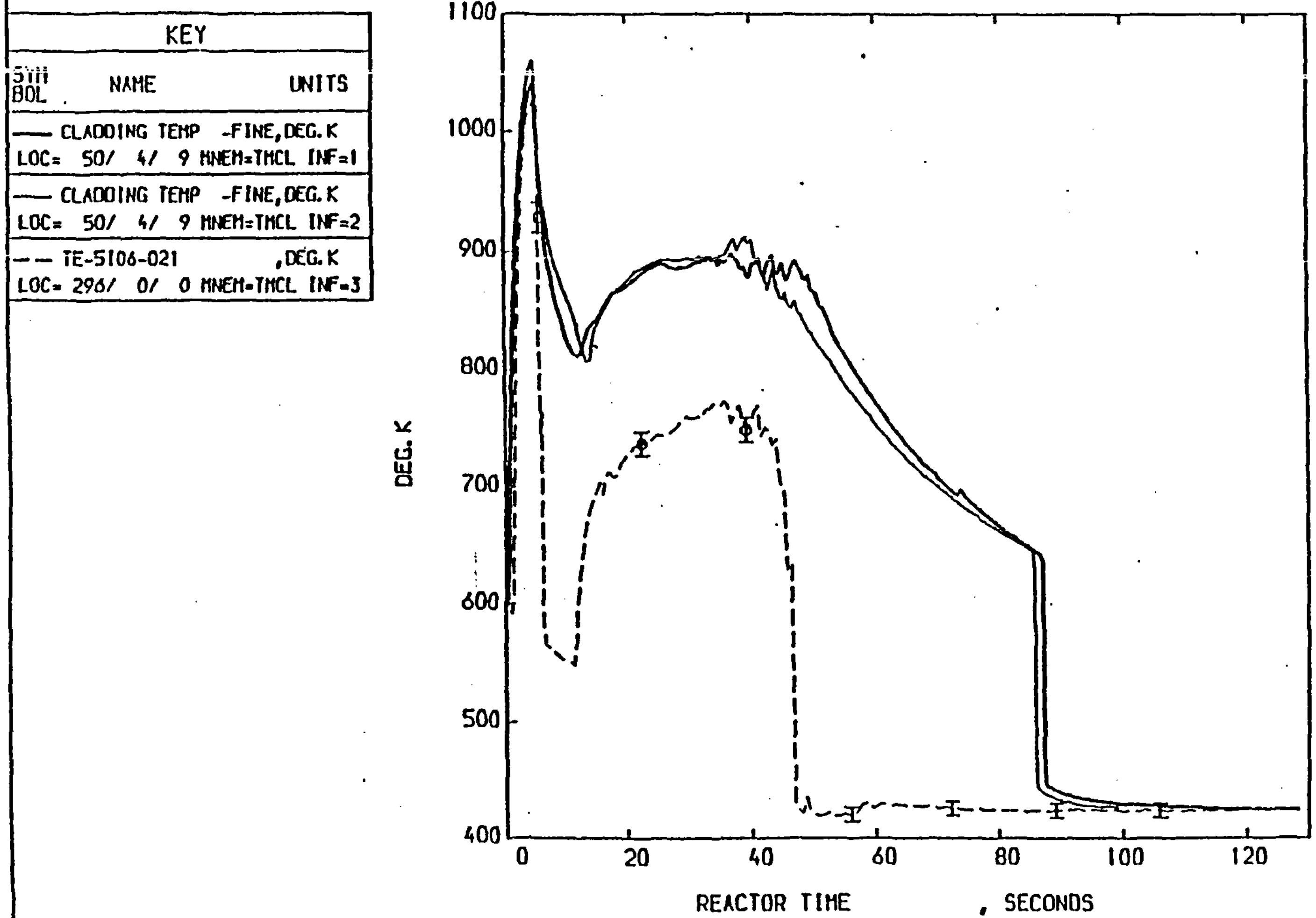

FIGURE 197 INF 1 ISHARP, INF 2 ZEROGAP, INF 3 EXP
CENTRAL FUEL BUNDLE CLADDING TEMPERATURES

Winfrith

THE FOLLOWING ARE PLOTTED AGAINST REACTOR TIME

CLADDING TEMP -FINE,TE-5H06-024

KEY		
SYMBOL	NAME	UNITS
——	CLADDING TEMP -FINE, LOC= 50/ 1/ 10 MNEM=THCL INF=1	DEG.K
——	CLADDING TEMP -FINE, LOC= 50/ 1/ 10 MNEM=THCL INF=2	DEG.K
– –	TE-5H06-024, LOC= 285/ 0/ 0 MNEM=THCL INF=3	DEG.K

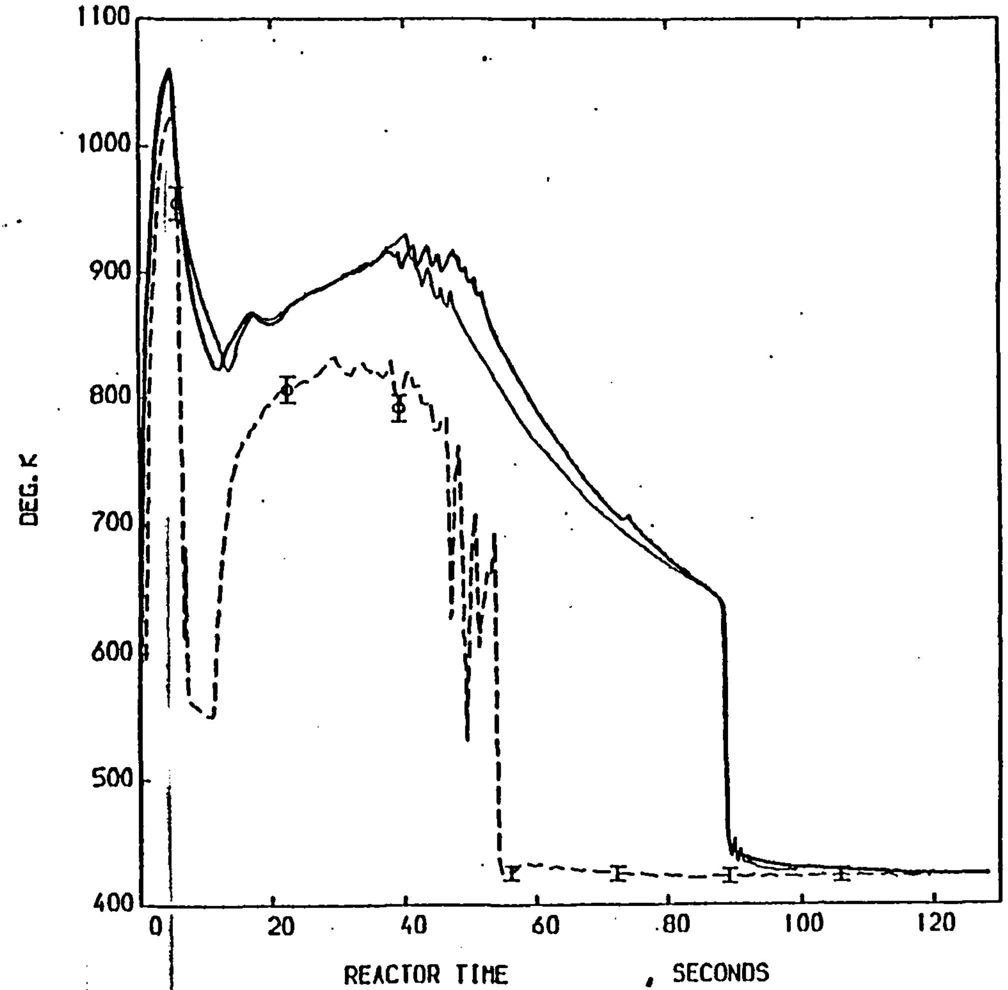

FIGURE 198 INF 1 ISHARP, INF 2 ZEROGAP, INF 3 EXP
CENTRAL FUEL BUNDLE CLADDING TEMPERATURES

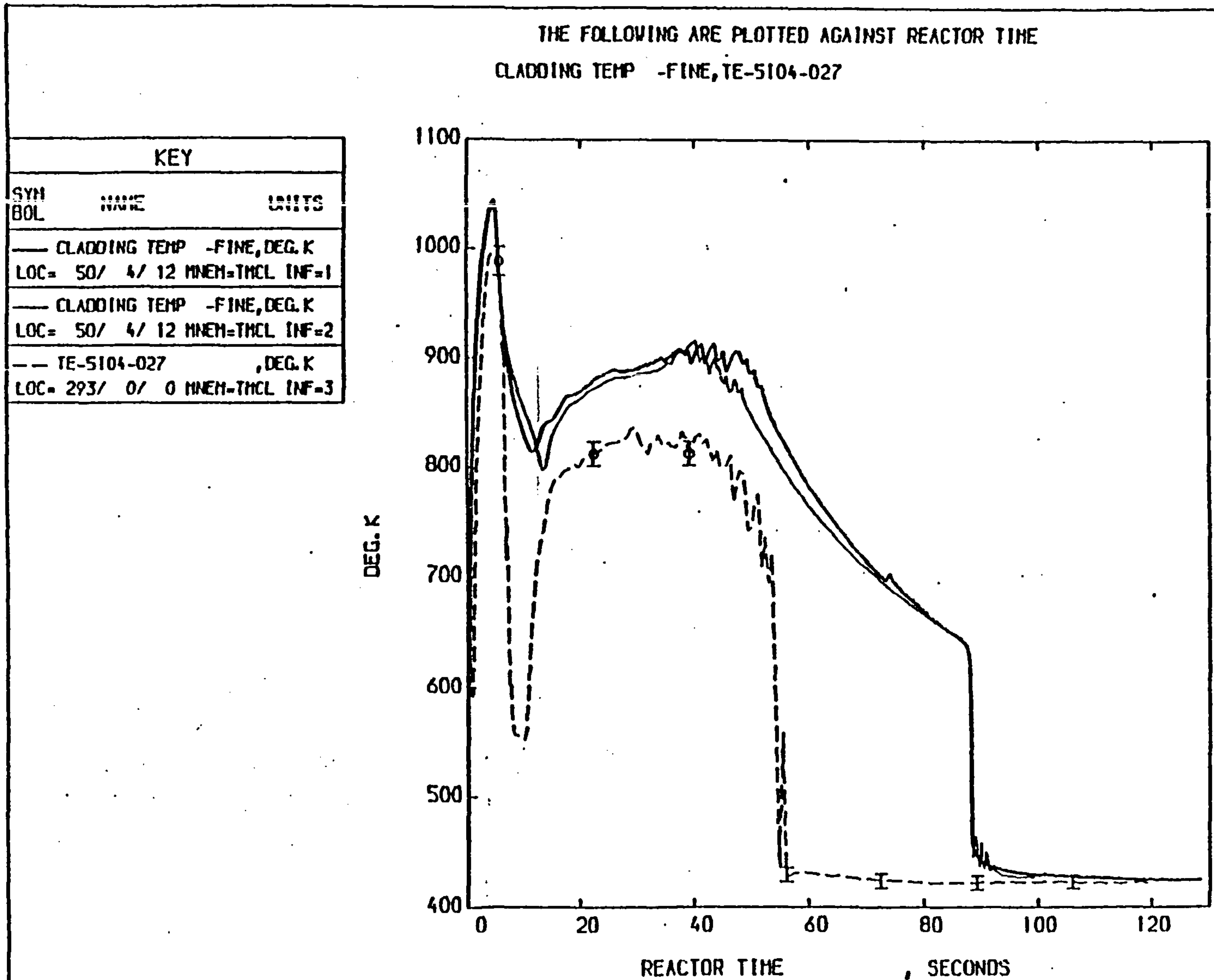

Winfrith

FIGURE 199 INF 1 ISHARP, INF 2 ZEROGAP, INF 3 EXP
CENTRAL FUEL BUNDLE CLADDING TEMPERATURES

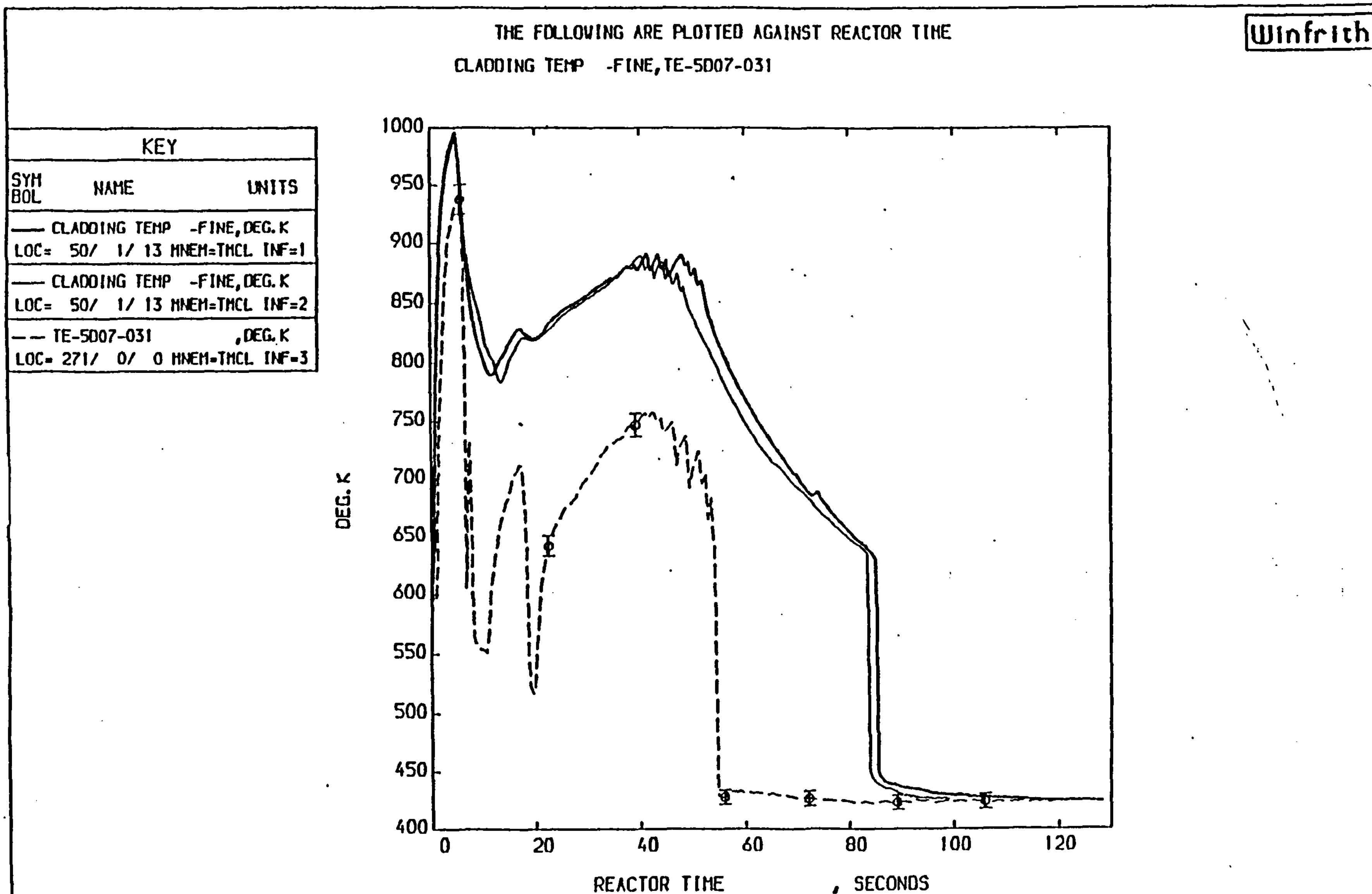

FIGURE 200 INF 1 ISHARP, INF 2 ZEROGAP, INF 3 EXP
CENTRAL FUEL BUNDLE CLADDING TEMPERATURES

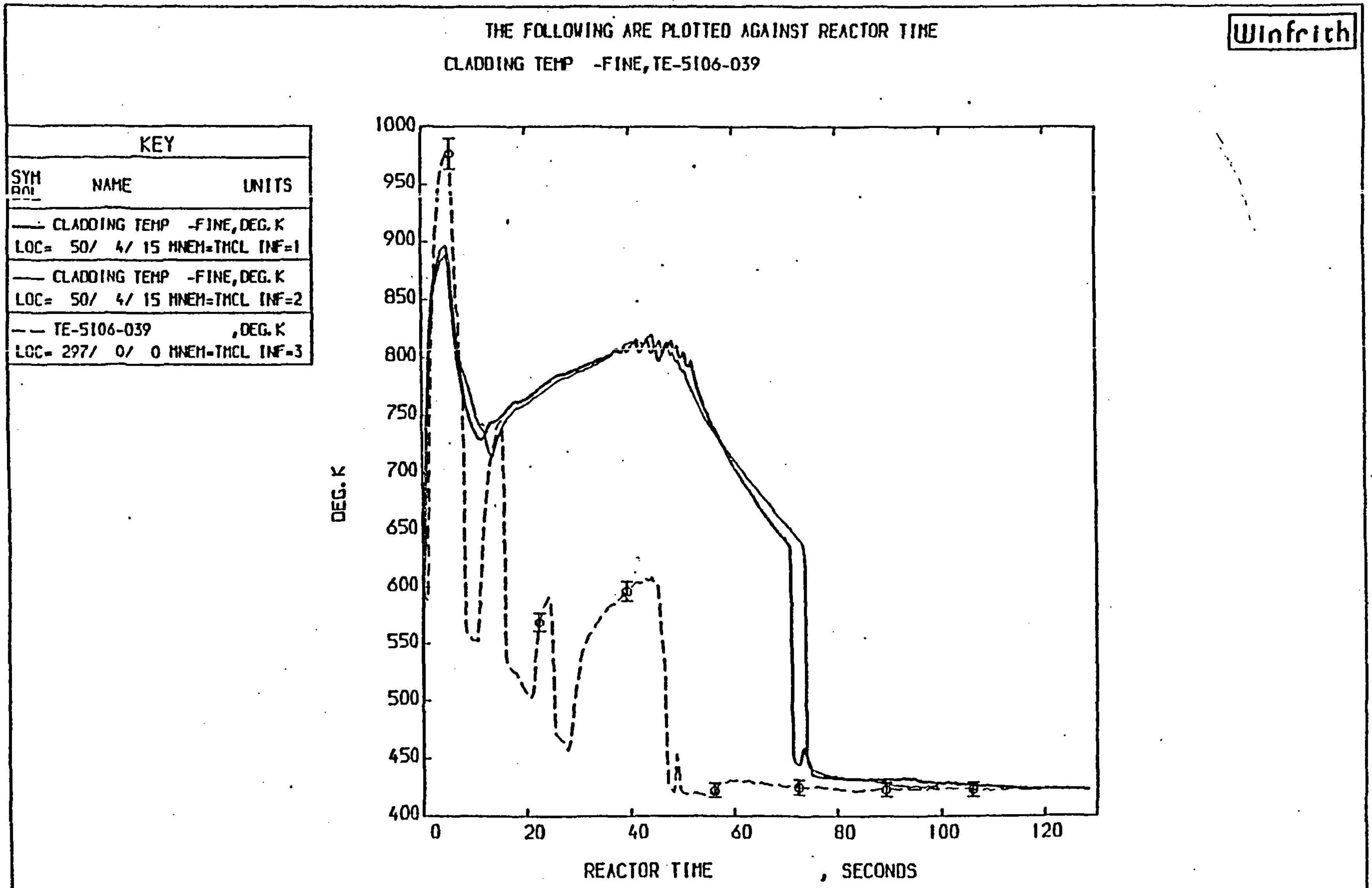

FIGURE 201 INF 1 ISHARP, INF 2 ZEROGAP, INF 3 EXP
CENTRAL FUEL BUNDLE CLADDING TEMPERATURES

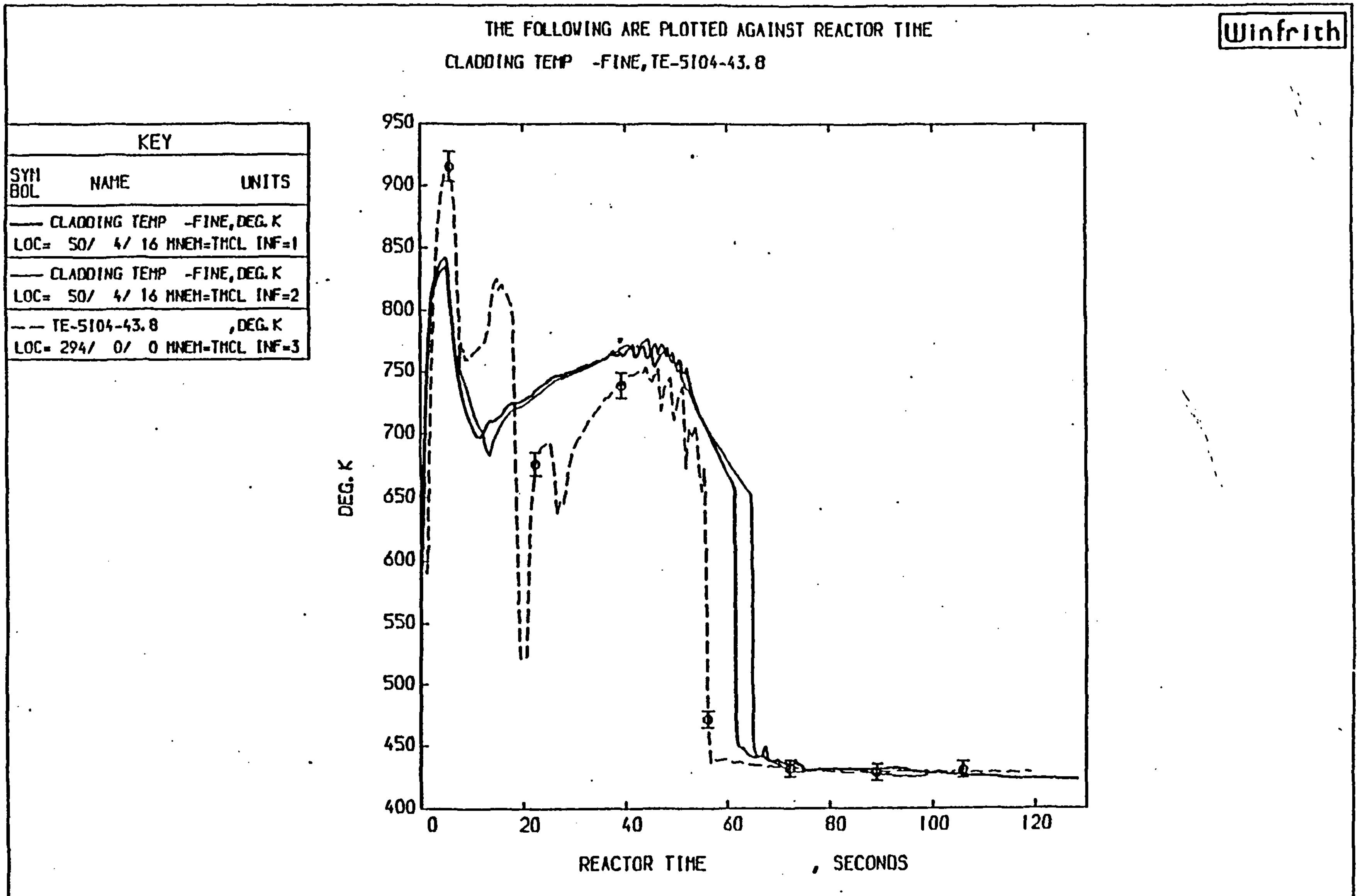

FIGURE 202 INF 1 ISHARP, INF 2 ZEROGAP, INF 3 EXP
CENTRAL FUEL BUNDLE CLADDING TEMPERATURES

Winfrith

THE FOLLOWING ARE PLOTTED AGAINST REACTOR TIME

CLADDING TEMP -FINE,TE-5H05-049

KEY		
SYMBOL	NAME	UNITS
——	CLADDING TEMP -FINE,	DEG.K
	LOC= 50/ 1/ 17 MNEM=THCL INF=1	
——	CLADDING TEMP -FINE,	DEG.K
	LOC= 50/ 1/ 17 MNEM=THCL INF=2	
– –	TE-5H05-049	,DEG.K
	LOC= 284/ 0/ 0 MNEM=THCL INF=3	

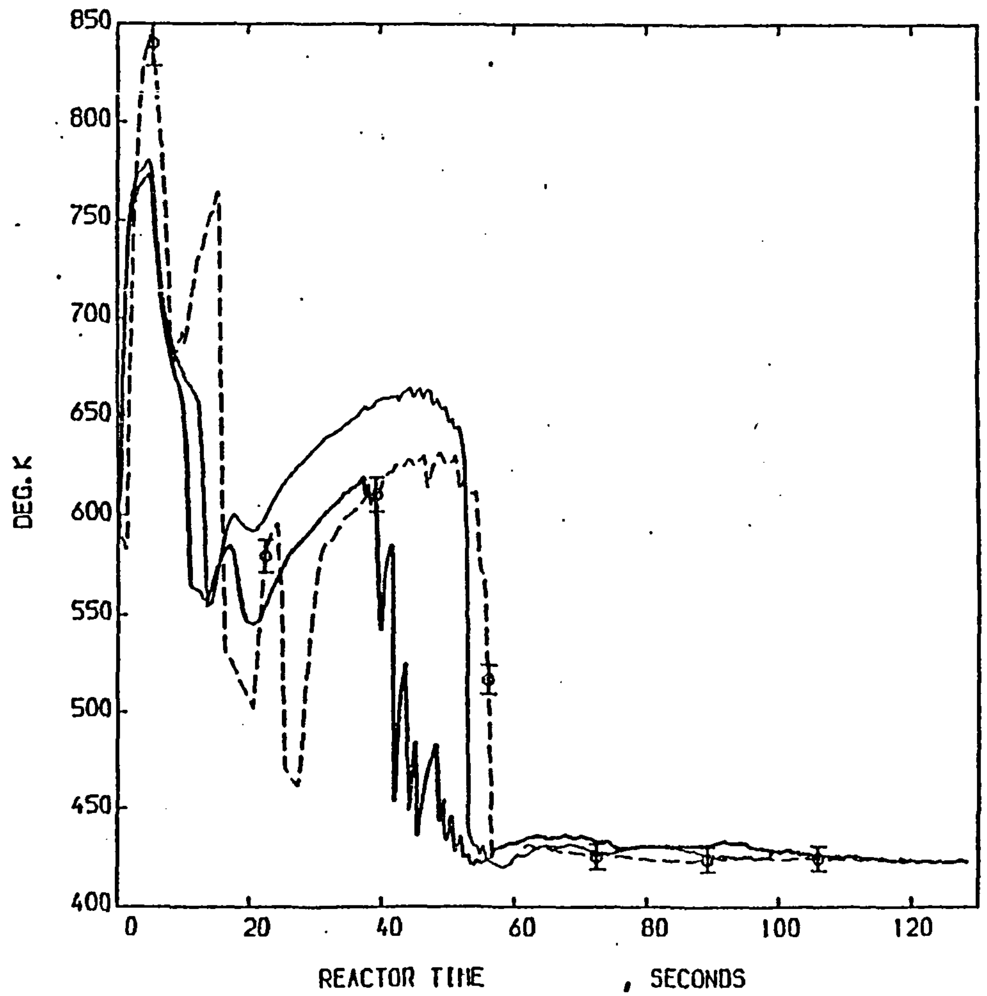

FIGURE 203 INF 1 ISHARP, INF 2 ZEROGAP, INF 3 EXP
CENTRAL FUEL BUNDLE CLADDING TEMPERATURES

AEEW - M 2464

240

THE FOLLOWING ARE PLOTTED AGAINST REACTOR TIME

CLADDING TEMP -FINE,TE-5G06-062

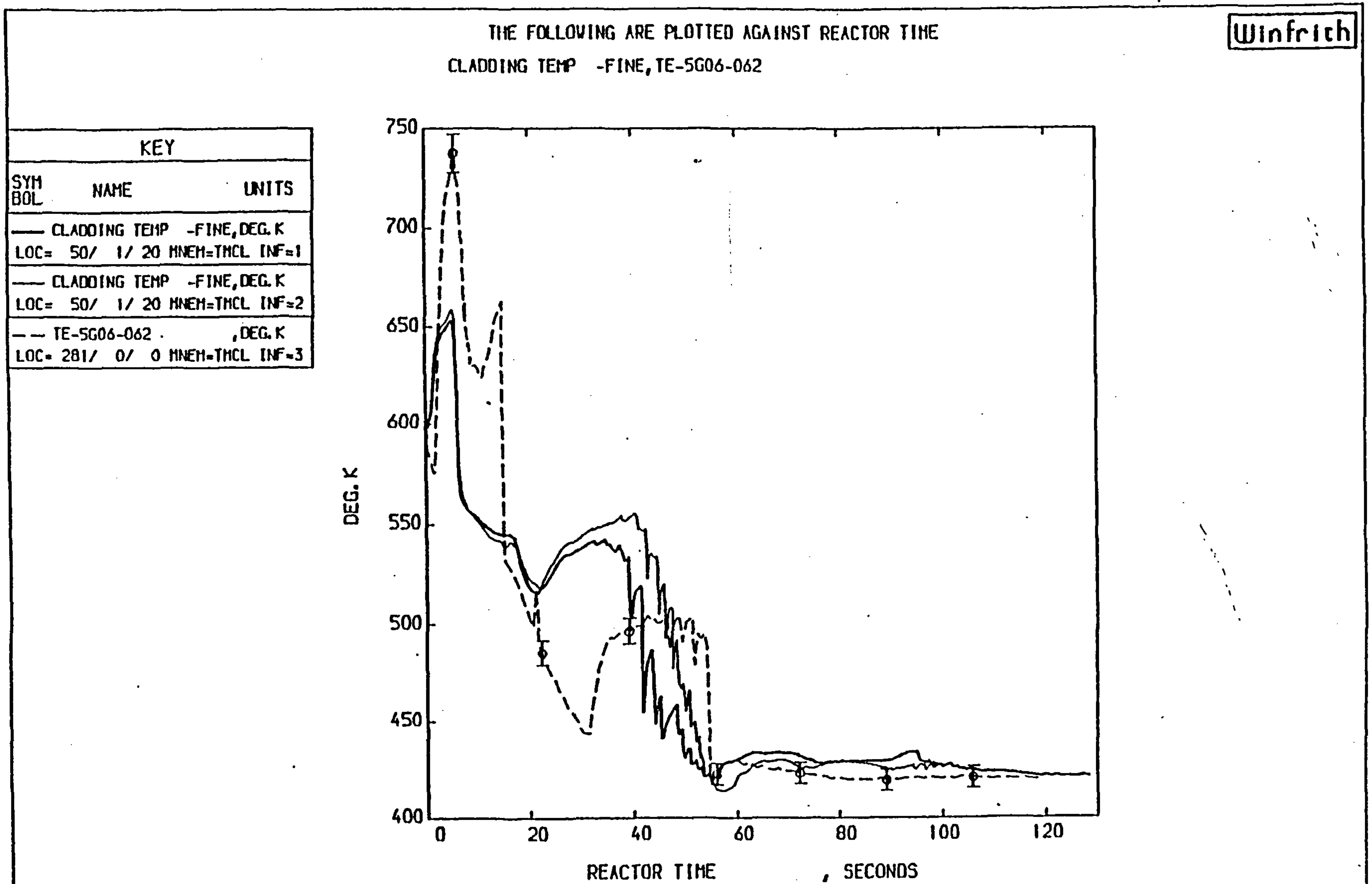

FIGURE 204 INF 1 ISHARP, INF 2 ZEROGAP, INF 3 EXP
CENTRAL FUEL BUNDLE CLADDING TEMPERATURES

THE FOLLOWING ARE PLOTTED AGAINST REACTOR TIME

ROD CENTRE TEMP-FINE, TC-5D07-27 , TC-5D09-27
TC-5D10-27

Winfrith

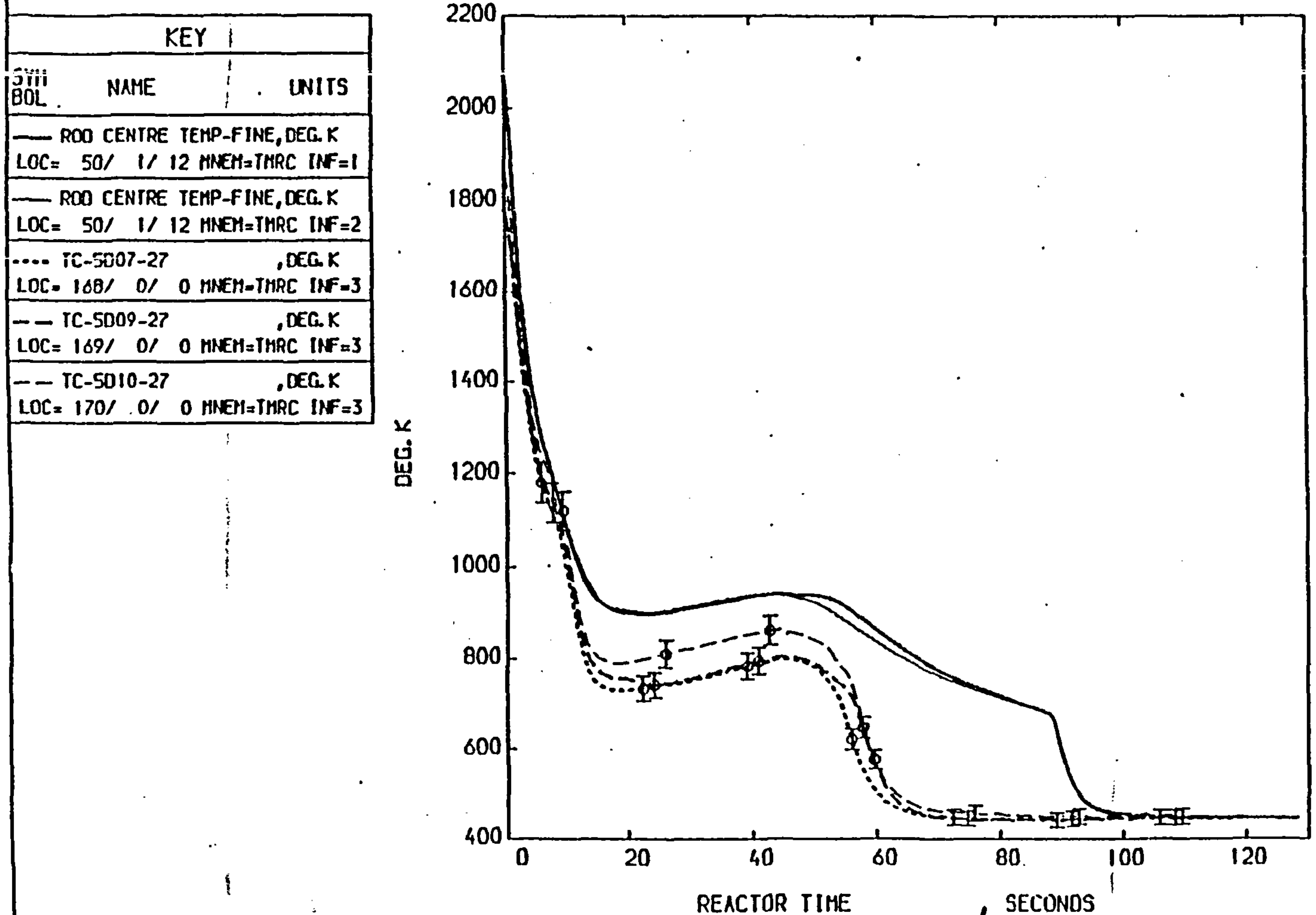

FIGURE 205 INF 1 ISHARP, INF 2 ZEROGAP, INF 3 EXP
CENTRELINE FUEL TEMPERATURE

Winfrith

THE FOLLOWING ARE PLOTTED AGAINST REACTOR TIME

CLADDING TEMP -FINE, TE-2G14-011

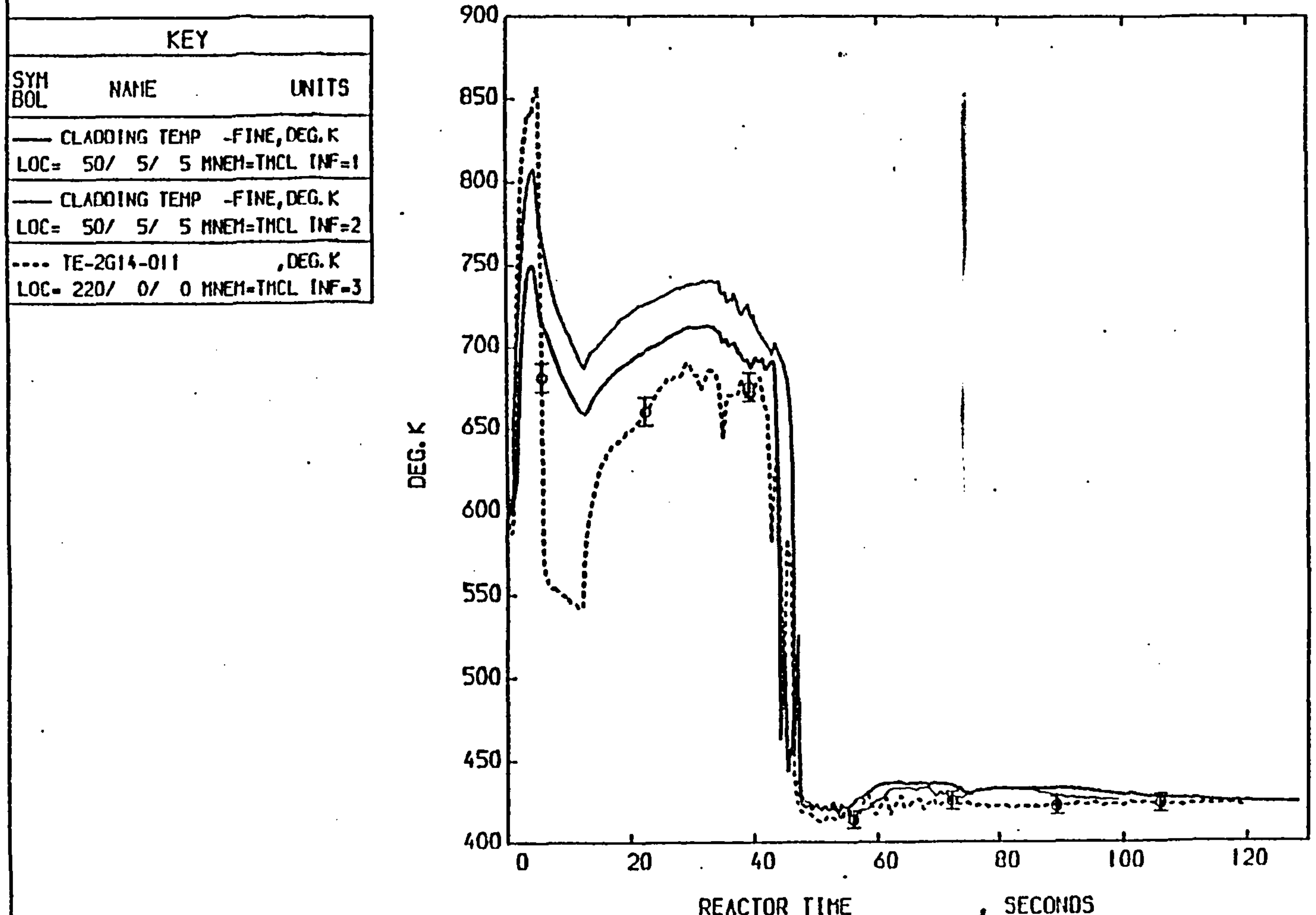

FIGURE 206 INF 1 ISHARP, INF 2 ZEROGAP, INF 3 EXP
FUEL ROD CLADDING TEMPERATURES - PERIPHERAL BUNDLES

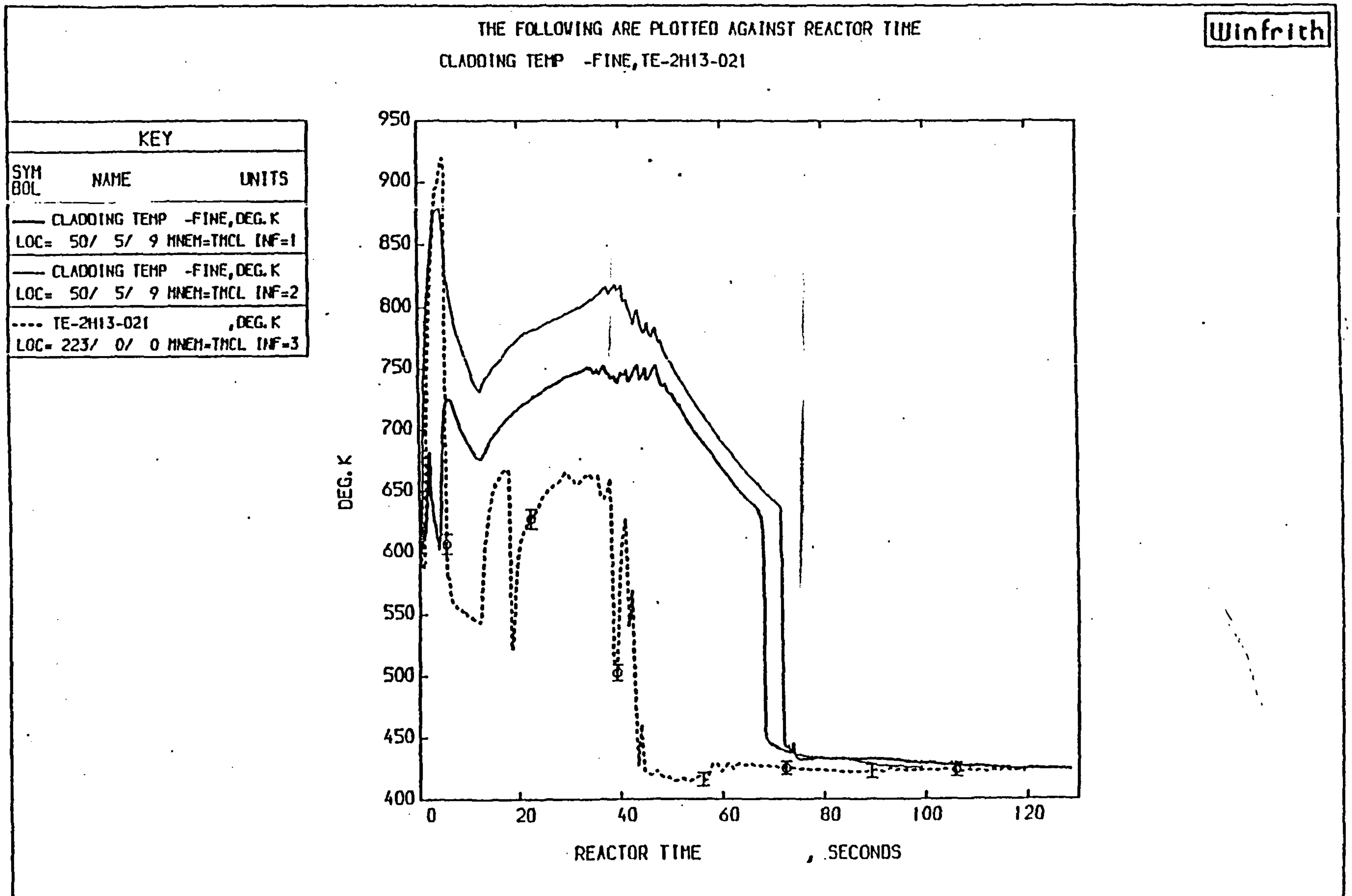

FIGURE 207 INF 1 ISHARP, INF 2 ZEROGAP, INF 3 EXP
FUEL ROD CLADDING TEMPERATURES - PERIPHERAL BUNDLES

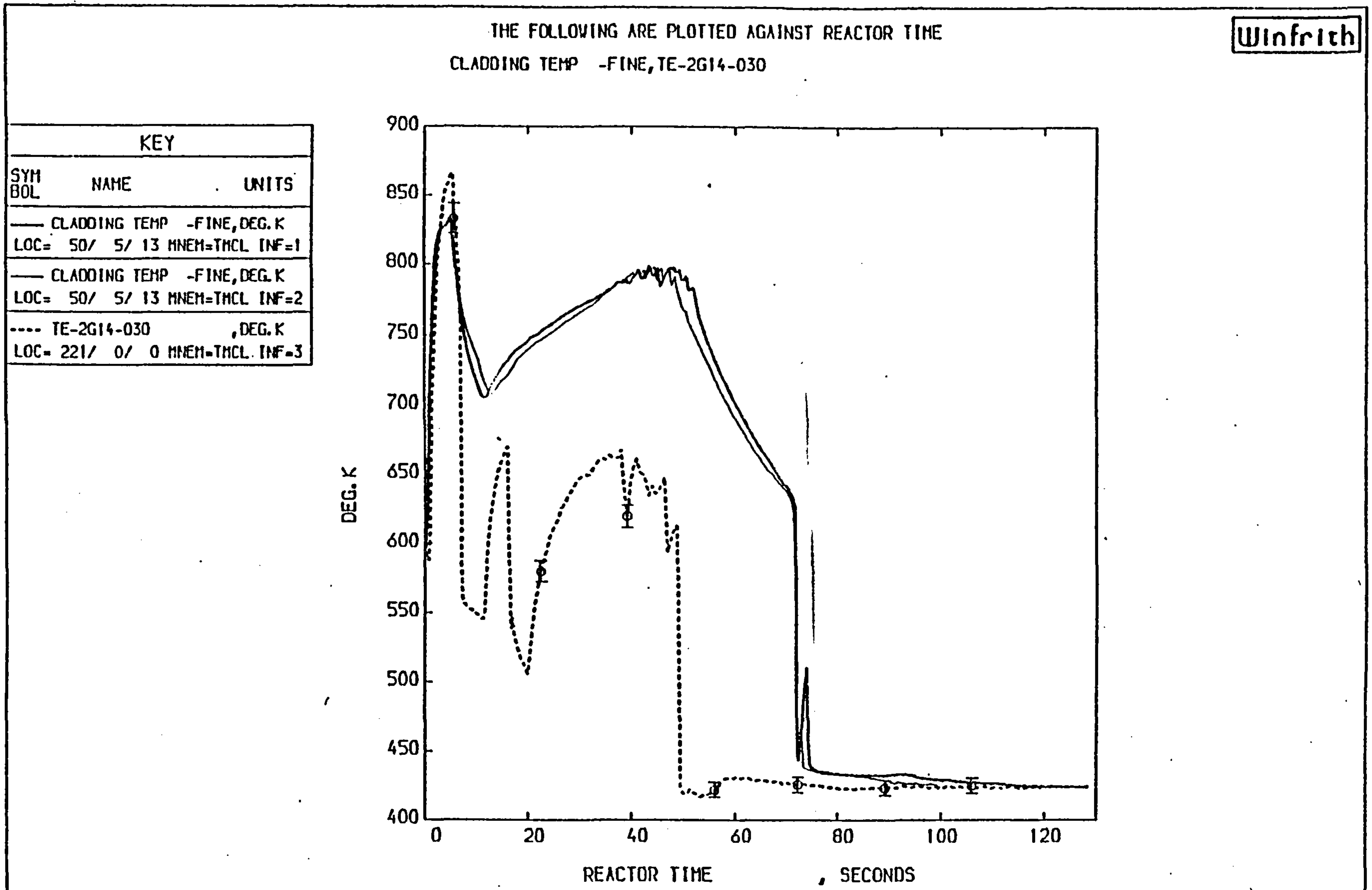

FIGURE 208 INF 1 ISHARP, INF 2 ZEROGAP, INF 3 EXP
FUEL ROD CLADDING TEMPERATURES - PERIPHERAL BUNDLES

Winfrith

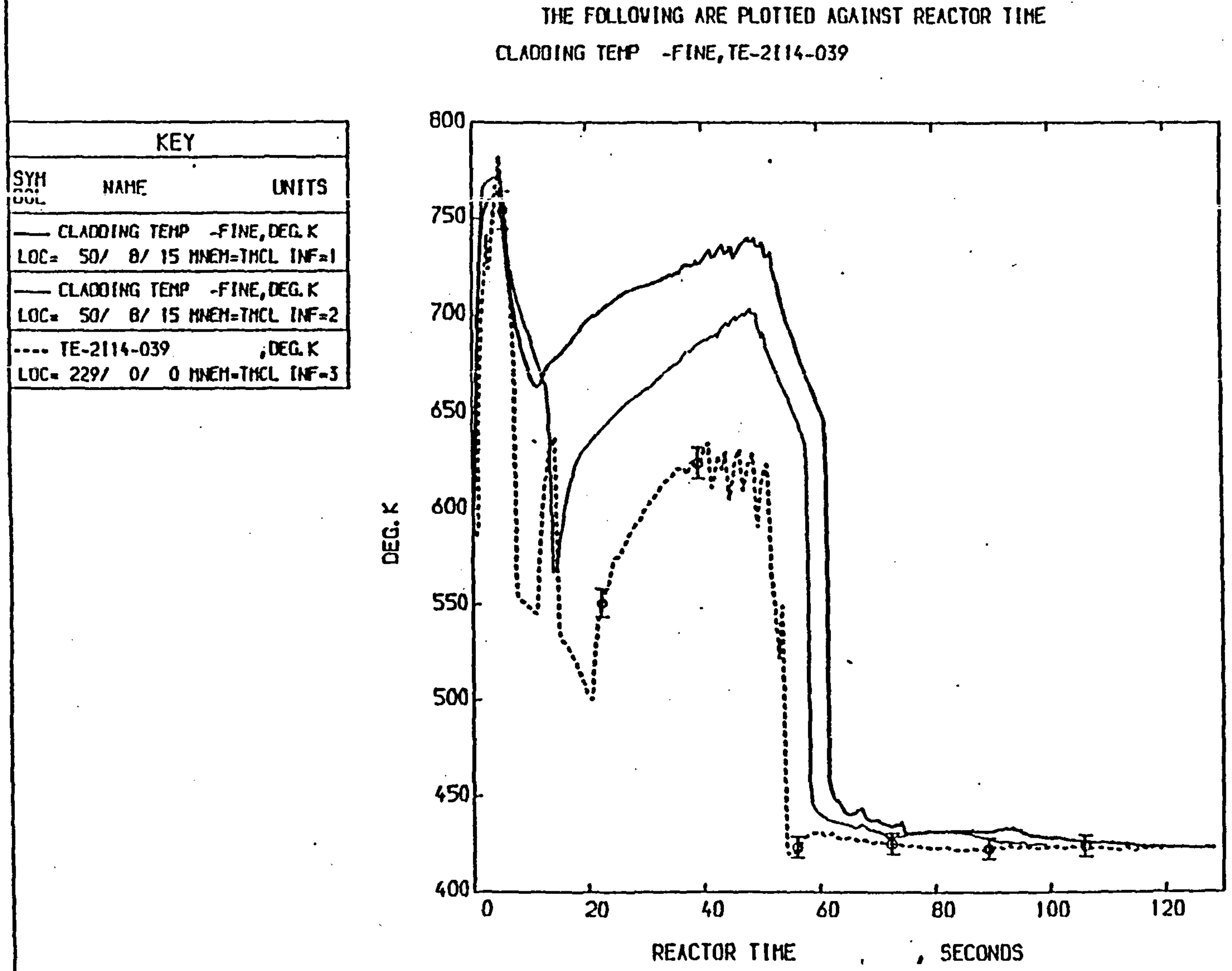

FIGURE 209 INF 1 ISHARP, INF 2 ZEROGAP, INF 3 EXP
FUEL ROD CLADDING TEMPERATURES - PERIPHERAL BUNDLES

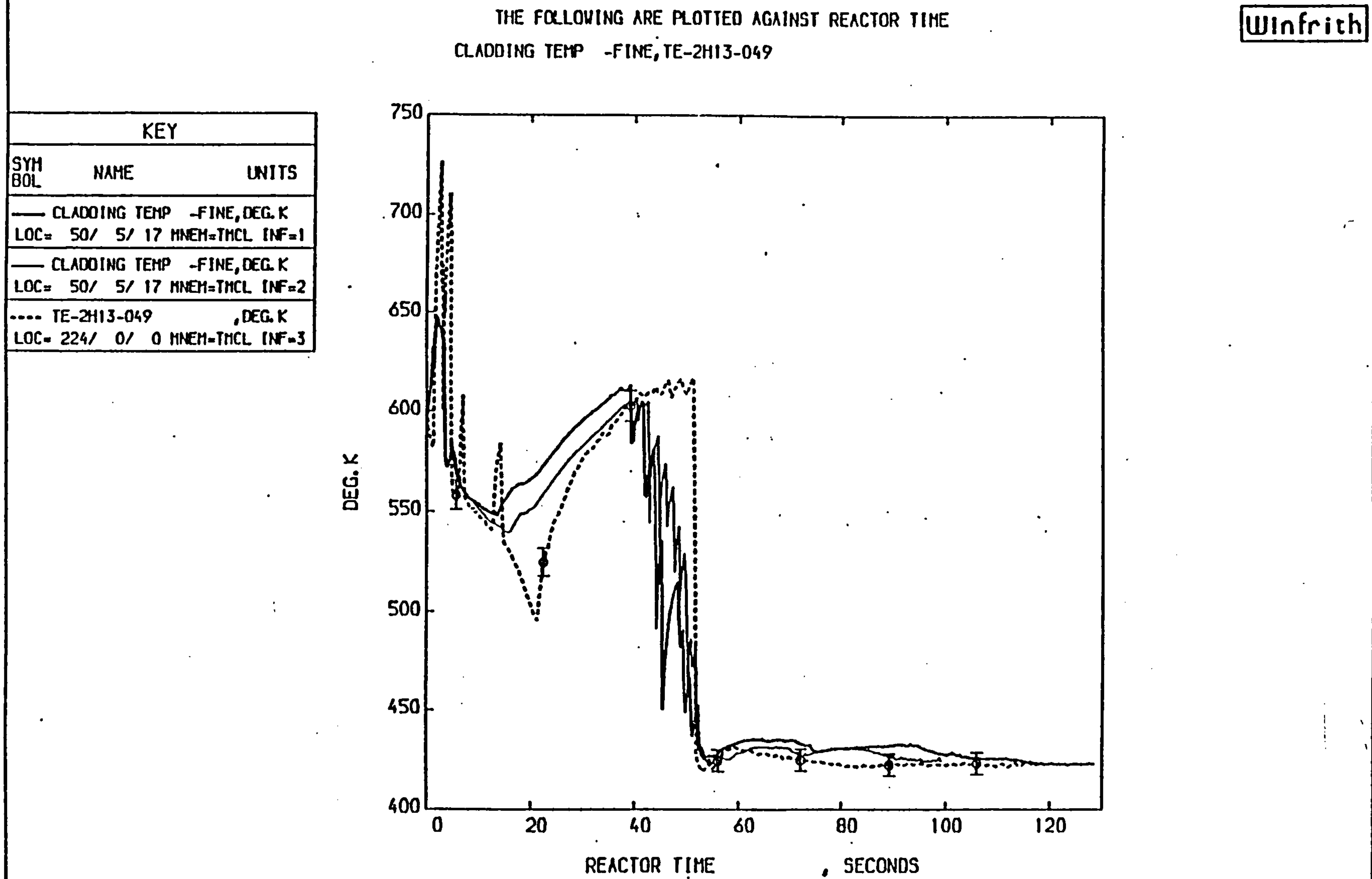

FIGURE 210 INF 1 ISHARP, INF 2 ZEROGAP, INF 3 EXP
FUEL ROD CLADDING TEMPERATURES - PERIPHERAL BUNDLES

THE FOLLOWING ARE PLOTTED AGAINST REACTOR TIME

CLADDING TEMP -FINE, TE-4G14-011

Winfrith

KEY		
SYMBOL	NAME	UNITS
——	CLADDING TEMP -FINE,	DEG.K
LOC= 50/ 6/ 5 MNEM=THCL INF=1		
——	CLADDING TEMP -FINE,	DEG.K
LOC= 50/ 6/ 5 MNEM=THCL INF=2		
·····	TE-4G14-011	,DEG.K
LOC= 249/ 0/ 0 MNEM=THCL INF=3		

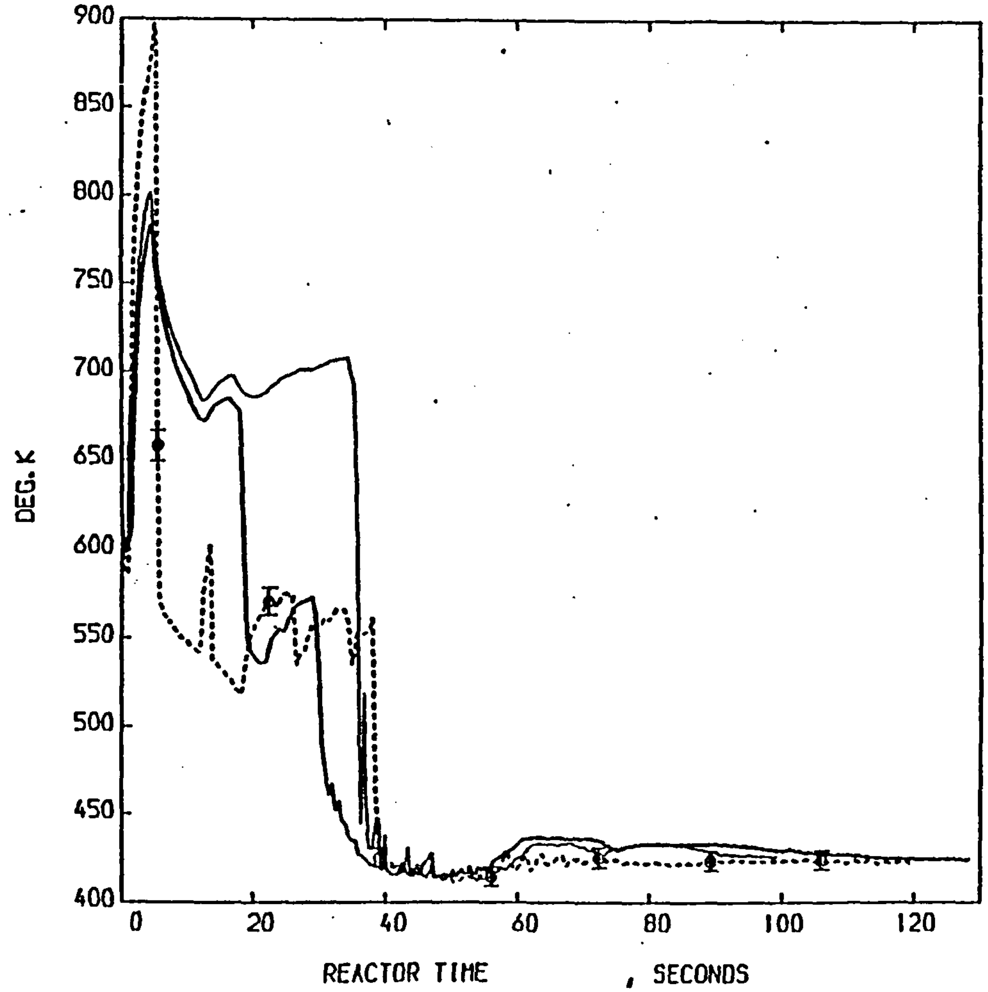

FIGURE 211 INF 1 ISHARP, INF 2 ZEROGAP, INF 3 EXP
FUEL ROD CLADDING TEMPERATURES - PERIPHERAL BUNDLES

Winfrith

THE FOLLOWING ARE PLOTTED AGAINST REACTOR TIME

CLADDING TEMP -FINE,TE-4G08-021

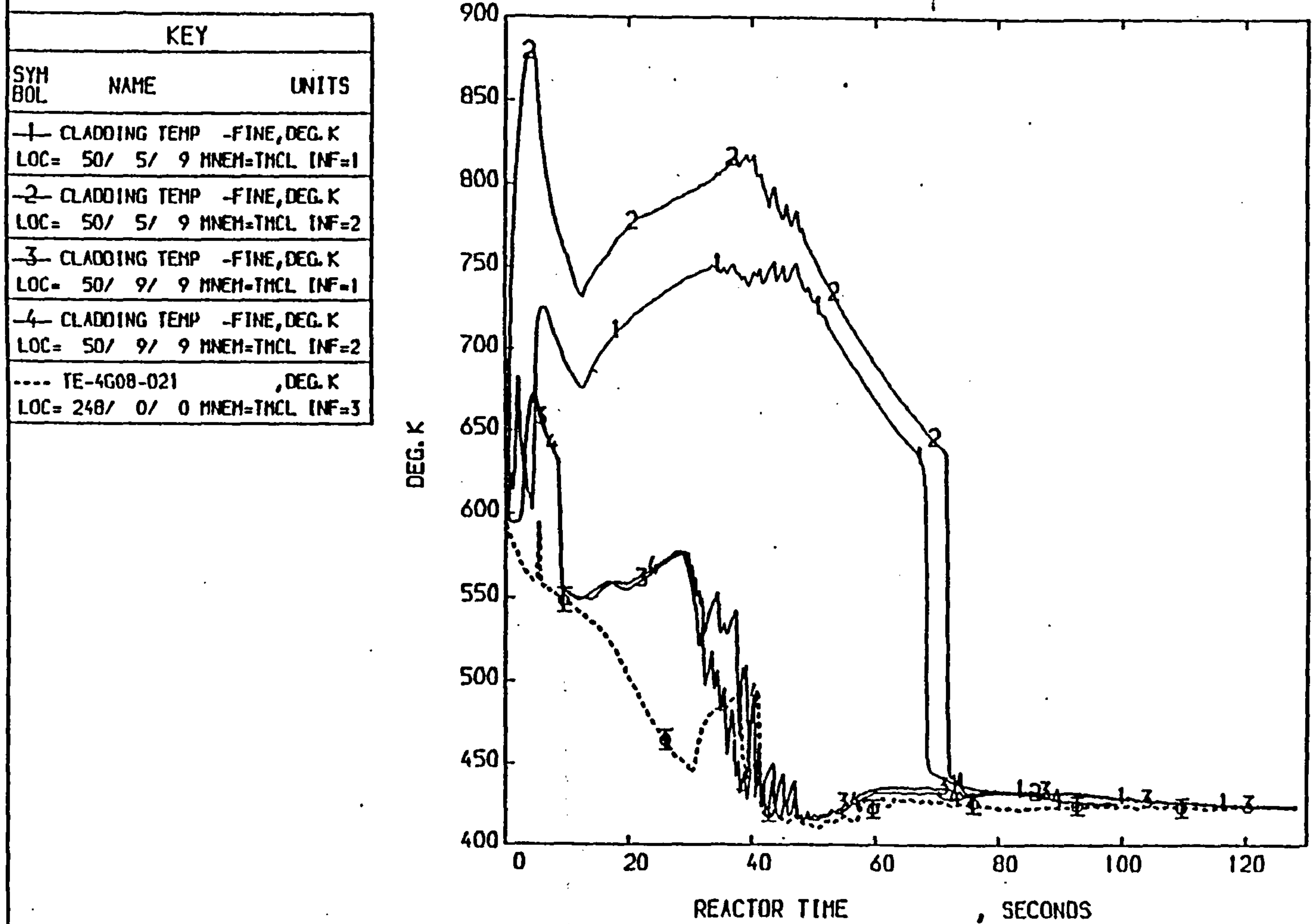

FIGURE 212 INF 1 ISHARP, INF 2 ZEROGAP, INF 3 EXP
FUEL ROD CLADDING TEMPERATURES - PERIPHERAL BUNDLES

THE FOLLOWING ARE PLOTTED AGAINST REACTOR TIME

CLADDING TEMP -FINE,TE-4H14-028

Winfrith

KEY		
SYMBOL	NAME	UNITS
——	CLADDING TEMP -FINE,	DEG.K
	LOC= 50/ 6/ 12 MNEM=THCL INF=1	
——	CLADDING TEMP -FINE,	DEG.K
	LOC= 50/ 6/ 12 MNEM=THCL INF=2	
----	TE-4H14-028	,DEG.K
	LOC= 253/ 0/ 0 MNEM=THCL INF=3	

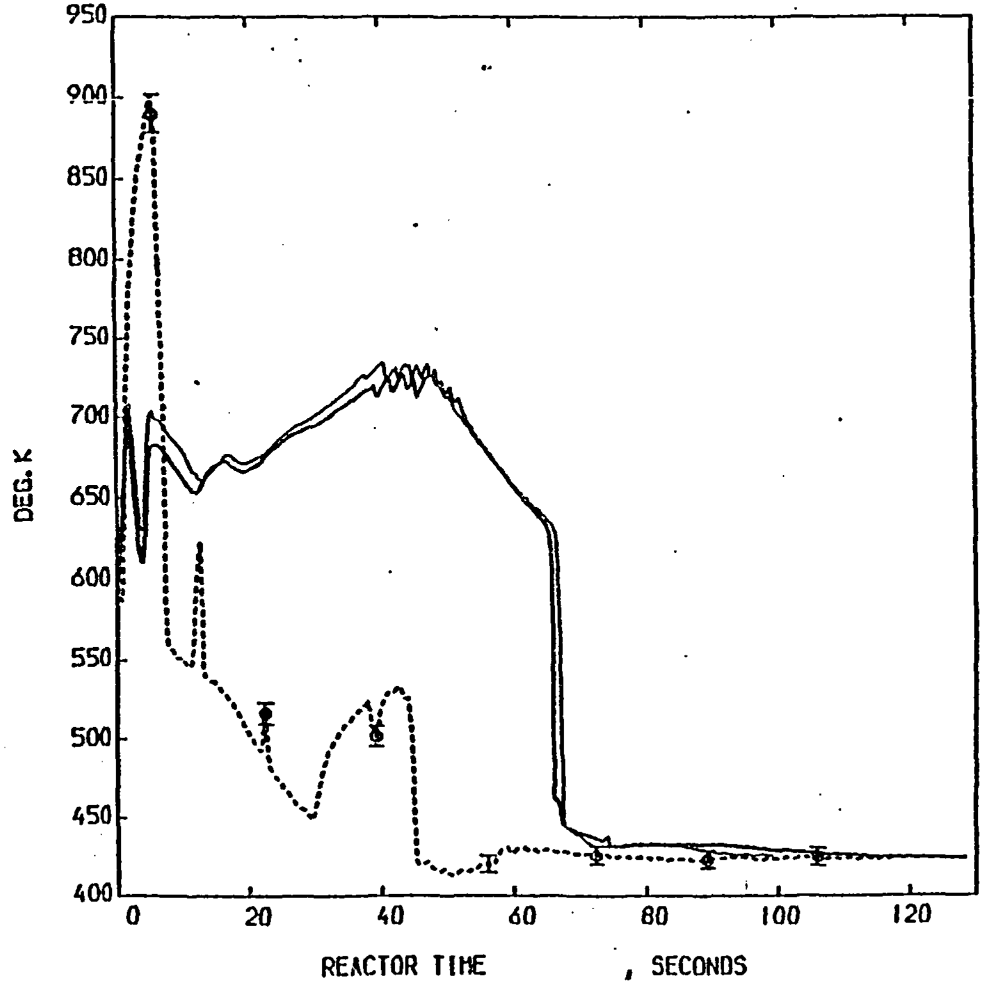

FIGURE 213 INF 1 ISHARP, INF 2 ZEROGAP, INF 3 EXP
FUEL ROD CLADDING TEMPERATURES - PERIPHERAL BUNDLES

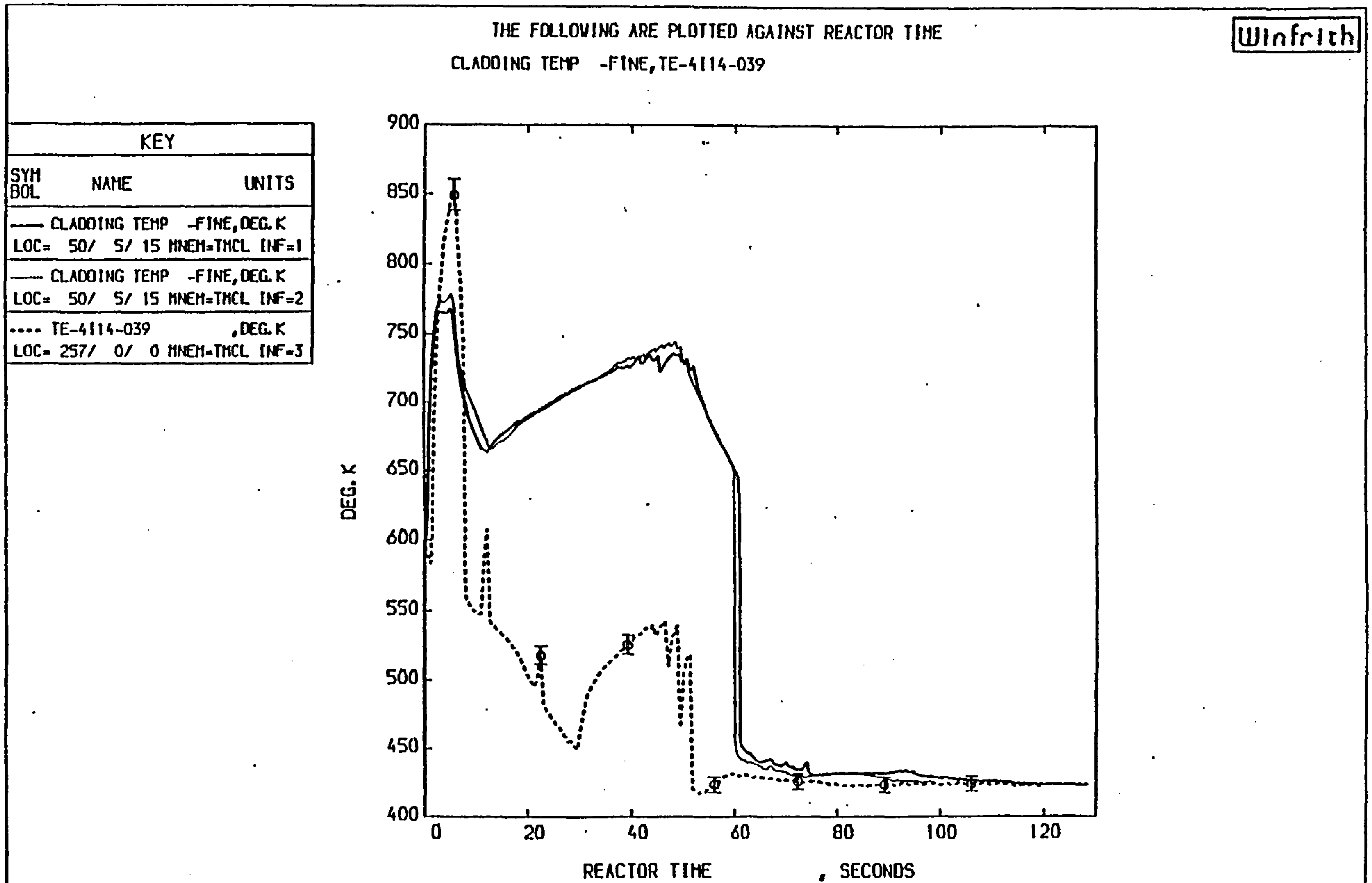

FIGURE 214 INF 1 ISHARP, INF 2 ZEROGAP, INF 3 EXP
FUEL ROD CLADDI"^ TEMPERATURES - PERIPHERAL BUNDLES

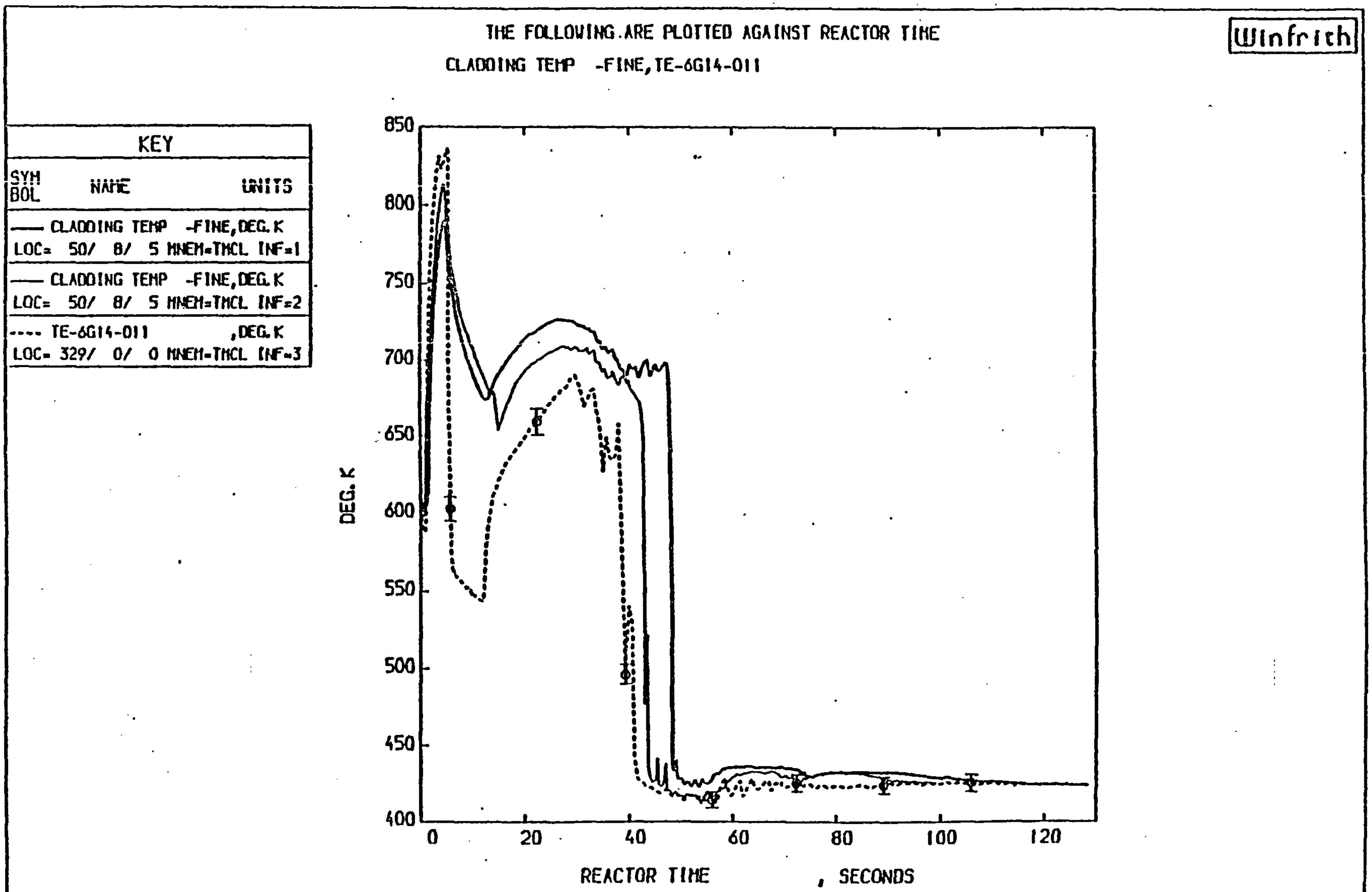

FIGURE 215 INF 1 ISHARP, INF 2 ZEROGAP, INF 3 EXP
FUEL ROD CLADDING TEMPERATURES - PERIPHERAL BUNDLES

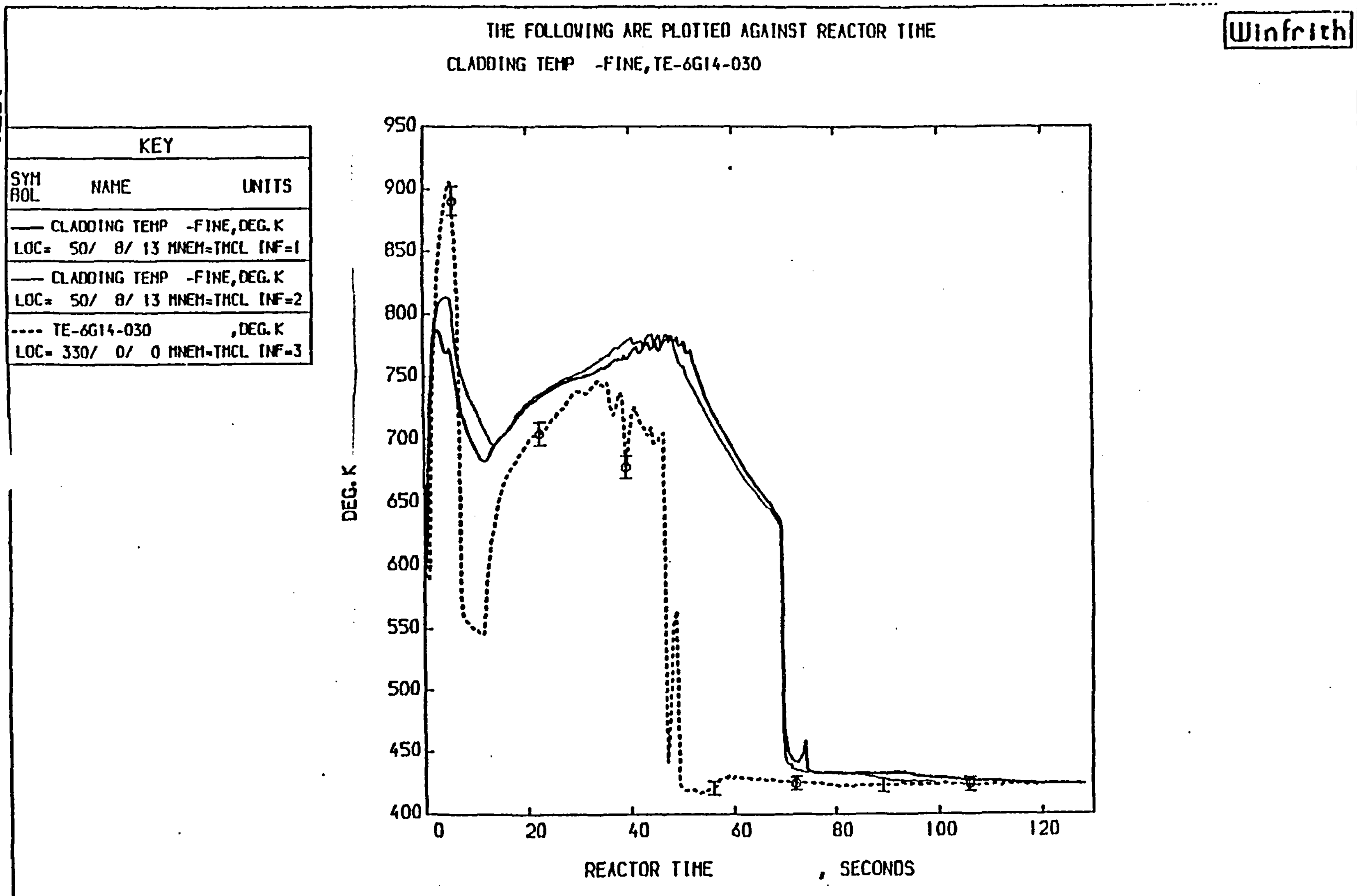

FIGURE 216 INF 1 ISHARP, INF 2 ZEROGAP, INF 3 EXP
FUEL ROD CLADDING TEMPERATURES - PERIPHERAL BUNDLES

Winfrith

THE FOLLOWING ARE PLOTTED AGAINST REACTOR TIME
CLADDING TEMP -FINE, TE-6H15-026

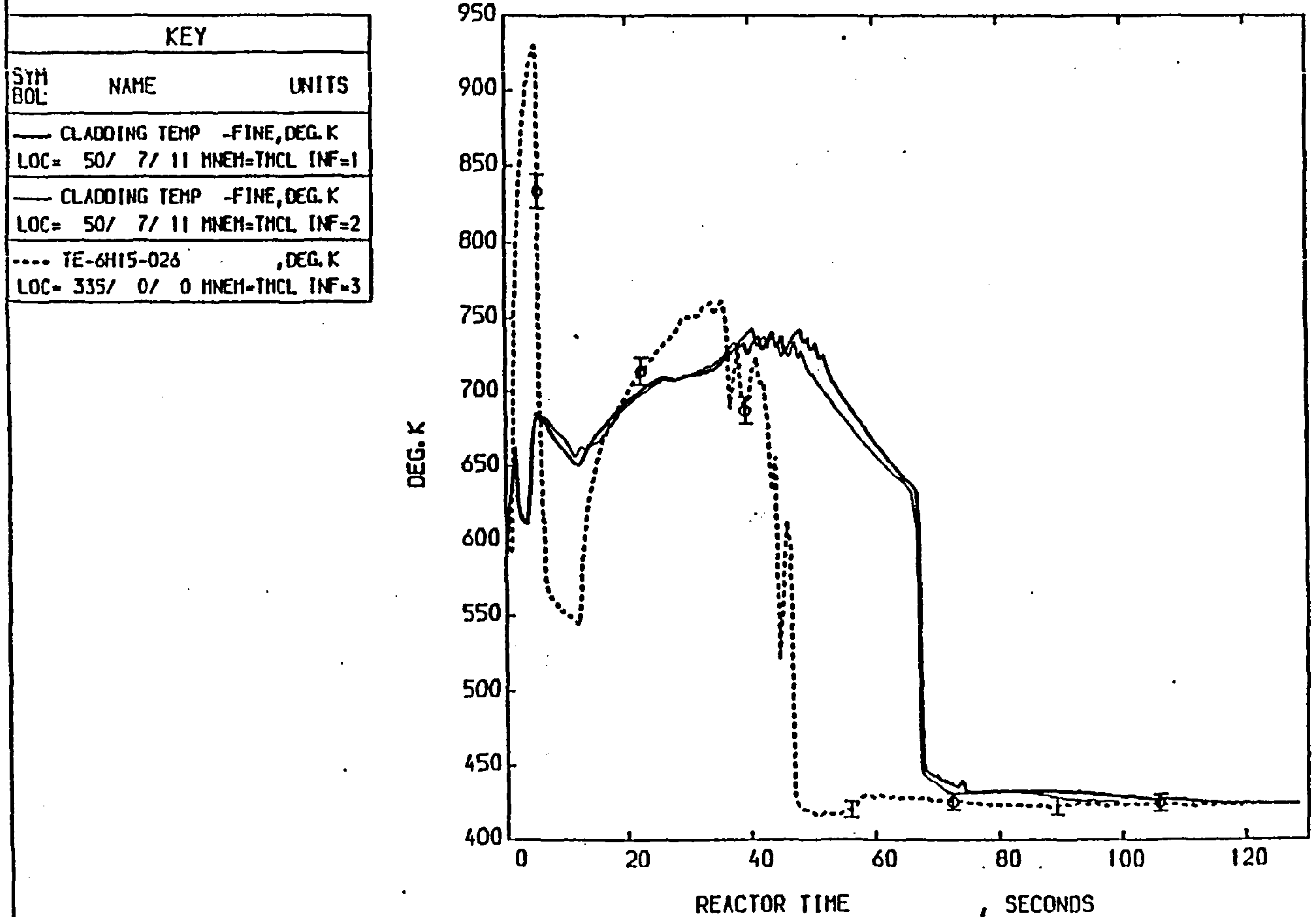

FIGURE 217 INF 1 ISHARP, INF 2 ZEROGAP, INF 3 EXP
FUEL ROD CLADDING TEMPERATURES - PERIPHERAL BUNDLES

THE FOLLOWING ARE PLOTTED AGAINST REACTOR TIME

CLADDING TEMP -FINE,TE-6114-039

Winfrith

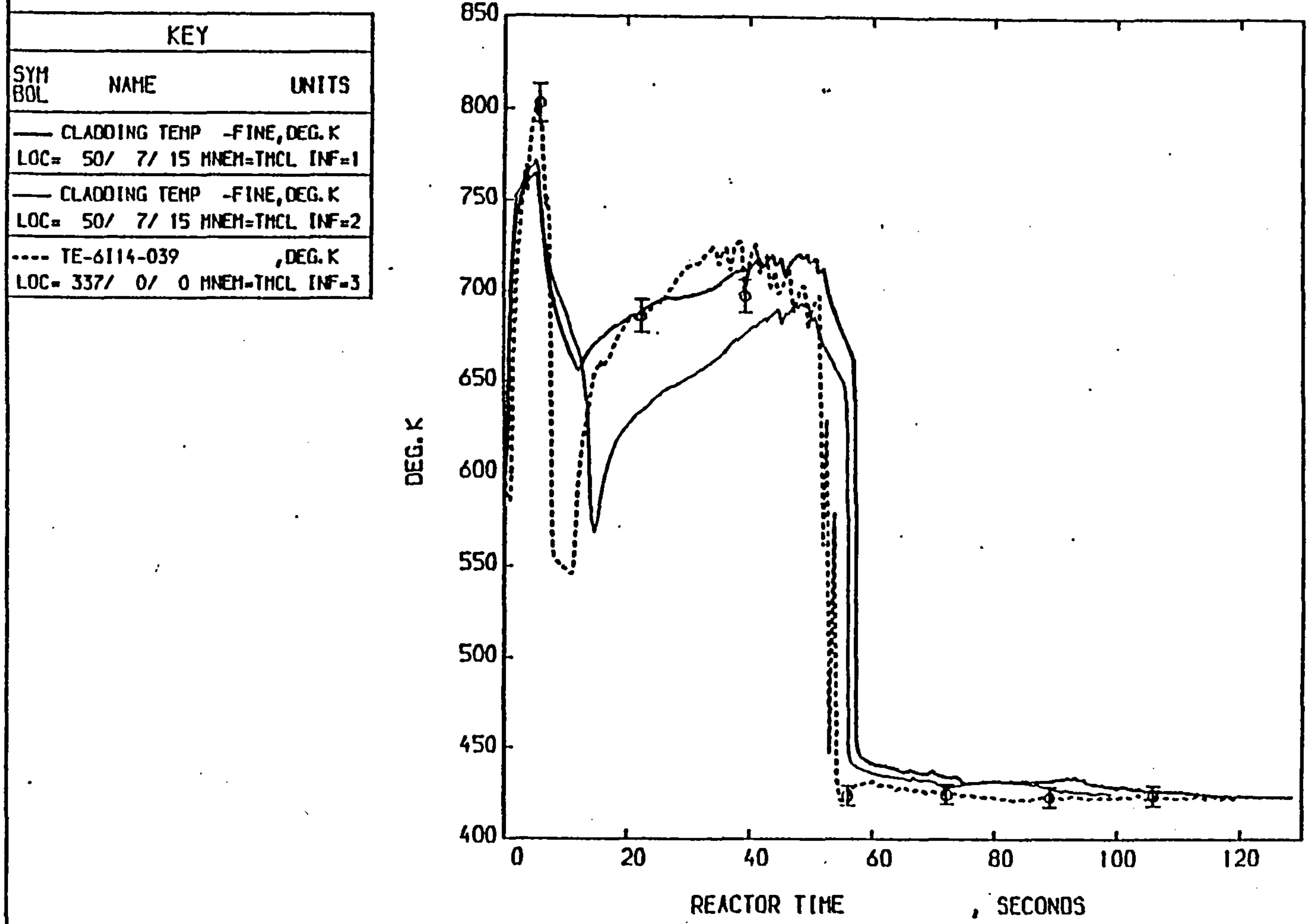

FIGURE 218 INF 1 ISHARP, INF 2 ZEROGAP, INF 3 EXP
FUEL ROD CLADDING TEMPERATURES - PERIPHERAL BUNDLES

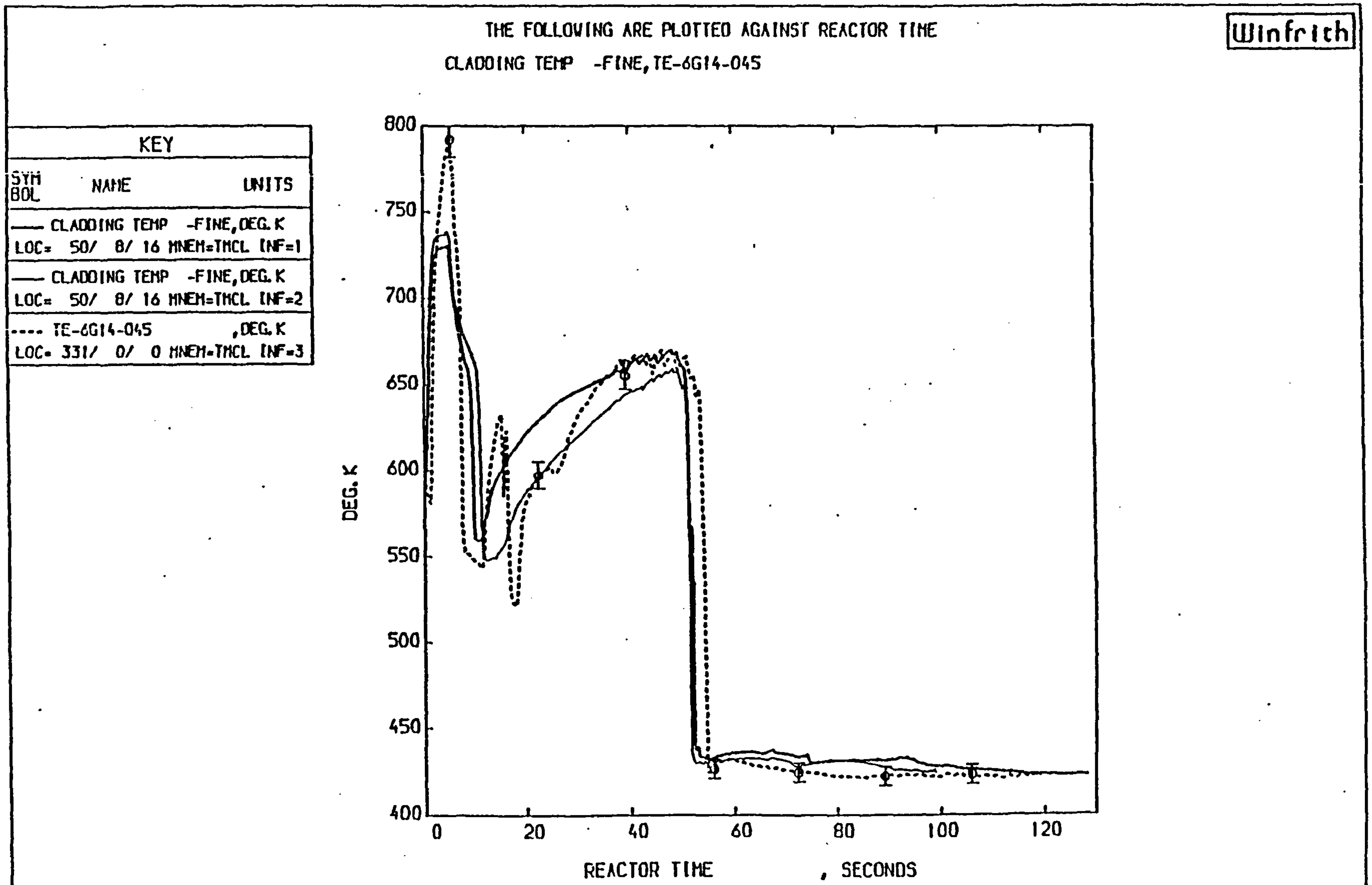

FIGURE 219 INF 1 ISHARP, INF 2 ZEROGAP, INF 3 EXP
FUEL ROD CLADDING TEMPERATURES - PERIPHERAL BUNDLES

DISTRIBUTION

PWR HEAT TRANSFER AND HYDRAULICS WORKING GROUP

Mr M W E Coney	CEGB	CERL Kelvin Avenue, Leatherhead, Surrey
Dr M J Bird	AEEW	338/B41
Dr A J Wickett	AEEW	214/A32
Mr I Brittain	AEEW	201/A32
Mr K G Pearson	AEEW	333/B41
Dr D B Utton	NNC	c/o Reports Section, Library, Booths Hall, Chelford Road, Knutsford, Cheshire WA16 9QZ
Mr K Routledge	NNC	c/o Reports Section, Library, Booths Hall, Chelford Road, Knutsford, Cheshire
Mr D Coucill	BNF	Springfields Works, Salwick, Preston, Lancs
Mr P C Hall	CEGB	Barnett Way, Barnwood, Gloucestershire
Dr P R Farmer	CEGB	HSD, Courtenay House, 18 Warwick Lane, London EC4P 3EB
Dr L C Daniels	UKAEA	Bldg 392, AERE Harwell
Dr T J Haste	UKAEA	Springfields NPDL, Salwick, Preston, Lancs
Mr D W McLaughlin	UKAEA	CLF 125, SRD Culcheth, Warrington
Mr B Chojnowski	CEGB	Marchwood Engineering Labs, Marchwood, Southampton
Dr M El-Shanawany	CEGB	HSD, Nuclear Safety Branch, Courtenay House, 18 Warwick Lane, London EC4P 3EB

ADDITIONAL

AEE WINFRITH, DORCHESTER, DORSET, DT2 8DH

Mr M H Butterfield	309/B41	(Summary Only)
Dr I H Gibson	236/A32	
Dr G R Kimber	221/A32	(Summary Only)
Dr P Coddington	270/A32	(5 copies)
Mr R Potter	209/A32	
Mr A Neill	267/A32	(Summary Only)
Miss E Allen	266/A32	(Summary Only)
Dr C Richards	260/A32	
Dr D A Williams	210/A32	(Summary Only)
Dr A L Nichols	102/A50	(Summary Only)
Dr S R Kinnersly	203/A32	
Dr J N Lillington	217/A32	(Summary Only)
Mr C R Gill	229/A32	(3 copies)

UKAEA, SAFETY AND RELIABILITY DIRECTORATE, WIGSHAW LANE, CULCHETH, WARRINGTON

Mr R N H McMillan	CLF 112	(Summary Only)
Dr A A Debenham	CLC 002	(Summary Only)
Mr P Clough		(Summary Only)

UKAEA, RISLEY NPDE, WARRINGTON, WA3 6AT

Reports Library		
Mr A Parry	E417	(Summary Only)

UKAEA, AERE HARWELL, DIDCOT, OXON, OX11 ORA

Dr D Hicks	G35, Bldg 77	
Mr M R Everett	Bldg 329	(Summary Only)
Dr G F Hewitt	TH 392.7	

UKAEA, RISLEY, NPDL, WARRINGTON, WA3 6AT

Dr W E Gardner	3/103	
Dr N Davies	CH481	(Summary Only)

UKAEA SPRINGFIELDS NPDL, SALWICK, PRESTON, PR3 ORR

Mr R D Stacey	Bldg 321	(Summary Only)
Mr A J Manley		(Summary Only)

UKAEA, WINDSCALE NL, SELLAFIELD, SEASCALE, CUMBRIA

Mr A Garlick		(Summary Only)

BNFL, SPRINGFIELDS WORKS, SALWICK, PRESTON, PR3 OXJ

Mr D A Howl	Bldg 382	(Summary Only)
Mr J P Cooch	Bldg 382	(Summary Only)

NNC, BOOTH'S HALL, CHELFORD ROAD, KNUTSFORD, CHESHIRE

Dr K R Barry		(Summary Only)
Mr R J Tinsley		(Summary Only)

NNC Risley, Warrington Road, Risley, Warrington

Dr D Briney		(Summary Only)

CEGB, COMPUTING BUREAU, 85 PARK STREET, LONDON SE1

Mr L Wilson		(Summary Only)

CEGB, HEALTH AND SAFETY DEPARTMENT, NUCLEAR SAFETY BRANCH, 18 WARWICK LANE LONDON, EC4 4EB

Mr J R Harrison		(Summary Only)

LOFT PROGRAMME REVIEW GROUP

TECHNICAL RESEARCH CENTER OF FINLAND (VTT), NUCLEAR ENGINEERING LABORATORY, POB 169, SF-00181 HELSINKI 18, FINLAND

Mr Heikke Holmstrom

EIDGENÖSSISCHES INSTITUT FÜR REAKTORFORSCHUNG, CH-8303 WÜRENLINGEN, SWITZERLAND

Mr O M Mercier

ÖSTERREICHISCHES FORSCHUNGSZENTRUM, SEIBERSDORF GESELLSCHAFT MBH, C/O EG&G IDAHO INC, PO BOX 1625, IDAHO FALLS, ID 83415, USA

Dipl Phys S Michael Modro

UNIDAD ELECTRICA SA, C/ FRANCISCO GERVAS 3, E-28020 MADRID, SPAIN

Mr Jose Puga

OFFICE OF NUCLEAR REACTOR REGULATION, US NUCLEAR REGULATORY COMMISSION, WASHINGTON DC 20555, USA

Dr Brian Sheron

JAPAN ATOMIC ENERGY RESEARCH INSTITUTE, TOKAI-MURA, NAKA-GUN, IBARAKI-KEN 219-11, JAPAN

Dr Kanji Tasaka

US DEPARTMENT OF ENERGY, OFFICE OF NUCLEAR POWER SYSTEMS, MS B-107, WASHINGTON DC 20555, USA

Mr D F Giessing

EPRI, PO BOX 10412, PALO ALTO, CA 94304, USA

Mr M Merilo

ENTE NAZIONALE ENERGIE ALTERNATIVE, CRE CASACCIA, SP ANGUILLARESE KM 1 + 300, CP NR 2400, I-00100 ROME, ITALY

Dr Giorgio Palazzi

CEGB, PROJECT MANAGEMENT TEAM, BOOTHS HALL, CHELFORD ROAD, KNUTSFORD, CHESHIRE

Mr N Buttery	
Mr M E Durham	(Summary Only)
Dr M M Chestnutt	(Summary Only)
Mr P George	(Summary Only)
Dr R Garnsey	(Summary Only)

CEGB, CERL, KELVIN AVENUE, LEATHERHEAD, SURREY

Dr G C Gardner	(Summary Only)
Mr N Newman	(Summary Only)

CEGB, BERKELEY NUCLEAR LABORATORIES, BERKELEY, GLOUCESTERSHIRE, GL13 9PB

Dr D Witherington	(Summary Only)
Dr S J Board	(Summary Only)
Ms J P Longworth	(Summary Only)

CEGB, GDCD BARNWOOD, BARNETT WAY GLOUCESTER, GLOUCESTERSHIRE, GL4 7RS

Mr C Harwood	(Summary Only)
Mr I Pugh	(Summary Only)
Mr P D Jenkins	(Summary Only)
Mr K H Ardron	
Mr J R D Jones	(Summary Only)

CEGB, MARCHWOOD ENGINEERING LABORATORIES, SOUTHAMPTON, HAMPSHIRE, S04 4ZB

Dr B Chojnowski	(Summary Only)

SOUTH OF SCOTLAND ELECTRICITY BOARD, CATHCART HOUSE, SPEAN STREET, GLASGOW, SCOTLAND

Mr D R Reeks	(Summary Only)

NUCLEAR INSTALLATIONS INSPECTORATE, HEALTH AND SAFETY EXECUTIVE, ST PETERS HOUSE, STANLEY PRECINCT, BALLIOL ROAD, BOOTLE, L20 3LZ

Mr C Potter
Mr J F Campbell
Dr S A Harbison

STUDSVIK ENERGITEKNIK AB, S-61182 NYKOPING, SWEDEN

Mr O Sandervaag

US NUCLEAR REGULATORY COMMISSION, WASHINGTON DC 20555, USA

Dr Robert Van Houten

EG&G, IDAHO INC, PO BOX 1625, IDAHO FALLS, ID 83415, USA

Dr D Croucher

OECD NUCLEAR ENERGY AGENCY, 38 BOULEVARD SUCHET, F-75016 PARIS, FRANCE

Mr Ralph Caruso

1 MELSTOCK AVENUE, DORCHESTER, DORSET

Mr J Fell

INTERNATIONAL CODE ASSESSMENT AND APPLICATIONS PROGRAMME

USNRC, SILVER SPING, WASHINGTON DC 20555, USA

Mr D Bessette
Mr L Shotkin

LOS ALAMOS NATIONAL LABORATORY, PO BOX 1663, LOS ALAMOS, NEW MEXICO 87545, USA

Dr R Jenks
Mr D Liles

EG&G (IDAHO) INC, INEL, PO BOX 1625, IDAHO FALLS, IDAHO 83415, USA

Mr G Wilson

LIBRARIES

Dounreay	-2
Harwell	-2
Risley	-4
Springfields	-2
Windscale	-2
Winfrith	-4

NRC FORM 335

U.S. NUCLEAR REGULATORY COMMISSION

BIBLIOGRAPHIC DATA SHEET

1. REPORT NUMBER (Assigned by NRC. Add Vol., Supp., Rev., and Addendum Numbers, if any.)

NUREG/IA-0027
AEEW-M 2464

2. TITLE AND SUBTITLE

TRAC-PF1/MOD1 Calculations of LOFT Experiment LP-02-6

3. DATE REPORT PUBLISHED

April 1992

4. FIN OR GRANT NUMBER

A4682

5. AUTHOR(S)

P. Coddington, C. Gill

6. TYPE OF REPORT

Technical

7. PERIOD COVERED

8. PERFORMING ORGANIZATION – NAME AND ADDRESS (If NRC, provide Division, Office or Region, U.S. Nuclear Regulatory Commission, and mailing address; if contractor, provide name and mailing address.)

Winfrith Technology Centre
United Kingdom Atomic Energy Authority
Winfrith, Dorchester
Dorset, England DT 28 DH

9. SPONSORING ORGANIZATION – NAME AND ADDRESS (If NRC, type "Same as above"; if contractor, provide NRC Division, Office or Region, U.S. Nuclear Regulatory Commission, and mailing address.)

Office of Nuclear Regulatory Research
U. S. Nuclear Regulatory Commission
Washington, DC 20555

10. SUPPLEMENTARY NOTES

11. ABSTRACT (200 words or less)

Experiment LP-02-6 was the First Large Break (200% Double Ended Cold Leg) Loss-of-Coolant Accident (LOCA) Experiment carried out in the Loss-Of Fluid Test (LOFT) Facility under the auspices of the Organization For Economic Cooperation and Development (OECD).

This report contains a comparison of the results of experiment LP-02-6 with those of TRAC-PF1/MOD1 calculation.

12. KEY WORDS/DESCRIPTORS (List words or phrases that will assist researchers in locating the report.)

ICAP Program, TRAC-PF1, LP-02-6, LOCA, Large Break

13. AVAILABILITY STATEMENT

Unlimited

14. SECURITY CLASSIFICATION

(This Page)
Unclassified

(This Report)
Unclassified

15. NUMBER OF PAGES

16. PRICE

NRC FORM 335 (2-89)

THIS DOCUMENT WAS PRINTED USING RECYCLED PAPER

UNITED STATES
NUCLEAR REGULATORY COMMISSION
WASHINGTON, D.C. 20555

OFFICIAL BUSINESS
PENALTY FOR PRIVATE USE, $300

SPECIAL FOURTH-CLASS RATE
POSTAGE & FEES PAID
USNRC

PERMIT No. G-67